Ai-Jie Wang · Bin Liang · Zhi-Ling Li
Hao-Yi Cheng **Editors**

Bioelectrochemistry Stimulated Environmental Remediation

From Bioelectrorespiration to
Bioelectrodegradation

Springer

Bioelectrochemistry Stimulated Environmental Remediation

Ai-Jie Wang • Bin Liang • Zhi-Ling Li
Hao-Yi Cheng

Editors

Bioelectrochemistry Stimulated Environmental Remediation

From Bioelectrorespiration to
Bioelectrodegradation

Springer

Editors
Ai-Jie Wang
Key Laboratory of Environmental
Biotechnology, Research Center for
Eco-Environmental Sciences
Chinese Academy of Sciences
Beijing, China

State Key Laboratory of Urban Water
Resource and Environment, School of
Environment
Harbin Institute of Technology
Harbin, China

Zhi-Ling Li
School of Municipal and Environmental
Engineering
Harbin Institute of Technology
Harbin, China

Bin Liang
Research Center for Eco-Environmental
Sciences
Chinese Academy of Sciences
Beijing, China

Hao-Yi Cheng
Research Center for Eco-Environmental
Sciences
Chinese Academy of Sciences
Beijing, China

Foreword

No doubt, there is an urgent need for advanced treatment of recalcitrant environmental chemicals. The general public gets every day more concerned, and even nervous, about various types of *so-called micro-pollutants*. Actually, chemical pollutants in the effluents of used water treatment plants are often still a factor 10–100 times above the Predicted No Effect Level (Margot et al., WIREs Water 2015, 2:457–487). Several micropollutants remain unchanged even after long-term bank filtration (Hamann et al., Sci. Total Environ. 2016, 545:629–640). To preserve the quality of life of the next generations, we need to come to new developments which open perspectives to bring forward strongly enhanced environmental remediation. We should not be at ease about this.

Scientific curiosity has, about two decades ago, re-launched the generic interest in bioelectrochemistry (Park and Zeikus, Appl. Environ. Microbiol. 2000, 66:1292–1297). The developments have ever since been startling and exponential in terms of perspectives and potential applications. Not only the insights in basic microbiology but also the progress in various aspects of technology have allowed to think forward with respect to new types of treatments of various environmental pollutants. Time has come *to implement the excellent scientific progress into valuable applications* which will demonstrate to the general public the significance of basic and applied research, particularly in this interphase where biology and electrochemistry meet in a most intriguing way.

This book is in many respects remarkable. It brings together in a comprehensive way the various advances of bioelectrochemistry in relation to environmental technology. It covers not only various aspects of microbial insights on physiology and ecology, but bridges these with the engineering and the implementation of various types of reactor systems. It addresses issues concerning a variety of contaminants. Moreover, it covers a whole set of matrices ranging from clean to polluted and from liquid and solid environments, such as drinking and wastewaters, industrial wastes, sediments, and soils. *Search and you will find your topic of interest*.

Most importantly, this book has the ambition to generate further scientific and technologiccal endeavor; it stimulates to think "break new grounds." The demands for better environmental quality are of such nature and such priority that all of us

should embark on renewed fresh thinking about what potentials this dynamic field will reveal in the future. We should dare to hope that this is the beginning of *the combination of a variety of new developments in microbial, electrotechnical, and environmental upgrading*.

Ghent University   Willy Verstraete
Gent, Belgium

Contents

Chapter 1
Bioengineering of Bacterial Extracellular Electron Transfer Towards Sustainable Wastewater Treatment

Zhen Fang, Jamile Mohammadi Moradian, Yan-Zhai Wang, Yang-Yang Yu, Xiang Liu, and Yang-Chun Yong

1.1 Introduction

Electron transfer is an essential process for life which is vital to nearly all cell metabolisms. Different electron transfer pathways related to substrate metabolism, energy metabolism, cofactor recycling, and aerobic/anaerobic respiration have been identified in prokaryotic cells. However, most of these electron transfer processes occurred intracellularly, and most of the electron acceptors are water soluble molecules or gases. Surprisingly, it was found that some bacterial species had a very unique electron transfer process by using the solid metal oxide or conductive material as the electron acceptor [1–5]. More recently, it was found that some species could uptake the electrons from the extracellular solid electrode [6]. To highlight the unique extracellular electron exchange capability of bacteria, it was termed as extracellular electron transfer (EET). To date, EET has been proved to play important roles in geochemical cycling and pollutants transfromation processes [7]. More impressively, by integrating traditional electrochemical systems with bacterial EET-based modules, various bioelectrochemical systems (BES) have been developed for environmental applications [8].

BES are unique systems that couples microbial metabolism with extracellular electrochemical reactions. It can employ microbes as catalysts to convert the organic waste including low-strength wastewaters into electricity at the anode [9]. Meanwhile, pollutant bioreduction, hydrogen generation, or other products including carbohydrates from CO_2 fixation can be achieved at the cathode. So, BES can be divided into two major categories based on the EET direction [10, 11] (Fig. 1.1). One is anodic BES (bacterial intracellular electrons passed to the electrode, e.g., microbial fuel cell (MFC)) that harnesses electrical current from the microbial

Z. Fang · J. M. Moradian · Y.-Z. Wang · Y.-Y. Yu · X. Liu · Y.-C. Yong (✉)
Biofuels Institute, School of Environment and Safety Engineering, Jiangsu University, Zhenjiang, China
e-mail: ycyong@ujs.edu.cn
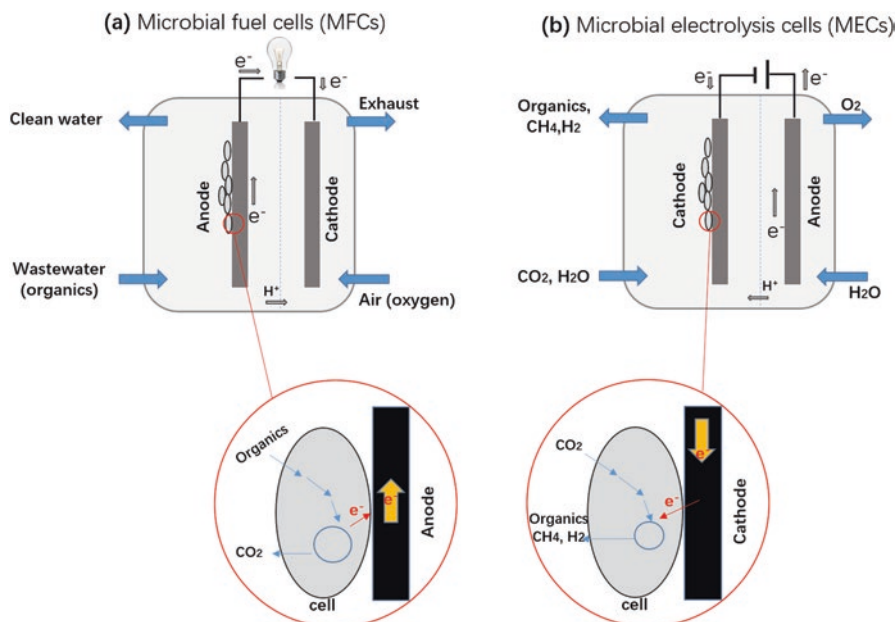
Fig. 1.1 Bioelectrochemical wastewater treatment with different electron transfer directions. Schematic representation of a typical configuration of the two most common bioelectrochemical wastewater treatment systems: the microbial fuel cell (MFC) for outward EET with organic consumption (**a**) and the microbial electrolysis cell (MEC) for inward EET with hydrogen, methane, and organic production in cathode (**b**). (This schematic is modified from Ref. [11])

oxidation of organic matter by using solid electrode as an electron acceptor. The other one is cathodic BES (uptake extracellular electrons from electrode by bacteria, e.g., microbial electrolysis cell (MEC)) that utilizes the cathodic electrons to power the bacterial catalysis such as pollutant bioreduction and chemical production. To date, BES have been successfully used for accelerating pollutant biodegradation/bioreduction, electricity harvesting from wastewater, resources (metal, nitrogen, phosphate, etc.) recovery from wastewater, hydrogen production, CO_2 upgrading, and other value-added chemical productions [8, 12, 13]. Besides, BES have also been adapted as various biosensing systems that can be used even for self-power online environment monitoring [10]. Therefore, BES have been considered as an energy-saving, emission-reducing, and economic feasible platform technology for sustainable wastewater treatment and environment protection. However, the performance of BES is still needed to be improved to meet the requirement of the practical applications. As EET is the fundamental and most important process in BES [14, 15], EET efficiency augmentation became the top priority for BES improvement. In this chapter, we would introduce the molecular pathway of EET and how bioengineering strategies improve the EET efficiency.

1.2 Molecular Pathways for EET

1.2.1 Outward EET Pathway

In anodic BES, bacteria produced intracellular electrons by cellular metabolism and passed across the membrane to the solid electrode. As for cells, the EET process is the electron outward transport from intracellular compartment to the extracellular electrode, which can be considered as outward EET. There are three main types of outward EET in electroactive bacteria. One is direct EET through cell and electrode surface interaction, one is indirect EET through bioactive shuttles and mediators between the cell and electrode, and another one is to use pili as nanowire for EET [16]. In this section, we would like to introduce the representative outward EET pathways in three model exoelectrogens, i.e., *Shewanella oneidensis*, *Geobacter sulfurreducens*, and *Pseudomonas aeruginosa*.

The main and most extensively studied outward EET pathway in *S. oneidensis* is called Mtr pathway, which contains a series of cytochromes like CymA, MtrA, MtrB, MtrC, and OmcA [17]. CymA attaches to the inner membrane by a single α-helix, while the MtrCAB complex crossing the outer membrane mainly responds to the Fe (III) reduction [18, 19]. The first step of the outward electron transfer is the formation of NADH or $FADH_2$ from the TCA cycle. Then NADH dehydrogenase or succinate dehydrogenase can oxidize NADH or $FADH_2$ and transfer electron into quinol pool which is a small electron carrier and is able to further transfer electron to inner membrane cytochromes [20]. CymA plays the main role to accept electron from quinone pool, causing it to transfer electron to other periplasmic cytochromes, such as DmsEF, NapAB, NrfA, FccA, MtrA, and SirA [15]. In those cytochromes, two complexes can support the transfer of electrons between the inner membrane and outer membrane or even the anode electrode. One complex is the DmsABEF which is able to reduce DMSO to DMS [21]. The other one is MtrCAB complex. Some reports mentioned that there are lots of homologues of MtrCAB like MtrFDE and OmcA according to the genome annotation of *S. oneidensis* [22, 23]. The Mtr pathway can easily transfer electron extracellularly by MtrC/OmcA, and the EET rate can be greatly improved with the outer membrane cytochrome-bound flavin semiquinones [24]. The electrode could accept electron directly from cytochrome protein MtrC/OmcA or indirectly from flavin when flavins were secreted outside the outer membrane and set as an electron shuttle molecule [19, 25].

G. sulfurreducens is a gram-negative obligate anaerobic δ-proteobacteria and widely used as a model electroactive microorganism. It is assumed that several electron transport pathways existed in *G. sulfurreducens* since more than 100 genes are coding the putative *c*-type cytochromes [26–28]. Similar to *S. oneidensis*, the main target of EET is to create a proton gradient for energy conservation by redox equivalents between the cellular menaquinone (MQ) pool and the extracellular insoluble metals or anode electrode [29]. The outward EET pathway consists of three parts.

MacA, a diheme cytochrome c peroxidase, transfers electron from the inner membrane to periplasmic c-type cytochrome (PpcA) [26]. And PpcA can pass the electrons to the outer membrane cytochromes, termed as OMCs (e.g., OmcB, OmcC, OmcS, OmcZ) [15]. It has been proved that extracellular cytochrome OmcZ secreted from *Geobacter* strains contributed 90% electron transfer to electrode, while OmcS and OmcB are essential for Fe(III) reduction [30]. In addition, nanowire, also called e-pili, is another efficient EET pathway for *Geobacter* that enables physical connection between cells or cells and surface of the electrode [31]. It was also found that the e-pili or pilus-like conductive filaments existed in other microorganisms besides *Geobacter* [32]. Malvankar et al. proposed that π-stacking of aromatic amino acid residues is the main factor enabling electron delocalization [16]. The conductivity of the e-pili also can be tuned by manipulating the aromatic content [33]. However, the structure and electron transport mechanism of e-pili are still unclear, and more efforts should be made in the near future.

P. aeruginosa is another model electroactive bacterial species with typical electron shuttle-mediated outward electron transfer pathway. Recent researches proved that the electron transport of *P. aeruginosa* mainly depends on electron shuttles but not c-type cytochromes [34, 35]. Those shuttles, like pyocyanin and phenazine carboxamide, can be synthesized by *P. aeruginosa* and reduced intracellularly. Reductive shuttles could be secreted out of the cell and be oxidized on the electrode surface, and the electron was passed to the electrode. Next, the oxidized shuttles could go across the cell membrane and back to the cytoplasm for further reduction and shuttling of the electron transport across the cell membrane [36].

In summary, a handful of organisms are known to be able to interact with electrodes; however, the exact mechanisms of EET processes haven't been fully understood yet. Typically, there are three different EET pathways based on the interactions between cell and the electrode: (i) direct EET based on direct contact between cell surface and the electrode, (ii) direct EET via special conductive cell appendant such as pili or nanowires, or (iii) indirect EET by mediating substances that act as electron shuttle. Biofilm development on electrode surface is the common method for direct electron transport [35]. Indirect or mediated electron transfer is another important EET pathway which mediates shuttles to transfer charge between electrode and organism like *P. aeruginosa*.

1.2.2 *Inward EET Pathway*

Generally, inward EET also called reverse electron chain pathway means electroactive cells accept electron from cathode. Those strains are also called electrotrophic microorganisms that can perform electroreductions to environmental pollutants (e.g., NO_3^-) and chemical fuel precursors (e.g., H^+ and CO_2) [37]. Though cathodic EET has been into focus of many research communities within the last decade, the mechanism of inward EET pathway is complex and still unclear. Interestingly, some reports have showed that the abovementioned two model microorganisms

S. oneidensis and *G. sulfurreducens* can form current-consuming biofilms. By adding fumarate to *Shewanella*, a sudden onset of cathodic currents can be observed in 3D biofilms, suggesting inward EET really happened [38]. The proposed inward EET pathway in *Shewanella* is related to a series of c-type cytochromes (such as MtrCAB complex), and the EET direction is controlled by the flavin redox bifurcation [39]. The pathway is the opposite of outward EET of *Shewanella* and probably transmits electron as follows: MtrC-MtrB-MtrA-CymA-FccA [18]. Since those cytochromes share approximate redox potential and distance, electron can be easily transferred from one c-type cytochrome to another [40]. On the other hand, it was observed that a *Geobacter* gene GSU3274 encoding a putative monoheme c-type cytochrome was strongly expressed in cathodic biofilms [41]. So, it is possible that OMC on the outer membrane is to accept electron and further transmits electron to GSU3274 in periplasmic space, while GSU3274 is mobilizable and transmits electron to the IMC.

Rhodopseudomonas palustris TIE-1 owns the phototrophic iron oxidation (Pio) pathway which absorbs electron from extracellular Fe(II) and delivers it into cytoplasm for CO_2 fixation. It has proved that *R. palustris* TIE-1 also can directly utilize electron from electrode [42, 43]. The deduced inward EET pathway is PioABC complex which consists of PioA (an MtrA homologue), PioB (an MtrB homologue), and PioC (an iron-sulfur protein with a high redox potential). The photoreaction center is located at the inner membrane to accept electron from PioC and exchange electron with quinone pool [40].

Sideroxydans lithotrophicus ES-1 is another metal-oxidizing autotrophic strain with the hypothesized inward EET pathway. *S. lithotrophicus* ES-1 oxidizes Fe(II) at pH 7 and transmits electron inward. From genome analysis, an *mto* gene cluster was found, and the encoding proteins share high homology with MtrCAB complex of *Shewanella* [44]. The inward EET of *S. lithotrophicus* ES-1 has four possible parts of cytochromes as the following pathway, MtoB (an MtrB homologue)-MtoA (an MtrA homologue)-MtoD (a gene that encodes a monohaem cytochrome)-CymA. The EET pathway can pass through from extracellular Fe(II) to the quinone pool of inner membrane [45].

1.3 Bioengineering of EET

Since BES are an excellent platform for sustainable wastewater treatment, it has received a tremendous boost for over a decade [14]. As the performance of BES greatly depends on the efficiency of bacterial EET, EET engineering is of great importance for BES optimization. During the past decades, great efforts have been made, and various strategies have been developed for EET engineering. As a modern biological technology, bioengineering showed great success in EET improvement and also holds great promise for further advancing the application of bacterial EET and BES. In this section, we would like to introduce bioengineering strategies to improve EET efficiency and BES performance.

1.3.1 Metabolic Engineering

For outward EET, the main process could be described as electron extraction, electron relay, and transmembrane electron transport [37]. So, the EET pathway usually contained five modules, including substrate oxidation, NADH recycling, quinone recycling, shuttle redox reaction, and transmembrane electron transport (Fig. 1.2). With the development of metabolic engineering technique, it is efficient to genetically modify the above five modules to facilitate EET and improve BES performance.

Genetically modified strains can produce a much higher and more stable electricity output than its parental strain in MFCs. The successful example is engineered *Escherichia coli* with enhanced TCA cycle [46]. The TCA cycle, also called citric acid cycle, is the center of metabolism to supply sufficient ATP and NAD(P)H for cell physiological activity. However, it was discovered that under MFC microaerobic condition, cells produce insufficient ATP and NAD(P)H which are essential for quinone reduction and EET [35]. The *arcA* gene, a global regulatory gene in *E. coli* mediating repression of enzymes in aerobic pathways, is the key factor to adjust TCA cycle [47]. Through the knockout of *arcA*, it can easily improve TCA cycle and initial substrate utilization of glycerol oxidation with the mutant *E. coli* (arcA⁻).
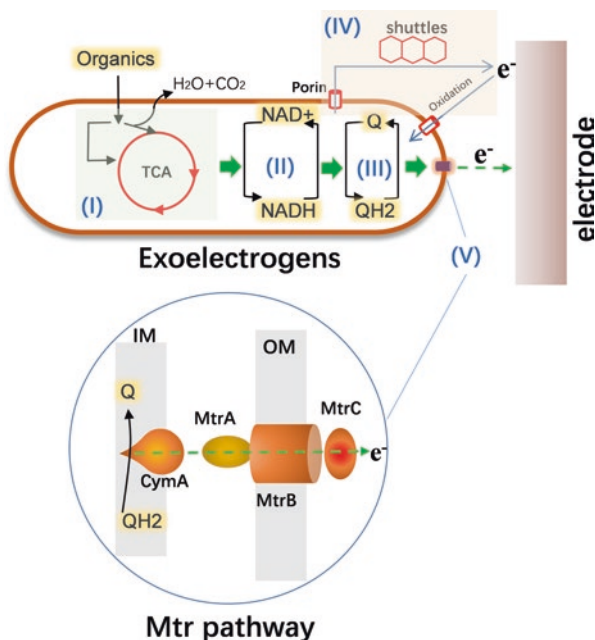

Fig. 1.2 Five modules in electroactive bacteria for EET. (*I*) The oxidation of organics (initial electron donor) and TCA cycle; (*II*) the redox of NADH; (*III*) the redox of quinone pool; (*IV*) electron transfer to extracellular electrode by shuttles through porin complex; and (*V*) the representative *Shewanella* metal-reducing (Mtr) pathway for EET

In addition, without the repression of aerobic pathway, the mutant arcA⁻ showed much higher power density than the wild type, and it was found that the enhanced secretion of a diffusive electron mediator (hydroxyl quinone derivative) may also contribute to the EET [46]. So, the first module of substrate oxidization in TCA cycle can affect the third module and integrally improve MFC work efficiency.

Changing the metabolic flux into electron production or extraction may be the fastest way to increase EET between bacteria and anodes. In anaerobic conditions, *E. coli* could store glucose electrons into reductive metabolites to balance their intracellular redox state [48, 49]. The by-product lactate, containing much electrons from glucose, may inhibit bioelectricity output in MFCs. It was found that the abolishment of the key enzyme LdhA in lactate synthesis pathway increased the ratio of NADH/NAD⁺, which is the precondition to increase intracellular releasable electrons. Subsequently, the *ldhA* knockout mutant transferred endogenous electron to the anode *by* a secreted diffusive electron shuttle [50]. Besides, genetic engineering, such as coexpressing flavin biosynthesis genes (*rib*D-*rib*C-*rib*BA-*rib*E) and EET pathway conduit biosynthesis genes (*mtr*C-*mtr*A-*mtr*B), can be explored in *S. oneidensis* MR-1 which exhibited an improved EET capacity [51]. The engineered strain enlarged the utilization of substrate lactate and rapidly removed methyl orange. This work demonstrates that coupling of improved synthesis of mediators and metal-reducing conduits could be an efficient strategy to enhance EET in *S. oneidensis* MR-1 for environmental remediation, wastewater treatment, and bioenergy recovery from wastes.

We also can improve the substrate (initial electron donor) utilization to enhance aerobic respiration and NADH regeneration. *Shewanella* always prefers to use lactate in MFC; however, the utilization efficiency is very low because of the low absorbency [52]. It has reported that the lactate oxidation ability and bioelectron production rate of *Shewanella* can be obviously improved by constructing engineered strain [53]. The crucial strategy is overexpressing SO1522 gene, the intrinsic inner membrane (IM) lactate transporter. The mutant can digest 55 ± 5 mM D-lactate, 61% higher than that by wild type. It proved that effectively substrate oxidation rate is corresponding to electron production rate.

The second module of EET pathway is to recycle the intracellular cofactor pool of NADH. The availability of cofactor is essential to improve power output in MFCs [54]. By overexpression of *nadE* (NAD synthetase gene) in *P. aeruginosa*, the electrochemical activity and power output were significantly increased as well as the concentration of the electron shuttle (pyocyanin, PYO) which is the main shuttle to accomplish extracellular redox and EET. So, increasing the second module of EET pathway by metabolic engineering has direct and indirect positive effect on power output. Another method is to increase electron mediator (shuttles) pool as showed in the fourth EET pathway module. In *P. aeruginosa* system, when *phzM* (methyltransferase encoding gene) was overexpressed, there was a 1.6-fold improvement of PYO concentration, and the maximum power density of MFC can be increased to a fourfold of the original strain, and it finally achieved the enhanced electricity power output (EPT) [55]. In Schmitz et al.'s work, they tried seven core phenazine biosynthesis genes *phzA-G* and the two specific genes *phzM* and *phzS* for PYO synthesis

[56]. The PYO overproduction mutant of *P. putida* KT2440 showed visible blue color and could adapt to oxygen-limited conditions for 2 weeks. So, the manipulation of electron shuttle synthesis pathways could be an efficient approach to improve the EET efficiency.

In addition, there are other bioengineering strategies to enhance EET pathway, like anoxic metabolic engineering. In *P. aeruginosa*, the 2-heptyl-3,4-dihydroxyquinoline (PQS) quorum-sensing (QS) system can regulate the biosynthesis of the redox shuttle phenazines [57, 58]. However, PQS makes trouble for anaerobic growth and EET pathway in MFC. Using the PQS negative Δ*pqsC* mutant to overexpress PqsE effector, *P. aeruginosa* produced higher concentrations of phenazines and exhibited an improved electrical performance under anaerobic conditions [57]. These results indicate that targeting cell-cell communication by genetic engineering of quorum sensing regulation is a suitable technique to improve power output of BES. *P. putida* F1 is a promising host for the biodegradation of chemicals and MFCs, but its industrial applications are significantly limited because of its obligate aerobic character [59]. So, it is meaningful to empower its anoxic metabolism into anaerobic respiration. Lai et al. realized *P. putida* F1 lives under anaerobic and limited biofilm conditions by increasing the redox potential of the mediator [60]. They propose that a growth limitation under anaerobic conditions is due to a shortage of NADPH. So, anoxic metabolic engineering can broaden the application of electroactive strains in BES.

1.3.2   Physiological Manipulation

In order to obtain the maximum power output or EET of electroactive strain, physiological manipulation is also important. Generally, there are many related methods, such as additions of surfactant, heavy metal ion, electron shuttles, integrated aerobic-anaerobic strategy, high cell density strategy, pH, optimization, and so on.

Firstly, we would like to introduce how to regulate electrochemical cell by enhancing cell membrane permeability. In *P. aeruginosa* MFC system, electron shuttle (PYO) is the main factor to complete EET, and its transport efficiency is based on cell membrane permeability [55, 61]. Surfactant addition may be a one choice since some researchers have mentioned that enhanced endogenous biosurfactant could improve the electron transfer rate and power output of MFC [62]. It observed that RhlA overexpressed *P. aeruginosa* mutant had high yields of biosurfactant rhamnolipids and PYO which were proposed to the main contributors of higher power density output [62]. Except for endogenous surfactant, we can directly add exogenous surfactant like sophorolipid to enhance the performance of electrochemical active bacterial in MFC with the high level secretion of PYO [63]. In addition, it is found that adding a trace level of heavy metal ions (Cu^{2+} and Cd^{2+}) has a positive effect on power output [64]. The main reason may be related to the change

of physiological activity which allows plenty of riboflavin to be secreted out of the cell and contributes a higher power output performance. It suggested that addition of biosurfactant or inorganic salt could be a promising way to enhance the energy generation in MFCs.

Using electrochemically active bacteria (EAB) is promising to treat wastewater in MFC; however, its application can be limited with the scale-up problem [65, 66]. One problem to restrict scale-up is the low cell density and biofilm [65]. With a higher biomass, biofilm on anode surface and riboflavin concentration significantly increased in MFC [67]. So, increase cell density would be a simple and practical strategy for EET and power density output. We also can increase electron mediator titer and biofilm formation by an integrated aerobic-anaerobic strategy in *P. aeruginosa*-inoculated MFC system, which is more favorable to support biofilm formation and PYO production [68]. So, promoted EET from EAB to the anode can be more easily achieved with the integrated aerobic-anaerobic strategy.

The pH of electrolyte tremendously affects the electricity output of MFCs [69, 70]. However, its underlying molecular mechanism remains elusive, in particular for *S. oneidensis* MR-1. One possible reason is related to the redox potentials of various c-type cytochromes, and electron mediators are sensitive to environmental pH [71, 72]. Some researchers have found that MFCs were able to deliver different electricity outputs in a wide range of pH (from 6 to 10) and cyclic voltammetry analysis showed that the underlying mechanism was related to the riboflavin concentration which was synthesized by *Shewanella* and showed a good correlation with the electricity output of MFCs at different pH [73]. Another example, with an anodic pH of 10.0 and a cathodic pH of 2.0, the tubular MFC provided an open-circuit voltage of 1.04 V and a maximum power density of 29.9 W/m^3, which were, respectively, 1.5 and 3.8 times higher than those obtained in the same MFC working at neutral pH [74]. pH also can affect the biofilm formation as well as the cell metabolism [75, 76]. The pH optimization strategy in both chambers provides a promising improvement in MFC performance.

Besides, cell-cell communication that enables synchronized population behaviors (e.g., shuttle secretion and extracellular electron transport) in microbial communities can be explored in the MFC system for bioremediation and bioenergy generation. It found that the quorum-sensing systems, which play the essential role for cell-cell communication, can control the aromatics biodegradation and the electricity harvest of *Pseudomonas* and QS is a generic cell-cell communication mechanism [58, 77, 78]. The synthesis of electron mediator phenazines is regulated by QS systems at the late exponential growth stage of *Pseudomonas* [79]. By overexpressing *rhl* gene to regulate QS system, the *Pseudomonas* strains showed great activity to produce PYO and phenazine-1-carboxylate [58]. It seemed that cell-cell communication mainly helps bacteria to overproduce shuttles and enhance electrochemical activity.

1.3.3 Synthetic Biology

Recently, the synthetic biology technique has attracted much attention since it can design and construct a new biological system or redesign artificial biological pathways for useful purpose [80]. Along with the perception of EET pathway and the genome decoding of exoelectrogenic bacteria (*S. oneidensis* MR-1 and *G. sulfurreducens* PCA), we can clearly find the corresponding genes [27, 81]. The wild-type exoelectrogens have many limitations like the strictly anaerobic and low growth rate, which might be overcome with synthetic biology approaches [82, 83]. To date, there are two categories of synthetic biology approaches which have been reported on exoelectrogens. One is to modify the native exoelectrogens to enhance electron flux by adding useful pathways, while the other is to introduce the complete EET pathway into non-native exoelectrogens [84]. There are several successful examples about using synthetic biology to enhance EET pathway as summarized in the following sections.

1.3.3.1 Synthetic Biology Enhancing EET in Native Exoelectrogens

Native exoelectrogenic microbes (*S. oneidensis*, *G. sulfurreducens*, and *P. aeruginosa*) are the first choice for genetic modification because they have many advantages, such as released genome sequence and partially known EET pathway. The only drawbacks can include the genetic tools that are not well-developed in those strains and the limited knowledge of how to adjust physiology with genetic modifications [51, 85]. For example, some scientists raised that *S. oneidensis* lacks proton-motive force to supply sufficient lactate which is the initial electron donor. By expression of a light-driven proton pump to increase proton-motive force, the electricity generation from this engineered strain was enhanced with light illumination [86]. Since the TCA cycle is the center metabolic pathway to produce NADH and ATP, the current production is related to the flux balance of exoelectrogen, and an artificial ATP drain into *G. sulfurreducens* probably increases power output [87].

Using synthetic biology to drive cells to produce plenty electron shuttle is an efficient method to enhance electron transfer rates in the fourth EET module. A riboflavin synthesis pathway from *Bacillus subtilis* was incorporated into *S. oneidensis*, *which s*ecreted 25-fold more flavins as well as 15-fold higher current production than wild-type strain [88]. Another typical case about synthesizing electron mediator is the phenazine overproduction in *P. aeruginosa*. The main strategy is modifying QS systems which finally achieved twofold phenazine titer and fivefold current production [57]. The work on *P. aeruginosa* seems more like metabolic engineering since the wild type can produce phenazine with itself. However, it suggests that producing electron shuttles is a tractable strategy for improving electrochemical performance and has great potential in non-native or native exoelectrogens [83]. Min et al. greatly improved the EET efficiency of *S. oneidensis* by engineering the c-type cytochrome protein-based conduit and riboflavin synthesis pathway,

which substantially proved the power of bioengineering/synthetic biology on EET manipulation [51].

Enhancing the biofilm formation by synthetic biology is another efficient method to modify EET. Generally, the biomass of biofilm on electrode is essential for EET and final electric output. Kouzuma et al. improved the biofilms of *S. oneidensis* by random genetic modifications of transposon mutagenesis libraries, and they showed more than 90% improvement of current [89]. Since the c-di-GMP (bis-(3′-5′)-cyclic dimeric guanosine monophosphate) has the function to promote the adhesive matrix components, Liu et al. tried to overproduce c-di-GMP with a heterologous gene *ydeH* in *S. oneidensis* and obtained a rich biofilm and a maximum power density of 2.8 times increase compared to the wild type [90]. The biofilm properties of *G. sulfurreducens* and its EET rate also can be improved by deletion of its pilin regulatory domain [91]. Furthermore, the most interesting field is to make native exoelectrogenesis to form biofilm on common electrode materials like gold. Kane et al. expressed a synthetic gold-binding peptide on the cell surface of *S. oneidensis* to improve its binding ability to gold [92].

However, with limited knowledge on EET and the biology of exoelectrogens, attempts to engineering EET with synthetic biology or metabolic engineering approaches are still scarce and are quite challenging. So, it needs more understanding to introduce new pathway in exoelectrogens and optimize the expression of multiple complex proteins by synthetic biology or metabolic engineering. In addition, we also need new genetic tools for synthetic biology in exoelectrogens. Though there is a big advance in synthetic biology, the limited understanding of exoelectrogen physiology might limit its application. The commonly used plasmids in *S. oneidensis* MR-1 derived from the broad-host-range (bhr) cloning vector pBBR1MCS with the *mob* (mobilization gene) and promoter *lac* [90]. Recently, Song group has developed CRISPRi–sRNA to regulate transcription–translation of EET in *S. oneidensis* and broke the ice of lacking efficient genome regulation tools in exoelectrogen [85]. CRISPRi means clustered regularly interspaced short palindromic repeats interference and is used to repress the expression levels of EET pathway-related genes like *mtrCAB* and electroactive biofilm genes. Moreover, they established a translational regulation technology of Hfq-dependent small regulatory RNA (sRNA) to repress MtrA. And it was able to regulate the EET pathway efficiently by a single plasmid in *S. oneidensis*. With the development of synthetic biology methods, more engineering applications in native and non-native exoelectrogens can be expected in the near future.

1.3.3.2   EET Pathway Assembling in Non-native Exoelectrogens

The well-studied industrial microbes like *E. coli* have many similar morphological characteristics to electroactive *S. oneidensis*; however, *E. coli* strains belong to non-native exoelectrogens and may not have EET pathway for direct power output [93]. One strategy is to add adventitious redox carriers and increase membrane permeability which helps release redox-active compounds from the periplasm to the

electrode. Yong et al. overexpressed an outer membrane porin (OprF from *P. aeruginosa* PAO1) in *E. coli* BL21 to drive more intracellular electron outflow by riboflavin [94]. Though synthetic porins could be an efficient strategy to enhance bioelectricity generation, the non-native exoelectrogens still lack efficient EET pathway such as the Mtr pathway.

Introducing a heterologous electron transport pathway into *E. coli* is an interesting approach of synthetic biology to create new electroactive strains. The earliest example of this approach is the active expression of MtrA with a native cytochrome c maturation pathway (Ccm) in *E. coli* [95]. The recombinant cells are capable of reducing soluble Fe(III) but cannot transfer electron through the outer membrane. Subsequently, inner membrane CymA was successfully expressed by integrating into *E. coli* genome, and cells could increase biomass with the reduction of soluble Fe(III) [96]. In 2010, Jensen and co-workers firstly reported that they succeeded to express the outer membrane spanning porin-cytochrome complex MtrCAB and that new strain exhibited an extracellular electron flux [93]. They proved that native NapC could fill the role of CymA, and overexpression of MtrCAB could impair EET in *E. coli* [97]. In 2013 and 2014, the four cytochromes (CymA, MtrA, MtrC, and MtrB) of Mtr pathway were all expressed and allowed *E. coli* to produce substantially more current than previous strains [98]. It was found that engineered exoelectrogen *E. coli* could adjust central metabolism of TCA cycle through Mtr pathway. Besides, Sturm-Richter et al. realized EET by adding exogenous electron shuttle (methylene blue) and expressing STC (a periplasmic c-type cytochrome) as well as CymA and MtrA in *E. coli* [99]. They all showed that *E. coli* have the capability to be exoelectrogen and do electrode-assisted fermentation.

TerAvest and Ajo-Frankin have mentioned that constructing new exoelectrogens or expressing functional EET pathways by synthetic biology is meaningful in bioengineering and industrial application since EET pathway could maintain redox balance either in wastewater treatment or chemical production [80]. However, there still has a long way to walk. For example, the outward electron transfer has not yet been shown to support cell growth or set as a respiratory mechanism, which greatly restrict the utilization of engineered electroactive strains. It indicates that we need additional understanding of how native exoelectrogens utilize EET pathway to conserve energy balance and central metabolism [15].

1.3.4 Bio-nano-hybrid System

To realize efficient EET between cells and electrode, sophisticated electrode materials and electrode modification procedures are usually required, which may result in high cost and may be time-consuming. In addition, the biofilm formation on electrode surface is also important for EET and BES performance. Therefore, many techniques focused on biohybrid system which may share the light of simple self-assembling strategy.

One of the interesting biohybrid systems is the self-assembly bioelectrode, which is formed by graphene oxide and *S. oneidensis* MR-1 [38]. The system is an electro-active, reduced-graphene-oxide-hybridized, three-dimensional macroporous bio-film and able to bi-directionally and efficiently transfer electron between *Shewanella* and electrodes. This 3D macroporous rGO/bacteria hybrid biofilm system delivered a 25-fold increase in the outward current and a 74-fold increase in the inward cur-rent. Inspired by this biohybrid system, Hu group explored the application of graphene-hybrid biofilm in MFC. They found that graphene-modified anode exhib-ited obvious antibacterial activity in initial growth stage of biofilm and had no effect on MFC performance [100]. Graphene hybridized biocathode increased MFC power density and decreased interfacial charge transfer resistance [101]. Then, they prepared dual graphene-modified bioelectrode in situ and polarity reversion in MFC, in which bioanode showed higher rate of substrate oxidation and biocathode was of higher efficiency of catalyzing oxygen reduction [102]. They also used that graphene modified bioelectrode to enrich bacterial community and found that Firmicutes occupied 48.75% in graphene modified bioanode, while Proteobacteria occupied 62.99% in graphene-modified biocathode [103]. It indicated that high bio-mass incorporation and enhanced direct contact with reduced graphene oxide are essential to improve EET and have great promise in wastewater treatment.

To construct biocompatible electrode is the first step to realize the EET application in effluent treatment. Lv et al. used a novel three-stage hybrid nano-bimetallic system, which consisted of nZVI/Pd reduction, nZVI/Pd-O_2 oxidation, and biodegradation by *P. putida*, to mineralize polybrominated diphenyl ethers [104]. According to the previ-ous reports, the 3D carbonaceous materials with high surface area, conductivity, bio-compatibility, and stability are attractive for application [105, 106]. A biohybrid system with immobilized bacteria can reduce cell leakage and cellular damage for bioremediation of hydrocarbon-contaminated water. Li et al. constructed such biohy-bridized system by pre-immobilization of bacteria on sawdust followed by coating a silica layer through vapor deposition (Silica-IC), which was able to maintain long-term storage stability and shelf life for phenanthrene degradation [107].

Immobilization of exoelectrogen is also promising. Exoelectrogen immobiliza-tion was developed to construct a conductive artificial biofilm (CAB) on the anode of MFC. The MFCs equipped with an optimized CAB exhibited an 11-fold increase in power output compared with natural biofilms [108]. Besides, using graphite/algi-nate granules, the MFC had a 0.8–1.7 times improvement on coulombic efficiency as well as dramatically decreased internal resistance [109]. Moreover, the cell immobilized MFC showed a much higher tolerance to the shock of high salt con-centration than the MFC with suspension cells. The results substantiated that biohy-brid system of immobilization is promising for practical application in energy harvesting from wastewater by MFCs.

Addition of nanomaterials in vitro to build biohybrid system is also feasible. It was found that introduction of carbon nanotubes (CNTs) in *S. oneidensis* MR-1 cell-immobilized alginate beads could change electron flow route [110]. The nitrobenzene (NB) reduction was shifted from intracellular to extracellular reaction with 74% improvement.

1.4   Conclusion

BES, which have the potential to accelerate pollutant treatment, harvest energy from wastewater, recover resources from waste, and recycle the CO_2 emission of wastewater treatment, hold great promise to develop sustainable technology for wastewater treatment. In this chapter, we reviewed the recent progress of BES and highlighted the mechanistic and bioengineering research on bacterial EET (the key limiting step for BES). To date, two different EETs termed as outward EET and inward EET have been identified in exoelectrogens. With the focus on addressing the limiting steps of EET, bioengineering strategies including metabolic engineering, physiological manipulation, synthetic biology approach, and bio-nano-hybridized system construction have been developed and showed great success to improve the EET efficiency and the BES performance. Though the genetic manipulation in most of the exoelectrogens is still difficult, the developing biotechnology may provide plenty of feasible strategies in the near future. It is expected that with more knowledge on EET mechanism and more bioengineering strategies on EET manipulation, multifunctional and more powerful BES will be explored, and more sustainable wastewater treatment technology will be developed in the near future.

References

1. Schroder U (2007) Anodic electron transfer mechanisms in microbial fuel cells and their energy efficiency. Phys Chem Chem Phys 9(21):2619–2629. https://doi.org/10.1039/B703627M
2. Reguera G, McCarthy KD, Mehta T, Nicoll JS, Tuominen MT, Lovley DR (2005) Extracellular electron transfer via microbial nanowires. Nature 435(7045):1098–1101. https://doi.org/10.1038/nature03661
3. Potter MC (1911) Electrical effects accompanying the decomposition of organic compounds. Proc Roy Soc London 84(571):260–276
4. Logan BE (2009) Exoelectrogenic bacteria that power microbial fuel cells. Nat Rev Microbiol 7(5):375–381. https://doi.org/10.1038/nrmicro2113
5. Lovley DR (2006) Bug juice: harvesting electricity with microorganisms. Nat Rev Microbiol 4(7):497–508. https://doi.org/10.1038/nrmicro1442
6. Nevin KP, Woodard TL, Franks AE, Summers ZM, Lovley DR (2010) Microbial electrosynthesis: feeding microbes electricity to convert carbon dioxide and water to multicarbon extracellular organic compounds. MBio 1(2):e00103-10. https://doi.org/10.1128/mBio.00103-10
7. Shi L, Dong H, Reguera G, Beyenal H, Lu A, Liu J, Yu H-Q, Fredrickson JK (2016) Extracellular electron transfer mechanisms between microorganisms and minerals. Nat Rev Microbiol 14(10):651–662. https://doi.org/10.1038/nrmicro.2016.93

8. Logan BE, Rabaey K (2012) Conversion of wastes into bioelectricity and chemicals by using microbial electrochemical technologies. Science 337(6095):686–690. https://doi.org/10.1126/science.1217412

9. Rabaey K, Rozendal RA (2010) Microbial electrosynthesis—revisiting the electrical route for microbial production. Nat Rev Microbiol 8:706–716. https://doi.org/10.1038/nrmicro2422

10. Bajracharya S, Sharma M, Mohanakrishna G, Dominguez Benneton X, Strik DPBTB, Sarma PM, Pant D (2016) An overview on emerging bioelectrochemical systems (BESs): technology for sustainable electricity, waste remediation, resource recovery, chemical production and beyond. Renew Energy 98:153–170. https://doi.org/10.1016/j.renene.2016.03.002

11. Rozendal RA, Hamelers HVM, Rabaey K, Keller J, Buisman CJN (2008) Towards practical implementation of bioelectrochemical wastewater treatment. Trends Biotechnol 26(8):450–459. https://doi.org/10.1016/j.tibtech.2008.04.008

12. Wang H, Ren ZJ (2013) A comprehensive review of microbial electrochemical systems as a platform technology. Biotechnol Adv 31(8):1796–1807. https://doi.org/10.1016/j.biotechadv.2013.10.001

13. Sadhukhan J, Lloyd JR, Scott K, Premier GC, Yu EH, Curtis T, Head IM (2016) A critical review of integration analysis of microbial electrosynthesis (MES) systems with waste biorefineries for the production of biofuel and chemical from reuse of CO. Renew Sust Energ Rev 56:116–132. https://doi.org/10.1016/j.rser.2015.11.015

14. Arends JBA (2018) The next step towards usable microbial bioelectrochemical sensors? Microb Biotechnol 11(1):20–21. https://doi.org/10.1111/1751-7915.12590

15. Kracke F, Vassilev I, Krömer JO (2015) Microbial electron transport and energy conservation – the foundation for optimizing bioelectrochemical systems. Front Microbiol 6:575. https://doi.org/10.3389/fmicb.2015.00575

16. Malvankar NS, Vargas M, Nevin KP, Franks AE, Leang C, Kim B-C, Inoue K, Mester T, Covalla SF, Johnson JP, Rotello VM, Tuominen MT, Lovley DR (2011) Tunable metallic-like conductivity in microbial nanowire networks. Nat Nanotechnol 6(9):573–579. https://doi.org/10.1038/nnano.2011.119

17. Coursolle D, Gralnick JA (2010) Modularity of the Mtr respiratory pathway of *Shewanella oneidensis* strain MR-1. Mol Microbiol 77(4):995–1008. https://doi.org/10.1111/j.1365-2958.2010.07266.x

18. Ross DE, Flynn JM, Baron DB, Gralnick JA, Bond DR (2011) Towards electrosynthesis in *Shewanella*: energetics of reversing the Mtr pathway for reductive metabolism. PLoS One 6:e16649. https://doi.org/10.1371/journal.pone.0016649

19. Clarke TA, Edwards MJ, Gates AJ, Hall A, White GF, Bradley J, Reardon CL, Shi L, Beliaev AS, Marshall MJ, Wang Z, Watmough NJ, Fredrickson JK, Zachara JM, Butt JN, Richardson DJ (2011) Structure of a bacterial cell surface decaheme electron conduit. Proc Natl Acad Sci U S A 108(23):9384–9389. https://doi.org/10.1073/pnas.1017200108

20. Firer-Sherwood M, Pulcu GS, Elliott SJ (2008) Electrochemical interrogations of the Mtr cytochromes from *Shewanella*: opening a potential window. JBIC J Biol Inorg Chem 13(6):849. https://doi.org/10.1007/s00775-008-0398-z

21. Fonseca Bruno M, Paquete Catarina M, Neto Sónia E, Pacheco I, Soares Cláudio M, Louro Ricardo O (2013) Mind the gap: cytochrome interactions reveal electron pathways across the periplasm of *Shewanella oneidensis* MR-1. Biochem J 449(1):101–108. https://doi.org/10.1042/bj20121467

22. Kolker E, Picone AF, Galperin MY, Romine MF, Higdon R, Makarova KS, Kolker N, Anderson GA, Qiu X, Auberry KJ, Babnigg G, Beliaev AS, Edlefsen P, Elias DA, Gorby YA, Holzman T, Klappenbach JA, Konstantinidis KT, Land ML, Lipton MS, McCue L-A, Monroe M, Pasa-Tolic L, Pinchuk G, Purvine S, Serres MH, Tsapin S, Zakrajsek BA, Zhu W, Zhou J, Larimer FW, Lawrence CE, Riley M, Collart FR, Yates JR, Smith RD, Giometti CS, Nealson KH, Fredrickson JK, Tiedje JM (2005) Global profiling of *Shewanella oneidensis* MR-1: expression of hypothetical genes and improved functional annotations. Proc Natl Acad Sci U S A 102(6):2099–2104. https://doi.org/10.1073/pnas.0409111102

23. Beliaev AS, Klingeman DM, Klappenbach JA, Wu L, Romine MF, Tiedje JM, Nealson KH, Fredrickson JK, Zhou J (2005) Global transcriptome analysis of *Shewanella oneidensis* MR-1 exposed to different terminal electron acceptors. J Bacteriol 187(20):7138–7145. https://doi.org/10.1128/jb.187.20.7138-7145.2005

24. Okamoto A, Hashimoto K, Nealson KH, Nakamura R (2013) Rate enhancement of bacterial extracellular electron transport involves bound flavin semiquinones. Proc Natl Acad Sci U S A 110:7856. https://doi.org/10.1073/pnas.1220823110

25. Ross DE, Brantley SL, Tien M (2009) Kinetic characterization of OmcA and MtrC, terminal reductases involved in respiratory electron transfer for dissimilatory iron reduction in Shewanella oneidensis MR-1. Appl Environ Microbiol 75(16):5218–5226. https://doi.org/10.1128/aem.00544-09

26. Lloyd JR, Leang C, Hodges Myerson AL, Coppi MV, Ciufo S, Methé B, Sandler SJ, Lovley DR (2003) Biochemical and genetic characterization of PpcA, a periplasmic c-type cytochrome in Geobacter sulfurreducens. Biochem J 369:153–161. https://doi.org/10.1042/bj20020597

27. Methé BA, Nelson KE, Eisen JA, Paulsen IT, Nelson W, Heidelberg JF, Wu D, Wu M, Ward N, Beanan MJ, Dodson RJ, Madupu R, Brinkac LM, Daugherty SC, DeBoy RT, Durkin AS, Gwinn M, Kolonay JF, Sullivan SA, Haft DH, Selengut J, Davidsen TM, Zafar N, White O, Tran B, Romero C, Forberger HA, Weidman J, Khouri H, Feldblyum TV, Utterback TR, Van Aken SE, Lovley DR, Fraser CM (2003) Genome of Geobacter sulfurreducens: metal reduction in subsurface environments. Science 302:1967–1969. https://doi.org/10.1126/science.1088727

28. Segura D, Mahadevan R, Juárez K, Lovley DR (2008) Computational and experimental analysis of redundancy in the central metabolism of Geobacter sulfurreducens. PLoS Comput Biol 4(2):e36. https://doi.org/10.1371/journal.pcbi.0040036

29. Santos TC, Silva MA, Morgado L, Dantas JM, Salgueiro CA (2015) Diving into the redox properties of *Geobacter sulfurreducens* cytochromes: a model for extracellular electron transfer. Dalton Trans 44(20):9335–9344. https://doi.org/10.1039/C5DT00556F

30. Aklujkar M, Krushkal J, DiBartolo G, Lapidus A, Land ML, Lovley DR (2009) The genome sequence of *Geobacter metallireducens:* features of metabolism, physiology and regulation common and dissimilar to *Geobacter sulfurreducens*. BMC Microbiol 9(1):109. https://doi.org/10.1186/1471-2180-9-109

31. Reguera G, Nevin KP, Nicoll JS, Covalla SF, Woodard TL, Lovley DR (2006) Biofilm and nanowire production leads to increased current in *Geobacter sulfurreducens* fuel cells. Appl Environ Microbiol 72(11):7345–7348. https://doi.org/10.1128/aem.01444-06

32. Walker DJF, Adhikari RY, Holmes DE, Ward JE, Woodard TL, Nevin KP, Lovley DR (2018) Electrically conductive pili from pilin genes of phylogenetically diverse microorganisms. ISME J 12:48–58. https://doi.org/10.1038/ismej.2017.141

33. Vargas M, Malvankar NS, Tremblay P-L, Leang C, Smith JA, Patel P, Synoeyenbos-West O, Nevin KP, Lovley DR (2013) Aromatic amino acids required for pili conductivity and long-range extracellular electron transport in Geobacter sulfurreducens. MBio 4(2):e00105. https://doi.org/10.1128/mBio.00105-1

34. Wang Y, Kern SE, Newman DK (2010) Endogenous phenazine antibiotics promote anaerobic survival of *Pseudomonas aeruginosa* via extracellular electron transfer. J Bacteriol 192(1):365–369. https://doi.org/10.1128/jb.01188-09

35. Rabaey K, Verstraete W (2005) Microbial fuel cells: novel biotechnology for energy generation. Trends Biotechnol 23(6):291–298. https://doi.org/10.1016/j.tibtech.2005.04.008

36. Watanabe K, Manefield M, Lee M, Kouzuma A (2009) Electron shuttles in biotechnology. Curr Opin Biotechnol 20(6):633–641. https://doi.org/10.1016/j.copbio.2009.09.006

37. Kumar A, Hsu LH-H, Kavanagh P, Barrière F, Lens PNL, Lapinsonnière L, Lienhard VJH, Schröder U, Jiang X, Leech D (2017) The ins and outs of microorganism–electrode electron transfer reactions. Nat Rev Chem 1:0024. https://doi.org/10.1038/s41570-017-0024

38. Yong Y-C, Yu Y-Y, Zhang X, Song H (2014) Highly active bidirectional electron transfer by a self-assembled electroactive reduced-graphene-oxide-hybridized biofilm. Angew Chem Int Ed 53(17):4480–4483. https://doi.org/10.1002/anie.201400463

39. Okamoto A, Hashimoto K, Nealson KH (2014) Flavin redox bifurcation as a mechanism for controlling the direction of electron flow during extracellular electron transfer. Angew Chem Int Ed 53(41):10988–10991. https://doi.org/10.1002/anie.201407004

40. Bird LJ, Bonnefoy V, Newman DK (2011) Bioenergetic challenges of microbial iron metabolisms. Trends Microbiol 19(7):330–340. https://doi.org/10.1016/j.tim.2011.05.001

41. Strycharz SM, Glaven RH, Coppi MV, Gannon SM, Perpetua LA, Liu A, Nevin KP, Lovley DR (2011) Gene expression and deletion analysis of mechanisms for electron transfer from electrodes to *Geobacter sulfurreducens*. Bioelectrochemistry 80(2):142–150. https://doi.org/10.1016/j.bioelechem.2010.07.005

42. Bose A, Gardel EJ, Vidoudez C, Parra EA, Girguis PR (2014) Electron uptake by iron-oxidizing phototrophic bacteria. Nat Commun 5:3391. https://doi.org/10.1038/ncomms4391

43. Doud DFR, Angenent LT (2014) Toward electrosynthesis with uncoupled extracellular electron uptake and metabolic growth: enhancing current uptake with *Rhodopseudomonas palustris*. Environ Sci Technol Lett 1(9):351–355. https://doi.org/10.1021/ez500244n

44. Liu J, Wang Z, Belchik SM, Edwards MJ, Liu C, Kennedy DW, Merkley ED, Lipton MS, Butt JN, Richardson DJ, Zachara JM, Fredrickson JK, Rosso KM, Shi L (2012) Identification and characterization of MtoA: a decaheme c-type cytochrome of the neutrophilic Fe(II)-oxidizing bacterium *Sideroxydans lithotrophicus* ES-1. Front Microbiol 3:37. https://doi.org/10.3389/fmicb.2012.00037

45. Shi L, Rosso Kevin M, Zachara John M, Fredrickson James K (2012) Mtr extracellular electron-transfer pathways in Fe(III)-reducing or Fe(II)-oxidizing bacteria: a genomic perspective. Biochem Soc Trans 40(6):1261–1267. https://doi.org/10.1042/bst20120098

46. Liu J, Yong Y-C, Song H, Li CM (2012) Activation enhancement of citric acid cycle to promote Bioelectrocatalytic activity of *arcA* knockout *Escherichia coli* toward high-performance microbial fuel cell. ACS Catal 2(8):1749–1752. https://doi.org/10.1021/cs3003808

47. Shalel-Levanon S, San K-Y, Bennett GN (2005) Effect of oxygen, and ArcA and FNR regulators on the expression of genes related to the electron transfer chain and the TCA cycle in Escherichia coli. Metab Eng 7(5):364–374. https://doi.org/10.1016/j.ymben.2005.07.001

48. Singh A, Lynch MD, Gill RT (2009) Genes restoring redox balance in fermentation-deficient E. coli NZN111. Metab Eng 11(6):347–354. https://doi.org/10.1016/j.ymben.2009.07.002

49. Vemuri GN, Altman E, Sangurdekar DP, Khodursky AB, Eiteman MA (2006) Overflow metabolism in *Escherichia coli* during steady-state growth: transcriptional regulation and effect of the redox ratio. Appl Environ Microbiol 72(5):3653–3661. https://doi.org/10.1128/aem.72.5.3653-3661.2006

50. Yong Y-C, Yu Y-Y, Yang Y, Li CM, Jiang R, Wang X, Wang J-Y, Song H (2012) Increasing intracellular releasable electrons dramatically enhances bioelectricity output in microbial fuel cells. Electrochem Commun 19:13–16. https://doi.org/10.1016/j.elecom.2012.03.002

51. Min D, Cheng L, Zhang F, Huang X-N, Li D-B, Liu D-F, Lau T-C, Mu Y, Yu H-Q (2017) Enhancing extracellular electron transfer of *Shewanella oneidensis* MR-1 through coupling improved flavin synthesis and metal-reducing conduit for pollutant degradation. Environ Sci Technol 51(9):5082–5089. https://doi.org/10.1021/acs.est.6b04640

52. Tang YJ, Hwang JS, Wemmer DE, Keasling JD (2007) *Shewanella oneidensis* MR-1 Fluxome under various oxygen conditions. Appl Environ Microbiol 73(3):718–729. https://doi.org/10.1128/aem.01532-06

53. Zhu G, Yang Y, Liu J, Liu F, Lu A, He W (2017) Enhanced photocurrent production by the synergy of hematite nanowire-arrayed photoanode and bioengineered *Shewanella oneidensis* MR-1. Biosens Bioelectron 94:227–234. https://doi.org/10.1016/j.bios.2017.03.006

54. Yong X-Y, Feng J, Chen Y-L, Shi D-Y, Xu Y-S, Zhou J, Wang S-Y, Xu L, Yong Y-C, Sun Y-M, Shi C-L, OuYang P-K, Zheng T (2014) Enhancement of bioelectricity generation by cofactor manipulation in microbial fuel cell. Biosens Bioelectron 56:19–25. https://doi.org/10.1016/j.bios.2013.12.058

55. Yong X-Y, Shi D-Y, Chen Y-L, Jiao F, Lin X, Zhou J, Wang S-Y, Yong Y-C, Sun Y-M, OuYang P-K, Zheng T (2014) Enhancement of bioelectricity generation by manipulation of the electron shuttles synthesis pathway in microbial fuel cells. Bioresour Technol 152:220–224. https://doi.org/10.1016/j.biortech.2013.10.086

56. Schmitz S, Nies S, Wierckx N, Blank LM, Rosenbaum MA (2015) Engineering mediator-based electroactivity in the obligate aerobic bacterium *Pseudomonas putida* KT2440. Front Microbiol 6:284. https://doi.org/10.3389/fmicb.2015.00284

57. Wang VB, Chua S-L, Cao B, Seviour T, Nesatyy VJ, Marsili E, Kjelleberg S, Givskov M, Tolker-Nielsen T, Song H, Loo JSC, Yang L (2013) Engineering PQS biosynthesis pathway for enhancement of bioelectricity production in *Pseudomonas aeruginosa* microbial fuel cells. PLoS One 8(5):e63129. https://doi.org/10.1371/journal.pone.0063129

58. Yong Y-C, Yu Y-Y, Li C-M, Zhong J-J, Song H (2011) Bioelectricity enhancement via over-expression of quorum sensing system in *Pseudomonas aeruginosa*-inoculated microbial fuel cells. Biosens Bioelectron 30(1):87–92. https://doi.org/10.1016/j.bios.2011.08.032

59. Friman H, Schechter A, Nitzan Y, Cahan R (2012) Effect of external voltage on *Pseudomonas putida* F1 in a bio electrochemical cell using toluene as sole carbon and energy source. Microbiology 158(2):414–423. https://doi.org/10.1099/mic.0.053298-0

60. Lai B, Yu S, Bernhardt PV, Rabaey K, Virdis B, Krömer JO (2016) Anoxic metabolism and biochemical production in *Pseudomonas putida* F1 driven by a bioelectrochemical system. Biotechnol Biofuels 9(1):39. https://doi.org/10.1186/s13068-016-0452-y

61. Al-Tahhan RA, Sandrin TR, Bodour AA, Maier RM (2000) Rhamnolipid-induced removal of lipopolysaccharide from *Pseudomonas aeruginosa*: effect on cell surface properties and interaction with hydrophobic substrates. Appl Environ Microbiol 66(8):3262–3268. https://doi.org/10.1128/aem.66.8.3262-3268.2000

62. Zheng T, Xu Y-S, Yong X-Y, Li B, Yin D, Cheng Q-W, Yuan H-R, Yong Y-C (2015) Endogenously enhanced biosurfactant production promotes electricity generation from microbial fuel cells. Bioresour Technol 197:416–421. https://doi.org/10.1016/j.biortech.2015.08.136

63. Shen H-B, Yong X-Y, Chen Y-L, Liao Z-H, Si R-W, Zhou J, Wang S-Y, Yong Y-C, OuYang P-K, Zheng T (2014) Enhanced bioelectricity generation by improving pyocyanin production and membrane permeability through sophorolipid addition in *Pseudomonas aeruginosa*-inoculated microbial fuel cells. Bioresour Technol 167:490–494. https://doi.org/10.1016/j.biortech.2014.05.093

64. Xu Y-S, Zheng T, Yong X-Y, Zhai D-D, Si R-W, Li B, Yu Y-Y, Yong Y-C (2016) Trace heavy metal ions promoted extracellular electron transfer and power generation by *Shewanella* in microbial fuel cells. Bioresour Technol 211:542–547. https://doi.org/10.1016/j.biortech.2016.03.144

65. Dewan A, Beyenal H, Lewandowski Z (2008) Scaling up microbial fuel cells. Environ Sci Technol 42(20):7643–7648. https://doi.org/10.1021/es800775d

66. Liu H, Cheng S, Huang L, Logan BE (2008) Scale-up of membrane-free single-chamber microbial fuel cells. J Power Sources 179(1):274–279. https://doi.org/10.1016/j.jpowsour.2007.12.120

67. Zhai D-D, Li B, Sun J-Z, Sun D-Z, Si R-W, Yong Y-C (2016) Enhanced power production from microbial fuel cells with high cell density culture. Water Sci Technol 73(9):2176–2181. https://doi.org/10.2166/wst.2016.059

68. Yong X-Y, Yan Z-Y, Shen H-B, Zhou J, Wu X-Y, Zhang L-J, Zheng T, Jiang M, Wei P, Jia H-H, Yong Y-C (2017) An integrated aerobic-anaerobic strategy for performance enhancement of *Pseudomonas aeruginosa*-inoculated microbial fuel cell. Bioresour Technol 241:1191–1196. https://doi.org/10.1016/j.biortech.2017.06.050

69. Raghavulu SV, Mohan SV, Goud RK, Sarma PN (2009) Effect of anodic pH microenvironment on microbial fuel cell (MFC) performance in concurrence with aerated and ferricyanide catholytes. Electrochem Commun 11(2):371–375. https://doi.org/10.1016/j.elecom.2008.11.038

70. He Z, Huang Y, Manohar AK, Mansfeld F (2008) Effect of electrolyte pH on the rate of the anodic and cathodic reactions in an air-cathode microbial fuel cell. Bioelectrochemistry 74(1):78–82. https://doi.org/10.1016/j.bioelechem.2008.07.007

71. Hartshorne RS, Jepson BN, Clarke TA, Field SJ, Fredrickson J, Zachara J, Shi L, Butt JN, Richardson DJ (2007) Characterization of *Shewanella oneidensis* MtrC: a cell-surface deca-heme cytochrome involved in respiratory electron transport to extracellular electron acceptors. JBIC J Biol Inorg Chem 12(7):1083–1094. https://doi.org/10.1007/s00775-007-0278-y

72. Okamoto A, Kalathil S, Deng X, Hashimoto K, Nakamura R, Nealson KH (2014) Cell-secreted flavins bound to membrane cytochromes dictate electron transfer reactions to surfaces with diverse charge and pH. Sci Rep 4:5628. https://doi.org/10.1038/srep05628

73. Yong Y-C, Cai Z, Yu Y-Y, Chen P, Jiang R, Cao B, Sun J-Z, Wang J-Y, Song H (2013) Increase of riboflavin biosynthesis underlies enhancement of extracellular electron transfer of Shewanella in alkaline microbial fuel cells. Bioresour Technol 130:763–768. https://doi.org/10.1016/j.biortech.2012.11.145

74. Zhuang L, Zhou S, Li Y, Yuan Y (2010) Enhanced performance of air-cathode two-chamber microbial fuel cells with high-pH anode and low-pH cathode. Bioresour Technol 101(10):3514–3519. https://doi.org/10.1016/j.biortech.2009.12.105

75. Yuan Y, Zhao B, Zhou S, Zhong S, Zhuang L (2011) Electrocatalytic activity of anodic bio-film responses to pH changes in microbial fuel cells. Bioresour Technol 102(13):6887–6891. https://doi.org/10.1016/j.biortech.2011.04.008

76. Sasaki D, Sasaki K, Tsuge Y, Kondo A (2016) Comparative metabolic state of microflora on the surface of the anode electrode in a microbial fuel cell operated at different pH conditions. AMB Express 6(1):125. https://doi.org/10.1186/s13568-016-0299-4

77. Alagappan G, Cowan RM (2004) Effect of temperature and dissolved oxygen on the growth kinetics of *Pseudomonas putida* F1 growing on benzene and toluene. Chemosphere 54:1255–1265. https://doi.org/10.1016/j.chemosphere.2003.09.013

78. Yong Y-C, Wu X-Y, Sun J-Z, Cao Y-X, Song H (2015) Engineering quorum sensing signaling of *Pseudomonas* for enhanced wastewater treatment and electricity harvest: a review. Chemosphere 140:18–25. https://doi.org/10.1016/j.chemosphere.2014.10.020

79. Yong Y-C, Zhong J-J (2013) Impacts of quorum sensing on microbial metabolism and human health. In: Zhong J-J (ed) Future trends in biotechnology. Springer, Berlin/Heidelberg, pp 25–61. https://doi.org/10.1007/10_2012_138

80. TerAvest MA, Ajo-Franklin CM (2016) Transforming exoelectrogens for biotechnology using synthetic biology. Biotechnol Bioeng 113(4):687–697. https://doi.org/10.1002/bit.25723

81. Heidelberg JF, Paulsen IT, Nelson KE, Gaidos EJ, Nelson WC, Read TD, Eisen JA, Seshadri R, Ward N, Methe B, Clayton RA, Meyer T, Tsapin A, Scott J, Beanan M, Brinkac L, Daugherty S, DeBoy RT, Dodson RJ, Durkin aS, Haft DH, Kolonay JF, Madupu R, Peterson JD, Umayam LA, White O, Wolf AM, Vamathevan J, Weidman J, Impraim M (2002) Genome sequence of the dissimilatory metal ion-reducing bacterium Shewanella oneidensis. Nat Biotechnol 20:1118–1123. https://doi.org/10.1038/nbt749

82. Jensen HM, TerAvest MA, Kokish MG, Ajo-Franklin CM (2016) CymA and exogenous flavins improve extracellular electron transfer and couple it to cell growth in Mtr-expressing *Escherichia coli*. ACS Synth Biol 5(7):679–688. https://doi.org/10.1021/acssynbio.5b00279

83. Tschirhart T, Kim E, McKay R, Ueda H, Wu H-C, Pottash AE, Zargar A, Negrete A, Shiloach J, Payne GF, Bentley WE (2017) Electronic control of gene expression and cell behaviour in *Escherichia coli* through redox signalling. Nat Commun 8:14030. https://doi.org/10.1038/ncomms14030

84. Schuergers N, Werlang C, Ajo-Franklin CM, Boghossian AA (2017) A synthetic biology approach to engineering living photovoltaics. Energy Environ Sci 10(5):1102–1115. https://doi.org/10.1039/C7EE00282C

85. Cao Y, Li X, Li F, Song H (2017) CRISPRi–sRNA: transcriptional–translational regulation of extracellular electron transfer in Shewanella oneidensis. ACS Synth Biol 6(9):1679–1690. https://doi.org/10.1021/acssynbio.6b00374

86. Johnson ET, Baron DB, Naranjo B, Bond DR, Schmidt-Dannert C, Gralnick JA (2010) Enhancement of survival and electricity production in an engineered bacterium by light-driven proton pumping. Appl Environ Microbiol 76(13):4123–4129. https://doi.org/10.1128/aem.02425-09

87. Izallalen M, Mahadevan R, Burgard A, Postier B, Didonato R, Sun J, Schilling CH, Lovley DR (2008) Geobacter sulfurreducens strain engineered for increased rates of respiration. Metab Eng 10(5):267–275. https://doi.org/10.1016/j.ymben.2008.06.005

88. Yang Y, Ding Y, Hu Y, Cao B, Rice SA, Kjelleberg S, Song H (2015) Enhancing bidirectional electron transfer of *Shewanella oneidensis* by a synthetic flavin pathway. ACS Synth Biol 4(7):815–823. https://doi.org/10.1021/sb500331x

89. Kouzuma A, Meng XY, Kimura N, Hashimoto K, Watanabe K (2010) Disruption of the putative cell surface polysaccharide biosynthesis gene SO3177 in *Shewanella oneidensis* MR-1 enhances adhesion to electrodes and current generation in microbial fuel cells. Appl Environ Microbiol 76:4151–4157. https://doi.org/10.1128/aem.00117-10

90. Liu T, Yu Y-Y, Deng X-P, Ng CK, Cao B, Wang J-Y, Rice SA, Kjelleberg S, Song H (2015) Enhanced Shewanella biofilm promotes bioelectricity generation. Biotechnol Bioeng 112(10):2051–2059. https://doi.org/10.1002/bit.25624

91. Leang C, Malvankar NS, Franks AE, Nevin KP, Lovley DR (2013) Engineering *Geobacter sulfurreducens* to produce a highly cohesive conductive matrix with enhanced capacity for current production. Energy Environ Sci 6(6):1901–1908. https://doi.org/10.1039/C3EE40441B

92. Kane AL, Bond DR, Gralnick JA (2013) Electrochemical analysis of *Shewanella oneidensis* engineered to bind gold electrodes. ACS Synth Biol 2(2):93–101. https://doi.org/10.1021/sb300042w

93. Jensen HM, Albers AE, Malley KR, Londer YY, Cohen BE, Helms BA, Weigele P, Groves JT, Ajo-Franklin CM (2010) Engineering of a synthetic electron conduit in living cells. Proc Natl Acad Sci U S A 107(45):19213–19218. https://doi.org/10.1073/pnas.1009645107

94. Yong Y-C, Yu Y-Y, Yang Y, Liu J, Wang J-Y, Song H (2013) Enhancement of extracellular electron transfer and bioelectricity output by synthetic porin. Biotechnol Bioeng 110(2):408–416. https://doi.org/10.1002/bit.24732

95. Pitts KE, Dobbin PS, Reyes-Ramirez F, Thomson AJ, Richardson DJ, Seward HE (2003) Characterization of the *Shewanella oneidensis* MR-1 decaheme cytochrome MtrA: expression in *Escherichia coli* confers the ability to reduce soluble Fe(III) chelates. J Biol Chem 278(30):27758–27765. https://doi.org/10.1074/jbc.M302582200

96. Gescher JS, Cordova CD, Spormann AM (2008) Dissimilatory iron reduction in *Escherichia coli*: identification of CymA of *Shewanella oneidensis* and NapC of *E. coli* as ferric reductases. Mol Microbiol 68(3):706–719. https://doi.org/10.1111/j.1365-2958.2008.06183.x

97. Goldbeck CP, Jensen HM, TerAvest MA, Beedle N, Appling Y, Hepler M, Cambray G, Mutalik V, Angenent LT, Ajo-Franklin CM (2013) Tuning promoter strengths for improved synthesis and function of electron conduits in *Escherichia coli*. ACS Synth Biol 2(3):150–159. https://doi.org/10.1021/sb300119v

98. TerAvest MA, Zajdel TJ, Ajo-Franklin CM (2014) The Mtr pathway of *Shewanella oneidensis* MR-1 couples substrate utilization to current production in *Escherichia coli*. ChemElectroChem 1(11):1874–1879. https://doi.org/10.1002/celc.201402194

99. Sturm-Richter K, Golitsch F, Sturm G, Kipf E, Dittrich A, Beblawy S, Kerzenmacher S, Gescher J (2015) Unbalanced fermentation of glycerol in *Escherichia coli* via heterologous production of an electron transport chain and electrode interaction in microbial electrochemical cells. Bioresour Technol 186:89–96. https://doi.org/10.1016/j.biortech.2015.02.116

100. Chen J, Deng F, Hu Y, Sun J, Yang Y (2015) Antibacterial activity of graphene-modified anode on *Shewanella oneidensis* MR-1 biofilm in microbial fuel cell. J Power Sources 290:80–86. https://doi.org/10.1016/j.jpowsour.2015.03.033

101. Chen J, Hu Y, Huang W, Zhang L (2017) Enhanced electricity generation for biocathode microbial fuel cell by in situ microbial-induced reduction of graphene oxide and polarity reversion. Int J Hydrog Energy 42(17):12574–12582. https://doi.org/10.1016/j.ijhydene.2017.03.012

102. Chen J, Hu Y, Tan X, Zhang L, Huang W, Sun J (2017) Enhanced performance of microbial fuel cell with in situ preparing dual graphene modified bioelectrode. Bioresour Technol 241:735–742. https://doi.org/10.1016/j.biortech.2017.06.020

103. Chen J, Zhang L, Hu Y, Huang W, Niu Z, Sun J (2017) Bacterial community shift and incurred performance in response to in situ microbial self-assembly graphene and polarity reversion in microbial fuel cell. Bioresour Technol 241:220–227. https://doi.org/10.1016/j.biortech.2017.05.123

104. Lv Y, Zhang Z, Chen Y, Hu Y (2016) A novel three-stage hybrid nano bimetallic reduction/oxidation/biodegradation treatment for remediation of 2,2′4,4′-tetrabromodiphenyl ether. Chem Eng J 289:382–390. https://doi.org/10.1016/j.cej.2015.12.097

105. Yang X, Ma X, Wang K, Wu D, Lei Z, Feng C (2016) Eighteen-month assessment of 3D graphene oxide aerogel-modified 3D graphite fiber brush electrode as a high-performance microbial fuel cell anode. Electrochim Acta 210:846–853. https://doi.org/10.1016/j.electacta.2016.05.215

106. Wang H, Wang G, Ling Y, Qian F, Song Y, Lu X, Chen S, Tong Y, Li Y (2013) High power density microbial fuel cell with flexible 3D graphene-nickel foam as anode. Nanoscale 5(21):10283–10290. https://doi.org/10.1039/C3NR03487A

107. Li J, Guo C, Liao C, Zhang M, Liang X, Lu G, Yang C, Dang Z (2016) A bio-hybrid material for adsorption and degradation of phenanthrene: bacteria immobilized on sawdust coated with a silica layer. RSC Adv 6(109):107189–107199. https://doi.org/10.1039/C6RA22683C

108. Yu Y-Y, Chen H-l, Yong Y-C, Kim D-H, Song H (2011) Conductive artificial biofilm dramatically enhances bioelectricity production in *Shewanella*-inoculated microbial fuel cells. Chem Commun 47(48):12825–12827. https://doi.org/10.1039/C1CC15874K

109. Yong Y-C, Liao Z-H, Sun J-Z, Zheng T, Jiang R-R, Song H (2013) Enhancement of coulombic efficiency and salt tolerance in microbial fuel cells by graphite/alginate granules immobilization of *Shewanella oneidensis* MR-1. Process Biochem 48(12):1947–1951. https://doi.org/10.1016/j.procbio.2013.09.008

110. Yan F-F, He Y-R, Wu C, Cheng Y-Y, Li W-W, Yu H-Q (2014) Carbon nanotubes alter the electron flow route and enhance nitrobenzene reduction by *Shewanella oneidensis* MR-1. Environ Sci Technol Lett 1(1):128–132. https://doi.org/10.1021/ez4000093

Chapter 2
Bioelectrocatalysis Favorable Electrode Materials for Environmental Remediation

Xiaoshuai Wu and Yan Qiao

2.1 Fundamentals of Electrode Process in Bioelectrocatalysis

2.1.1 Electrode Process in BES

Electrode process here means transfer of an electric charge between a solid and liquid phase, which is a fundamental course of an electrochemical device. Generally, it includes a couple of steps like mass transfer, redox reaction, ion adsorption/desorption, etc. For the bioelectrocatalysis in bioelectrochemical system (BES) device, the electrode process is much more complicated than a typical one since it contains microbial electrocatalysis, a complicated and flexible energy conversion process based on a cascade of redox reactions that involve both microbes and electrodes. In general, three consecutive and interactional processes are carried out for the microbial electrocatalysis in BES: (i) a biocatalytic process within electroactive microbes, in which the organic substrates are oxidized via a suite of oxidases along with the release of electrons to extracellular region; (ii) an interfacial electron transfer process, in which microbes are able to transport electrons into (or out of) the cells from (or to an) electrode through diverse pathways; and (iii) an electrocatalytic process on an electrode, where electrochemical oxidation or reduction take place. Except process (i), which is mostly dependent on the catalytic capability of the microorganism cells, the other two processes would rely on the electrode design such as the microstructures and the surface properties.

X. Wu · Y. Qiao (✉)
Faculty of Materials and Energy, Institute for Clean Energy and Advanced Materials, Southwest University, Chongqing, People's Republic of China

Chongqing Key Laboratory for Advanced Materials and Technologies of Clean Energies, Chongqing, People's Republic of China
e-mail: yanqiao@swu.edu.cn

2.1.2 Anodic Interfacial Electron Transfer

Quite a few microorganisms including gram-negative and gram-positive bacteria as well as eukaryotic microbes and microalgae have been identified to be able to harvest electricity via decomposition of carbon sources in anaerobic anode of BES. As the envelope of the microbe cells is insulation, there has to be specific transport pathways for the cells to deliver electrons to the extracellular solid electrode. Up to date, some typical exoelectrogens (e.g., *Geobacter* species and *Shewanella* species) are well investigated to understand their extracellular electron transfer (EET) mechanisms [1–3]. Generally, electron transfer from exoelectrogens to an anode is carried out by two primary mechanisms: direct electron transfer (DET) via outer membrane (OM) electroactive proteins such as c-type cytochromes (c-Cyts) or conductive pili (termed as nanowires) and mediated electron transfer (MET) via endogenous electron mediators (e.g., flavin).

2.1.2.1 Direct Electron Transfer (DET)

G. sulfurreducens and *S. oneidensis* are the famous exoelectrogen species that could pass electrons inside the cells directly to the extracellular solid electrode and achieve great power generation performance in MFCs. According to the analysis of functional genes of these species, some EET pathways have been proposed and proved in previous reports [2–4]. For example, multi-heme c-cytochromes located on outer membrane of the bacteria cells have been regarded as one of the primary conduits for DET, which enables the direct transport of electrons from cellular quinone pool located at the cytoplasm inner membrane to the extracellular insoluble acceptors. It has been reported that the deletion of OM c-Cyt OmcZ that is abundant in *G. sulfurreducens* biofilm grown on an electrode resulted in almost 70–90% current decrease [5, 6]. For *S. oneidensis*, a well-known Mtr respiration pathway encoded by *mtrDEF-omcA-mtrCAB* gene cluster is identified to take in charge of the DET pathway for reducing extracellular insoluble electron acceptors [3, 7, 8]. *S. oneidensis* mutants lacking the involved c-Cyts genes have been detected to generate less than 20% of the current produced by the wild-type strain, while 35% increase in current production has been observed when *mtrC* cytochrome was overexpressed in the wild-type strain [9]. Nevertheless, the rate of electron transfer between redox-active proteins and the electrode surface is found out to decrease exponentially with their distance once larger than 14 Å [10]. In this case, the OM c-Cyts-governed DET pathway might only take place in the innermost layer of the biofilm. Alternatively, these exoelectrogens can produce nanowires, electrically conductive appendages (e.g., pili formed by protein filaments or outer membrane extensions) for promoting electron transfer through the thick biofilm within a relatively long distance [11–14].

2.1.2.2   Mediated Electron Transfer (MET)

In comparison to DET, the MET through endogenous electron shuttles is more common in the exoelectrogens. A great deal of microbes can use some of their metabolites as redox mediators to execute the extracellular electron transfer without physical contact. The MET mechanism varies with the natures of endogenous electrons mediators and exoelectrogens. According to the reports in last 15 years, the MET pathways in *Shewanella* species and *Pseudomonas* species are more discussed due to their available pure cultures and the well-established genetic manipulation techniques. *Shewanella* species are well-known for their capability of reducing insoluble metals at a distance [15] with flavins (including flavin mononucleotide (FMN) and riboflavin (RF)) as the main extracellular electron shuttles [16, 17]. Some research has demonstrated that MET enabled by flavins is responsible for delivering the charge of more than 70% of total EET for *Shewanella* species [18–20]. That is to say, the flavin-enabled MET pathway may be a more effective pathway to achieve fast EET within a long distance. Further, flavins have also been proved as bound cofactors on MtrC and/or OmcA of *S. oneidensis* MR-1 to synergistically accelerate electron transfer from a monolayer cells to a flat indium tin-oxide electrode recently [21–24]. Although *Geobacter* species behave with a typical organism relying on DET pathway for extracellular electron transfer, they have also been reported to use flavins even other redox-active molecules as either electron shuttles or cofactors of OM c-Cyts to achieve else EET pathways [24–26].

Another interesting genus of exoelectrogens relying on MET pathway is *Pseudomonas* species that are able to secrete phenazine derivatives (e.g., phenazine-1-carboxylic acid, phenazine-1-carboxamide, and pyocyanin) as electron shuttles. Rabaey et al. reveal that the EET rate of *P. aeruginosa* strain KRP1 isolated from the anode compartment of an MFC is greatly accelerated by pyocyanin and phenazine-1-carboxamide, while the deficiency of phenazine biosynthesis in mutant strains results in almost 95% decrease in power output [27]. Moreover, the secreted phenazine could be used not only by *P. aeruginosa* itself but also by other bacterial species to boost EET ability in a mixed culture [28, 29]. For those nontypical exoelectrogens like *Escherichia coli* species, which are not innately electroactive, they can use some unknown metabolites to achieve EET in an anaerobic MFC after long-term operation [30–32]. In evidence, these electron mediator-enabled EET mechanisms have universal scientific significance for anaerobic respirations of extensive microbes toward extracellular insoluble electron acceptors.

2.1.3   Interfacial Electron Transfer in Biocathode

Intriguingly, some microbes have been observed to take up electrons from an electrode as an electron donor to drive their metabolism, which is known as a microbial electrosynthesis process, enabling microbes to synthesize high-value biofuels and chemicals such as acetate, ethanol, and butyrate from reuse of low-cost matters

(e.g., CO_2) on the biocathode [33–37]. In comparison to the EET mechanism from exoelectrogens to an anode, much less is yet known about this reverse process although considerable effort has been paid to explore very recently. Likewise, two types of mechanisms, namely, DET pathway and MET pathway, have been proposed to be involved in cathodic electron transfer process. Evidently, the DET pathway in the charge of bacteria OM c-Cyts from a cathode to exoelectrogens may be not a simple reversal of DET in the microbial anode. In contrast to current-producing biofilms, current-consuming biofilms of *G. sulfurreducens* accompanied with fumarate reduction have much lower expression of OM c-Cyts and conductive pili. It is still under debates whether a c-Cyts-based electron conduit possesses a dual function for both outward and inward DET mechanisms in *Geobacter* biofilms [38, 39]. A *S. oneidensis* biofilm adhering on a graphite electrode was also observed to take up electrons for fumarate reduction, and the Mtr pathway may be functionally reversible and electrons probably flow from OM c-Cyts into the quinone pool [40]. More exact roles of these proteins involving in DET process from electrode surface into bacterial cells are still not fully understood.

For the MET pathway, riboflavin has been demonstrated to greatly accelerate electron transfer from an electrode to wild-type *S. oneidensis* MR-1 and even its mutants lacking c-Cyts [40]. More recently, the increase in concentration of flavins was reported to greatly improve the inward current from an electrode to *S. oneidensis* MR-1 [41]. What's more, hydrogen has been regarded as an alternative redox mediator in microbial electrosynthesis systems, which can be substantially generated from cathode reactions [42, 43]. The CO_2 reduction to butyrate in a biocathode was also found to be a hydrogen-driven process [36]. In particular, an electron flux from the cathode to CO_2 for acetate production was proposed to be driven by biologically induced hydrogen [44]. Therefore, the MET mechanism mediated by endogenous electron shuttles also plays a significant role in the reverse electron transfer in cathodic bioelectrocatalysis.

2.1.4   Biofilm Promoted EET

The biofilm adhesion is the characteristic feature of the electrodes in BES. It is known that the biofilm is formed by aggregation of microorganisms within a self-produced matrix of extracellular polymeric substances adhered to a surface to against unpleasant environmental conditions. While for a bioelectrocatalytic electrode, the biofilm guarantees the physical contact of bacteria cells to the solid electrode for DET. It has been reported that the biofilm-anchoring exoelectrogens are able to achieve multiple electron transfer pathways through bacterial OM c-Cyts, bacterial nanowires, endogenously secreted electron shuttles, and other immobile components of the biofilm matrix [45, 46]. Additionally, the long-range electron transfer between the outer layer of biofilm and the electrode can be supported by an efficient conductive network in the biofilm matrix composed of bacterial pili, bound c-Cyts, extracellular polysaccharides, humic substances, electron shuttles, and so

on [47–50]. On the other hand, the biofilm formation on the electrode also can promote MET-based interfacial charge transfer. It has been demonstrated that the activity of some key enzymes for flavins biosynthesis and secretion is higher in *Shewanella* biofilm than that in planktonic cells [51, 52]. Meanwhile, the biofilm formation could accumulate electron shuttles on the electrode surface to accelerate the MET, which has been reported in MFCs catalyzed by *S. putrefaciens* CN32 [53] and *P. aeruginosa* species [54, 55]. So far, few of literatures have paid attention to cathodic biofilms, but we still notice that a viably electroactive biofilm is also essential for efficient cathodic bioelectrocatalysis based on reviewing the existing literatures [56–58].

According to above introduction about fundamentals of bioelectrocatalysis, it should be noted that the electrode design is quite important for a BES device as it will greatly affect the key steps of the interfacial electron transfer process as well as the bioelectrocatalytic performance. In the following paragraphs, different kinds of electrode materials applied for bioelectrocatalysis will be reviewed to show their pros and cons in BES devices.

2.2 Traditional Carbon-Based Electrode Materials

Traditional carbon materials such as carbon cloth, carbon felt, graphite rod, etc. are most widely used electrode materials in BES since they possess good electric conductivity, stability, and biocompatibility. In the meantime, these carbon materials are commercial products with reliable quality so that they are often used as standard electrode materials for device performance evaluation.

2.2.1 Fiber-Based Electrodes

Fiber-based carbon electrodes including carbon paper, carbon cloth, carbon felt, etc. are the most popular electrode materials in polymer electrolyte membrane (PEM) fuel cells, which are always constructed with membrane electrode assemblies (MEA). These fiber-based carbon electrodes not only provide good support for noble metal catalysts but also possess nice pores for gas diffusion after water proof treatment. While for biocatalytic electrodes in BES, the availability for biofilm adhesion and accessibility for electron mediators are more important. In this case, the non-waterproofing carbon fiber electrodes are the widely used electrode materials in BES devices especially before 2010 as they have good porous structure and biocompatible surface properties for biofilm formation and long-term stability during the operation.

Carbon paper is a kind of non-woven carbon fiber electrode with rigid properties. It has often been used as anode and cathode materials in dual-chamber or single-chamber MFCs for wastewater treatment. In 2004, Liu and Logan reported a

prototype of single-chamber MFC that is used for wastewater treatment [59], in which the carbon paper was used as anode material. The highest performance of plain carbon paper-based MFC might be the one reported by Min and Logan in 2005, which treated swine wastewater and delivered 261 mW/m^2 maximum power density and 92% COD removal in a single-chamber device [60]. In another work reported in 2009, an air-cathode MFC with carbon paper anode/cathode and starch processing wastewater as substrate delivered similar maximum power density (239.4 mW/m^2) and 98% COD removal [61]. Comparing to carbon cloth or carbon felt, carbon paper is fragile and lacks durability, so it is not suitable for long-term operation and those specific MFC devices like tubular MFCs. That is the reason that the carbon paper is not as popular as those flexible carbon fiber electrodes in BES devices.

Carbon cloth and carbon felt are carbon fiber textile electrodes with different weaving methods. Carbon cloth is usually woven with carbon yarns made from polyacrylonitrile (PAN), while carbon felt is produced in a laying and needle-punching process [62]. Generally, the carbon cloth is regarded as "2D" carbon fiber electrode, while the carbon felt is regarded as "3D" electrode. However, it has been proved that the carbon cloth and carbon felt exhibit similar performance in a wastewater-driven MFC although the adhered biofilm pattern is different [63]. Carbon cloth could deliver higher-power generation performance than carbon paper since a similar single-chamber MFC with carbon cloth anode achieved maximum power density of 483 mW/m^2 (12 W/m^3) and 89% COD removal for beer brewery wastewater treatment [64].

In 2008, Zhao et al. [65] reported that an MFC with activated carbon cloth anode showed excellent performance in sulfate removal and also delivered quite high power density (5100 mW/m^{-2}). This activated carbon cloth is a cloth woven by activated carbon fiber, which is obtained through an activation process like being heated in CO_2 atmosphere [66]. Similar with the activated carbon power, the activated carbon fiber possesses quite high specific surface area as there are lots of micropores (pore size <2 nm) on the fiber surface. Therefore, the activated carbon cloth could provide large surface area for sulfate oxidation and thus achieve high current density in the MFC. The activated carbon felt also exhibits good catalytic performance when it was used as cathode for oxygen reduction reaction in MFCs [67]. However, the application of activated carbon fiber electrodes in BES is not extensive as expected. The reason might be that the large surface area of these activated carbon fiber electrodes is not fully accessible, which will be discussed in Sect. 2.3.3.

Up to date, the most favorable fiber-based carbon electrode should be graphite fiber brush electrode, which was developed by Logan et al. in 2007 [68]. The fiber brush electrode was made of carbon fibers cut to a set length and wound into a twisted core consisting of two titanium wires. In this work, the graphite fiber brush electrode was applied as anode in cubic air-cathode MFCs and delivered a maximum power produced of 2400 mW/m^2 (73 W/m^3), which is more than twofold of carbon cloth. After this report, the carbon fiber brush electrode was widely used in BES for waste treatment [69–71] or hydrogen production [72–75]. The excellent bioelectrocatalytic performance should be due to its high surface area and low elec-

trode resistance. It is interesting that up to 65% of the graphite fiber could be removed from the brush electrode without decreasing power generation, but the start-up time will increase [76]. Logan et al. also developed multi-brush anode [77] and found that enlarging the brush size or moving the center of the brush closer to the cathode could greatly improve the power production [78].

2.2.2   Other Carbon Electrodes

At early stage of MFC development, graphite rods have been used as anode materials. In 2004, Logan's group also built a single cylindrical chamber MFC with eight graphite rods as anode [79] before the air-cathode MFC with carbon paper anode was reported. A maximum power of 26 mWm^{-2} and 80% COD removal were fulfilled, using sewage from the primary sedimentation tank of a treatment plant as fuel. However, these solid graphite electrodes are too expensive that they can only be used in lab-scale device, which is not suitable for waste treatment. Similarly, the high cost of carbon fiber materials also limits their application in large-scale BES devices, which are more useful for waste treatment or environmental remediation. In this case, a couple of low-cost carbon electrodes were developed by different research groups. Wang et al. [80] use carbon mesh as MFC anode, which costs only one tenth of carbon cloth. It has a more open structure than cloth electrodes due to a more open weave and delivered similar or better power generation performance than carbon cloth after appropriate surface treatment. Granular carbon/graphite is also a kind of non-expensive carbon electrode that has been used in MFCs. He et al. [81] reported an upflow MFC with granular carbon anode, which produced a maximum volumetric power of 29.2 W/m^3 at a volumetric loading rate of 3.40 kg COD/ (m^3 day). Granular activated carbon is a cost-effective electrode material that has been reported in large-scale MFC [82] or even pilot-scale test [83].

2.2.3   Surface Modification on Traditional Carbon Electrodes

Generally, the carbon electrodes mentioned above are the commercial carbon materials, which have standard physical and chemical properties and purchasable in different regions. However, these commercial carbon materials did not deliver satisfying performances in BES so that researchers always tried to increase their bioelectrocatalytic ability through different kinds of modification or fabrication techniques. In 2007, Cheng and Logan [84] reported that ammonia gas treatment of a carbon cloth anode increased the surface charge of the electrode and thus improved the power generation performance and reduced the start-up time of a domestic water MFC. Inspired by this work, Feng et al. [85] investigated the effect of acid soaking on performance of carbon fiber brush electrode and proposed that power increases are related to higher N1s/C1s ratios and a lower C-O composition. Zhu et al. tried to

use nitric acid soaking and ethylenediamine (EDA) treatment to improve the performance of activated carbon fiber electrode [86], and it turns out that both of the treatment could greatly improve the maximum power densities and shorten the start-up. From these works, it could be verified that functional groups like lactam, imide, amide, and ammonium nitrate promote the bacteria adhesion to the anode and facilitated electron transfer from bacteria to electrodes. Therefore, introducing functional groups to the surface of traditional carbon electrodes is a quite effective strategy to enhance the performance of bioelectrocatalysis. For example, Liu et al. [87] tried to introduce amide groups to the surface of carbon cloth by using electrochemical oxidation method, which increased the electrochemical active surface area by 2.9 times and improved the exchange current density by 41%.

Besides the wet chemistry methods, plasma treatment is also a feasible way to modify the surface of carbon electrodes. The first attempt was reported by He et al. [88], who treated the carbon paper with plasma-based N^+ ion implantation. The treatment increases the hydrophilicity of the carbon paper and promotes the interfacial charge transfer as well as the biofilm adhesion. Recently, Chang et al. [89] investigated electrocatalytic properties of the carbon cloth modified by using atmospheric pressure plasma jets, a recently developed method enabling operations under moderate pressure. The treated carbon cloth under nitrogen gas possessed abundant carboxyl and ammonium functional groups on the surface, which improve the biofilm adhesion and the power generation performance.

According to the above discussion, we can find that the surface chemistry of the electrode will affect the biofilm adhesion and interfacial electron transfer, which are the dominant factors for power generation or waste treatment. In this case, surface treatment or modification of traditional carbon electrodes are feasible approaches to make them deliver higher performance in BES devices. However, the increment on the performance by this way is quite limited due to the disadvantages of their microstructures like relative low surface area for bacteria loading and inadequate active sites for interfacial redox reactions. To solve this problem, various kinds of porous materials have been developed and applied in BES devices (Table 2.1), which will be discussed in details in the following parts.

2.3 Newly Developed Porous Materials

2.3.1 Graphene-Based Electrodes

Graphene is one of the most hot carbon nanomaterials in last 10 years. Due to its fascinating properties in terms of electronic and thermal conductivity, chemical plasticity, and mechanical strength and extensibility, it has been extensively studied to modify conventional planar electrodes for BES applications. Zhang et al. [90] found that graphene-modified stainless steel mesh (GSM) anode delivers a maximum power density of 2668 mW m^{-2} in *Escherichia coli* MFC, which is 18 times

Table 2.1 Summary of newly developed porous electrode materials applied in BESs

Material	Pore size	Inoculum	Nutritional substrate	Performance	Refs.
Graphene					
Graphene-modified stainless steel mesh (GAM)	–	*Escherichia coli*	Glucose	2668 mW m^{-2} (18-fold vs. SSM)	[90]
Graphene/carbon cloth	–	*P. aeruginosa* (ATCC 9027)	Glucose	52.5 mW m^{-2} (2.7-fold vs. CC)	[91]
Graphene sponge (GS)	Dozens of microns	Anaerobic sludge	Wastewater	427.0 W m^{-3} (15-fold vs. CF)	[92]
Chitosan/vacuum-stripped graphene (CHI/VSG) scaffold	<50 μm	*P. aeruginosa*	Glucose	1530 mW m^{-2} (78-fold vs. CC)	[94]
Graphene-sponge-stainless steel (G-S-SS)	Hundreds of microns	Evolved MFC anolyte	Glucose	1570 mW m^{-2} (14-fold vs. SS) 394 W m^{-3} (14-fold vs. SS)	[95]
Reduced graphene oxide-nickel (rGO-Ni) foam	Hundreds of microns	*S. oneidensis* MR-1	Trypticase soy broth (TSB)	661 W m^{-3} (19-fold vs. Ni foam, 29-fold vs. CF, 55-fold vs. CP, 16-fold vs. CF)	[96]
3D graphene scaffolds	100–200 μm	*Geobacter sulfurreducens*	Sodium acetate medium	11,220 W m^{-3}	[98]
Carbonizing natural biomass					
Ordered 3D carbon material (3D-KSC)	Hundreds of microns	Natural microbial consortium	Domestic wastewater	32.5 A m^{-2}	[99]
Reticulated carbon foam derived from pomelo peel (RCF-PP)	>100 μm	Natural microbial consortium	Domestic wastewater	40 A m^{-2} (5-fold vs. RVC)	[100]
Layered corrugated carbon (LCC)	Millimeter scale	Natural microbial consortium	Domestic wastewater	70, 200 and 390 A m^{-2} for 1, 3, and 6 layers, respectively	[101]
Carbon electrode derived from corn stem (CECS)	2–7 μm	Mixed biofilm formation	Acetate	31.2A m^{-2} (8-fold vs. plate graphite)	[102]
Carbonized kapok (kapok_c)	10–20 μm	Anaerobic sludge	Acetate	1738.1 mW m^{-2} COD removal: 92.9 ± 2.1%	[103]
Nitrogen-enriched carbon NPs/loofah sponge carbon (NCP/LSC)	20–200 μm	Evolved anodic effluent	Sodium acetate	1090 ± 72 mW m^{-2} (1.9-fold vs. CF, 2.8-folds vs. GP, 1.7-fold vs. RVC)	[104]

Table 2.1 (continued)

Material	Pore size	Inoculum	Nutritional substrate	Performance	Refs.
Carbonized chestnut shell (CSE)	Hundreds of microns	Anaerobic sludge	Acetate	759 ± 38 mW m^{-2}	[105]
				Coulombic efficiencies: 75% 12%	
Activated chestnut shell powder (act-powder)	Hundreds of microns	Municipal wastewater	Sodium acetate	23.6 W m^{-3} (2.3-fold vs. CC)	[106]
Carbonized silk cocoon	~2 μm	Anaerobic sludge	Acetate	8.6 ± 0.1 mWg^{-1} (2.5-fold vs. CC)	[107]
Carbon nanofiber (CNF) aerogel	Several microns	S. putrefaciens CN32	Sodium acetate	1747 mW m^{-2} (4-fold vs. CNT, 14-fold vs. CC)	[46]
Nanostructured materials					
Mo$_2$C@CF	2.56 nm	S. putrefaciens CN32	Sodium acetate	1025 mW m^{-2} (5-fold vs. CF)	[108]
3D hierarchically nanostructured carbon (HN-C)	Macropores (ca., 400 nm) and mesopores (ca., 4 nm)	Anaerobic sludge	Sucrose	1034 mW m^{-2}	[109]
				COD removal: 92.1%	
20 wt.% CNT/PANI	Hundreds of nanometers	E. coli K12 (ATCC 29181)	Glucose	42 mW m^{-2}	[111]
PANI/mesoporous TiO$_2$	6–8 nm	E. coli K12 (ATCC 29181)	Glucose	1495 mW m^{-2}	[110]
PANI/m-WO$_3$	–	E. coli	Glucose	980 mW m^{-2}	[113]
PPy nanosucker array (nano-SA)	Tens of nanometers	Anaerobic sludge	Glucose	727.8 mW m^{-2}	[115]
TiO$_2$/rGO	3–4 nm	S. putrefaciens CN32	Sodium acetate	540 mW m^{-2}	[119]
TiO$_2$-NSs	–	Anaerobic sludge	Acetate	690 mW m^{-2}	[120]
RuO$_2$-coated carbon felt	–	Shewanella decolorationis S12	Lactate	3.08 W m^{-2}	[123]
NiO/graphene	~5 μm	S. putrefaciens CN32	Sodium acetate	3632 mW m^{-2}	[124]
MWCNTs/SnO$_2$	–	E. coli (ATCC 11775)	Glucose	1421 mW m^{-2}	[126]

larger than that obtained from the MFC with the stainless steel mesh anode. Liu et al. [91] used an electrodeposition approach to obtain graphene nanosheet modified carbon cloth and applied it as anode in a *P. aeruginosa* MFC. The graphene-modified carbon cloth not only promotes the interfacial electron transfer but also stimulates excretion of mediating molecules for higher electron transfer rate. As a result, the anode delivered a 2.7-fold higher power density and a threefold higher energy conversion efficiency than a plain carbon cloth anode. In these two works, the graphene

nanosheets were just used for surface modification rather than structure fabrication.

Since the graphene oxide (GO) nanosheets are easy to self-assemble into macroporous or scaffold structure during reduction process under appropriate conditions, these assembled three-dimensional (3D) reduced graphene oxide (rGO) materials may be good candidates for BES electrodes. Chen et al. [92] fabricated a 3D macroporous graphene sponge (GS) via chemical reduction of GO aqueous suspension with addition of $NaHSO_3$ as reducing agent, which resulted in a self-assembled rGO aerogels after freeze-drying. The macroporous structure of this prepared 3D rGO sponge enabled the microbes to easily diffuse into and propagate inside the electrode, leading to much higher performance than a conventional carbon felt (CF) in MFC. It should be noticed that the reducing condition will not only affect the porous structure but also the surface properties of the rGO aerogels. To get a biocompatible surface on the rGO, we have tried to use L-cysteine as reducing agent to prepare the rGO aerogel [93]. The obtained rGO aerogels delivered higher power density in *Shewanella* MFC than that of the rGO aerogels prepared with hydrothermal method.

For these self-assembled 3D rGO electrodes, the pore size distribution is not uniform and some part of the inner surface is not accessible for exoelectrogen cells. Thus, a neat and ordered 3D structure with abundant macropores could to be more preferable for promoting microbial colonization and accelerating mass transport. He et al. [94] utilize the ice segregation-induced self-assembly technique to prepare a novel 3D chitosan/vacuum-stripped graphene (CHI/VSG) scaffold with hierarchically and orderly porous structure, in which the aligned macropores were produced by layered-branched architecture from chitosan template and mesopores from porous VSG were embedded in the wall of macropores. The pore size in the range of 30 to 50 μm of the produced self-supported spongelike 3D graphene scaffold was large enough to allow microbe swimming into its interior. Meanwhile, the mesopores from porous VSG were suggested to augment the active surface area for accepting electrons from electron shuttles produced by exoelectrogens. Expectedly, the optimized CHI/VSG anode delivered an outstanding maximum power density of 1530 mW m^{-2} in a dual-chamber MFC inoculated with *P. aeruginosa*, which was 78-fold higher than a conventional carbon cloth anode.

Besides the self-assembly with the assistance of various soft templates, the impregnation of graphene nanosheets into scaffold substrate with open macropores has attracted attentions recently. Xie et al. [95] selected low-cost synthetic sponges from polyurethane as substrates and coated them with graphene via a simple dipping and drying process to prepare 3D graphene sponge electrodes. Due to the open and continuous macroporous structure of sponges with a pore size range of 300–500 μm for efficient microbial colonization and fast electrolyte transport, the prepared 3D graphene sponge electrode showed great advantages in MFC in terms of current production, durability, and cost of electrode. Besides, Ni foam is also an often used hard template to build 3D graphene-based electrodes. The GO nanosheets could be deposited on the Ni scaffold [96] or self-assembled in the macropores [97] to produce 3D rGO/Ni composite electrodes after a hydrothermal reduction. Another frequently used approach to prepare 3D macroporous and monolithic graphene

scaffold electrodes is direct growth of continuous graphene film on nickel foam substrate by chemical vapor deposition (CVD). Ren et al. [98] prepared a macroporous graphene scaffold anode prepared by CVD technique, which delivered a very high power density over 10,000 W m^{-3} in a miniaturized MFC. Undoubtedly, the 3D graphene-based materials are promising candidates to build highly effective bioelectrodes for BES applications.

2.3.2 Carbonized Materials from Natural Biomass

Production of porous carbon materials from carbonized porous biomass is a cost-effective way to obtain large amount of electrode materials for BES. These biomass-derived 3D macroporous electrodes generally produced high current densities and/or power densities in MFCs. Chen et al. [99] used crop plant kenaf as raw material in the preparation of a macroporous carbon for high-performance MFC anodes; the current density generated by the 3D order porous carbon reached 3.25 mA cm^{-2}. Later, they prepared a reticulated carbon foam by direct carbonization of the sponge-like natural product pomelo peel [100]. Attributed to the reticulated macroporous architecture with high porosity (97%), large pore size (>100 μm), and wrinkled electrode surface with excellent wetting property, this anode generated a high current density of 4.02 mA cm^{-2}. Furthermore, they also chose the corrugated cardboard as raw materials to prepare layered corrugated carbon with millimeter pores [101], which delivered a current density of 7.28 mA cm^{-2} with only single layer. It has also been reported that carbonized king mushroom, wild mushroom, and corn stem [102] and a hollow natural fiber (kapok)-derived anode [103] exhibited good bioelectrocatalytic properties. For these carbonized materials, an easy way for surface fabrication is to introduce some specific precursors before carbonization. Yuan et al. [104] reported a loofah sponge carbon decorated with nitrogen-enriched carbon nanoparticles that are fabricated by co-carbonizing with nanosize polyaniline. The nitrogen-enriched carbon nanoparticle coating on the surface could promote interfacial charge transfer between the bacteria and the electrode.

Besides the common plants with porous structures, some plants with special structures were also used as carbonization precursors. For instance, a hierarchically structured urchin-like anode derived from chestnut shells was fabricated by Chen et al. [105]. When the carbonized chestnut was connected to a titanium wire, it looked like spherical carbon brush, which provided large surface area for bacterial loading. In another work, an activation process was introduced after the chestnut was carbonization to obtain mesoporous and microporous structure [106]. The authors believed that the chemical activation process not only created more mesopores and micropores but also decreased the O-content and pyridinic/pyrrolic N groups on the biomass anode, which were beneficial for improving charge transfer efficiency between the anode surface and microbial biofilm. In addition, some fibrous natural materials have been used to prepare carbonized electrode materials for BES. Recently, Lu et al. [107] reported a nitrogen-enriched pseudographitic

anode derived from silk cocoon, and this anode delivered ~2.5-fold maximum gravimetric power density than that of MFCs with commonly used carbon cloth anodes. Zou et al. [46] found that the carbon nanofiber (CNF) aerogel derived from a bacterial cellulose pellicle possessed relatively smaller macropore size than other reported biomass-derived porous materials but achieved more biofilm loading. It is possible that the pores constructed by 1D nanofibers were open in almost all directions, which would promote bacterial access and substrate transport into the inner surface of CNF aerogel electrode. In a word, carbonizing natural and recyclable materials provides an excellent green approach for electrode preparation in BES devices.

2.3.3   Nanostructured Electrodes

The development of 3D hierarchically porous electrode with tailored macroporous structure and good biocompatibility indeed opens an effective channel for enhancing biofilm growth and boosting microbial electrocatalysis on anode. The introduced nanostructure which originated from the integrated nanoscale materials in the 3D macroscopic electrode apparently also plays an extraordinary role in enabling the high performance of almost all reported 3D hierarchically macroporous electrodes. Recently, Zou et al. [108] reported a nanoporous molybdenum carbide (Mo_2C) functionalized carbon felt electrode with rich 3D hierarchical porous architecture; they proposed that the introduction of rough Mo_2C nanostructural interface into macroporous carbon architecture would promote microbial growth with great excretion of endogenous electron shuttles (flavins) and the rich available nanopores would enlarge electrochemically active surface area. Liu et al. [109] developed a 3D hierarchically nanostructured carbon with well-patterned macropores (~400 nm) and ordered mesopores (~4 nm) via a dual-templating strategy, which showed higher power density and COD removal than both the macroporous carbon and the mesoporous carbon in MFCs. The reason could be the combination of macropores for the bacteria adhesion and efficient mass transport and the large specific surface area of mesopores for fast electron transfer. In generally, an excellent electrode for microbial electrocatalysis should be a 3D hierarchically porous structure composed of ordered, open macropores that are large enough (at least a few microns) to allow microbe swarming into and then colonization together with rich mesopores that can provide a large available surface area for electrochemical reaction, thereby leading to remarkable increases in both biocatalysis and electrocatalysis at the same time.

Actually, the nanoporous structure (especially the mesopores with diameter between 2 and 50 nm) of an electrode has been found to be crucial to the electrocatalytic reaction of small-sized redox molecules in diverse biotic or abiotic systems. Qiao et al. demonstrated that a unique nanostructured PANI/TiO_2 composite [110] with large specific surface area and uniform mesopores distribution could greatly improve the performance of *E. coli* MFC, which delivered much higher power density than the similar MFC with PANI/CNT anode reported in their previous work [111]. Notably, conducting polymers as well as their composite

materials such as polypyrrole/anthraquinone-2,6-disulphonic disodium salt (PPy/AQDS) [112], polyaniline/mesoporous tungsten trioxide (PANI/m-WO₃) [113], and graphene/poly(3,4-ethylenedioxythiophene) (G/PEDOT) [114] have been used to modify anodes to improve the performance of MFC owing to their facile synthesis process, good electronic conductivity, easily forming diverse nanostructures, and excellent biocompatibility and environmental stability. A polypyrrole nanotubular structure vertically grown on the surface of carbon textile electrode has been reported by Wang et al. [115]. They found that this electrode could capture microbial cells rather than only passively provide attachment sites for microbial attachment and EET kinetics could be promoted. Ding et al. proposed that the PANI [116] or PPy [117] nanowire arrays could sever as tunable terminal polymeric mediator for bacterial EET process rather than only as a current collector. The aligned nanostructure of size-matchable PANI or PPy nanowires could enable a local topological interaction with microbes along with a more efficient interfacial electronic interaction.

Besides the conducting polymers, transition metal compounds, including their oxides and carbides, have also attracted great research interest in BES owing to their versatile properties. Wen et al. [118] reported a nanohybrid of anatase TiO_2 nanoparticle-decorated CNTs (CNTs@TiO_2) that exhibited a much higher current density, power density, and coulombic efficiency in comparison to pure CNTs and TiO_2 NPs alone when used as anode materials in mixed consortia-derived MFCs. Zou et al. [119] synthesized a TiO_2 nanocrystal/rGO hybrid as MFC anode. They proposed that the improved hydrophilicity and large surface area of TiO_2/rGO hybrid could promote bacterial adhesion and biofilm formation. It is interesting that the TiO_2 nanocrystals could stimulate the endogenous production of flavins from *S. putrefaciens* CN32 biofilm and meanwhile the highly conductive rGO could enable fast redox reaction of these electron shuttles with a short diffusion distance. Besides, several studies have also demonstrated that the nanostructured TiO_2 promoted biofilm formation and interfacial EET rate could be tailored by its morphology, size, and pore structure [120, 121]. Furthermore, other transition metal oxides such as Fe_3O_4 [122], RuO_2 [123], NiO [124], MnO_2 [125], and SnO_2 [126], which possess multiple redox reactions and diverse nanostructure, have been reported to hold a promising potential in electrode functionalization for facilitating interfacial electron transfer in bioelectrocatalytic process.

2.4 Future Electrode Design for Bioremediation

According to the above discussion about the electrode materials used for bioelectrocatalysis, it is noted that the newly developed electrode materials, especially the ones with hierarchical porous structures and biocompatible surface properties, could always exhibit great bioelectrocatalytic performance. Therefore, a high-performance BES electrode should provide not only adequate surface (macropores or open structures) for biofilm loading but also large area of active sites (mesopores)
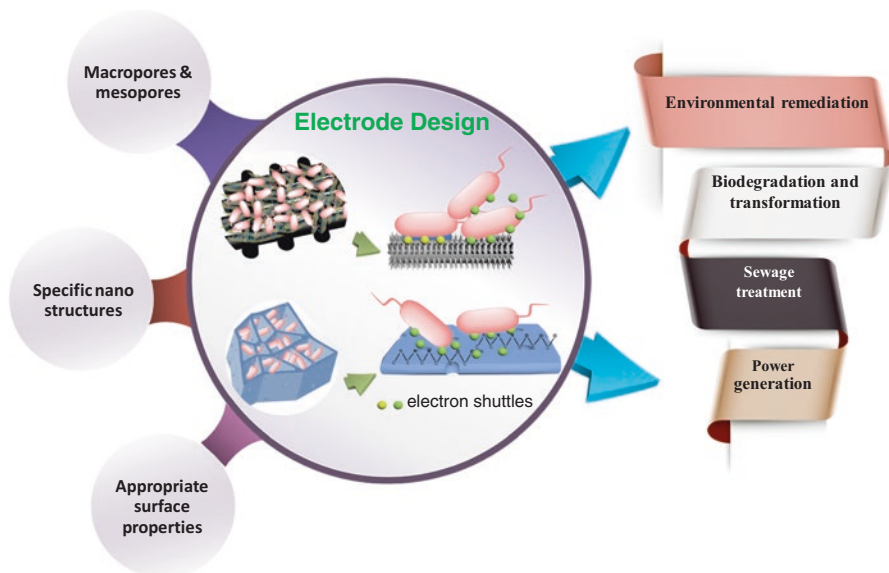
Fig. 2.1   Schematic summary of electron design for environmental remediation

for interfacial electron transfer (MET and DET). Meanwhile, the surface of the favorable electrodes should be hydrophilic and possess appropriate functional groups. As the development of material science, synthesis of such kind of materials in laboratory scale is not difficult. However, the mass production of these superior electrode materials is still not easy so the cost will be quite high when used in large-scale electrodes. While for the BES devices used in bioremediation, the small-scale models are obviously not feasible.

On the other hand, most of these newly developed electrode materials are powders, which are required being pasted or coated on a current collector before used in BES devices. Apparently, this pasting process will affect the electrode performance especially when the polymer binders are used, and it is hard to build a standard process for all kinds of powder materials. To solve this problem, an in situ growth of nano- or microstructures on traditional electrodes or current collectors could be a feasible strategy. There have been some examples like gold-sputtered carbon paper [127], NiO nanorod array-modified carbon cloth [128], and the abovementioned rGO/Ni composite. It still needs further exploration to find an optimal hybrid with low-cost current collector or substrate and highly effective decoration part that can be obtained through mass production.

In summary, according to the characters of bioelectrocatalysis, the BES electrode design should involve both structure fabrications and the surface functionalization, which are important issues for interfacial electron transfer and the devices' performance. As summarized in Fig. 2.1, the cost-effective hierarchical porous electrodes with macropores and mesopores or the fabric electrodes with specific nanostructures could be good candidates for BES electrodes especially after appro-

priate surface modification. The excellent electrode design could greatly improve the capability of BES devices for biodegradation, waste treatment, electrosynthesis, and power generation.

References

1. Logan BE (2009) Exoelectrogenic bacteria that power microbial fuel cells. Nat Rev Microbiol 7(5):375–381
2. Kumar R, Singh L, Zularisam A (2016) Exoelectrogens: recent advances in molecular drivers involved in extracellular electron transfer and strategies used to improve it for microbial fuel cell applications. Renew Sust Energ Rev 56:1322–1336
3. Shi L, Dong HL, Reguera G, Beyenal H, Lu AH, Liu J, Yu HQ, Fredrickson JK (2016) Extracellular electron transfer mechanisms between microorganisms and minerals. Nat Rev Microbiol 14(10):651–662. https://doi.org/10.1038/nrmicro.2016.93
4. Sydow A, Krieg T, Mayer F, Schrader J, Holtmann D (2014) Electroactive bacteria—molecular mechanisms and genetic tools. Appl Microbiol Biotechnol 98(20):8481–8495
5. Nevin KP, Kim B-C, Glaven RH, Johnson JP, Woodard TL, Methé BA, DiDonato RJ Jr, Covalla SF, Franks AE, Liu A (2009) Anode biofilm transcriptomics reveals outer surface components essential for high density current production in Geobacter sulfurreducens fuel cells. PLoS One 4(5):e5628
6. Richter H, Nevin KP, Jia H, Lowy DA, Lovley DR, Tender LM (2009) Cyclic voltammetry of biofilms of wild type and mutant Geobacter sulfurreducens on fuel cell anodes indicates possible roles of OmcB, OmcZ, type IV pili, and protons in extracellular electron transfer. Energy Environ Sci 2(5):506–516
7. Okamoto A, Nakamura R, Hashimoto K (2011) In-vivo identification of direct electron transfer from Shewanella oneidensis MR-1 to electrodes via outer-membrane OmcA–MtrCAB protein complexes. Electrochim Acta 56(16):5526–5531
8. Breuer M, Rosso KM, Blumberger J, Butt JN (2015) Multi-haem cytochromes in Shewanella oneidensis MR-1: structures, functions and opportunities. J R Soc Interface 12(102):20141117. https://doi.org/10.1098/rsif.2014.1117
9. Bretschger O, Obraztsova A, Sturm CA, Chang IS, Gorby YA, Reed SB, Culley DE, Reardon CL, Barua S, Romine MF (2007) Current production and metal oxide reduction by Shewanella oneidensis MR-1 wild type and mutants. Appl Environ Microbiol 73(21):7003–7012
10. Leys D, Scrutton NS (2004) Electrical circuitry in biology: emerging principles from protein structure. Curr Opin Struct Biol 14(6):642–647
11. Reguera G, McCarthy KD, Mehta T, Nicoll JS, Tuominen MT, Lovley DR (2005) Extracellular electron transfer via microbial nanowires. Nature 435(7045):1098–1101 doi:http://www.nature.com/nature/journal/v435/n7045/suppinfo/nature03661_S1.html
12. El-Naggar MY, Wanger G, Leung KM, Yuzvinsky TD, Southam G, Yang J, Lau WM, Nealson KH, Gorby YA (2010) Electrical transport along bacterial nanowires from Shewanella oneidensis MR-1. Proc Natl Acad Sci U S A 107(42):18127–18131. https://doi.org/10.1073/pnas.1004880107
13. Strycharz-Glaven SM, Snider RM, Guiseppi-Elie A, Tender LM (2011) On the electrical conductivity of microbial nanowires and biofilms. Energy Environ Sci 4(11):4366–4379. https://doi.org/10.1039/C1EE01753E
14. Pirbadian S, Barchinger SE, Leung KM, Byun HS, Jangir Y, Bouhenni RA, Reed SB, Romine MF, Saffarini DA, Shi L (2014) Shewanella oneidensis MR-1 nanowires are outer membrane and periplasmic extensions of the extracellular electron transport components. Proc Natl Acad Sci U S A 111(35):12883–12888

15. Lies DP, Hernandez ME, Kappler A, Mielke RE, Gralnick JA, Newman DK (2005) Shewanella oneidensis MR-1 uses overlapping pathways for iron reduction at a distance and by direct contact under conditions relevant for biofilms. Appl Environ Microbiol 71(8):4414–4426

16. Marsili E, Baron DB, Shikhare ID, Coursolle D, Gralnick JA, Bond DR (2008) Shewanella Secretes flavins that mediate extracellular electron transfer. Proc Natl Acad Sci U S A 105(10):3968–3973. https://doi.org/10.1073/pnas.0710525105

17. von Canstein H, Ogawa J, Shimizu S, Lloyd JR (2008) Secretion of flavins by Shewanella species and their role in extracellular electron transfer. Appl Environ Microbiol 74(3):615–623. https://doi.org/10.1128/aem.01387-07

18. Kotloski NJ, Gralnick JA (2013) Flavin electron shuttles dominate extracellular electron transfer by Shewanella oneidensis. MBio 4(1). https://doi.org/10.1128/mBio.00553-12

19. Coursolle D, Baron DB, Bond DR, Gralnick JA (2010) The Mtr respiratory pathway is essential for reducing Flavins and electrodes in Shewanella oneidensis. J Bacteriol 192(2):467–474. https://doi.org/10.1128/jb.00925-09

20. Jiang X, Hu J, Fitzgerald LA, Biffinger JC, Xie P, Ringeisen BR, Lieber CM (2010) Probing electron transfer mechanisms in Shewanella oneidensis MR-1 using a nanoelectrode platform and single-cell imaging. Proc Natl Acad Sci U S A 107(39):16806–16810. https://doi.org/10.1073/pnas.1011699107

21. Okamoto A, Hashimoto K, Nealson KH, Nakamura R (2013) Rate enhancement of bacterial extracellular electron transport involves bound flavin semiquinones. Proc Natl Acad Sci U S A 110(19):7856–7861. https://doi.org/10.1073/pnas.1220823110

22. Okamoto A, Hashimoto K, Nealson KH (2014) Flavin redox bifurcation as a mechanism for controlling the direction of electron flow during extracellular electron transfer. Angew Chem Int Ed 53(41):10988–10991. https://doi.org/10.1002/anie.201407004

23. Xu S, Jangir Y, El-Naggar MY (2016) Disentangling the roles of free and cytochrome-bound flavins in extracellular electron transport from Shewanella oneidensis MR-1. Electrochim Acta 198:49–55

24. Okamoto A, Nakamura R, Nealson KH, Hashimoto K (2014) Bound Flavin model suggests similar electron-transfer mechanisms in Shewanella and Geobacter. ChemElectroChem 1(11):1808–1812

25. Maithreepala RA, Doong R-A (2009) Transformation of carbon tetrachloride by biogenic iron species in the presence of Geobacter sulfurreducens and electron shuttles. J Hazard Mater 164(1):337–344 https://doi.org/10.1016/j.jhazmat.2008.08.007

26. Okamoto A, Saito K, Inoue K, Nealson KH, Hashimoto K, Nakamura R (2014) Uptake of self-secreted flavins as bound cofactors for extracellular electron transfer in Geobacter species. Energy Environ Sci 7(4):1357–1361. https://doi.org/10.1039/c3ee43674h

27. Rabaey K, Boon N, Höfte M, Verstraete W (2005) Microbial Phenazine production enhances electron transfer in biofuel cells. Environ Sci Technol 39(9):3401–3408. https://doi.org/10.1021/es048563o

28. Boon N, De Maeyer K, Höfte M, Rabaey K, Verstraete W (2008) Use of Pseudomonas species producing phenazine-based metabolites in the anodes of microbial fuel cells to improve electricity generation. Appl Microbiol Biotechnol 80(6):985–993

29. Wang Y, Kern SE, Newman DK (2010) Endogenous phenazine antibiotics promote anaerobic survival of Pseudomonas aeruginosa via extracellular electron transfer. J Bacteriol 192(1):365–369

30. Zhang T, Cui C, Chen S, Ai X, Yang H, Shen P, Peng Z (2006) A novel mediatorless microbial fuel cell based on direct biocatalysis of Escherichia coli. Chem Commun 21:2257–2259

31. Qiao Y, Li CM, Bao S-J, Lu Z, Hong Y (2008) Direct electrochemistry and electrocatalytic mechanism of evolved Escherichia coli cells in microbial fuel cells. Chem Commun (11):1290–1292. https://doi.org/10.1039/b719955d

32. Zhang T, Cui C, Chen S, Yang H, Shen P (2008) The direct electrocatalysis of Escherichia coli through electroactivated excretion in microbial fuel cell. Electrochem Commun 10(2):293–297 https://doi.org/10.1016/j.elecom.2007.12.009

33. Nevin KP, Woodard TL, Franks AE, Summers ZM, Lovley DR (2010) Microbial electrosynthesis: feeding microbes electricity to convert carbon dioxide and water to multicarbon extracellular organic compounds. MBio 1(2):e00103–e00110

34. Rabaey K, Rozendal RA (2010) Microbial electrosynthesis—revisiting the electrical route for microbial production. Nat Rev Microbiol 8(10):706–716

35. Rosenbaum M, Aulenta F, Villano M, Angenent LT (2011) Cathodes as electron donors for microbial metabolism: which extracellular electron transfer mechanisms are involved? Bioresour Technol 102(1):324–333

36. Ganigué R, Puig S, Batlle-Vilanova P, Balaguer MD, Colprim J (2015) Microbial electrosynthesis of butyrate from carbon dioxide. Chem Commun 51(15):3235–3238

37. Sadhukhan J, Lloyd JR, Scott K, Premier GC, Eileen HY, Curtis T, Head IM (2016) A critical review of integration analysis of microbial electrosynthesis (MES) systems with waste biorefineries for the production of biofuel and chemical from reuse of CO_2. Renew Sust Energ Rev 56:116–132

38. Strycharz SM, Glaven RH, Coppi MV, Gannon SM, Perpetua LA, Liu A, Nevin KP, Lovley DR (2011) Gene expression and deletion analysis of mechanisms for electron transfer from electrodes to Geobacter sulfurreducens. Bioelectrochemistry 80(2):142–150

39. Dantas JM, Tomaz DM, Morgado L, Salgueiro CA (2013) Functional characterization of PccH, a key cytochrome for electron transfer from electrodes to the bacterium Geobacter sulfurreducens. FEBS Lett 587(16):2662–2668

40. Ross DE, Flynn JM, Baron DB, Gralnick JA, Bond DR (2011) Towards electrosynthesis in Shewanella: energetics of reversing the Mtr pathway for reductive metabolism. PLoS One 6(2):e16649

41. Yang Y, Ding Y, Hu Y, Cao B, Rice SA, Kjelleberg S, Song H (2015) Enhancing bidirectional electron transfer of Shewanella oneidensis by a synthetic flavin pathway. ACS Synth Biol 4(7):815–823. https://doi.org/10.1021/sb500331x

42. Kundu A, Sahu JN, Redzwan G, Hashim MA (2013) An overview of cathode material and catalysts suitable for generating hydrogen in microbial electrolysis cell. Int J Hydrog Energy 38(4):1745–1757. https://doi.org/10.1016/j.ijhydene.2012.11.031

43. Kadier A, Simayi Y, Kalil MS, Abdeshahian P, Hamid AA (2014) A review of the substrates used in microbial electrolysis cells (MECs) for producing sustainable and clean hydrogen gas. Renew Energy 71:466–472. https://doi.org/10.1016/j.renene.2014.05.052

44. Jourdin L, Lu Y, Flexer V, Keller J, Freguia S (2016) Biologically induced hydrogen production drives high rate/high efficiency microbial electrosynthesis of acetate from carbon dioxide. ChemElectroChem 3:581

45. Yoho RA, Popat SC, Rago L, Guisasola A, Torres CI (2015) Anode biofilms of Geoalkalibacter ferrihydriticus exhibit electrochemical signatures of multiple electron transport pathways. Langmuir 31(45):12552–12559

46. Zou L, Qiao Y, Wu Z-Y, Wu X-S, Xie J-L, Yu S-H, Guo J, Li CM (2016) Tailoring unique mesopores of hierarchically porous structures for fast direct electrochemistry in microbial fuel cells. Adv Energy Mater 6(4):1501535. https://doi.org/10.1002/aenm.201501535

47. Reguera G, Nevin KP, Nicoll JS, Covalla SF, Woodard TL, Lovley DR (2006) Biofilm and nanowire production leads to increased current in Geobacter sulfurreducens fuel cells. Appl Environ Microbiol 72(11):7345–7348. https://doi.org/10.1128/aem.01444-06

48. Borole AP, Reguera G, Ringeisen B, Wang Z-W, Feng Y, Kim BH (2011) Electroactive biofilms: current status and future research needs. Energy Environ Sci 4(12):4813–4834. https://doi.org/10.1039/c1ee02511b

49. Rollefson JB, Stephen CS, Tien M, Bond DR (2011) Identification of an extracellular polysaccharide network essential for cytochrome anchoring and biofilm formation in Geobacter sulfurreducens. J Bacteriol 193(5):1023–1033

50. Sun D, Cheng S, Wang A, Li F, Logan BE, Cen K (2015) Temporal-spatial changes in viabilities and electrochemical properties of anode biofilms. Environ Sci Technol 49(8):5227–5235

51. Cao B, Shi L, Brown RN, Xiong Y, Fredrickson JK, Romine MF, Marshall MJ, Lipton MS, Beyenal H (2011) Extracellular polymeric substances from Shewanella sp. HRCR-1 biofilms: characterization by infrared spectroscopy and proteomics. Environ Microbiol 13(4):1018–1031. https://doi.org/10.1111/j.1462-2920.2010.02407.x

52. De Vriendt K, Theunissen S, Carpentier W, De Smet L, Devreese B, Van Beeumen J (2005) Proteomics of Shewanella oneidensis MR-1 biofilm reveals differentially expressed proteins, including AggA and RibB. Proteomics 5(5):1308–1316

53. Zou L, Qiao Y, Wu X-S, Li CM (2016) Tailoring hierarchically porous graphene architecture by carbon nanotube to accelerate extracellular electron transfer of anodic biofilm in microbial fuel cells. J Power Sources 328:143–150. https://doi.org/10.1016/j.jpowsour.2016.08.009

54. Qiao Y, Qiao Y-J, Zou L, Ma C-X, Liu J-H (2015) Real-time monitoring of phenazines excretion in Pseudomonas aeruginosa microbial fuel cell anode using cavity microelectrodes. Bioresour Technol 198:1–6

55. Qiao Y-J, Qiao Y, Zou L, Wu X-S, Liu J-H (2017) Biofilm promoted current generation of Pseudomonas aeruginosa microbial fuel cell via improving the interfacial redox reaction of phenazines. Bioelectrochemistry 117:34–39. https://doi.org/10.1016/j.bioelechem.2017.04.003

56. Jourdin L, Freguia S, Donose BC, Chen J, Wallace GG, Keller J, Flexer V (2014) A novel carbon nanotube modified scaffold as an efficient biocathode material for improved microbial electrosynthesis. J Mater Chem A 2(32):13093–13102

57. Jourdin L, Freguia S, Donose BC, Keller J (2015) Autotrophic hydrogen-producing biofilm growth sustained by a cathode as the sole electron and energy source. Bioelectrochemistry 102:56–63. https://doi.org/10.1016/j.bioelechem.2014.12.001

58. Patil SA, Arends JB, Vanwonterghem I, Van Meerbergen J, Guo K, Tyson GW, Rabaey K (2015) Selective enrichment establishes a stable performing community for microbial electrosynthesis of acetate from CO_2. Environ Sci Technol 49(14):8833–8843

59. Liu H, Logan BE (2004) Electricity generation using an air-cathode single chamber microbial fuel cell in the presence and absence of a proton exchange membrane. Environ Sci Technol 38(14):4040–4046. https://doi.org/10.1021/es0499344

60. Min B, Kim J, Oh S, Regan JM, Logan BE (2005) Electricity generation from swine wastewater using microbial fuel cells. Water Res 39(20):4961–4968. https://doi.org/10.1016/j.watres.2005.09.039

61. Lu N, Zhou S-G, Zhuang L, Zhang J-T, Ni J-r (2009) Electricity generation from starch processing wastewater using microbial fuel cell technology. Biochem Eng J 43(3):246–251. https://doi.org/10.1016/j.bej.2008.10.005

62. Minke C, Kunz U, Turek T (2017) Carbon felt and carbon fiber – a techno-economic assessment of felt electrodes for redox flow battery applications. J Power Sources 342:116–124. https://doi.org/10.1016/j.jpowsour.2016.12.039

63. Blanchet E, Erable B, De Solan M-L, Bergel A (2016) Two-dimensional carbon cloth and three-dimensional carbon felt perform similarly to form bioanode fed with food waste. Electrochem Commun 66:38–41. https://doi.org/10.1016/j.elecom.2016.02.017

64. Wang X, Feng YJ, Lee H (2008) Electricity production from beer brewery wastewater using single chamber microbial fuel cell. Water Sci Technol 57(7):1117

65. Zhao F, Rahunen N, Varcoe JR, Chandra A, Avignone-Rossa C, Thumser AE, Slade RCT (2008) Activated carbon cloth as anode for sulfate removal in a microbial fuel cell. Environ Sci Technol 42(13):4971–4976. https://doi.org/10.1021/es8003766

66. Suzuki M (1994) Activated carbon fiber: fundamentals and applications. Carbon 32(4):577–586. https://doi.org/10.1016/0008-6223(94)90075-2

67. Deng Q, Li X, Zuo J, Ling A, Logan BE (2010) Power generation using an activated carbon fiber felt cathode in an upflow microbial fuel cell. J Power Sources 195(4):1130–1135. https://doi.org/10.1016/j.jpowsour.2009.08.092

68. Logan B, Cheng S, Watson V, Estadt G (2007) Graphite fiber brush anodes for increased power production in air-cathode microbial fuel cells. Environ Sci Technol 41(9):3341–3346. https://doi.org/10.1021/es062644y

69. Feng Y, Yang Q, Wang X, Liu Y, Lee H, Ren N (2011) Treatment of biodiesel production wastes with simultaneous electricity generation using a single-chamber microbial fuel cell. Bioresour Technol 102(1):411–415. https://doi.org/10.1016/j.biortech.2010.05.059

70. Hays S, Zhang F, Logan BE (2011) Performance of two different types of anodes in membrane electrode assembly microbial fuel cells for power generation from domestic wastewater. J Power Sources 196(20):8293–8300. https://doi.org/10.1016/j.jpowsour.2011.06.027

71. Kim K-Y, Yang W, Logan BE (2015) Impact of electrode configurations on retention time and domestic wastewater treatment efficiency using microbial fuel cells. Water Res 80:41–46. https://doi.org/10.1016/j.watres.2015.05.021

72. Cheng S, Logan BE (2007) Sustainable and efficient biohydrogen production via electro-hydrogenesis. Proc Natl Acad Sci U S A 104(47):18871–18873. https://doi.org/10.1073/pnas.0706379104

73. Call D, Logan BE (2008) Hydrogen production in a single chamber microbial electrolysis cell lacking a membrane. Environ Sci Technol 42(9):3401–3406. https://doi.org/10.1021/es8001822

74. Logan BE, Call D, Cheng S, Hamelers HVM, Sleutels THJA, Jeremiasse AW, Rozendal RA (2008) Microbial electrolysis cells for high yield hydrogen gas production from organic matter. Environ Sci Technol 42(23):8630–8640. https://doi.org/10.1021/es801553z

75. Wagner RC, Regan JM, Oh S-E, Zuo Y, Logan BE (2009) Hydrogen and methane production from swine wastewater using microbial electrolysis cells. Water Res 43(5):1480–1488. https://doi.org/10.1016/j.watres.2008.12.037

76. Hutchinson AJ, Tokash JC, Logan BE (2011) Analysis of carbon fiber brush loading in anodes on startup and performance of microbial fuel cells. J Power Sources 196(22):9213–9219. https://doi.org/10.1016/j.jpowsour.2011.07.040

77. Lanas V, Logan BE (2013) Evaluation of multi-brush anode systems in microbial fuel cells. Bioresour Technol 148:379–385. https://doi.org/10.1016/j.biortech.2013.08.154

78. Lanas V, Ahn Y, Logan BE (2014) Effects of carbon brush anode size and loading on microbial fuel cell performance in batch and continuous mode. J Power Sources 247:228–234. https://doi.org/10.1016/j.jpowsour.2013.08.110

79. Liu H, Ramnarayanan R, Logan BE (2004) Production of electricity during wastewater treatment using a single chamber microbial fuel cell. Environ Sci Technol 38(7):2281–2285. https://doi.org/10.1021/es034923g

80. Wang X, Cheng S, Feng Y, Merrill MD, Saito T, Logan BE (2009) Use of carbon mesh anodes and the effect of different pretreatment methods on power production in microbial fuel cells. Environ Sci Technol 43(17):6870–6874. https://doi.org/10.1021/es900997w

81. He Z, Wagner N, Minteer SD, Angenent LT (2006) An upflow microbial fuel cell with an interior cathode: assessment of the internal resistance by impedance spectroscopy. Environ Sci Technol 40(17):5212–5217. https://doi.org/10.1021/es060394f

82. Jiang D, Li B (2009) Granular activated carbon single-chamber microbial fuel cells (GAC-SCMFCs): a design suitable for large-scale wastewater treatment processes. Biochem Eng J 47(1):31–37. https://doi.org/10.1016/j.bej.2009.06.013

83. Logan BE (2010) Scaling up microbial fuel cells and other bioelectrochemical systems. Appl Microbiol Biotechnol 85(6):1665–1671. https://doi.org/10.1007/s00253-009-2378-9

84. Cheng S, Logan BE (2007) Ammonia treatment of carbon cloth anodes to enhance power generation of microbial fuel cells. Electrochem Commun 9(3):492–496. https://doi.org/10.1016/j.elecom.2006.10.023

85. Feng Y, Yang Q, Wang X, Logan BE (2010) Treatment of carbon fiber brush anodes for improving power generation in air–cathode microbial fuel cells. J Power Sources 195(7):1841–1844. https://doi.org/10.1016/j.jpowsour.2009.10.030

86. Zhu N, Chen X, Zhang T, Wu P, Li P, Wu J (2011) Improved performance of membrane free single-chamber air-cathode microbial fuel cells with nitric acid and ethylenediamine surface modified activated carbon fiber felt anodes. Bioresour Technol 102(1):422–426. https://doi.org/10.1016/j.biortech.2010.06.046

87. Liu J, Liu J, He W, Qu Y, Ren N, Feng Y (2014) Enhanced electricity generation for microbial fuel cell by using electrochemical oxidation to modify carbon cloth anode. J Power Sources 265:391–396. https://doi.org/10.1016/j.jpowsour.2014.04.005

88. He Y-R, Xiao X, Li W-W, Sheng G-P, Yan F-F, Yu H-Q, Yuan H, Wu L-J (2012) Enhanced electricity production from microbial fuel cells with plasma-modified carbon paper anode. Phys Chem Chem Phys 14(28):9966–9971. https://doi.org/10.1039/C2CP40873B

89. Chang S-H, Liou J-S, Liu J-L, Chiu Y-F, Xu C-H, Chen B-Y, Chen J-Z (2016) Feasibility study of surface-modified carbon cloth electrodes using atmospheric pressure plasma jets for microbial fuel cells. J Power Sources 336:99–106. https://doi.org/10.1016/j.jpowsour.2016.10.058

90. Zhang Y, Mo G, Li X, Zhang W, Zhang J, Ye J, Huang X, Yu C (2011) A graphene modified anode to improve the performance of microbial fuel cells. J Power Sources 196(13):5402–5407. https://doi.org/10.1016/j.jpowsour.2011.02.067

91. Liu J, Qiao Y, Guo CX, Lim S, Song H, Li CM (2012) Graphene/carbon cloth anode for high-performance mediatorless microbial fuel cells. Bioresour Technol 114:275–280. https://doi.org/10.1016/j.biortech.2012.02.116

92. Chen W, Huang Y-X, Li D-B, Yu H-Q, Yan L (2014) Preparation of a macroporous flexible three dimensional graphene sponge using an ice-template as the anode material for microbial fuel cells. RSC Adv 4(41):21619–21624. https://doi.org/10.1039/c4ra00914b

93. Qiao Y, Wen G-Y, Wu X-S, Zou L (2015) L-Cysteine tailored porous graphene aerogel for enhanced power generation in microbial fuel cells. RSC Adv 5(72):58921–58927. https://doi.org/10.1039/c5ra09170e

94. He Z, Liu J, Qiao Y, Li CM, Tan TTY (2012) Architecture engineering of hierarchically porous chitosan/vacuum-stripped graphene scaffold as bioanode for high performance microbial fuel cell. Nano Lett 12(9):4738–4741. https://doi.org/10.1021/nl302175j

95. Xie X, Yu G, Liu N, Bao Z, Criddle CS, Cui Y (2012) Graphene-sponges as high-performance low-cost anodes for microbial fuel cells. Energy Environ Sci 5(5):6862–6866. https://doi.org/10.1039/c2ee03583a

96. Wang H, Wang G, Ling Y, Qian F, Song Y, Lu X, Chen S, Tong Y, Li Y (2013) High power density microbial fuel cell with flexible 3D graphene-nickel foam as anode. Nanoscale 5(21):10283–10290. https://doi.org/10.1039/c3nr03487a

97. Qiao Y, Wu X-S, Ma C-X, He H, Li CM (2014) A hierarchical porous graphene/nickel anode that simultaneously boosts the bio- and electro-catalysis for high-performance microbial fuel cells. RSC Adv 4(42):21788–21793. https://doi.org/10.1039/c4ra03082f

98. Ren H, Tian H, Gardner CL, Ren T-L, Chae J (2016) A miniaturized microbial fuel cell with three-dimensional graphene macroporous scaffold anode demonstrating a record power density of over 10 000 W m(−3). Nanoscale 8(6):3539–3547. https://doi.org/10.1039/c5nr07267k

99. Chen S, He G, Hu X, Xie M, Wang S, Zeng D, Hou H, Schroeder U (2012) A three-dimensionally ordered macroporous carbon derived from a natural resource as anode for microbial bioelectrochemical systems. ChemSusChem 5(6):1059–1063. https://doi.org/10.1002/cssc.201100783

100. Chen S, Liu Q, He G, Zhou Y, Hanif M, Peng X, Wang S, Hou H (2012) Reticulated carbon foam derived from a sponge-like natural product as a high-performance anode in microbial fuel cells. J Mater Chem 22(35):18609–18613. https://doi.org/10.1039/c2jm33733a

101. Chen S, He G, Liu Q, Harnisch F, Zhou Y, Chen Y, Hanif M, Wang S, Peng X, Hou H, Schroeder U (2012) Layered corrugated electrode macrostructures boost microbial bioelectrocatalysis. Energy Environ Sci 5(12):9769–9772. https://doi.org/10.1039/c2ee23344d

102. Karthikeyan R, Wang B, Xuan J, Wong JWC, Lee PKH, Leung MKH (2015) Interfacial electron transfer and bioelectrocatalysis of carbonized plant material as effective anode of microbial fuel cell. Electrochim Acta 157:314–323. https://doi.org/10.1016/j.electacta.2015.01.029

103. Zhu H, Wang H, Li Y, Bao W, Fang Z, Preston C, Vaaland O, Ren Z, Hu L (2014) Lightweight, conductive hollow fibers from nature as sustainable electrode materials for microbial energy harvesting. Nano Energy 10:268–276. https://doi.org/10.1016/j.nanoen.2014.08.014

104. Yuan Y, Zhou S, Liu Y, Tang J (2013) Nanostructured macroporous bioanode based on polyaniline-modified natural loofah sponge for high-performance microbial fuel cells. Environ Sci Technol 47(24):14525–14532. https://doi.org/10.1021/es404163g

105. Chen S, Tang J, Jing X, Liu Y, Yuan Y, Zhou S (2016) A hierarchically structured urchin-like anode derived from chestnut shells for microbial energy harvesting. Electrochim Acta 212:883–889. https://doi.org/10.1016/j.electacta.2016.07.077

106. Chen Q, Pu W, Hou H, Hu J, Liu B, Li J, Cheng K, Huang L, Yuan X, Yang C, Yang J (2017) Activated microporous-mesoporous carbon derived from chestnut shell as a sustainable anode material for high performance microbial fuel cells. Bioresour Technol 249:567–573. https://doi.org/10.1016/j.biortech.2017.09.086

107. Lu M, Qian Y, Yang C, Huang X, Li H, Xie X, Huang L, Huang W (2017) Nitrogen-enriched pseudographitic anode derived from silk cocoon with tunable flexibility for microbial fuel cells. Nano Energy 32:382–388. https://doi.org/10.1016/j.nanoen.2016.12.046

108. Zou L, Lu Z, Huang Y, Z-e L, Qiao Y (2017) Nanoporous Mo_2C functionalized 3D carbon architecture anode for boosting flavins mediated interfacial bioelectrocatalysis in microbial fuel cells. J Power Sources 359:549–555. https://doi.org/10.1016/j.jpowsour.2017.05.101

109. Liu M, Zhou M, Ma L, Yang H, Zhao Y (2016) Architectural design of hierarchically meso-macroporous carbon for microbial fuel cell anodes. RSC Adv 6(33):27993–27998. https://doi.org/10.1039/c5ra26420k

110. Qiao Y, Bao S-J, Li CM, Cui X-Q, Lu Z-S, Guo J (2008) Nanostructured polyaniline/titanium dioxide composite anode for microbial fuel cells. ACS Nano 2(1):113–119. https://doi.org/10.1021/nn700102s

111. Qiao Y, Li CM, Bao S-J, Bao Q-L (2007) Carbon nanotube/polyaniline composite as anode material for microbial fuel cells. J Power Sources 170(1):79–84. https://doi.org/10.1016/j.jpowsour.2007.03.048

112. Feng C, Ma L, Li F, Mai H, Lang X, Fan S (2010) A polypyrrole/anthraquinone-2,6-disulphonic disodium salt (PPy/AQDS)-modified anode to improve performance of microbial fuel cells. Biosens Bioelectron 25(6):1516–1520. https://doi.org/10.1016/j.bios.2009.10.009

113. Wang Y, Li B, Zeng L, Cui D, Xiang X, Li W (2013) Polyaniline/mesoporous tungsten trioxide composite as anode electrocatalyst for high-performance microbial fuel cells. Biosens Bioelectron 41:582–588. https://doi.org/10.1016/j.bios.2012.09.054

114. Wang Y, C-e Z, Sun D, Zhang J-R, Zhu J-J (2013) A graphene/poly(3,4-ethylenedioxythiophene) hybrid as an anode for high-performance microbial fuel cells. ChemPlusChem 78(8):823–829. https://doi.org/10.1002/cplu.201300102

115. Wang W, You S, Gong X, Qi D, Chandran BK, Bi L, Cui F, Chen X (2016) Bioinspired nanosucker array for enhancing bioelectricity generation in microbial fuel cells. Adv Mater 28(2):270–275. https://doi.org/10.1002/adma.201503609

116. Ding C, Liu H, Zhu Y, Wan M, Jiang L (2012) Control of bacterial extracellular electron transfer by a solid-state mediator of polyaniline nanowire arrays. Energy Environ Sci 5(9):8517–8522. https://doi.org/10.1039/c2ee22269h

117. Ding C, Liu H, Lv M, Zhao T, Zhu Y, Jiang L (2014) Hybrid bio-organic interfaces with matchable nanoscale topography for durable high extracellular electron transfer activity. Nanoscale 6(14):7866–7871. https://doi.org/10.1039/c4nr01338g

118. Wen Z, Ci S, Mao S, Cui S, Lu G, Yu K, Luo S, He Z, Chen J (2013) TiO2 nanoparticles-decorated carbon nanotubes for significantly improved bioelectricity generation in microbial fuel cells. J Power Sources 234:100–106. https://doi.org/10.1016/j.jpowsour.2013.01.146

119. Zou L, Qiao Y, Wu X-S, Ma C-X, Li X, Li CM (2015) Synergistic effect of titanium dioxide nanocrystal/reduced graphene oxide hybrid on enhancement of microbial electrocatalysis. J Power Sources 276:208–214. https://doi.org/10.1016/j.jpowsour.2014.11.127

120. Yin T, Lin Z, Su L, Yuan C, Fu D (2015) Preparation of vertically oriented TiO_2 nanosheets modified carbon paper electrode and its enhancement to the performance of MFCs. ACS Appl Mater Inter 7(1):400–408. https://doi.org/10.1021/am506360x

121. C-e Z, Wang W-J, Sun D, Wang X, Zhang J-R, Zhu J-J (2014) Nanostructured graphene/TiO_2 hybrids as high-performance anodes for microbial fuel cells. Chem Eur J 20(23):7091–7097. https://doi.org/10.1002/chem.201400272

122. Peng X, Yu H, Wang X, Zhou Q, Zhang S, Geng L, Sun J, Cai Z (2012) Enhanced performance and capacitance behavior of anode by rolling Fe_3O_4 into activated carbon in microbial fuel cells. Bioresour Technol 121:450–453. https://doi.org/10.1016/j.biortech.2012.06.021

123. Lv Z, Xie D, Yue X, Feng C, Wei C (2012) Ruthenium oxide-coated carbon felt electrode: a highly active anode for microbial fuel cell applications. J Power Sources 210:26–31. https://doi.org/10.1016/j.jpowsour.2012.02.109

124. Wu X, Shi Z, Zou L, Li CM, Qiao Y (2018) Pectin assisted one-pot synthesis of three dimensional porous NiO/graphene composite for enhanced bioelectrocatalysis in microbial fuel cells. J Power Sources 378:119–124. https://doi.org/10.1016/j.jpowsour.2017.12.023

125. Zhang C, Liang P, Yang X, Jiang Y, Bian Y, Chen C, Zhang X, Huang X (2016) Binder-free graphene and manganese oxide coated carbon felt anode for high-performance microbial fuel cell. Biosens Bioelectron 81:32–38. https://doi.org/10.1016/j.bios.2016.02.051

126. Mehdinia A, Ziaei E, Jabbari A (2014) Multi-walled carbon nanotube/SnO_2 nanocomposite: a novel anode material for microbial fuel cells. Electrochim Acta 130:512–518. https://doi.org/10.1016/j.electacta.2014.03.011

127. Sun M, Zhang F, Tong Z-H, Sheng G-P, Chen Y-Z, Zhao Y, Chen Y-P, Zhou S-Y, Liu G, Tian Y-C, Yu H-Q (2010) A gold-sputtered carbon paper as an anode for improved electricity generation from a microbial fuel cell inoculated with Shewanella oneidensis MR-1. Biosens Bioelectron 26(2):338–343. https://doi.org/10.1016/j.bios.2010.08.010

128. Qiao Y, Wu X-S, Li CM (2014) Interfacial electron transfer of Shewanella putrefaciens enhanced by nanoflaky nickel oxide array in microbial fuel cells. J Power Sources 266:226–231. https://doi.org/10.1016/j.jpowsour.2014.05.015

Chapter 3
Electrode-Respiring Microbiomes Associated with the Enhanced Bioelectrodegradation Function

Bin Liang, Mengyuan Qi, Hui Yun, Youkang Zhao, Yang Bai, Deyong Kong, and Ai-Jie Wang

3.1 Introduction

Bioelectrochemical systems (BESs), using electrochemically active microorganisms to catalyze oxidative or reductive reactions in the anode or cathode, respectively, have attracted growing attention in recent decades [1–4]. Microbial electrode-respiration process has been proved to significantly enhance the microbial oxidation (with anode serving as electron acceptor) or microbial reduction (with cathode serving as electron donor) of various hazardous organic contaminants [5–13]. Currently, the major foci of BESs studies have been on the engineering of electrode materials [14, 15] and reactor constructure design [6, 16–20] as well as striving for optimization and integration of microbial electrode-respiration processes [21–27].

B. Liang · H. Yun
Key Laboratory of Environmental Biotechnology, Research Center for Eco-Environmental Sciences, Chinese Academy of Sciences, Beijing, China

M. Qi · Y. Zhao · Y. Bai
State Key Laboratory of Urban Water Resource and Environment, Harbin Institute of Technology, Harbin, China

D. Kong
Key Laboratory of Environmental Biotechnology, Research Center for Eco-Environmental Sciences, Chinese Academy of Sciences, Beijing, China

Shenyang Academy of Environmental Sciences, Shenyang, China

A.-J. Wang (✉)
Key Laboratory of Environmental Biotechnology, Research Center for Eco-Environmental Sciences, Chinese Academy of Sciences, Beijing, China

State Key Laboratory of Urban Water Resource and Environment, School of Environment, Harbin Institute of Technology, Harbin, China
e-mail: waj0578@hit.edu.cn; ajwang@rcees.ac.cn
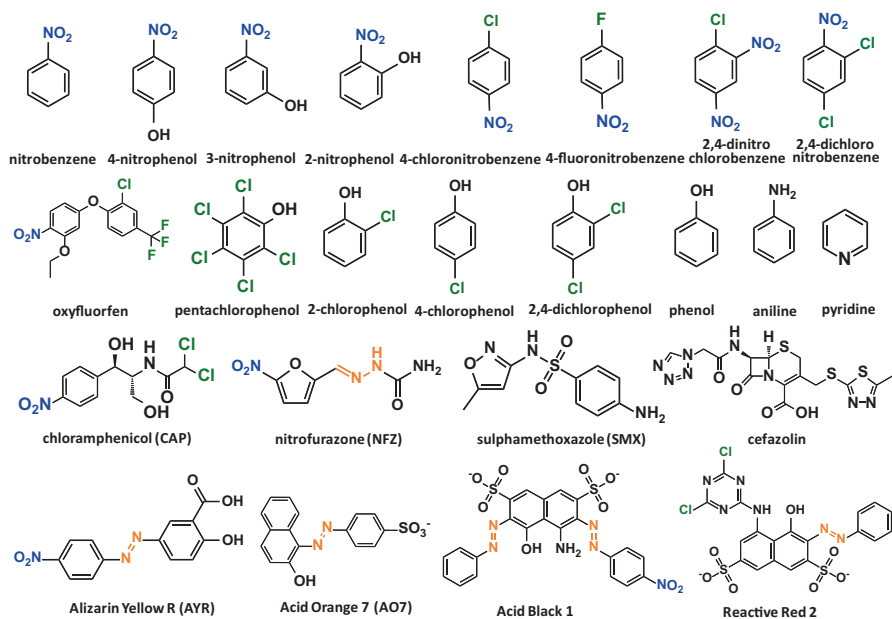
Fig. 3.1 Chemical structures of various hazardous organic compounds discussed in this chapter

Microbial ecology is devoted to understanding the dynamics, structure, activity, and interaction of microorganisms in natural and engineering ecosystems [28]. Undoubtedly, disclosing the microbial ecology and physiology of the involved electrode-associated multispecies biofilms is essential for the maintenance and enhancement of the catalytic function of BESs. However, the comprehensive information of the complex electrode-respiring microbiomes associated with microbial electrode-respiration bioelectrodegradation function remains largely untapped and poorly understood.

In this chapter, we summarize the advances of the electrode-respiring biofilm microbiomes involving in the catalysis of various hazardous organic contaminants, such as microbial reduction of nitroaromatics (nitrobenzene and nitrophenols), azo dyes (Alizarin Yellow R, acid orange 7, and acid black 1), halogenated organics (2-chlorophenol, tetrachloroethylene, trichloroethylene, 2,4-dinitrochlorobenzene, *p*-chloronitrobenzene, *p*-fluoronitrobenzene, and 2,4-dichloronitrobenzene), and antibiotics (chloramphenicol and nitrofurazone) at the cathode side and microbial oxidation of N-heterocyclic compounds, aromatic amines, (chlor)phenols, and antibiotics (e.g., aniline, phenol, pyridine, pentachlorophenol, 4-chlorophenol, 2,4-dichlorophenol, oxyfluorfen, sulfamethoxazole, cefazolin, and chloramphenicol) at the anode side. The chemical structures of the organic compounds discussed in this chapter are illustrated in Fig. 3.1. We also highlight the challenges and outlook for the electrode-respiring biofim microbomes research. From the perspective of microbial ecology, understanding the comprehensive information of the

electrode-respiring microbiomes, including biofilm structure, composition, dynamics, activity, diversity, potential functional microbes, and interaction, is potentially necessary for regulating and scaling-up the microbial electrode-respiration-based engineering systems as well as the management of bioremediation applications.

3.2   Microbial Ecology of Functional Bioanode Microbiomes

Recently, numerous researches have focused on microbial fuel cells (MFCs), since MFCs have performed well on the sustainable energy production and wastewater treatment [1, 2]. Especially, the bioelectrodegradation of bioanode MFCs has been proved to have the ability to remove many organic contaminants that present in wastewater. In this part, the bioelectrodegradation efficiency, pathway, and functional microbes involved in the bioanode microbiomes would be discussed.

3.2.1   (Chloro/Nitro) Phenols

Phenol and its derivatives (2,4-dichlorophenol, 2,4-DCP; 4-chlorophenol, 4-CP; pentachlorophenol, PCP; and *p*-nitrophenol, PNP) are considered as refractory hazardous pollutants in wastewater. Due to the discharge of waste effluents of many industrial processes, phenolics have become one of the most frequently detected contaminants in the aqueous environment [29]. As reported, one of its derivatives PCP could be bioelectrotransformed into tetrachlorohydroquinone (TeCHQ), 2,3,4,5-tetrachlorophenol (TeCP), trichlorophenol, dichlorophenol, and phenol with co-substrates (acetate or glucose) in MFCs [30]. Besides, *Bacillus subtilis* is able to dehalogenate 2,4-DCP to 4-CP with approximately 60% degradation efficiency [31]. In another research, 4-CP was degraded via the formation of phenol, which was further mineralized with a bioanode dominated by uncultured *Desulfobulbus* [32]. Based on the 16S rRNA gene clone library and qPCR analysis, *Geobacter* sp. was dominant on the anode biofilm upon feeding phenol as carbon source and electron donor [33]. A previous study proved that *Geobacter metallireducens* ATCC 53774 could metabolize phenol with Fe(III) as electron acceptor [34]. Another pure strain isolated from bioanode was identified as *Bacillus cereus*. It can degrade 500 mg/L phenol with 86.44% degradation efficiency within 41 h [35]. As for the nitro-substituted derivative PNP, *Pseudomonas monteilii* LZU-3 is able to utilize PNP as the sole carbon and energy source accompanied with power production at an aerobic MFC condition [36]. *Cupriavidus basilensis*-formed bioanode also can generate current (310 mA m^{-2}) in a MFC using phenol (1.06 mM) as a carbon source at a microaerobic condition (the dissolved oxygen concentration at the beginning of the experiment was 8.4 mg L^{-1}) [37].

Under different inoculation conditions, the performance of MFCs varied. With industrial microbial consortium (IMC) as inoculum, the power production was

higher than that of with domestic microbial consortium (DMC), but the 2,4-DCP reduction rate was much lower. 16S rRNA gene-based analysis showed that the DMC was dominated by bacteria classified as *Arcobacter*, *Aeromonas*, *Pseudomonas*, *Acinetobacter*, *Cloacibacterium*, and *Shewanella*, which were found to be vital for 2,4-DCP degradation and electron transfer, while IMC was enriched mainly with *Bacillus* sp. (83.6%), which contributed to the higher electricity production. 4-Chlorophenol, phenol, 3,5-dichlorocatechol, and benzoic acid were identified as intermediate products during the bioelectrodegradation of 2,4-DCP [38]. The 2,4-DCP degradation in MFC was also related to the catholyte. A recent study showed that with potassium persulfate as catholyte, the MFC established with *Bacillus subtilis* exhibited the highest current generation (64 mA/m^2) and 2,4-DCP degradation efficiency compared to NaCl and water, since potassium persulfate had high capability of solving diffusional and electrochemical restriction by *Bacillus subtilis* [29]. Zhao et al. showed that approximately 81% of 50 mg/L PNP was degraded within 24 h by a bioanode, which was dominated by *Corynebacterium* (32.75%), *Comamonas* (31.29%), *Bacteroides* (7.48%), *Chryseobacterium* (6.05%), *Petrimonas* (4.38%), and *Rhodococcus* (3.40%) based on the 16S rRNA gene sequencing analysis. Interestingly, this biofilm is also able to degrade chloramphenicol, benzofluorfen, fluoxastrobin, and flubendiamide [39].

3.2.2   Antibiotics and Pesticides

Antibiotics are among the most commonly used and the most successful group of pharmaceuticals applied in humans and animals [40]. Also, pesticides are widely used all over the world, leading to the frequent detection in surface water and underground water. Faced with this fact, challenge has been called out that methods are urgently needed to solve the problem. Recently, some researches have paid attention to the microbial electrode-respiration-based biodegradation process. Sulfamethoxazole (SMX) is a cheap, effective, and broad-spectrum antibiotic that is largely consumed in the breeding industry [12]. It was observed that SMX is quite hard to remove when it was initially added into the MFCs. But after 10-month acclimation, the bioanode performance for degrading SMX was rapidly increased and reached a steady state. Approximately 85% of 20 mg/L SMX disappeared in MFCs bioanode within 12 h and undetectable after 48 h [12]. The similar situation was observed in an experiment dealing with oxyfluorfen. After 10-month acclimation with oxyfluorfen, the anode biofilm is able to effectively degrade oxyfluorfen (50 mg/L) with 77% removal efficiency within 24 h and nearly completely degraded within 96 h [41]. With applied voltage, the acclimation period could be reduced. A research reported that with an applied voltage of 0.8 V, the bioanode degradation rates for SMX and tetracycline (TC) could reach 93.5% and 95.6%, respectively [40]. Another research has found that after a long lag period (>300 h), more than 70% of cefazolin sodium (CFZ) was removed with CFZ loading below 100 mg/L [42]. Even with co-substrate, it still took a long period to obtain a mature biofilm for

biodegradation. When supplied with acetate in a MFC bioanode for the chloramphenicol (CAP) cometabolic degradation, a mature bioanode with 6-month acclimation could remove approximately 84% of 50 mg/L CAP within 12 h [13].

For these emerging contaminants, most of the biodegradation mechanisms with bioanode communities are related to the nitro-group (if containing) reduction or acetylation. Some of the products were further transformed by the bioanode. As the biodegradation of CAP, the nitro-group of CAP was reduced to form aromatic amine ($AMCl_2$). And the 3-hydroxy group of CAP occurred acetylation with formation of acetylated-CAP which finally transferred to $AMCl_2$. Then $AMCl_2$ was further degraded via *meta*-cleavage [13]. Oxyfluorfen was also firstly transformed into a nitro-group reduction product and subsequently acetylated to *N*-[4-(2-chloro-4-trifluoromethyl-phenoxy)-2-ethoxy-6-hydroxy-phenyl]-acetamide that underwent a further degradation [41]. The mechanism for SMX degradation was different. At first, the S-N bond was broken with formation of 4-amino benzene sulfinic acid and 3-amino-5-methylisoxazole (3A5MI). Then the 4-amino benzene sulfinic acid could be further transformed into benzene sulfinic acid or 4-aminobenzenethiol. The other part 3A5MI could be highly utilized by anodophilic microbes in the form of isopropanol which was from the N–O and the C–C double bonds broken. With further transformation, even CH_4 could form [12]. The SMX-degrading bioanode mainly consists of *Methanobacterium*, *Methanosaeta*, *Treponema*, *Achromobacter* (a SMX degrader), and an unnamed genus (belonging to the Porphyromonadaceae family). Methanogens *Methanobacterium* and *Methanosaeta* may contribute to the mineralization of some degradation products of SMX [43]. The composition of bioanode community for CAP degradation included exoelectrogenic *Azonexus* (19.94%), exoelectrogenic *Comamonas* (19.41%), *Nitrososphaera* (12.15%), *Azoarcus* (3.10%), *Rhodococcus* (1.91%), and *Chryseobacterium* (8.86%). Importantly, *Comamonas* is an electroactive aromatic amines degrader. *Azoarcus* and *Rhodococcus* could work on various aromatics degradation via a ring cleavage pathway under anaerobic conditions [13]. The predominant bacteria in the oxyfluorfen-degrading bioanode community were *Arcobacter* (40.31%), *Acinetobacter* (30.56%), *Azospirillum* (20.39%), *Spirochaeta* (1.67%), *Azonexus* (1.65%), and *Comamonas* (1.46%). Among them, the functional degraders were inferred to be *Acinetobacter*, *Azospirillum*, and *Comamonas* [41]. The CFZ-degrading bioanode community was enriched of electroactive/biodegradative bacteria (*Geobacter*, 18.71%; *Acinetobacter*, 15.82%; *Stenotrophomonas*, 2.85%; *Lysinibacillus*, 3.22%) and fermentative bacteria (*Dysgonomonas*, 5.36%; *Proteiniphilum*, 5.28%) [42].

The fate of antibiotic resistance genes (ARGs) during the bioreactor treatment process is of great importance for the evaluation of an antibiotic-degrading approach. To gain the response of ARGs of a SMX-TC treatment reactor, the relative abundances of three *sul* and five *tet* genes were investigated. These target genes (*sulI*, *sulII*, *sulIII*, *tetA*, *tetC*, *tetO*, *tetQ*, and *tetW*) in the biocathode were present at a higher concentration than in the bioanode of the reactors, implying bioanode was more suitable for the inhibition of ARGs' spread. A clearly increased trend in the relative abundances of all target ARGs was observed during the treatment processes [40].

3.2.3   N-Heterocyclic and Aromatic Amine Compounds

Nitroaromatics, halogenated nitroaromatics, and some azo dyes could be efficiently transformed to corresponding aromatic amines with electrode biofilm microbiomes. The generated aromatic amines need to be further degraded. Cheng et al. found that the introduction of limited dissolved oxygen (1 mg/L) can significantly stimulate the microbial electrode-respiration process for aromatic amine aniline mineralization and electricity generation simultaneously in a bioanode community. The anode biofilm community was predominated by several aerobic aniline degraders (*Comamonas*, 12.95%; *Variovorax*, 4.56%; *Stenotrophomonas*, 2.15%; and *Diaphorobacter*, 2.20%) and anode-respiration bacteria (*Comamonas*, 12.95%; *Aquamicrobium*, 7.85%; *Geothrix*, 4.51%; *Geobacter*, 3.59%; and *Ochrobactrum*, 0.99%), which likely cooperated with each other and finally featured the energy recovery from aniline mainly through electron shuttle mechanism [5]. In another study, N-heterocyclic pyridine mineralization was also benefitted from the micro-aerobic environment in a bioanode community, which was enriched with several potential pyridine degraders (*Desulfovibrio*, 4.50%; *Dokdonella*, 15.43%; *Hydrogenophaga*, 9.45%; and *Paracoccus*, 11.36%) [44].

3.3   Establishment of Functional Biocathode Microbiomes

3.3.1   Cathode Biofilm Establishment Methods

Biocathode microbiomes play important roles in various biotransformation processes. Though cathode biofilms are self-renewable and potentially cost-effective to some extent, they are hard to establish, particularly under anaerobic conditions. Two main methods for the establishment of cathode biofilm were discussed as the following. The first method is a traditional time-consuming procedure that uses the pre-enriched functional consortium working as inoculum for biocathode microbiomes establishment. Based on previous studies, the enrichment of consortium for targeted organic contaminants transformation (e.g., nitrobenzene, chloramphenicol, and nitrofurazone) needs 3–4 weeks, and then the establishment of biocathode with the functional consortium costs another 2–3 weeks. The whole process totals at least 5–7 weeks [7–11]. Some studies generally employ the anaerobic sludge from the long-running-targeted contaminants-treatment bioreactors working as biocathode establishment inoculum [23, 25, 45]. It is worth mentioning that some electrochemically active bacteria (EAB) are probably eliminated during such non-electrode selection and acclimation stage, for which inevitable co-substrate would potentially enrich more fermentative bacteria [3]. However, many variables could potentially affect the startup time of different functional biocathode microbiomes, including targeted contaminant category, electrode material, applied potential, electrolyte component, co-substrate type, reactor configuration, and so on.

The second method is a novel procedure that establishes functional biocathode microbiomes by direct polarity inversion after the bioanode microbiomes establishment. Several electron acceptors such as CO_2, proton, O_2, and nitrate had been utilized for methane and hydrogen production, oxygen reduction, as well as denitrification by these bidirectional microbial communities [46–49]. Based on the anode biofilm acclimation and polarity inversion, some EAB can be effectively selected. These EAB, such as *Geobacter*, could use the electrode as electrons donor for the reduction of various contaminants [50]. Yun et al. demonstrated that the electroactive microbes of antibiotic chloramphenicol-acclimated bioanode could perform the bidirectional electron transfer for chloramphenicol reduction [51]. Yun et al. also proved that the enhanced biocathodic reduction of toxic aromatic pollutants (nitroaromatic nitrobenzene and azo dye acid orange 7) is feasible with a directly inverted bioanode. The cytochrome *c* of EAB *Geobacter* involved in the backward electrons transfers from electrode to nitrobenzene [3]. Importantly, the biocathode establishment time (about 12 days) was obviously decreased under this protocol, and the developed biocathode microbiome likely worked on various reducible contaminants by diverse reductases and electrons transfer-related proteins of EAB. Generally, many kinds of organic or inorganic pollutants coexist in practical wastewaters, such as nitro- and halo-aromatics, dyes, or heavy metals in the oxidation state accompanied with nitrate, perchlorate, or sulfate [3]. Very recently, Yun et al. found that a biocathode with efficient multi-pollutant removal capabilities (nitrate, nitrobenzene, and acid orange 7) could be enriched based on a polarity inverted bioanode established with domestic wastewater. Other pollutants, such as perchlorate, sulfate, heavy metals, and halogenated organics, may also work as potential electron acceptors based on the biocathode community analysis (Fig. 3.2) [52]. These studies offer new insights into the rapid establishment and modularization of non-specific functional biocathode microbiomes and the improvement of the biocathode community multifunctionality by polarity inversion for the potential treatment of complicated electron acceptors-coexisting wastewaters [3, 51, 52].

3.3.2   Microbial Ecology of Functional Biocathode Microbiomes

3.3.2.1   Antibiotic Chloramphenicol (CAP) and Nitrofurazone (NFZ)

Antibiotic chloramphenicol (CAP) is a frequently detected environmental pollutant [53]. It can be efficiently transformed to aromatic amine product $AMCl_2$ firstly and then dechlorinated to partially dechlorinated product AMCl by the biocathode communities [9, 10, 51, 54]. AMCl could be completely dechlorinated to dechlorinated product AM with an abiotic cathode under a lower potential condition (such as −1.25 V vs standard hydrogen electrode, SHE) [53]. PCR-DGGE-based bacterial community analysis indicated that the dominant bacteria on a CAP-reducing biocathode community belonged to α, β, and γ-*Proteobacteria* (e.g., *Enterobacter*,
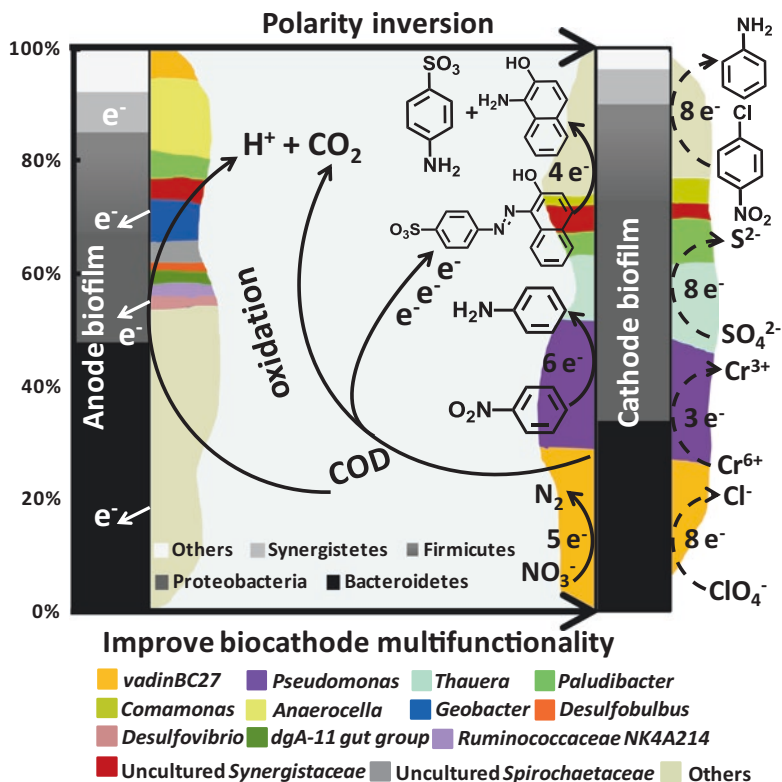
Fig. 3.2 A concept model for improving biocathode microbiome multifunctionality by polarity inversion for simultaneous bioelectroreduction processes in domestic wastewater. (Reprinted from Ref. [52], Copyright 2018, with permission from Elsevier)

Stenotrophomonas, *Pseudomonas*, *Devosia*, *Ochrobactrum*, *Dechloromonas*) [9]. 16S rRNA gene-based Illumina MiSeq sequencing found that functional bacteria, including *Geobacter* (67.6%), *Desulfovibrio* (3.49%), and *Pseudomonas* (2.29%), are obviously enriched in a biocathode community that is established by the polarity inversion of a CAP-acclimated bioanode community (Table 3.1). These three genera are responsible for the bidirectional electron transfer and nitroaromatics reduction [51]. Recently, we found that low-temperature acclimation with electrical stimulation could enhance the biocathode functioning stability for CAP detoxification. The cold-adapted functional bacteria such as *Aeromonas* (33.2%), *Vagococcus* (22.25%), and *Citrobacter* (3.13%) were dominated in the low-temperature 10 °C-performed biocathode. In the 25 °C-performed biocathodes, the nitroaromatic reducers *Raoultella* (62.1%) and *Enterococcus* (9.00%) were obviously enriched (Table 3.1). Further analysis with a functional genes microarray (GeoChip v4.6) showed that the function stability of 10 °C-performed biocathode was maintained mainly through selectively enriching cold-adapted functional species, coexisting metabolically

Table 3.1 The summary of dominant genera from cathode-respiring microbiomes involved in the bioelectrotransformation of various organic pollutants. Each line of dominant genus and class is the corresponding relationship

Dominant genus	Class	Cathode potential (V vs SHE)	Electron acceptor	Reduction products	References
Anaeromyxobacter dehalogenans 2CP-1	*γ-Proteobacteria*	−0.30	2-Chlorophenol	Phenol	[72]
Shewanella oneidensis MR-1	*γ-Proteobacteria*	−0.41	Acid orange 7 (AO7)	Sulfanilic acid (SA)	[80]
Geobacter lovleyi SZ	*δ-Proteobacteria*	−0.30	Tetrachloroethylene	*cis*-dichloroethylene	[101]
Pseudomonas sp. WYZ–2	*γ-Proteobacteria*	−0.55	Acid black 1	Aromatic amines	[73]
Enterococcus (75.8%)	*Bacilli*	Switching −0.80 to −0.40	Nitrobenzene	Aniline (AN)	[11]
Enterococcus (38.4% for glucose fed)	*Bacilli*	−0.54	Nitrobenzene	AN	[8]
Psychrobacter (18.1% for glucose fed)	*γ-Proteobacteria*				
Enterobacter (7.6% for glucose fed)	*γ-Proteobacteria*				
Paracoccus (30.9% for bicarbonate fed)	*α-Proteobacteria*				
Variovorax (10.6% for bicarbonate fed)	*β-Proteobacteria*				
Raoultella (11.1% for glucose fed)	*γ-Proteobacteria*				
Enterococcus (54.62%)	*Bacilli*	−0.40	Nitrobenzene	AN	[60]
Desulfovibrio (7.72%)	*δ-Proteobacteria*				
Klebsiella (6.73%)	*γ-Proteobacteria*				

(continued)

Table 3.1 (continued)

Dominant genus	Class	Cathode potential (V vs SHE)	Electron acceptor	Reduction products	References
Geobacter (67.6%)	δ-*Proteobacteria*	−0.40	Chloramphenicol	Aromatic amine (AMCl2) and dechlorinated AMCl2 (AMCl)	[51]
Desulfovibrio (3.49%)	δ-*Proteobacteria*				
Pseudomonas (2.29%)	γ-*Proteobacteria*				
Geobacter (6.1%)	δ-*Proteobacteria*	Switching −0.45 to −0.40	Nitrobenzene, AO7	AN, SA	[3]
Acinetobacter (1.88%)	γ-*Proteobacteria*				
Desulfovibrio (2.79%)	δ-*Proteobacteria*				
Pseudomonas (23.42%)	γ-*Proteobacteria*	−0.40	Nitrobenzene, AO7, and nitrate	AN, SA, and N$_2$	[52]
Thauera (11.38%)	β-*Proteobacteria*				
Comamonas (2.15%)	β-*Proteobacteria*				
Raoultella (62.1% for 25 °C)	γ-*Proteobacteria*	−0.70	Chloramphenicol	AMCl2 and AMCl	[10]
Aeromonas (33.2% for 10 °C)	γ-*Proteobacteria*				
Vagococcus (22.25% for 10 °C)	*Bacilli*				
Enterococcus (9.00% for 25 °C)	*Bacilli*				
Citrobacter (3.13% for 10 °C)	γ-*Proteobacteria*				
Klebsiella (62.5%)	γ-*Proteobacteria*	−0.45	Nitrofurazone (NFZ)	Mainly accumulation of [(5-amino-2-furyl)-Methylene]-hydrazinecarboxamide (AMN) and (5-nitro-2-furyl) methenamine (NFF) at both with and without glucose modes	[7]
Enterococcus (2.76%)	*Bacilli*				
Citrobacter (12.16%)	γ-*Proteobacteria*				
Desulfovibrio (1.64%)	δ-*Proteobacteria*				
Pseudomonas (1.20%)	γ-*Proteobacteria*				
Actinobaculum (1.96%)	*Actinomycetales*				

Genus (%)	Class	Compound	Value	Notes	Ref
Klebsiella (57.0%)	γ-Proteobacteria	Nitrofurazone	−0.65	Mainly accumulation of NFF and AMN without glucose supply	[7]
Enterococcus (8.19%)	Bacilli				
Citrobacter (9.40%)	γ-Proteobacteria				
Desulfovibrio (1.89%)	δ-Proteobacteria				
Actinobaculum (1.02%)	Actinomycetales				
Enterococcus (56.3%)	Bacilli	Nitrofurazone	−0.86	Mainly production of linear chain products: 5-hydroxycadaverine and 5-amino-pentanamide at both with and without glucose modes	[7]
Actinobaculum (20.49%)	Actinomycetales				
Klebsiella (6.36%)	γ-Proteobacteria				
Desulfovibrio (2.04%)	δ-Proteobacteria				
Pseudomonas (3.44%)	γ-Proteobacteria				
Dehalobacter (2.63% for 190 days and 1.14% for 240 days)	Clostridia	2,4-Dinitrochlorobenzene	−1.30	m-Phenylenediamine	[25]
Desulfovibrio (1.28% for 190 days and 1.38% for 240 days)	δ-Proteobacteria				
Geobacter (0.23% for 190 days and 0.61% for 240 days)	δ-Proteobacteria				
Desulfovibrio (2.01%)	δ-Proteobacteria	o-Nitrophenol (ONP)	−0.50	o-Aminophenol	[45]
Geobacter (1.98%)	δ-Proteobacteria				
Desulfovibrio (1.47%)	δ-Proteobacteria	m-Nitrophenol (MNP)	−0.50	m-Aminophenol	[45]
Geobacter (7.76%)	δ-Proteobacteria				
Pseudomonas (2.56%)	γ-Proteobacteria	p-Nitrophenol (PNP)	−0.50	p-Aminophenol	[45]
Desulfovibrio (1.29%)	δ-Proteobacteria				
Geobacter (2.53%)	δ-Proteobacteria				
Ochrobactrum (1.33%)	α-Proteobacteria				

(continued)

Table 3.1 (continued)

Dominant genus	Class	Cathode potential (V vs SHE)	Electron acceptor	Reduction products	References
Desulfovibrio (1.30%)	δ-*Proteobacteria*	−0.64	*p*-Chloronitrobenzene	AN and it was further transformed into benzoic acid via reductive deamination	[64]
Halanaerobium (7.20%)	*Clostridia*				
Desulfobacterales (4.56%)	δ-*Proteobacteria*				
Citrobacter (29.24%)	γ-*Proteobacteria*	−0.70	Alizarin Yellow R	*p*-Phenylenediamine and 5-aminosalicylic acid	[75]
Acinetobacter (17.79%)	γ-*Proteobacteria*				
Achromobacter (6.39%)	β-*Proteobacteria*				
Enterococcus (14.66%)	*Bacilli*				
Alkaliflexus (9.22%)	*Bacteroidia*				
Delftia (9.44%)	β-*Proteobacteria*				
Comamonas (2.47%)	β-*Proteobacteria*				
Pseudomonas (7.76%)	γ-*Proteobacteria*				
Aeromonas (3.04%)	γ-*Proteobacteria*				
Enterobacter (40.06%)	γ-*Proteobacteria*	−0.79	Alizarin Yellow R	*p*-Phenylenediamine and 5-aminosalicylic acid	[74]
Desulfovibrio (8.16%)	δ-*Proteobacteria*				
Enterococcus (5.93%)	*Bacilli*				
Lactococcus (4.96%)	*Bacilli*				
Klebsiella (3.98%)	γ-*Proteobacteria*				
Enterococcus (6.71%)	*Bacilli*	−0.72	Alizarin Yellow R	*p*-Phenylenediamine and 5-aminosalicylic acid	[23]
Enterobacter (16.89%)	γ-*Proteobacteria*				
Desulfovibrio (6.26%)	δ-*Proteobacteria*				
Lactococcus (4.36%)	*Bacilli*				
Geobacter (1.02%)	δ-*Proteobacteria*				
Klebsiella (2.85%)	γ-*Proteobacteria*				

Genus	Class	Value	Compound	Description	Ref
Enterococcus (21.07%)	*Bacilli*	−0.83	Alizarin Yellow R	*p*-Phenylenediamine and 5-aminosalicylic acid	[23]
Enterobacter (5.79%)	*γ-Proteobacteria*				
Desulfovibrio (10.72%)	*δ-Proteobacteria*				
Lactococcus (2.29%)	*Bacilli*				
Geobacter (5.01%)	*δ-Proteobacteria*	−0.72	Alizarin Yellow R	*p*-Phenylenediamine and 5-aminosalicylic acid	[16]
Syntrophus (17.91%)	*δ-Proteobacteria*				
Desulfovibrio (0.96%)	*δ-Proteobacteria*				
Delftia (28.86%)	*β-Proteobacteria*	−0.75	*p*-nitrophenol	*p*-Aminophenol	[62]
Diaphorobacter (9.4%)	*β-Proteobacteria*				
Aquamicrobium (7.1%)	*α-Proteobacteria*				
Raoultella (5.78%)	*γ-Proteobacteria*				
Shinella (5.55%)	*α-Proteobacteria*				
Halobacterium (56.8%)	Halobacteria	−0.58	*p*-Fluoronitrobenzene	AN and it was further partially mineralized	[65]
Spirochaeta (6.9%)	Spirochaetales				
Clostridium (2.6%)	*Clostridia*				
Pseudomonas (1.2%)	*γ-Proteobacteria*				
Halanaerobium (7.2%)	*Clostridia*	Not given	*p*-Chloronitrobenzene	AN and it was further mineralized	[64]
Desulfobacterales (4.56%)	*δ-Proteobacteria*				
Desulfovibrio (1.3%)	*δ-Proteobacteria*				
Propionimicrobium(0.8%)	Unidentified Actinobacteria				
Dehalobacter (7.9%)	*Clostridia*	Not given	2,4-Dichloronitrobenzene	AN	[26]
Dehalococcoides (8.4%)	*Dehalococcoidia*				
Syntrophus (21.9%)	*δ-Proteobacteria*				
Clostridium (4.3%)	*Clostridia*				

similar nitroaromatic reducers and maintaining the relative abundance of key electrons transfer genes (cytochrome *c* and hydrogenase genes) [10].

It is necessary to assess the fate and abundance of ARGs during the biological treatment of antibiotic wastewater. However, the response of ARGs of antibiotic-degrading electrode microbiomes to the electrical stimulation under different operational modes remains poorly understood. Only a few studies have investigated the fate of ARGs such as CAP resistance and integrase-encoding genes during the bio-electrotransformation of CAP in biocathode communities. A recent study found that a higher CAP concentration (20 and 50 mg/L compared to 10 mg/L) and less negative cathode potential (−0.5 V vs SHE, with the lowest CAP reduction efficiency compared to that of the −1.25 and −1.0 V operational modes) enhanced the expression of CAP resistance genes (e.g., *floR* and *cmlA*) [55]. Over 50% *Proteobacteria* were enriched in the established biocathode communities. *Pseudomonas* and *Methylobacillus* (the sum of the relative abundances over 40%) dominated in −1.25 V and −1.0 V operational modes or high CAP concentration mode (50 mg/L) [55]. Another recent work showed that the relative abundances of potential hosts of ARGs were strongly affected by salinity, which further determined the alteration in ARGs' abundances under different salinities. The relative abundances of *cmlA*, *floR*, *intI1*, and *sul1* under low salinity group were significantly higher than those of the control and high salinity group, although the control (88.3%) and high 6% salinity group (49.5%) showed lower CAP reduction efficiency than that of the low 0.5% salinity group (92.5%) [56]. *Lysinibacillus* and *Pseudomonas* were dominant potential hosts collected at 0.5% salinity group. With the increase of salinity, these two genera were weeded out from the biocathode communities. Interestingly, the relative abundance of *tetC* significantly increased as salinity increased, with the maximal abundance at 6% salinity among all the tested ARGs. In addition, the spread of ARGs could be inhibited under moderate cathode potential (−1.0 V), 2% salinity and mesophilic condition (above 15 °C) due to the shift of ARGs' potential hosts, resulting in the lowest ARGs abundances except for *tetC* [56].

The ecological response of nitrofurans nitrofurazone (NFZ)-degrading biocathode communities to different cathode potentials (−0.45 ± 0.01, −0.65 ± 0.01, and −0.86 ± 0.05 V vs SHE, with applied cell voltages of 0.2, 0.5, and 0.8 V, respectively) was studied. The bioelectrotransformation efficiency and degree of NFZ were highly related to different cathode potentials. The 0.2 V- and 0.5 V-performed biocathode communities were similar (both enriched a Gram-negative electroactive nitroaromatic reducer *Klebsiella* >55%) but significantly differed from that of 0.8 V supply (enriched a Gram-positive electroactive nitroaromatic reducer *Enterococcus* by 56%) (Table 3.1) and open circuit modes (enriched a Gram-negative nitroaromatic reducer *Pseudomonas* by 82%) [7]. These mentioned studies provide valuable insights into the antibiotic-transforming biocathode microbiomes feature as well as the fate and mechanisms of antibiotic resistance in biocathode BES treating antibiotic-containing wastewater [9, 10, 51, 55, 56].

3.3.2.2 Nitroaromatics

Nitroaromatics and halogenated nitroaromatics are priority controlled organic pollutants in environments. Nitrobenzene (NB) can be efficiently reduced to aniline (AN) with the established biocathode communities [8, 11, 57]. Selective bioelectrotransformation of NB to AN was maintained (over 90%) after carbon source switchover (co-substrate glucose was replaced by $NaHCO_3$) although the rate obviously decreased. 16S rRNA gene-based clone library and Illumina MiSeq sequencing analysis of the cathode biofilms found that the biocathode communities are dominated by the nitroaromatic reducers such as *Enterococcus*, *Desulfovibrio*, *Klebsiella*, *Enterobacter*, *Raoultella*, *Pseudomonas*, and *Clostridium* [8, 11, 58–60] (Table 3.1). Based on the GeoChip analysis, how key functional genes of the NB-reducing biocathode communities responded to carbon source switchover was studied. An increase of cytochrome *c* gene intensity was observed in the cathode biofilms compared to that of inoculum, which likely caused by the stimulation of cathodic extracellular electron transfer (EET) due to the poised cathode potential. Moreover, relatively higher multiheme cytochrome *c* and carbon fixation genes in the $NaHCO_3$-fed biocathode likely met the requirement of the energy conservation and maintained the selective NB bioelectroreduction capability after carbon source switchover. Extracellular pilin (Msh and PilA), which are important for biofilm formation and potential conductivity, had a higher gene abundance in the glucose-fed biocathode, corresponding to the enhancement of electro-catalysis activity for NB reduction with glucose supply [8].

Nitrophenols (NPs) can be efficiently reduced to aminophenols with the established biocathode communities [45, 61, 62]. Different NPs (*o*-nitrophenol, ONP; *m*-nitrophenol, MNP; and *p*-nitrophenol, PNP) could affect the bioelectroreduction efficiency, and they presented in the following order: ONP > MNP > PNP. The type of NPs rather than the polarity of the electrode significantly affected the electrode biofilm community structure and composition. Electroactive nitroaromatic reducers *Desulfovibrio* (1.29–2.01%) and *Geobacter* (1.98–7.76%) were dominant genera in the cathodic biofilms [45]. *Geobacter* and *Desulfovibrio* were also identified from the organic pollutants (NB, CAP, and azo dye) reducing biocathode communities that are established by the polarity inversion of the traditional bioanode communities [3, 51], suggesting these important electroactive genera generally come from anode biofilms by man-made polarity inversion regulation or microbial self-drift (due to no membrane between the anode and cathode chambers) [63]. Interestingly, another study showed that a PNP-reducing biocathode community is dominated by different electroactive genera (e.g., *Delftia*, *Diaphorobacter*, and *Aquamicrobium*) [62] (Table 3.1).

3.3.2.3 Halogenated Nitroaromatics and Phenols

Halogenated nitroaromatics including *p*-chloronitrobenzene (CNB), *p*-fluoronitrobenzene (FNB), 2,4-dinitrochlorobenzene (DNCB), and 2,4-dichloronitrobenzene (DCNB) can be efficiently reduced to aromatic amines with the acclimated biocathode communities [25–27, 64–67]. Liu et al. found that direct electron transfer from electrode to EAB was responsible for the biocathodic dechlorination of pentachlorophenol (PCP) [68]. Electroactive genera including *Clostridium* (8.04%), *Stenotrophomonas* (2.34%), *Pseudomonas* (0.84%), and *Citrobacter* (0.57%) [69–71] and fermentative genera such as *Dysgonomonas* (15.42%) and *Proteiniphilum* (11.64%) dominated in the PCP-dechlorinating biocathode community [68]. In the upflow anaerobic sludge blanket (UASB) with built-in BES reactors, microbial communities derived from the cathode districts could perform the nitro-group reduction and dehalogenation reactions. The synergistic mechanism was responsible for the enhanced bioelectrotransformation of CNB/DNCB/DCNB to aniline/*m*-phenylenediamine/aniline in the biocathode districts by the cooperation between fermentative-related species (e.g., *Acetobacterium*, *Kosmotoga*, *Petrimonas*, *Syntrophus*, *Clostridium*, *Longilinea*, and *Sarcina*) and electroactive nitroaromatic reducers/dehalogenators (*Desulfovibrio*, *Pseudomonas*, *Dehalobacter*, *Dehalococcoides*, *Anaeromyxobacter*, and *Geobacter*) [25–27, 66]. Feng et al. found that electrical stimulation could significantly improve microbial salinity resistance and FNB degradation in BES. The corresponding halotolerant FNB-degrading biocathode community was selectively enriched by *Halobacterium*, *Spirochaeta*, *Clostridium*, and *Pseudomonas* [65]. Peng et al. proposed that CNB was first converted into aniline in a biocathode community through nitro-group reduction and dechlorination reactions by functional δ-*Proteobacteria*, *Clostridia*, and unidentified *Actinobacteria* (e.g., *Desulfovibrio*, *Propionimicrobium*, *Halanaerobium*, and low abundance *Geobacter*), and then aniline was further transformed into phthalic acid derivative by *Desulfobacterales* [64]. At the cathode potential of −0.30 V vs SHE, *Anaeromyxobacter dehalogenans* 2CP-1-formed biocathode was capable of dechlorinating 2-chlorophenol to phenol with an electrode as the sole electron donor [72] (Table 3.1).

3.3.2.4 Azo Dyes

Azo dyes (e.g., Alizarin Yellow R, acid orange 7, acid black 1, and Congo red) can be efficiently decolorized with the acclimated biocathode communities [23, 73–76]. Sun et al. found that co-substrate types could significantly affect the cathodic decolorizing performances of Alizarin Yellow R (AYR) and the corresponding biocathode community structure and composition. The glucose-fed biocathode showed higher AYR decolorization and *p*-phenylenediamine generation rates than those of the acetate-fed biocathode. The glucose-fed group was enriched by *Citrobacter* (29.24%), *Enterococcus* (14.66%), *Alkaliflexus* (9.22%), and *Aeromonas* (3.04%), while *Acinetobacter* (17.8%), *Achromobacter* (6.40%), *Stenotrophomonas* (2.74%), and

Comamonas (2.47%) were dominant in the acetate-fed biocathode. Some electroactive or azo dye-decolorizing genera, like *Pseudomonas*, *Delftia*, and *Dechloromonas*, were commonly enriched [75]. Most of the dominant genera own azo dye decolorization or electrochemical activity [75, 77, 78]. Cui et al. reported the effects of electrode position on AYR decolorization in an upflow hybrid anaerobic digestion reactor with built-in BES. *Enterobacter*, *Desulfovibrio*, and *Enterococcus*, which are capable of bidirectional EET and azo dye decolorization, were found to be the dominant genera in both anode and cathode biofilms [23, 74]. Concretely, the bioanode and the biocathode microbiomes enriched 40.05% and 29.86% of these three functional genera, respectively, in the mode that the anode and cathode installed in liquid phase, while the corresponding proportion were 26.65% and 37.58% in the mode that the anode and cathode installed in sludge phase [23]. Interestingly, neither the polarity nor the position of the electrodes obviously altered the electrode microbiomes structure in the mode of two anodes and two cathodes in an upflow BES. *Enterobacter* obviously enriched in the electrode communities (30.61–40.06%). *Desulfovibrio* occupied >5% of relative abundance in the electrode communities. *Enterococcus* dominated in both anodes (5.93% for down and 5.19% for up) and decreased in cathodes (2.55% and 2.88% for down and up, respectively). Some electroactive or azo dye-decolorizing genera, like *Klebsiella*, *Citrobacter*, and *Lactococcus*, were commonly identified with the relative abundance >1%. It is likely that these mentioned genera with bidirectional EET capability enriched in the anode biofilms first and then migrated to the cathodes due to the electrodes immersing in the same chamber [74]. In a hybrid anaerobic reactor built-in with sleeve-type bioelectrocatalyzed modules, fermentative *Syntrophus* (17.91%), electroactive nitroaromatic/azo dye-reducing *Geobacter* (5.01%), and *Desulfovibrio* (0.96%) dominated in the AYR-decolorizing biocathode community (Table 3.1). The corresponding bioanode community also enriched these three functional genera (*Geobacter* for 7.60%, *Desulfovibrio* for 3.25%, and *Syntrophus* for 11.91%) [16]. In microbial fuel cell-coupled constructed wetlands (CW-MFC), the azo dye reactive red 2 was efficiently decolorized. Electroactive *Geobacter* (azo dye reducer), *Desulfobulbus*, and *Desulfuromonas* enriched in the bioanode community (14.25%, 1.10%, and 5.31%, respectively). The 20-cm-plant and 27.5-cm CW-MFC cathode biofilms shared the most similar microflora but different from the anode and 20-cm CW-MFC cathode biofilms. *Geobacter*, *Hyphomicrobium*, and *Lactococcus* enriched by 8.69%, 1.31%, and 3.58%, respectively, in the 27.5-cm CW-MFC cathode biofilm (an anoxic zone), while they were 2.03%, 0.32%, and 0.21% in the 20-cm CW-MFC cathode biofilm (an aerobic environment). Facultative bacteria *Aeromonas* and *Flavobacterium* were identified in the 20-cm-plant cathode biofilm, which likely attributed to the release of oxygen by the plant roots [79]. For pure cultures, *Shewanella oneidensis* MR-1 (the cathode potential of −0.41 V vs SHE) and *Pseudomonas* sp. WYZ-2 (the cathode potential of −0.55 V vs SHE) could form an azo dye-decolorizing biocathode with an electrode as the electron donor [73, 80].

A phylogenetic tree for some representative dominant genera based on the identified OTUs from functional biocathode communities was shown in Fig. 3.3. Collectively, the nitroaromatics, halogenated nitroaromatics, azo dyes, and antibiot-
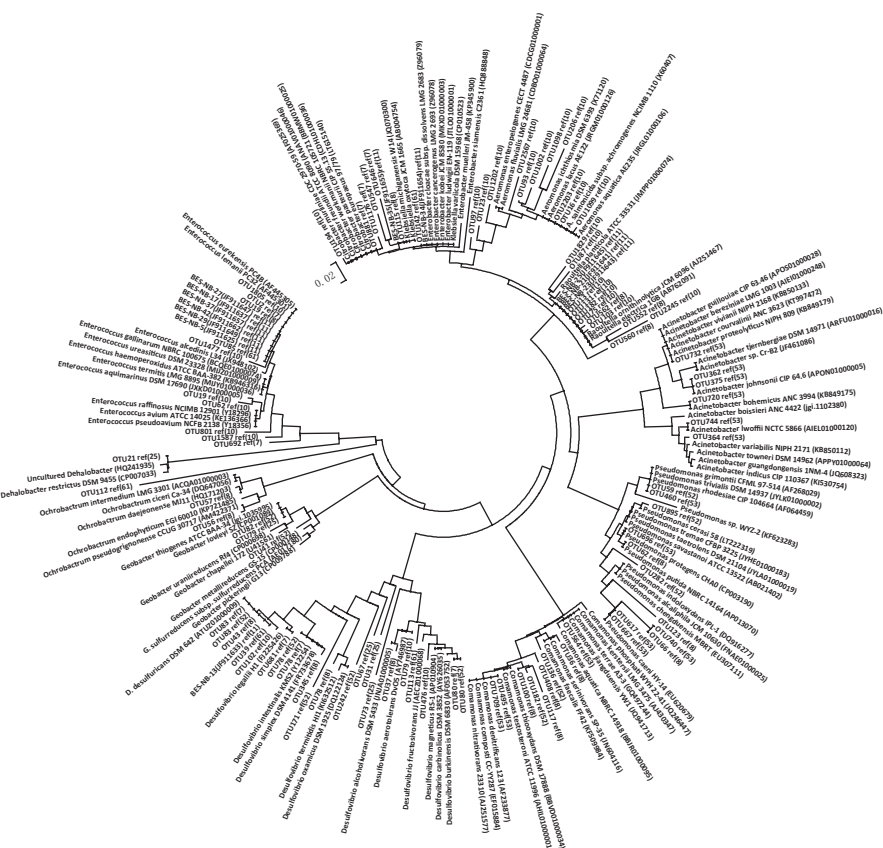
Fig. 3.3 Phylogenetic tree constructed using the neighbor-joining method based on the identified OTUs belonging to representative dominant genera from functional biocathode communities and homologous type strains from different hosts

ics reducers in the biocathode communities mainly belonged to α-, β-, γ-, and δ-*Proteobacteria* (e.g., *Geobacter*, *Citrobacter*, *Pseudomonas*, *Enterobacter*, *Raoultella*, *Desulfovibrio*, *Klebsiella*, and *Comamonas*), *Clostridia* (e.g., *Dehalobacter* and *Clostridium*), and *Bacilli* (e.g., *Enterococcus* and *Lactococcus*). Most of them have the electrochemical activity. In addition, the functional biocathode communities also enriched a number of fermentative-related bacteria (*Acetobacterium*, *Kosmotoga*, *Petrimonas*, *Syntrophus*, *Cloacibacillus*, *Paludibacter*, *Dysgonomonas*, etc.) [3, 16, 25, 52]. The synergistic interaction among these functional bacteria provides an important guarantee for the enhanced bioelectrotransformation of nitro-, halo-, and azo-aromatic pollutants.

3.4   Challenges and Outlook for Electrode Biofilm Microbiomes

As summarized above, most of the electrode-respiring biofilm microbiomes studies related to organic contaminants biodegradation were confined to the phylogenetic level. However, taxonomic information alone may be not enough to reflect the functional aspects of microbial microbiomes (e.g., electrode and plankton microbiomes), as not all members of certain taxon carry similar functional genes, making it difficult to accurately predict the electrode-respiring biofilm function [81]. Until now, only a few biocathode microbiomes were analyzed by the high-throughput 16S rRNA gene-based sequencing combining with GeoChip-based functional gene array technologies [8, 10]. Although phylogenetic and functional genes information can be derived from these representative studies, more analysis including the microbial community activity, metabolic network, key functional microbes interaction, and microbial community dynamics and succession are needed to confidently delineate the bioelectrodegradation process and mechanism within the complex electrode-respiring biofilm microbiomes.

It is well-known that in practical wastewater treatment systems, refractory organic pollutants often need to be treated by multiple reaction steps, such as hydrolysis, reduction, and oxidation, to achieve deep degradation and mineralization [82]. Therefore, understanding the synergistic degradation process and mechanism of functional microbiomes in the acclimated BESs is crucial to enhance the efficiency and function stability of wastewater treatment. The rapid development of microbial ecology undoubtedly provides various techniques targeting different phylogenetic and functional gene levels. Metagenomics, metatranscriptomics, and metaproteomics analysis that focus on the entire DNA, RNA, or expressed protein level, respectively, could reveal the presence of certain metabolic capacities and abundance information of functional microbial communities. The potential metabolic pathways in the microbial community can be identified and assigned to individual dominant species [28, 83, 84]. DNA-stable isotope probing (SIP) coupled with 16S rRNA and functional genes sequencing, genome-centric metagenomics, metatranscriptomics, and metaproteomics technologies could further clarify and identify which microorganisms actually involved in the organics biodegradation process [85–87]. More elaborately, in situ identification of the metabolic activity of functional biofilm communities at single cell level may be realized by using nanoscale secondary ion mass spectrometry fluorescence in situ hybridization (nanoSIMS-FISH) and nanometer-scale stable isotope probing (NanoSIP). NanoSIP might also identify metabolic interactions and nutrient fluxes within syntrophic associations [28, 88] in the complex electrode-respiring biofilms (e.g., biocathode and bioanode microbiomes for organics mineralization). In order to understand the potential metabolic function of the dominant genus in the electrode-respiring biofilm microbiomes, researchers also need to isolate and culture those dominant functional bacteria using high-throughput methods such as microfluidic streak plates (MSP) method and magnetic nanoparticle-mediated isolation (MMI) method [89, 90], and then try to establish pure culture, co-culture, or constructed model electrode biofilms in

BESs, which potentially provides valuable information to reveal the confusing electron transfer mechanism within complex electrode communities at the relatively simple condition [91, 92]. Although anodic electron transfer mechanisms of some typical electroactive bacterial are clear, the microbial uptake of electrons at the cathode (inward EET) tends to be different from the electron donation at the anode (outward EET) [93–99], and the electron transfer mechanism requires more pure culture studies. From the ecological, microbial single cell, and molecular perspectives, there is an urgent need to understand and reveal the molecular ecological network characteristics and synergistic biodegradation mechanism of functional groups (e.g., electroactive microbes, biodegradative microbes, and volatile acid-producing fermentative microbes) within the biofilm and plankton microbiomes in the future.

In addition, more biological replicates are needed to accurately reveal the complex interaction among the functional electrode-respiring microbiomes. However, many environmental engineering studies currently have no replicates or do not have enough replicates for microbial ecology analysis [100]. An important work has indicated that unpredictability in replicate reactors is a consequence of stochastic processes in microbiome assembly and that the experimental replicates could improve the chances of obtaining desirable microbial biofilm microbiomes for environmental engineering purposes [100]. Collectively, in combination with the comprehensive genetic information of microbiomes, (electro) chemical data, and physiological characteristics of core functional strains, the enhanced bioelectrodegradation mechanisms in the electrode-respiring microbiomes would be further understood. The knowledge about the presence, function, activity, interaction, and physiology of the core functional microorganisms in the electrode-respiring biofilm and plankton microbiomes is therefore necessary to guide the improvement and optimization of microbial electrode-respiration-based bioremediation systems.

References

1. Wang H, Ren ZJ (2013) A comprehensive review of microbial electrochemical systems as a platform technology. Biotechnol Adv 31(8):1796–1807. https://doi.org/10.1016/j.biotechadv.2013.10.001
2. Wang H, Luo H, Fallgren PH, Jin S, Ren ZJ (2015) Bioelectrochemical system platform for sustainable environmental remediation and energy generation. Biotechnol Adv 33(3):317–334. https://doi.org/10.1016/j.biotechadv.2015.04.003
3. Yun H, Liang B, Kong DY, Cheng HY, Li ZL, Gu YB, Yin HQ, Wang AJ (2017) Polarity inversion of bioanode for biocathodic reduction of aromatic pollutants. J Hazard Mater 331:280–288. https://doi.org/10.1016/j.jhazmat.2017.02.054
4. Daghio M, Aulenta F, Vaiopoulou E, Franzetti A, Arends JB, Sherry A, Suarez-Suarez A, Head IM, Bestetti G, Rabaey K (2017) Electrobioremediation of oil spills. Water Res 114:351–370. https://doi.org/10.1016/j.watres.2017.02.030

5. Cheng HY, Liang B, Mu Y, Cui MH, Li K, Wu WM, Wang AJ (2015) Stimulation of oxygen to bioanode for energy recovery from recalcitrant organic matter aniline in microbial fuel cells (MFCs). Water Res 81:72–83. https://doi.org/10.1016/j.watres.2015.05.012

6. Cui MH, Cui D, Gao L, Wang AJ, Cheng HY (2016) Azo dye decolorization in an up-flow bioelectrochemical reactor with domestic wastewater as a cost-effective yet highly efficient electron donor source. Water Res 105:520–526. https://doi.org/10.1016/j.watres.2016.09.027

7. Kong D, Yun H, Cui D, Qi M, Shao C, Cui D, Ren N, Liang B, Wang A (2017) Response of antimicrobial nitrofurazone-degrading biocathode communities to different cathode potentials. Bioresour Technol 241:951–958. https://doi.org/10.1016/j.biortech.2017.06.056

8. Liang B, Cheng H, Van Nostrand JD, Ma J, Yu H, Kong D, Liu W, Ren N, Wu L, Wang A, Lee DJ, Zhou J (2014) Microbial community structure and function of nitrobenzene reduction biocathode in response to carbon source switchover. Water Res 54:137–148. https://doi.org/10.1016/j.watres.2014.01.052

9. Liang B, Cheng HY, Kong DY, Gao SH, Sun F, Cui D, Kong FY, Zhou AJ, Liu WZ, Ren NQ, Wu WM, Wang AJ, Lee DJ (2013) Accelerated reduction of chlorinated nitroaromatic antibiotic chloramphenicol by biocathode. Environ Sci Technol 47(10):5353–5361. https://doi.org/10.1021/es400933h

10. Liang B, Kong D, Ma J, Wen C, Yuan T, Lee DJ, Zhou J, Wang A (2016) Low temperature acclimation with electrical stimulation enhance the biocathode functioning stability for antibiotics detoxification. Water Res 100:157–168. https://doi.org/10.1016/j.watres.2016.05.028

11. Wang AJ, Cheng HY, Liang B, Ren NQ, Cui D, Lin N, Kim BH, Rabaey K (2011) Efficient reduction of nitrobenzene to aniline with a biocatalyzed cathode. Environ Sci Technol 45(23):10186–10193. https://doi.org/10.1021/es202356w

12. Wang L, Liu Y, Ma J, Zhao F (2016) Rapid degradation of sulphamethoxazole and the further transformation of 3-amino-5-methylisoxazole in a microbial fuel cell. Water Res 88:322–328. https://doi.org/10.1016/j.watres.2015.10.030

13. Zhang Q, Zhang Y, Li D (2017) Cometabolic degradation of chloramphenicol via a meta-cleavage pathway in a microbial fuel cell and its microbial community. Bioresour Technol 229:104–110. https://doi.org/10.1016/j.biortech.2017.01.026

14. Guo K, Prevoteau A, Patil SA, Rabaey K (2015) Engineering electrodes for microbial electrocatalysis. Curr Opin Biotechnol 33:149–156. https://doi.org/10.1016/j.copbio.2015.02.014

15. Wang HC, Cheng HY, Cui D, Zhang B, Wang SS, Han JL, Su SG, Chen R, Wang AJ (2017) Corrugated stainless-steel mesh as a simple engineerable electrode module in bioelectrochemical system: hydrodynamics and the effects on decolorization performance. J Hazard Mater 338:287–295. https://doi.org/10.1016/j.jhazmat.2017.05.048

16. Cui D, Cui M-H, Lee H-S, Liang B, Wang H-C, Cai W-W, Cheng H-Y, Zhuang X-L, Wang A-J (2017) Comprehensive study on hybrid anaerobic reactor built-in with sleeve type bioelectrocatalyzed modules. Chem Eng J 330:1306–1315. https://doi.org/10.1016/j.cej.2017.07.167

17. Cui D, Guo YQ, Cheng HY, Liang B, Kong FY, Lee HS, Wang AJ (2012) Azo dye removal in a membrane-free up-flow biocatalyzed electrolysis reactor coupled with an aerobic biocontact oxidation reactor. J Hazard Mater 239–240:257–264. https://doi.org/10.1016/j.jhazmat.2012.08.072

18. Kong F, Wang A, Liang B, Liu W, Cheng H (2013) Improved azo dye decolorization in a modified sleeve-type bioelectrochemical system. Bioresour Technol 143:669–673. https://doi.org/10.1016/j.biortech.2013.06.050

19. Sun Q, Li Z, Wang Y, Cui D, Liang B, Thangavel S, Chung JS, Wang A (2015) A horizontal plug-flow baffled bioelectrocatalyzed reactor for the reductive decolorization of Alizarin Yellow R. Bioresour Technol 195:73–77. https://doi.org/10.1016/j.biortech.2015.06.086

20. Wang AJ, Cui D, Cheng HY, Guo YQ, Kong FY, Ren NQ, Wu WM (2012) A membrane-free, continuously feeding, single chamber up-flow biocatalyzed electrolysis reactor for nitrobenzene reduction. J Hazard Mater 199–200:401–409. https://doi.org/10.1016/j.jhazmat.2011.11.034

21. Cui D, Guo YQ, Lee HS, Wu WM, Liang B, Wang AJ, Cheng HY (2014) Enhanced decolorization of azo dye in a small pilot-scale anaerobic baffled reactor coupled with biocata-

lyzed electrolysis system (ABR-BES): a design suitable for scaling-up. Bioresour Technol 163:254–261. https://doi.org/10.1016/j.biortech.2014.03.165

22. Cui MH, Cui D, Gao L, Cheng HY, Wang AJ (2016) Efficient azo dye decolorization in a continuous stirred tank reactor (CSTR) with built-in bioelectrochemical system. Bioresour Technol 218:1307–1311. https://doi.org/10.1016/j.biortech.2016.07.135

23. Cui MH, Cui D, Lee HS, Liang B, Wang AJ, Cheng HY (2016) Effect of electrode position on azo dye removal in an up-flow hybrid anaerobic digestion reactor with built-in bioelectrochemical system. Sci Rep 6:25223. https://doi.org/10.1038/srep25223

24. Cui MH, Cui D, Gao L, Wang AJ, Cheng HY (2017) Evaluation of anaerobic sludge volume for improving azo dye decolorization in a hybrid anaerobic reactor with built-in bioelectrochemical system. Chemosphere 169:18–22. https://doi.org/10.1016/j.chemosphere.2016.11.034

25. Jiang X, Shen J, Han Y, Lou S, Han W, Sun X, Li J, Mu Y, Wang L (2016) Efficient nitro reduction and dechlorination of 2,4-dinitrochlorobenzene through the integration of bioelectrochemical system into upflow anaerobic sludge blanket: a comprehensive study. Water Res 88:257–265. https://doi.org/10.1016/j.watres.2015.10.023

26. Chen H, Gao X, Wang C, Shao J, Xu X, Zhu L (2017) Efficient 2,4-dichloronitrobenzene removal in the coupled BES-UASB reactor: effect of external voltage mode. Bioresour Technol 241:879–886. https://doi.org/10.1016/j.biortech.2017.06.010

27. Chen L, Shao J, Chen H, Wang C, Gao X, Xu X, Zhu L (2018) Cathode potential regulation in a coupled bioelectrode-anaerobic sludge system for effective dechlorination of 2,4-dichloronitrobenzene. Bioresour Technol 254:180–186. https://doi.org/10.1016/j.biortech.2018.01.092

28. Koch C, Korth B, Harnisch F (2018) Microbial ecology-based engineering of microbial electrochemical technologies. Microb Biotechnol 11(1):22–38. https://doi.org/10.1111/1751-7915.12802

29. Hassan H, Jin B, Dai S, Ma T, Saint C (2016) Chemical impact of catholytes on *Bacillus subtilis*-catalysed microbial fuel cell performance for degrading 2,4-dichlorophenol. Chem Eng J 301:103–114. https://doi.org/10.1016/j.cej.2016.04.077

30. Wang S, Huang L, Gan L, Quan X, Li N, Chen G, Lu L, Xing D, Yang F (2012) Combined effects of enrichment procedure and non-fermentable or fermentable co-substrate on performance and bacterial community for pentachlorophenol degradation in microbial fuel cells. Bioresour Technol 120:120–126. https://doi.org/10.1016/j.biortech.2012.06.022

31. Hassan H, Schulte-Illingheim L, Jin B, Dai S (2016) Degradation of 2,4-dichlorophenol by *Bacillus subtilis* with concurrent electricity generation in microbial fuel cell. Proc Eng 148:370–377. https://doi.org/10.1016/j.proeng.2016.06.473

32. Huang L, Sun Y, Liu Y, Wang N (2013) Mineralization of 4-chlorophenol and analysis of bacterial community in microbial fuel cells. Procedia Environ Sci 18:534–539. https://doi.org/10.1016/j.proenv.2013.04.072

33. Zhang D, Li Z, Zhang C, Zhou X, Xiao Z, Awata T, Katayama A (2017) Phenol-degrading anode biofilm with high coulombic efficiency in graphite electrodes microbial fuel cell. J Biosci Bioeng 123(3):364–369. https://doi.org/10.1016/j.jbiosc.2016.10.010

34. Zhang T, Tremblay P-L, Chaurasia AK, Smith JA, Bain TS, Lovley DR (2013) Anaerobic benzene oxidation via phenol in *Geobacter metallireducens*. Appl Environ Microbiol 79(24):7800–7806. https://doi.org/10.1128/aem.03134-13

35. Wei G, Xia D, Li-Li W, Hong Y (2018) Isolation, selection, and biological characterization research of highly effective electricigens from MFCs for phenol degradation. Folia Microbiol 63(1):73–83. https://doi.org/10.1007/s12223-017-0536-5

36. Chen Z, Niu Y, Zhao S, Khan A, Ling Z, Chen Y, Liu P, Li X (2016) A novel biosensor for *p*-nitrophenol based on an aerobic anode microbial fuel cell. Biosens Bioelectron 85:860–868. https://doi.org/10.1016/j.bios.2016.06.007

37. Friman H, Schechter A, Ioffe Y, Nitzan Y, Cahan R (2013) Current production in a microbial fuel cell using a pure culture of *Cupriavidus basilensis* growing in acetate or phenol as a carbon source. Microb Biotechnol 6(4):425–434. https://doi.org/10.1111/1751-7915.12026

38. Hassan H, Jin B, Donner E, Vasileiadis S, Saint C, Dai S (2018) Microbial community and bioelectrochemical activities in MFC for degrading phenol and producing electricity: microbial consortia could make differences. Chem Eng J 332:647–657. https://doi.org/10.1016/j.cej.2017.09.114

39. Zhao H, Kong C-H (2018) Enhanced removal of *p*-nitrophenol in a microbial fuel cell after long-term operation and the catabolic versatility of its microbial community. Chem Eng J. https://doi.org/10.1016/j.cej.2018.01.158

40. Zhang S, Song H-L, Yang X-L, Yang K-Y, Wang X-Y (2016) Effect of electrical stimulation on the fate of sulfamethoxazole and tetracycline with their corresponding resistance genes in three-dimensional biofilm-electrode reactors. Chemosphere 164:113–119. https://doi.org/10.1016/j.chemosphere.2016.08.076

41. Zhang Q, Zhang L, Wang H, Jiang Q, Zhu X (2017) Simultaneous efficient removal of oxyfluorfen with electricity generation in a microbial fuel cell and its microbial community analysis. Bioresour Technol 250:658–665. https://doi.org/10.1016/j.biortech.2017.11.091

42. Zhang E, Yu Q, Zhai W, Wang F, Scott K (2017) High tolerance of and removal of cefazolin sodium in single-chamber microbial fuel cells operation. Bioresour Technol 249:76–81. https://doi.org/10.1016/j.biortech.2017.10.005

43. Wang L, Wu Y, Zheng Y, Liu L, Zhao F (2015) Efficient degradation of sulfamethoxazole and the response of microbial communities in microbial fuel cells. RSC Adv 5(69):56430–56437. https://doi.org/10.1039/C5RA08438E

44. Jiang X, Shen J, Xu K, Chen D, Mu Y, Sun X, Han W, Li J, Wang L (2018) Substantial enhancement of anaerobic pyridine bio-mineralization by electrical stimulation. Water Res 130:291–299. https://doi.org/10.1016/j.watres.2017.12.005

45. Jiang X, Shen J, Lou S, Mu Y, Wang N, Han W, Sun X, Li J, Wang L (2016) Comprehensive comparison of bacterial communities in a membrane-free bioelectrochemical system for removing different mononitrophenols from wastewater. Bioresour Technol 216:645–652. https://doi.org/10.1016/j.biortech.2016.06.005

46. Rozendal RA, Jeremiasse AW, Hamelers HV, Buisman CJ (2008) Hydrogen production with a microbial biocathode. Environ Sci Technol 42(2):629–634

47. Cheng KY, Ho G, Cord-Ruwisch R (2010) Anodophilic biofilm catalyzes cathodic oxygen reduction. Environ Sci Technol 44(1):518–525. https://doi.org/10.1021/es9023833

48. Cheng KY, Ho G, Cord-Ruwisch R (2011) Novel methanogenic rotatable bioelectrochemical system operated with polarity inversion. Environ Sci Technol 45(2):796–802. https://doi.org/10.1021/es102482j

49. Pous N, Carmona-Martínez AA, Vilajeliu-Pons A, Fiset E, Bañeras L, Trably E, Balaguer MD, Colprim J, Bernet N, Puig S (2016) Bidirectional microbial electron transfer: switching an acetate oxidizing biofilm to nitrate reducing conditions. Biosens Bioelectron 75:352–358. https://doi.org/10.1016/j.bios.2015.08.035

50. Lovley DR (2011) Powering microbes with electricity: direct electron transfer from electrodes to microbes. Environ Microbiol Rep 3(1):27–35. https://doi.org/10.1111/j.1758-2229.2010.00211.x

51. Yun H, Kong D, Liang B, Cui M, Li Z, Wang A (2016) Response of anodic bacterial community to the polarity inversion for chloramphenicol reduction. Bioresour Technol 221:666–670. https://doi.org/10.1016/j.biortech.2016.09.047

52. Yun H, Liang B, Kong D, Wang A (2018) Improving biocathode community multifunctionality by polarity inversion for simultaneous bioelectroreduction processes in domestic wastewater. Chemosphere 194:553–561. https://doi.org/10.1016/j.chemosphere.2017.12.030

53. Kong D, Liang B, Yun H, Cheng H, Ma J, Cui M, Wang A, Ren N (2015) Cathodic degradation of antibiotics: characterization and pathway analysis. Water Res 72:281–292. https://doi.org/10.1016/j.watres.2015.01.025

54. Sun F, Liu H, Liang B, Song R, Yan Q, Wang A (2013) Reductive degradation of chloramphenicol using bioelectrochemical system (BES): a comparative study of abiotic cathode and biocathode. Bioresour Technol 143:699–702. https://doi.org/10.1016/j.biortech.2013.06.084

55. Guo N, Wang Y, Yan L, Wang X, Wang M, Xu H, Wang S (2017) Effect of bio-electrochemical system on the fate and proliferation of chloramphenicol resistance genes during the treatment of chloramphenicol wastewater. Water Res 117:95–101. https://doi.org/10.1016/j.watres.2017.03.058

56. Guo N, Wang Y, Tong T, Wang S (2018) The fate of antibiotic resistance genes and their potential hosts during bio-electrochemical treatment of high-salinity pharmaceutical wastewater. Water Res 133:79–86. https://doi.org/10.1016/j.watres.2018.01.020

57. Zhang J, Zhang Y, Quan X (2015) Bio-electrochemical enhancement of anaerobic reduction of nitrobenzene and its effects on microbial community. Biochem Eng J 94:85–91. https://doi.org/10.1016/j.bej.2014.11.018

58. Roldan MD, Perez-Reinado E, Castillo F, Moreno-Vivian C (2008) Reduction of polynitroaromatic compounds: the bacterial nitroreductases. FEMS Microbiol Rev 32(3):474–500. https://doi.org/10.1111/j.1574-6976.2008.00107.x

59. Marvin-Sikkema FD, de Bont JA (1994) Degradation of nitroaromatic compounds by microorganisms. Appl Microbiol Biotechnol 42(4):499–507

60. Qi M, Liang B, Chen R, Sun X, Li Z, Ma X, Zhao Y, Kong D, Wang J, Wang A (2018) Effects of surface charge, hydrophilicity and hydrophobicity on functional biocathode catalytic efficiency and community structure. Chemosphere 202:105–110. https://doi.org/10.1016/j.chemosphere.2018.03.065

61. Zhang L, Jiang X, Shen J, Xu K, Li J, Sun X, Han W, Wang L (2016) Enhanced bioelectrochemical reduction of p-nitrophenols in the cathode of self-driven microbial fuel cells. RSC Adv 6(35):29072–29079. https://doi.org/10.1039/C6RA04293G

62. Wang X, Xing D, Ren N (2016) p-nitrophenol degradation and microbial community structure in a biocathode bioelectrochemical system. RSC Adv 6(92):89821–89826. https://doi.org/10.1039/C6RA17446A

63. Wang YZ, Wang AJ, Liu WZ, Kong DY, Tan WB, Liu C (2013) Accelerated azo dye removal by biocathode formation in single-chamber biocatalyzed electrolysis systems. Bioresour Technol 146:740–743. https://doi.org/10.1016/j.biortech.2013.07.082

64. Peng X, Pan X, Wang X, Li D, Huang P, Qiu G, Shan K, Chu X (2017) Accelerated removal of high concentration p-chloronitrobenzene using bioelectrocatalysis process and its microbial communities analysis. Bioresour Technol 249:844–850. https://doi.org/10.1016/j.biortech.2017.10.068

65. Feng H, Zhang X, Guo K, Vaiopoulou E, Shen D, Long Y, Yin J, Wang M (2015) Electrical stimulation improves microbial salinity resistance and organofluorine removal in bioelectrochemical systems. Appl Environ Microbiol 81(11):3737–3744. https://doi.org/10.1128/AEM.04066-14

66. Xu X, Shao J, Li M, Gao K, Jin J, Zhu L (2016) Reductive transformation of p-chloronitrobenzene in the upflow anaerobic sludge blanket reactor coupled with microbial electrolysis cell: performance and microbial community. Bioresour Technol 218:1037–1045. https://doi.org/10.1016/j.biortech.2016.07.037

67. Feng H, Wang Y, Zhang X, Shen D, Li N, Chen W, Huang B, Liang Y, Zhou Y (2017) Degradation of p-fluoronitrobenzene in biological and bioelectrochemical systems: differences in kinetics, pathways, and microbial community evolutions. Chem Eng J 314:232–239. https://doi.org/10.1016/j.cej.2016.12.097

68. Liu D, Lei L, Yang B, Yu Q, Li Z (2013) Direct electron transfer from electrode to electrochemically active bacteria in a bioelectrochemical dechlorination system. Bioresour Technol 148:9–14. https://doi.org/10.1016/j.biortech.2013.08.108

69. Kumar R, Singh L, Wahid ZA, Din MFM (2015) Exoelectrogens in microbial fuel cells toward bioelectricity generation: a review. Int J Energy Res 39(8):1048–1067. https://doi.org/10.1002/er.3305

70. Galai S, Pérez de los Ríos A, Hernández-Fernández FJ, Kacem SH, Ramírez FM, Quesada-Medina J (2015) Microbial fuel cell application for azoic dye decolorization with simultane-

ous bioenergy production using *Stenotrophomonas* sp. Chem Eng Technol 38(9):1511–1518. https://doi.org/10.1002/ceat.201400608

71. Logan BE (2009) Exoelectrogenic bacteria that power microbial fuel cells. Nat Rev Microbiol 7:375. https://doi.org/10.1038/nrmicro2113

72. Strycharz SM, Gannon SM, Boles AR, Franks AE, Nevin KP, Lovley DR (2010) Reductive dechlorination of 2-chlorophenol by *Anaeromyxobacter dehalogenans* with an electrode serving as the electron donor. Environ Microbiol Rep 2(2):289–294. https://doi.org/10.1111/j.1758-2229.2009.00118.x

73. Wang YZ, Wang AJ, Zhou AJ, Liu WZ, Huang LP, Xu MY, Tao HC (2014) Electrode as sole electrons donor for enhancing decolorization of azo dye by an isolated *Pseudomonas* sp. WYZ-2. Bioresour Technol 152:530–533. https://doi.org/10.1016/j.biortech.2013.11.001

74. Cui M-H, Cui D, Gao L, Cheng H-Y, Wang A-J (2016) Analysis of electrode microbial communities in an up-flow bioelectrochemical system treating azo dye wastewater. Electrochim Acta 220:252–257. https://doi.org/10.1016/j.electacta.2016.10.121

75. Sun Q, Li ZL, Wang YZ, Yang CX, Chung JS, Wang AJ (2016) Cathodic bacterial community structure applying the different co-substrates for reductive decolorization of Alizarin Yellow R. Bioresour Technol 208:64–72. https://doi.org/10.1016/j.biortech.2016.02.003

76. Kong F, Wang A, Cheng H, Liang B (2014) Accelerated decolorization of azo dye Congo red in a combined bioanode-biocathode bioelectrochemical system with modified electrodes deployment. Bioresour Technol 151:332–339. https://doi.org/10.1016/j.biortech.2013.10.027

77. Mahmood S, Khalid A, Arshad M, Mahmood T, Crowley DE (2016) Detoxification of azo dyes by bacterial oxidoreductase enzymes. Crit Rev Biotechnol 36(4):639–651. https://doi.org/10.3109/07388551.2015.1004518

78. Liu G, Zhou J, Wang J, Zhang X, Dong B, Wang N (2015) Reductive decolorization of azo dye by bacteria. In: Singh SN (ed) Microbial degradation of synthetic dyes in wastewaters. Springer, Cham, pp 111–133. https://doi.org/10.1007/978-3-319-10942-8_5

79. Fang Z, Cao X, Li X, Wang H, Li X (2017) Electrode and azo dye decolorization performance in microbial-fuel-cell-coupled constructed wetlands with different electrode size during long-term wastewater treatment. Bioresour Technol 238:450–460. https://doi.org/10.1016/j.biortech.2017.04.075

80. Gao S-H, Peng L, Liu Y, Zhou X, Ni B-J, Bond PL, Liang B, Wang A-J (2016) Bioelectrochemical reduction of an azo dye by a *Shewanella oneidensis* MR-1 formed biocathode. Int Biodeter Biodegr 115:250–256. https://doi.org/10.1016/j.ibiod.2016.09.005

81. He Z, Zhang P, Wu L, Rocha AM, Tu Q, Shi Z, Wu B, Qin Y, Wang J, Yan Q, Curtis D, Ning D, Van Nostrand JD, Wu L, Yang Y, Elias DA, Watson DB, Adams MWW, Fields MW, Alm EJ, Hazen TC, Adams PD, Arkin AP, Zhou J (2018) Microbial functional gene diversity predicts groundwater contamination and ecosystem functioning. mBio 9 (1). doi:https://doi.org/10.1128/mBio.02435-17

82. Yun H, Liang B, Qiu J, Zhang L, Zhao Y, Jiang J, Wang A (2017) Functional characterization of a novel amidase involved in biotransformation of triclocarban and its dehalogenated congeners in *Ochrobactrum* sp. TCC-2. Environ Sci Technol 51(1):291–300. https://doi.org/10.1021/acs.est.6b04885

83. Ishii S, Suzuki S, Norden-Krichmar TM, Tenney A, Chain PS, Scholz MB, Nealson KH, Bretschger O (2013) A novel metatranscriptomic approach to identify gene expression dynamics during extracellular electron transfer. Nat Commun 4:1601. https://doi.org/10.1038/ncomms2615

84. Eddie BJ, Wang Z, WJt H, Leary DH, Malanoski AP, Tender LM, Lin B, Strycharz-Glaven SM (2017) Metatranscriptomics supports the mechanism for biocathode electroautotrophy by "Candidatus Tenderia electrophaga". mSystems 2(2):e00002–e00017. https://doi.org/10.1128/mSystems.00002-17

85. Coyotzi S, Pratscher J, Murrell JC, Neufeld JD (2016) Targeted metagenomics of active microbial populations with stable-isotope probing. Curr Opin Biotechnol 41:1–8. https://doi.org/10.1016/j.copbio.2016.02.017

86. Kowalczyk A, Eyice O, Schafer H, Price OR, Finnegan CJ, van Egmond RA, Shaw LJ, Barrett G, Bending GD (2015) Characterization of para-nitrophenol-degrading bacterial communities in river water by using functional markers and stable isotope probing. Appl Environ Microbiol 81(19):6890–6900. https://doi.org/10.1128/AEM.01794-15

87. Ziels RM, Sousa DZ, Stensel HD, Beck DAC (2018) DNA-SIP based genome-centric metagenomics identifies key long-chain fatty acid-degrading populations in anaerobic digesters with different feeding frequencies. ISME J 12(1):112–123. https://doi.org/10.1038/ismej.2017.143

88. Musat N, Musat F, Weber PK, Pett-Ridge J (2016) Tracking microbial interactions with NanoSIMS. Curr Opin Biotechnol 41:114–121. https://doi.org/10.1016/j.copbio.2016.06.007

89. Jiang CY, Dong L, Zhao JK, Hu X, Shen C, Qiao Y, Zhang X, Wang Y, Ismagilov RF, Liu SJ, Du W (2016) High-throughput single-cell cultivation on microfluidic streak plates. Appl Environ Microbiol 82(7):2210–2218. https://doi.org/10.1128/AEM.03588-15

90. Zhang D, Berry JP, Zhu D, Wang Y, Chen Y, Jiang B, Huang S, Langford H, Li G, Davison PA, Xu J, Aries E, Huang WE (2014) Magnetic nanoparticle-mediated isolation of functional bacteria in a complex microbial community. ISME J 9(3):603–614. https://doi.org/10.1038/ismej.2014.161

91. McAnulty MJ, Poosarla VG, Kim KY, Jasso-Chavez R, Logan BE, Wood TK (2017) Electricity from methane by reversing methanogenesis. Nat Commun 8:15419. https://doi.org/10.1038/ncomms15419

92. Liu Y, Ding M, Ling W, Yang Y, Zhou X, Li B-Z, Chen T, Nie Y, Wang M, Zeng B, Li X, Liu H, Sun B, Xu H, Zhang J, Jiao Y, Hou Y, Yang H, Xiao S, Lin Q, He X, Liao W, Jin Z, Xie Y, Zhang B, Li T, Lu X, Li J, Zhang F, Wu X-L, Song H, Yuan Y-J (2017) A three-species microbial consortium for power generation. Energy Environ Sci 10(7):1600–1609. https://doi.org/10.1039/C6EE03705D

93. Lovley DR (2012) Electromicrobiology. Annu Rev Microbiol 66:391–409. https://doi.org/10.1146/annurev-micro-092611-150104

94. Nealson KH, Rowe AR (2016) Electromicrobiology: realities, grand challenges, goals and predictions. Microb Biotechnol 9(5):595–600. https://doi.org/10.1111/1751-7915.12400

95. Yu L, Yuan Y, Rensing C, Zhou S (2018) Combined spectroelectrochemical and proteomic characterizations of bidirectional *Alcaligenes faecalis*-electrode electron transfer. Biosens Bioelectron 106:21–28. https://doi.org/10.1016/j.bios.2018.01.032

96. Strycharz SM, Glaven RH, Coppi MV, Gannon SM, Perpetua LA, Liu A, Nevin KP, Lovley DR (2011) Gene expression and deletion analysis of mechanisms for electron transfer from electrodes to *Geobacter sulfurreducens*. Bioelectrochemistry 80(2):142–150. https://doi.org/10.1016/j.bioelechem.2010.07.005

97. Sekar N, Wang J, Zhou Y, Fang Y, Yan Y, Ramasamy RP (2018) Role of respiratory terminal oxidases in the extracellular electron transfer ability of cyanobacteria. Biotechnol Bioeng. https://doi.org/10.1002/bit.26542

98. Kawaichi S, Yamada T, Umezawa A, McGlynn SE, Suzuki T, Dohmae N, Yoshida T, Sako Y, Matsushita N, Hashimoto K, Nakamura R (2018) Anodic and cathodic extracellular electron transfer by the filamentous bacterium *Ardenticatena maritima* 110S. Front Microbiol 9:68. https://doi.org/10.3389/fmicb.2018.00068

99. Bose A, Gardel EJ, Vidoudez C, Parra EA, Girguis PR (2014) Electron uptake by iron-oxidizing phototrophic bacteria. Nat Commun 5:3391. https://doi.org/10.1038/ncomms4391

100. Zhou J, Liu W, Deng Y, Jiang YH, Xue K, He Z, Van Nostrand JD, Wu L, Yang Y, Wang A (2013) Stochastic assembly leads to alternative communities with distinct functions in a bio-reactor microbial community. mBio 4(2). doi:https://doi.org/10.1128/mBio.00584-12

101. Strycharz SM, Woodard TL, Johnson JP, Nevin KP, Sanford RA, Loffler FE, Lovley DR (2008) Graphite electrode as a sole electron donor for reductive dechlorination of tetra-chlorethene by *Geobacter lovleyi*. Appl Environ Microbiol 74(19):5943–5947. https://doi.org/10.1128/AEM.00961-08

Chapter 4
Acceleration of Microbial Dehalorespiration with Electrical Stimulation

Fan Chen, Zhi-Ling Li, and Ai-Jie Wang

4.1 Introduction

Halogenated organic compounds (HOCs) constitute one of the most ubiquitous contaminants in the environment due to their widespread use and improper disposal [1]. HOCs are mainly comprised of chlorinated, brominated, and fluorinated organic pollutants. Some of the HOCs which have attracted great attention are listed in Table 4.1. For example, polychlorinated biphenyls (PCBs) are mainly used as electrical insulating, heat transfer, and lubricating fluids in industry, which exhibit both toxicity and carcinogenic/mutagenic properties [2, 3]. δ-Hexachlorocyclohexane (lindane), dichlorodiphenyl trichloroethane (DDT), and pentachlorophenol (PCP), extensively used as agricultural organochlorine pesticides, are ubiquitously found in aquifers, soils, and sediments [4–6]. Tetrachloroethylene (PCE), trichloroethylene (TCE), and 1,2-dichloroethane (1,2-DCA), widely used as industrial solvent and metal degreaser due to their excellent solvent properties, have been the most popular groundwater contaminants [7, 8]. Brominated flame retardants, such as polybrominated diphenyl ethers (PBDEs), tetrabromobisphenol A (TBBPA), and hexabromocyclododecane (HBCD), are extensively found in the environment and recognized to cause adverse effects to ecosystems and human health [3, 9, 10]. Perfluorinated compounds such as perfluorooctane sulfonate (PFOS) and perfluorooctanoic acid (PFOA) have been also extensively utilized as flame retardants, surfactants, and lubricants in many industrial and consumer products [3, 11].

F. Chen · Z.-L. Li (✉)
State Key Laboratory of Urban Water Resource and Environment,
Harbin Institute of Technology, Harbin, China

A.-J. Wang
Key Laboratory of Environmental Biotechnology, Research Center for Eco-Environmental Sciences, Chinese Academy of Sciences, Beijing, China
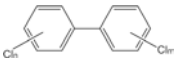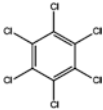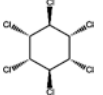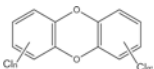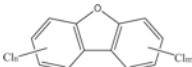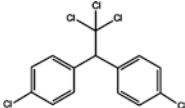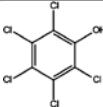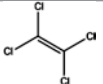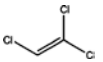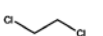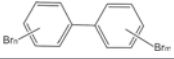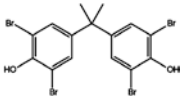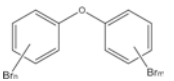
State Key Laboratory of Urban Water Resource and Environment, School of Environment, Harbin Institute of Technology, Harbin, China
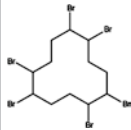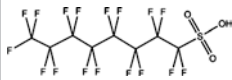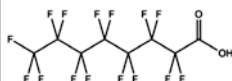
Table 4.1 Representative halogenated organic compounds of major concern worldwide

Compounds	Uses/origins	Chemical structures	References
Polychlorinated biphenyls (PCBs)	Electrical insulating, heat transfer, and lubricating fluids		[2]
Hexachlorobenzene (HCB)	Fungicide		[12]
γ-Hexachlorocyclohexane (lindane)	Insecticide		[4]
Polychlorinated dibenzodioxins (PCDDs)	Pyrolysis or incineration of chlorine-containing substances		[3]
Polychlorinated dibenzofurans (PCDFs)	Pyrolysis or incineration of chlorine-containing substances		[3]
Dichlorodiphenyltrichloroethane (DDT)	Insecticide		[5]
Pentachlorophenol (PCP)	Pesticides and disinfectants		[6]
Tetrachloroethylene (PCE)	Industrial solvent and metal degreaser		[7]
Trichloroethene (TCE)	Industrial solvent and metal degreaser		[7]
1,2-Dichloroethane (1,2-DCA)	Industrial solvent and metal degreaser		[8]
Polybrominated biphenyls (PBBs)	Flame retardants		[9]
Tetrabromobisphenol A (TBBPA)	Flame retardants		[13]
Polybrominated diphenyl ethers (PBDEs)	Flame retardants		[9]

(continued)

Table 4.1 (continued)

Compounds	Uses/origins	Chemical structures	References
Hexabromocyclododecane (HBCD)	Flame retardants		[13]
Perfluorooctane sulfonate (PFOS)	Flame retardants, surfactants, lubricants		[11]
Perfluorooctanoic acid (PFOA)	Flame retardants, surfactants, lubricants		[11]

Most of HOCs are liposoluble, bioaccumulative, and toxic to human beings and animals. For example, the toxic effects of chlorophenols are directly proportional to the degree of chlorination, and they accumulate mostly in the liver and kidney of experimental animals and to a lesser degree in the brain, muscle, and fat [14]. Acute poisoning by pentachlorophenol is characterized by general weakness, fatigue, ataxia, headache, anorexia, sweating, hyperpyrexia, nausea, vomiting, tachycardia, abdominal pain, terminal spasms, and death [15]. Because of their refractory characteristics and large application, they have created serious contamination to various environments including soil, aquifers, sediments, and groundwater through tank leakages, accidental spills, and illegal dumping [3]. The majority of them were defined as persistent organic pollutants (POPs). In total, 69 types of HOCs have been classified as priority pollutants by the United States Environmental Protection Agency, which accounted for 54.8% of the total compounds list [16].

Therefore, a number of HOCs remediation approaches, including biodegradation [17], absorption [18], thermal incineration [19], advanced oxidation processes [20], chemical reductive dechlorination (e.g., sulfidated nanoscale zerovalent iron reduction) [21, 22], and mechanochemical destruction [3], have been developed and implemented in the past decades. Among them, bioremediation via anaerobic reductive dehalogenation by organohalide-respiring bacteria (OHRB), which utilizes HOCs as terminal electron acceptors for metabolism, has been regarded as one of the most sustainable and viable alternatives during in situ remediation of anoxic/anaerobic contaminated sites (e.g., sediments, aquifers, groundwater, etc.) [23, 24]. The anaerobic reductive dehalogenation process would effectively reduce the HOCs toxicity and remove HOCs from the contaminated sites cost-effectively and environmentally friendly; however, it is frequently restricted by time-consuming metabolic rate, the narrow dechlorination range, and lack of effective in situ electron donors [25–30].

Bioelectrochemical systems (BES), which utilize electrochemically active microorganisms to catalyze the reductive reactions in cathode, have recognized as one
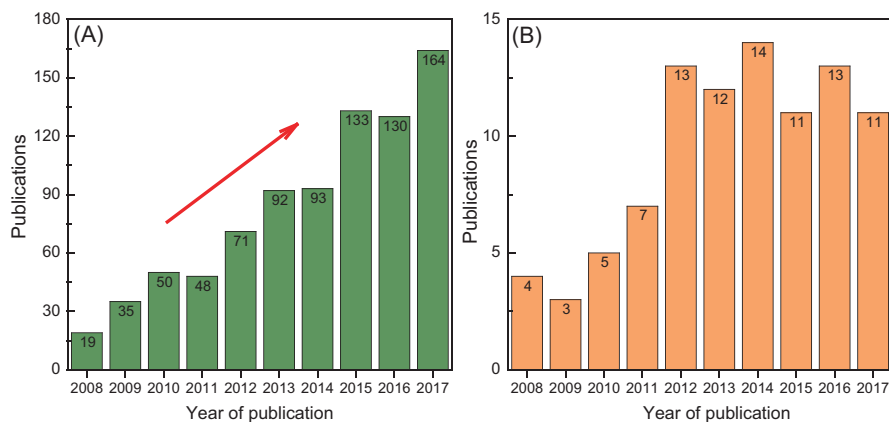
Fig. 4.1 Published papers related to biocathode (**a**) and biocathode reductive dehalogenation (**b**) in recent years

solid approach for the enhanced reduction of various refractory organic pollutants [31–33]. In previous studies, stimulated microbial reductive dechlorination of HOCs with electrode serving as available electron donor for the organohalide-respiring strains or enriched consortia continues to be a subject of intense investigation (Fig. 4.1). In this chapter, firstly, anaerobic reductive dehalogenation of HOCs via OHRB is briefly described. Secondly, the enhanced HOCs dehalogenation performance by biocathodes and types of organohalide-respiring biocathode-related microorganisms are overviewed. Thirdly, extracellular electron transfer (EET) mechanisms involved in the HOCs bio-dehalogenation at cathode are outlined. Finally, the challenges and outlook for bioelectrochemical stimulated microbial reductive dehalogenation of HOCs are highlighted from mechanism and application perspectives.

4.2   Anaerobic Reductive Dehalogenation of HOCs

Bioremediation of HOCs via anaerobic dehalogenation is considered relatively cheap and generally applicable [34–41]. Microbial reductive dehalogenation is the process by which anaerobic microorganisms utilize HOCs as the terminal electron acceptor of respiratory chain to respire and generate energy [42]. These organisms, known as OHRB, are found mostly in contaminated deep soils or sediments and are widely reported for the reduction and decomposition of HOCs such as chlorinated aliphatic hydrocarbons, chlorophenols, polychlorinated biphenyls [25, 42–45]. For example, He et al. [46] have reported the complete vinyl chloride (VC) detoxification by an anaerobic enrichment culture and identified the reductively dechlorinating population as a *Dehalococcoides* spp.

To date, several typical strains employed in HOCs dehalogenation were summarized in Table 4.2. Currently known OHRB mainly include *Geobacter*, *Dehalobacter*,

Table 4.2 HOCs dehalogenation by some typical OHRB

OHRB	HOCs	References
Dehalococcoides ethenogenes 195	Chlorinated ethenes (PCE, TCE), 1,2-dichloroethane, PBDEs, PCBs, 1,2,3,4-tetrachlorodibenzo-p-dioxin, 2,3,4,5,6-pentachlorobiphenyl, hexachlorobenzene, 1,2,3,4-tetrachloronaphthalene	[25, 62–65]
Dehalococcoides mccartyi CBDB1	Oligocyclic phenolic bromoaromatics, chlorinated aromatic compounds (chlorobenzenes, chlorinated dioxins, Aroclor 1260), chlorobenzene congeners, PCB, brominated aromatics	[37, 48, 66–69]
Dehalobium chlorocoercia DF-1	Aroclor 1260, hexachlorobenzene, PCB	[70, 71]
Acetobacterium sp. AG	Debrominates octa- /pentabrominated diphenyl ether	[72]
Dehalobacter species	TBBPA	[73]
Shewanella sp. XB	TBBPA	[74]
Pseudomonas sp. fz	TBBPA	[75]
A co-culture of *Dehalococcoides* and *Desulfovibrio* species	Tetra- /pentabrominated diphenyl ethers	[76]
A sediment-free culture containing *Dehalococcoides* and *Dehalobacter*	PCBs, PBDEs, 2,4,6-TCP, PCE, 1,2-DCA	[77]
Desulfitobacterium sp. PCE1	Tetrachloroethene/ortho-chlorinated phenols	[78]
Desulfitobacterium frappieri PCP-1	Chlorophenols	[79]
Desulfomonile tiedjei DCB-1	3-Chlorobenzoate	[47]
Desulfovibrio sp. TBP-1	2,4,6-Tribromophenol	[80]
Geobacter lovleyi SZ	Tetrachloroethene	[81]

Desulfovibrio, *Desulfitobacterium*, *Desulfomonile*, *Pseudomonas*, *Acetobacterium*, *Shewanella*, *Dehalococcoides*, and *Sulfurospirillum* and belong to three bacterial phyla (*Proteobacteria*, *Firmicutes*, and *Chloroflexi*). HOCs dehalogenation is catalyzed by reductive dehalogenases (RDase), and 3-chlorobenzoate RDase of *Desulfomonile tiedjei* strain DCB-1 was firstly biochemically characterized [47]. RDase-encoding genes have been identified in a variety of anaerobic bacteria (*Dehalococcoides* [48], *Dehalobacter* [49], *Desulfitobacterium* [50], and *Sulfurospirillum* [51]) and few aerobic bacteria [52, 53]. For example, the *cprA*-type and *crdA*-type RDases genes were identified in typical pentachlorophenol and chlorophenols-dechlorinating bacteria (e.g., *Desulfitobacterium hafniense* PCP and *Desulfitobacterium dehalogenans* JW/IU-DC1) [50, 54]. The *pceA* and *tceA* genes of *Dehalococcoides mccartyi* 195 encode RDases catalyzing PCE and TCE reductive dechlorination, respectively [55, 56]. In addition, the analysis of RDases crystal structure is benefit to resolve how RDases participate in HOCs dehalogenation and understand the organohalide-respiring mechanism [53, 57]. For example, X-ray

crystal structures of PceA reveal how a cobalamin supports a reductive halo elimination exploiting a conserved B_{12}-binding scaffold capped by a highly variable substrate-capturing region [57]. RDases associated with HOCs dehalogenation were also investigated in anaerobic reactors, which facilitates the understanding of microbial activity, genetic diversity, and contaminant transformation [58, 59]. It is worth mentioning that members of *Dehalococcoides* genus are considered to play key roles in bioremediation of the HOCs-contaminated sites and its consortia have been successfully used for bioaugmentation in practical application [60]. Therefore, the appearance of various OHRB and RDases in contaminated sites provides basic conditions for anaerobic dehalogenation of HOCs.

It has been found that dehalogenation is the first step for HOCs decomposition and transformation in anaerobic/anoxic environment [25, 43]. After dehalogenation, the toxicity of HOCs is greatly reduced and is easily degraded and transformed by other microorganisms. However, there are many limitations for HOCs anaerobic reduction by OHRB. Firstly, the complex chemical structure and toxicity of HOCs lead to the limited utilization by OHRB, with the much slower metabolic rates and longer decomposition periods [3]. At present, the dehalogenation processes of most OHRB are over 7 days and some even up to hundreds of days [24, 25]. Secondly, lack of exogenous electron donor leads to the low electron transfer efficiencies around the cell and the poor dehalogenation and detoxification capacities [24]. Most HOCs have a high octanol-water partition coefficient, strong lipophilicity and hydrophobicity, and low bioavailability, which limit the caption and further degradation by OHRB [1]. As the terminal electron donor of dehalogenation respiration process, available H_2 to be utilized by OHRB directly determines the dehalogenation efficiency. In most of reductive dechlorination systems, the traditional way of H_2 supply is completed by addition of short-chain fatty acids, and H_2 is generated by short-chain fatty acids fermentation and subsequent H_2 hydrolyzes [24]. However, this method is restrictive in operation, which may easily lead to problems such as uneven distribution of dosing chemicals or inducing the secondary contamination [24]. Meanwhile, some non-dehalogenation respiration microorganisms, such as hydrogen-utilizing methanogens, and denitrifying bacteria will also participate in organic substrate competition, further restricting the electron transfer efficiency of OHRB [61]. This leads to an increase in energy consumption, the incomplete dehalogenation capacity, and generation of toxic end products.

4.3   Enhanced HOCs Dehalogenation in Biocathode Systems

Compared with the soluble electron donors (organic acids, H_2, etc.), the direct electron transfer from electrodes to attached OHRB may be more efficient for stimulating the HOCs dehalogenation [82–84]. The approach of utilizing electrode as the potential electron donor for enhanced dehalogenation of HOCs with OHRB possesses the following advantages: (i) supplying the sustained electrons/redox environment and (ii) avoiding electron competition derived from addition of hydrogen-generated organic acids. Previously, several biocathode systems have

Table 4.3 Summary of HOCs dehalogenation by dehalorespiring biocathode systems

HOCs	Inoculation sources	Redox mediators	End products	Operation modes	Cathode potential vs SHE/current density	References
1,2-Dichloroethane (1,2-DCA)	Activated sludge	Anthraquinone-2,6-disulfonate (AQDS)	Ethene	Two-chamber batch-fed BESs	−300 mV	[85]
2,3,4,5-Tetrachlorobiphenyl (PCB 61)	River sediment	–	PCB 29 and PCB 23	Two-chamber batch-fed BESs	−450 mV	[86]
Pentachlorophenol (PCP)	Domestic wastewater	–	Phenol	Two-chamber batch-fed BESs	2.5 ± 0.03 W/m^3	[87]
Tetrachloroethene (PCE)	*Geobacter lovleyi* SZ	–	*cis*-Dichloroethene	Two-chamber batch-fed BESs	−300 mV	[88]
2-Chlorophenol	*Anaeromyxobacter dehalogenans* 2CP-1	–	Phenol	Two-chamber batch-fed BESs	−300 mV	[82]
Trichloroethene (TCE)	*Dehalococcoides* spp. enrichment culture	Methyl viologen	*cis*-DCE (14%), VC (81%), sum of ethene and ethane (5%)	Two-chamber batch-fed BESs	−500 mV	[89]
Trichloroethene (TCE)	*Desulfitobacterium* sp. enrichment culture	Methyl viologen	*cis*-DCE, VC, ethene and ethane	Two-chamber batch-fed BESs	−450 mV	[90]
Trichloroethene (TCE)	Enriched culture	–	*cis*-DCE, VC, ethene	Two-chamber batch-fed BESs	−550 mV	[91]
Trichloroethene (TCE)	Mixed dechlorinating culture	–	*cis*-DCE, VC, ethene	Two-chamber batch-fed BESs	−450 mV	[84]
Trichloroethene (TCE)	*Geobacter lovleyi* SZ	–	*cis*-DCE	Two-chamber batch-fed BESs	−450 mV	[84]

(continued)

Table 4.3 (continued)

HOCs	Inoculation sources	Redox mediators	End products	Operation modes	Cathode potential vs SHE/current density	References
Chloramphenicol (CAP)	Biofilms enriched from anode	–	Aromatic amine (AMCl$_2$) and dechlorinated AMCl$_2$ (AMCl)	Two-chamber batch-fed BESs	–400 mV	[92]
Chloramphenicol (CAP)	Municipal sludge and pre-enriched CAP-reducing consortium	–	AMCl$_2$ and AMCl	Two-chamber batch-fed BESs	–700 mV	[93]
2,4-Dichloronitrobenzene (DClNB)	Sludge	COD (500 g·m^{-3}·day^{-1})	Aniline	Microbial electrosynthesis-up flow anaerobic sludge reactor	–450/–660/–870 mV	[94]
4-Chloronitrobenzene (4-CNB)	Enriched 4-CNB degrading inoculums	Glucose (500 mg/L)	*para*-Chloroaniline (4-CAN) and aniline	Two-chamber/ batch-fed	–500 mV	[95]
Trichloroethene (TCE)	TCE-to-ethene dechlorinating culture	–	*cis*-DCE and VC	Continuous-flow reactor	–250 to –750 mV	[96]
Pentachlorophenol (PCP)	PCP dechlorination culture	–	–	Two-chamber batch-fed BESs	–100 to –600 mV	[97]
Pentachlorophenol (PCP)	PCP-to-phenol dechlorinating culture	Humin	Monochlorophenol (MCP) and phenol	Two-chamber batch-fed BESs	–500 mV	[98]

been constructed for HOCs dehalogenation by acclimating *Geobacter*, *Dehalococcoides*, or the highly enriched dehalorespiration cultures. The favorable dehalogenation activities have been observed in either batch-scale or the continuous-flow biocathode reactors (Table 4.3). These studies have demonstrated the potential of using electrode as an electron donor for OHRB respiration during reductive dehalogenation of HOCs.

4.3.1 Dehalorespiring Biocathodes Constructed by Organohalide-Respiring Strains

Evaluation OHRB metabolism by pure culture constructed biocathode system is helpful to understand the dehalogenation process and electron transfer mechanism. To date, the identified cathode respiring OHRB includes *Geobacter lovleyi* SZ and *Anaeromyxobacter dehalogenans* 2CP-1 for PCE and 2-chlorophenol dechlorination, respectively [82, 88]. Pure culture studies have primarily focused on *Geobacter* spp., which are often found as the predominant bacterial species attached to electrode and able to transfer electrons with electrode bidirectionally [99]. At the cathode potential of −300 mV vs SHE, *G. lovleyi* effectively dechlorinates PCE to *cis*-DCE with an electrode serving as a sole electron donor, and the maximum dechlorination rate of 25 µM/day was achieved, which was comparable to the condition when applying acetate as electron donor [81, 88]. Compared with biofilm on the anode, bacterial cells were less abundant on cathodes [88]. Genome sequencing of *G. lovleyi* SZ revealed the presence of a gene cluster related to organohalide respiration and genes encoding *c*-type cytochromes [100]. These functional genes are most probably to play important roles in HOCs dechlorination by respiring electrode.

Strain 2CP-1 was reported one typical 2-chlorophenol dechlorination and acetate-respiring dechlorinator [101]. When cathode was applied with a potential of −300 mV vs SHE, strain 2CP-1 could also reductively dechlorinate 2-chlorophenol to phenol with the maximum dechlorination rate of ca. 40 µM/day without the addition of acetate [82]. Strain 2CP-C genome has up to 68 putative *c*-type cytochrome genes [102], probably indicating *A. dehalogenans* species that contain the electrode-respiring ability at genetic level. The finding that dehalogenators other than *Geobacter* spp. utilizing electrode as sole electron donor for HOCs dehalogenation indicate the capacity for electrode-respiring dehalogenation could possibly work in a wide range and types of dehalogenators and HOCs.

4.3.2   Dehalorespiring Biocathode Constructed by Highly Enriched Cultures

Other than pure cultures, the majority of dehalorespiring studies were conducted in biocathode systems constructed by mixed cultures. The efficient dechlorination was achieved through electron transfer from electrode (at cathode potential of −450/−500 mV vs SHE) to highly enriched cultures (containing *Dehalococcoides* sp. and *Desulfitobacterium* sp.) assisted by a low-dose methyl viologen (MV) as redox mediator and finally resulted in the quickly reductive dechlorination of TCE to harmless end products (such as ethene and ethane) [89, 90]. On the other hand, the conditions without exogenous redox mediators require the much lower cathodic potential to initiate TCE dechlorination [91].

Aulenta et al. [96] constructed a continuous-flow bioelectrochemical reactor, and TCE continuous dechlorination capacity was investigated for about 570 days at the different cathode potentials ranging from −250 to −750 mV vs SHE. With cathode potential of −250 mV vs SHE, TCE dechlorination was efficiently maintained via the direct extracellular electron transfer from electrode to OHRB. Under these conditions, methanogenesis was almost completely suppressed [96]. Although a higher TCE dechlorination rate was achieved at cathode potentials lower than −450 mV, methanogenesis composed one dominant bioprocess which consumed over 60% of electric current [96].

When set cathode potential is more reducing than the electrolytic hydrogenation potential of −0.421 V vs SHE (the cathode overpotentials might decrease due to the lower partial pressure by microbial catalysis) [103], HOCs dechlorination with H_2 mediated by electrochemical dehydrogenation has been demonstrated. For example, TCE dechlorination was supported by H_2 generation by proton reduction inoculated with *Dehalococcoides*-enriched culture, and the balance between H_2 generation and dechlorination consumption could be achieved through controlling cathodic potentials [104]. The formation of H_2 on the cathode could also generate highly reducing conditions to induce HOCs dehalogenation, which has been demonstrated for the bio-dehalogenation of 2,6-dichlorophenol (2,6-DCP) [105].

Besides chlorinated aliphatic hydrocarbons, the reductive dechlorination capacities of chlorinated aromatic compounds in biocathode were also investigated. Accelerated reduction of chloramphenicol (CAP) was observed in a biocathode system inoculated with a CAP-reducing enriched consortium [106]. Nitro-reduction combined with dehalogenation enhanced the detoxification capacity and efficiency of CAP [106]. The stimulated microbial reductive dechlorination of pentachlorophenol (PCP) has also been studied in (humin-mediated) biocathode systems inoculating with the enriched dechlorination cultures. Favorable PCP dechlorination efficiencies were achieved in these constructed systems [87, 97, 98]. Although, compared with pure culture, a mixed culture holds the potential to reduce HOCs to more reduced products, these systems would attribute some other electrochemically active bacteria (EAB) and metabolic activities (e.g., methanogenesis), which would
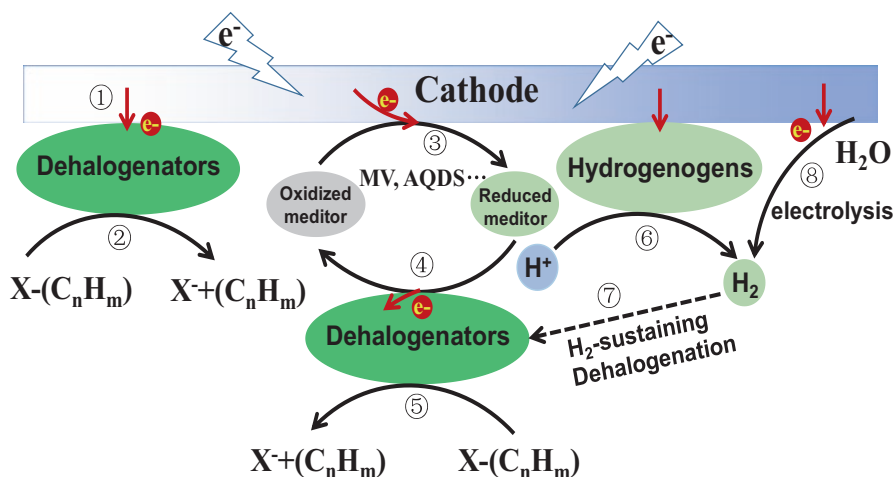
Fig. 4.2 Simplified representations of EET mechanisms from electrodes to dehalorespiring bacteria in biocathodes. ①② represent direct electron transfer process via membrane-bound cytochromes; ③④⑤ represent indirect electron transfer process assisted by exogenous/endogenous redox mediator; ⑤⑥⑦⑧ represent the indirect electron transfer via generated H_2

potentially reduce the electron utilization efficiency and increase the potential system cost [88, 96].

4.4 Dehalorespiring Bacteria-Related EET Mechanism

Biocathode has been extensively investigated for HOCs reduction, but the EET from cathode to dehalorespiring bacteria-related molecular mechanism remains unclear [107]. To date, the EET mechanisms which have been proposed or proven mainly include (i) direct electron transfer from the electrode surface and (ii) indirect electron transfer via soluble redox mediators (Fig. 4.2). Based on the ability of *Geobacter* species to directly accept electrons from cathode surface for HOCs dehalogenation [61, 88], the direct electron transfer mechanism is proposed (① and ② processes in Fig. 4.2). A close physical contact between dehalogenators and the electrodic surface is necessary for direct electron transfer [31]. The strong expression of a *Geobacter* gene (GSU3274) encoding a putative monoheme (*c*-type cytochrome) was observed in cathodic biofilms, suggesting GSU3274 cytochrome may serve as an intermediary in electron transfer between the outer cell surface and the inner membrane [108]. The *Shewanella* has a dual directional electronic conduit involving 40 heme redox centers in flavin-binding outer-membrane *c*-type cytochromes [109]. So, it is proposed that *c*-type cytochromes might play an important role in direct cathodic EET [105]. The direct electron transfer process without adding any exogenous agents is very attractive for in situ applications.

Indirect electron transfer mechanism via redox shuttling molecule is also presented (③, ④, and ⑤ processes in Fig. 4.2). The redox mediator is reduced to get electrons from the cathode surface ③ and further reoxidized by dehalogenation microorganism ④. In principal, redox mediator works as the electron carrier, which would be continuously recycled and never be consumed during HOCs dehalogenation and electron transfer with cathode.

Various added redox mediators, such as neutral red, cobalt sepulchrate, methyl viologen (MV), and 2,6-anthraquinone disulfonate (AQDS), have been applied to improve the electron transfer capacity from cathode to bacterial species [89, 110–113]. Among of them, MV was one of the most commonly used to mediate the electron transfer from electrode to typical OHRB, like *Dehalococcoides* spp. [89]. As previously reported, MV could penetrate the outer membrane of microorganisms, but it was unable to cross the cytoplasmatic membrane [114]. With the addition of reduced MV in cathode, cellular electron carriers or redox enzymes such as cythochromes and NAD^+ were probably being reduced at -500 mV vs SHE to act as internal electron donors for dechlorination [89]. In addition, using a highly enriched hydrogenotrophic dechlorinating culture in cathode with a potential of -450 mV vs SHE, TCE dechlorination and H_2 evolution were simultaneously stimulated at higher MV concentrations (>750 μM) [90]. Since the standard redox potential of MV (-446 mV) is closed to that of electrochemical dehydrogenation (-414 mV), MV would possibly be used as a redox partner of hydrogenases and donate electrons directly to periplasmic hydrogenase for MV-mediated biocathodic H_2 generation (⑥ and ⑦ processes in Fig. 4.2), which finally facilitate *Desulfitobacterium* sp. dechlorinating TCE with a high efficiency by utilizing H_2 [90, 107]. Although the addition of exogenous mediators could facilitate EET from a cathode to a microorganism, it also generates additional costs and negative environmental impact due to the toxicity and unsustainability of their chemical structures [31, 115].

Meanwhile, some electroactive bacteria perform indirect electron transfer through their self-secreted redox mediators. Although many microbial self-secreted redox mediators have been identified in bioanode, only small portions of them were identified that could function in biocathodes, such as phenazines [116], flavin derivatives [117], and quinones [118]. Some studies have given the positive evidence that the self-secreted redox mediators play important roles in promoting the bio-dehalogenation processes in constructed biocathode systems via mediating EET from electrode to the dechlorinating bacteria [84]. Right now, it has been confirmed that the self-secreted redox mediators could react at multiple sites, including the cell periplasm, cytoplasmic membrane, and even within the cytoplasm [107]. In addition, the shared utilization of redox mediators between other bacteria and their secretors may enhance the metabolic activity of the cathode community [107].

Besides, the indirect electron transfer also includes H_2 generation through electrochemical dehydrogenation, and then H_2 was employed for HOCs dehalogenation (⑦ and ⑧ processes in Fig. 4.2). As far, H_2-sustained HOCs dehalogenation was considered much less efficient than the direct capture of electrons from electrode by cathode-utilizing dehalogenators, attributed to the low H_2 solubility and H_2 hydrolysis capacities [96, 119].

4.5 Challenges and Perspectives

So far, biocathode dehalogenation has been employed for limited kinds of HOCs, majorly focusing on some kinds of chlorinated aliphatic compounds and a few kinds of chlorinated aromatic compounds. However, its applicability to other types of HOCs, like brominated flame retardants or perfluorinated compounds, requires further demonstration. It is worth mentioning that EET-related molecular mechanisms in biocathode are still poorly understood. The characterization of functional genes in related with EET and RDases is necessary to better understand the electron transfer-related mechanism at the genetic level and give theory instructions on construction of more efficient systems.

Facing the removal of HOCs in practical field application, the startup of biocathode systems for efficient dehalogenation remains a time-consuming process, and how to quickly establish a dehalorespiring biocathode systems remains the application challenges [31, 106, 120]. Some studies have attempted to accelerate the startup and enhance biocathode reactor performance by optimizing cathode potential and improving the surface characteristics and area of electrode [121, 122]. Also, polarity inversion strategy has been proposed to accelerate the establishment of a biocathode for aromatic compound reduction [33]. However, a systematic research on the rapid startup strategy remains lacking. Whether the above-discussed methods are conducive to the rapid construction of dehalorespiring biocathode systems remains to be explored, and the more applicable cost-effective approaches are expected.

Moreover, some operation parameters, such as cathodic potential, were regarded as one vital factor to manipulate redox environment and favor the electron transfer between electrode and bacteria [123]. Some studies found that both the dechlorination rate and extent could be greatly affected by the fine-tuning of the cathodic potential [96]. In addition, electron transfer pathways varied partially laying on the applied cathodic potential [96, 124, 125]. How these operation parameters regulate HOCs dehalogenation in related to the microbial electron transfer mechanism is not yet understood.

Besides, most of the abovementioned studies focused on the efficient system construction to obtain the favorable HOCs dehalogenation ability by inoculating either the dehalorespiring isolates or the highly enriched cultures [61, 82, 85, 88, 91, 96]. In view of application, the use of dehalogenating isolates or cultures is restrictive because of (i) the narrow ecological niches or strict nutrients/redox potential demands [27, 29, 126] and (ii) the unknown EET capacity with electrode [31]. To improve the applicability, it is worth to understand whether the enhanced dehalogenation activity could be obtained with the conventional, easy-to-obtain, and less restrictive microbial sources, such as raw activated sludge.

References

1. Kirk KL (1991) Biochemistry of halogenated organic compounds. Plenum, New York
2. Erickson MD, Kaley RG (2011) Applications of polychlorinated biphenyls. Environ Sci Pollut Res 18(2):135–151
3. Cagnetta G, Robertson J, Huang J, Zhang K, Yu G (2016) Mechanochemical destruction of halogenated organic pollutants: a critical review. J Hazard Mater 313:85–102
4. Chaurasia AK, Adhya TK, Apte SK (2013) Engineering bacteria for bioremediation of persistent organochlorine pesticide lindane (γ-hexachlorocyclohexane). Bioresour Technol 149:439–445
5. Turusov V, Rakitsky V, Tomatis L (2002) Dichlorodiphenyltrichloroethane (DDT): ubiquity, persistence, and risks. Environ Health Perspect 110(2):125
6. Li Z, Inoue Y, Suzuki D, Ye L, Katayama A (2013) Long-term anaerobic mineralization of pentachlorophenol in a continuous-flow system using only lactate as an external nutrient. Environ Sci Technol 47(3):1534–1541
7. Lu C, Bjerg PL, Zhang F, Broholm MM (2011) Sorption of chlorinated solvents and degradation products on natural clayey tills. Chemosphere 83(11):1467–1474
8. van der Zaan B, de Weert J, Rijnaarts H, de Vos WM, Smidt H, Gerritse J (2009) Degradation of 1, 2-dichloroethane by microbial communities from river sediment at various redox conditions. Water Res 43(13):3207–3216
9. Wang J, Ma Y-J, Chen S-J, Tian M, Luo X-J, Mai B-X (2010) Brominated flame retardants in house dust from e-waste recycling and urban areas in South China: implications on human exposure. Environ Int 36(6):535–541
10. Feng Y, Colosi LM, Gao S, Huang Q, Mao L (2013) Transformation and removal of tetrabromobisphenol A from water in the presence of natural organic matter via laccase-catalyzed reactions: reaction rates, products, and pathways. Environ Sci Technol 47(2):1001–1008
11. Ahrens L, Yeung LW, Taniyasu S, Lam PK, Yamashita N (2011) Partitioning of perfluorooctanoate (PFOA), perfluorooctane sulfonate (PFOS) and perfluorooctane sulfonamide (PFOSA) between water and sediment. Chemosphere 85(5):731–737
12. Cooney MA, Louis GMB, Hediger ML, Vexler A, Kostyniak PJ (2010) Organochlorine pesticides and endometriosis. Reprod Toxicol 30(3):365–369
13. Feng A-H, Chen S-J, Chen M-Y, He M-J, Luo X-J, Mai B-X (2012) Hexabromocyclododecane (HBCD) and tetrabromobisphenol A (TBBPA) in riverine and estuarine sediments of the Pearl River Delta in southern China, with emphasis on spatial variability in diastereoisomer-and enantiomer-specific distribution of HBCD. Mar Pollut Bull 64(5):919–925
14. Baynes RE, Brooks JD, Mumtaz M, Riviere JE (2002) Effect of chemical interactions in pentachlorophenol mixtures on skin and membrane transport. Toxicol Sci 69(2):295–305
15. Proudfoot AT (2003) Pentachlorophenol poisoning. Toxicol Rev 22(1):3–11
16. Agency USEP Toxic and priority pollutants under the clean water act. https://www.epagov/eg/toxic-and-priority-pollutants-under-clean-water-act
17. Perelo LW (2010) In situ and bioremediation of organic pollutants in aquatic sediments. J Hazard Mater 177(1–3):81–89
18. Liang J, Liu J, Yuan X, Dong H, Zeng G, Wu H, Wang H, Liu J, Hua S, Zhang S (2015) Facile synthesis of alumina-decorated multi-walled carbon nanotubes for simultaneous adsorption of cadmium ion and trichloroethylene. Chem Eng J 273:101–110
19. Matsukami H, Kose T, Watanabe M, Takigami H (2014) Pilot-scale incineration of wastes with high content of chlorinated and non-halogenated organophosphorus flame retardants used as alternatives for PBDEs. Sci Total Environ 493:672–681
20. Bokare AD, Choi W (2014) Review of iron-free Fenton-like systems for activating H2O2 in advanced oxidation processes. J Hazard Mater 275:121–135
21. Rajajayavel SRC, Ghoshal S (2015) Enhanced reductive dechlorination of trichloroethylene by sulfidated nanoscale zerovalent iron. Water Res 78:144–153

22. Li D, Mao Z, Zhong Y, Huang W, Wu Y, Pa P (2016) Reductive transformation of tetrabromo-bisphenol A by sulfidated nano zerovalent iron. Water Res 103:1–9
23. Adrian L, Loeffler FE (2016) Organohalide-respiring bacteria, vol 85. Springer, Berlin
24. Bhatt P, Kumar MS, Mudliar S, Chakrabarti T (2007) Biodegradation of chlorinated compounds—a review. Crit Rev Environ Sci Technol 37(2):165–198
25. Wang S, Chng KR, Wilm A, Zhao S, Yang K-L, Nagarajan N, He J (2014) Genomic characterization of three unique Dehalococcoides that respire on persistent polychlorinated biphenyls. Proc Natl Acad Sci 111(33):12103–12108
26. Wang S, Zhang W, Yang K-L, He J (2014) Isolation and characterization of a novel Dehalobacter species strain TCP1 that reductively dechlorinates 2, 4, 6-trichlorophenol. Biodegradation 25(2):313–323
27. Cheng D, He J (2009) Isolation and characterization of "Dehalococcoides" sp. strain MB, which dechlorinates tetrachloroethene to trans-1, 2-dichloroethene. Appl Environ Microbiol 75(18):5910–5918
28. Adrian L, Hansen SK, Fung JM, Görisch H, Zinder SH (2007) Growth of Dehalococcoides strains with chlorophenols as electron acceptors. Environ Sci Technol 41(7):2318–2323
29. He J, Sung Y, Krajmalnik-Brown R, Ritalahti KM, Löffler FE (2005) Isolation and characterization of Dehalococcoides sp. strain FL2, a trichloroethene (TCE)-and 1, 2-dichloroethene-respiring anaerobe. Environ Microbiol 7(9):1442–1450
30. He J, Sung Y, Dollhopf ME, Fathepure BZ, Tiedje JM, Löffler FE (2002) Acetate versus hydrogen as direct electron donors to stimulate the microbial reductive dechlorination process at chloroethene-contaminated sites. Environ Sci Technol 36(18):3945–3952
31. Huang L, Regan JM, Quan X (2011) Electron transfer mechanisms, new applications, and performance of biocathode microbial fuel cells. Bioresour Technol 102(1):316–323
32. Mu Y, Rozendal RA, Rabaey K, Keller Jr (2009) Nitrobenzene removal in bioelectrochemical systems. Environ Sci Technol 43(22):8690–8695
33. Yun H, Liang B, Kong D-Y, Cheng H-Y, Li Z-L, Gu Y-B, Yin H-Q, Wang A-J (2017) Polarity inversion of bioanode for biocathodic reduction of aromatic pollutants. J Hazard Mater 331:280–288
34. Mohn WW, Tiedje JM (1992) Microbial reductive dehalogenation. Microbiol Rev 56(3):482–507
35. Linkfield TG, Suflita J, Tiedje J (1989) Characterization of the acclimation period before anaerobic dehalogenation of halobenzoates. Appl Environ Microbiol 55(11):2773–2778
36. Kuhn EP, Suflita JM (1989) Dehalogenation of pesticides by anaerobic microorganisms in soils and groundwater—a review. In: Reactions and movement of organic chemicals in soils. Soil Science Society of America, Madison, pp 111–180
37. Bunge M, Adrian L, Kraus A, Opel M, Lorenz WG, Andreesen JR, Görisch H, Lechner U (2003) Reductive dehalogenation of chlorinated dioxins by an anaerobic bacterium. Nature 421(6921):357
38. Bunge M, Lechner U (2009) Anaerobic reductive dehalogenation of polychlorinated dioxins. Appl Microbiol Biotechnol 84(3):429–444
39. Haest PJ, Springael D, Smolders E (2010) Dechlorination kinetics of TCE at toxic TCE concentrations: assessment of different models. Water Res 44(1):331–339
40. Li Z, Yang S, Inoue Y, Yoshida N, Katayama A (2010) Complete anaerobic mineralization of pentachlorophenol (PCP) under continuous flow conditions by sequential combination of PCP-dechlorinating and phenol-degrading consortia. Biotechnol Bioeng 107(5):775–785
41. Li Z, Suzuki D, Zhang C, Yang S, Nan J, Yoshida N, Wang A, Katayama A (2014) Anaerobic 4-chlorophenol mineralization in an enriched culture under iron-reducing conditions. J Biosci Bioeng 118(5):529–532
42. Sun B, Griffin BM, Ayala del Rio HL, Hashsham SA, Tiedje JM (2002) Microbial dehalorespiration with 1, 1, 1-trichloroethane. Science 298(5595):1023–1025
43. Yoshida N, Ye L, Baba D, Katayama A (2009) A novel Dehalobacter species is involved in extensive 4, 5, 6, 7-tetrachlorophthalide dechlorination. Appl Environ Microbiol 75(8):2400–2405

44. Li Z, Suzuki D, Zhang C, Yoshida N, Yang S, Katayama A (2013) Involvement of Dehalobacter strains in the anaerobic dechlorination of 2, 4, 6-trichlorophenol. J Biosci Bioeng 116(5):602–609

45. Li Z, Yoshida N, Wang A, Nan J, Liang B, Zhang C, Zhang D, Suzuki D, Zhou X, Xiao Z (2015) Anaerobic mineralization of 2, 4, 6-tribromophenol to CO_2 by a synthetic microbial community comprising Clostridium, Dehalobacter, and Desulfatiglans. Bioresour Technol 176:225–232

46. He J, Ritalahti KM, Aiello MR, Löffler FE (2003) Complete detoxification of vinyl chloride by an anaerobic enrichment culture and identification of the reductively dechlorinating population as a Dehalococcoides species. Appl Environ Microbiol 69(2):996–1003

47. Dolfing J (1990) Reductive dechlorination of 3-chlorobenzoate is coupled to ATP production and growth in an anaerobic bacterium, strain DCB-1. Arch Microbiol 153(3):264–266

48. Hölscher T, Görisch H, Adrian L (2003) Reductive dehalogenation of chlorobenzene congeners in cell extracts of Dehalococcoides sp. strain CBDB1. Appl Environ Microbiol 69(5):2999–3001

49. Holliger C, Hahn D, Harmsen H, Ludwig W, Schumacher W, Tindall B, Vazquez F, Weiss N, Zehnder AJ (1998) Dehalobacter restrictus gen. nov. and sp. nov., a strictly anaerobic bacterium that reductively dechlorinates tetra-and trichloroethene in an anaerobic respiration. Arch Microbiol 169(4):313–321

50. van de Pas BA, Smidt H, Hagen WR, van der Oost J, Schraa G, Stams AJ, de Vos WM (1999) Purification and molecular characterization of ortho-chlorophenol reductive dehalogenase, a key enzyme of halorespiration in Desulfitobacterium dehalogenans. J Biol Chem 274(29):20287–20292

51. Neumann A, Scholz-Muramatsu H, Diekert G (1994) Tetrachloroethene metabolism of Dehalospirillum multivorans. Arch Microbiol 162(4):295–301

52. Chen K, Huang L, Xu C, Liu X, He J, Zinder SH, Li S, Jiang J (2013) Molecular characterization of the enzymes involved in the degradation of a brominated aromatic herbicide. Mol Microbiol 89(6):1121–1139

53. Payne KA, Quezada CP, Fisher K, Dunstan MS, Collins FA, Sjuts H, Levy C, Hay S, Rigby SE, Leys D (2015) Reductive dehalogenase structure suggests a mechanism for B12-dependent dehalogenation. Nature 517(7535):513

54. Bisaillon A, Beaudet R, Lépine F, Villemur R (2011) Quantitative analysis of the relative transcript levels of four chlorophenol reductive dehalogenase genes in Desulfitobacterium hafniense PCP-1 exposed to chlorophenols. Appl Environ Microbiol 77(17):6261–6264

55. Magnuson JK, Romine MF, Burris DR, Kingsley MT (2000) Trichloroethene reductive dehalogenase from Dehalococcoides ethenogenes: sequence of tceA and substrate range characterization. Appl Environ Microbiol 66(12):5141–5147

56. Yan J, Ritalahti KM, Wagner DD, Löffler FE (2012) Unexpected specificity of interspecies cobamide transfer from Geobacter spp. to organohalide-respiring Dehalococcoides mccartyi strains. Appl Environ Microbiol 78(18):6630–6636

57. Bommer M, Kunze C, Fesseler J, Schubert T, Diekert G, Dobbek H (2014) Structural basis for organohalide respiration. Science 346:455–458 1258118

58. Z-L L, Nan J, Yang J-Q, Jin X, Katayama A, Wang A-J (2015) Temporal distributions of functional microbes and putative genes associated with halogenated phenol anaerobic dehalogenation and further mineralization. RSC Adv 5(108):89157–89163

59. Li Z-L, Nan J, Huang C, Liang B, Liu W-Z, Cheng H-Y, Zhang C, Zhang D, Kong D, Kanamaru K (2016) Spatial abundance and distribution of potential microbes and functional genes associated with anaerobic mineralization of pentachlorophenol in a cylindrical reactor. Sci Rep 6:19015

60. Löffler FE, Yan J, Ritalahti KM, Adrian L, Edwards EA, Konstantinidis KT, Müller JA, Fullerton H, Zinder SH, Spormann AM (2013) Dehalococcoides mccartyi gen. nov., sp. nov., obligately organohalide-respiring anaerobic bacteria relevant to halogen cycling and bioremediation, belong to a novel bacterial class, Dehalococcoidia classis nov., order

Dehalococcoidales ord. nov. and family Dehalococcoidaceae fam. nov., within the phylum Chloroflexi. Int J Syst Evol Microbiol 63(2):625–635

61. Aulenta F, Majone M (2010) Bioelectrochemical systems (BES) for subsurface remediation. Bioelectrochemical Systems, IWA Publishing, London

62. Fennell DE, Nijenhuis I, Wilson SF, Zinder SH, Häggblom MM (2004) Dehalococcoides ethenogenes strain 195 reductively dechlorinates diverse chlorinated aromatic pollutants. Environ Sci Technol 38(7):2075–2081

63. He J, Robrock KR, Alvarez-Cohen L (2006) Microbial reductive debromination of polybrominated diphenyl ethers (PBDEs). Environ Sci Technol 40(14):4429–4434

64. Maymó-Gatell X, Anguish T, Zinder SH (1999) Reductive dechlorination of chlorinated ethenes and 1, 2-dichloroethane by "Dehalococcoides ethenogenes" 195. Appl Environ Microbiol 65(7):3108–3113

65. Maymó-Gatell X, Nijenhuis I, Zinder SH (2001) Reductive dechlorination of cis-1, 2-dichloroethene and vinyl chloride by "Dehalococcoides ethenogenes". Environ Sci Technol 35(3):516–521

66. Yang C, Kublik A, Weidauer C, Seiwert B, Adrian L (2015) Reductive dehalogenation of oligocyclic phenolic bromoaromatics by Dehalococcoides mccartyi strain CBDB1. Environ Sci Technol 49(14):8497–8505

67. Adrian L, Szewzyk U, Wecke J, Görisch H (2000) Bacterial dehalorespiration with chlorinated benzenes. Nature 408(6812):580

68. Adrian L, Dudková V, Demnerová K, Bedard DL (2009) "Dehalococcoides" sp. strain CBDB1 extensively dechlorinates the commercial polychlorinated biphenyl mixture Aroclor 1260. Appl Environ Microbiol 75(13):4516–4524

69. Wagner A, Cooper M, Ferdi S, Seifert J, Adrian L (2012) Growth of Dehalococcoides mccartyi strain CBDB1 by reductive dehalogenation of brominated benzenes to benzene. Environ Sci Technol 46(16):8960–8968

70. May HD, Miller GS, Kjellerup BV, Sowers KR (2008) Dehalorespiration with polychlorinated biphenyls by an anaerobic ultramicrobacterium. Appl Environ Microbiol 74(7):2089–2094

71. Wu Q, Milliken CE, Meier GP, Watts JE, Sowers KR, May HD (2002) Dechlorination of chlorobenzenes by a culture containing bacterium DF-1, a PCB dechlorinating microorganism. Environ Sci Technol 36(15):3290–3294

72. Ding C, Chow WL, He J (2013) Isolation of Acetobacterium sp. strain AG, which reductively debrominates octa-and pentabrominated diphenyl ether technical mixtures. Appl Environ Microbiol 79(4):1110–1117

73. Zhang C, Li Z, Suzuki D, Ye L, Yoshida N, Katayama A (2013) A humin-dependent Dehalobacter species is involved in reductive debromination of tetrabromobisphenol A. Chemosphere 92(10):1343–1348

74. Wang J, Fu Z, Liu G, Guo N, Lu H, Zhan Y (2013) Mediators-assisted reductive biotransformation of tetrabromobisphenol-A by Shewanella sp. XB. Bioresour Technol 142:192–197

75. Gu C, Wang J, Liu S, Liu G, Lu H, Jin R (2016) Biogenic fenton-like reaction involvement in cometabolic degradation of tetrabromobisphenol A by Pseudomonas sp. fz. Environ Sci Technol 50(18):9981–9989

76. Lee LK, Ding C, Yang K-L, He J (2011) Complete debromination of tetra-and pentabrominated diphenyl ethers by a coculture consisting of Dehalococcoides and Desulfovibrio species. Environ Sci Technol 45(19):8475–8482

77. Wang S, He J (2013) Dechlorination of commercial PCBs and other multiple halogenated compounds by a sediment-free culture containing Dehalococcoides and Dehalobacter. Environ Sci Technol 47(18):10526–10534

78. Gerritse J, Renard V, Gomes TP, Lawson PA, Collins MD, Gottschal JC (1996) Desulfitobacterium sp. strain PCE1, an anaerobic bacterium that can grow by reductive dechlorination of tetrachloroethene or ortho-chlorinated phenols. Arch Microbiol 165(2):132–140

79. Dennie D, Gladu I, Lépine F, Villemur R, Bisaillon J-G, Beaudet R (1998) Spectrum of the reductive dehalogenation activity of Desulfitobacterium frappieri PCP-1. Appl Environ Microbiol 64(11):4603–4606

80. Boyle AW, Phelps CD, Young L (1999) Isolation from estuarine sediments of a Desulfovibrio strain which can grow on lactate coupled to the reductive dehalogenation of 2, 4, 6-tribromophenol. Appl Environ Microbiol 65(3):1133–1140

81. Sung Y, Fletcher KE, Ritalahti KM, Apkarian RP, Ramoshernández N, Sanford RA, Mesbah NM, Löffler FE (2006) Geobacter lovleyi sp. nov. strain SZ, a novel metal-reducing and tetrachloroethene-dechlorinating bacterium. Appl Environ Microbiol 72(4):2775–2782

82. Strycharz SM, Gannon SM, Boles AR, Franks AE, Nevin KP, Lovley DR (2010) Reductive dechlorination of 2-chlorophenol by Anaeromyxobacter dehalogenans with an electrode serving as the electron donor. Environ Microbiol Rep 2(2):289–294

83. Gregory KB, Bond DR, Lovley DR (2004) Graphite electrodes as electron donors for anaerobic respiration. Environ Microbiol 6(6):596

84. Aulenta F, Canosa A, Reale P, Rossetti S, Panero S, Majone M (2009) Microbial reductive dechlorination of trichloroethene to ethene with electrodes serving as electron donors without the external addition of redox mediators. Biotechnol Bioeng 103(1):85

85. Leitão P, Rossetti S, Danko AS, Nouws H, Aulenta F (2016) Enrichment of Dehalococcoides mccartyi spp. from a municipal activated sludge during AQDS-mediated bioelectrochemical dechlorination of 1, 2-dichloroethane to ethene. Bioresour Technol 214:426–431

86. Wan H, Yi X, Liu X, Feng C, Dang Z, Wei C (2018) Time-dependent bacterial community and electrochemical characterizations of cathodic biofilms in the surfactant-amended sediment-based bioelectrochemical reactor with enhanced 2, 3, 4, 5-tetrachlorobiphenyl dechlorination. Environ Pollut 236:343–354

87. Huang L, Chai X, Quan X, Logan BE, Chen G (2012) Reductive dechlorination and mineralization of pentachlorophenol in biocathode microbial fuel cells. Bioresour Technol 111:167–174

88. Strycharz SM, Woodard TL, Johnson JP, Nevin KP, Sanford RA, Löffler FE, Lovley DR (2008) Graphite electrode as a sole electron donor for reductive dechlorination of tetrachloroethene by Geobacter lovleyi. Appl Environ Microbiol 74(19):5943–5947

89. Aulenta F, Catervi A, Majone M, Panero S, Priscilla Reale A, Rossetti S (2007) Electron transfer from a solid-state electrode assisted by methyl viologen sustains efficient microbial reductive dechlorination of TCE. Environ Sci Technol 41(7):2554–2559

90. Aulenta F, Canosa A, Majone M, Panero S, Reale P, Rossetti S (2008) Trichloroethene dechlorination and H2 evolution are alternative biological pathways of electric charge utilization by a dechlorinating culture in a bioelectrochemical system. Environ Sci Technol 42(16):6185–6190

91. Aulenta F, Reale P, Canosa A, Rossetti S, Panero S, Majone M (2010) Characterization of an electro-active biocathode capable of dechlorinating trichloroethene and cis-dichloroethene to ethene. Biosens Bioelectron 25(7):1796–1802

92. Yun H, Kong D, Liang B, Cui M, Li Z, Wang A (2016) Response of anodic bacterial community to the polarity inversion for chloramphenicol reduction. Bioresour Technol 221:666–670

93. Liang B, Kong D, Ma J, Wen C, Yuan T, Lee D-J, Zhou J, Wang A (2016) Low temperature acclimation with electrical stimulation enhance the biocathode functioning stability for antibiotics detoxification. Water Res 100:157–168

94. Chen H, Gao X, Wang C, Shao J, Xu X, Zhu L (2017) Efficient 2,4-dichloronitrobenzene removal in the coupled BES-UASB reactor: effect of external voltage mode. Bioresour Technol 241:879

95. Guo W-Q, Guo S, Yin R-L, Yuan Y, Ren N-Q, Wang A-J, Qu D-X (2015) Reduction of 4-chloronitrobenzene in a bioelectrochemical reactor with biocathode at ambient temperature for a long-term operation. J Taiwan Inst Chem Eng 46:119–124

96. Aulenta F, Tocca L, Verdini R, Reale P, Majone M (2011) Dechlorination of trichloroethene in a continuous-flow bioelectrochemical reactor: effect of cathode potential on rate, selectivity, and electron transfer mechanisms. Environ Sci Technol 45(19):8444–8451

97. Liu D, Lei L, Yang B, Yu Q, Li Z (2013) Direct electron transfer from electrode to electrochemically active bacteria in a bioelectrochemical dechlorination system. Bioresour Technol 148:9–14

98. Zhang D, Zhang C, Li Z, Suzuki D, Komatsu DD, Tsunogai U, Katayama A (2014) Electrochemical stimulation of microbial reductive dechlorination of pentachlorophenol using solid-state redox mediator (humin) immobilization. Bioresour Technol 164:232–240

99. Lovley DR, Nevin KP (2011) A shift in the current: new applications and concepts for microbe-electrode electron exchange. Curr Opin Biotechnol 22(3):441–448

100. Wagner DD, Hug LA, Hatt JK, Spitzmiller MR, Padilla-Crespo E, Ritalahti KM, Edwards EA, Konstantinidis KT, Löffler FE (2012) Genomic determinants of organohalide-respiration in Geobacter lovleyi, an unusual member of the Geobacteraceae. BMC Genomics 13(1):200

101. Sanford RA, Cole JR, Tiedje JM (2002) Characterization and description of Anaeromyxobacter dehalogenans gen. nov., sp. nov., an aryl-halorespiring facultative anaerobic Myxobacterium. Appl Environ Microbiol 68(2):893

102. Thomas SH, Wagner RD, Arakaki AK, Skolnick J, Kirby JR, Shimkets LJ, Sanford RA, Löffler FE (2008) The mosaic genome of Anaeromyxobacter dehalogenans strain 2CP-C suggests an aerobic common ancestor to the delta-proteobacteria. PLoS One 3(5):e2103

103. Logan BE, Call D, Cheng S, Hamelers HV, Sleutels TH, Jeremiasse AW, Rozendal RA (2008) Microbial electrolysis cells for high yield hydrogen gas production from organic matter. Environ Sci Technol 42(23):8630–8640

104. Aulenta F, Reale P, Catervi A, Panero S, Majone M (2008) Kinetics of trichloroethene dechlorination and methane formation by a mixed anaerobic culture in a bio-electrochemical system. Electrochim Acta 53(16):5300–5305

105. Skadberg B, Geoly-Horn SL, Sangamalli V, Flora JR (1999) Influence of pH, current and copper on the biological dechlorination of 2, 6-dichlorophenol in an electrochemical cell. Water Res 33(9):1997–2010

106. Liang B, Cheng HY, Kong DY, Gao SH, Sun F, Cui D, Kong FY, Zhou AJ, Liu WZ, Ren NQ, Wu WM, Wang AJ, Lee DJ (2013) Accelerated reduction of chlorinated nitroaromatic antibiotic chloramphenicol by biocathode. Environ Sci Technol 47(10):5353–5361. https://doi.org/10.1021/es400933h

107. Rosenbaum M, Aulenta F, Villano M, Angenent LT (2011) Cathodes as electron donors for microbial metabolism: which extracellular electron transfer mechanisms are involved? Bioresour Technol 102(1):324–333

108. Strycharz SM, Glaven RH, Coppi MV, Gannon SM, Perpetua LA, Liu A, Nevin KP, Lovley DR (2011) Gene expression and deletion analysis of mechanisms for electron transfer from electrodes to Geobacter sulfurreducens. Bioelectrochemistry 80(2):142–150

109. Okamoto A, Hashimoto K, Nealson KH (2014) Flavin redox bifurcation as a mechanism for controlling the direction of electron flow during extracellular electron transfer. Angew Chem Int Ed 53(41):10988–10991

110. Thrash JC, Coates JD (2008) Direct and indirect electrical stimulation of microbial metabolism. Environ Sci Technol 42(11):3921–3931

111. Patil SA, Hägerhäll C, Gorton L (2012) Electron transfer mechanisms between microorganisms and electrodes in bioelectrochemical systems. In: Advances in chemical bioanalysis. Springer, pp 71–129

112. Thrash JC, Van Trump JI, Weber KA, Miller E, Achenbach LA, Coates JD (2007) Electrochemical stimulation of microbial perchlorate reduction. Environ Sci Technol 41(5):1740–1746

113. Moscoviz R, Toledo-Alarcón J, Trably E, Bernet N (2016) Electro-fermentation: how to drive fermentation using electrochemical systems. Trends Biotechnol 34(11):856–865

114. Jones RW, Garland PB (1977) Sites and specificity of the reaction of bipyridylium compounds with anaerobic respiratory enzymes of *Escherichia coli*. Effects of permeability barriers imposed by the cytoplasmic membrane. Biochem J 164(1):199–211

115. Huang L, Angelidaki I (2008) Effect of humic acids on electricity generation integrated with xylose degradation in microbial fuel cells. Biotechnol Bioeng 100(3):413–422
116. Venkataraman A, Rosenbaum M, Arends JB, Halitschke R, Angenent LT (2010) Quorum sensing regulates electric current generation of Pseudomonas aeruginosa PA14 in bioelectrochemical systems. Electrochem Commun 12(3):459–462
117. Marsili E, Baron DB, Shikhare ID, Coursolle D, Gralnick JA, Bond DR (2008) Shewanella secretes flavins that mediate extracellular electron transfer. Proc Natl Acad Sci 105(10):3968–3973
118. Freguia S, Tsujimura S, Kano K (2010) Electron transfer pathways in microbial oxygen biocathodes. Electrochim Acta 55(3):813–818
119. Luijten ML, Roelofsen W, Langenhoff AA, Schraa G, Stams AJ (2004) Hydrogen threshold concentrations in pure cultures of halorespiring bacteria and at a site polluted with chlorinated ethenes. Environ Microbiol 6(6):646–650
120. Liang B, Cheng H, Van Nostrand JD, Ma J, Yu H, Kong D, Liu W, Ren N, Wu L, Wang A, Lee DJ, Zhou J (2014) Microbial community structure and function of nitrobenzene reduction biocathode in response to carbon source switchover. Water Res 54:137–148. https://doi.org/10.1016/j.watres.2014.01.052
121. Oh S-E, Logan BE (2006) Proton exchange membrane and electrode surface areas as factors that affect power generation in microbial fuel cells. Appl Microbiol Biotechnol 70(2):162–169
122. Wei J, Liang P, Huang X (2011) Recent progress in electrodes for microbial fuel cells. Bioresour Technol 102(20):9335–9344
123. Ter Heijne A, Strik DP, Hamelers HV, Buisman CJ (2010) Cathode potential and mass transfer determine performance of oxygen reducing biocathodes in microbial fuel cells. Environ Sci Technol 44(18):7151–7156
124. Di Battista A, Verdini R, Rossetti S, Pietrangeli B, Majone M, Aulenta F (2012) CARD-FISH analysis of a TCE-dechlorinating biocathode operated at different set potentials. New Biotechnol 30(1):33–38
125. Leitão P, Rossetti S, Nouws HP, Danko AS, Majone M, Aulenta F (2015) Bioelectrochemically-assisted reductive dechlorination of 1, 2-dichloroethane by a Dehalococcoides-enriched microbial culture. Bioresour Technol 195:78–82
126. Lee PK, Cheng D, West KA, Alvarez-Cohen L, He J (2013) Isolation of two new Dehalococcoides mccartyi strains with dissimilar dechlorination functions and their characterization by comparative genomics via microarray analysis. Environ Microbiol 15(8):2293–2305

Chapter 5
Bioelectrodegradation of Hazardous Organic Contaminants from Industrial Wastewater

Xinbai Jiang, Jinyou Shen, Yang Mu, Libin Zhang, and Lianjun Wang

5.1 Introduction

5.1.1 Industrial Wastewater Treatment

Rapid development of industrialization directly leads to widespread use of multifarious organic compounds, substantial part of which are complex, synthetic, and refractory. The major industries, such as pulp and paper mills, food, pharmaceutical, electroplating, textile, photographic, mining, and agriculture, usually generate complex streams including kinds of chemicals and biological compositions. Besides, many industrial products such as paints, adhesives, gasoline, and plastics are also toxic in themselves. Their disposal not only results in contaminant concentrations increase in the environment and brings great pollution risk to the environment but also poses a threat to human health [1, 2]. Therefore, prevention of industrial pollution and deep treatment of industrial wastewaters are currently a major focus of environmentalists.

Developing innovative and efficient wastewater treatment technology is the key to guarantee water environment safety. Many researchers have devoted efforts to the exploration of more sustainable and economic alternatives, which could avoid hazardous chemicals addition and replace expensive methods. Conventionally, to remove organic contaminants in situ, various physical and chemical engineering

X. Jiang · J. Shen (✉) · L. Zhang · L. Wang
Jiangsu Key Laboratory of Chemical Pollution Control and Resources Reuse,
School of Environmental and Biological Engineering, Nanjing University of Science
and Technology, Nanjing, Jiangsu Province, China
e-mail: shenjinyou@mail.njust.edu.cn

Y. Mu
CAS Key Laboratory of Urban Pollutant Conversion, Collaborative Innovation
Centre of Suzhou Nano Science and Technology, Department of Chemistry,
University of Science and Technology of China, Hefei, Anhui Province, China

techniques have been applied, including physical adsorption, condensation, advanced oxidation processes, and electrochemical methods. However, these traditional wastewater treatment techniques face several drawbacks or limitations: (i) physical adsorption only immobilizes the pollutants onto solid adsorbents instead of degrading them into harmless materials; (ii) condensation and/or biofiltration shows relatively low efficiency, and only a limited number of pollutants can be removed in this manner; (iii) catalytic destruction processes are normally carried out under harsh conditions, such as extremely low pH; and (iv) these methods may cause secondary contamination. Moreover, these conventional methods usually require high cost due to chemicals addition and a large amount of energy consumption. Thus, the physical and chemical approaches for refractory pollutants removal from industrial wastewaters always encounter conflicts between efficiency and economy [3].

Biological methods for organic contaminants degradation are environmentally friendly and cost effective, which are able to overcome the various deficiencies of the physicochemical methods. Aerobic biological processes have been typically utilized for industrial wastewater treatment. In the last century, the activated sludge process has been the mainstay of wastewater treatment. However, it is a very energy-intensive process, and, according to an estimate, the amount of electricity needed to provide oxygen in activated sludge processes in the USA is equivalent to almost 2% of the total US electricity consumption [4]. Fortunately, the contaminants can be reduced to innocuous forms of compounds by anaerobic processes. Apparently, the anaerobic treatment of refractory compounds is more economic than the aerobic method, but anaerobic processes have shown much slower treatment rate for refractory wastewater compared to aerobic ones, accounting for the limited application of anaerobic technologies.

5.1.2 Bioelectrochemical Systems: From Energy Generation to Wastewater Treatment

Bioelectrochemical systems (BESs) including microbial fuel cell (MFC), microbial electrolysis cell (MEC), microbial electrosynthesis (ME), microbial desalination cell (MDC), or microbial solar cell (MSC) have been extensively explored recently. BESs are interesting and constantly expanding fields of science and technology that combine biological catalytic redox activity with classic abiotic electrochemical reactions and physics, and their application accelerates electrochemical reactions that occur either at the anode or cathode surfaces [5].

The knowledge indicating that bacteria are able to generate electric current was first reported by Potter. Since then, interest in BESs has grown exponentially, especially at the beginning of the twenty-first century, as illustrated by the number of publications and related citations [5] (Fig. 5.1). MFC and MEC are two typical types of BESs, which are categorized according to the direction of electron transfer. In a MFC, electroactive microorganisms (i.e., exoelectrogens) on the anode oxidize

Total Publications

9,298

(A)

Sum of Times Cited per Year	*h*-index	Sum of Times Cited	Citing articles
	187	**226,045**	**65,101**
1999 2018	Average citations per item	Without self citations	Without self citations
	24.31	**89,689**	**57,429**

Total Publications

1,360

(B)

Sum of Times Cited per Year	*h*-index	Sum of Times Cited	Citing articles
	77	**28,696**	**11,790**
1999 2018	Average citations per item	Without self citations	Without self citations
	21.1	**18,621**	**10,728**

Fig. 5.1 The number of journal papers on MFCs (**a**) and MECs (**b**). The number of articles is based on a "Web of Science" search using "Microbial fuel cell" (**a**) and "microbial electrolysis cell" (**b**) as keywords in November 2017

biodegradable organic compounds (mainly acetate) in renewable energy sources, such as wastewaters, extracellularly transferring electrons to the anode and producing an electrical current. Microorganisms function as the biocatalyst in these systems, advocating the electron flux from the metabolic reactions and playing a pivotal role in the bio-electrogenic activity [6].

Hence, MFCs are regarded as a promising energy source when treating waste/ wastewater. MFCs can utilize a wide range of soluble or dissolved complex organic molecules, including solid wastes, wastewaters, and renewable biomass, as the substrate (anolyte). The use of mixed consortia as the biocatalyst and wastewater as the feedstock is an economically viable option to upgrade MFCs in the existing effluent treatment units, which will have the dual benefits of treating the wastewater and generating bioelectricity [7]. While interesting, researchers are realizing that the economic and environmental value of electricity from MFCs cannot compete with that of other energy sources (e.g., biogas) at this stage. Therefore, developments have recently been initiated to broaden the scope of MFCs for more value-added applications, such as contaminants remediation by MECs [8]. Slightly different from the MFC, the bioelectrocatalysis reaction in such a system does not occur spontaneously, and a small power supply (0.2–0.8 V in practice) needs to be supplied between two electrodes to reduce the thermodynamic barrier for the biorefinery of the wastes and the bioconversion of the electrofuels [9]. A broad range of waste substrates with different biodegradability can be used in MEC, from model carbon sources, such as volatile acids, methanol, glucose, glycerol, and starch, to real wastewaters, including domestic, swine, human urine, fermentation, saline, and winery wastewaters, landfill leachate, and liquid fraction of pressed municipal solid waste [9]. Similar to the development of MFCs, the research interest of MECs in the early stage lies in one direction, i.e., H_2 production. The alternative applications of MECs that have emerged include recalcitrant pollutants removal, resources recovery, chemicals synthesis, bioelectrochemical research platforms, and biosensors. With an electricity supply, the cathode potential of MECs can be controlled, and thus recalcitrant pollutants such as nitrobenzene and 4-chlorophenol, in addition to H^+, can be reduced as electron acceptors at the cathode. Compared to conventional electrochemical reduction, the removal of these pollutants in MECs consumes much less energy. Furthermore, electroactive microorganisms as the catalysts on the anode or cathode of MECs could greatly lower the overpotential of electrochemical reactions and lead to higher removal efficiencies/rates [10, 11]. Thus, another application possibility for MECs is in the removal of recalcitrant contaminants [3].

5.2   Degradation of Organic Contaminants in the Anode of BESs

Anaerobic degradation of refractory organic pollutants is challenging to current water treatment technologies, especially biological processes due to their resistance to microbial respiration and the natural environment. While in the anode of the BESs, microorganisms are capable of converting a wide variety of organic compounds into CO_2, water, and energy. Microbes interact through a variety of mechanisms with an electrode. The electrode acts as an electron sink in what is in essence

an anaerobic respiration. Due to the driving force from cathode reactions, many studies have demonstrated that using BES as a remediation technology can accelerate pollutants degradation process and shorten reaction time. Anode-respiring bacteria (ARB) in syntrophy with fermenters could anaerobically oxidize biodegradable compounds [12]. One aspect of the electro-catalytic ability of biofilms is related to the presence of some specific bacterial strains (e.g., *Geobacter sulfurreducens*, *Rhodoferax ferrireducens*, and *Shewanella* sp.) that are able to exchange electrons with solid substrata (i.e., electrodes) [5]. Heterotrophic bacteria can oxidize a wide variety of organic molecules (substrates) by producing useful energy for their growth and maintenance of their metabolism. The substrate then serves for the bacteria as a source of carbon energy. The substrates used by electro-catalytic biofilms can be any kind of organic matter, from simple molecules (e.g., glucose, acetate, and carbohydrates) to complex compounds (e.g., cellulose and molasses) as well as the organic matter contained in the wastewater treatment plants, agricultural wastes (e.g., dairies and manure), domestic wastes, and any type of fermentable substrate. Thus, BESs can complement existing anaerobic treatment processes well. Various investigations have been carried out for the possible application of BES technology in the effective treatment of industrial wastewater containing hazardous organic contaminants.

5.2.1 N-Heterocyclic Compounds

N-Heterocyclic compounds have potential applications in the manufacturing of dyestuffs, pesticides, agrochemicals, and disinfectants. Due to their toxicity, mutagenicity, and carcinogenicity, they constitute a danger for the natural biogenic environment and have severe odor potential [13]. Furthermore, most of the N-heterocyclic compounds are difficult for microorganisms to degrade under aerobic and anaerobic conditions and have an adverse impact on the conventional biological wastewater treatment system due to their toxicity to bacteria. Several studies demonstrated that BESs or MFCs can solve problems of scarcity of electron acceptor or create the right environment to significantly stimulate and enhance N-heterocyclic compounds degradation accompanied by energy production. Some previous studies have indicated the effectiveness of BES in the oxidative degradation of three representative N-heterocyclic compounds (pyridine, indole, and quinoline) and in the subsequent electricity generation from wastewater streams. Maximum power densities of 228.8, 203.4, and 142.1 mW m^{-2} were obtained from pyridine, quinoline, and indole, respectively. Meanwhile, the maximum degradation efficiency of these substrates and COD removal were up to 90% and 88%, respectively [14–17]. Jiang et al. also investigated the feasibility of electrical stimulation for enhanced biodegradation of pyridine in anaerobic systems [18]. The ability to resist environmental stress, such as a high pyridine concentration, a short HRT, and a low acetate dosage, was strengthened in the BES system.

5.2.2   Aromatic Compounds

Aromatic compounds and their derivatives are the persistent organic compounds, which are toxic or not easy to degrade. The US EPA has listed benzene, nitrobenzene, phenol, and their derivatives as priority pollutants, and the European Union also regarded several phenols as priority pollutants [19]. These aromatic compounds are common pollutants discharged by petrochemical, chemical, coking plants, oil refineries, and pharmaceutical industries [20, 21]. Therefore, the removal of aromatic compounds from wastewater is of environmental interest [22]. In BESs, electrodes are potentially attractive electron acceptors for stimulating the anaerobic degradation of aromatic hydrocarbon contaminants because they can provide a low-cost, low-maintenance, and continuous sink for electrons. Li et al. developed a BES anode with an extra gas diffusion layer and polytetrafluoroethylene layer at the gas side for the efficient treatment of gaseous toluene. The BES showed a maximum toluene elimination capacity of 274.5 g m^{-3} h^{-1}, which was higher than the values usually reported for biofiltration systems and comparable with those with biotrickling filters [23]. The MFC inoculated using glucose exhibited the highest power density (31.3 mW m^{-2}) when phenol was used as the sole substrate for the MFC. The corresponding biodegradation kinetic constant was obtained at 0.035 h^{-1}, at an initial phenol concentration of 600 mg L^{-1}. Moreover, the phenol degradation rates in this MFC with a closed circuit were 9.8–16.5% higher than those in the MFC with an opened circuit, which might be mainly attributed to the anodic microbial community enriched from the different acclimation methods [24]. Al-Shehri recently evaluated the recalcitrant mixture of naphthalene and benzidine that resulted in a maximum power density of 292.60 mWm^{-2} and 100% mixture removal at optimal conditions [25]. Toluene supplemented with pyocyanin achieved a 3.64-fold increase in maximum power density from 4.69 to 21.7 mWm^{-2} and a 13-fold increase in CE from 0.83% to 11.62% in comparison to the only-toluene feed in a study by Wu et al. [26]. Cheng et al. demonstrated that electricity generation from aniline, a typical recalcitrant organic matter under the anaerobic condition, was remarkably facilitated by employing oxygen into the bioanodes of MFCs. By exposing the bioanode to air, electrons of 47.2 ± 6.9 C were recovered with an aniline removal efficiency of 91.2 ± 2.2% in 144 h [27]. Another study also proved that pure culture *Cupriavidus basilensis* formed anode biofilm could generate electricity with phenol as the sole carbon source under the low dissolved oxygen level [28]. These results provided a new insight into the biodegradation of recalcitrant organics on the anode, as well as electricity generation simultaneously.

5.2.3   Azo Dyes

Azo dyes constitute the largest chemical class of synthetic dyes and are extensively present in effluent from dye-manufacturing industries and textile industries. Along with recalcitrant organics, toxic, mutagenic, or carcinogenic chemicals usually

characterize the dye effluent. Their removal from these effluents before discharge is of paramount importance [29]. Recently, efforts have been made to utilize these dyes as a substrate in BES anode, leading to color removal from such dye-containing wastewaters and generating electricity. Co-metabolism has been demonstrated as the main removal mechanism for azo dye in the anaerobic anode chamber, or the anode side in the single-chamber BES or MFC. Fang et al. demonstrated electricity production from azo dye wastewater using an BES coupled with a constructed wetland, a device adapted to treat the wastewater and produce energy, which has increased wastewater treatment volume and is easier to maintain than other BESs [30]. The highest power density reached in this case was 0.852 W m^{-3}. Sun et al. reported accelerated decolorization of active brilliant red X-3B (ABRX3) in a BES anode when glucose and confectionary wastewater were used as co-substrates. Higher dye concentrations (even up to 1500 mg L^{-1}) did not inhibit their decolorization; however, electricity generation from glucose was affected by higher concentrations of ABRX3 (>300 mg L^{-1}), which could be attributed to the competition between azo dye and the anode for electrons from carbon sources [31]. Thus, the simultaneous treatment of azo dye-containing wastewater and readily biodegradable organic matter-containing wastewater could be achieved by mixing two kinds of wastewater in the MFCs, with the advantage of saving both cost and energy. However, the system still requires considerable improvements in terms of finding an appropriate bacterial community that is capable of utilizing a mixture of dyes and other simple carbon sources to make BESs a realistic solution for this type of wastewater. Moreover, azo dyes can also be degraded in the BES cathode chamber by receiving electrons from the cathode without additional electron donor supply, which would be emphasized in the following chapters.

5.2.4 Pharmaceutical Wastewater

Pharmaceutical factories, medical facilities, the breeding industry, and patients discharge a large quantity of antibiotics, but few water treatment plants have strictly implemented current standards, resulting in discharge of residual antibiotics into the environment. The complex composition and high toxicity make pharmaceutical wastewater difficult to treat by conventional technologies [32]. Synthetic penicillin wastewater in an air-cathode single-chamber MFC was evaluated by Wen et al. 1 g L^{-1} glucose+50 mg L^{-1} penicillin resulted in a maximum power density of 101.2 W m^{-2}, which was sixfold higher than the sum of that for 1 g L^{-1} glucose (14.7 W m^{-2}) and 50 mg L^{-1} penicillin (2.1 W m^{-3}) as the sole fuel [32]. Wang et al. demonstrated that sulfamethoxazole, a broad-spectrum antibiotic, and its degradation product 3-amino-5-methylisoxazole could be effectively degraded in BES reactors, with 85% of 20 mg L^{-1} sulfamethoxazole degraded within 12 h [33]. Chloramphenicol-containing toxic effluent has been treated in a BES anode with acetate as the electron donor. Approximately 84% of 50 mg L^{-1} CAP was degraded within 12 h via a *meta*-cleavage pathway [34]. Steroidal drug production wastewater has been

investigated and resulted in the maximum COD, total nitrogen, and sulfate removal efficiency of 82%, 62%, and 26%, respectively. And the maximum power density approached to 22.3 W m^{-3} [35]. These results indicated that toxic and biorefractory organic matter-containing wastes, such as antibiotic wastewater, might also be a good resource for BES technology.

5.2.5 Others

5.2.5.1 Petrochemical Industry Wastewater

A few investigations have been carried out for the possible application of BES technology in the effective treatment of petroleum hydrocarbons contaminated sites and refinery effluents. Purified terephthalic acid (PTA) is a raw material for petrochemical products manufacturing with a high strength in organic materials. Foad Marashi et al. first examined the raw wastewater of PTA from a petrochemical plant in a membraneless single-chamber MFC, resulting in the maximum power density of 31.8 mW m^{-2} (normalized per cathode area) and a coulombic efficiency (CE) of 2.05% for a COD removal of 74% during 21 days at an acidic pH (4.45), while a higher maximum power density (65.6 mW m^{-2}) was achieved under an alkaline condition (pH 8.5) [36]. Real-field petroleum sludge has been reported as an electron donor leading to power generation of 53.11 mW m^{-2}. Approximately 31 mW m^{-2} (cathode surface area) of maximum power density was generated during diesel degradation in the anode compartment of a dual chambered MFC [37].

5.2.5.2 Biorefinery Wastewater

In the general manufacturing process, biodiesel is manufactured through transesterification of lipids with alcohol. Acyl groups of triglycerides produce 1 mol of glycerin for every 3 mol of ester. During the biorefinery process, typically, four to ten times more water is utilized than the amount of biofuel generated. Biorefinery wastewater is characterized by residual sugars, 5-furfural, phenolics, and other pretreatment and fermentation byproducts. Post-fermentation biorefinery stream containing phenolic compounds and furan aldehyde derivatives from conversion has been tried as substrate in MFCs. Using biocathode MFCs, electricity generation from glycerin-containing biodiesel side stream achieved a maximum P_d of 23 W m^{-3} [38]. In another study, a maximum power density of 2110 mW m^{-2} (cathode surface area) with a biodiesel waste blended with 200 mM PBS with the heat-treated carbon brush anode was reported [39].

5.2.5.3 Paper Recycling Industry Wastewater

Wastewater from paper industries contains soluble organics and particulate matter such as cellulose, which cannot be effectively treated with traditional wastewater technologies. Sustainable agriculture and bio-based industries have led to the use of an efficient method for treating cellulose-containing wastewater. In MFCs, the treatment efficiency of such wastewater was limited by its conductivity. Evaluation of full-strength paper mill effluent for electricity generation in a mediator-less MFC resulted in a maximum power density of 24 mW m^{-2}. To overcome this problem, different buffers were tested. Fifty percent PBS reached maximum power density of 501 mW m^{-2}, CE of 16%, and total COD removal of 76% [40]. Cellulose removal was 96%. Higher power densities, for instance, a maximum power density of 1070 mW m^{-2} (cathode surface area) in a single-chamber and 880 mW m^{-2} in two-chamber air-cathode MFCs with CE up to 50% and COD removal up to 70%, have been reported with cellulose, which is a by-product of the paper manufacturing industry [41].

5.2.6 Bioelectrodegradation Mechanism in Bioanode

So far, the electron transfer mechanisms for most studies of organic contaminants degradation in the anode of BESs could be summarized as the following (Fig. 5.2). On the one hand, the electrode can serve as an electron acceptor for the anaerobic oxidation of contaminants, and providing an electrode as an electron acceptor can stimulate the anaerobic oxidation of contaminants. One significant advantage is that electrodes represent a continuous long-term electron acceptor. Soluble electron acceptors, such as oxygen, nitrate, sulfate, or chelated Fe (III), rapidly diffuse away from the point of application. In contrast, electrodes can be permanently located at the point of application. Furthermore, poriferous electrodes readily adsorb diverse types of organic contaminants [42]. Thus, when a graphite electrode is provided as an electron acceptor, it has the additional benefit of concentrating the contaminant at the source of the electron acceptor. It is expected that the microorganisms utilizing the contaminants will also attach to the electrode surface. Therefore, graphite electrodes have the unique capability of co-localizing the contaminants, electron acceptor, and degradative microorganisms on the same surface. The contaminants could be directly degraded in the BES anode. On the other hand, co-metabolism has been demonstrated as the main removal mechanism for contaminants in the anaerobic anode chamber, or the anode side in the single-chamber BES or MFC [43]. Co-substrates provide electrons for both the degradation of refractory compounds and electricity production. BESs anodes can provide anaerobic conditions and electrons for the reduction of oxidizing groups. The existence of the anode promoted the degradation of biorefractory compounds, and the electricity production consumed
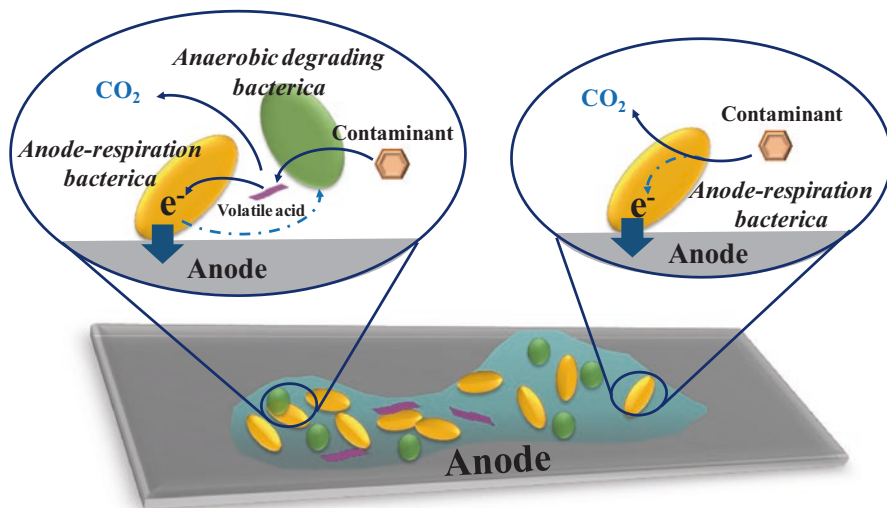
Fig. 5.2 Possible schematic of organic contaminants degradation in the anode of BESs

the co-substrates. The co-substrates could be consumed by the anode-respiration bacteria (ARB) and other anaerobic bacteria to stimulate their own growth and metabolism. The degradation of contaminants might be enhanced through the anode biofilm acclimation to toxicity. Anode-respiring bacteria in syntrophy with fermenters anaerobically oxidize biodegradable compounds. Syntrophic interaction by anodic consortium was suggested as a strategy to utilize the complex substrates as electron donors [27]. In summary, these studies expand the range of known electron acceptors that can support anaerobic oxidation of hazardous organic contaminants. The finding that compounds such as aromatic hydrocarbons, which are often considered to be recalcitrant to anaerobic degradation, can readily be oxidized with electron transfer to electrodes further emphasizes the potential for electrode-based systems as an effective waste treatment option in the absence of oxygen.

5.3 Reduction of Organic Contaminants in the Cathode of BESs

5.3.1 Abiotic Reduction

In BESs, electricity can be harvested from wastewater, and simultaneously complex organic pollutants in wastewater can be substantially removed by oxidation with the help of biocatalysts. However, there are still some contaminants that cannot be degraded by the anodic oxidation process owing to their highly positive redox potentials. Nevertheless, it is feasible to reduce them at cathode of BESs with or

without power supply. Cathodes can provide non-exhaustible electrons for the reduction of diverse organic pollutants, including nitroaromatics, azo dyes, haloaromatics, and reducible antibiotics. Therefore, reduction of organics at cathode extensively expands the application of BES technology.

5.3.1.1 Azo Dyes

Azo dyes contain one or more azo groups (–N = N–), which are the most labile portions in the molecular structure that can be reduced and cleaved resulting in mutagenic or carcinogenic degradation products. Azo dyes removal in traditional treatment systems is limited, but recent studies showed that many of the dyes can be degraded in both anode chamber and cathode chamber of BES reactors. Azo bonds are broken at the cathode by reduction, while organics undergo microbial oxidation at the anode, which simultaneously provides electrons for reduction at the cathode. Compared with conventional electrochemical and anaerobic biological processes, the energy consumption and electron donor requirements are significantly lower in BESs. Mu et al. investigated the use of a BES to abiotically cathodic decolorize Acid Orange 7 (AO7). The AO7 decolorization rate was significantly enhanced when the BES was supplied with power, reaching 13.18 mol m^{-3} NCC day^{-1} at an energy consumption 0.012 kWh mol^{-1} AO7 at a controlled cathode potential of −400 mV vs SHE) [44]. Compared with conventional anaerobic biological methods, the required dosage of the organic co-substrate was significantly reduced in the BES. Liu et al. ranked methyl orange (MO) > Orange I > Orange II as azo dye-feeding cathodes and concluded catholyte pH and dye structure are key factors affecting system performance [45].

5.3.1.2 Nitroaromatic Compounds

Nitroaromatic compounds (NACs), including nitrobenzene, 2,4,6-trinitrotoluene, 2,4-dinitrotoluene, and 2,6-dinitrotoluene, are extensively used in industrial segments. Many NACs are toxic and potentially carcinogenic at relatively low concentrations. However, NACs are usually recalcitrant to biodegradation due to nitro groups. BES has shown to be effective in the reduction of NACs. At the cathode of BES, the nitro groups could be reduced to aromatic amine compounds efficiently [22]. Mu et al. investigated nitrobenzene removal at cathode of BES coupled with microbial acetate oxidation at anode. Effective reduction of nitrobenzene at rates up to 1.29 mol m^{-3} TCC day^{-1} (total cathodic compartment, TCC) was achieved with aniline formation rate of 1.14 mol m^{-3} TCC day^{-1} and with energy recovery simultaneously. With small power supply, nitrobenzene removal and aniline formation rates were significantly enhanced, which reached 8.57 and 6.68 mol m^{-3} TCC day^{-1}, respectively. The energy consumption was 17.06 W m^{-3} TCC (current density at 59.5 A m^{-3} TCC), and the required dosage of organic co-substrate was significantly reduced comparing to conventional anaerobic biological methods [46]. Shen et al.

applied BES for recalcitrant *p*-nitrophenol (PNP) removal. Effective removal of PNP at rates up to 9.14 ± 0.48 mol m^{-3} day^{-1} was achieved at an energy consumption as low as 0.010 ± 0.002 kWh mol^{-1} PNP. The PNP removal rate was enhanced with negative cathode potential, increased influent PNP concentration, and shortened hydraulic retention time (HRT) [47]. Moreover, the reduction of the three nitrophenols (*o*-nitrophenol (ONP), *m*-nitrophenol (MNP), and *p*-nitrophenol (PNP)) followed in the order of ONP > MNP > PNP in the BESs. Both quantum chemical calculation using density function theory and cyclic voltammetry analysis confirmed the reductive sequence of the three nitrophenols. In addition, the acute toxicity of the nitrophenol effluent significantly decreased, while its biodegradability was enhanced after treatment in the BES [48].

5.3.1.3 Halogenated Aromatic Compounds

Halogenated aromatic compounds, such as trichloroethylene (TCE), tetrachloroethylene, and polychlorinated biphenyls, are well-known chemicals that are highly toxic to human health and the environment. A critical step in degradation of organohalides is the cleavage of the carbon-halogen bond [49]. Thus halogenated aromatic compounds would be more easily degraded under strictly anaerobic conditions [50]. BESs (MEC style) have been applied to TCE and iodinated contrast medium diatrizoate (diaI3) [51]. With 0.8 V power supply, TCE was degraded into chloride and ethane at a rate of 0.58 mol m^{-3} (reactor volume) day^{-1} with a bio-Pd coated cathode (5 mg g^{-1} electrode) [51]. Wen et al. proved the feasibility of 4-chlorophenol removal in two-chamber BES (MFC style) with small amount of electricity production. However, the dechlorination efficiency of the 4-CP was only 50.3%. It was significantly enhanced to 92.5% with 0.7 V power input (MEC style). The maximum dechlorination rate reached 0.38 mol m^{-3} day^{-1} with energy consumption of 0.549 kWh mol^{-1} 4-CP. The energy requirement was 50% lower than that of electrochemical methods (1.17 kWh mol^{-1} 4-CP) [8]. Mu et al. reported that iopromide could be completely dehalogenated in BESs when the potential of granular graphite cathode was controlled at -800 mV vs SHE or lower [52]. Similarly, diatrizoate dechlorination was degraded into 3,5-diacetamidobenzoate at an abiotic cathode [53]. Therefore, BESs offer an alternative and promising method to dehalogenate pharmaceuticals and thereby significantly decrease the environmental burden of pharmaceutical point sources, such as hospital wastewaters [53]. It is noteworthy that the studies by Liang and Kong have shown that chlorinated nitroaromatic antibiotic chloramphenicol (CAP) could be efficiently reduced to antibacterial inactivity products by the abiotic cathode. Moreover, the biocatalyzed cathode had higher CAP reduction efficiency than that of the abiotic cathode. However, under a cathode potential of approximately -0.7 V (vs SHE), the reductive dechlorination of the nitro group did not reduce the product of the CAP (aromatic amine product AMCl2) to an AM (dechlorinated product of AMCl2) [10, 54]. With the lower cathode potential (such as -1.25 V vs SHE), partially dechlorinated product AMCl from CAP can be further dechlorinated to AM with an abiotic cathode [54]. In addition,

halogenated antibiotic florfenicol (FLO) can also be dehalogenated efficiently with an abiotic cathode (below -0.75 V vs SHE) [54].

5.3.2 Biocathode Reduction

Researchers have shifted their focus from abiotic cathodes toward the implementation of biotic cathodes due to their biocatalyzed activity, economic viability, and environmental sustainability. A microbial community or a single strain is used as the biocatalyst to catalyze the reduction reactions upon acceptance of electrons from the cathode. Electroactive microorganisms as the catalysts on the cathode of BES could greatly lower the overpotential of electrochemical reactions and lead to higher removal efficiencies/rates. The application of biocathodes might achieve better BES performance, which could overcome the limitations of the electron transfer from the cathode to the microorganism, and then reduce the biological overpotentials of those stubborn compounds [55]. The biocathode had significantly higher efficiency and selectivity to pollutants reduction than that of the abiotic cathode. Moreover, using organic wastes, which were abundant and easily accessible, as the carbon source of biocathode, could be another option to further reduce BES operating costs. Various studies have been carried out using biocathodes for the reduction of azo dyes, nitroaromatic compounds, and halogenated aromatic compounds [6].

5.3.2.1 Azo Dyes

A large number of BESs with biocathode were employed for azo dyes reduction. Using activated carbon (GAC) as a redox mediator, reactive red 272 was efficiently reduced with 95% degradation rate without external electron donors. The use of low-cost granular activated carbon is allowed for buffering of OCP and pH in the solution, which is useful for removal rates improvement [56]. Liu et al. demonstrated that the decolorization efficiency and COD removal of the Reactive Brilliant Red X-3B in biocathode BESs, with activated carbon fiber attached to steel as the cathode, were significantly higher than the sum of those values in a single biological reactor and a single electrochemical reactor, which indicated that there was a synergistic effect between the electrode reaction and biodegradation [57]. Kong et al. modified the configuration of BES to be a sleeve-type with a compact structure for Acid Orange 7 decolorization. The decolorization efficiency was enhanced to be higher than 98% from 0.14 to 2.00 mM. The advantages of the sleeve-type BES might be due to the reduction in the distance between anode and cathode and the large proton exchange area, both of which would decrease the internal resistance of BESs [58]. Gao et al. demonstrated that pure culture *Shewanella oneidensis* MR-1 formed biocathode could enhance the capture of electrons from the cathode for the reduction of Acid Orange 7 with or without co-substrate lactate [59]. Wang et al. developed a corrugated stainless-steel mesh electrode module that showed better

hydrodynamic characteristic and azo dye decolorization performance comparing to the conventional planar electrodes module. BES with the corrugated electrode spacing of 2 mm had the highest efficiencies of azo dye AO7 decolorization ($90.9 \pm 0.4\%$) and COD removal efficiencies ($36.8 \pm 3.8\%$) at HRT of 8 h, which were 30.7% and 15.2% higher than that with electrode spacing of 8 mm, respectively. These results highlight the corrugated stainless-steel mesh electrode module holding great potential for engineering application of BES [60, 61].

5.3.2.2 Nitroaromatic Compounds

It may be attractive to use a biologically catalyzed cathode, as a number of bacteria are known to selectively and completely convert nitroaromatics to their corresponding aromatic amine compounds, with less-toxic intermediate products generation. Wang et al. reported the conversion of NB to aniline (AN) by using fed-batch BESs with biocathodes. When a voltage of 0.5 V was applied in the presence of glucose, 88.2% of NB (0.5 mM) was transformed to AN within 24 h, which was 10.25 and 2.90 times higher than those with abiotic cathode and with open circuit, respectively. AN was the only product detected during the bioelectrochemical reduction of NB (maximum efficiency 98.70%), whereas in abiotic conditions, nitrosobenzene was observed as an intermediate of the NB reduction to AN (decreased efficiency to 73.75%) [62]. A membraneless, upflow MEC-type BES (0.5 V power supply) was developed to reduce NB with 98% removal efficiency obtained at cathode zone, resulting in a maximum removal rate of 3.5 mol m^{-3} day^{-1}. The main product from NB degradation was aniline, and the production rate reached 3.06 mol m^{-3} day^{-1}. The overall energy requirement for this process was less than 0.075 kWh mol^{-1} NB [63]. The biocathode BESs (bioc-BESs) were used for p-nitrophenol (PNP) degradation with sodium bicarbonate as the carbon source. The PNP degradation efficiency in bioc-BES reached 96.1% within 72 h with an applied voltage of 0.5 V, which was much higher than that obtained in the biocathode BES without applied voltage (bioc-BES-NAP), open circuit biocathode BES (OC-bioc-BES), or abiotic cathode BES (abioc-BES) [64]. Liang et al. found that selective transformation of NB to AN maintained with biocathode communities after carbon source switchover. Continuous electrical field stimulation and carbon source switchover had markedly influences on the microbial community succession [65].

5.3.2.3 Halogenated Aromatic Compounds

Microorganisms can reduce some halogenated aromatic compounds by using them as terminal electron acceptors under highly reducing conditions in the BES cathode. Some studies have investigated the use of BESs to stimulate microbial dechlorination processes. Electrodes poised at potentials low enough to serve as an electron donor for microbial respiration, but high enough to avoid the production of hydrogen, have been proposed as an alternative to the use of soluble electron donors for

stimulating the bioremediation of chlorinated contaminants. Liang and Sun et al. demonstrated the higher peak currents and lower overpotentials for CAP reduction at the biocathode compared with abiotic cathode. Importantly, the antibacterial activity of CAP was completely removed, and nitro group reduction combined with dechlorination reaction enhanced detoxification efficiency of CAP [10, 66, 67]. Aulenta et al. firstly reported that an electrochemical cell with a solid-state electrode polarized at −500 mV vs SHE, in combination with a low-potential redox mediator (methyl viologen), can efficiently transfer electrochemical reducing equivalents to microorganisms that respire using chlorinated solvents. Using this approach, the dechlorination of TCE into *cis*-dichloroethene has been reported, where lower amounts of vinyl chloride and ethane were observed as the end products at a maximum formation rate of 0.0112 mol m^{-3} day^{-1} [68]. It has been reported that *Geobacter lovleyi* can reduce tetrachloroethene to *cis*-dichloroethene with an electrode serving as the sole electron donor [69]. *Anaeromyxobacter dehalogenans* attached to the electrodes poised at −300 mV vs SHE reductively dechlorinated 2-chlorophenol to phenol. Nevertheless, there was no dechlorination in the absence of organisms, and the electrode-driven dechlorination stopped when the supply of electrons to the electrode was disrupted [42]. Feng et al. successfully improved the reduction and defluorination efficiency of *p*-fluoronitrobenzene (*p*-FNB) in a BES with graphite as the cathode. The reaction rate for *p*-FNB was higher than the sum of the rates of the two control systems, i.e., a biological system and an electrocatalytic system, by a maximum of 62.9% under a voltage of 1.4 V [3].

5.3.3 Mechanism

The processes of organic contaminants reduction in the cathodes of BESs could be summarized as the following two categories: abiotic cathode reduction and biocathode reduction (Fig. 5.3). At the abiotic cathode, organic contaminants could be reduced by using the proton and electron, resulting in the formation of less-toxic, reduced products. Nevertheless, the less-reduced intermediates that may be more toxic would accumulate in the system due to the incomplete reduction [70]. Moreover, the abiotic reduction process was usually slow, in particular for halogenated aromatic compounds, due to overpotentials of those stubborn compounds. Therefore, low pH and noble metal-modified electrodes were usually required for the selective reduction process, adding to the cost of the water treatment [71]. Regarding the biocathode reduction process, numerous electroactive bacteria, reduction-related bacteria, and fermentative-related bacteria were involved in the reduction of contaminants. The enriched reduction-related species were able to catalyze the reduction process, and the electroactive species could facilitate the electron transfer between the biocatalyst and the electrode. It was reported that electrodes could offer a continuous and finely controlled supply of electrons to microorganisms on the surface of electrodes [72]. In the biocathode, with the help of electroactive bacteria, reduction-related bacteria could obtain additional electrons from the
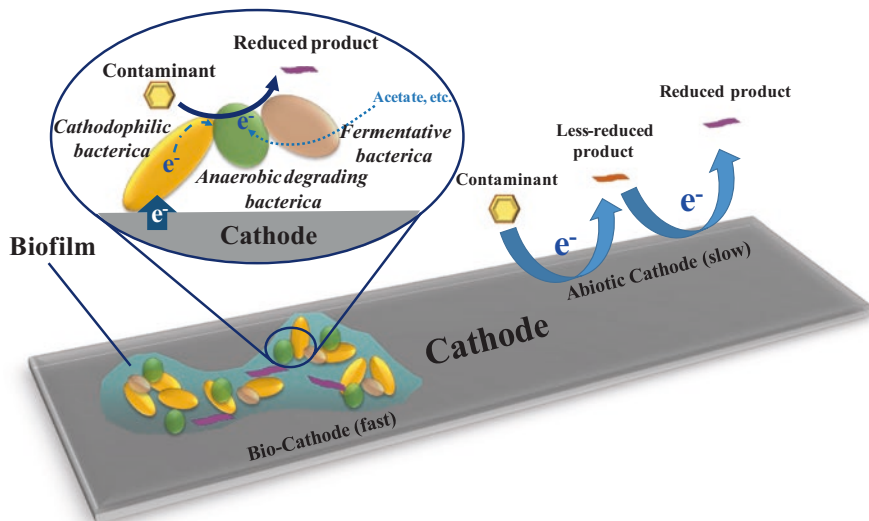
Fig. 5.3 Schematic of organic contaminants reduction in the cathode of BESs

electrode to catalyze the reduction process, which was more effective than obtaining electrons from the fermentation of organic matter. Fermentative-related bacteria in the BES cathode were able to utilize the reduced products as the sources of carbon and energy during growth, with fermentation products, such as fatty acids and electrons, generated. Due to the synergistic cooperation among reduction-related species, potential electroactive species, and fermentative-related species, the coupled reaction system could be driven close to thermodynamic equilibrium, resulting in higher-efficiency treatments than are obtained in a conventional electrochemical process [73]. Additionally, the microbial metabolic processes could also be facilitated due to the existence of a thermodynamic driving force, which came from the negative cathode potential [74]. Moreover, the viability of electricigens adhered to electrodes could be enhanced under a suitable micro-electric field. Thus, the redox ability of anaerobic microbes to the substrate was improved, and the electron transfer rate increased, which attributed to the enhanced reductive transformation [75].

5.4   Scope of Integration with Existing Technologies

Although BES technology showed great potential for wastewater treatment, it may not be sufficient as a stand-alone wastewater treatment technology to achieve high effluent quality and may be better used in conjunction with current technologies. The reported coupled systems are summarized as the following two categories: one mode is linking BES as a separate process with other treatment systems, and another mode is introducing electrode modules into existing treatment processes, such as
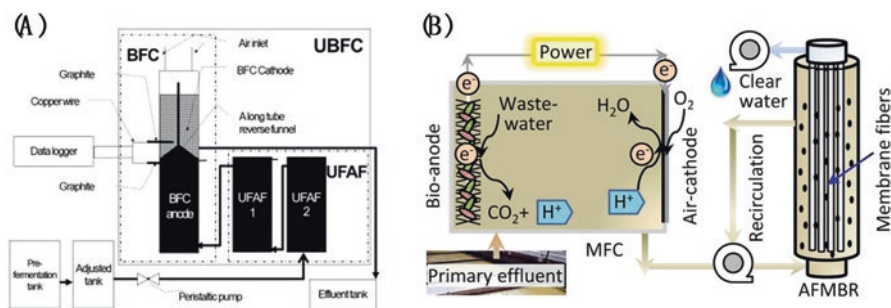
Fig. 5.4 Schematic of the upflow biofilter circuit (UBFC) system (**a**) [77] (Reprinted from Ref. [77], Copyright 2011, with permission from Elsevier) and BC reactor with conductive UF membrane used as the air-biocathode (**b**) [83] (Reprinted with the permission from Ref. [83]. Copyright 2014 American Chemical Society)

anaerobic sludge blanket reactor, bio-contact, and Fenton system [76]. BES as a polishing strategy could increase the quality of the effluent, either by reducing its organic matter content or by removing nutrients.

5.4.1 Linking BES as a Separate Process

Several methods, through linking BES as a separate process with other treatment systems, have been proposed to improve industrial wastewater treatment. For instance, a membraneless upflow bioreactor combined with the immobilization of microorganisms on granular activated carbon electrode surface as biocatalyst, called an upflow biofilter circuit, was renovated and reinvented for treating biodiesel wastewater without chemical treatment or nutrient supplementation. The developed system was combined with a pre-fermentation, influent adjustment, upflow anaerobic filter and biofilter circuit connected sequentially (as seen in Fig. 5.4a). The optimal conditions were operated with an organic loading rate (OLR) of 30.0 g COD L^{-1} day, a HRT of 1.04 day, maintained at a pH level of 6.5–7.5, and aerated at 2.0 L min^{-1}. The capital cost was \$118,380 per ton of treated COD, less than the AD capital cost, and the power consumption was 0.152 kW kg^{-1} of treated COD, close to the aerated lagoon operational cost [77].

Other methods, such as integrating BES (MFC-type) with nitrification step [78], submerging the electrode modules in the aeration tank of an activated sludge process [79], combining the BES with a sequencing batch reactor [80] or a membrane-aerated biofilm process [81], or integrating it into a rotating biological contactor [82], have also been proposed. The main problem with these combined systems, however, is that in all cases, the effluent quality is poor without subsequent sedimentation or filtration to remove particulates, and some of these systems also require wastewater aeration. Logan et al. has developed a two-stage laboratory-scale combined treatment process, consisting of microbial fuel cells and an anaerobic fluidized

bed membrane bioreactor (MFC-AFMBR), to produce high-quality effluent with minimal energy demands (Fig. 5.4b). The combined system was operated continuously for 50 days feeding with domestic wastewater at room temperature, resulting in 92.5% overall COD removal with >99% removal of TSS to a final effluent concentration of <1 mg L^{-1}. The energy requirement of the AFMBR is much less than that needed for aerobic MBRs with internal membranes that require air sparging to control membrane fouling [83]. These results showed that a combined MFC-AFMBR system could be used to effectively treat domestic primary effluent at ambient temperatures, producing high effluent quality with low energy requirements.

5.4.2 Introducing Electrode Modules into Existing Treatment System

5.4.2.1 Aerobic Process

Integrating BES as an individual component into an aeration tank will not require additional land space in a wastewater treatment plant. Coupling MFCs with the activated sludge process, the most widely used biological wastewater treatment technology so far, is considered a promising way to achieve energy-efficient wastewater treatment and deliver a scaled-up application of MFCs. Especially, the sequencing batch reactor (SBR), attributed to its operating flexibility and high adaptability to automatic control, shows great potential to combine with an MFC. Yu et al. reported an integrated MFC-SBR (sequencing batch reactor) process (Fig. 5.5) with enhanced electricity generation by optimizing COD loading distribution between the MFC and SBR modules. The results showed that the performances of individual modules in this system were linked through the "food chain" and the overall system performance was governed by COD loading distribution. By increasing HRT from 10 to 40 min, the COD removal rate in the MFC increased by 52.4%, and the maximum power density increased from 3.9 to 4.5 W m^{-3} [84].

In addition, there are several other potential benefits by installing MFCs into an aeration tank. First, a portion of wastewater can be treated under anaerobic condition at anodes of MFCs, and thus the requirement of aeration, as well as energy consumption, is greatly reduced. Second, the effluent from MFCs contains much lower concentrations of suspended solids. Therefore, the secondary sludge production will be lower than that of activated sludge treatment only. Third, MFCs can produce some electric energy (although low currently), which can be potentially applied to offset the energy consumption by the treatment process. Fourth, MFCs may physically act as solid media to form a hybrid attached/suspended growth system, with advantages demonstrated in previous integrated fixed-film-activated sludge processes. These potential benefits cannot be verified or examined at the current stage of research because of the small scales of MFCs; however, it is beneficial to consider them for future studies [85]. Meanwhile, most of the existing
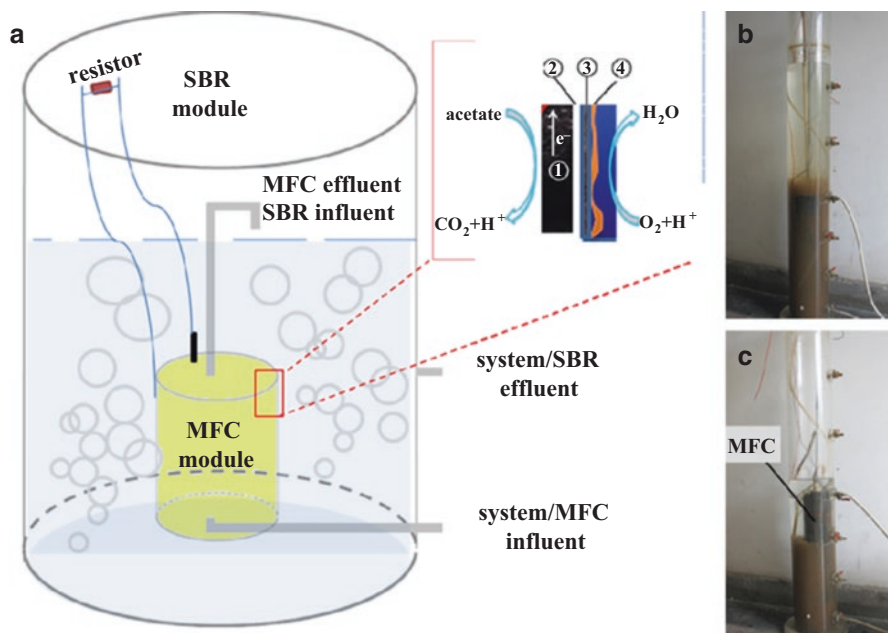
Fig. 5.5 Schematic of the MFC-SBR system (**a**) and photos of the integrated system during the operation period of settling (**b**) and withdrawn. (**c**) Numbered items: (1) granular graphite anode, (2) nonwoven separator, (3) graphite felt cathode, and (4) biofilm [84] (Reprinted from Ref. [84], Copyright 2014, with permission from Elsevier)

BES-based aerobic processes focused on maximizing COD removal and energy recovery from high organic substance-containing wastewater, with minimal notice having been paid to the removal of recalcitrant compounds.

5.4.2.2 Anaerobic Process

The successful application of BES to wastewater treatment inevitably depends on the improvement of performance and the reduction of costs at a scaled-up level. Considering that anaerobic active sludge processes are widely used in wastewater treatment for refractory contaminant degradation, the combination of BES with an anaerobic active sludge reactor may be a great potential application, especially with BES module embedding into the traditional anaerobic sludge reactor. This integrated process will allow electrons produced at the anode to be a driving force for removing pollution at the cathode as a part of the energy-saving process. Moreover, the most recent research has focused on the performance of BES with membrane-less configurations to increase contaminants degradation and reduce the construction and operation costs such as membrane fouling replacement [76]. In general, an ion exchange membrane is one of the costly components of BESs, for either

operational maintenance or replacement during long-term operation for wastewater treatment. In addition, the installation of a membrane could cause pH gradient and increase internal resistance. Development of a membrane-free BES could be a cost-effective approach for potential applications and further enhancements of power density or to decrease the potential loss by reducing the resistance. Attempts to develop membrane-free, single-chamber reactors have been reported on MFCs for power generation and MEC for hydrogen production. Most of the reported configurations were set up by installing anode and cathode vertically in one chamber. The electrogenic microorganisms on the anode might be inhibited if the influent contained inhibitory or toxic compounds. Penetration of the cathode content to the anode chamber is a design and operational issue for cathodic reduction-type BES treatment of toxic metals and other compounds for reductive detoxification. To solve the abovementioned problems, Wang et al. developed a membrane-free, continuously feeding, single-chamber upflow biocatalyzed electrolysis reactor (UBER) by setting the cathode below the anode (Fig. 5.6a). The oxidative toxic chemical, i.e., nitrobenzene (NB), was reductively transformed into a less- or nontoxic reduced form in the cathode zone with the oxidation of an electron donor in the anode zone. After NB is reduced to AN, the toxicity is significantly reduced. Aromatic amines are 500 times less inhibitory, on average, than their corresponding nitroaromatics. An external power source (0.5 V) was provided between the anode and cathode to enhance electrochemical reactions. The results demonstrated the feasibility of NB reduction in the novel system at volumetric loading rate (LR) at 3.5 mol m^{-3} day^{-1} with >98% NB removal efficiency. The additional energy required was less than 0.075 kWh mol^{-1} NB [63]. Shen et al. developed a coupled bioelectrochemical system (BES)-upflow anaerobic sludge blanket (UASB) for enhanced p-nitrophenol (PNP) removal. Three-electrode systems, i.e., the cathode, anode, and reference electrode, were horizontally installed in the sludge bed of the UASB system for applied potential or current control (Fig. 5.6b). Compared to the control UASB reactor, both PNP removal and the formation of its final reductive product p-aminophenol (PAP) were notably improved in the UASB-BES process. More importantly, the required dosage of organic co-substrate was significantly reduced comparing to that in the UASB reactor. Organic carbon flux analysis suggested that biogas production from the organic co-substrate was seriously suppressed, while direct anaerobic reduction of PNP was not remarkably affected by the current input in the UASB-BES system [86]. Based on this work, Shen and Jiang subsequently developed another two-electrode UASB-BES system (Fig. 5.6c) for enhancing nitro reduction and dechlorination of recalcitrant 2,4-dinitrochlorobenzene, with the optimization of key operation parameters, the system stability, and the microbial biodiversity emphasized. The ability to resist shock loading was strengthened in the UASB-BES system in comparison with the control UASB system. The enhanced reduction of DNCB in UASB-BES could be attributed to higher microbial diversity and the enrichment of reduction-related species, potential electroactive species, and fermentative species. The observed efficient and stable performance highlights the potential for long-term operation and full-scale application of the UASB-BES coupled system, particularly for highly recalcitrant pollutants removal [74]. Wang et al.
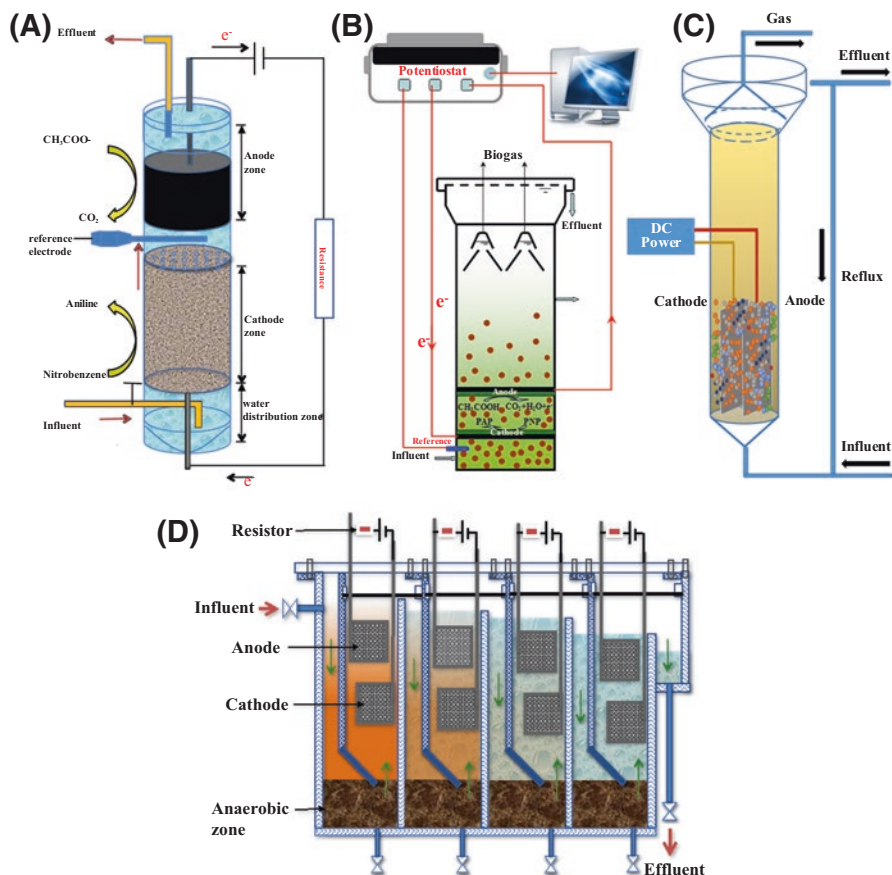
Fig. 5.6 Schematic diagram of the BES-anaerobic system for recalcitrant pollutants removal: single-chamber upflow biocatalyzed electrolysis reactor (UBER) (**a**) [63] (Reprinted from Ref. [63], Copyright 2012, with permission from Elsevier), coupled BES-upflow anaerobic sludge blanket (UASB) system (**b**) [86] (Reprinted from Ref. [86], Copyright 2014, with permission from Elsevier), UASB-BES [74] (Reprinted from Ref. [74], Copyright 2016, with permission from Elsevier) and anaerobic baffled reactor (ABR)-BES [87] (Reprinted from Ref. [87], Copyright 2014, with permission from Elsevier)

developed an integrated system incorporating BES with an anaerobic baffled reactor (ABR) by installing membraneless BES modules into four compartments of ABR (called ABR-BES) (Fig. 5.6d) and tested this process at a small pilot scale for the treatment of azo dye (alizarin yellow R: AYR) wastewater. The decolorization efficiency of AYR was significantly improved in ABR-BES with electrolysis compared with ABR-BES without electrolysis. Higher power supply (0.7 V) led to higher AYR decolorization efficiency and current density. The novel membrane-free ABR-BES provided a new concept for BES scaling-up to the energy-efficient treatment of azo dye wastewater [87].

5.5   Conclusions and Future Perspectives

BESs can be a promising technology for wastewater treatment, due to decreased energy demand and sludge production, and for resource recovery. The unique feature of BESs for hazardous organic contaminants degradation is the use of electrodes as non-exhaustible electron acceptors, or even donors, for contaminant degradation, requiring very little to zero external energy or external chemical amendments. Electrons generated microbially from the anode of BES enable bioremediation processes for removing persistent pollutants in wastewater with energy recovery. Co-metabolism has been demonstrated as the main removal mechanism for contaminants in the anaerobic anode chamber. Highly oxidized hazardous organic contaminants, which are resistant to microbial oxidative degradation in the anode, could be efficiently reduced at abiotic/biocathode driven by bioanodes. Moreover, the biocathode could greatly lower the overpotential of electrochemical reactions and lead to higher efficiency and selectivity to pollutants reduction than that of the abiotic cathode. Although BES technology has the potential to replace traditional treatment technologies, it may not be sufficient as a stand-alone wastewater treatment technology to achieve high effluent quality and may be better used in conjunction with current technologies. Coupling BESs with other conventional processes by introducing electrode modules into existing treatment system is considered a promising way to achieve energy-efficient wastewater treatment and deliver scaled-up applications of BESs. There are still some challenges for the BES-based technology application, including the optimization of the integrated system, the long-term operation for practical wastewater treatment, and the tolerance issues in the integrated system.

So far, most of BES studies have been conducted at laboratory scale from 1.5 μL to several liters. Large-scale BESs ($\sim$1 m^3) were tested for power generation or contaminants degradation [12]. Despite its success in laboratory-scale studies, if BES is to become a practical wastewater treatment technology, many of the economic and technological issues around its scaling-up must be addressed. These BES systems pose significant challenges toward up-scaling and practical applications, among which cost is the most critical issue. The current cost of a BES, due to the use of expensive electrode materials, membranes, and reactors, is approximately 100 times than that of a conventional anaerobic digester, making the generation of a small amount of electricity in such systems insufficient to justify their cost. Further effort is still needed to study new modification in electrodes and to explore low-cost membranes, which is essential to develop a successful BES system. In addition, there are stability issues, such as the logging of electrodes and membrane fouling, during long-term operation for practical wastewater treatment. Future progress in the above aspects will not only improve the wastewater treatment performance in BES but also have high theoretical research value and practical significance in the construction and application of the integrated process [76]. Bioelectrochemical degradation of hazardous organic contaminants will yield even more impressive results when we move beyond the limitations of the current systems.

References

1. Kang JW (2014) Removing environmental organic pollutants with bioremediation and phytoremediation. Biotechnol Lett 36(6):1129–1139

2. Mahlambi MM, Ngila CJ, Mamba BB (2015) Recent developments in environmental photocatalytic degradation of organic pollutants: the case of titanium dioxide nanoparticles—a review. J Nanomater 2015:1–29

3. Feng H, Zhang X, Liang Y, Wang M, Shen D, Ding Y, Huang B, Shentu J (2014) Enhanced removal of *p*-fluoronitrobenzene using bioelectrochemical system. Water Res 60:54–63

4. Pant D, Van Bogaert G, Diels L, Vanbroekhoven K (2010) A review of the substrates used in microbial fuel cells (MFCs) for sustainable energy production. Bioresour Technol 101(6):1533–1543

5. Santoro C, Arbizzani C, Erable B, Ieropoulos I (2017) Microbial fuel cells: from fundamentals to applications. A review. J Power Sources 356:225–244

6. Butti SK, Velvizhi G, Sulonen MLK, Haavisto JM, Oguz Koroglu E, Yusuf Cetinkaya A, Singh S, Arya D, Annie Modestra J, Vamsi Krishna K, Verma A, Ozkaya B, Lakaniemi A-M, Puhakka JA, Venkata Mohan S (2016) Microbial electrochemical technologies with the perspective of harnessing bioenergy: maneuvering towards upscaling. Renew Sust Energ Rev 53:462–476

7. Zhang Q, Hu J, Lee D-J (2016) Microbial fuel cells as pollutant treatment units: research updates. Bioresour Technol 217:121–128

8. Zhang Y, Angelidaki I (2014) Microbial electrolysis cells turning to be versatile technology: recent advances and future challenges. Water Res 56:11–25

9. Zhen G, Lu X, Kumar G, Bakonyi P, Xu K, Zhao Y (2017) Microbial electrolysis cell platform for simultaneous waste biorefinery and clean electrofuels generation: current situation, challenges and future perspectives. Prog Energ Combust 63:119–145

10. Liang B, Cheng HY, Kong DY, Gao SH, Sun F, Cui D, Kong FY, Zhou AJ, Liu WZ, Ren NQ, Wu WM, Wang AJ, Lee DJ (2013) Accelerated reduction of chlorinated nitroaromatic antibiotic chloramphenicol by biocathode. Environ Sci Technol 47(10):5353–5361

11. Yun H, Liang B, Kong DY, Cheng HY, Li ZL, Gu YB, Yin HQ, Wang AJ (2017) Polarity inversion of bioanode for biocathodic reduction of aromatic pollutants. J Hazard Mater 331:280–288

12. Cui D, Cui M-H, Lee H-S, Liang B, Wang H-C, Cai W-W, Cheng H-Y, Zhuang X-L, Wang A-J (2017) Comprehensive study on hybrid anaerobic reactor built-in with sleeve type bioelectrocatalyzed modules. Chem Eng J. https://doi.org/10.1016/j.cej.2017.07.167

13. Kaiser JP, Feng Y, Bollag JM (1996) Microbial metabolism of pyridine, quinoline, acridine, and their derivatives under aerobic and anaerobic conditions. Microbiol Rev 60(3):483–498

14. Hu W-J, Niu C-G, Wang Y, Zeng G-M, Wu Z (2011) Nitrogenous heterocyclic compounds degradation in the microbial fuel cells. Process Saf Environ 89(2):133–140

15. Zhang C, Li M, Liu G, Luo H, Zhang R (2009) Pyridine degradation in the microbial fuel cells. J Hazard Mater 172(1):465–471

16. Zhang C, Liu G, Zhang R, Luo H (2010) Electricity production from and biodegradation of quinoline in the microbial fuel cell. J Environ Sci Health A Toxic/Hazard Subst Environ Eng 45(2):250–256

17. Rezaei F, Xing D, Wagner R, Regan JM, Richard TL, Logan BE (2009) Simultaneous cellulose degradation and electricity production by *Enterobacter cloacae* in a microbial fuel cell. Appl Environ Microbiol 75(11):3673–3678

18. Jiang X, Shen J, Xu K, Chen D, Mu Y, Sun X, Han W, Li J, Wang L (2017) Substantial enhancement of anaerobic pyridine bio-mineralization by electrical stimulation. Water Res 130:291–299

19. Wu Z, Webley PA, Zhao D (2010) Comprehensive study of pore evolution, mesostructural stability, and simultaneous surface functionalization of ordered mesoporous carbon (FDU-15) by wet oxidation as a promising adsorbent. Langmuir 26(12):10277–10286

20. Zhang T, Gannon SM, Nevin KP, Franks AE, Lovley DR (2010) Stimulating the anaerobic degradation of aromatic hydrocarbons in contaminated sediments by providing an electrode as the electron acceptor. Environ Microbiol 12(4):1011–1020
21. Britto JM, Oliveira SB, Rabelo D, Rangel MC (2008) Catalytic wet peroxide oxidation of phenol from industrial wastewater on activated carbon. Catal Today 133–135:582–587
22. Fu F, Dionysiou DD, Liu H (2014) The use of zero-valent iron for groundwater remediation and wastewater treatment: a review. J Hazard Mater 267:194–205
23. Li J, Li M, Zhang J, Ye D, Zhu X, Liao Q (2013) A microbial fuel cell capable of converting gaseous toluene to electricity. Biochem Eng J 75:39–46
24. Song TS, Wu XY, Zhou CC (2014) Effect of different acclimation methods on the performance of microbial fuel cells using phenol as substrate. Bioprocess Biosyst Eng 37(2):133–138
25. Alshehri ANZ (2015) Employment of microbial fuel cell technology to biodegrade naphthalene and benzidine for bioelectricity generation. Int J Curr Microbiol App Sci 4(1):134–149
26. Wu CH, Yet-Pole I, Chiu YH, Lin CW (2014) Enhancement of power generation by toluene biodegradation in a microbial fuel cell in the presence of pyocyanin. J Taiwan Inst Chem E 45(5):2319–2324
27. Cheng HY, Liang B, Mu Y, Cui MH, Li K, Wu WM, Wang AJ (2015) Stimulation of oxygen to bioanode for energy recovery from recalcitrant organic matter aniline in microbial fuel cells (MFCs). Water Res 81:72–83
28. Friman H, Schechter A, Ioffe Y, Nitzan Y, Cahan R (2013) Current production in a microbial fuel cell using a pure culture of Cupriavidus basilensis growing in acetate or phenol as a carbon source. Microb Biotechnol 6(4):425–434
29. Husain Q (2010) Peroxidase mediated decolorization and remediation of wastewater containing industrial dyes: a review. Rev Environ Sci Biotechnol 9(2):117–140
30. Fang Z, Song HL, Cang N, Li XN (2015) Electricity production from Azo dye wastewater using a microbial fuel cell coupled constructed wetland operating under different operating conditions. Biosens Bioelectron 68(68):135–141
31. Sun J, Hu YY, Bi Z, Cao YQ (2009) Simultaneous decolorization of azo dye and bioelectricity generation using a microfiltration membrane air-cathode single-chamber microbial fuel cell. Bioresour Technol 100(13):3185–3192
32. Wen Q, Kong F, Zheng H, Cao D, Ren Y, Yin J (2011) Electricity generation from synthetic penicillin wastewater in an air-cathode single chamber microbial fuel cell. Chem Eng J 168(2):572–576
33. Wang L, Liu Y, Ma J, Zhao F (2016) Rapid degradation of sulphamethoxazole and the further transformation of 3-amino-5-methylisoxazole in a microbial fuel cell. Water Res 88:322–328
34. Zhang Q, Zhang Y, Li D (2017) Cometabolic degradation of chloramphenicol via a meta-cleavage pathway in a microbial fuel cell and its microbial community. Bioresour Technol 229:104–110
35. Liu R, Gao C, Zhao YG, Wang A, Lu S, Wang M, Maqbool F, Huang Q (2012) Biological treatment of steroidal drug industrial effluent and electricity generation in the microbial fuel cells. Bioresour Technol 123:86–91
36. Marashi SK, Kariminia HR, Savizi IS (2013) Bimodal electricity generation and aromatic compounds removal from purified terephthalic acid plant wastewater in a microbial fuel cell. Biotechnol Lett 35(2):197–203
37. Chandrasekhar K, Venkata Mohan S (2012) Bio-electrochemical remediation of real field petroleum sludge as an electron donor with simultaneous power generation facilitates bio-transformation of PAH: effect of substrate concentration. Bioresour Technol 110:517–525
38. Clauwaert P, van der Ha D, Verstraete W (2008) Energy recovery from energy rich vegetable products with microbial fuel cells. Biotechnol Lett 30(11):1947–1951
39. Feng Y, Yang Q, Wang X, Liu Y, Lee H, Ren N (2011) Treatment of biodiesel production wastes with simultaneous electricity generation using a single-chamber microbial fuel cell. Bioresour Technol 102(1):411–415

40. Kassongo J, Togo CA (2013) Evaluation of full-strength paper mill effluent for electricity generation in mediator-less microbial fuel cells. Afr J Biotechnol 10(69):15564–15570

41. Cheng S, Kiely P, Logan BE (2011) Pre-acclimation of a wastewater inoculum to cellulose in an aqueous-cathode MEC improves power generation in air-cathode MFCs. Bioresour Technol 102(1):367–371

42. Strycharz SM, Gannon SM, Boles AR, Franks AE, Nevin KP, Lovley DR (2010) Reductive dechlorination of 2-chlorophenol by Anaeromyxobacter dehalogenans with an electrode serving as the electron donor. Environ Microbiol Rep 2(2):289–294

43. Wang H, Luo H, Fallgren PH, Jin S, Ren ZJ (2015) Bioelectrochemical system platform for sustainable environmental remediation and energy generation. Biotechnol Adv 33(3–4):317–334

44. Mu Y, Rabaey K, Rozendal RA, Yuan Z, Keller J (2009) Decolorization of azo dyes in bioelectrochemical systems. Environ Sci Technol 43(13):5137–5143

45. Liu L, Li FB, Feng CH, Li XZ (2009) Microbial fuel cell with an azo-dye-feeding cathode. Appl Microbiol Biotechnol 85(1):175–183

46. Mu Y, Rozendal RA, Rabaey K, Keller J (2009) Nitrobenzene removal in bioelectrochemical systems. Environ Sci Technol 43(22):8690–8695

47. Shen J, Feng C, Zhang Y, Jia F, Sun X, Li J, Han W, Wang L, Mu Y (2012) Bioelectrochemical system for recalcitrant *p*-nitrophenol removal. J Hazard Mater 209–210:516–519

48. Shen J, Zhang Y, Xu X, Hua C, Sun X, Li J, Mu Y, Wang L (2013) Role of molecular structure on bioelectrochemical reduction of mononitrophenols from wastewater. Water Res 47(15):5511–5519

49. Haggblom MM, Knight VK, Kerkhof LJ (2000) Anaerobic decomposition of halogenated aromatic compounds. Environ Pollut 107(2):199–207

50. Ghattas AK, Fischer F, Wick A, Ternes TA (2017) Anaerobic biodegradation of (emerging) organic contaminants in the aquatic environment. Water Res 116:268–295

51. Hennebel T, Benner J, Clauwaert P, Vanhaecke L, Aelterman P, Callebaut R, Boon N, Verstraete W (2011) Dehalogenation of environmental pollutants in microbial electrolysis cells with biogenic palladium nanoparticles. Biotechnol Lett 33(1):89–95

52. Mu Y, Radjenovic J, Shen J, Rozendal RA, Rabaey K, Keller J (2010) Dehalogenation of iodinated X-ray contrast media in a bioelectrochemical system. Environ Sci Technol 45(2):782–788

53. De GB, Hennebel T, Vanhaecke L, Soetaert M, Desloover J, Wille K, Verbeken K, Verstraete W, Boon N (2011) Biogenic palladium enhances diatrizoate removal from hospital wastewater in a microbial electrolysis cell. Environ Sci Technol 45(13):5737–5745

54. Kong D, Liang B, Yun H, Cheng H, Ma J, Cui M, Wang A, Ren N (2015) Cathodic degradation of antibiotics: characterization and pathway analysis. Water Res 72:281–292

55. Chen GW, Choi SJ, Lee TH, Lee GY, Cha JH, Kim CW (2008) Application of biocathode in microbial fuel cells: cell performance and microbial community. Appl Microbiol Biotechnol 79(3):379–388

56. Cardenas-Robles A, Martinez E, Rendon-Alcantar I, Frontana C, Gonzalez-Gutierrez L (2013) Development of an activated carbon-packed microbial bioelectrochemical system for azo dye degradation. Bioresour Technol 127:37–43

57. Liu S, Song H, Wei S, Liu Q, Li X, Qian X (2015) Effect of direct electrical stimulation on decolorization and degradation of azo dye reactive brilliant red X-3B in biofilm-electrode reactors. Biochem Eng J 93:294–302

58. Kong F, Wang A, Liang B, Liu W, Cheng H (2013) Improved azo dye decolorization in a modified sleeve-type bioelectrochemical system. Bioresour Technol 143:669–673

59. Gao S-H, Peng L, Liu Y, Zhou X, Ni B-J, Bond PL, Liang B, Wang A-J (2016) Bioelectrochemical reduction of an azo dye by a Shewanella oneidensis MR-1 formed biocathode. Int Biodeterior Biodegrad 115(Supplement C):250–256

60. Wang HC, Cheng HY, Cui D, Zhang B, Wang SS, Han JL, Su SG, Chen R, Wang AJ (2017) Corrugated stainless-steel mesh as a simple engineerable electrode module in bio-

electrochemical system: hydrodynamics and the effects on decolorization performance. J Hazard Mater 338:287–295

61. Wang HC, Cui D, Yang LH, Ding YC, Cheng HY, Wang AJ (2017) Increasing the bio-electrochemical system performance in azo dye wastewater treatment: reduced electrode spacing for improved hydrodynamics. Bioresour Technol 245:962–969

62. Wang AJ, Cheng HY, Liang B, Ren NQ, Cui D, Lin N, Kim BH, Rabaey K (2011) Efficient reduction of nitrobenzene to aniline with a biocatalyzed cathode. Environ Sci Technol 45(23):10186–10193

63. Wang A-J, Cui D, Cheng H-Y, Guo Y-Q, Kong F-Y, Ren N-Q, Wu W-M (2012) A membrane-free, continuously feeding, single chamber up-flow biocatalyzed electrolysis reactor for nitrobenzene reduction. J Hazard Mater 199–200:401–409

64. Wang X, Xing D, Ren N (2016) p-Nitrophenol degradation and microbial community structure in a biocathode bioelectrochemical system. RSC Adv 6(92):89821–89826

65. Liang B, Cheng H, Van Nostrand JD, Ma J, Yu H, Kong D, Liu W, Ren N, Wu L, Wang A, Lee DJ, Zhou J (2014) Microbial community structure and function of nitrobenzene reduction biocathode in response to carbon source switchover. Water Res 54:137–148

66. Sun F, Liu H, Liang B, Song R, Yan Q, Wang A (2013) Reductive degradation of chloramphenicol using bioelectrochemical system (BES): a comparative study of abiotic cathode and biocathode. Bioresour Technol 143:699–702

67. Liang B, Kong D, Ma J, Wen C, Yuan T, Lee DJ, Zhou J, Wang A (2016) Low temperature acclimation with electrical stimulation enhance the biocathode functioning stability for antibiotics detoxification. Water Res 100:157–168

68. Aulenta F, Catervi A, Majone M, Panero S, Reale P, Rossetti S (2007) Electron transfer from a solid-state electrode assisted by methyl viologen sustains efficient microbial reductive dechlorination of TCE. Environ Sci Technol 41(7):2554–2559

69. Strycharz SM, Woodard TL, Johnson JP, Nevin KP, Sanford RA, Löffler FE, Lovley DR (2008) Graphite electrode as a sole electron donor for reductive dechlorination of tetrachlorethene by Geobacter lovleyi. Appl Environ Microbiol 74(19):5943–5947

70. Cui D, Guo YQ, Cheng HY, Liang B, Kong FY, Lee HS, Wang AJ (2012) Azo dye removal in a membrane-free up-flow biocatalyzed electrolysis reactor coupled with an aerobic bio-contact oxidation reactor. J Hazard Mater 239–240:257–264

71. Deng Q, Li X, Zuo J, Ling A, Logan BE (2010) Power generation using an activated carbon fiber felt cathode in an upflow microbial fuel cell. J Power Sources 195(4):1130–1135

72. Chun CL, Payne RB, Sowers KR, May HD (2013) Electrical stimulation of microbial PCB degradation in sediment. Water Res 47(1):141–152

73. Jiang X, Shen J, Lou S, Mu Y, Wang N, Han W, Sun X, Li J, Wang L (2016) Comprehensive comparison of bacterial communities in a membrane-free bioelectrochemical system for removing different mononitrophenols from wastewater. Bioresour Technol 216:645–652

74. Jiang X, Shen J, Han Y, Lou S, Han W, Sun X, Li J, Mu Y, Wang L (2016) Efficient nitro reduction and dechlorination of 2,4-dinitrochlorobenzene through the integration of bioelectrochemical system into upflow anaerobic sludge blanket: a comprehensive study. Water Res 88:257–265

75. Zhu L, Gao K, Qi J, Jin J, Xu X (2014) Enhanced reductive transformation of p-chloronitrobenzene in a novel bioelectrode–UASB coupled system. Bioresour Technol 167:303–309

76. Kong F, Wang A, Ren HY (2014) Improved azo dye decolorization in an advanced integrated system of bioelectrochemical module with surrounding electrode deployment and anaerobic sludge reactor. Bioresour Technol 175C:624–628

77. Sukkasem C, Laehlah S, Hniman A, O'Thong S, Boonsawang P, Rarngnarong A, Nisoa M, Kirdtongmee P (2011) Upflow bio-filter circuit (UBFC): biocatalyst microbial fuel cell (MFC) configuration and application to biodiesel wastewater treatment. Bioresour Technol 102(22):10363–10370

78. Virdis B, Rabaey K, Rozendal RA, Yuan Z, Keller J (2010) Simultaneous nitrification, denitrification and carbon removal in microbial fuel cells. Water Res 44(9):2970–2980

79. Cha J, Choi S, Yu H, Kim H, Kim C (2010) Directly applicable microbial fuel cells in aeration tank for wastewater treatment. Bioelectrochemistry 78(1):72–79

80. Liu XW, Wang YP, Huang YX, Sun XF, Sheng GP, Zeng RJ, Li F, Dong F, Wang SG, Tong ZH, Yu HQ (2011) Integration of a microbial fuel cell with activated sludge process for energy-saving wastewater treatment: taking a sequencing batch reactor as an example. Biotechnol Bioeng 108(6):1260–1267

81. Yu CP, Liang Z, Das A, Hu Z (2011) Nitrogen removal from wastewater using membrane aerated microbial fuel cell techniques. Water Res 45(3):1157–1164

82. Cheng KY, Ho G, Cord-Ruwisch R (2011) Novel methanogenic rotatable bioelectrochemical system operated with polarity inversion. Environ Sci Technol 45(2):796–802

83. Ren L, Ahn Y, Logan BE (2014) A two-stage microbial fuel cell and anaerobic fluidized bed membrane bioreactor (MFC-AFMBR) system for effective domestic wastewater treatment. Environ Sci Technol 48(7):4199–4206

84. Wang Y-P, Zhang H-L, Li W-W, Liu X-W, Sheng G-P, Yu H-Q (2014) Improving electricity generation and substrate removal of a MFC–SBR system through optimization of COD loading distribution. Biochem Eng J 85:15–20

85. Zhang F, Ge Z, Grimaud J, Hurst J, He Z (2013) In situ investigation of tubular microbial fuel cells deployed in an aeration tank at a municipal wastewater treatment plant. Bioresour Technol 136:316–321

86. Shen J, Xu X, Jiang X, Hua C, Zhang L, Sun X, Li J, Mu Y, Wang L (2014) Coupling of a bioelectrochemical system for p-nitrophenol removal in an upflow anaerobic sludge blanket reactor. Water Res 67C:11–18

87. Cui D, Guo YQ, Lee HS, Wu WM, Liang B, Wang AJ, Cheng HY (2014) Enhanced decolorization of azo dye in a small pilot-scale anaerobic baffled reactor coupled with biocatalyzed electrolysis system (ABR-BES): a design suitable for scaling-up. Bioresour Technol 163:254–261

Chapter 6
Recovery of Metals from Wastes Using Bioelectrochemical Systems

Liping Huang, Qian Zhou, and Xie Quan

6.1 Introduction

The decline of valuable metal resources, together with the increased future valuable metals demand, is likely to provide future impetus for increased metal recovery from wastes such as fly ash, sewage sludge, spent batteries, and electronic scrap materials, as well as hydroprocessing catalysts. The recovery and reuse of these wastes usually require the conversion from an insoluble to a soluble form. While a number of pyrometallurgical methods have been employed to achieve dissolution of the metal oxides, the emission of toxic gases into the environment, high energy costs, and associated expensive capital equipment costs decrease its desirable attraction. The hydrometallurgical process is thus more favorable from an environment conservation viewpoint. However, this process requires large amounts of reagents and thus augments the operational costs. In addition, it also results in the co-dissolution of other metals, increasing the complexity and cost of recovering value-added metals and treatment of unwanted elements. A biohydrometallurgical process or bioleaching offers attractive features for the extraction of metals from solid materials due to lower cost and energy requirements, environmental safety, and operational flexibility [1]. However, there are additional remaining challenges for using this approach, such as increasing leaching rates and reducing sludge generation. Electrochemical reduction is regarded as a potential strategy for the separation of the dissolved metals from solutions owing to multiple merits such as effectiveness, selectivity, robustness, versatility, controllability, less sludge production, easy operation, short retention time, reusability of the effluent, and amenability to automation and control [2]. However, electrochemical processes have high energy requirements

L. Huang (✉) · Q. Zhou · X. Quan
Key Laboratory of Industrial Ecology and Environmental Engineering,
Ministry of Education (MOE), School of Environmental Science and Technology,
Dalian University of Technology, Dalian, China
e-mail: lipinghuang@dlut.edu.cn

and can require expensive catalysts to decrease electrode overpotentials. Development of more environmentally benign and less energy-demanding technologies would therefore be useful for treating these metal wastes and wastewaters with simultaneous value-added metal recovery.

Bioelectrochemical systems (BESs) is a newly developed technology for wastes and wastewaters treatment based on the integration of biological processes, electrochemical reduction, material science, engineering, and many related area together. BESs have recently attracted much attention owing to its high efficiency, low cost, environmental sustainability, and ambient operating temperatures with biologically compatible materials [3, 4]. BESs present potential opportunities for the microbially catalyzed conversion of electrical current into attractive value-added products, providing significant environmental benefits through the displacement of chemical production by conventional means [3–8]. Following this exploration, an emerging research field recovering metals from wastes using BESs, namely, metallurgical BESs, is being developed in an early stage and shows the most promising prospects due to its beneficial for both limited resource and environmental ecosystem. There are a few reviews about BES technologies for metal recovery [9–13]. In an effort to minimize overlap, this review gives a condensed overview of our current knowledge of metal recovery from wastes using these next-generation technologies, highlighting recent discoveries of the so-called self-driven BES processes for mixed metal recovery and discussing critically the influence of different processes and design parameters for recovery efficiencies.

6.2 Bioelectrochemical Systems (BESs)

A BES is called a microbial fuel cell (MFC) if electricity is generated and the overall reaction is exothermic. When the overall reaction is endothermic, power is needed to drive the non-spontaneous reaction, and this BES is regarded as a microbial electrolysis cell (MEC) [7]. It is reasonably believed that microbial electrosynthesis is being emerged as an alternative option to provide reducing/oxidizing power for biochemical production via electricity [4]. In terms of metal recovery, the specific cathodic condition in BESs provides preferable situation for metal reduction, and this metallurgical BES technology has thus widened the application range of BESs [14]. In the following sections, latest experimental results on bioelectroreduction for heavy metals and the developments of two aspects, namely, abiotic cathodes and biocathodes, will be briefly summarized. The newly developed MFC-MEC self-driven systems for multiple metal recovery will be emphatically discussed. Influencing factors and electron transfer mechanisms in these systems, as well as the scientific and technical challenges that have yet to be faced in the future, will be reviewed in detail.

6.3 Abiotic Cathodes

The reducing environment in the BES cathode, which is a sink for electrons originally coming from organic compounds in the anode, holds an advantage for the treatment of oxidized metal pollutants. In most cases, the oxidative electron acceptors contact with the electrode surface directly and receive the electrons released from the cathode. In addition, cathodic electrons can be also indirectly transferred through mediators such as anthraquinone analogues, riboflavin, Fe(III), and O_2 (Fig. 6.1 and Table 6.1) [15–52]. These direct and indirect electron transfer processes generally occur on the cathodes due to the high redox potentials of oxidative metal electron acceptors. Take the extensively explored Cr(VI) reduction in MFCs, for example (Table 6.1). Cr(VI) can be directly reduced to the less toxic $Cr(OH)^{2+}$ and $Cr(OH)_2^+$ in addition to $Cr(OH)_3$ on the abiotic cathodes of MFCs [15, 22]. Alternatively, Cr(VI) also indirectly accepts electrons through the in situ generated hydrogen peroxide from oxygen oxidation [15] or the external added riboflavin or Fe(III) [17, 18], which receives electrons either directly from the abiotic cathodes or via the mediator of anthraquinone-2,6-disulfonate. These mediated electron transfers explain the accelerated Cr(VI) reduction on the abiotic cathodes.

6.3.1 Individual Metal Recovery

By controlling operating conditions, some desirable metals or products can be generated from the cathode chamber. BESs thus could be used as not only an environmental remediation technology, but also a tool to produce metals from low-grade

Fig. 6.1 Electron transfer pathways in the abiotic cathodes of BESs
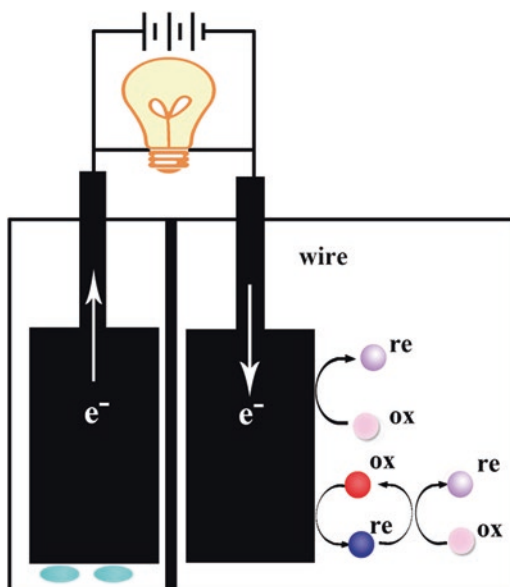
Table 6.1 Metals removed/reduced in the abiotic cathodes of BESs

Type of substrate	Electron donor	Reactor	Anode	Cathode	Operation mode	Initial pH in catholyte	Electron acceptor	Removal/reduction rate[a]	Product	Power production (W/m³)[b] or applied voltage (V)[c]	References
Ag(I)	Acetate and yeast	Two-chamber MFC	Carbon fiber	Carbon cloth	Batch	7.0	Ag(I)	6.2–25	Ag	9.4[b]	[19]
Ag(I)	Acetate	Two-chamber MFC	Graphite plate	Graphite plate	Continuous	4.0	Ag(I)	18	Ag	9.8[b]	[20]
Ag(I) thiosulfate	Acetate	Two-chamber MFC	Graphite plate	Graphite plate	Continuous	10.0	Ag(I)	8.8	Ag and Ag₂O	3.2[b]	
Tetrachloroaurate	Acetate and yeast	Two-chamber MFC	Carbon fiber	Carbon cloth	Batch	2.0	Au(III)	8.3–15	Au	3.3–7.1[b]	[21]
Cr(VI)	Acetate	Two-chamber MFC	Graphite plate	Graphite plate	Batch	2.0	Cr(VI)	0.67	Cr(OH)₃	2.2[b]	[22]
	Acetate	Two-chamber MFC	Carbon felt	Graphite paper	Batch	2.5	Cr(VI)	8.1	Cr(OH)₃	16[b]	[23]
	Acetate	Two-chamber MFC	Graphite plate	Rutile-coated graphite	Batch with light irradiation	2.0	Cr(VI)	0.97	Not provided	0.25[b]	[24]
	Acetate	Two-chamber MFC	Graphite plate	Rutile-coated graphite	Batch in the dark	2.0	Cr(VI)	0.61	Not provided	0.12[b]	

	Substrate	Reactor	Anode	Cathode	Mode	pH	Species		Product	Rate	Ref
	Glucose	Two-chamber MFC	Carbon felt	Carbon felt	Batch	2.0	Cr(VI)+O$_2$	2.9	Cr(III)	2.5[b]	[15]
	Glucose and anthraquinone-2,6-disulfonate	Two-chamber MFC	Carbon felt	Carbon felt	Batch	2.0	Cr(VI)+O$_2$	4.9	Cr(III)	Not provided	
	Glucose	Two-chamber MFC	Carbon felt	Carbon felt	Batch	2.0	Cr(VI)	0.35	Cr(III)	0.3[b]	
Cu(II)	Acetate	Two-chamber MFC	Graphite plate	Graphite foil	Continuous	3.0	Cu(II)	6.9	Cu	1.2[b]	[14]
	Acetate	Two-chamber MFC	Graphite plate	Graphite foil	Continuous	3.0	Cu(II)+O$_2$	5.9	Cu	2.2[b]	
	Glucose	Two-chamber MFC	Graphite plate or graphite felt	Graphite plate	Batch	4.7	Cu(II)	7.1	Cu	0.34[b]	[25]
	Glucose	Membrane-free baffled MFC	Graphite plate or graphite felt	Graphite plate	Batch	7.0	Cu(II)	1.3–4.9	Cu and Cu$_2$O	0.05–0.31[b]	[26]
	Acetate	Membrane-free MFC	Graphite felt	Graphite disk	Batch	2.0	Cu(II)	0.12–0.19	Cu and Cu$_2$O	0.02–0.06[b]	[27]
	Acetate	Two-chamber MFC	Graphite felt	Graphite plate	Batch	9.0	Cu(II)	36	Cu and Cu$_2$O	3.8[b]	[28]

(continued)

Table 6.1 (continued)

Type of substrate	Electron donor	Reactor	Anode	Cathode	Operation mode	Initial pH in catholyte	Electron acceptor	Removal/reduction rate[a]	Product	Power production (W/m^3)[b] or applied voltage (V)[c]	References
	Acetate	One-chamber air-cathode MFC	Carbon fiber brush	Graphite rod	Batch	2.0	Cu(II)	13–15	Cu	18.8[b]	[29]
	Acetate	Four-chamber microbial desalination cell	Carbon felt	Graphite plate	Batch	3.0	Cu(II)	4.5–34.2	Cu and Cu$_2$O	1.0–5.0[b]	[30]
	Acetate	Two-chamber MFC	Graphite felt	Carbon rod, stainless steel mesh, titanium sheet, or copper sheet	Multiple batch cycle	2.0	Cu(II)	Carbon rod: 4.1 (1st cycle) −6.8 (12th cycle), stainless steel mesh: 6.1 (1st cycle) −7.3 (12th cycle), copper sheet: 8.3 (1st cycle) −7.3 (12th cycle)	Cu	1.9–2.6[b]; 1.82–3.1[b]; 1.91–6.5[b]; 3.2–10.8[b]	[31]

Hg(II)	Acetate and yeast	Two-chamber MFC	Graphite felt	Carbon paper	Batch	2.0	Hg(II)	9.8	Hg	7.6[b]	[32]
Mn(VI)	Glucose	Two-chamber MFC	Carbon paper	Carbon cloth	Batch	3.6	Mn(VI)	5.8	MnO$_2$	2.2[b]	[33]
	Glucose	Bushing MFC	Carbon paper	Carbon cloth	Batch	3.6	Mn(VI)	Not provided	MnO$_2$	80[b]	
V(V)	Glucose and Na$_2$S	Two-chamber MFC	Carbon fiber felt	Carbon fiber felt	Batch	2.0	V(V)	1.8	V(IV)	3.7[b]	[34]
	Glucose and Na$_2$S	Two-chamber MFC	Carbon fiber felt	Carbon fiber felt	Batch	1.0	V(V)	1.8	V(IV)	3.9[b]	[35]
Co(III)	Acetate	Two-chamber MEC	Graphite felt	Graphite felt	Batch	2.0	Co(III)	3.6	Co(II)	0.2[c]	[36]
	Acetate	Two-chamber MFC	Graphite felt	Graphite felt	Batch	2.0	Co(III)	2.6	Co(II)	0.2[b]	[37]
	Acetate	Two-chamber MFC	Graphite felt	Graphite felt	Batch	2.0	Co(III) catalyzed by Cu(II)	8.0	Co(II)	0.8[b]	[38]
Co(II)	Acetate	Two-chamber MEC	Graphite felt	Graphite felt	Batch	6.2	Co(II)	7.9	Co and H$_2$	0.5[c]	[39]

(continued)

Table 6.1 (continued)

Type of substrate	Electron donor	Reactor	Anode	Cathode	Operation mode	Initial pH in catholyte	Electron acceptor	Removal/reduction rate[a]	Product	Power production (W/m^3)[b] or applied voltage (V)[c]	References
	Acetate	Two-chamber MEC	Graphite felt	Nickel foam	Batch	5.8–6.0	Co(II)	1.4–6.7	Co and H$_2$	0.2–0.7[c]	[40]
				Stainless steel woven mesh				2.5–6.5			
				Titanium sheet				3.0–6.7			
				Carbon cloth				2.5–7.0			
				Nickel foam + graphene				2.5–6.7			
	Acetate	Two-chamber MEC self-driven by MFC	Graphite felt in MFC and MEC	Graphite felt in MFC and carbon rod in MEC	Batch	2.0 in MFC and 6.0 in MEC	Co(III) in MFC and Co(II) in MEC	Co(III): 4.2; Co(II): 3.7	Co(II) in MFC and Co in MEC	–	[41]
Ni(II)	Acetate	Two-chamber MEC	Carbon felt	Stainless steel mesh	Batch	3.0–6.0	Ni(II)	13–19	Ni	0.5–1.1[c]	[42]

Zn(II)	Acetate	One-chamber air-cathode MFC with supported liquid membrane extraction	Carbon cloth	Carbon cloth coated with Pt	Batch	5.4	O_2	5.2	Zn(II)	4.5[a]	[43]
		One-chamber air-cathode MFC alone						2.8		1.9[a]	
Cr(VI), V(V)	Glucose	Two-chamber MFC	Carbon fiber felt	Carbon fiber felt	Batch	2.0	Cr(VI), V(V)	0.8	Cr(III) and V(IV)	6.2[b]	[44]
Cu(II), Pb(II), Cd(II), Zn(II)	Acetate	Two-chamber MEC	Carbon felt	Titanium wire	Batch	2 M HCl	Cu(II), Pb(II), Cd(II), Zn(II)	Cu(II): 8.9; Pb(II): 2.3; Cd(II): 2.8; Zn(II): 1.2	Cu, Pb, Cd, Zn	0–1.7[c]	[5]
Cu(II), Ni(II), Fe(II)	Acetate	Two-chamber MEC	Graphite brush	Carbon cloth coated with Pt	Batch	2.9	Cu(II), Ni(II), Fe(II)	Cu(II): 16, Ni(II): 6.3, Fe(II): 5.0	Cu, Ni, H_2	1.0[c]	[45]

(continued)

Table 6.1 (continued)

Type of substrate	Electron donor	Reactor	Anode	Cathode	Operation mode	Initial pH in catholyte	Electron acceptor	Removal/reduction rate[a]	Product	Power production (W/m^3)[b] or applied voltage (V)[c]	References
Cr(VI), Cd(II)	Acetate	Two-chamber MEC driven by MFC	Carbon brush	Carbon cloth	Batch	2.0 and 6.0	Cr(VI), Cd(II)	Cr(VI): 0.5–1.0; Cd(II): 0.03–0.7	Cr(III) in MFC; Cd in MEC	–	[46]
Zn(II), Cd(II)	Acetate	One-chamber air-cathode MFC	Carbon cloth	Carbon cloth coated with Pt	Batch	7.0	O$_2$	Zn(II): 0.6–0.7; Cd(II): 0.5–0.7	ZnS and CdS	60.7–67.7	[47]
Cr(VI), Cu(II), Cd(II)	Acetate	Two-chamber MEC driven by MFC	Graphite felt in MFC and MEC	Carbon rod in MFC and titanium sheet in MEC / Carbon rod in both MFC and MEC	Batch	2.0	Cr(VI) in MFC, Cu(II) in MFC, and Cd(II) in MEC	Cr(VI): 7.0–7.2; Cu(II): 5.8–7.5; Cd(II): 3.2–3.6; Cr(VI): 8.5; Cu(II):7.6; Cd(II): 0.0	Cr(III) in MFC; Cu in MFC, and Cd and H$_2$ in MEC	–	[48]
	Acetate	Two-chamber MEC driven by MFC	Graphite felt in MFC and MEC	Carbon rod in MFC and titanium sheet in MEC	Continuous	2.0	Mixed influent of Cr(VI), Cu(II), and Cd(II)	Cr(VI): 0.3–1.3; Cu(II): 0.3– –1.3; Cd(II): 1.3	Cr(III) and Cu in MFC, and Cd in MEC	–	[49]

Cu(II), Co(II)	Acetate	Two-chamber MEC driven by MFC	Graphite felt in MFC and MEC	Carbon rod in MFC, carbon rod, stainless steel mesh, or titanium sheet in MEC	Batch	2.0	Cu(II) in MFC and Co(II) in MEC	Cu(II): 5.6, Co(II): 3.5, 3.3, or 3.8 (carbon rod, stainless steel mesh, or titanium sheet in MEC)	Cu in MFC and Co in MEC	—	[50]
Cu(II), Co(II) and Li(I)	Acetate	Two-chamber MEC driven by MFC	Graphite felt in MFC and MEC	Various mesh size stainless steel	Continuous	2.0	Mixed influent of Cu(II), Co(II) and Li(I)	Cu(II) or Co(II): 1.1, and Li(I): 0.3 (mesh size 60#)	Cu in MFC, Co in MEC, and Li(I) in effluent	—	[51]
Cu(II) and Cd(II)	Acetate	Two-chamber MFC shifted to two-chamber MEC	Graphite felt	Carbon rod, titanium sheet, or nickel foam	Batch	2.0	Mixed Cu(II) and Cd(II)	Cu(II): 4.8–4.9, Cd(II): 5.9 (carbon rod), 5.3 (titanium sheet) and 5.0 (nickel foam)	Cu in MFC mode, Cd and H$_2$ in MEC mode	6.4[b] in MFC mode; 0.5[c] in MEC mode	[52]

aCalculated on the basis of net cathodic compartment (mg/L/h)
bPower output calculated on the basis of net cathodic compartment (W/m³)

ores in hydrometallurgical processes. Great attention has been paid to the finding of metals possibly used as cathodic electron acceptors in BESs. Diverse aqueous metals including Cr(VI) [18, 22, 23], V(V) [34, 35, 44], Mn(VII) [33], Hg(II) [32], Ni(II) [42], Cu(II) [14, 25–31], Ag(I) [19, 20], Au(III) [21], and Co(II) [39, 40] have been individually reduced, whereas Cd(II) was removed through biosorption, and Zn(II) was formed as sulfides precipitation or separated through supported liquid membrane extraction in one-chamber air-cathode BESs [43, 47] (Table 6.1). This list does not seem to have an end so far. Besides aqueous metal ions, metals in dissoluble particles such as Co(III) in particles $LiCoO_2$, major component of the extensively applied lithium-ion batteries, can be also reduced on the cathodes of both MFCs and MECs [36, 37]. Cathodic electrons play a synergetic interaction with HCl for cobalt leaching, leading to the decrease of apparent activation energy of cobalt leaching in both MFCs (30.6 kJ/mol) [37] and MECs (16.6 kJ/mol) [36], in comparison with the 30.8–98.7 kJ/mol in open circuit controls (OCC). The presence of Cu(II) catalyst further decreases the apparent activation energy of cobalt leaching in MFCs to 11.8 kJ/mol [38]. These results demonstrate the more efficiency of BES technologies than conventional chemical processes, and thus provide new efficient approaches for recovery of metals in solid wastes and broaden the applicable BESs for recycling spent lithium-ion batteries. In terms of net energy production/consumption, BES technologies show appreciable advantages over conventional electrochemical processes due to the always free fuels in the anodes [4]. Taking silver metal, for example, an abiotic cathode MFC can achieve recovery of pure silver metal and electrical production at a rate of 0.0143 kWh per kg of silver (69.9 kg silver per kWh energy output) in comparison with an electricity spending of 3.81 kWh per kg of silver at an optimum condition in a conventional electrowinning [19]. Thus the use of abiotic cathode MFCs for metal recovery would be to use the "green" electricity produced in the MFC to supply power for electrowinning. This process has the advantage to keep the reactions take place in only one system and thus reduce the overall energy losses. Besides, abiotic cathode BESs can also achieve higher metal removal efficiency and product purity than conventional electrolysis reactors [20, 26, 27]. In terms of endurance to high metal concentrations and acidic environments, abiotic cathodes show advantages over biological processes, in which microorganisms can only endure to a certain metal concentration at neutral or close to neutral pHs, after which inhibition of the biological processes takes over [39, 53]. Another striking feature is that abiotic cathodes can work well at a wide range of metal concentration compared to either a maximal metal concentration for conventional biological processes or a minimal metal concentration required for conventional electrolysis process [20, 26, 27]. All of these aforementioned above demonstrate the advantages of BESs over conventional technologies for individual metal leaching and/or subsequent recovery from aqueous phase to solid phase.

6.3.2   Multiple Metal Recovery and Self-Driven BESs

While numerous initiatives have attempted to develop abiotic cathodes for individual metal recovery, there is a trend of switch to recover multiple metals, making BES a more practical application (Table 6.1). Species of V(V) and Cr(VI), co-present in wastewaters from vanadium mining and vanadium pentoxide manufacture, are recently proved to be, respectively, reduced on the abiotic cathodes of MFCs [44]. Cr(VI) is firstly reduced as an electron acceptor due to its higher electrochemical redox potential than V(V), which leads to Cr(VI) decreasing and Cr(III) depositing, and the electrochemical redox potential of V(V) then exceeds that of Cr(VI) and begins to act as an electron acceptor to be converted into soluble V(IV). This repeatable and alternative reduction of Cr(VI) and V(V) provides an applicable abiotic cathode MFCs for separating Cr(VI) from V(V) in practical wastewaters. Closely following this report and by varying the cathode potentials of MECs, multiple metals of Cu, Pb, Cd, and Zn are selectively and sequentially separated from a simulated municipal solid waste incineration ash leachate, providing an approach for cathodic recovery of metals from municipal solid waste incineration ash leachate [5]. Similarly, simulating fly ash leachate containing multiple metals of Zn(II), Pb(II), and Cu(II) can be also successfully recovered with Zn(0) and Pb(0) in electrolysis cells and Cu(0) in MFCs [54]. While Cu(0) and Ni(0) are deposited on the same cathodes of MECs at an applied voltage of 1.0 V [45], the Cu(0) deposited in MFC mode substantially enhances the subsequent Cd(II) reduction on the same cathode but in MEC mode [52], stressing the critical catalysis role of previously deposited copper in Cd(II) reduction. Cu(0) deposited on the cathodes of titanium sheet or stainless steel woven mesh has also been observed to improve electricity generation and Cu(II) removal from cathoyte of MFCs over prolonged time [31]. Obviously, competition of electrons among protons, Cu(II), Ni(II), and Fe(II) on the cathodes of MECs was also observed, explaining the delay of each metal ion reduction in comparison with individual Cu(II), Ni(II), or Fe(II) reduction on the same cathodes [45]. While MFCs or MECs as wastes treatment methods could be potentially used for treating ash leachates, metallurgical wastewaters, and landfill leachates, the products with multiple metals require the subsequent separation of these mixed metals unless otherwise specially used. In addition, these MFCs, MECs, and electrolysis cells were separately operated, in which not only electricity generated from MFCs was not utilized but also external applied voltages of 1.0–6.0 V were required for MECs and electrolysis cells [45, 54]. In view of this point and enlightened from MFC-MEC coupled system for hydrogen production [55], a self-driven MFC-MEC system successfully carried out the two processes of Co(II) firstly released from particles $LiCoO_2$ on the cathodes of MFCs and subsequently reduced on the cathodes of the connected MECs, which are completely powered by the cobalt leaching MFCs [41]. This self-driven system thus provides a new process of linking MFCs to MECs for complete recovery of cobalt and recycle of spent

lithium-ion batteries with no any external energy consumption. To develop the concept of self-driven system, Cr(VI)-reduced MFCs and Cu(II)-reduced MFCs are connected in parallel or series to successfully power Cd(II)-reduced MECs with simultaneous Cr(VI), Cu(II), and Cd(II) recovery, despite the individual metal influents in each reactor units [48]. Appropriately adjusting the composite of mixed metals of Cr(VI), Cu(II), and Cd(II) under continuous operating condition can achieve complete separation of Cr(VI), Cu(II), and Cd(II) from the mixed influents using this self-driven MFC-MEC systems [49]. For W and Mo deposition, stacked MFC-MEC made of one MEC unit serially connected with three parallel-connected MFC units outperformed other modules, achieving depositions of 27.6% (W) and 75.4% (Mo) with a separation factor of 8.1 and hydrogen production of 0.34 $m^3/m^3/day$ in the MEC unit, compared to 12.3% (W), 52.6% (Mo), and 7.9 (separation factor) in the MFC unit [56]. In the controls of either MEC or MFC unit only, only 15.3% (W) and 60.1% (Mo) (MFC only) and 12.9% (W) and 56.1% (Mo) (MEC only) were deposited from a mixture of W(VI) and Mo(VI). Thus, this process provides a truly sustainable strategy for applicable recovery of multiple metals from electroplating wastewater and ore dressing wastewater used during W and Mo extraction processes with no need for external energy input. Ingenious designs of self-driven MFC-MEC coupled systems together with appropriate influent composites, solution chemistry, and operation modes provide guarantee for sequential metal recovery and complete separation from mixed influents using these zero energy consumption technologies. While metals deposited on the electrodes may need to be peeled from the electrode to achieve their final recovery, the in situ utilization of these deposits for photocatalytic processes may become an attractive strategy for reuse, since many metal oxides exhibit excellent photocatalytic properties [56, 57]. Multiple parameters including initial metal concentration, initial pH, electrode material, electrode distance, exoelectrogenic activities, and the copresence of multiple electron acceptors can particularly affect system performance as well as final products. It is thus essential to discuss these parameters in the following sections.

6.3.3   Critical Factors Influencing System Performance

6.3.3.1   Initial Metal Concentration

A decrease in initial metal concentration resulted in a decrease in cathode potential and an increase in internal resistance of BESs. As a result, cell voltage, current density, and cathodic efficiency decreased as well [14, 19, 20, 25–27]. Thus a high initial metal concentration will generally benefit for BES system performance [14, 29, 30]. However, in view of reduction products, this high initial metal concentration can lead to the deficient cathodic reducibility, which may change the products formed. For example, high initial Cu(II) concentrations of 500–6400 mg/L have led to the formation of non-reductive product of $Cu_4(OH)_6SO_4$ compared to the reductive products of Cu_2O and Cu at a low initial Cu(II) concentration of 200 mg/L

[25–27]. It is thus essential to control initial metal concentration in order for the formation of desirable products and in particular the preferable low metal concentrations for pure reductive metals. However, even at the same initial concentration and the identical metal ion, the variety of metal compounds also affect metal reduction rate, power production, as well as product purity. For example, at identical initial Ag(I) concentrations in the same MFC reactors, species of Ag(I) ions achieved apparent higher reduction rate and power production than Ag(I) thiosulfate complex $(AgS_2O_3)^-$ in addition to the pure Ag in the former and trace Ag_2O in the latter (Table 6.1) [20], stressing the complexity of metal reduction on the cathodes as well as the importance of various metal compounds on system performance.

6.3.3.2   Initial pH

A comparatively high cathode pH is in favor of the reduction of oxidized contaminants that require higher pH, while a low cathode pH benefits to the reduction of oxidized substrates in need of more acidic conditions. In most cases, metal reduction in the abiotic cathode requires an acidic pH such as 2.0–3.0 (Table 6.1). For example, Cr(VI) was reduced to Cr(III) in the abiotic cathode MFCs, during which a low pH substantially improved reduction rate according to Eq. 6.1 [22].

$$Cr_2O_7^{2-} + 14H^+ + 6e^- \rightarrow 2Cr^{3+} + 7H_2O \tag{6.1}$$
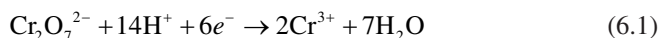
However, in the case of Ag(I) reduction, the pH effect was dependent on the original form of Ag(I) electron acceptor, in which a higher pH of 10 was favorable for the reduction of Ag(I) thiosulfate complex than the pH 4.0 for ion Ag(I) [20]. Different from this, Co(II) reduction in MECs was improved at a range of 85–97% with an increase in initial pHs from 3.8 to 6.2, mainly due to the beneficial acidic environment for hydrogen-producing process and reasonably disadvantage to its electron competitor of Co(II) reduction [39]. These results in concert imply the complex interrelated effects of initial pH, original form of metal, and hydrogen evolution on reducing metals to the same final products. Besides the aforementioned above, the formations of reductive products are also influenced by initial pH. At the tested range of low pHs, pure crystals of copper [14, 25–27], vanadium [34, 35], and mercury [32] with no trace of other corresponding oxides and hydrates were formed on the cathodes because a high pH made these metal ions precipitate as metal oxide and was unavailable for reduction. Considering the fact of low pHs in these metal containing waste streams, the chemical conditions of such wastewaters are suitable for them to act as electron acceptors in the abiotic cathodes, which prefer low pHs and directly reduce metals from wastes with no pH adjustment. However, a bioanode covered by exoelectrogens was preferably operated at near neutral pH to achieve higher power generation from MFCs [4]. A bipolar membrane was therefore more effective to prevent the pH in the catholyte from increasing and the anolyte pH from dropping although part of the energy was lost for maintaining the pH difference [58].

6.3.3.3 Electrode Material

Cathode electrode materials and their design were the most challenging aspects of BESs using air as a final electron acceptor [4]. In this case, cathodic reactions took place on the three-phase surface of solid electrode, liquid catholyte, and gaseous oxygen. Increasing cathode surface area and retaining a small anode relative to the cathode area can keep cathodic reactions from limiting rates of electron transfer at the bioanode and therefore improve power production from MFCs [4]. For soluble metal reduction on the abiotic cathodes, a certain concentration of highly soluble metals such as Cu(II) >200 mg/L at acidic conditions can preserve faster mass transfer in comparison with the occurring of mass transfer limitations of oxygen as a result of low oxygen solubility in air-cathode MFCs [14]. The overpotential for soluble metal reduction is thus much lower than that of oxygen reduction reaction. Consequently, much more porous electrode materials commonly used in aqueous air-cathodes such as granule graphite and graphite felt are not always necessary for abiotic cathodes for recovery of metals at high concentrations. Instead, carbon-based cathodes with equally apparent sizes of anodes like graphite plate and graphite foil are usually accepted [14, 20, 25–27]. However, under the mediation of dissolved oxygen, which is heavily dependent on electrode materials, reduction of metal ions such as Cr(VI) is reasonably related with cathode materials [15]. In addition, metal ions at low concentrations exhibit high overpotentials, resulting in the occurrence of electron competition with other species. For example, hydrogen is well known to be evolved in MECs, and the efficiency is heavily dependent on electrode materials [59, 60]. As a consequence, the reduction of Co(II) as low as 50 mg/L in MECs is indirectly related with electrode material via competition with hydrogen evolution [40]. In view of these considerations, species in the catholyte such as dissolved O_2 or hydrogen evolution should be carefully investigated to ensure efficient metal reduction.

In the case of self-driven MFC-MEC system for multiple metal recovery and separation, cathode material in MEC is crucial for efficient metal recovery, morphology, and crystal form of final products due to its substantial effects on electrode potential and circuit current [48, 50, 51]. Carbon rod as the cathodes of MECs cannot lead to Cd(II) or Co(II) reduction inside regardless of the serial or parallel-connected Cr(VI)-reduced MFCs and/or Cu(II)-reduced MFCs, mainly ascribed to the unsatisfied low voltage output from the MFCs and the consequent high cathode potentials unfavorable for Cd(II) reduction in MECs [50]. Conversely, titanium sheet or stainless steel mesh is a suitable cathode material used successfully for proceeding Cd(II) or Co(II) reduction in MECs with simultaneous Cr(VI) and/or Cu(II) reduction in the serially or parallel-connected MFCs [50]. Even for the same material of stainless steel mesh, Mesh #60 instead of #20 and #120 can achieve the best and complete separation of Cu(II), Co(II), and Li(I) [51]. In addition, the morphology and crystal form of final Co(II)-reduced products are substantially different and heavily dependent on the MEC cathode materials of carbon rod, titanium sheet, and stainless steel mesh [50]. These results in concert stress the importance of MEC

cathode materials for multiple metal recovery and separation in the self-driven MFC-MEC systems, which should be conditionally considered as the aforementioned.

6.3.3.4 Initial Concentration and Ratio of Different Metals

The ratios of different metals in the influent of MFC-MEC coupled system play critical roles in the separation of these metals from mixed influents. Mixed Cu(II) and Co(II) at a same concentration of 50 mg/L was firstly fed in the cathodes of MFCs, followed by the cathodes of the connected MECs. This sequential MFC-MEC cannot achieve the complete separation of Cu(II) and Co(II), leading to the mixed reduced products of Cu(0) and Co(0) on the same cathodes of MECs [50]. Similarly, metals of Cr(VI), Cu(II), and Cd(II) with each of 5 mg/L cannot be completely removed using the self-driven MFC-MEC system, whereas a composite of either 5 mg/L Cr(VI), 1 mg/L Cu(VI), and 5 mg/L Cd(II) or 1 mg/L Cr(VI), 5 mg/L Cu(II), and 5 mg/L Cd(II) can be completely and sequentially recovered from the mixed metals, illustrating the importance of metal composite and ratios for complete metal recovery and separation [49].

6.3.3.5 Electrode Distance

A properly closed anode and cathode distance can decrease internal resistance and thus improve electron transportation from anode to the cathode, and consequently benefit to completely metal reduction. For example, in a pilot and membrane-free MFC using Cu(II) as an electron acceptor, the internal resistance can be decreased from 1694 Ω at a distance of 65 cm to 304 Ω at 35 cm [25]. It was thus concluded that a close anode and cathode created a high circuit current and provided more sufficient electrons for Cu(II) reduction for pure copper, whereas the limited electrons or lower currents at a far anode and cathode distance resulted in the less reduced copper species such as partial Cu(II) reduction to Cu_2O or CuCl [25]. In terms of reactor size, however, a far anode and cathode distance is generally observed in large reactors and results in the consequent low system performances. For example, a large volume up to 16 L in pilot-scale membrane-free MFC substantially decreased system performance for both Cu(II) reduction and power generation compared to other smaller volume MFCs (Table 6.1) [25]. In view of practical application, scale-up reactors with large volumes will satisfy the requirement of large amount wastewater treatment. Based on these considerations, performance in stack cells where many small reactors are connected in parallel or in series may be an alternative choice. However, the variability in the capacity for individual reactor in the stack may lead to voltage reversal in some reactors [61]. In view of this point, a same hydraulic condition and a same substrate concentration are beneficial for less voltage reversal [62]. In addition, various types of control circuit for each cell in the

stack system may also avoid this phenomenon [63]. Much effort is still in great need along this direction for more efficient and practically applied metal recovery from wastes.

6.3.3.6   Exoelectrogenic Activities

Cathodic electrons originally come from organic compounds oxidized by exoelectrogens on the anodes. Exoelectrogenic activities reasonably affect metal reduction on the abiotic cathodes. For example, bioanodes catalyzed by either *Shewanella decolorationis* S12 or *Klebsiella pneumoniae* L17 exhibited slower Cr(VI) reduction than anaerobic activated sludge, mainly ascribed to their different exoelectrogenic activities [15]. In the case of Co(III) reduction on the abiotic cathodes, exoelectrogenic activities were substantially different from those using pentachlorophenol as an electron acceptor in the cathodes in spite of their similar microbial community compositions [37, 64], stressing the changes of exoelectrogenic activities with cathodic electron acceptors. While bacterial community collaboration may occur among many other bacteria and exoelectrogens on the anodes [4, 65], exoelectrogenic activities in linkage with cathodic metal acceptors have attracted less attention. Further investigation of the exoelectrogenic activities of bacteria with diverse metal reductions on the cathodes is still needed.

6.3.3.7   Other Electron Acceptors

Other electron acceptors such as oxygen can heavily affect system performance due to its higher redox potential and competitive ability than the metals present in the cathode. In the case of Cu(II) or Co(II) reduction, the presence of oxygen also consumed electrons and consequently resulted in adverse effects on Cu(II) or Co(II) reduction as well as low cathodic efficiencies [14, 40]. For W(VI) and Mo(VI) deposition in MFCs, however, the presence of oxygen can enhance W and Mo deposition through the in situ produced H_2O_2 and the consequent predominant peroxotungstate and peroxo-polymolybdate despite the always occurrence of competition between oxygen reduction and metal deposition for H^+ ions [66]. The purity of reduced products was also dependent on aerobic and anaerobic environments, where pure copper crystals were attributable to the anaerobic condition, and CuO and Cu_2O other than Cu(0) were formed under an aerobic environment [25–27]. In terms of power production, it is understandable that the multiple electron acceptors of oxygen and Cu(II) had higher current densities than the Cu(II) individually due to a high redox potential of 0.8 V for oxygen [13, 14]. In fact, in view of oxygen reduction, copper here may also function as a catalyst, although the catalysis mechanism was still unclear [14]. Quantitative competition between metal ions and other electron acceptors for electrons transferred from the anode may need to be further

reinforced to stress the greater efficiencies and advantages of abiotic cathodes compared to conventional processes for metal recovery.

6.4 Biocathodes

6.4.1 Recovered Metal

While an abiotic cathode employed as a direct electron donor in the reduction of metals has been proposed, development of microbially catalyzed cathodes (microbial cathodes or biocathodes) revealed that certain electrochemically active bacteria (electrotrophs) are capable of "picking" electrons from the surface of cathodic electrodes and using them to metabolically reduce the oxidative metals in the catholytes. The use of bacteria can avoid some of the drawbacks such as much acidic condition and low sustainability in abiotic cathodes [67, 68]. Metal reduction on the biocathodes can be dated back to 2005, in which Gregory and Lovley [69] demonstrated the occurrence of U(VI) reduction on a graphite plate cathode at a poised potential of −0.3 V (vs SHE) under the catalysis of either *Geobacter sulfurreducens* or enrichment culture (Table 6.2). A substantially higher U(VI) reduction rate of 0.58–0.77 mg/L/h with the presence of *G. sulfurreducens* implies the preferable *G. sulfurreducens* instead of enrichment culture to U(VI) reduction. The pure culture of *G. sulfurreducens* can get energy from reducing or adding electrons to U(VI) and reduce uranium dissolved in groundwater and thus make this metal much less soluble and abate the spread of its contamination. Similar to U(VI) reduction, *Shewanella species* was recently proved to use electrode as electron donor for Cr(VI) reduction [17, 70]. Instead of pure culture, Tandukar et al. [71] constructed a complete biological MFC with mixed culture at both the anode and the cathode and achieved a Cr(VI) reduction rate of 0.17–0.42 mg/L/h on the cathode with spontaneous electricity production of 0.9 W/m³ (Table 6.2). The Cr(VI)-reducing biocathode was further demonstrated with preferable electrode materials for electrotrophic attachment [67], modifications to reactor architecture [72], and minimization of start-up period and enhancement of system performance [73]. The newly established biocathode MECs dominantly composed of *G. psychrophilus*, *Acidovorax ebreus*, *Diaphorobacter oryzae*, *Pedobacter duraquae*, and *Prolixibacter bellariivorans* provide a new approach for aqueous Co(II) recovery concomitant with production of other biomaterials such as gaseous methane and liquefied acetate [53]. Besides metal recovery and other biomaterials production with simultaneous wastes treatment and environmental remediation, another potentially applicable field for biocathodes is metal nanoparticles synthesis, which is a very exciting field because of its potential application in bioenergy, catalysis, electronics, optics, medicine, and environmental remediation. While a large number of bacteria including *Shewanella oneidensis* have been illustrated to act as nanofactories, showing advantages over chemical methods due to the consumption of strong reducing agents and large

quantities of chemicals that can contaminate the nanoparticles [74], biocathodes are expected to develop microbial consortia or pure culture exhibiting both electrotrophic activities and synthesizing metal nanoparticle abilities [75]. However, this concept is still not extensively proved in BESs, and metal-reducing biocathodes are demonstrated in very limited literature (Table 6.2), in which only metals of U(V), Cr(VI), Se(VI), Co(II), Cu(II), and Cd(II) together with a narrow range of operating conditions including initial metal concentration, initial pH, anodic acetate dose, cathodic electrode material, and optimal start-up time were reported [69–73, 76–85]. In addition, OH^- generated from oxygen-reducing biocathode MFCs in situ reacted with Co(II) to form precipitated $Co(OH)_2$, providing a new clean approach for the production of cobalt dihydroxide with simultaneous electricity generation (Table 6.2) [81]. It is very recent that a directed production of selenium-containing nanoparticles in *S. oneidensis* MR-1 cells, with fine-tuned composition and subcellular synthetic location, was achieved by modifying the extracellular electron transfer chain, leading to the development of fine-controllable nanoparticles biosynthesis technologies [75]. Much work is still needed to be paid on this emerging alternative and inexpensive technology for devising new microbial cathode systems for efficient metal reduction and broadening applicable fields of BESs as well. On the other hand, the recovery of metals by biocathodes will likely not displace existing methods of electrochemical or chemical-physical processes, especially for high-strength metal recovery, because of detrimental effects of high concentration of metals on electrotrophic activities. Biocathodes will likely be more appropriate for treatment of relatively low-strength or dilute metal effluents [53, 81, 85]. The overall advantages of biocathodes for recovery of metals from wastes could make them an important method for metal reduction in the near future. Factors including bacterial origin and evolution, initial pH, and metal concentration can particularly influence biocathode performance since environmental conditions can shape microbial consortia in terms of various bacterial roughness, biocompatibilities, electron transfer efficiencies, and stimulus to microbial consortia [53]. In addition, electron transfer mechanisms on the biocathodes, properly different from the bioanodes, are still debatable [68, 86]. In the following sections, these aspects in linkage with metal recovery will be in particular addressed.

6.4.2   Bacterial Origin and Evolution

Microbial consortia inoculated from different sites exhibit various Cr(VI) reduction rates, in which bacteria from a wastewater treatment plant achieved a specific Cr(VI) reduction rate of 0.30 mg/g biomass/h [71] compared to 2.4 mg/g biomass/h obtained from a Cr(VI) contaminated site [72]. Although other factors including reactor architecture and electrode material may also contribute to these differences in Cr(VI) reduction rate, microbial consortia well developed at a Cr(VI) contaminated site is presumably more adaptive and favorable for the Cr(VI) environment in the biocathodes and thus attribute to more efficient Cr(VI) reduction [72]. Further

Table 6.2 Metals removed/reduced in the biocathodes of BESs

Electron acceptor	Biocatalyst	Mediator	Reactor	Anode electrode	Cathode electrode	Carbon source in catholyte	Operation mode	Initial pH	Removal/ reduction rate[a]	Product	Power production (W/ m³)[b], poised potential (V)[c] or applied voltage (V)[d]	References
U(VI)	*Geobacter sulfurreducens*	–	Two-chamber	Graphite plate	Graphite plate	$NaHCO_3$	Batch	6.9	0.58–0.77	U(IV)	–0.3[c]	[69]
	Enrichment culture	–	Two-chamber	Graphite plate	Graphite plate	$NaHCO_3$	Batch	6.9	0.02	U(IV)	–0.3[c]	
Cr(VI)	Enrichment culture	–	Two-chamber	Graphite plate	Graphite plate	$NaHCO_3$	Batch	7.2–7.6	0.17–0.42	$Cr(OH)_3$	0.9[b]	[71]
	Enrichment culture	–	Two-chamber	Graphite plate	Graphite granule	$NaHCO_3$	Batch	7.0	4.4–5.3	$Cr(OH)_3$	2.4[b]	[72]
	Enrichment culture	–	Two-chamber and tubular	Graphite fiber	Graphite granule	$NaHCO_3$	Batch	7.0	3.5	$Cr(OH)_3$	2.0[b]	[73]
		–	Two-chamber and tubular	Graphite fiber	Graphite felt	$NaHCO_3$	Batch	7.0	3.1	$Cr(OH)_3$	3.8[b]	
		–	Two-chamber and tubular	Graphite fiber	Graphite fiber	$NaHCO_3$	Batch	7.0	3.6	$Cr(OH)_3$	4.5[b]	
	Shewanella oneidensis MR-1	–	Two-chamber	Reticulated vitreous carbon	Reticulated vitreous carbon	–	Batch	7.0	0.04	$Cr(OH)_3$	0.03[b]	[70]

(continued)

Table 6.2 (continued)

Electron acceptor	Biocatalyst	Mediator	Reactor	Anode electrode	Cathode electrode	Carbon source in catholyte	Operation mode	Initial pH	Removal/reduction rate[a]	Product	Power production (W/m^3)[b], poised potential (V)[c] or applied voltage (V)[d]	References
	Shewanella putrefaciens W3–18-1	–	Two-chamber	Reticulated vitreous carbon	Reticulated vitreous carbon	–	Batch	7.0	0.04	$Cr(OH)_3$	0.16[b]	
	Shewanella amazonensis SB2B	–	Two-chamber	Reticulated vitreous carbon	Reticulated vitreous carbon	–	Batch	7.0	0.03	$Cr(OH)_3$	0.13[b]	
	Shewanella sp. ANA-3	–	Two-chamber	Reticulated vitreous carbon	Reticulated vitreous carbon	–	Batch	7.0	0.04	$Cr(OH)_3$	0.08[b]	
	Shewanella loihica PV-4	–	Two-chamber	Reticulated vitreous carbon	Reticulated vitreous carbon	–	Batch	7.0	0.03	$Cr(OH)_3$	0.03[b]	
	Shewanella sp. MR-4	–	Two-chamber	Reticulated vitreous carbon	Reticulated vitreous carbon	–	Batch	7.0	0.03	$Cr(OH)_3$	0.08[b]	
	Shewanella oneidensis MR-1	Riboflavin	Two-chamber	Graphite felt	Graphite felt	Lactate	Batch	7.0	1.3–2.0	$Cr(OH)_3$ and Cr(III)-lactate	–0.3[c]	[17]
	–	Riboflavin	Two-chamber	Graphite felt	Graphite felt	Lactate	Batch	7.0	0.17	$Cr(OH)_3$ and Cr(III)-lactate	Not provided	
	–	–	Two-chamber	Graphite felt	Graphite felt	Lactate	Batch	7.0	0.13	$Cr(OH)_3$ and Cr(III)-lactate	0.43[b]	

	Organism		Two-chamber				Batch	5.8			Reference
	Stenotrophomonas sp. YS1	–	Two-chamber	Graphite felt	Graphite felt	NaHCO$_3$	Batch	5.8	2.9	Intracellular Cr(III) ions	1.0	[76]
	Stenotrophomonas maltophilia YS2								3.0	Intracellular Cr(III) ions	1.2	
	Serratia marcescens YS3								3.4	Intracellular Cr(III) ions	2.9	
	Achromobacter xylosoxidans YS8								3.1	Intracellular Cr(III) ions	1.6	
Cu(II)	*Stenotrophomonas maltophilia* JY1	–	Two-chamber	Graphite felt	Graphite felt	NaHCO$_3$	Batch	5.8	2.9	Intracellular Cu(II) ions	0.4	[77, 78]
	Citrobacter sp. JY3								3.5	Intracellular Cu(II) ions	0.4	
	Pseudomonas aeruginosa JY5								3.6	Intracellular Cu(II) ions	0.5	
	Stenotrophomonas sp. JY6								3.6	Intracellular Cu(II) ions	1.1	
Cd(II)	*Ochrobactrum* sp. X1	–	Two-chamber	Graphite felt	Graphite felt	NaHCO$_3$	Batch	5.8	3.1	Intracellular Cd(II) ions	0.5[d]	[79]
	Pseudomonas sp. X3								3.3	Intracellular cd(II) ions	0.5[d]	
	Pseudomonas delhiensis X5								3.2	Intracellular Cd(II) ions	0.5[d]	
	Ochrobactrum anthropi X7								3.1	Intracellular Cd(II) ions	0.5[d]	

(continued)

Table 6.2 (continued)

Electron acceptor	Biocatalyst	Mediator	Reactor	Anode electrode	Cathode electrode	Carbon source in catholyte	Operation mode	Initial pH	Removal/ reduction rate[a]	Product	Power production (W/ m³)[b], poised potential (V)[c] or applied voltage (V)[d]	References
Se(IV)	Enrichment culture	–	One-chamber air-cathode MFC	Carbon cloth	Carbon cloth coated with Pt	Glucose	Batch	7.0	1.3	Se	25[b]	[80]
						Acetate			0.47		18[b]	
Co(II)	Enrichment culture	–	Two-chamber	Graphite felt	Graphite felt	NaHCO₃	Batch	6.2	2.9	Co	0.2[d]	[53]
	Enrichment culture	–	Two-chamber oxygen-reducing MFC	Graphite felt	Graphite felt	Acetate	Batch	5.6	4.7	Co(OH)₂	1.5[b]	[81]
	Enrichment culture	–	Two-chamber MFCs driven by MECs	Graphite felt	Graphite felt	NaHCO₃	Batch	MFC: 2.0	Cu: 6.0	MFC: Cu	0.0	[82]
								MEC: 6.2	Co: 5.3	MEC: Co		
Cd(II)	M	–	Two-chamber	Graphite felt	Graphite felt	NaHCO₃	Batch	5.8	6.56	Cd and Cd(II)	0.5[d]	[83]
						Acetate			7.33			

	Inoculum		Reactor type	Anode	Cathode	Substrate	Mode	pH	Removal	Products		Reference
Cr(VI), Fe(III)	Enrichment culture	–	One-chamber air-cathode MFC	Carbon brush	Carbon cloth coated with Pt	Acetate	Batch	6.5	Cr(VI): 0.08 Fe(III): 0.4	Cr(III)	0.8–1.3[b]	[84]
Cr(VI), Cu(II), Cd(II)	Enrichment culture	–	Two-chamber MFC and	Graphite felt	Graphite felt	NaHCO$_3$	Batch	5.8	Cr(VI): 1.24 Cu(II): 1.07 Cd(II): 0.98	Cr(III) Cu Cd	0.45–0.58[b] 0.5[d]	[85]

[a]Calculated on the basis of net cathodic compartment (mg/L/h)

[b]Calculated on the basis of net cathodic liquid volume (W/m^3)

[c]vs standard hydrogen electrode (SHE). Values reported vs Ag/AgCl were converted to SHE by adding 0.195 V

exploration should use the same reactor architecture with identical electrode material to compare effects of different bacterial origins on metal reduction in order to deeply understand relations between microbial consortia and metal reduction.

Another important issue about the catalysts of microbial consortia is the efficient evolution strategies for specific microbial consortia. It has long been recognized that mixed species biofilm of *Klebsiella pneumoniae*, *Pseudomonas fluorescens*, and *Pseudomonas aeruginosa* grown in a flow cell fitted with two platinum wire electrodes remained changeable with the alternative anode and cathode. The biofilm expanded by approximately 4% when the wire was cathodic but was reduced to 74% of the original thickness when the wire was anodic, explained by electrostatic interactions between negatively charged groups in the biofilm and the charged wire which caused biofilm expansion when the wire was cathodic and contraction when the wire was anodic [87]. It is thus reasonably feasible to apply an optimal selected cathode potential for shortened start-up period and enhanced Cr(VI) reduction on the biocathodes of MFCs [73] based on the roles of applied electrode potential on microbial physiology, which include changing the cell surface properties, increasing the enzyme activity, as well as shortening the doubling time of the bacteria [88]. Similarly and in the case of Co(II) reduction on the biocathodes of MECs, applied voltages of 0.1–0.7 V achieved different cathode potentials, electric currents, and cathodic distributions of charges for Co(II) reduction, hydrogen evolution, methane and acetate production, as well as bacterial growth [53], reasonably resulting in diverse microbial community compositions. However, at the same applied voltage of 0.2 V, the composition of bacterial community developed for 1 month exhibited a somewhat shift from that evolved for 3 months in spite of similar Co(II) reduction [53]. Different from the strategy of applied voltage for bacterial community, carbon sources of acetate or $NaHCO_3$ at long-term bacterial community acclimation (6 months) and elevated Cd(II) concentrations (20–50 mg/L) can also enhance Cd(II) removal with simultaneous hydrogen production [83]. Cd(II) removal of 7.33 mg/L/h (acetate) and 6.56 mg/L/h ($NaHCO_3$) and hydrogen production of 0.301 m^3/m^3/day (acetate) and 0.127 m^3/m^3/day ($NaHCO_3$) were achieved at an initial Cd(II) of 50 mg/L with the observation of the same predominant species but in different proportions in the acetate or $NaHCO_3$ biofilms. Deeper understanding of the microbial consortia effects on biocathode performance is thus critical to maintain a healthy operation, and proper control of the composition of microbial consortia will also be necessary.

6.4.3 Initial pH and Metal Concentration

Initial pH and metal concentration extensively stressed in abiotic cathodes also affect the performance of biocathodes [53, 67, 71, 85] since initial pH and metal concentration are primarily responsible for structuring whole communities, and the diverse microbial taxa response differently to various environmental conditions [89]. It is generally recognized electrotrophs can only endure an appropriate metal

concentration, after which inhibition of the electrotrophic activities takes over [53, 67, 85]. Take Cr(VI), for example. The presently reported Cr(VI) concentrations in the biocathodes ranged from 2.5 mg/L with pure culture of *Shewanella* to 40 mg/L with enrichment culture (Table 6.2) [70, 73], reflecting the applicable biocathodes for reducing Cr(VI) at these concentration levels. In terms of microbial characters, the pH changes may have affected the surface properties of the cells, including cell surface hydrophobicity, net surface electrostatic charge, cell surface shape and polymers, cell morphology, cell size at cell division, time to division, as well as biofilm structure [87, 88], and consequently influenced the bio-catalytic activity on electron transfer from cathode to bacteria and the subsequent metal reduction. A neutral condition is more beneficial for electrotrophic activities, whereas a more alkaline environment is inclined to form metal precipitates and not only influences electrotrophic activities but also augments metal reduction overpotential. A more acidic condition, however, favors for hydrogen evolution and detrimental to electrotrophic activities. Optimal pHs and initial metal concentrations thus benefit to both electrotrophic activities and metal reduction via electrochemical and biological reactions [53, 67, 70, 85]. Investigation is necessary to better clarify the nature of the competitive processes on the biocathodes and achieve efficient system performance for metal recovery.

6.4.4 Electron Transfer Mechanism

In contrast to electron transfer mechanisms in the bioanodes, the exact mechanisms of electron transfer from the cathode, through the bacteria, and finally, to the terminal electron acceptors in biocathodes have not yet been studied in detail. There are actually close interactions between microorganisms and the cathodic electrodes. Gene expression and deletion analysis demonstrate that the mechanisms for electron transfer from electrodes to *G. sulfurreducens* differed significantly from the mechanisms for electron transfer to electrodes [90]. To date, two main mechanisms, namely, direct and indirect electron transfers, have been reported (Fig. 6.2), which are more complex than those in abiotic cathodes (Fig. 6.1). Direct electron transfer on the biocathodes requires a physical contact between the bacterial cell membrane and the cathode electrode surface, and electrons from the electrode are directly received by the outer membrane redox macromolecules such as cytochromes (Fig. 6.2). *G. sulfurreducens* is one of the few microorganisms available in pure culture known to directly accept electrons from a negative poised electrode. It is believed that c-type cytochromes inside bacteria are essential electron-transferring proteins, and outer membrane cytochromes have the ability to catalyze the last step of the respiratory chains. Alternatively, a versatile bacterium of *S. putrefaciens* in anodic electron transfer through excreted flavins and menaquinone-related redox mediators as well as outer membrane cytochromes can utilize an outer membrane-bound redox compound for electron transfer in microbially cathodic oxygen reduction although this compound was still unidentified. In both cases, c-type cytochromes

are essential electron-transferring proteins. They make the journey of respiratory electrons from the cytoplasmic membrane through periplasm and over the outer membrane possible [91]. Similarly, the absence of ferrous iron repressed the transcription of genes encoding outer membrane cytochromes necessary for the reduction of metals such as MnO_2, reflecting the importance of outer membrane cytochromes in *S. oneidensis* MR-1 for MnO_2 reduction [92]. With the presence of lactate and electrode, *S. oneidensis* MR-1 can use both as the electron donor for accelerated Cr(VI) reduction because (i) the forming chelates of Cr(III)-lactate interaction delayed the electrode deactivation by $Cr(OH)_3$ precipitate, (ii) electron mediators produced mediated electrons from the electrode to Cr(VI) and promoted indirect Cr(VI) reduction, and (iii) the presence of lactate and redox mediators produced enabled *S. oneidensis* MR-1 to be actively involved in the electrode oxidation process and drive direct or indirect Cr(VI) reduction [17]. With the help of noninvasive imaging technique of a naphthalimide-rhodamine-based Cr(III) fluorescent probe [93], four Gram-negative electrotrophs *Stenotrophomonas* sp. YS1, *Stenotrophomonas maltophilia* YS2, *Serratia marcescens* YS3, and *Achromobacter xylosoxidans* YS8 isolated from previously well-developed mixed culture biocathodes for Cr(VI) reduction [85] were imaginably and quantitatively mapped for intracellular Cr(III) ions [76]. These electrotrophs were intracellularly accumulated by chromium, shown as a total of 45.1–60.5% with a composite of Cr(III) ions (23.7–27.3%) and other forms of chromium complex (18.7–32.2%), compared to 10.2–11.7% (Cr(III) ions: 8.2–9.5%; other forms: 0.2–0.3%) in the controls in the absence of cathodic electrons, implying the direction of cathodic electrons for more intracellular chromium. In parallel, another four indigenous Gram-negative electrotrophs *Stenotrophomonas maltophilia* JY1, *Citrobacter* sp. JY3, *Pseudomonas aeruginosa* JY5, and *Stenotrophomonas* sp. JY6 isolated from well-adapted mixed cultures on the MFC cathodes for Cu(II) reduction [85] were proved to play diverse functions between cellular electron transfer processes and either Cu(II) reduction or circuital current [77]. Strains JY1 and JY5 exhibited a weak correlation between circuital current and Cu(II) reduction, whereas a much stronger correlation was observed for strain JY3 followed by strain JY6. In the presence of electron transfer inhibitor of 2,4-dinitrophenol or rotenone, significant inhibition on strain JY6 activity and a weak effect on strains JY1, JY3, and JY5 were observed, confirming a strong correlation between cellular electron transfer processes and either Cu(II) reduction or circuital current. With the help of a rhodamine-based Cu(II) fluorescent probe [94], Cu(II) ions were imaginably and quantitatively tracked in these electrotrophic subcellular sites [78]. Similar to the imaginable Cr(III) ions in the corresponding electrotrophs [76], cathodic electrons also led to more Cu(II) ions in the intracellular site compared to the prolonged appearance of more Cu(II) ions in the controls in the absence of cathodic electrons. For Cd(II) removal on the biocathodes of MECs and with the help of a quinoline-based Cd(II) fluorescent probe [95], four indigenous electrotrophs of *Ochrobactrum* sp. X1, *Pseudomonas* sp. X3, *Pseudomonas delhiensis* X5, and *Ochrobactrum anthropi* X7 isolated from mixed culture for Cd(II) removal [85] imaginably exhibited diverse distributions of Cd(II) ions at the subcellular level with heavy dependence on current and electron transfer

inhibitor of 2,4-dinitrophenol (2,4-DNP) [79]. These results in concert may provide evidence for explaining the previous always observation of more efficient biocathodes for heavy metals removal at the subcellular level [53, 67, 70, 85].

In comparison with Gram-negative bacteria, little is known about Gram-positive bacteria for dissimilatory metal reduction. *Thermincola potens*, isolated from a MFC and reserving unusual abundance of multiheme c-type cytochromes localized to the cell wall or cell surface, can couple acetate oxidation to the reduction of hydrous ferric oxides or anthraquinone-2,6-disulfonate [96]. This result provides direct evidence for cell wall-associated cytochromes and supports multiheme c-type cytochromes involvement in conducting electrons across the cell envelope of a Gram-positive bacterium. In addition, a wide variety of microbially induced extracellular mechanisms have been used to explain the role of microorganisms in the increase of surface potential on passive metals, such as the generation of protons and hydrogen peroxide near the surface and the production of organometallic catalysts of metal reduction, specific enzymes, and passivating siderophores [15, 88, 89]. All the aforementioned enriches the electron transfer mechanisms in the biocathodes.

Compared with the increasing attention being paid on the electron transfer mechanisms between cathodic electrodes and microorganisms, present information about the subsequent link between the electrons derived from the electrodes and the terminal electron acceptors of metals is minimal and debatable (Fig. 6.2). Even for the extensively investigated electron acceptor of oxygen, it has not yet been demonstrated that the electron transfer is a respiratory mechanism in which electrons derived from the cathode serve as an energy-yielding electron donor for oxygen reduction, and there are a variety of other possible mechanisms by which cells
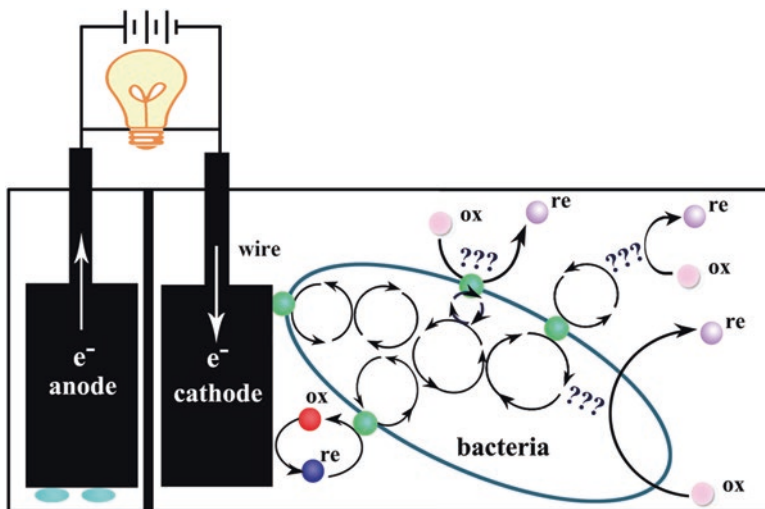

Fig. 6.2 Electron transfer pathways in the biocathodes of BESs

might catalyze enhanced oxygen reduction [68]. Riboflavin, an electron mediator naturally produced by *S. oneidensis* MR-1, was found to have a positive impact in potentiostatically controlled cathodes [17], implying its function as a mediator for electron transfer between *S. oneidensis* MR-1 and Cr(VI). While Gram-negative bacteria of *Shewanella* and *Geobacter* are model organisms enabling the dissimilatory reduction of extracellular electron acceptors, it is recently found that *G. sulfurreducens* can donate electrons through pili, a type of metal-like conductive nanofilaments or nanowires and made from protein produced by themselves, photosynthetic cyanobacteria, and thermophilic methanogens, to the external electron acceptor of uranium [97]. The bacterial pili can move charges over thousands of times the bacterium's length. Compared to the no-pili controls, in which *G. sulfurreducens* reduced uranium within the cell envelope and thus poisoned the cell in the process, the great surface area of pili had provided more occurrence of the precipitation around the pili and thus greatly increased the amount of uranium that *G. sulfurreducens* was able to remove [98]. While this result provides evidence for long-range electron transfer along the pili, *G. sulfurreducens* analogous to *S. oneidensis* [99] can reduce U(VI) much as it reduced the soluble, extracellular electron acceptors of anthraquinone-2,6-disulfonate and Fe(III) citrate without the requirement of pili, and a number of outer-surface c-type cytochromes contribute to U(VI) reduction. These results support the conclusion that pili were necessarily required for long-range electron transport to insoluble electron acceptor such as Fe(III) oxides in the *Geobacter* species [100, 101] and electron exchange between syntrophic partners [102], as well as electron conduction through current-producing biofilms [103]. Based on this observation and after fine-tuning the properties of the pili or adding different functional groups on the pili, these amended pili may be also used to precipitate other metal elements. In view of this point, the discovery of conductive pili is not only an important new principle in biology but also in materials science.

While biocathodes are presently limited to reduce U(VI), Cr(VI), Se(IV), Cu(II), Cd(II), and Co(II), few attempts have been made to elucidate the basic aspects of microbial activities such as interaction of substrate metabolism and electron transfers in the biocathodes. Although gene expression and deletion analysis are usually used for clarifying electron transfer mechanisms in U(VI)-reducing and pure-culture biocathodes [100–103], whether the cathodic electrons are the only energy source for the organisms forming the biofilm, which would make these microorganisms electrochemical lithotrophs, and what function this property plays in nature remain to be elucidated. Development of novel noninvasive imaging techniques to characterize the structure and biochemical composition of the electrotrophic biofilm is of particular importance. That a number of highly selective metal ion-sensitive fluorescence probes are synthesized and combined with confocal laser scanning microscopy for metal detection in cell biology [104] will potentially provide critical insights into metal distribution and electron transfer within the electrotrophs, as well as tools to characterize the mechanisms of electron transfer, leading to a better understanding of the electrotrophic roles in electron transfer mechanisms [76, 78, 79].

6.5 Conclusion

Metallurgical BES processes have been proved in labs and will be well established. However, these technologies are still far from finding real applications in wastes treatment. In addition, much is known about recovering single metals from individual abiotic cathodes; more attention should be paid to MFC-MEC coupled systems and/or BES-other technology combined processes for sequential metal recovery from wastes. Electron transfer mechanisms on the biocathodes are ultimately required to be elucidated in order to understand their limitations and hence maximize metal recovery in the near future.

References

1. Xin B, Zhang D, Zhang X et al (2009) Bioleaching mechanism of Co Li from spent lithium-ion battery mixed culture acidophilic sulfur-oxidizing iron-oxidizing bacteria. Bioresour Technol 100:6163–6169
2. Chen G (2004) Electrochemical technologies in wastewater treatment. Sep Purif Technol 38:11–41
3. Rabaey K, Rozendal RA (2010) Microbial electrosynthesis-revisiting the electrical route for microbial production. Nat Rev Microbiol 8:706–716
4. Logan BE, Rabaey K (2012) Conversion of wastes into bioelectricity and chemicals by using microbial electrochemical technologies. Science 337:686–690
5. Modin O, Wang X, Wu X et al (2012) Bioelectrochemical recovery of Cu, Pb, Cd, and Zn from dilute solutions. J Hazard Mater 235:291–297
6. Huang L, Yang X, Quan X et al (2010) A microbial fuel cell–electro-oxidation system for coking wastewater treatment and bioelectricity generation. J Chem Technol Biotechnol 85:621–627
7. Huang L, Cheng S, Chen G (2011) Bioelectrochemical systems for efficient recalcitrant wastes treatment. J Chem Technol Biotechnol 86:481–491
8. Kelly PT, He Z (2014) Nutrients removal and recovery in bioelectrochemical systems: a review. Bioresour Technol 153:351–360
9. Wang H, Ren Z (2014) Bioelectrochemical metal recovery from wastewater: a review. Water Res 66:219–232
10. Nancharaiah YV, Mohan SV, Lens PNL (2015) Metals removal and recovery in bioelectrochemical systems: a review. Bioresour Technol 195:102–114
11. Nancharaiah YV, Mohan SV, Lens PNL (2016) Biological and bioelectrochemical recovery of critical and scarce metals. Trends Biotechnol 34:137–155
12. Lu Z, Chang D, Ma J (2015) Behavior of metal ions in bioelectrochemical systems: a review. J Power Sources 275:243–260
13. He C, Mu Z, Yang H et al (2015) Electron acceptors for energy generation in microbial fuel cells fed with wastewaters: a mini-review. Chemosphere 140:12–17
14. Ter Heijne A, Liu F, van der Weijden R et al (2010) Copper recovery combined with electricity production in a microbial fuel cell. Environ Sci Technol 44:4376–4343
15. Liu L, Yuan Y, Li F et al (2011) In-situ Cr(VI) reduction with electrogenerated hydrogen peroxide driven by iron-reducing bacteria. Bioresour Technol 102:2468–2473

16. Pang Y, Xie D, Wu B et al (2013) Conductive polymer-mediated Cr(VI) reduction in a dual-chamber microbial fuel cell under neutral conditions. Synth Met 183:57–62

17. Xafenias N, Zhang Y, Banks CJ (2013) Enhanced performance of hexavalent chromium reducing cathodes in the presence of Shewanella oneidensis MR-1 and lactate. Environ Sci Technol 47:4512–4520

18. Wang Q, Huang L, Pan Y et al (2017) Impact of Fe(III) as an effective mediator for enhanced Cr(VI) reduction in microbial fuel cells: reduction of diffusional resistances and cathode overpotentials. J Hazard Mater 321:896–906

19. Choi C, Cui Y (2012) Recovery of silver from wastewater coupled with power generation using a microbial fuel cell. Bioresour Technol 107:522–525

20. Tao H, Gao Z, Ding H et al (2012) Recovery of silver from silver(I)-containing solutions in bioelectrochemical reactors. Bioresour Technol 111:522–525

21. Choi C, Hu N (2013) The modeling of gold recovery from tetrachloroaurate wastewater using a microbial fuel cell. Bioresour Technol 133:589–598

22. Wang G, Huang L, Zhang Y (2008) Cathodic reduction of hexavalent chromium [Cr(VI)] coupled with electricity generation in microbial fuel cells. Biotechnol Lett 30:1959–1966

23. Li Z, Zhang X, Lei L (2008) Electricity production during the treatment of real electroplating wastewater containing Cr(VI) using microbial fuel cell. Process Biochem 43:1352–1358

24. Li Y, Lu A, Ding H et al (2009) Cr(VI) reduction at rutile-catalyzed cathode in microbial fuel cells. Electrochem Commun 11:1496–1499

25. Tao H, Zhang L, Gao Z et al (2011) Copper reduction in a pilot-scale membrane-free bioelectrochemical reactor. Bioresour Technol 102:10334–10339

26. Tao H, Li W, Liang M et al (2011) A membrane-free baffled microbial fuel cell for cathodic reduction of Cu(II) with electricity generation. Bioresour Technol 102:4774–4778

27. Tao H, Liang M, Li W et al (2011) Removal of copper from aqueous solution by electrodeposition in cathode chamber of microbial fuel cell. J Hazard Mater 189:186–192

28. Zhang Q, Wei Z, Liu C et al (2012) Copper-doped cobalt oxide electrodes for oxygen evolution reaction prepared by magnetron sputtering. Int J Hydrog Energy 37:822–830

29. Cheng S, Wang B, Wang Y (2013) Increasing efficiencies of microbial fuel cells for collaborative treatment of copper and organic wastewater by designing reactor and selecting operating parameters. Bioresour Technol 147:115–121

30. An Z, Zhang H, Wen Q et al (2014) Desalination combined with copper(II) removal in a novel microbial desalination cell. Desalination 346:115–121

31. Wu D, Huang L, Quan X et al (2016) Electricity generation and bivalent copper reduction as a function of operation time and cathode electrode material in microbial fuel cells. J Power Sources 307:705–714

32. Wang Z, Lim B, Choi C (2011) Removal of Hg^{2+} as an electron acceptor coupled with power generation using a microbial fuel cell. Bioresour Technol 102:6304–6307

33. You S, Zhao Q, Zhang J et al (2006) A microbial fuel cell using permanganate as the cathodic electron acceptor. J Power Sources 162:1409–1415

34. Zhang B, Zhao H, Shi C et al (2009) Simultaneous removal of sulfide and organics with vanadium (V) reduction in microbial fuel cells. Technol Biotechnol 84:1780–1786

35. Zhang B, Zhou S, Zhao H et al (2010) Factors affecting the performance of microbial fuel cells for sulfide and vanadium (V) treatment. Bioprocess Biosyst Eng 33:187–194

36. Huang L, Guo R, Jiang L et al (2013) Cobalt leaching from lithium cobalt oxide in microbial electrolysis cells. Chem Eng J 220:72–80

37. Huang L, Li T, Liu C et al (2013) Synergetic interactions improve cobalt leaching from lithium cobalt oxide in microbial fuel cells. Bioresour Technol 128:539–546

38. Liu Y, Shen J, Huang L et al (2013) Copper catalysis for enhancement of cobalt leaching and acid utilization efficiency in microbial fuel cells. J Hazard Mater 262:1–8

39. Jiang L, Huang L, Sun Y (2014) Recovery of flakey cobalt from aqueous Co(II) with simultaneous hydrogen production in microbial electrolysis cells. Int J Hydrog Energy 39:654–663

40. Wang Q, Huang L, Yu H et al (2015) Assessment of five different cathode materials for Co(II) reduction with simultaneous hydrogen evolution in microbial electrolysis cells. Int J Hydrog Energy 40(2015):184–196

41. Huang L, Yao B, Wu D et al (2014) Complete cobalt recovery from lithium cobalt oxide in self-driven microbial fuel cell-microbial electrolysis cells systems. J Power Sources 259:54–64

42. Qin B, Luo H, Liu G et al (2012) Nickel ion removal from wastewater using the microbial electrolysis cell. Bioresour Technol 121:458–461

43. Fradler KR, Michie I, Dinsdale RM et al (2014) Augmenting microbial fuel cell power by coupling with supported liquid membrane permeation for zinc recovery. Water Res 55:115–125

44. Zhang B, Feng C, Ni J et al (2012) Simultaneous reduction of vanadium (V) and chromium (VI) with enhanced energy recovery based on microbial fuel cell technology. J Power Sources 204:34–39

45. Luo H, Liu G, Zhang R et al (2014) Heavy metal recovery combined with H_2 production from artificial acid mine drainage using the microbial electrolysis cell. J Hazard Mater 270:153–159

46. Choi C, Hu N, Lim B (2014) Cadmium recovery by coupling double microbial fuel cells. Bioresour Technol 170:361–369

47. Abourached C, Catal T, Liu H (2014) Efficacy of single-chamber microbial fuel cells for removal of cadmium and zinc with simultaneous electricity production. Water Res 51:228–233

48. Zhang Y, Yu L, Wu D et al (2015) Dependency of simultaneous Cr(VI), Cu(II) and Cd(II) reduction on the cathodes of microbial electrolysis cells self-driven by microbial fuel cells. J Power Sources 273:1103–1113

49. Li M, Pan Y, Huang L et al (2017) Continuous flow operation with appropriately adjusting composites in influent for recovery of Cr(VI), Cu(II) and Cd(II) in self-driven MFC-MEC system. Environ Technol 38:615–628

50. Wu D, Pan Y, Huang L et al (2015) Comparison of Co(II) reduction on three different cathodes of microbial electrolysis cells driven by Cu(II)-reduced microbial fuel cells under various cathode volume conditions. Chem Eng J 266:121–132

51. Wu D, Pan Y, Huang L et al (2015) Complete separation of Cu(II), Co(II) and Li(I) using self-driven MFCs-MECs with stainless steel mesh cathodes under continuous flow conditions. Sep Purif Technol 147:114–124

52. Wang Q, Huang L, Pan Y et al (2016) Cooperative cathode electrode and in situ deposited copper for subsequent enhanced Cd(II) removal and hydrogen evolution in bioelectrochemical systems. Bioresour Technol 200:565–571

53. Huang L, Jiang L, Wang Q et al (2014) Cobalt recovery with simultaneous methane and acetate production in biocathode microbial electrolysis cells. Chem Eng J 253:281–290

54. Tao H, Lei T, Shi G et al (2014) Removal of heavy metals from fly ash leachate using combined bioelectrochemical systems and electrolysis. J Hazard Mater 264:1–7

55. Sun M, Sheng G, Zhang L et al (2008) An MEC-MR-coupled system for biohydrogen production from acetate. Environ Sci Technol 42:8095–8100

56. Huang L, Li M, Pan Y et al (2017) Efficient W and Mo deposition and separation with simultaneous hydrogen production in stacked bioelectrochemical systems. Chem Eng J 327:584–596

57. Ramabhadran RO, Mann JE, Waller SE et al (2013) New insights on photocatalytic H_2 liberation from water using transition-metal oxides: lessons from cluster models of molybdenum and tungsten oxides. J Am Chem Soc 135:17039–17051

58. Chen Q, Liu J, Liu Y et al (2013) Hydrogen production on TiO_2 nanorod arrays cathode coupling with bio-anode with additional electricity generation. J Power Sources 238:345–349

59. Kundu A, Sahu JN, Redzwan G et al (2013) An overview of cathode material and catalysts suitable for generating hydrogen in microbial electrolysis cell. Int J Hydrog Energy 38:1745–1757

60. Ribot-Llobet E, Nam JY, Tokash JC et al (2013) Assessment of four different cathode materials at different initial pHs using unbuffered catholytes in microbial electrolysis cells. Int J Hydrog Energy 38:2951–2956

61. Oh SE, Logan BE (2007) Voltage reversal during microbial fuel cell stack operation. J Power Sources 167:11–17

62. Modin O, Fukushi K (2014) Development and testing of bioelectrochemical reactors converting wastewater organics into hydrogen peroxide. Water Sci Technol 69:1359–1372

63. Kim Y, Hatzell MC, Hutchinson AJ et al (2011) Capturing power at higher voltages from arrays of microbial fuel cells without voltage reversal. Energy Environ Sci 4:4662–4667

64. Huang L, Chai X, Quan X et al (2012) Reductive dechlorination and mineralization of pentachlorophenol in biocathode microbial fuel cells. Bioresour Technol 111:167–174

65. Wang H, Ren Z (2013) A comprehensive review of microbial electrochemical systems as a platform technology. Biotechnol Adv 31:1796–1807

66. Wang Q, Huang L, Quan X et al (2017) Preferable utilization of in-situ produced H_2O_2 rather than externally added for efficient deposition of tungsten and molybdenum in microbial fuel cells. Electrochim Acta 247C:880–890

67. Huang L, Chai X, Cheng S et al (2011) Evaluation of carbon-based materials in tubular biocathode microbial fuel cells in terms of hexavalent chromium reduction and electricity generation. Chem Eng J 166:652–661

68. Huang L, Regan JM, Quan X (2011) Electron transfer mechanisms, new applications, and performance of biocathode microbial fuel cells. Bioresour Technol 102:316–323

69. Gregory KB, Lovley DR (2005) Remediation and recovery of uranium from contaminated subsurface environments with electrodes. Environ Sci Technol 39:8943–8947

70. Hsu L, Masuda SA, Nealson KH et al (2012) Evaluation of microbial fuel cell *Shewanella* biocathodes for treatment of chromate contamination. RSC Adv 2:5844–5855

71. Tandukar M, Huber SJ, Onodera T et al (2009) Biological chromium(VI) reduction in the cathode of a microbial fuel cell. Environ Sci Technol 43:8159–8165

72. Huang L, Chen J, Quan X et al (2010) Enhancement of hexavalent chromium reduction and electricity production from a biocathode microbial fuel cell. Bioprocess Biosyst Eng 33:937–945

73. Huang L, Chai X, Chen G et al (2011) Effect of set potential on hexavalent chromium reduction and electricity generation from biocathode microbial fuel cells. Environ Sci Technol 45:5025–5031

74. De Windt W, Boon N, van den Bulcke J et al (2006) Biological control of the size and reactivity of catalytic Pd(0) produced by *Shewanella oneidensis*. Antonie Van Leeuwenhoek 90:377–389

75. Tian LJ, Li WW, Zhu TT et al (2017) Directed biofabrication of nanoparticles through regulating extracellular electron transfer. J Am Chem Soc 139:12149–12152

76. Xue H, Zhou P, Huang L et al (2017) Cathodic Cr(VI) reduction by electrochemically active bacteria sensed by fluorescent probe. Sensor Actuat B Chem 243:303–310

77. Shen J, Huang L, Zhou P et al (2017) Correlation between circuital current, Cu(II) reduction and cellular electron transfer in EAB isolated from Cu(II)-reduced biocathodes of microbial fuel cells. Bioelectrochemistry 114:1–7

78. Tao Y, Xue H, Huang L et al (2017) Fluorescent probe based subcellular distribution of Cu(II) ions in living electrotrophs isolated from Cu(II)-reduced biocathodes of microbial fuel cells. Bioresour Technol 225:316–325

79. Huang L, Xue H, Zhou Q et al (2018) Imaging and distribution of Cd(II) ions in electrotrophs and its response to current and electron transfer inhibitor in microbial electrolysis cells. Sensor Actuat B Chem 255:244–254

80. Catal T, Bermek H, Liu H (2009) Removal of selenite from wastewater using microbial fuel cells. Biotechnol Lett 31:1211–1216

81. Huang L, Liu Y, Yu L et al (2015) A new clean approach for production of cobalt dihydroxide from aqueous Co(II) using oxygen-reducing biocathode microbial fuel cells. J Clean Prod 86:441–446

82. Shen J, Sun Y, Huang L et al (2015) Microbial electrolysis cells with biocathodes and driven by microbial fuel cells for simultaneous enhanced Co(II) and Cu(II) removal. Front Environ Sci Eng 9:1084–1095

83. Chen Y, Shen J, Huang L et al (2016) Enhanced Cd(II) removal with simultaneous hydrogen production in biocathode microbial electrolysis cells in the presence of acetate or NaHCO$_3$. Int J Hydrog Energy 41:13368–13379

84. Li Y, Wu Y, Puranik S et al (2014) Metals as electron acceptors in single-chamber microbial fuel cells. J Power Sources 269:430–439

85. Huang L, Wang Q, Jiang L et al (2015) Adaptively evolving bacterial communities for complete and selective reduction of Cr(VI), Cu(II) and Cd(II) in biocathode bioelectrochemical systems. Environ Sci Technol 49:9914–9924

86. Rosenbaum MA, Franks AE (2014) Microbial catalysis in bioelectrochemical technologies: status quo, challenges and perspectives. Appl Microbiol Biotechnol 98:509–518

87. Stoodley P, De Beer D, Lappin-Scott HM (1997) Influence of electric fields and pH on biofilm structure as related to the bioelectric effect. Agent Chemother 41:1876–1879

88. Luo Q, Wang H, Zhang X et al (2005) Effect of direct electric current on the cell surface properties of phenol-degrading bacteria. Appl Environ Microbiol 71:423–427

89. Liu J, Hua Z, Chen L et al (2014) Correlating microbial diversity patterns with geochemistry in an extreme and heterogeneous environment of mine tailings. Appl Environ Microbiol 80:3677–3686

90. Strycharz SM, Glaven RH, Coppi MV et al (2011) Gene expression and deletion analysis of mechanisms for electron transfer from electrodes to *Geobacter sulfurreducens*. Bioelectrochemistry 80:142–150

91. Richter K, Schicklberger M, Ge scher J (2012) Dissimilatory reduction of extracellular electron acceptors in anaerobic respiration. Appl Environ Microbiol 78:913–921

92. Kouzuma A, Hashimoto K, Watanabe K (2012) Roles of siderophore in manganese-oxide reduction by *Shewanella oneidensis* MR-1. FEMS Microbiol Lett 326:91–98

93. Mao J, Wang L, Dou W et al (2007) Tuning the selectivity of two chemosensors to Fe(III) and Cr(III). Org Lett 9:4567–4570

94. Zhao Y, Zhang X, Han Z et al (2009) Highly sensitive and selective colorimetric and off-on fluorescent chemosensor for Cu^{2+} in aqueous solution and living cells. Anal Chem 81:7022–7030

95. Xu L, He MI, Yang HB et al (2013) A simple fluorescent probe for Cd^{2+} in aqueous solution with high selectivity and sensitivity. Dalton Trans 42:8218–8222

96. Carlson HK, Iavarone AT, Gorur A et al (2012) Surface multiheme c-type cytochromes from Thermincola potens and implications for respiratory metal reduction by gram- positive bacteria. Proc Natl Acad Sci U S A 109:1702–1707

97. Cologgi DL, Lampa-Pastirk S, Speers AM et al (2011) Extracellular reduction of uranium via *Geobacter* conductive pili as a protective cellular mechanism. Proc Natl Acad Sci U S A 108:15248–15252

98. Orellana R, Leavitt JJ, Comolli LR et al (2013) U(VI) reduction by diverse outer surface c-type cytochromes of *Geobacter sulfurreducens*. Appl Environ Microbiol 79:6369–6374

99. Marshall MJ, Beliaev AS, Dohnalkova AC et al (2006) c-type cytochrome-dependent formation of U(IV) nanoparticles by *Shewanella oneidensis*. PLoS Biol 4:e268

100. Reguera G, McCarthy KD, Mehta T et al (2005) Extracellular electron transfer via microbial nanowires. Nature 435:1098–1101

101. Smith JA, Lovley DR, Tremblay PL (2013) Outer cell surface components essential for Fe(III) oxide reduction by *Geobacter metallireducens*. Appl Environ Microbiol 79:901–907

102. Summers ZM, Fogarty HE, Leang C et al (2010) Direct exchange of electrons within aggregates of an evolved syntrophic coculture of anaerobic bacteria. Science 330:1413–1415
103. Malvankar NS, Vargas M, Nevin KP et al (2011) Tunable metallic-like conductivity in microbial nanowire networks. Nat Nanotechnol 6:573–579
104. Hao L, Li J, Kappler A et al (2013) Mapping of heavy metal ion sorption to cell-extracellular polymeric substance-mineral aggregates by using metal-selective fluorescent probes and confocal laser scanning microscopy. Appl Environ Microbiol 79:6524–6534

Chapter 7
Removal and Recovery of Nitrogen Pollutants in Bioelectrochemical System

Yuxiang Liang and Huajun Feng

Abbreviations

AD-MFC	Anode denitrification microbial fuel cell
AEM	Anion-exchange membrane
AMO	Ammonia monooxygenase
AOB	Ammonia-oxidizing bacteria
AO-MFC	Ammonia oxidation microbial fuel cell
BES	Bioelectrochemical system
CEM	Cation-exchange membrane
COD	Chemical oxygen demand
CW	Constructed wetland
CW-MFC	Constructed wetland microbial fuel cell
DET	Direct electron transfer
DO	Dissolved oxygen
HAO	Hydroxylamine oxidoreductase
IET	Indirect electron transfer
MEC	Microbial electrolysis cell
MFC	Microbial fuel cell
NOB	Nitrite-oxidizing bacteria
PA-MFC	Photosynthetic algae microbial fuel cell
PBR	Photobioreactor
PMFC	Photomicrobial fuel cell
SMDDC	Submerged microbial desalination-denitrification cell
SMFC	Sediment microbial fuel cell
SND	Simultaneous nitrification and denitrification
UBER	Upflow bioelectrochemical reactor

Y. Liang · H. Feng (✉)
Zhejiang Provincial Key Laboratory of Solid Waste Treatment and Recycling, School of
Environmental Science and Engineering, Zhejiang Gongshang University, Hangzhou, China
e-mail: fenghuajun@mail.zjgsu.edu.cn

7.1   Background

Nitrogen is the most abundant chemical element in the Earth's atmosphere, and a crucial component of biomolecules. The increased availability of inorganic nitrogen in the environment has boosted biotic production and primary productivity. Ammonium (NH_4^+), nitrite (NO_2^-), and nitrate (NO_3^-) are the most common forms of inorganic nitrogen in the terrestrial environment [1]. These ions can be generated naturally, for example, via nitrogen fixation by prokaryotes (cyanobacteria and rhizobium), atmospheric deposition, and dissolution of nitrogen-rich geological deposits [2]. The total rate of nitrogen production via these natural processes is in the range of 300–500 Tg N year^{-1}, and 25–50% of which is fixed on land [3–5].

During the past two centuries, particularly in recent decades, human activities have substantially accelerated the global nitrogen cycle. By 2000, the rate of anthropogenic inorganic nitrogen production was ~165 Tg N year^{-1}. This increased the total rate of reactive nitrogen formation by 33–55%, which exceeded the needs of industry and agriculture [6]. If these high levels of inorganic nitrogen cannot be assimilated by the functioning of ecological systems, there will be serious adverse effects on the natural environment, especially aquatic ecosystems. There are several ways in which inorganic nitrogen derived from human activities can enter aquatic ecosystems. The largest sources of nitrogen pollution are crop farming, animal farming, municipal sewage, and industrial sewage (Table 7.1). Among them, human and animal wastes contribute 60% of nitrogen pollution. In addition, nonpoint sources of nitrogen such as acid rain are generally more damaging than point sources because they occur on a larger scale and are more difficult to control.

Inorganic nitrogenous pollutants in groundwater and surface water have significant negative effects on many aquatic organisms, thus contributing to the degradation of aquatic ecosystems. In the past few decades, there has been a massive increase in eutrophication on a global scale. Eutrophication is the process in which additional nutrients stimulate the rapid growth of phytoplankton, resulting in wide-

Table 7.1 Major anthropogenic sources of inorganic nitrogen in aquatic ecosystems [1, 7–9]

Major anthropogenic sources		Emissions (Tg N year^{-1})
Crop farming	Runoff from chemical fertilizer and animal manure	~1.01
Animal farming	Wastewater from livestock (cattle, pigs, chickens)	~4.21
	N releases from aquaculture (fish, prawns, shrimps)	~0.15
Municipal sewage	Runoff and infiltration from waste disposal sites	~2.41
	Urine	~3.97
	Effluents from sewage treatment plants	~0.12
Industrial sewage	Dairy, fertilizer, and food processing sewage and so on	~1.76
Air pollution transfer	Acid rain caused by NO_X and SO_2	/

spread hypoxia and anoxia, changes in the food-web structure, habitat degradation, and loss of biodiversity [6]. Inorganic nitrogen pollution also markedly increases the concentration of hydrogen ions in freshwater, resulting in acidification of those ecosystems. Furthermore, nitrate in drinking water with high concentrations (>10 mg N L^{-1}) can be converted into nitrite in animal intestines, which could result in methemoglobinemia of the animal and possible death [10, 11]. Therefore, effective methods to reduce nitrogen pollution are urgently required.

The existing biological treatments (nitrification and denitrification) to remove nitrogen require energy and a carbon source, which greatly increase the costs of wastewater treatment [12, 13]. These biological denitrification methods also produce large amounts of waste sludge, which presents a new environmental problem to be solved. In recent years, MFC have been widely used as an alternative technology to reduce nitrogen pollution. The advantages of MFC are that they do not require energy or a carbon source, generate less sludge, and have a flexible electron transfer process [14–17]. In this chapter, we summarize recent research on nitrogen removal/recovery in BES focusing on wastewater treatment. We describe the nitrogen removal pathways, reaction mechanisms, and new developments in these technologies and discuss the challenges in creating BES that efficiently and effectively remove nutrients from wastewater.

7.2 Nitrate Removal and Recovery

Nitrate concentrations in the environment have increased worldwide because of the increased use of nitrogen fertilizers and increased emissions of industrial and domestic wastewater. Nitrate is a health risk to both animals and humans and can cause methemoglobinemia (blue-baby syndrome) when it is absorbed by infants [10]. Therefore, many researchers have focused on developing biological and physicochemical processes to remove nitrate from water.

7.2.1 Autotrophic Denitrification at Biocathodes

Biological denitrification can remove almost 100% of nitrate from water, so it is an excellent choice for nitrogen removal. There are four stages in the conversion of nitrate to nitrogen gas (N$_2$) during this process:

$$NO_3^- \rightarrow NO_2^- \rightarrow NO \rightarrow N_2O \rightarrow N_2 \tag{7.1}$$
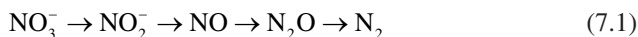
Since denitrification is a microbial metabolic process, an oxidizable substrate or electron donor is necessary. There are two types of biological denitrification [12]: autotrophic and heterotrophic. Heterotrophic denitrification bacteria can use

carbon-containing compounds like ethanol, methanol, acetate, or insoluble carbon sources such as wheat straw as oxidizable substrates [18–20]. The disadvantage of heterotrophic denitrification is that it produces biomass. Autotrophic denitrification bacteria utilize hydrogen, iron, or sulfur chemical compounds as sources of carbon dioxide and power, or bicarbonate as the carbon source. The biotic process involving ferrous ions (Fe^{2+}) decreases nitrate to nitrite autotrophically in low-iron surroundings [21]. Based on this reaction, researchers proposed that the cathode could serve as the electron source.

In 1992, successful denitrification was achieved at the cathode of BES [22]. From that study, most researchers believed that nitrate moved from the bulk mass into the cathode biofilm and was reduced to nitrogen gas biologically using the hydrogen generated from the electrolysis of water in the biofilm. It was proposed that the efficiency of hydrogen production was 100% and that the hydrogen generated by the electrolysis of water was used completely in the denitrification process. In 2005, Park et al. obtained a maximal denitrification rate of 434.78 mg NO_3-N h^{-1} (2.16×10^{-5} mol H_2 h^{-1}) in their biological cathode denitrification system [23]. However, they obtained a maximal hydrogen production rate of 1.38×10^{-7} mol H_2 h^{-1} (with an applied current of 200 mA), which was 100-fold lower than the nitrate reduction rate. Those results demonstrated that hydrogen is not needed to drive complete cathode denitrification. Different from conventional denitrification that relies on hydrogen, hydrogenotrophic denitrifying bacteria can directly accept electrons from the cathode of BES. This discovery would advance denitrifying process at biocathode in MFC technology, as it led to the development of systems with effective nitrate removal and simultaneous electricity generation.

7.2.1.1   Electron Transfer Between Biocathodes and Denitrifying Bacteria

Higher removal efficiencies can be achieved by autotrophic denitrification. The power conversion and efficiency of nitrogen pollution treatment are determined by electron transfer between microbes and electrodes. Studies in recent decades have revealed details of the anode electron transfer process, but the electron transfer process between the cathode and microorganisms is still poorly understood. Researchers have proposed two mechanisms of autotrophic denitrification at the cathode (Fig. 7.1) [24]:

The first proposed mechanism of autotrophic denitrification is DET. In this process, hydrogen is not needed to drive complete cathode denitrification, and hydrogenotrophic denitrifying bacteria can directly accept electrons from the cathode of BES in the absence of organic substances [23, 25]. So far, the best-researched anode DET is the extracellular respiration of dissimilatory metal-reducing *Shewanella* and *Geobacter* bacteria. In these bacteria, electrons are transferred via a chain of *c*-type cytochromes (heme-type proteins) across the cell envelope to extracellular electron acceptors [26]. Similarly, *c*-type cytochromes are involved in direct cathode DET. The uptake of electrons from electron donors by *c*-type cytochromes is a common process in nature, especially in acidic situations such as drains in mines, where
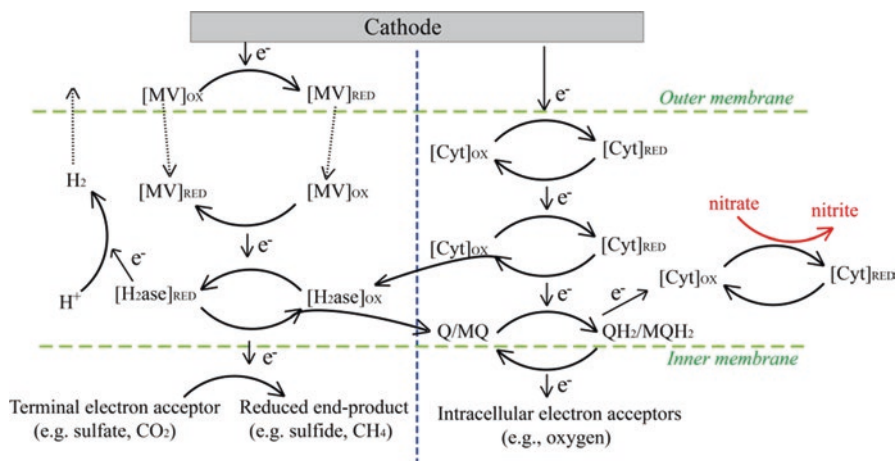
Fig. 7.1 Proposed cathode extracellular electron transfer mechanisms and associated energy gains for biocathode microorganisms: (right) DET involving *c*-type cytochrome electron transfer chains; (left) mediated electron transfer. [Cyt], *c*-type cytochrome; [MV], methyl (redox mediator); [H₂ase], hydrogenase; Q/MQ, functional enzyme. (This schematic is modified from [24])

chemolithotrophic iron II and sulfur oxidization are the dominant microbial actions [27–29]. For example, Yarzabal et al. showed that *Acidithiobacillus ferrooxidans* can accept electrons directly from Fe (II) minerals (pyrite) through the outer membrane Cyc2 (+0.560 V; the highest potential recorded for a *c*-type cytochrome). Then, Cyc2 further transfers the electrons to an electron transport chain with oxygen reduction as the final reaction step. Cytochrome (Cyt572) has been abundantly found in iron (II) oxidation conditions, where its role is to carry the heme that ultimately binds to *c*-type cytochromes [29].

The *c*-type cytochrome of cathodic microorganisms may also have the similar function for electron transfer. The process mainly depends on the redox potential, which affects cytochromes and their eventual association with the electron transfer chain. In bioelectrochemical denitrification systems, the final reaction is nitrate reduction, which has broad potential to provide electrons for uptake by microorganisms [30–32]. The potential difference generated in this process may be sufficient to power the energy-conserving reactions between the electrode and the electron acceptor such as nitrate, oxygen, or chlorinated organic compounds [30–32]. Hence, the immobilization of denitrifying bacteria on the cathode surface is necessary for electron exchange.

Artificial redox mediators can be used to facilitate electron transfer between the cathode and microorganisms, as the cathode itself cannot transfer electrons. The most commonly used redox mediators are neutral red, anthraquinone-2,6-disulfonate, and methyl viologen [33–36]. The results of several studies have suggested that artificial mediators not only enhance electron transfer but also promote microbial growth and metabolism at biocathodes. However, more research is

required to confirm this additional role of redox mediators in the bioelectrochemical denitrification process.

The second proposed mechanism of autotrophic denitrification is IET, in which hydrogen gas is used as a general electron donor. However, in traditional biological denitrification systems, the crucial hydrogen concentration appeared to be 0.2 mg L^{-1}, because incomplete denitrification occurred at lower hydrogen concentrations [11]. During bioelectrochemical denitrification, denitrifying bacteria are immobilized on the cathode surface and utilize the hydrogen gas produced from the electrolysis of electrolytes. The effective contact area between bacteria and cathode is much larger than that of traditional hydrogen diffusion [37], so the electron transfer process is relatively straightforward.

In addition, some bacteria contain hydrogenases that can catalyze the reversible consumption (oxidation) and production (reduction) of hydrogen. Tatsumi et al. and Lojou et al. firstly reported hydrogen gas production by bacterial electrocatalysis [38, 39]. They showed that *Desulfovibrio vulgaris* Hildenborough produced hydrogen gas with a carbon electrode as the electron donor in the presence of a low-potential redox mediator (methyl viologen) ($E = 446$ mV). The hydrogen requirement of the autotrophic denitrification process may be more easily met by bacterial electrocatalysis than by direct electrolysis of an electrolyte. However, further research is required to test this idea.

7.2.1.2 Factors Controlling Denitrification at the Biocathode

The main factors that influence the biocathode denitrification are cathode potential, electrode material, reactor configuration, pH, ionic strength, initial nitrate concentration, and the carbon source.

7.2.1.2.1 Cathode Potential

During the DET denitrification process, an applied cathode potential below 150 mV is theoretically sufficient for autotrophic denitrification (Table 7.2). However, the potential should be more negative in practice because of the loss of overpotential [40]. Pous et al. reported an increase in the nitrate reduction rate as the cathode potential decreased from 0 to −300 mV [41]. In their study, 93.9% of the nitrate was

Table 7.2 Summary of DET denitrification reactions and theoretical potential [42, 43]

Process	Cathode reduction reaction	E_o (mV vs. Ag/AgCl)
Nitrate reduction	$NO_3^- + 2\ e^- + 2\ H^+ \rightarrow NO_2^- + H_2O$	+233
Nitrite reduction	$NO_2^- + e^- + 2\ H^+ \rightarrow NO + H_2O$	+150
Nitric oxide reduction	$NO + e^- + H^+ \rightarrow 0.5\ N_2O + 0.5\ H_2O$	+975
Nitrous oxide reduction	$0.5\ N_2O + 5\ e^- + 6\ H^+ \rightarrow 0.5\ N_2 + 0.5\ H_2O$	+1155

Table 7.3 Summary of mediated electron transfer denitrification reactions and theoretical potential [12, 44]

Process	Cathode reduction reaction	E_o (mV vs Ag/AgCl)
Hydrogen evolution reaction	$10\ H_2O + 10e^- \rightarrow 5\ H_2 + 10\ OH^-$	-611
Nitrate reduction	$2\ NO_3^- + 2\ H_2 \rightarrow 2\ NO_2^- + 2\ H_2O$	/
Nitrite reduction	$2\ NO_2^- + 2\ H_2 \rightarrow 2\ N_2O + H_2O + 2\ OH^-$	/
Nitrous oxide reduction	$N_2O + H_2 \rightarrow N_2 + H_2O$	/

converted into nitrogen gas or absorbed by bacteria at -300 mV, but 6.1% was converted into nitrous oxide (N_2O) as an intermediate. Their results also showed that the production of nitrous oxide and nitrite, two undesirable denitrification intermediates, varied with cathode potential and was lower at potentials lower than about -500 mV. This phenomenon may have resulted from competition for electrons among different denitrifying enzymes. Therefore, an unlimited source of electrons from the electrode to denitrifying bacteria can avoid the accumulation of nitrite and nitrous oxide.

The hydrogen formation rate at the cathode is also controlled by the cathode potential, which plays a critical function because hydrogen is necessary in the mediated electron transfer denitrification process (Table 7.3). The standard hydrogen evolution potential (pH = 7) is -611 mV, that is, a more negative cathode potential is required for autotrophic denitrification [44]. However, the higher current density resulting from a lower cathode potential will increase the denitrification rate but decrease the current–denitrification efficiency because of the incomplete consumption of hydrogen gas [45]. In addition, when the cathode potential is too low, the hydrogen gas yield by electrolysis increases, leading to effervescence. The resulting gas bubbles form a dry space on the surface of the electrode. This blocks electron transfer and inhibits biofilm formation, thus lowering denitrification performance [46].

7.2.1.2.2 Electrode Substrate

The electrode functions as both the electron acceptor and the carrier for microorganisms. Therefore, electrodes directly affect the power output, bacterial attachment, hydrogen production, and nitrogen removal efficiency of a system. A summary of the types of cathode materials used in MFC and their nitrogen removal performance is provided in Table 7.4.

Carbon-based materials are the most versatile anode materials because of their high specific surface area and excellent biocompatibility. Li et al. developed an integrated shortcut nitrification and autotrophic denitrification MFC with carbon cloth as the cathode [47]. The removal efficiency of total nitrogen (50 mg N L^{-1}) was 99.9%, and the power output was 294.9 mW m^{-2}. Zhang et al. built a two-chamber BES consisting of heterotrophic denitrifying microorganisms immobilized on a cathode with a plain carbon paper surface [48]. The concentration of NO_3^-–N in the wastewater was 60 mg N L^{-1}. The applied voltage was controlled by another

Table 7.4 Cathode substrates and modifications in bioelectrochemical denitrification systems

Cathode substrate	NO_3^--N (mg L^{-1})	Feed solution	Experimental conditions	Nitrogen removal (%)	References
Carbon brushes	TN = 50	Synthetic wastewater	HRT = 4 h; shortcut nitrification and autotrophic denitrification MFC	99.9	[47]
Carbon paper	60	Synthetic wastewater	HRT = 3 h; BES; V = 700 mV	100	[48]
Graphite felt	20	Synthetic wastewater	HRT = 4 h; BES; carbon source: NaHCO$_3$	98	[55]
Stainless steel mesh	20	Synthetic wastewater	HRT = 3 d; BES (750 mL); I = 1 mA	>50	[50]
Stainless steel multi-electrode	15–20	Synthetic wastewater	HRT = 6 h; BES (eight and two pieces of cylindrical, expanded metal electrodes, acting as cathodes and anodes, respectively); I = 80 mA	>90	[51]
Stainless steel	20.9–22	Groundwater	HRT = 4.2 h; combined bioelectrochemical and sulfur autotrophic denitrification system; I = 30–1200 mA	95–100	[56]
Stainless steel	20	Contaminated water	HRT = 6–36 h; UBER; I = 20 mA	100	[44]
Cylindrical stainless steel	30	Drinking water	HRT = 1.9–5 h; combined bioelectrochemical and sulfur autotrophic denitrification system; I = 2–20 mA	90–100	[57]
Stainless steel	24	Groundwater	HRT = 10 h; BES; I = 10 mA	>95	[58]
Stainless steel	TN = 68	Municipal sewage	HRT = 6 h; BES; I = 20–120 mA	75	[59]
Carbon felt/ multi-wall carbon nanotube	25–100	Synthetic wastewater	HRT = 6 h; BES (2 L); I = 15 mA cm^{-2}; ORP −100 mV; pH 7	Modified: 93 / Unmodified: 76	[60]
Humin-containing cathode	19	Synthetic wastewater	HRT = 1 h; BES (300 mL); P = −500 mV	Modified: 90 / Unmodified: 60	[61]

MFC. With voltage outputs ranging from 500 to 700 mV and a maximal power output of 502.5 mW m^{-2}, nitrate removal was significantly accelerated, with almost no accumulation of intermediates. Although carbon-based materials are the most extensively used electrodes in MFC, they have limited use in practical situations because of their high capital cost and poor ductility (low current density) [49].

Consequently, metal-based electrodes, such as gold, silver, copper, nickel, cobalt, stainless steel, and titanium, have been tested as electrodes. Among them, stainless steel is a widely used industrial metal with excellent mechanical properties, sufficiently unusual electrical conductivity, and long-term resistance to corrosion, as well as being commercially available. In 1998, Cast and Flora compared heterotrophic denitrification rates between two cathode materials (a stainless steel rod wrapped with stainless steel mesh and a graphite rod wrapped with polypropylene) in a water treatment experiment [50]. They found that both electrode substances were suitable for microbial attachment and showed similar denitrification efficiencies. Sakakibara compared porous and expanded stainless steel multi-electrode systems in a continuous denitrification experiment [51]. The hydraulic retention times and electric currents ranged from 6 to 2 h and from 80 to 960 mA, respectively. When the electrical current was increased, the effluent nitrite concentration was decreased to less than 0.5 mg N L^{-1} (influent nitrite concentration was 20 mg N L^{-1}). However, the use of metals as electrodes for denitrification is limited by their poor biocompatibility. In the past few decades, there have been very few reports on the use of metal electrodes as cathodes in bioelectrochemical denitrification systems. Instead, there has been increasing interest in the discovery and design of inexpensive, stable, and effective electrode substances for BES.

Some active metals such as iron, nickel, zinc, and copper have been used in electrochemical denitrification systems. This non-biological approach has been shown to effectively remove nitrate at a broad range of initial concentrations (up to 100 g/L) from diverse wastewaters. The reaction in which zinc and sulfamic acid reduce nitrate to nitrogen gas is as follows (7.2) [52]:

$$NO_3^- + Zn + H^+ + NH_2SO_3H \rightarrow N_2 + SO_4^{2-} + Zn^{2+} 2H_2O \qquad (7.2)$$
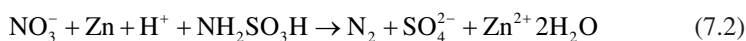
The Zn^{2+} ions produced in (7.2) reform into solid zinc on the cathode via electrolysis. Consequently, the zinc metal itself is not consumed in the reaction and is reusable afterward as a metal catalyst, whereas the sulfamic acid is consumed in the reaction.

Several recent studies have focused on boron-doped diamond (BDD) [53, 54] as a high-performance anode substrate for removal of emerging pollutants and other refractory pollutants and for electrochemical disinfection. This substance has excellent electrochemical properties including its wide functional potential, its stable and low voltammetric background drift, its unusual overpotential to form oxygen and hydrogen in aqueous electrolytes, and its stability. Ghazouani et al. [53] studied non-biological denitrification in a system with a BDD anode/cathode and found that the current efficiency was higher and the energy consumption was lower than those of other systems. Therefore, the use of BDD may be a fresh approach in the engineering of bioelectrochemical denitrification systems.

7.2.1.2.3   Electrode Modifications

Modifications to the surface of the anode can enhance the current densities of BES. Such modifications include carbon particle coating, conductive polymer coating, mediator grafting, heat treatment, and hydrophilic modification of graphite or metal electrode substrates. Similarly, the cathode surface can be modified to improve its performance in bioelectrochemical denitrification (Table 7.4). To increase the microbial load on the electrode surface, Abbas et al. used a carbon felt cathode modified with a multi-wall carbon nanotube (CF/MWCNT) to enhance the efficiency of bioelectrochemical denitrification [59]. The highest nitrate removal efficiency in the CF/MWCNT system under optimum conditions was 92.7% within 4 h, compared with a nitrate removal efficiency of 76.4% within 4 h with an unmodified cathode. In another study, carbon felt modified with a polypyrrole film (CF/PPy) was used as a cathode in a bioelectrochemical denitrification system [61]. The CF/PPy films formed evenly and stably on the CF electrode using the potentiostatic electropolymerization method. Compared with the unmodified electrode, the CF/PPy electrode showed a 24.7% enhancement in the nitrate removal rate. More biomass was attached to the CF/PPy electrode than to the unmodified electrode, indicating that this modification could improve bacterial adhesion on the cathode.

The low extracellular electron transfer rate between the cathode and bacteria is a major limitation in bioelectrochemical denitrification. To accelerate electron transfer, melted electron shuttles can be added to the cathode. However, electron shuttles are toxic and/or unstable and consequently are a poor fit for these systems environmentally. Thus, it is important to use fixed electron shuttles for denitrification in BES. In this context, Xiao et al. showed that a graphite cathode merged with solid-phase humin supported electron transfer to *Pseudomonas stutzeri* for denitrification in BES [60]. The solid-phase humin served as a redox mediator to donate electrons to the denitrifying bacterium at −700 mV. Nitrogen gas as the final product accounted for 94.6% of the initial nitrate, and no nitrous oxide accumulated.

Several modifications that enhance cathode denitrification performance have also been reported. Studies have shown that electron exchange between the microbe and the cathode can be improved by introducing a positive charge at the electrode surface, for example, by treatment with cyanuric chloride, ammonia gas, chitosan, 3-aminopropyltriethoxysilane, melamine, or polyaniline [61, 62]. Thin layers of nickel, gold, or palladium catalysts were shown to reduce the activation energy threshold for electron transfer from electrodes to bacteria [62]. Fabrics coated with carbon nanotubes provide open, three-dimensional, matrices that are conducive to microbial growth. Among such materials, carbon cloth modified with thin layers of gold, palladium, or nickel nanoparticles were shown to increase electrosynthesis rates by 4.5-, 4.7-, or sixfold, respectively, in microbial electrosynthesis systems [63], compared with the unmodified carbon cloth. These modifications led to significant increase in cathode performance. Consequently, the design, discovery, and optimization of cheap and stable modifications may increase the efficiency of denitrification in BES.
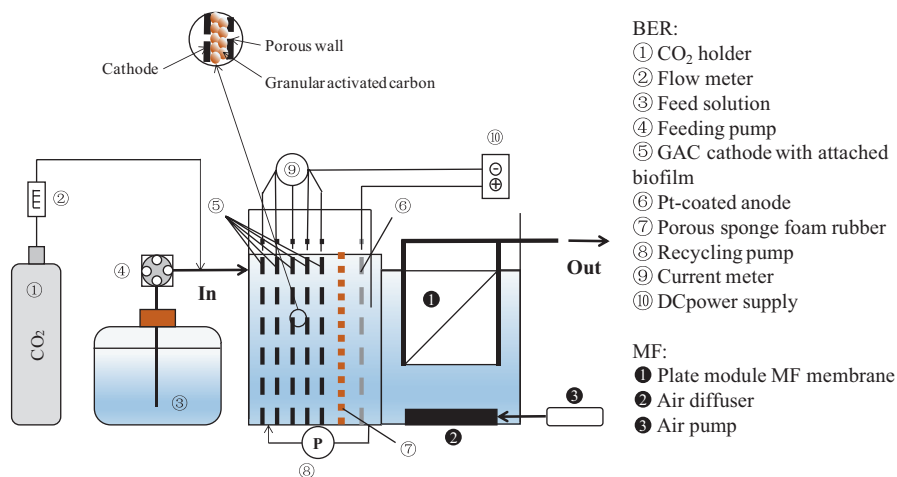
Fig. 7.2 Multi-cathode biofilm-electrode reactor combined with microfiltration. (Reprinted from [45], Copyright 2002, with permission from Elsevier)

7.2.1.2.4 Electrode Structure

Brushes, rods, and plates are the most popular structures of carbon-based electrodes [64]. The typical electrode system is a flat-parallel configuration of plate electrodes. Its advantages are the uniform current and readily available materials [65], but its disadvantage is its small surface area that severely limits biofilm formation. By contrast, carbon felt and carbon brushes have larger surface areas for immobilizing denitrifiers.

A multi-cathode biofilm electrode provides a large surface area for immobilizing denitrifiers. Prosnansky et al. developed a multi-cathode biofilm-electrode reactor merged with microfiltration and used it to treat nitrate-contaminated water in a laboratory-scale experiment (Fig. 7.2) [45]. The multi-cathode electrodes consisted of multi-granular activated carbon that provided a large surface area for the attachment of bacteria. The denitrification rate was enhanced by 3–60 times in comparison with those reported in previous studies.

The use of three-dimensional (3D) cathodes in BES has led to higher efficiency as a result of the increased surface area for hydrogen production and the growth of denitrifying microbes, as well as the larger contact area with contaminants. Generally, 3D cathodes are constructed by adding conductive filler between the anode and the cathode. Zhang et al. designed a 3D BES [66] equipped with a stainless steel anode and cathode and added functional polyurethane foam (specific surface area, 35,000 $m^2 m^{-3}$) and activated carbon to immobilize microorganisms in the cathode chamber. Compared with a traditional two-dimensional (2D) reactor, this 3D system enhanced the removal efficiencies of both organic matter and nitrate and significantly reduced the formation of nitrite as a by-product. In the 3D reactor constructed by Zhou et al., the denitrification rate was about 2.4-fold higher than that of

a 2D reactor. Furthermore, it showed excellent and stable performance in a range of conditions, indicating its suitability for use in wastewater treatment systems.

7.2.1.2.5 Reactor Configuration

In the review of Kelly et al., the reactor configuration for nutrient removal and recovery has been summarized in detail [64]. The specifications of reactor design play a significant role in the denitrification rate. The double chamber is one of the most common reactor configurations, and its superior features are its biofilm selectivity and uniform current [65]. In this system, the anode generates electricity from biodegradable organic matter in an anaerobic environment. The cathode works anaerobically and consumes electrons to reduce nitrate to nitrogen gas via the activity of hydrogenotrophic denitrifying bacteria. However, since most wastewaters contain ammonia rather than nitrate, most reactors focus on the removal of total nitrogen. Therefore, the conversion of ammonia to nitrate will facilitate the subsequent bioelectrochemical denitrification.

The first report of complete nitrogen removal in BES involved a separate biofilm-based aerobic reactor (Fig. 7.3a) [67]. In this system, the organic pollutant was efficiently metabolized by microbes in the anode chamber, and this reaction provided electrons for the cathode reduction reaction. Then, the anode effluent with a high ammonia concentration moved into a separate aerobic reactor for the nitration reaction in which ammonia was oxidized to nitrate. Finally, the secondary effluent flowed into a cathode chamber in which nitrate was reduced to nitrogen gas. This system developed by Virdis et al. achieved a high nitrogen removal rate of 0.41 kg m^{-3} day^{-1} and a maximum power density of 34.6 W m^{-3}. However, its main disadvantage was that a high concentration of ammonium could enter the cathode chamber via diffusion through the CEM.

To solve this problem, Virdis et al. designed a simultaneous nitrification and SND in which integrated aerobic nitrification occurred in the cathode chamber (Fig. 7.3b) [68]. In this system, the cathode biofilm included two layers: nitrifying bacteria in the outer layer and denitrifying bacteria in the inner layer. The outer biofilm could consume DO, thereby creating a micro-anoxic environment on the surface of the cathode for the denitrification process. To reduce the cost and internal resistance of reactors associated with ion-exchange membranes, several studies focused on SND in simplified single BES. In such systems, the denitrification process is similar to that of a cathode SND, which relies on an oxygen gradient (oxygen concentration decreasing from the anode to the cathode) to produce aerobic and anoxic zones in a single reactor. The aerobic zone is located in the anode chamber, where oxygen is produced by anode oxygen evolution or active aeration. Ammonia is reduced to nitrate in the anode chamber, and nitrate moves to the cathode for the next denitrification reaction. Although such systems can remove nitrogen, the residual DO severely restricts bioelectrochemical denitrification. In addition, the spread of organic compounds into the cathode chamber can lead to serious heterotrophic denitrification.
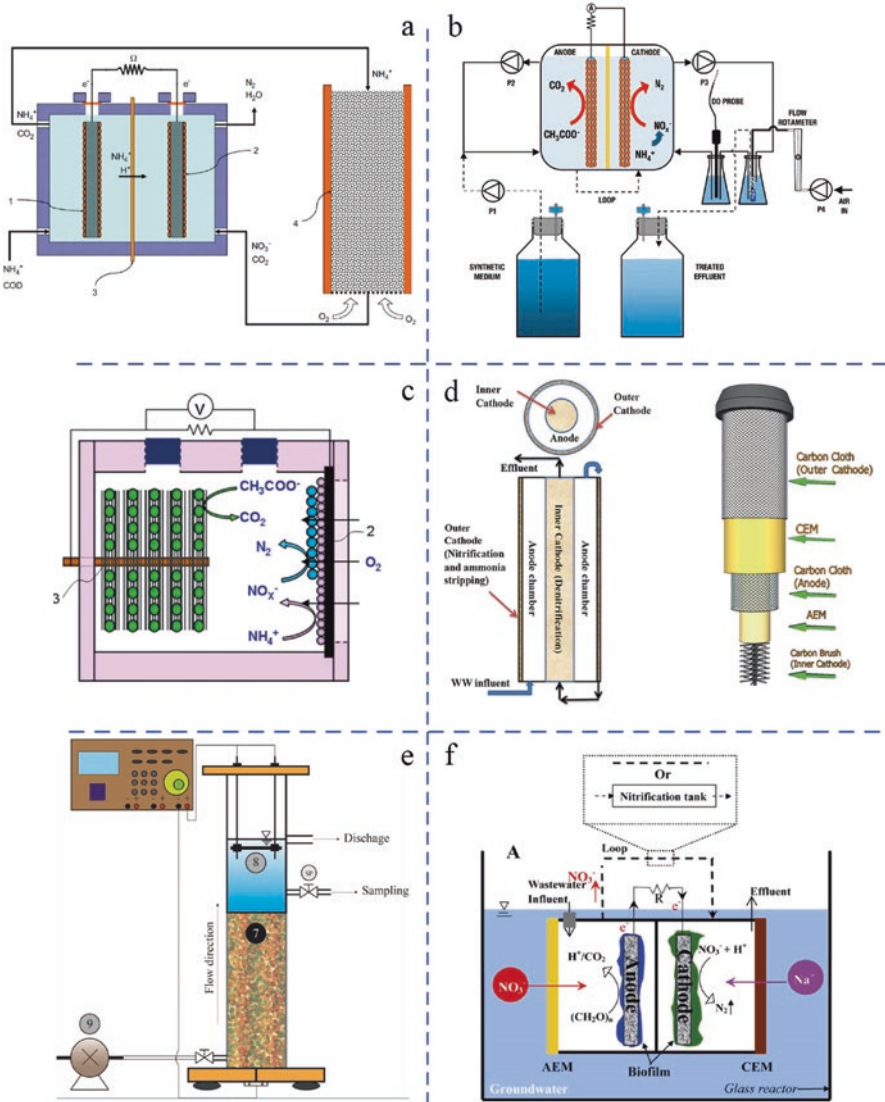
Fig. 7.3 BES designed for complete nitrogen removal by nitrification and bioelectrochemical denitrification: (**a**) BES plus an external nitrifying bioreactor. (Reprinted from [67], Copyright 2008, with permission from Elsevier). (**b**) SND at the cathode of BES. (Reprinted from [68], Copyright 2010, with permission from Elsevier). (**c**) Single-chamber air-cathode MFC. (Reprinted from [71], Copyright 2012, with permission from Elsevier). (**d**) Tubular MFC with dual cathodes. (Reprinted from [72], Copyright 2012, with permission from Elsevier). (**e**) UBER with palm shell activated carbon as cathode material. (Reprinted from [73], Copyright 2009, with permission from Elsevier). (**f**) SMDDC to remove nitrate from groundwater in situ. (Reprinted from [74], Copyright 2013, with permission from Elsevier)

Because SND reactors have a high prerequisite for DO, several kinds of BES systems have been designed (dual-cathode MFC) with discrete anoxic and aerobic cathodes for denitrification and nitrification, respectively [69]. These systems have an anoxic cathode and an aerobic cathode on each side of the anode chamber. First, the nitrogen-containing wastewater flows into the anode chamber of both BES. Then, the anode effluent is collectively fed into the aerobic biocathode chamber. Finally, the cathode effluent moves into the anoxic biocathode chamber. To explore the engineering applications of this system, Liang et al. designed a 50-L MFC comprising an oxic-anoxic two-stage biocathode and activated-semicoke-packed electrodes [70]. This system simultaneously generated power and removed nitrogen and organic substances. The nitrogen removal efficiency was higher than 84% in continuous mode, and the average maximum power density was 43.1 W m^{-3}.

A single-chamber BES with an air cathode pre-enriched with a nitrifying biofilm can also achieve denitrification and simultaneous nitrification, without additional power input for aeration. In a single-chamber MFC, the nitrifying biofilm adheres to the surface of the air cathode and then oxidizes ammonia to nitrate via the activities of nitrifying bacteria. The nitrate is further reduced to nitrogen gas by heterotrophic denitrifiers (Fig. 7.3c) [71]. Nitrogen removal is further enhanced by increasing the gas diffusion area. Although this system removes nitrogen, the process is not necessarily relevant to current output.

There are many other special designs of BES for nitrogen removal. The tubular configuration appears to be the most extensively studied reactor structure. In such systems, an individual anode is located at the reactor's axial center and is encircled by the cathode; this is the best configuration to maximize the area of cathode in a volume-limited reactor. Zhang et al. developed a system with a tubular batch-operated dual-cathode configuration (Fig. 7.3d) [72]. The wastewater moved from the anode to the aerobic cathode and finally to the anoxic cathode. The ion-exchange membranes in the system consisted of a CEM between the aerobic cathode and the anode, and an AEM between the anoxic cathode and the anode.

When scaling up BES, UBER may be an appropriate configuration to slow mass transfer in an enormous cathode zone (Fig. 7.3e) [73]. Such systems use particulates such as granular activated carbon as the cathode and biocarrier and contain hydrogenotrophic denitrifying bacteria. Wastewater flows into the cathode zone and contacts the 3D cathode with a large surface area (granular activated carbon). The wide distribution of nitrate is spontaneous in the cathode zone, because of the velocity of the influent. However, the increase in pH at the cathode zone inhibits nitrite reduction, and so nitrite is not reduced to satisfactory levels. This is the common disadvantage of all single-chamber reactors.

Several studies have focused on the removal of nitrogen from groundwater using BES. Nitrate is one of the pollutants in groundwater that poses a threat to human and animal health but is difficult to remove in situ. The uses of BES to treat groundwater require a pump, which requires energy input. Angelidaki et al. designed a SMDDC to remove nitrate from groundwater in situ (Fig. 7.3f) [74]. The reactor included an anode chamber and a cathode chamber on opposite sides of a polycarbonate plate. A CEM and an AEM were placed against the outer side of the cathode

chamber and anode chamber to insulate the interior of the chambers against the outside environment. The whole reactor was submerged below the groundwater surface. Wastewater flowed into the anode and the effluent was directly fed into the cathode. Under the action of an electric field force, nitrate was transferred to the anode chamber and then to the cathode chamber for the denitrification reaction.

7.2.1.2.6 pH Control

The pH of wastewater is unstable, and this is one of the main factors affecting the performance of hydrogenotrophic denitrification. Therefore, to increase biocatalytic denitrification, the pH must be maintained at an appropriate level because the microorganisms that catalyze these reactions deteriorate in the conditions that result from their activities [64]. In many autotrophic denitrification systems, the denitrification reaction can significantly slow or even stop under lower (<6) or higher pH (>9) conditions. The pH in the cathode chamber will increase significantly because of proton consumption during the denitrification process [75]. Villano et al. found that the biocathode pH increased rapidly from 8.40 to 11.43 during the first 15 days of operation [76]. Clauwaert et al. reported that only 26% of nitrate was reduced without pH adjustment, but nitrate removal increased under a stable neutral pH [77]. Therefore, the pH at the cathode must be continuously adjusted during the denitrification process. A pH between 6.5 and 8.0 is optimal for denitrification systems.

The pH affects denitrification performance mainly via its effects on the microbial community [78]. Wang et al. reported that the *Clostridia* community was the most significant nitrate remover at pH 7.0–8.0, followed by members of *α-Proteobacteria*, *γ-Proteobacteria*, and *Bacilli*. Lee et al. showed that *Clostridia* was the principal community in autotrophic denitrification and that *Clostridia* displayed denitrifying activity in the cathode chamber of BES. At pH 9.0, *Bacilli* was the most abundant class, since its members grow well under alkaline conditions. *γ-Proteobacteria* was the main class at pHs below pH 6.0, indicating that acidic conditions favor this class.

The pH of the electrolyte is normally adjusted by phosphoric acid during a batch denitrification process [50]. The pH is also adjusted by the carbon dioxide produced during the denitrification process [79], as the carbon dioxide gas dissolves in water to produce carbonic acid. This reacts with hydroxyl radicals (OH^-) to form bicarbonate (HCO_3^-), which buffers against the increase in pH [45].

7.2.1.2.7 Ionic Strength

Several studies have shown that nitrate removal is promoted at high ionic strength. Zhang et al. studied the effects of conductivity on BES performance and showed that the nitrate removal efficiency was higher at a high ionic strength (99%; 2200 μS cm^{-1}; added 1000 mg L^{-1} NaCl) than at a low ionic strength (91%; 900 μS cm^{-1}) [74]. The higher denitrification efficiency at high ionic strength was likely caused

by the decrease in internal resistance, which resulted in higher current density and coulombic efficiency. This is the main reason why nitrate removal from groundwater is incomplete. Zhang et al. found that anionic species like chloride ions (Cl^-) did not negatively affect the performance of denitrification systems. These results indicated that the addition of exogenous electrolytes (2000–11,000 μS cm^{-1}) is an effective way to increase denitrification efficiency at the cathode [74].

Incomplete nitrate removal is caused by the accumulation of denitrification intermediates (NO_2^- and N_2O). With regard to high conductivity, the electrons produced by the oxidation of organic substances in the anode chamber move to the cathode, where they are used to reduce nitrogen-containing compounds. Nitrogenous gases (NO and N_2O) are formed as intermediates at low conductivity. These gases increase resistance in the system, thus limiting proton and electron transport and promoting the accumulation of denitrification intermediates.

7.2.1.2.8   Initial Nitrate Loadings

Biological denitrification has been used to treat wastewater with comparatively low nitrate concentrations (10–200 mg N L^{-1}). However, the nitrate concentrations in wastewater frequently exceed this level, especially wastewater from industries in small- and medium-sized communities (150–12,500 mg N L^{-1}) [80]. Very high nitrate concentrations can be toxic to denitrifying bacteria [81, 82]. Zhang et al. showed that, at an initial nitrate concentration of 100 mg N L^{-1}, nitrate was nearly completely reduced within 21 h, and the denitrification process was similar to that occurring at a lower initial nitrate concentration (70 mg N L^{-1}). However, at a much higher initial nitrate concentration (150 mg N L^{-1}), denitrification was slightly inhibited, and the denitrification rate was significantly decreased [83]. Another study showed that denitrification was completely inhibited when the initial nitrate concentration was higher than 1350 mg N L^{-1} [80].

7.2.1.2.9   Carbon Source

Organic compounds are the most abundant pollutants in wastewater. Bioelectrochemical denitrification accepts electrons from the cathode and from organic compounds at the cathode [13]. In the cathode of BES fed with organic substances, both autotrophic and heterotrophic denitrifying bacteria exist simultaneously, and the nitrogen reduction pathway varies depending on the carbon source. The carbon/nitrogen ratio (C/N) affects the electron supply and, hence, affects the nitrogen removal rate and pathways. In previous studies [84], heterotrophic denitrifying bacteria were dominant if organic matter was abundant (C/N >1), but autotrophic denitrifying bacteria were dominant when the C/N was below 0.75. To avoid secondary pollution produced by the incomplete use of methanol, the C/N ratio ought to lower than 0.75. The nitrate removal efficiency can be enhanced by the cooperation of autotrophic denitrification and heterotrophic microorganisms.

Table 7.5 Summary of carbon sources in bioelectrochemical denitrification systems

Carbon source	Initial NO_3^--N (mg L^{-1})	C/N ratio	Experimental conditions	Nitrate removal rate (g N m^{-3} day^{-1})	References
Ethanol	20	0.95	HRT = 4 h; a three-dimensional reactor (0.6 L); I = 15 mA	120	[90]
Sodium acetate	35	1	HRT = 8 h; BES (2.5 L); I = 80 mA	105	[91]
Methanol	20	Enough	HRT = 5.3 h; membrane bioreactor (4 L)	81	[92]
Methanol	50–100	1.25	HRT = 8 h; a fiber-based biofilm reactor (12 L)	149	[93]
Methanol	50	0.75	HRT = 8 h; BES (12 L); I = 40 mA	146	[85]
Glucose	30	3.5	HRT = 24 h; single-chamber BES (0.45 L); I = 3.5–5 mA	22.8	[86]
Starch	30	3.5	HRT = 24 h; single-chamber BES (0.45 L); I = 3.5–5 mA	26.4	[86]
$NaHCO_3$	30	3.5	HRT = 24 h; single-chamber BES (0.45 L); I = 3.5–5 mA	10.5	[86]
Phenol	/	/	HRT = 70 h; phenol concentration 1400 mg L^{-1}; BES (0.05 L); initial NH_4^+-N 230 mg L^{-1};	TN = 0 mg L^{-1}	[89]

Three kinds of carbon sources have been used in previous studies: inorganic (e.g., sodium bicarbonate, $NaHCO_3$), simple (e.g., methanol, glucose, and acetate), and complex/refractory (e.g., starch and phenol) (Table 7.5). Inorganic carbon sources are more favorable for autotrophic denitrification than for heterotrophic denitrification. Feng et al. found that BES fed with sodium bicarbonate accumulated nitrite and showed lower nitrogen removal efficiency than those of systems with other organic carbon sources [85, 86]. In this system, most of the nitrogen removal was attributed to hydrogenotrophic denitrification. However, a different nitrogen removal mechanism operated when organic carbon sources were added. In BES fed with simple carbon sources, the carbon sources were direct electron donors for heterotrophic denitrification [87].

However, in BES fed with complex carbon sources, the specific nitrogen pathways are probably different. For example, soluble microbial products and nitrite accumulated in BES which is fed with starch [85, 86], but not in BES fed with simple carbon sources. Further research is required to explore the mechanisms operating in each system. Phenol, another refractory carbon source, cannot be degraded by denitrifying bacteria. Therefore, the concomitant removal of phenol and total

nitrogen can be achieved by the combined activities of phenol-degrading bacteria and denitrifying bacteria [88]. In such systems, small-molecule metabolites are the direct electron donors for heterotrophic denitrification. In addition, bioelectrochemical denitrification accepts electrons from direct cell-cell electron transfer.

7.2.1.2.10   Microbial Communities in Cathode Biofilm

Denitrifying bacteria belong to taxonomically and biochemically diverse categories of anaerobic bacteria, which obtain energy for biosynthesis and upkeep from electrons transported from donors to acceptors (NO_2^-, N_2O, and NO_3). Many studies have focused on the microbial ecology of biocathode denitrification systems in which the cathode microbial community is separated from mixed cultures of hydrogenotrophic microorganisms. The microbial community is complex and comprises species involved in denitrification and other species with different functions (e.g., species that consume organic compounds synthesized during autotrophic denitrification) [64]. *Nitrosomonas* sp. is a denitrifying bacterium that can oxidize ammonia to nitrite or reduce nitrite to nitric oxide [93]. The active denitrifying bacterial community in biocathodes was compared between an MFC with an annular association (anode effluent moved into the cathode) and a dual MFC with separate cathode and anode chambers. The loop MFC showed higher performance in both its nitrogen removal rate and current generation; this was probably because of its evenness and greater bacterial richness and the dominance of members of the *Firmicutes* and *Proteobacteria* in the cathode biofilm [94–98]. The main participants in the bioelectrochemical denitrification process are *Proteobacteria*, *Firmicutes*, and *Clostridia*. Wrighton et al. found that *Proteobacteria* and *Firmicutes* were the dominant phyla in a denitrification system, indicating that these classes have strong potential for nitrate removal. Sotres et al. also found that members of the *Firmicutes*, *Proteobacteria*, and *Actinobacteria* displayed efficient denitrification activities in a biocathode denitrification system.

Proteobacteria are typical hydrogen-oxidizing denitrifiers. *Paracoccus denitrificans*, which belongs to the α-subclass of *Proteobacteria*, is one of the most widely studied denitrifying microorganisms [11, 99]. *β-Proteobacteria* such as *Thauera* sp., *Hydrogenophaga* sp. [100], and *Rhodocyclus* [101] have also been isolated from mixed microbial communities. In IET denitrification, *Proteobacteria* may dominate the biofilm during the start-up and substrate limitation (hydrogen) phases. However, in DET denitrification, denitrifiers must be able to transfer extracellular electrons through a chain of *c*-type cytochromes. Previous studies have shown that *c*-type cytochromes are present in *Halochromatium salexigens* and other *Proteobacteria* [101] and in some purple denitrifying microorganisms, including *Rhodocyclus* [102]. Wodara et al. identified two *c*-type cytochromes and a flavoprotein in *P. denitrificans* [103]. These results indicated that most denitrifying microorganisms on the cathode are able to transfer electrons extracellularly.

The difference in degradation efficiency among different denitrifying microorganisms may be due to differences in the expression patterns of genes in the

denitrification pathway. The main nitrate reductase genes are *napA* and *narG*, the main nitrite reductase genes are *nirS* and *nirK,* and the main NO and N_2O reductase genes are *norB* and *nosZ*, respectively [78]. *napA* is a periplasmic nitrate reductase that can easily link to the outside electron flow because of its short distance to the outer membrane. Doan et al. reported that the expression of *napA* and *narG* was unaffected by increasing current density [104], whereas those of *nirS* and *nirK* slowly increased to reach a peak in expression as the current density increased. The rate-limiting step in the denitrification pathway was found to be that catalyzed by NO and N_2O reductases (encoded by *norB* and *nosZ*). Expression of these two genes was shown to increase rapidly as the current density increased, and denitrification intermediates other than N_2O did not accumulate. Finally, N_2O accumulation and the low expression of *nosZ* supported the conclusion that the NO-to-N_2O transformation is the rate-limiting step in the denitrification pathway.

7.2.1.2.11   Influence of Other Pollutants

As well as nitrogenous and organic compounds, wastewater contains many other types of pollutants, such as heavy metals, surfactants, sulfides, and nanoparticles. Heavy metal ions and surfactants can inhibit the self-purification of soil and groundwaters in nature [105]. Surfactants are widely used to create emulsions of various compounds such as lubricants and oils. However, the amount of surfactants seeping into the environment has increased. These substances may lead to the accumulation of secondary pollutants and dissolve pollutants that are usually insoluble in polar solvents [106]. As an example, the denitrification rate of a standard medium containing APDA (N-N-Bis (3-aminopropyl) dodecylamine – disinfectant and cleaning agent, a biocide used in the food and cosmetics industry) at 2 mg L^{-1} by *Bacillus licheniformis* was similar to that of the standard medium without APDA. However, the denitrification rate decreased with increasing APDA concentrations (inhibiting concentration 2–8 mg L^{-1}). At the toxic concentration of APDA (8 mg L^{-1}), the denitrification process almost completely stopped.

Unlike surfactants, heavy metals can be reduced and detoxified at the surface of the cathode. Thus, the inhibitory effects of heavy metals probably differ between bioelectrochemical denitrification and biological denitrification. Watanabe et al. attempted to use a bioelectrochemical reactor to treat nitrogen pollutants directly in wastewater containing copper [107]. The copper ions and nitrogen pollutants could be removed simultaneously during a continuous operation by applying electric current and supplying acetate. In addition, wastewater containing high concentrations of nitrogen pollutants and hexavalent chromium was successfully treated by a laboratory-scale expanded granular sludge bed reactor [108]. Almost all nitrates were removed, even from wastewater containing a high level of hexavalent chromium (120 mg L^{-1}).

The treatment of nitrate-containing wastewater by the sulfur autotrophic denitrification process using BES has been studied for decades. In this process, sulfur autotrophic and hydrogen autotrophic steps are integrated for the following reasons:

bioelectrochemical hydrogen denitrification consumes the protons produced during sulfur denitrification to attain neutralization; and the sulfate concentration in the effluent can be controlled by adjusting the nitrogen load in the sulfur autotrophic denitrification step [109]. Using such a system, Cai et al. achieved nitrate and sulfide removal efficiencies of >90% when influent nitrate and sulfide concentrations were 780 mg L^{-1} and 135.49 mg N L^{-1}, respectively [110]. These processes are also strongly affected by pH; the sulfur autotrophic denitrification process is weaker than hydrogen denitrification in acid conditions, while hydrogen denitrification is enhanced under alkaline conditions.

Nanomaterials such graphene oxide, zinc oxide, nano-silver, and ferric oxide are used widely in industry and are potential pollutants in wastewater because of their strong dispersity [111]. Such nanomaterials have been shown to be toxic to microorganisms in the wastewater biochemical treatment process [112]. Chen et al. [113] designed a 3D bioelectrochemical denitrification system (3D-BEDS) to treat wastewater containing a high nitrate concentration and various concentrations of graphene oxide (GO; 0–150 mg L^{-1}). As the GO concentration increased (<100 mg L^{-1}), the nitrate removal efficiency decreased slightly from 99.52% to 94.81%. However, the denitrification efficiency dramatically decreased to 74.95% when the GO concentration increased to 150 mg L^{-1}. The authors also found that high GO concentrations changed the dominant bacterial communities and decreased community abundance.

Refractory organic pollutants are another class of hazardous contaminants that affect the nitrate removal efficiency of BES. Chen et al. found that an increase in the *p*-nitrophenol concentration (0–100 mg L^{-1}) in wastewater led to a decrease in denitrification efficiency (to 74.51%) [114]. Therefore, a high concentration of *p*-nitrophenol may be harmful to denitrifying microorganisms.

7.2.2   Denitrification at Bioanodes

As mentioned above, most previous studies have focused on SND in the limited-aeration cathode chamber of BES. The DO that is not consumed during nitrification will be harmful to denitrifying bacteria. The anode denitrification MFC (AD-MFC) is a novel type of MFC that removes nitrate and simultaneously generates electricity in the anode chamber [115, 116]. In these systems, SND occurs in separate anode and cathode chambers, rather than in the same cathode chamber. In an MFC that cathode nitrification was coupled to anode denitrification for nitrogen removal, an AEM allowed nitrate to move from the aerobic cathode chamber to the anaerobic anode chamber. Zhang et al. used an AD-MFC system to remove nitrate at various initial concentrations [116]. When the initial nitrate concentration in the anolyte was increased from 50.02 ± 0.03 to 3560 ± 36.80 mg L^{-1}, it was completely removed within 4.2–171.8 h. The results demonstrated that the AD-MFC was capable of treating wastewater containing nitrate, even at very high concentrations, while simultaneously generating electricity.

In anode exoelectrogen systems, the electron output from the anode is due to their ability to directly convert organic waste into electrical energy, and the final electron acceptor is oxygen. Such systems have been used to remove nitrogen, but they are not suitable for power generation because the denitrification process competes for electrons with biological electricity generation in the anode biofilm. In addition, high nitrate concentrations in the anolyte can inhibit or even stop electricity generation in this type of MFC [117].

7.2.3   Nitrate Removal by Constructed Wetland Coupled with MFC

CWs have been widely used to treat municipal sewage, livestock and agricultural wastewater, and leachates and mine drainage. The popularity of CWs has increased in the last 20 years because of their low installation, operation, and maintenance costs. Systems combining an MFC and CW-MFC are a new development in ecosystem wastewater treatment technology (Fig. 7.4) [118]. Such systems are considered to be a cost-effective and environmentally friendly method for generating bioenergy while simultaneously biodegrading organic matter and nitrate. Most CW-MFC has an upflow construction with the cathode buried below the surface layer or in the plant rhizosphere. This arrangement minimizes DO in the anode zone. In CW-MFC, plants play two roles: they provide organic chemical compounds in the rhizosphere and harbor microorganisms that generate power from those organic chemical compounds. The reported current output of a plant-MFC was 18-fold higher than that of a freshwater sediment MFC.
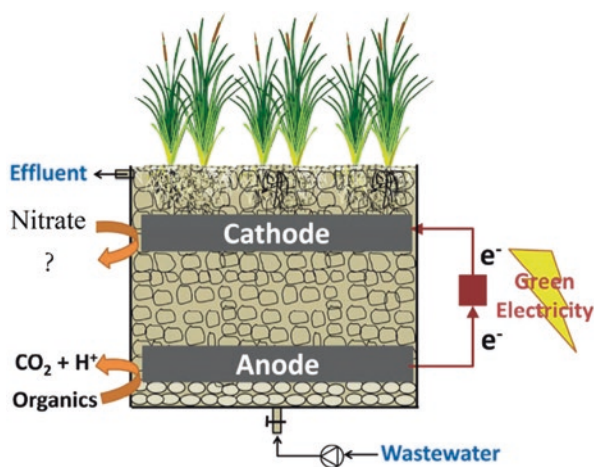

Fig. 7.4 Schematic diagram of simultaneous carbon and nitrogen removal in a CW-MFC. (Reprinted from [118], Copyright 2015, with permission from Elsevier)

The average COD and nitrate removal efficiency of a CW-MFC were 8.3% and 40.2% higher, respectively, than those of the original CW [119]. The relative abundance of *β-Proteobacteria*, nitrobacteria, and denitrifying bacteria was significantly increased in a closed-circuit CW-MFC, and dissimilatory nitrate reduction to ammonium, microbial immobilization, and plant uptake were all minor mechanisms of nitrate removal. Matheson et al. evaluated the relative importance of competing nitrate removal processes by measuring the degradation pathway of ^{15}N-labeled nitrate in a surface-flow CW [120]. They found that most of the nitrate was permanently removed through denitrification, while smaller proportions were removed by plant uptake (11%) and microbial immobilization (13%).

7.3 Ammonia Removal and Recovery

Ammonium pollution of water is a serious environmental problem because it causes eutrophication, which leads to the death of aquatic species. Kim et al. used an MFC to treat ammonia in wastewater containing organic pollutants [121]. The system removed ammonia while simultaneously generating electrons to produce energy, in a process completely different from traditional ammonia removal processes. Recently, there has been increasing interest in using MFC for ammonia recovery [122]. There are two mechanisms of ammonia removal in MFC. The first mechanism is the transfer of ammonium ions from the anode to another chamber (through ion-exchange membranes) under pressure generated by an electric field force. Then, the ammonium ions can be removed by various methods such as struvite precipitation ($MgNH_4PO_4 \cdot 6H_2O$) and blowing-stripping. The second mechanism is biological nitrification/denitrification, in which ammonium ions are oxidized to form nitrogen gas in a water-based bioelectrode mechanically supplied with oxygen.

7.3.1 Nitrification at Bioanodes

There are three biological oxidation steps in the nitrification process (Eq. 7.3) [123]. The limiting step is oxidation of ammonium ions to form nitrite, which is catalyzed by ammonium-oxidizing bacteria. Then, nitrite is rapidly oxidized to nitrate by nitrite-oxidizing bacteria in the presence of molecular oxygen:

$$NH_4^+ \xrightarrow{O_2} NH_2OH \xrightarrow{H_2O} NO_2^- \xrightarrow{O_2} NO_3^- \tag{7.3}$$
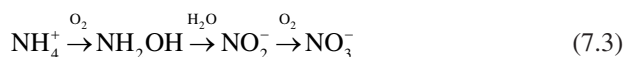
The reduction of ammonium ions to nitrite is a two-step reaction with hydroxylamine (NH_2OH) as the main intermediate product. In the first step, ammonia rather than ammonium ion is the real substrate; ammonia is oxidized to hydroxylamine by AMO. In the second process, hydroxylamine is further oxidized to nitrite by HAO [124].

Whereas oxygen is required for conventional nitrification, nitrifying bacteria can directly accept electrons from the anode in bioelectrochemical nitrification systems. Min et al. were the first to report the removal of ammonium at high concentrations from swine wastewater in an MFC under anaerobic conditions [125]. The maximum power density generated from swine wastewater was about 45 mW m^{-2} in a dual-chamber MFC but increased to 261 mW m^{-2} in a single-chamber MFC. This system removed approximately 83% of ammonia and 88% of soluble COD. Detailed analyses indicated that many extra ammonia elimination processes such as anaerobic ammonia oxidization and denitrification occurred in the system. However, the results did not clarify whether ammonia oxidation was coupled to electricity generation.

Later, Kim et al. tried to generate electricity from ammonia oxidation by intermittently injecting ammonia into the anaerobic anode chamber as the sole electron donor. No power was produced, indicating that ammonia could not serve as a substrate for electricity generation under anaerobic conditions [121]. In contrast, He et al. showed that ammonium could serve as the sole substrate for electricity generation as it could be used directly as an electron donor in anode chamber or indirectly as the substrate for nitrifiers to produce organic compounds for heterotrophs in a rotating-cathode MFC [126]. At present, there is no unanimous agreement as to whether ammonium is a substrate for electricity generation.

In 2013, Xie et al. further investigated the effects and mechanism of DO on nitrification and electricity generation in an AO-MFC [127]. In that system, the electrons originated from ammonia and flowed to AMO (which catalyzes the conversion of ammonia to hydroxylamine), Cyt aa3 oxidase (which catalyzes the reduction of oxygen), and the anode, which were used for triggering ammonia oxidation, synthesizing ATP, and generating electricity. Molecular oxygen was found to play a key role in distributing electrons among these three acceptors. Concentrations of DO that were too high (>6.45 mg L^{-1}) or too low (<0.5 mg L^{-1}) negatively affected electricity generation. However, the ammonia oxidation rate gradually increased as the DO concentration increased. Those results indicated that the electrons derived from ammonia simultaneously flow to oxygen and the electrode. The ammonia-electrode electron transformation was favored under low-DO conditions. However, since oxygen is a substrate for not only AMO but also Cyt aa3 oxidase, low-DO conditions can inhibit the activity of ammonia-oxidizing microorganisms.

7.3.1.1   Electron Transfer Between Bioanodes and Nitrifying Bacteria

Although many studies have focused on electron transfer mechanisms between the anode and bacteria, this process is still poorly understood. The current understanding is that, like in the cathode denitrification process, there are two mechanisms of electron transfer between the anode and bacteria: direct and mediated electron transfer (DET and MET, respectively). In the DET process, electrons are transferred through flavin, conductive pili, and *c*-type cytochromes. In the mediated electron transfer process, electrons are transferred through external electron mediators between the electrode and microorganisms [128].
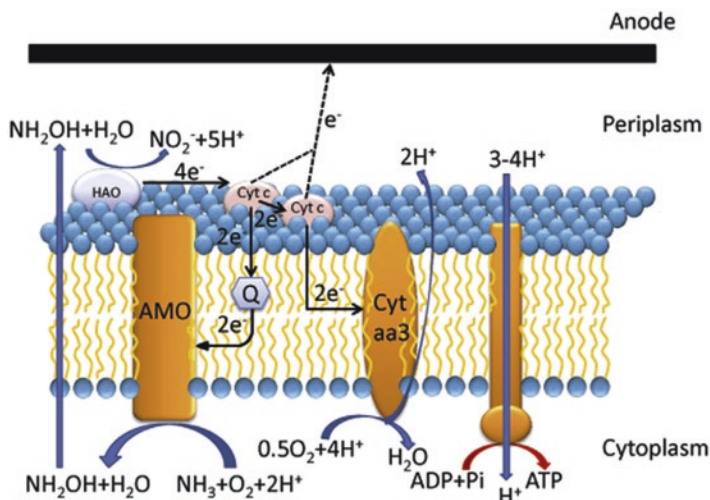
Fig. 7.5 Proposed cathode extracellular electron transfer mechanisms and associated energy gains for bioanode microorganisms. *Cytc* c-type cytochrome, *AMO* ammonia monooxygenase (which catalyzes conversion of ammonia to hydroxylamine), *HAO* hydroxylamine oxidoreductase (which catalyzes conversion of hydroxylamine to nitrite). (Reprinted from [127], Copyright 2013, with permission from Elsevier)

To date, three pathways have been proposed. In the first possible pathway, electrons released from ammonium oxidation and nitrite oxidations by nitrifying bacteria are transferred from the microbial cells to the anode to generate electricity [127]. As shown in Fig. 7.5, four electrons are produced from the conversion of hydroxylamine to nitrite by HAO. In traditional nitrification, half of those electrons are used to convert ammonia to hydroxylamine by AMO, and the other two are used to reduce oxygen by Cyt aa3 oxidase [129]. A different process occurs in anode nitrification, where the electrons for oxygen reduction are transferred to the anode via c-type cytochromes [127].

In the second possible pathway, nitrite is electrochemically oxidized into nitrate to generate electricity [130], and ammonia is oxidized in the same way as in the first pathway. In the third possible pathway, ammonium is assimilated by microorganisms into organic compounds, which serve as fuel to generate electricity.

7.3.1.2 Factors Controlling Nitrification at Bioanodes

7.3.1.2.1 pH Control

Both biological and electrochemical pathways depend on the anode pH. The electrochemically active bacteria in the anode chamber can be inhibited or even inactivated in acidic or alkaline conditions. In addition, in an alkali environment, ammonium ions are converted into free ammonia, which inhibits microbial activity.

Therefore, the ammonia removal efficiency depends on the anode pH of MFC systems [131]. Kim et al. investigated the pH dependence of ammonia removal in an MFC system (pH 7.0, 8.0, and 8.6) [132, 133]. In this MFC system, 23.3% (30.2 mg N L^{-1}) of total ammonia nitrogen (TAN) was removed via the electrochemical pathway during 192 h at a neutral pH. More ammonia was removed by biological pathways than by electrochemical pathways, and *Anammox* were the main functional bacteria. However, at the initial pH of 8.6, the proportion of free ammonia increased to 22.8%, which strongly inhibited ammonia removal by biological pathways. Therefore, a neutral pH was identified as being optimal for AO-MFC.

7.3.1.2.2 Initial Ammonia Loadings

Denitrifying systems have been tested using various types of wastewater, e.g., fermented wastewater, swine wastewater, leachates and wastewater from paper and brewing industries, and recycling wastewater [134]. The ammonia concentration in most real wastewaters far exceeds the capacity of the nitrifying process. Nam et al. studied the effect of free ammonia concentration on electricity generation in MFC and found that electricity generation was significantly inhibited by high concentrations of TAN (>500 mg N L^{-1}) [134, 135]. Further increases in TAN significantly inhibited AOB and NOB, resulting in a continuous decrease in maximum power density.

At low concentrations, ammonia functions as a sustainable proton shuttle. Therefore, a low concentration of ammonia can effectively stabilize the anolyte pH and enhance the current output of an MFC [136]. In these systems, the cathode remains anaerobic, thereby facilitating abiotic hydrogen gas formation. When the anolyte is neutral (pH 6.5–7.5), ammonia mainly exists as ammonium ions through combining with the protons produced by the biofilm on the anode. The ammonium ions are transferred into the cathode chamber through a CEM, and free volatile ammonia is produced in the catholyte (pH > 10).

7.3.1.2.3 Inhibition by Primary Intermediates

Ammonium is the original substrate of AO-MFC. The intermediates of nitrification, hydroxylamine, and nitrite, which can also donate electrons, may also serve as substrates in AO-MFC [137]. Chen et al. showed that hydroxylamine at concentrations lower than 3.0 mg L^{-1} promoted electricity generation in an AO-MFC but inhibited it at a higher concentration (7.2 mg L^{-1}). Since very little hydroxylamine accumulates during nitrification, its contribution to electricity generation will be negligible. Nitrite at concentrations lower than 100 mg N L^{-1} was shown to promote electricity generation in an AO-MFC but inhibited it at a higher concentration (150 mg N L^{-1}) because of its severe biotoxicity. The addition of nitrate to an AO-MFC was shown to decrease electricity generation.

7.3.1.2.4   Carbon Source

Organic compounds are the most abundant pollutants in wastewater and serve as electron donors. Therefore, there is competition for electron input between organic compounds and ammonium in the anode chamber [72]. Jadhav et al. found that ammonia and organic matter could be removed simultaneously under different COD/ammonium ratios (COD/NH_4^+ ratios of 1:1, 10:1, and 5:1) [138]. About 63% and 33% of NH_4^+-N was removed with a COD/ammonium ratio of 1:1 and 10:1, respectively. However, the highest volumetric power density (0.7 W m^{-3}) was in the MFC system with a COD/ammonium ratio of 10:1, indicating that COD benefited current output but inhibited ammonia removal.

7.3.1.2.5   Microbial Communities in Anode Biofilm

In the presence of ammonium and the absence of microbes, a chemical cell failed to generate electricity (ammonium in the anolyte; potassium permanganate in the catholyte). However, in the presence of ammonium and microbes, an AO-MFC system generated electricity. In other words, functional bacteria play a pivotal role in generating electricity in AO-MFC [139].

In the review of Ge et al., the detection of nitrifiers for wastewater treatment has been summarized in detail [12]. The AOB can be distinguished by their cell morphologies and Gram-negative multilayered cell walls, and some of them are motile (with flagella). Since the first isolation of AOB in 1890, five recognized genera of AOB in two phylogenetically distinct groups, the *γ*- and *β*-subclasses of *Proteobacteria*, have been reported [140]. Four genera of AOB, including clusters of *Nitrosomonas* (e.g., *Nitrosococcus mobilis*), *Nitrosolobus*, *Nitrosovibrio*, and *Nitrosospira*, are grouped in the β-subclass [141], and one *Nitrosococcus* cluster is in the *γ*-subclass [142]. To date, 25 AOB species have been cultured from various environments, and *Nitrosomonas* and *Nitrosospira* are the most extensively studied genera [143]. The majority of AOB obtain energy for growth from aerobic oxidation. However, some special AOB species can grow under both aerobic and anaerobic conditions. In high-DO conditions (DO > 0.8 mg L^{-1}), the main aerobic oxidation product of *Nitrosomonas eutropha* was nitrite, while nitrogen gas, nitrite, and nitric oxides were produced under low-DO conditions (DO < 0.8 mg L^{-1}) [144]. In the anode chamber, *N. eutropha* may play an important role in oxidizing ammonia and releasing electrons to the anode. Schmid and Bock demonstrated that *Nitrosomonas europaea* was able to anaerobically oxidize ammonia using nitrite as the acceptor, suggesting that oxygen is not indispensable for ammonia oxidation [145, 146]. He et al. showed that *N. europaea* could transfer electrons to the anode [147]. Zhan et al. found that *N. europaea* dominated the microbial community on the anode surface of BES [139].

The conversion from ammonia to nitrite via hydroxylamine is catalyzed by two key enzymes: AMO and HAO. The former is a membrane-bound heterotrimeric

copper-containing enzyme, with a broad substrate range and an acetylene-inhibitor profile [148]. The three subunits of AMO are encoded by *amoC*, *amoA*, and *amoB*, but only a portion of *amoA* performs as a functional gene in AOB [149, 150]. Although AMO is inactivated upon cell breakage, its activity can be tested in vitro. Compared with AMO, HAO has been characterized more extensively. The HAO enzyme is located in the periplasm and comprises multi-*c*-heme and homotrimer subunits [151]. It is encoded by the gene cluster *hao* (hydroxylamine oxidoreductase), which is highly conserved, especially in the *β*-subdivision [143]. *N. europaea* was found to contain three copies of *hao*, which were separate but identical (except for one nucleotide) and constituted 40% of the *c*-type heme [152].

Compared with AOB, NOB is more phylogenetically distinct and widespread among the *Proteobacteria*. Eight species of NOB have been cultured, and four phylogenetically distinct groups have been described. The genera *Nitrococcus* and *Nitrobacter* are assigned to the *α*-subclass and *γ*-subclass of *Proteobacteria*, respectively. The *Nitrospira* genus, which is in its own subdivision (phylum Nitrospira), groups closely with the *δ*-subclass. *Candidatus Nitrospira defluvii* was the first NOB to have its complete genome sequence determined. *Nitrospira* are the dominant and more specialized NOB in most wastewater treatment plants, including drinking water and soil water treatment plants [153–156]. Fukushima et al. found that *Nitrospira* was dominant in high inorganic carbon conditions, while *Nitrobacter* was dominant in low inorganic carbon conditions [157]. Moreover, *Nitrospira* was found to be a K-strategist (high substrate affinities and low maximum activity for nitrite and oxygen), while *Nitrobacter* were *γ*-strategists under substrate-limited conditions. *Nitrococcus* and *Nitrobacter* are able to utilize organic sources as they are facultative autotrophs and anaerobes [158].

The NOB obtains energy from the oxidation of nitrite to nitrate. Nitrite oxidoreductase (NXR) is the key enzyme in the nitrite-oxidizing systems of *Nitrobacter*, *Nitrococcus, Nitrospina,* and *Nitrospira*. An active form of the membrane-bound NXR isolated from *Nitrobacter hamburgensis* was shown to oxidize nitrite to nitrate in the presence of ferricyanide [159]. The NXR enzyme comprises two to three subunits (*α*-subunit, NorA, and *β*-subunit, NorB) containing various cofactors (iron, molybdenum, sulfur, and copper). It is thought that NorA contains the NOR catalytic site and NorB functions as an electron-channeling protein between NorA and the membrane-integrated electron-transport chain [159]. The molecular masses of NorB differ among NOB species, e.g., 65 kDa in *Nitrococcus* and *Nitrobacter*, 48 kDa in *Nitrospina*, and 46 kDa in *Nitrospira*. Analyses of NXRs have revealed their subcellular location and phylogenetic position as a monophyletic lineage in the tree of type II enzymes in the DMSO reductase family [154].

However, *Nitrobacter* have never been found in AO-MFC systems. Some studies have demonstrated that the nitrite in the anolyte and potassium permanganate in catholyte can establish a chemical cell to generate electricity, suggesting that biotic nitrite reduction may be negligible and that nitrite may be electrochemically oxidized into nitrate.

7.3.2 Ammonia Removal in Photosynthetic Algae MFC

The possibility of using light to promote electricity production in MFC has received more attention in the last decade, with the development of new systems to convert light into bioelectricity [160]. These systems, which are known as PMFC, can utilize free solar radiation to generate energy. The most widely studied concept is the use of microalgae in the cathode chamber to produce oxygen for the cathode reaction (photosynthetic algae MFC; PA-MFC) [161]. Typically, bacteria at the anode oxidize organic compounds and produce protons and electrons. The electrons are transferred from bacteria to the anode, and then to the cathode through an external circuit. At the cathode, microalgae use light and carbon dioxide to produce oxygen via photosynthesis. The oxygen combines with protons and electrons (from the anode compartment) to form water, thus completing the cathode reaction. The advantage of these systems is that they can treat biodegradable wastes (by bacteria in the anode), consume carbon dioxide, and fix nitrogen and phosphorus (by microalgae in the cathode) while simultaneously producing electricity.

Photosynthesis is a complex biological redox process that occurs in algae and plants. In this process, solar power is used to produce oxygen and carbohydrates via multiple redox reactions. Other chemical compounds produced during photosynthesis can also be used to produce power or to synthesize other molecules [162]. Microalgal growth depends on several parameters, such as light, temperature, nutrients, and pH. Light (quality, intensity, and dark/light regimes) is one of the most important parameters controlling the growth and composition of microalgae biomass (fatty acid and pigment profiles). Nutrients also affect the growth and composition of microalgae. Under nutrient-limited conditions (particularly nitrogen limitation), microalgae increase the production of lipids, carbohydrates, and/or pigments.

7.3.2.1 Electron Transfer Between Electrode and Microalgae

There are four possible electron transfer mechanisms between the electrode and microalgae: DET through the cathode to algae, direct carbon dioxide reduction at the cathode, reduction of oxygen generated by photosynthesis, and electron transfer via self-produced mediators (Fig. 7.6) [163]. Unfortunately, only the oxygen reduction mechanism has been thoroughly studied. First, a phototrophic biofilm comprising cyanobacteria, algae, and other bacteria develops at the cathode. Illumination provides photosynthetically manufactured oxygen as the last electron acceptor for the microbial-catalyzed cathode oxygen reaction [161]. During photosynthesis, nutrients such as nitrogen and phosphate are simultaneously consumed, but DET has not been detected in this mechanism.

Based on theoretic thermodynamic determinations, power output is impossible with end products such as acetate or glucose. The voltage only slightly increased by about 60 mV by directly injecting pure carbon dioxide into the cathode. Cao et al.
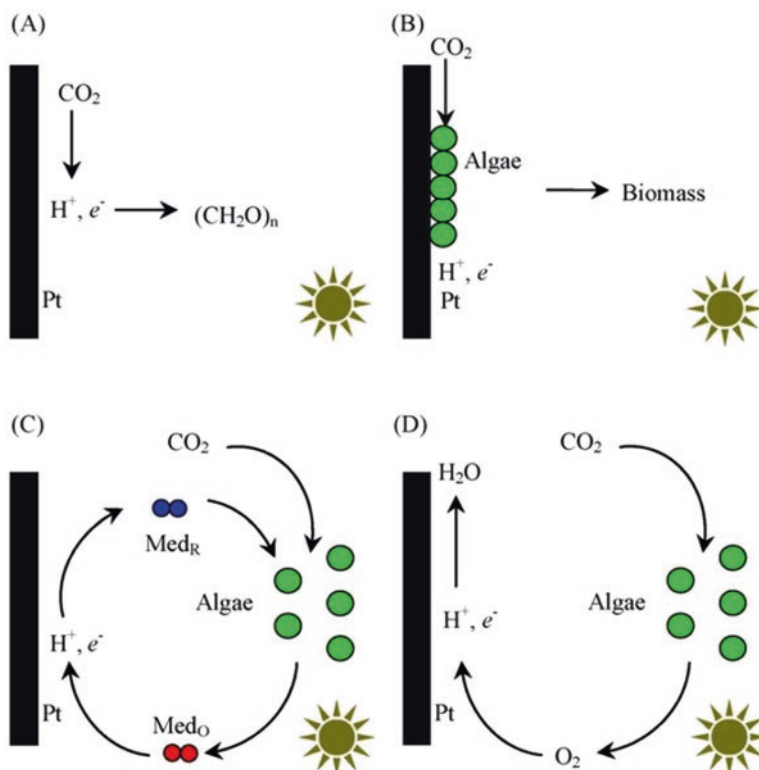
Fig. 7.6 Possible cathode reaction mechanisms in microbial carbon capture cells: direct carbon dioxide reduction (**a**), DET from cathode to algae (**b**), mediator-assisted electron transfer (**c**), and oxygen reduction (**d**). (Reprinted from [163], Copyright 2010, with permission from Elsevier)

studied the direct reduction of carbon dioxide in an MFC [164]. Their DO measurements indicated that no oxygen was produced, but there was an obvious reduction peak at around -40 mV, indicating that carbon dioxide was reduced at the biocathode. However, there was no peak before the *Chlorella vulgaris* biofilm formed on the biocathode. These results indicated that the biofilm is the main functional region for extracellular electron transfer [165].

7.3.2.2 Factors Controlling Photosynthesis

7.3.2.2.1 Light Intensity

Among the environmental factors affecting the growth rate of unicellular algae, light is the most important and is often supplied at abnormal levels. In essence, the intensity of natural light is much higher than the saturation point of the microorganism and may even inhibit growth. The inhibition by light depends on other factors such

as temperature, carbon dioxide levels, and nutrient supply. Therefore, in PA-MFC, a low light intensity (lower than that of sunlight, ~100 mW m^{-2}) is sufficient for photosynthesis [166]. In the appropriate range of light intensity, photosynthetic activity, microalgae biomass, and the oxygen production rate were shown to increase with higher light intensity, thereby maximizing the voltage output of the MFC [161]. In addition, the power coulombic efficiency of a PA-MFC was shown to be higher under low light than under high light, indicating that high light should be avoided if algal photosynthesis is the only source of oxygen in the cathode chamber.

7.3.2.2.2   Reactor Configurations

In the review of Elmekawy et al., the reactor configuration of PBR has been summarized in details [162]. An early photosynthetic microbial cathode cell was developed using *Chlorella vulgaris* as a direct electron acceptor at the surface of the cathode (Fig. 7.7a) [165, 167]. This design has been tested as a bioethanol-producing device and consists of an MFC coupled to an existing industrial yeast bioreactor as the anode chamber. This dual-benefit integrated system has been used to generate electricity in bioethanol plants while reducing carbon dioxide emissions. In this system, the carbon dioxide is used to produce biofuel via the photosynthesis of microalgae growing in the cathode PBR half-cell. In addition, biodiesel is produced as a by-product of microalgal growth. To obtain all the benefits of the system, a chemical mediator must be added to the anode half-cell to allow electrons to travel between the yeast cells and the electrodes. The cathode half-cell is supplied with air containing 10% carbon dioxide, which is injected directly into the cell culture. The PBR is irradiated by sunlight to promote microalgal photosynthesis.

This concept can be altered by connecting a glass PBR to the MFC to form a PA-MFC (Fig. 7.7b) [168]. Algal growth is initiated in the illuminated PBR, which is supplied with air pumped by the nebulizer in the reactor. The MFC has a double electrode separated by a CEM. The growing microalgae are converted to chemical energy in the form of biomass, while electrochemically active bacteria proliferate in the anode chamber of the MFC. Jiang et al. proposed a similar design [169], in which an upflow-type MFC coupled with a PBR simultaneously treated wastewater and generated power. The upflow MFC consisted of a plastic cylinder with a carbon fiber brush electrode and a glass wool/bead delamination between the anode and the cathode chamber. The outer-column PBR was coupled to the upflow MFC, and the effluent from the cathode chamber of the upflow MFC was pumped continuously into the column PBR. The microalgae culture was grown under continuous irradiation and supplied with air mixed with carbon dioxide (MFC effluent).

So far, the dual-chamber PA-MFC is the most common design. In this configuration, algal photosynthesis directly supplies oxygen in the cathode chamber (Fig. 7.7c) [170–173], and the two chambers may be separated by an ion-exchange membrane. Typically, activated sludge is used as the inoculum in the anode chamber. The anode chamber is covered during operation to block the light so that algae cannot grow. The cathode compartment containing the microalgae culture is irradiated for a certain period, e.g., 12 h per day. In systems with this configuration, the
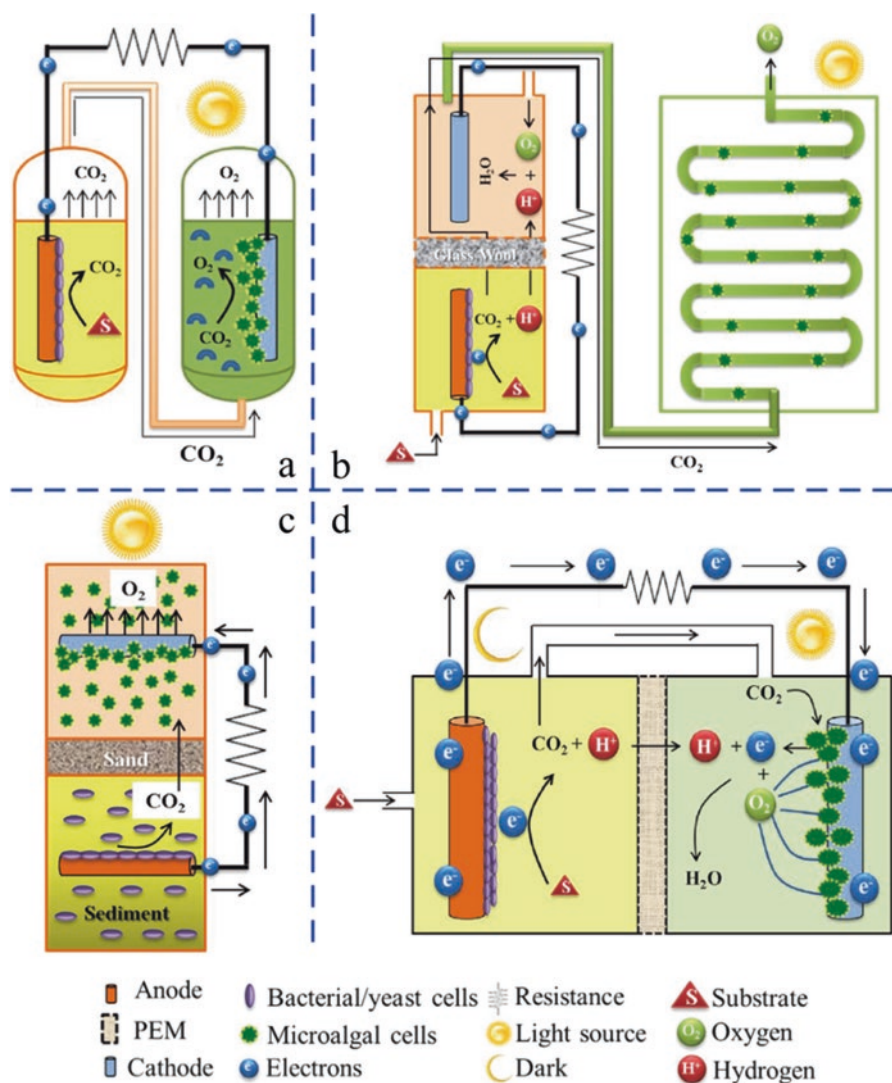
Fig. 7.7 Schematic configuration of coupled PA-MFC: (**a**) PBR-based design; (**b**) upflow MFC-based design; (**c**) dual-chamber PA-MFC; and (**d**) photosynthetic sediment MFC. (Reprinted from [162], Copyright 2014, with permission from Elsevier)

carbon dioxide produced in the anode chamber moves through a funnel-shaped gas collector at the top of the chamber through a tube to the cathode chamber, where it is used for algal photosynthesis and biomass production. Alternatively, microalgae can be used as a bioanode catalyst in a dual-chamber PA-MFC with an ion-exchange membrane separating the anode from the chemical cathode catalyst [174]. In general, the dual-chamber configuration requires the separate production of bacterial and microalgae cultures, microbial culturing instead of mechanical aeration, and a dynamic light/dark cycle for microalgal growth.

By using an anode buried in a deposit and a cathode in the water at the top of the deposit, energy can be generated by exploiting the naturally occurring potential difference [175]. This kind of system is known as a SMFC (Fig. 7.7d) [176]. The microorganisms obtain energy from the sediment through directly oxidizing organic matter or other inorganic complexes (i.e., sulfur-containing complexes). The cathode reaction of SMFC consists of the reduction of electron acceptors, such as oxygen dissolved in water. In photosynthetic SMFC, the cathode chamber contains microalgae and a biogenic substance [177]. The carbon dioxide generated by the anode bacteria is used by algal cells, and the oxygen generated by algae is used in the cathode chamber to generate the current output. Such systems are composed of an anode in a sediment layer, a sand layer, and a cathode chamber filled with microalgae culture medium. A light source is normally used to drive photosynthesis in photosynthetic SMFC.

7.3.2.2.3   Microbial Community of Anode Biofilm

Chlorella vulgaris is the most common microalgae species used in biological cathodes of PA-MFC. Powell et al. [165] tested the ability of *Chlorella vulgaris* to capture carbon dioxide as an electron acceptor in the cathode chamber of a PA-MFC. The maximum cell growth rate (3.6 mg L^{-1} h^{-1}) and a power density of 2.7 mW m^{-2} were obtained with a carbon dioxide concentration of 10%. Wang et al. [163] focused on reducing carbon dioxide emissions using a novel type of PA-MFC, a microbial carbon capture cell. All the carbon dioxide produced at the anode was moved into the catholyte, and the soluble inorganic carbon was converted to algal biomass. A PA-MFC with a co-culture of *Chlorella* and *Phormidium* was also tested.

A large proportion of the sequences (up to 50% of each sample) extracted from green algae (organellar DNA) at MFC cathodes was identified as "chloroplast." The combination of bacterial metabolic activities and algae in PA-MFC systems provides conditions that favor the growth of certain bacterial taxa. Xiao et al. found that 68–90% of the bacterial sequences identified in samples from a PA-MFC were from α-, *β*-, and *γ-Proteobacteria* and *Acidobacteria*_Gp3 [178].

7.3.3   Ammonia Recovery Through Struvite Precipitation in BES

In 1963, Taylor et al. successfully recycled struvite in the laboratory [179]. Struvite is a white crystalline material consisting of magnesium, ammonium, and phosphorus at equimolar concentrations ($MgNH_4PO_4 \cdot 6H_2O$). Occasionally, struvite precipitation is used to prevent the release of nitrogen as ammonia gas during composting of manure and corn stalks [180]. Due to the high concentration of struvite-forming ions (NH_4^+-N, Mg^{2+}, PO_4^{3-}) and high pH, struvite deposition is a common

operational problem in waste treatment plants, especially in anaerobic digestion tanks. When the molar ratio of Mg/N/P is less than 1:1:1, crystal deposition barely occurs. Although inadvertent struvite precipitation may be a serious problem in wastewater treatment, it can be used to produce valuable fertilizers (PO_4^{3-} and NH_4^+-N) from animal feces.

Struvite can be recovered from wastewater using several methods: electrolysis, chemical addition, or carbon dioxide stripping [181]. In most struvite-recycling studies, the pH has been controlled by adding chemicals (e.g., NaOH, $Mg(OH)_2$, and $Ca(OH)_2$) or by supplying carbon dioxide. However, these methods are not practical on a larger scale, because the operating costs of blower operation or chemical additions are excessive (about \$140–460 per L of struvite). In electrochemical systems, the localized pH can increase through the consumption of protons (via hydrogen evolution), allowing struvite precipitation to occur. The main drawback of this method is the energy cost to produce the voltage required for hydrogen evolution (theoretically about 1250 mV, but >1800 mV in practice).

To decrease the energy cost of electrochemical struvite precipitation, many studies have focused on simultaneously treating wastewater containing organic pollutants and recovering electricity with the help of a MEC [182]. In MECs, microbes convert organic and inorganic matter into current at a lower potential (about -400 mV), and an equal number of protons is released at the cathode. At neutral pH, the primary cationic species transported through the CEM are positive ions (e.g., NH_4^+, Na^+, and K^+) because of the low proton concentration. When an AEM is used, the charge is balanced by the transport of negatively charged materials (OH^-, HCO_3^-, HPO_4^{2-}, and Cl^-) [183]. In this process, all the ions required for struvite precipitation are concentrated in the same chamber.

There are two stages in struvite precipitation: nucleation and growth [184]. Nucleation occurs when constituent ions combine to form crystal embryos, and crystal growth continues until equilibrium is reached. In a continuous system, crystals may grow continuously. The struvite precipitation process is affected by pH, temperature, supersaturation, and other ions such as calcium. When the concentration of magnesium, ammonium, and phosphate ions exceeds the solubility of the product, crystal growth may also be affected. Thus, ionic activity and ionic strength affect the formation of struvite as a standard solubility product from a particular solution.

7.3.4 Factors Controlling Struvite Precipitation

7.3.4.1 Thermodynamic Equilibrium

Table 7.6 shows equilibrium calculations (as performed with the PHREEQC program) and thermodynamic data as reported elsewhere [185, 186]. The initial magnesium concentrations, $\triangle H$, and the standard solubility product were estimated in AQUASIM with the same set of equilibrium reactions.

Table 7.6 Thermodynamic equilibrium for a source-separated urine system

Equilibrium	pK
$Mg^{2+} + H_2PO_4^- \leftrightarrow MgPO_4^- + 2H^+$	12.96
$Na^+ + H_2PO_4^- \leftrightarrow NaHPO_4^- + H^+$	6.01
$Mg^{2+} + H_2PO_4^- \leftrightarrow MgHPO_4^- + H^+$	4.3
$NH_4^+ + HPO_4^- \leftrightarrow NH_4HPO_4^-$	−1.3
$Mg^{2+} + SO_4^{2-} \leftrightarrow MgSO_4$	−2.37
$NH_4^+ + SO_4^{2-} \leftrightarrow NH_4SO_4^-$	−1.03
$H_2PO_4^- \leftrightarrow HPO_4^{2-} + H^+$	7.21
$HPO_4^- \leftrightarrow PO_4^{2-} + H^+$	12.36
$Mg^{2+} + HCO_3^- \leftrightarrow MgHCO_3^-$	−1.07
$Mg^{2+} + HCO_3^- \leftrightarrow MgCO_3^- + H^+$	7.35
$HCO_3^- \leftrightarrow CO_3^- + H^+$	10.33
$NH_4^+ \leftrightarrow NH_3 + H^+$	9.24

Reprinted from [186], Copyright 2007, with permission from Elsevier

The standard solubility product is defined as follows:

$$pK_S^0 = -\log\left(K_S^0\right) \tag{7.4}$$

$$K_S^0 = f_1\left[NH_4^+\right]f_2\left[Mg^{2+}\right]f_3\left[PO_4^{3-}\right] \tag{7.5}$$

where $[NH_4^+]$, $[Mg^{2+}]$, and $[PO_4^{3-}]$ are the concentrations and *f1, f2,* and *f3* are the activity coefficients (Eq. 7.9) of the specific free ions of NH_4^+, Mg^{2+}, and PO_4^{3-}, respectively. When calculating the activities for the standard solubility product, speciation based on pH and all ions present must be taken into account, and the activity factors must be determined. This is a tedious task for a complex system like urine. Since undiluted stored urine has a consistent composition in terms of ionic strength and pH, we can work with a conditional solubility product, which is defined here as the product of calculated total concentrations in a system in equilibrium:

$$K_S^{cond} = \left[NH_4^+ + NH_3\right]\left[Mg\right]_{aq}\left[P\right]_{ortho} \tag{7.6}$$

where $[NH_4^+ + NH_3]$ represents the dissolved ammonia/ammonium concentration, $[Mg]_{aq}$ represents the total dissolved magnesium concentration, and $[P]_{ortho}$ represents the total dissolved orthophosphate concentration. Because K_s^{cond} is determined for a specific matrix with fixed pH and ionic strength, it is valid for this matrix only [187]. However, since K_s^{cond} is derived directly from the calculated total concentrations, speciation or activity calculations become redundant when estimating maximum dissolved total concentrations. Temperature corrections of the solubility product are performed with the Van't Hoff equation, as follows:

$$\frac{K_s\left(T2\right)}{K_s\left(T2\right)} = e^{(\Delta H/R)\left(\left(\frac{1}{T_1}\right)-\left(\frac{1}{T_2}\right)\right)} \tag{7.7}$$

where $K_s(T1)$ and $K_s(T2)$ are the solubility products at temperatures $T1$ and $T2$ in Kelvin, respectively, $R = 8.3145$ J mol^{-1} K^{-1}, and $\triangle H$ is the formation enthalpy. All concentrations are given in [M] or [mM].Most relevant equilibrium constants, such as solubility constants, are consequently influenced by the ionic strength, and activity coefficients must be considered for all chemical calculations. The ionic strength I is defined as follows:

$$I = \sum_i \left(c_i z_i^2\right) \tag{7.8}$$

$$-\log f_i = Az_i^2\left(\frac{\sqrt{I}}{1+\sqrt{I}} - BI\right) \tag{7.9}$$

where c_i is the concentration of ion i and z_i is the charge of ion i. A $= 0.509$ for water at 25 °C and B $= 0.2$ or 0.3 [186].

7.3.4.2 Reactor Configurations

Logan et al. introduced a method to simultaneously produce hydrogen and struvite based on bioelectrochemistry and microbial electrolysis-driven reactions of struvite crystals in the cathode of a single-chamber struvite-sedimentation cell [182, 188]. The anode was graphite fiber brushes covered with electro-active biofilm, and the cathode was stainless steel 304 flat plates or mesh. The electrons converted from organic and inorganic matter by microorganisms were used to generate hydrogen from water at the cathode. With the excessive consumption of protons, the pH of the cathode zone rapidly increased, thus achieving the simultaneous removal of ammonia nitrogen and the recovery of phosphate. Compared with flat plates, mesh cathodes resulted in higher ammonia removal efficiency. The accumulation of struvite crystals did not affect the hydrogen production rate. Both the hydrogen evolution rate and struvite crystallization rate depended on the extra applied voltage and the cathode material. The same concept was modified by connecting an air cathode as the direct electron acceptor and sediment adsorption carrier. When swine wastewater was treated with an air-cathode single-chamber MFC [189, 190], the maximum current density, maximum power density, coulombic efficiency, and average value of COD-removal efficiency were 6.0–7.0 A m^{-2}, 1–2.3 W m^{-2}, 37–47%, and 76–91%, respectively.

The dual-chamber MFC is the most common design used for ion transfer. Almatouq et al. designed a mediator-less dual-chamber MFC [191], in which hydroxide produced around the cathode increased the pH, leading to the precipita-

tion of nitrogen. A three-terminal MFC can be constructed by placing two membranes between the anode and cathode chambers, thereby forming a water-desalination intermediate chamber between the membranes [183]. In such systems, an AEM is placed near the anode and a CEM next to the cathode. When electrons are produced by bacteria on the anode, the ionic material in the anode and cathode chambers is transferred to the intermediate chamber, where nitrogen-containing substances precipitate. Similarly, a multi-pair ion-exchange membrane interposed between the anode chamber and the cathode chamber may improve the performance of the system to increase the charge transfer efficiency. This configuration is known as a stacked-structure MFC system.

7.3.5 Ammonia Recovery Through Blowing-Stripping in BES

Ammonia stripping is the best method to treat wastewater containing high concentrations of ammonia, such as kitchen garbage, human waste, poultry litter leachate, and chicken manure [192–194]. The method does not produce additional sludge, the cost is moderate, and the operation is simple. During this process, free ammonia is drained from wastewater and transferred to the gas phase after a large amount of additional aeration. The efficiency of ammonia stripping is strongly dependent on Henry's law equilibrium (Eq. 7.10) and on the ammonia dissociation equilibrium (Eqs. 7.11 and 7.12) [195]:

$$p = K_c c \tag{7.10}$$

$$NH_4^+ \leftrightarrow NH_3 + H^+ \tag{7.11}$$

$$\frac{[NH_3]}{[TNH_3]} = \left(1 + \frac{10 - pH}{10 - (0.09018 + 2729.92 / T(K))}\right) \tag{7.12}$$

where p is the partial pressure of ammonia gas, K_c is Henry's law constant, and c is its molar concentration in the liquid phase, $[NH_3]$ is the concentration of free ammonia, $[TNH_3]$ is the sum of free ammonia and ammonium ions, and $T(K)$ is temperature in Kelvin. As shown in Eq. (7.11), the free ammonia concentration in the aqueous phase depends on pH and temperature. Thus, higher pH and temperature lead to higher concentrations of free ammonia. Liao et al. showed that a high alkaline pH (10.5–11.5) and high temperature (80 °C) were required to remove ammonia from piggery slurry efficiently. The mass transfer rate of ammonia can also be controlled by the airflow rate. In the biogas removal during digestion of source-sorted food waste [192], the ammonia removal rate was increased by 4.5 times when the flow rate was increased from 0.125 to 0.375 L_{biogas} $L_{digestate}^{-1}$ min^{-1}.
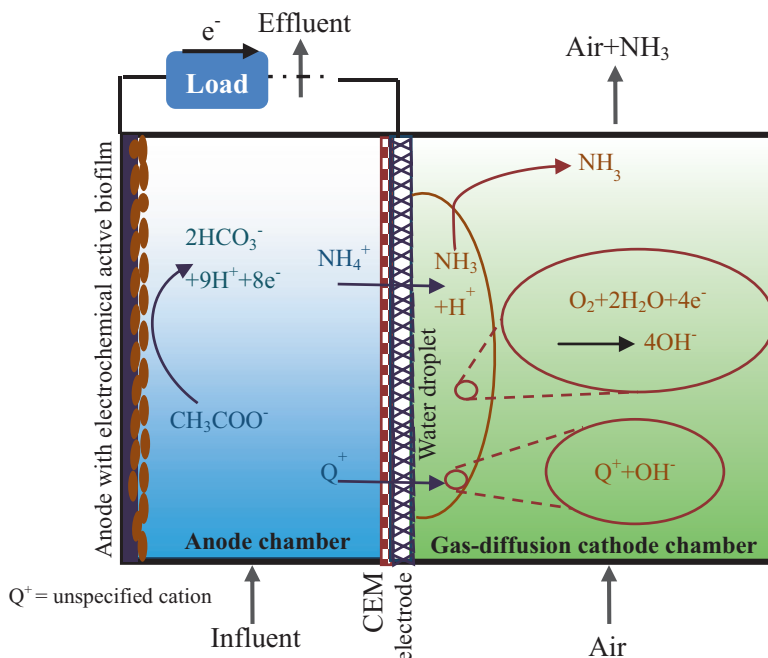
Fig. 7.8 Schematic representation of processes involved in ammonium recovery by blowing-stripping in an MFC. (Reprinted from [196], Copyright 2012, with permission from Elsevier)

Similar to the process described in Sect. 3.3, microorganisms convert the organic material into a current, the released electrons travel through the external circuit to the cathode, and oxygen is reduced in the anode chamber of the reactor (Fig. 7.8) [196]. In this process, ammonia is transferred to the cathode under the pressure of an electric field and then recycled using the blowing-stripping method. Kuntke et al. designed MFC equipped with gas diffusion cathodes in which the ammonia moves into the cathode chamber via the force of electric traction. In the cathode chamber, the ionized ammonium is converted to volatile ammonia under high pH. The ammonia is recovered from the liquid-gas boundary by evaporation, and the resulting acidic solution is absorbed.

Negative potential can be used to drive a thermodynamically unfavorable reaction in the cathode of an MEC to produce hydrogen gas, which can increase the pH of the cathode chamber [197]. For example, Wu et al. used BES to simultaneously produce hydrogen and recover ammonium from wastewater. More than 90% of the electrons generated in the anode chamber were used to produce hydrogen at the cathode. This rapidly increased the concentration of hydroxyl ions, resulting in a high ammonium recovery efficiency of 94% from synthetic wastewater [198].

7.4   Other Methods of Nitrogen Removal and Recovery

Nitrite and nitrogen oxides are the other two major nitrogen pollutants in the natural environment. Nitrite is an ozone-depleting compound with an oxidation state between those of ammonium and nitrate. Because it is easily oxidized, its concentration in oxygenated waters is typically less than 0.005 mg L^{-1}. However, certain human activities have increased the amount of nitrite in aquatic systems, leading to anoxia in fish and other aquatic organisms [199]. Nitrous oxides are important greenhouse gases whose global warming potential is about 300 times that of carbon dioxide and represent about 7.9% of the global greenhouse gas budget when expressed in carbon dioxide equivalents [200]. Therefore, it is important to mitigate nitrite and nitrogen oxide emissions.

In nitrification-denitrification systems, ammonium is oxidized to nitrite and then to nitrate, and finally nitrite and nitrate are reduced to nitrite, nitric oxide (NO), nitrous oxide (N_2O), and nitrogen gas in turn in the presence of electron donors [11]. Therefore, nitrite and nitrogen oxides are intermediates in the denitrification process. These two nitrogen pollutants can also be removed in BES using cathode denitrification technology. For example, Desloover et al. [201] found that BES equipped with autotrophic denitrifying biological cathodes removed nitrous oxide at rates ranging from 0.76 to 1.83 kg Nm^{-3} day^{-1}, proportional to the current rate of production, resulting in a high cathode coulombic efficiency of nearly 100%. That system operated for more than 115 days with nitrous oxide as the only electron acceptor, indicating that nitrous oxide respiration produces enough energy to sustain the biological process. Puig et al. studied autotrophic nitrite removal in the cathode of an MFC [47, 202] and found that nitrite could serve as the only electron acceptor in the process in which exoelectrogenic bacteria removed nitrogen from wastewater while producing electricity.

References

1. Camargo JA, Alonso A (2006) Ecological and toxicological effects of inorganic nitrogen pollution in aquatic ecosystems: a global assessment. Environ Int 32:831–849
2. Howarth RW (2003) Nutrient limitation of net primary production in marine ecosystems. Annu Rev Ecol Evol S 19:89–110
3. Vitousek PM, Aber J, Bayley SE et al (1997) Human alteration of the global nitrogen cycle: causes and consequences. Ecol Appl 7:737–750
4. Cleveland CC, Townsend AR, Schimel DS et al (1999) Global patterns of terrestrial biological nitrogen (N_2) fixation in natural systems. Glob Biogeochem Cycl 13:623–645
5. Karl D, Michaels Q, Bergman B et al (2002) Dinitrogen fixation in the world's oceans. Biogeochemistry 57(58):47–98
6. Howarth RW (2008) Coastal nitrogen pollution: a review of sources and trends globally and regionally. Harmful Algae 8:14–20
7. National Bureau of Statistics, Ministry of Environmental Protection (2014) China statistical yearbook on environment. China Statistics Press, China

8. Rousta MJ, Lotfi E, Shamsalam N et al (2010) Nitrate situation in some vegetables and the necessity of crop production via organic farming. Paper presented at 19th world congress of soil science, soil solutions for a changing world, Brisbane, Australia, 1–6
9. Vitousek PM, Aber JD, Howarth RW et al (1997) Human alteration of the global nitrogen cycle: sources and consequences. Ecol Appl 7:737–750
10. Gupta SK, Gupta RC, Seth AK et al (2000) Methaemoglobinaemia in areas with high nitrate concentration in drinking water. Natl Med J India 13:58–61
11. Lijinsky W, Conrad E, Bogart RVD (1972) Carcinogenic nitrosamines formed by drug-nitrite interactions. Nature 15:165–167
12. Ge S, Wang S, Yang X et al (2015) Detection of nitrifiers and evaluation of partial nitrification for wastewater treatment: a review. Chemosphere 140:85–98
13. Ghafari S, Hasan M, Aroua MK (2008) Bio-electrochemical removal of nitrate from water and wastewater—a review. Bioresour Technol 99:3965–3974
14. Karanasios KA, Vasiliadou IA, Pavlou S et al (2010) Hydrogenotrophic denitrification of potable water: a review. J Hazard Mater 180:20–37
15. Kim J, Benjamin MM (2004) Modeling a novel ion exchange process for arsenic and nitrate removal. Water Res 38:2053–2062
16. Schoeman JJ, Steyn A (2003) Nitrate removal with reverse osmosis in a rural area in South Africa. Desalination 155:15–26
17. Gain E, Laborie S, Viers P (2002) Ammonium nitrate wastewater treatment by coupled membrane electrolysis and electrodialysis. J Appl Electrochem 32:969–975
18. Aslan S (2005) Combined removal of pesticides and nitrates in drinking waters using biodenitrification and sand filter system. Process Biochem 40:417–424
19. Wasik E, Bohdziewicz J, Blaszczyk M (2001) Removal of nitrates from ground water by a hybrid process of biological denitrification and microfiltration. Process Biochem 37:57–64
20. Aslan S, Turkman A (2005) Combined biological removal of nitrate and pesticides using wheat straw as substrates. Process Biochem 40:935–943
21. Ernstsen V (1996) Reduction of nitrate by Fe^{2+} in clay minerals. Free Radic Res 44:599–608
22. Mellor RB, Ronnerrberg J, Campbell WH et al (1992) Reduction of nitrate and nitrite in water by immobilized enzymes. Nature 355:717–719
23. Park HI, Kim DK, Choi YJ et al (2005) Nitrate reduction using an electrode as direct electron donor in a biofilm-electrode reactor. Process Biochem 40:3383–3388
24. Rosenbaum M, Aulenta F, Villano M et al (2011) Cathodes as electron donors for microbial metabolism: which extracellular electron transfer mechanisms are involved? Bioresour Technol 102:324–333
25. Peter C, Korneel R, Peter A et al (2007) Biological denitrification in microbial fuel cells. Environ Sci Technol 41:3354–3360
26. Lovley DR (2012) Electromicrobiology. Annu Rev Microbiol 66:391–409
27. Butler CS, Nerenberg R (2010) Performance and microbial ecology of air-cathode microbial fuel cells with layered electrode assemblies. Appl Microbiol Biotechnol 86:1399–1408
28. Freguia S, Teh EH, Boon N et al (2010) Microbial fuel cells operating on mixed fatty acids. Bioresour Technol 101:1233–1238
29. Yarzabal A, Appia-Ayme C, Ratouchniak J et al (2004) Regulation of the expression of the *Acidithiobacillus ferrooxidans rus* operon encoding two cytochromes c, a cytochrome oxidase and rusticyanin. Microbiology 150:2113–2123
30. Freguia S, Tsujimura S, Kano K (2010) Electron transfer pathways in microbial oxygen biocathodes. Electrochim Acta 55:813–818
31. Lefebvre O, Al-Mamun A, Ng HY (2008) A microbial fuel cell equipped with a biocathode for organic removal and denitrification. Water Sci Technol 58:881–885
32. Aulenta F, Reale P, Canosa A (2010) Characterization of an electro-active biocathode capable of dechlorinating trichloroethene and cis-dichloroethene to ethene. Biosens Bioelectron 25:1796–1802

33. Aulenta F, Catervi A, Majone M (2007) Electron transfer from a solid-state electrode assisted by methyl viologen sustains efficient microbial reductive dechlorination of TCE. Environ Sci Technol 41:2554–2559

34. Steinbusch KJ, Hamelers HV, Schaap JD (2010) Bioelectrochemical ethanol production through mediated acetate reduction by mixed cultures. Environ Sci Technol 44:513–517

35. Hatch JL, Finneran KT (2008) Influence of reduced electron shuttling compounds on biological H_2 production in the fermentative pure culture *Clostridium beijerinckii*. Curr Microbiol 56:268–273

36. Park DH, Zeikus JG (1999) Utilization of electrically reduced neutral red by *Actinobacillus succinogenes*: physiological function of neutral red in membrane-driven fumarate reduction and energy conservation. J Bacteriol 181:2403–2410

37. Wei TM, Mohamed KTA, Mohammed HC (2013) A review on the effect of bio-electrodes on denitrification and organic matter removal processes in bio-electrochemical systems. J Ind Eng Chem 19:1–13

38. Tatsumi H, Takagi K, Fujita M (1999) Electrochemical study of reversible hydrogenase reaction of *Desulfovibrio vulgaris* cells with methyl viologen as an electron carrier. Anal Chem 71:1753–1759

39. Lojou E, Durand MC, Dolla A (2002) Hydrogenase activity control at *Desulfovibrio vulgaris* cell-coated carbon electrodes: biochemical and chemical factors influencing the mediated bioelectrocatalysis. Electroanalysis 14:913–922

40. Sanath K, Booki M (2013) Nitrate reduction with biotic and abiotic cathodes at various cell voltages in bioelectrochemical denitrification system. Bioprocess Biosyst Eng 36:231–238

41. Pous N, Puig S, Balaguer MD et al (2015) Cathode potential and anode electron donor evaluation for a suitable treatment of nitrate-contaminated groundwater in bioelectrochemical systems. Chem Eng J 263:151–159

42. Puig S, Coma M, Desloover J et al (2012) Autotrophic denitrification in microbial fuel cells treating low ionic strength waters. Environ Sci Technol 46:2309–2315

43. Chang CN, Cheng HB, Chao AC (2004) Applying the Nernst equation to simulate redox potential variations for biological nitrification and denitrification processes. Environ Sci Technol 38:1807–1812

44. Feleke Z, Araki K, Sakakibara et al (1998) Selective reduction of nitrate to nitrogen gas in a biofilm-electrode reactor. Water Res 32:2728–−2734

45. Prosnansky M, Sakakibara Y, Kuroda M (2002) High-rate denitrification and SS rejection by biofilm-electrode reactor (BER) combined with microfiltration. Water Res 36:4801–4810

46. Szekeres S, Kiss I, Bejerano TT et al (2001) Hydrogen-dependent denitrification in a two-reactor bio-electrochemical system. Water Res 35:715–719

47. Li Y, Williams I, Xu ZH et al (2016) Energy-positive nitrogen removal using the integrated short-cut nitrification and autotrophic denitrification microbial fuel cells (MFCs). Appl Energy 163:352–360

48. Zhang BG, Liu Y, Tong S et al (2014) Enhancement of bacterial denitrification for nitrate removal in groundwater with electrical stimulation from microbial fuel cells. J Power Source 268:423–429

49. Liang YX, Feng HJ, Shen DS et al (2016) Metal-based anode for high performance bioelectrochemical systems through photo-electrochemical interaction. J Power Source 324:26–32

50. Cast KL, Flora JRV (1998) An evaluation of two cathode materials and the impact of copper on bioelectrochemical denitrification. Water Res 32:63–70

51. Sakakibara Y, Nakayama T (2001) A novel multi-electrode system for electrolytic and biological water treatments: electric charge transfer and application to denitrification. Water Res 35:768–778

52. Sim J, Seo H, Kim J (2012) Electrochemical denitrification of metal-finishing wastewater: influence of operational parameters. Korean J Chem Eng 29:483–488

53. Ghazouani M, Akrout H, Bousselmi L (2014) Efficiency of electrochemical denitrification using electrolysis cell containing BDD electrode. Desalin Water Treat 53:1107–1117

54. Kesseru P, Kiss I, Bihari Z et al (2003) Biological denitrification in a continuous-flow pilot bioreactor containing immobilized *Pseudomonas butanovora* cells. Bioresour Technol 87:75–80
55. Wan D, Liu H, Qu J et al (2009) Using the combined bioelectrochemical and sulfur autotrophic denitrification system for groundwater denitrification. Bioresour Technol 100:142–148
56. Wang H, Qu J (2003) Combined bioelectrochemical and sulfur autotrophic denitrification for drinking water treatment. Water Res 37:3767–3775
57. Feleke Z, Sakakibara Y (2002) A bio-electrochemical reactor coupled with adsorber for the removal of nitrate and inhibitory pesticide. Water Res 36:3092–3102
58. Zhang L, Jia J, Zhu Y et al (2005) Electro-chemically improved bio-degradation of municipal sewage. Biochem Eng J 22:239–244
59. Zuo KC, Liiu H, Zhang QY et al (2016) Enhanced performance of nitrogen-doped carbon nanotube membrane-based filtration cathode microbial fuel cell. Electrochim Acta 211:199–206
60. Xiao ZX, Awata T, Zhang DD et al (2016) Enhanced denitrification of *Pseudomonas stutzeri* by a bioelectrochemical system assisted with solid-phase humin. J Biosci Bioeng 122:85–91
61. Liang YX, Feng HJ, Shen DD et al (2017) Enhancement of anodic biofilm formation and current output in microbial fuel cells by composite modification of stainless steel electrodes. J Power Source 342:98–104
62. Xie X, Criddle C, Cui Y (2015) Design and fabrication of bioelectrodes for microbial bioelectrochemical systems. Energy Environ Sci 8:3418–3441
63. Zhang T, Nie HR, Bain T (2013) Improved cathode materials for microbial electrosynthesis. Energy Environ Sci 6:217–224
64. Kelly PT, He Z (2013) Nutrients removal and recovery in bioelectrochemical systems: a review. Bioresour Technol 153:351–360
65. Ghafari B, Hasan M, Aroua MK (2008) Bio-electrochemical removal of nitrate from water and wastewater—a review. Bioresour Technol 99:3965–3974
66. Zhou MH, Wang W, Chi ML (2009) Enhancement on the simultaneous removal of nitrate and organic pollutants from groundwater by a three-dimensional bio-electrochemical reactor. Bioresour Technol 100:4662–4668
67. Virdis B, Rabaey K, Yuan ZG (2008) Microbial fuel cells for simultaneous carbon and nitrogen removal. Water Res 42:3013–3024
68. Virdis B, Rabaey K, Rozendal RA (2010) Simultaneous nitrification, denitrification and carbon removal in microbial fuel cells. Water Res 44:2970–2980
69. Xie S, Liang P, Chen Y (2011) Simultaneous carbon and nitrogen removal using an oxic/anoxic-biocathode microbial fuel cells coupled system. Bioresour Technol 102:348–354
70. Liang P, Wei JC, Li M (2013) Scaling up a novel denitrifying microbial fuel cell with an oxic-anoxic two stage biocathode. Front Environ Sci Eng 6:913–919
71. Yan HJ, Saito T, Regan JM (2012) Nitrogen removal in a single-chamber microbial fuel cell with nitrifying biofilm enriched at the air cathode. Water Res 46:2215–2224
72. Zhang F, He Z (2012) Integrated organic and nitrogen removal with electricity generation in a tubular dual-cathode microbial fuel cell. Process Biochem 47:2146–2151
73. Ghafari S, Hasan M, Aroua MK (2009) Nitrate remediation in a novel upflow bio-electrochemical reactor (UBER) using palm shell activated carbon as cathode material. Electrochim Acta 54:4164–4171
74. Zhang YF, Angelidaki I (2013) A new method for in situ nitrate removal from groundwater using submerged microbial desalination−denitrification cell (SMDDC). Water Res 47:1827–1836
75. Mook WT, Chakrabarti MH, Aroua MK et al (2012) Removal of total ammonia nitrogen (TAN), nitrate and total organic carbon (TOC) from aquaculture wastewater using electrochemical technology: a review. Desalination 285:1–13

76. Marianna V, Mario B, Davide D et al (2010) Effect of pH on the production of bacterial polyhydroxyalkanoates by mixed cultures enriched under periodic feeding. Process Biochem 45:714–−723

77. Clauwaert P, Desloover J, Shea C et al (2009) Enhanced nitrogen removal in bio-electrochemical systems by pH control. Biotechnol Lett 31:1537–1543

78. Chen D, Wei L, Zou ZC et al (2016) Bacterial communities in a novel three-dimensional bio-electrochemical denitrification system: the effects of pH. Appl Microbiol Biot 100:6805–6813

79. Sukkasem C, Xu S, Park S et al (2008) Effect of nitrate on the performance of single chamber air cathode microbial fuel cells. Water Res 42:4743–4750

80. Glass C, Silverstein JA (1998) Denitrification kinetics of high nitrate concentration water: pH effect on inhibition and nitrite accumulation. Water Res Oxford 32:831–839

81. Fernando CL, José CR, Barreiro MG (1998) Aluminium toxicity modulates nitrate to ammonia reduction. Photosynthetica 35:213–222

82. Fernándeznava Y, Marañón E, Soons J et al (2010) Denitrification of high nitrate concentration wastewater using alternative carbon sources. J Hazard Mater 173:682–688

83. Zhang Y, Zhong F, Xia S et al (2009) Effect of initial nitrate concentrations and heavy metals on autohydrogenotrohic denitrification. In: 2009 3rd International conference on bioinformatics and biomedical engineering

84. Zhao YX, Feng CP, Wang QG et al (2011) Nitrate removal from groundwater by cooperating heterotrophic with autotrophic denitrification in a biofilm–electrode reactor. J Hazard Mater 192:1033–1039

85. Huang BC, Feng HJ, Wang MZ et al (2013) The effect of C/N ratio on nitrogen removal in a bioelectrochemical system. Bioresour Technol 132:91–98

86. Huang BC, Feng HJ, Ding YC et al (2013) Microbial metabolism and activity in terms of nitrate removal in bioelectrochemical systems. Electrochim Acta 113:29–36

87. Pan YT, Ni BJ, Bond PL et al (2013) Electron competition among nitrogen oxides reduction during methanol-utilizing denitrification in wastewater treatment. Water Res 47:3273–3281

88. Feng C, Huang L, Yu H et al (2015) Simultaneous phenol removal, nitrification and denitrification using microbial fuel cell technology. Water Res 76:160–170

89. Zhou M, Fu W, Gu H et al (2007) Nitrate removal from groundwater by a novel three-dimensional electrode biofilm reactor. Electrochim Acta 52:6052–6059

90. Bao LS, Hao WS (2006) Removal of nitrate nitrogen using biofilm-electrode process. Ind Water Wastewater 6:45–47

91. Wasik E, Bohdziewicz J, Błaszczyk M (2001) Removal of nitrate ions from natural water using a membrane bioreactor. Sep Purif Technol 22:383–392

92. Wang Q, Feng C, Zhao Y et al (2009) Denitrification of nitrate contaminated groundwater with a fiber-based biofilm reactor. Bioresour Technol 100:2223–2227

93. Lemmer H, Zaglauer A, Neef A et al (1997) Denitrification in a methanol-fed fixed-bed reactor. Part 2: composition and ecology of the bacterial community in the biofilms. Water Res 31:1903–1908

94. Bonmatí A, Sotres A, Mu Y et al (2013) Oxalate degradation in a bioelectrochemical system: reactor performance and microbial community characterization. Bioresour Technol 143:147–153

95. Sotres A, Diaz-Marcos J, Guivernau M et al (2014) Microbial community dynamics in two-chambered microbial fuel cells: effect of different ion exchange membranes. J Chem Technol Biotechnol 90:1497–1506

96. Sotres A, Cerrillo M, Viñas M et al (2016) Nitrogen removal in a two-chambered microbial fuel cell: establishment of a nitrifying-denitrifying microbial community on an intermittent aerated cathode. Chem Eng J 285:905–916

97. Nguyen VK, Hong S, Park Y et al (2015) Autotrophic denitrification performance and bacterial community at biocathodes of bioelectrochemical systems with either abiotic or biotic anodes. J Biosci Bioeng 119:180–187

98. Wrighton KC, Virdis B, Clauwaert P et al (2010) Bacterial community structure corresponds to performance during cathodic nitrate reduction. ISME J 4:1443–1455

99. Liessens J, Vanbrabant J, De Vos P et al (1992) Mixed culture hydrogenotrophic nitrate reduction in drinking water. Microb Ecol 24:271–290

100. Park HI, Choi YJ, Pak D (2005) Autohydrogenotrophic denitrifying microbial community in a glass beads biofilm reactor. Biotechnol Lett 27:949–953

101. Zhang Y, Zhong F, Xia S et al (2009) Autohydrogenotrophic denitrification of drinking water using a polyvinyl chloride hollow fiber membrane biofilm reactor. J Hazard Mater 170:203–209

102. Driessche GV, Devreese B, Fitch J et al (2006) GHP, a new c-type green heme protein from *Halochromatium salexigens* and other proteobacteria. FEBS J 273:2801–2811

103. Archer M, Banci L, Dikaya E et al (1997) Crystal structure of cytochrome c' from *Rhodocyclus gelatinosus* and comparison with other cytochromes c'. J Biol Inorg Chem 2:611–622

104. Doan TV, Lee TK, Shukla SK et al (2013) Increased nitrous oxide accumulation by bioelectrochemical denitrification under autotrophic conditions: kinetics and expression of denitrification pathway genes. Water Res 47:7087–7097

105. Seifert K, Domka F (2005) Inhibiting effect of surfactants and heavy metal ions on the denitrification process. Pol J Environ Stud 14:87–93

106. Krzeminski S, Martin J, Brackett C (1973) The environmental impact of a quaternary ammonium bactericide. Household Pers Prod Ind 10:22

107. Watanabe T, Motoyama H, Kuroda M (2002) Denitrification and neutralization treatment by direct feeding of an acidic wastewater containing copper ion and high-strength nitrate to a bio-electrochemical reactor process. Water Res 35:4102–4110

108. Miao Y, Liao R, Zhang XX et al (2015) Metagenomic insights into Cr(VI) effect on microbial communities and functional genes of an expanded granular sludge bed reactor treating high-nitrate wastewater. Water Res 76:43–52

109. Nguyen VK, Park Y, Yang H et al (2016) Effect of the cathode potential and sulfate ions on nitrate reduction in a microbial electrochemical denitrification system. J Ind Microbiol Biot 43:783–793

110. Cai J, Zheng P, Zhang J et al (2013) Simultaneous anaerobic sulfide and nitrate removal coupled with electricity generation in microbial fuel cell. Bioresour Technol 129C:224–228

111. Geranio L, Heuberger M, Nowack B (2009) The behavior of silver nanotextiles during washing. Environ Sci Technol 43:8113–8118

112. Wiesner MR, Lowry GV, Alvarez P et al (2016) Assessing the risks of manufactured nanomaterials. Environ Sci Technol 40:4336–4345

113. Chen D, Wang XF, Yang K et al (2016) Response of a three dimensional bioelectrochemical denitrification system to the long-term presence of graphene oxide. Bioresour Technol 214:24–29

114. Chen D, Yang K, Wei L et al (2016) Microbial community and metabolism activity in a bioelectrochemical denitrification system under long-term presence of p-nitrophenol. Bioresour Technol 218:189–195

115. Drewnowski J, Fernandez-Morales F (2016) Heterotrophic anodic denitrification in microbial fuel cells. Sustain 86:561

116. Zhang JQ, Zhang P, Zhang M et al (2013) Kinetics of substrate degradation and electricity generation in anodic denitrification microbial fuel cell (AD-MFC). Bioresour Technol 149:44–50

117. Yenigün O, Demirel B (2013) Ammonia inhibition in anaerobic digestion: a review. Process Biochem 48:901–911

118. Doherty L, Zhao YQ, Zhao XH et al (2015) A review of a recently emerged technology: constructed wetland–microbial fuel cells. Water Res 85:38–45

119. Wang J, Song X, Wang Y et al (2016) Nitrate removal and bioenergy production in constructed wetland coupled with microbial fuel cell: establishment of electrochemically active bacteria community on anode. Bioresour Technol 221:358–365

120. Matheson FE, Sukias JP et al (2010) Nitrate removal processes in a constructed wetland treating drainage from dairy pasture. Ecol Eng 36:1260–1265
121. Kim JR, Zuo Y, Regan JM et al (2008) Analysis of ammonia loss mechanisms in microbial fuel cells treating animal wastewater. Biotechnol Bioeng 99:1120–1127
122. Kuntke P, Geleji M, Bruning H et al (2011) Effects of ammonium concentration and charge exchange on ammonium recovery from high strength wastewater using a microbial fuel cell. Bioresour Technol 102:4376–4382
123. Henze M, Van Loosdrecht MCM, Ekama GA et al (2008) Biological wastewater treatment: principles, modelling and design. IWA Publishing, London
124. Mctavish H, Fuchs JA, Hooper AB et al (1993) Sequence of the gene coding for ammonia monooxygenase in *Nitrosomonas europaea*. J Bacteriol 175:2436–2444
125. Ge SJ, Wang SY, Yang X et al (2015) Detection of nitrifiers and evaluation of partial nitrification for wastewater treatment: a review. Chemosphere 140:85–98
126. Min B, Kim J, Oh S et al (2005) Electricity generation from swine wastewater using microbial fuel cells. Water Res 39:4961–4968
127. Xie ZF, Chen H, Zheng P et al (2013) Influence and mechanism of dissolved oxygen on the performance of Ammonia-oxidation microbial fuel cell. Int J Hydrogen Energ 38:10607–10615
128. He Z, Kan JJ, Wang YB et al (2009) Electricity production coupled to ammonium in a microbial fuel cell. Environ Sci Technol 43:3391–3397
129. Schröder C (2012) Comparing reduced partial charge models with polarizable simulations of ionic liquids. Phys Chem Chem Phys 14:3089–3102
130. Sinha B, Annachhatre A (2007) Partial nitrification—operational parameters and microorganisms involved. Rev Environ Sci Biotechnol 6:285–313
131. Zöllig H, Morgenroth E, Udert KM (2015) Inhibition of direct electrolytic ammonia oxidation due to a change in local pH. Electrochim Acta 56:348–355
132. Kim DJ, Lee DI, Keller J (2006) Effect of temperature and free ammonia on nitrification and nitrite accumulation in landfill leachate and analysis of its nitrifying bacterial community by FISH. Bioresour Technol 97:459–468
133. Kim T, An J, Lee H (2016) pH-dependent ammonia removal pathways in microbial fuel cell system. Bioresour Technol 215:290–295
134. Bilanovic D, Battistoni P, Cecchi F (1999) Denitrification under high nitrate concentration and alternating anoxic conditions. Water Res 33:3311–3320
135. Nam JY, Kim HW, Shin HS (2010) Ammonia inhibition of electricity generation in single-chambered microbial fuel cells. J Power Sources 195:6428–6433
136. Nam JY, Kim HW, Shin HS (2011) Ammonia inhibition and microbial adaptation in continuous single-chamber microbial fuel cells. J Power Sources 196:6210–6213
137. Cordruwisch R, Law Y, Cheng KY (2011) Ammonium as a sustainable proton shuttle in bioelectrochemical systems. Bioresour Technol 102:9691–9696
138. Chen H, Zheng P, Zhang J et al (2014) Substrates and pathway of electricity generation in a nitrification-based microbial fuel cell. Bioresour Technol 161C:208–214
139. Jadhav DA, Ghangrekar MM et al (2015) Effective ammonium removal by anaerobic oxidation in microbial fuel cells. Environ Technol 36:767–775
140. Zhan G, Zhang L, Tao Y et al (2014) Anodic ammonia oxidation to nitrogen gas catalyzed by mixed biofilms in bioelectrochemical systems. Electrochim Acta 135:345–350
141. Purkhold U, Pommerening-Röser A, Juretschko S (2000) Phylogeny of all recognized species of ammonia oxidizers based on comparative 16S rRNA and amoA sequence analysis: implications for molecular diversity surveys. Appl Environ Microbiol 66:5368–5382
142. Woese CR, Weisburg WG, Paster BJ (1984) The phylogeny of purple bacteria: the beta subdivision. Syst Appl Microbiol 5:327–336
143. Junier P, Molina V, Dorador C (2010) Phylogenetic and functional marker genes to study ammonia-oxidizing microorganisms (AOM) in the environment. Appl Microbiol Biotechnol 85:425–440

144. Harms G, Layton AC, Dionisi HM (2003) Real-time PCR quantification of nitrifying bacteria in a municipal wastewater treatment plant. Environ Sci Technol 37:343–351
145. Schmidt I, Bock E (1997) Anaerobic ammonia oxidation with nitrogen dioxide by *Nitrosomonas eutropha*. Arch Microbiol 167:106–111
146. Schmidt I, Bock E (1998) Anaerobic ammonia oxidation by cell-free extracts of *Nitrosomonas eutropha*. Anton Leeuw Int J G 73:271–278
147. Bock E, Schmidt I, Stüven R et al (1995) Nitrogen loss caused by denitrifying Nitrosomonas cells using ammonium or hydrogen as electron donors and nitrite as electron acceptor. Arch Microbiol 163:16–20
148. He Z, Kan J, Wang Y et al (2009) Electricity production coupled to ammonium in a microbial fuel cell. Environ Sci Technol 43:3391–3397
149. Kuo DH, Robinson KG, Layton AC (2010) Transcription levels (amoA mRNA-based) and population dominance (amoA gene-based) of ammonia-oxidizing bacteria. J Ind Microbiol Biotechnol 37:751–757
150. Fukushima T, Wu YJ, Whang LM (2012) The influence of salinity and ammonium levels on amoA mRNA expression of ammonia-oxidizing prokaryotes. Water Sci Technol 65:2228–2235
151. Arp DJ, Sayavedra-Soto LA, Hommes NG (2002) Molecular biology and biochemistry of ammonia oxidation by *Nitrosomonas europaea*. Arch Microbiol 178:250–255
152. Hommes NG, Sayavedra-Soto LA, Arp DJ (2001) Transcript analysis of multiple copies of amo (encoding ammonia monooxygenase) and hao (encoding hydroxylamine oxidoreductase) in *Nitrosomonas europaea*. J Bacteriol 183:1096–1100
153. Fiencke C, Spieck E, Bock E (2005) In: Werner D, Newton W (eds) Nitrogen fixation in agriculture, forestry, ecology, and the environment. Springer, Netherlands, pp 255–276
154. Lucker S, Wagner M, Maixner F (2010) A *Nitrospira metagenome* illuminates the physiology and evolution of globally important nitrite-oxidizing bacteria. Proc Natl Acad Sci 107:13479–13484
155. Koops HP, Pommerening-Roser A (2001) Distribution and ecophysiology of the nitrifying bacteria emphasizing cultured species. FEMS Microbiol Ecol 37:1–9
156. Pommerening-Röser A, Rath G, Koops H-P (1996) Phylogenetic diversity within the genus *Nitrosomonas*. Syst Appl Microbiol 19:344–351
157. Fukushima T, Whang LM, Chiang TY (2013) Nitrifying bacterial community structures and their nitrification performance under sufficient and limited inorganic carbon conditions. Appl Microbiol Biotechnol 97:6513–6523
158. Schmidt I, Sliekers O, Schmid M (2003) New concepts of microbial treatment processes for the nitrogen removal in wastewater. FEMS Microbiol Rev 27:481–492
159. Sundermeyer-Klinger H, Meyer W, Warninghoff B (1984) Membrane-bound nitrite oxidoreductase of Nitrobacter: evidence for a nitrate reductase system. Arch Microbiol 140:153–158
160. Zhang YF, Noori JS, Angelidaki I (2011) Simultaneous organic carbon, nutrients removal and energy production in a photomicrobial fuel cell (PFC). Energy Environ Sci 4:4340–4346
161. Gouveia L, Neves C, Sebastião D et al (2014) Effect of light on the production of bioelectricity and added-value microalgae biomass in a photosynthetic alga microbial fuel cell. Bioresour Technol 154:171–177
162. Elmekawy A, Hegab HM, Vanbroekhoven K et al (2014) Techno-productive potential of photosynthetic microbial fuel cells through different configurations. Renew Sust Energ Rev 39:617–627
163. Wang X, Feng YJ, Liu J et al (2010) Sequestration of CO_2 discharged from anode by algal cathode in microbial carbon capture cells (MCCs). Biosens Bioelectron 25:2639–2643
164. Cao XX, Huang X, Liang P et al (2009) A completely anoxic microbial fuel cell using a photo-biocathode for cathodic carbon dioxide reduction. Energy Environ Sci 2:498–501
165. Powell EE, Mapiour ML, Evitts RW et al (2009) Growth kinetics of *Chlorella vulgaris* and its use as a cathodic half cell. Bioresour Technol 100:269–274

166. Sorokin C, Krauss RW (1958) The effects of light intensity on the growth rates of green algae. Plant Physiol 33:109–113
167. Powell EE, Hill GA (2009) Economic assessment of an integrated bioethanol–biodiesel–microbial fuel cell facility utilizing yeast and photosynthetic algae. Chem Eng Res Des 87:1340–1348
168. Strik DPBTB, Terlouw H, Hamelers HVM et al (2008) Renewable sustainable biocatalyzed electricity production in a photosynthetic algal microbial fuel cell (PAMFC). Appl Microbiol Biotechnol 81:659–668
169. Jiang H, Luo S, Shi X et al (2013) A system combining microbial fuel cell with photo bio-reactor for continuous domestic wastewater treatment and bioelectricity generation. J Cent South Univ 20:488–494
170. Lobato J, González del Campo A, Fernández FJ et al (2013) Lagooning microbial fuel cells: a first approach by coupling electricity-producing microorganisms and algae. Appl Energy 110:220–226
171. Rodrigo MA, Cañizares P, García H et al (2009) Study of the acclimation stage and of the effect of the biodegrade ability on the performance of a microbial fuel cell. Bioresour Technol 100:4704–4710
172. Gajda I, Stinchcombe A, Greenman J et al (2014) Algal lagoon effect for oxygenating MFC cathodes. Int J Hydrog Energy 39:21857–21863
173. Venkata MS, Srikanth S, Chiranjeevi P et al (2014) Algal biocathode for in situ terminal electron acceptor (TEA) production: synergetic association of bacteria-microalgae metabolism for the functioning of biofuel cell. Bioresour Technol 166:566–574
174. Raman K, Lan JCW (2012) Performance and kinetic study of photomicrobial fuel cells (PMFCs) with different electrode distances. Appl Energy 100:100–105
175. De Schamphelaire L, Rabaey K, Boeckx P et al (2008) Outlook for benefits of sediment microbial fuel cells with two bioelectrodes. Microb Biotechnol 1:446–462
176. Reimers CE, Girguis P, Stecher HA et al (2006) Microbial fuel cell energy from an ocean cold seep. Geobiology 4:123–136
177. Jeon HJ, Seo K, Lee SH et al (2012) Production of algal biomass (*Chlorella vulgaris*) using sediment microbial fuel cells. Bioresour Technol 109:308–311
178. Xiao L, Young EB, Berges JA et al (2012) Integrated photo-bioelectrochemical system for contaminants removal and bioenergy production. Environ Sci Technol 46:11459–11466
179. Taylor AW, Frazier AW, Gurney EL (1963) Solubility products of magnesium ammonium and magnesium potassium phosphate. Trans Faraday Soc 59:1580–1584
180. Ronteltap M, Maurer M, Hausher R et al (2010) Struvite precipitation from urine—influencing factors on particle size. Water Res 44:2038–2046
181. Kumar R, Pal P et al (2015) Assessing the feasibility of N and P recovery by struvite precipitation from nutrient-rich wastewater: a review. Environ Sci Pollut R 22:17453–17464
182. Cusick RD, Logan BE et al (2012) Phosphate recovery as struvite within a single chamber microbial electrolysis cell. Bioresour Technol 107:110–115
183. Cao XX, Huang X, Liang P et al (2009) A new method for water desalination using microbial desalination cells. Environ Sci Technol 43:7148–7152
184. Ronteltap M, Maurer M, Hausherr R et al (2010) Struvite precipitation from urine–influencing factors on particle size. Water Res 44:2038–2046
185. Martell AE, Smith RM, Motekaitis RJ (1997) Critical selected stability constants of metal complexes, Version 4.0. NIST
186. Ronteltap M, Maurer M, Gujer W (2007) Struvite precipitation thermodynamics in source-separated urine. Water Res 41:977–984
187. Stumm W, Morgan JJ (1996) Aquatic chem, 3rd edn. Wiley, New York
188. Huang H, Zhang P, Zhang Z (2016) Simultaneous removal of ammonia nitrogen and recovery of phosphate from swine wastewater by struvite electrochemical precipitation and recycling technology. J Clean Prod 127:302–310

189. Hirooka K, Ichihashi O (2013) Phosphorus recovery from artificial wastewater by microbial fuel cell and its effect on power generation. Bioresour Technol 137:368–375
190. Ichihashi O, Hirooka K (2012) Removal and recovery of phosphorus as struvite from swine wastewater using microbial fuel cell. Bioresour Technol 114:303–307
191. Almatouq A, Babatunde AO (2016) Concurrent phosphorus recovery and energy generation in mediator-less dual chamber microbial fuel cells: mechanisms and influencing factors. Int J Env Res Public Health 13:375
192. De la Rubia MÁ, Walker M, Heaven S et al (2010) Preliminary trials of in situ ammonia stripping from source segregated domestic food waste digestate using biogas: effect of temperature and flow rate. Bioresour Technol 101:9486–9492
193. Abouelenien F, Fujiwara W, Namba Y et al (2010) Improved methane fermentation of chicken manure via ammonia removal by biogas recycle. Bioresour Technol 101:6368–6373
194. Gangagni Rao A, Sasi Kanth Reddy T, Surya Prakash S et al (2008) Biomethanation of poultry litter leachate in UASB reactor coupled with ammonia stripper for enhancement of overall performance. Bioresour Technol 99:8679–8684
195. Bonmatí A, Flotats X (2003) Air stripping of ammonia from pig slurry: characterization and feasibility as a pre- or post-treatment to mesophilic anaerobic digestion. Waste Manag 23:261–272
196. Kuntke P, Śmiech KM8, Bruning H et al (2012) Ammonium recovery and energy production from urine by a microbial fuel cell. Water Res 46:2627–2636
197. Nancharaiah YV, Venkata Mohanb S, Lensc PNL (2016) Recent advances in nutrient removal and recovery in biological and bioelectrochemical systems. Bioresour Technol 215:173–185
198. Wu X, Modin O (2013) Ammonium recovery from reject water combined with hydrogen production in a bioelectrochemical reactor. Bioresour Technol 146C:530–536
199. William MLJ, Donald PM (2011) Toxicity of nitrite to fish: a review. Trans Am Fish Soc 115:183–195
200. Pan Y, Ni BJ, Bond PL et al (2013) Electron competition among nitrogen oxides reduction during methanol-utilizing denitrification in wastewater treatment. Water Res 47:3273–3281
201. Desloover J, Puig S, Virdis B et al (2011) Biocathodic nitrous oxide removal in bioelectrochemical systems. Environ Sci Technol 45:10557–10566
202. Puig S, Serra M, Vilarsanz A et al (2011) Autotrophic nitrite removal in the cathode of microbial fuel cells. Bioresource Technol 102:4462–4467

Chapter 8
Application of Redox Mediators in Bioelectrochemical System

Chunfang Zhang, Dongdong Zhang, and Zhixing Xiao

8.1 Electron Transfer Reactions and Redox Mediators

Electron transfer reactions are fundamental to metabolism. Regardless whether a microorganism is autotrophic or heterotrophic, free living or an obligate parasite, every cell must solve the energy-generation problem to survive. Electron transfer usually starts from the oxidation of electron donor (organic matter or some inorganic compounds), and then, electrons released from electron donors run to the most positive electron acceptor yielding the highest amount of energy. Thus, under the neutral condition, oxygen is a preferred electron acceptor for many microorganisms, followed by nitrate, Fe^{3+}, etc., with decreasing amounts of available energy (Table 8.1).

Since the 1990s, extensive research has been conducted to explore the effects of different redox mediators (RMs) on the biotransformation processes. RMs, also known as electron shuttles (Fig. 8.1), are compounds that could be used as electron carriers among multiple electron-mediating reactions as they can be reversibly oxidized and reduced [5]. RMs accelerate microbial reactions by enhancing the electron transfer rate or lowering the activation energy of the total reaction [1]. There are great potentials for the application of RMs on the reductive (bio)transformation of different kinds of pollutants in wastewaters, contaminated groundwater, as well as contaminated soils/sediments originated from different industrial sectors [5–7].

The majority of RMs studied so far are soluble compounds as shown in Fig. 8.2. The soluble RMs have been studied extensively for iron reduction, nitrate reduction, metal reduction, azo dye reduction, and so on. Recently, more and more studies

C. Zhang · D. Zhang (✉)
Institute of Marine Biology, Ocean College, Zhejiang University, Zhoushan, China
e-mail: zhangdongzju@zju.edu.cn

Z. Xiao (✉)
College of Urban Construction, Nanjing Tech University, Nanjing, China
e-mail: xzxcat@njtech.edu.cn

Table 8.1 Standard potentials of some selected redox couples, calculated at pH 7

Redox couple	E_0' (mV)	References
O_2/H_2O	+810	[1]
NO_3^-/N_2	+740	[1]
Cytochrome c ox/red	+250	[2]
Fe^{3+}/Fe^{2+}	+200	[1]
Ubiquinone ox/red	+113	[3]
Menaquinone ox/red	−75	[3]
AQDS/AHDS	−184	[3]
Lactate/pyruvate	−190	[1]
Acetate/CO_2	−280	[1]
Humic substances	−200 to +300	[4]
$NAD^+/NADH$	−320	[3]
$H_2/2H^+$	−420	[1]
Formate/CO_2	−430	[1]
Glucose/CO_2	−430	[1]
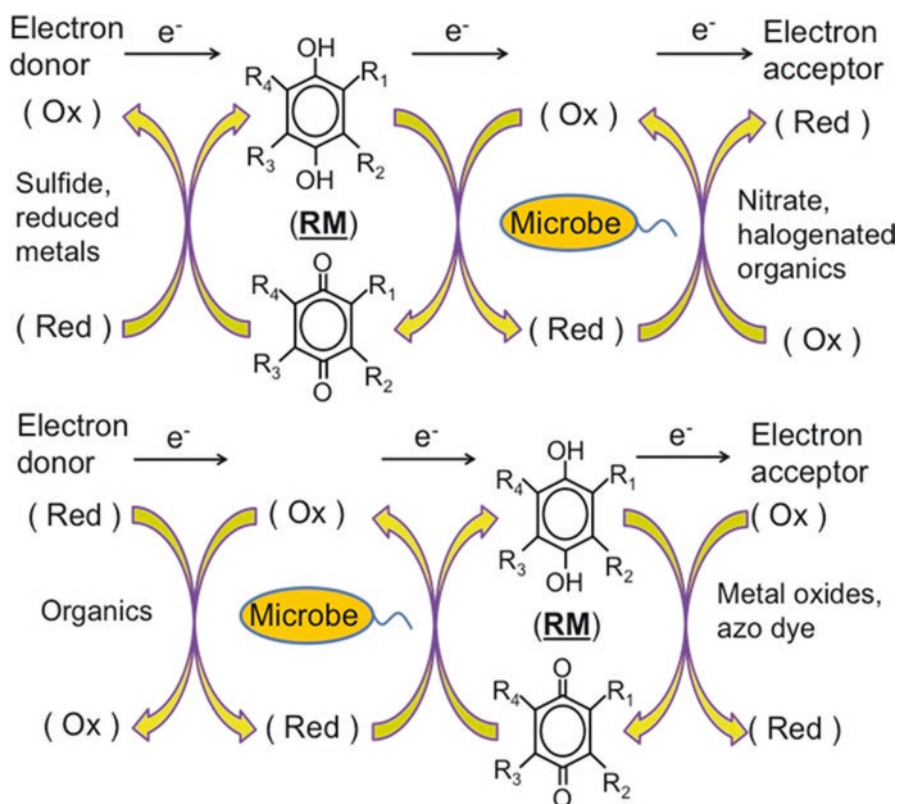
Fig. 8.1 RM-assisted microbial reactions. Ox denotes oxidized form; red denotes reduced form
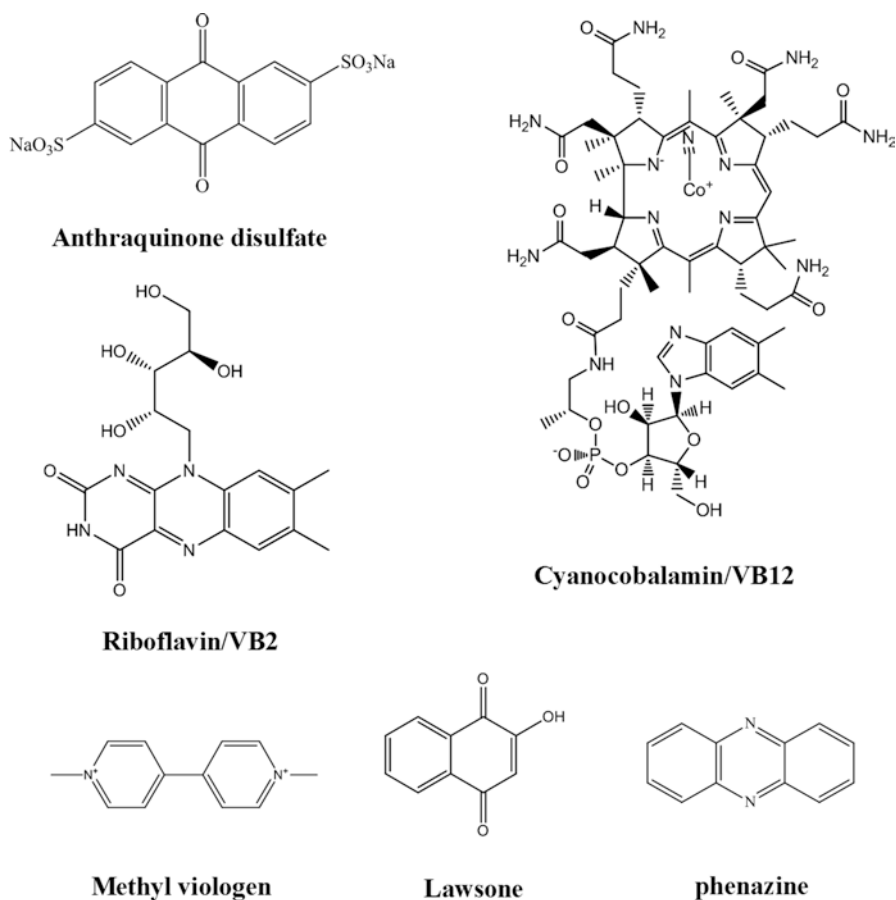
Fig. 8.2 Structure of the main redox mediators reported in the literature

have been reported for the application of non-soluble materials as RMs, e.g., activated carbon [8, 9], graphite [9], alginate beads with immobilized anthraquinone [10], and humin [11–15]. These solid-phase RMs have been shown to accelerate microbial reduction of organic pollutants such as azo dye and halogenated aromatic compounds. The clear difference in dye reduction kinetics obtained with activated carbon as compared to graphite suggested that activated carbon or other insoluble materials with surface-associated or entrapped redox-active functional groups can be considered the most ideal candidates as insoluble RMs. In the case of humin, it is natural origin, chemically stable and environmentally benign, which made it as a preferred RM for in situ bioremediation. The property of insoluble materials enables their use as biologically regenerable RMs in bioremediation, as these materials can be retained in the remediation sites for prolonged time. They are attractive alternatives to soluble RMs that would be flushed away and need to be dosed continuously.

A property of RMs that deserves attention is the ability to cross cell membranes. It has been demonstrated that the azo reductase activity of cell extracts can be much higher than that of intact cells and that the cell membrane forms a barrier for dyes and mediators [16]. Nevertheless, with the in-depth study of insoluble RMs, extracellular electron transfer (EET) through a solid-phase RMs was presumed as a natural occurrence and had attracted wide attention.

8.2   Application of Redox Mediators for Biotransformation

8.2.1   Dissolved RMs for Bioremediation

Several RMs have been reported to play an important role in the reductive (bio) transformation of priority pollutants. The large list of redox-active molecules includes 9,10-anthraquinone-2,6-disulfonate (AQDS) [17], quinones [18], porphyrins [19], cytochromes [20], cobalamins [21], flavines [22], pyridines [23], phenazines [24], methyl viologen (MV) [25], and so on (Table 8.2).

Among the reported RMs, quinones have been proposed as the most appropriate RM for the reductive (bio)transformation of some priority pollutants [18]. The main reason for considering quinones for redox (bio)transformation processes is that they are very abundant in humic substances (HSs), the most plentiful and cheaply available organic source in the biosphere.

8.2.2   Humic Substances and Their Role as Redox Mediators

Organic matter is at the very foundation of soil ecology and management. In the term of soil organic matter (SOM), it includes non-humic substances which are inherited from plant and animal residues entering the soil and HSs which are the stable fraction of organic matter accumulating from the decomposition of litter.

Non-humic substances, which mainly consist of (1) carbohydrates and their several derivatives such as cellulose, (2) amino acids, and (3) lipids, account for about 20–30% of the total SOM. They are relatively easily decomposed by microorganisms and persist in soil for a brief time.

HSs, which are the most widely spread natural complexing compounds occurring in nature, make up about 60–80% of the total SOM. They can be divided into three components, fulvic acids (FAs), humic acids (HAs), and humin, according to their solubility in aqueous solution at different pH (Fig. 8.3). They are complex substances of high molecular weight resulting from the biotransformation and (re) polymerization of phenolic and aromatic components in litter such as lignin, tannins, and secondary metabolites, which are resistant to further decomposition [31]. These highly condensed aromatic structures rich in quinone moieties are very recalcitrant to biodegradation. It was reported that the mean residence time of humus in soil varies from 250 to 1900 years [32].

Table 8.2 Impact of dissolved RMs on the microbial reduction of different kind of pollutants

Type of substrate[a]	Redox mediators[b]	Electron donor/system	Ratio pollutant/RM[c]	Results[d]	References
Fe(III) oxides	AQDS, AQS, lawsone, menadione	Acetate/*Geobacter metallireducens*	1000	The rate and extent of Fe(III) oxide reduction were greatly increased	[17]
Acid orange 7	MQ, AQDS	Starch derivative/SBR	1.43 or 0.77	Color removal efficiency increases from ~5% (no RM) to max. 25% (MQ) and ~70% and ~90% (AQDS conc, 1.43 and 0.77, resp.)	[26]
Vinyl chloride	AQDS, HA	VC/organic-rich stream sediment	1.25×10^{-3} (AQDS) 0.16 (HA)	Stimulated the mineralization of VC and the recovery of $^{14}CO_2$	[27]
Toluene	AQDS, HA	Enrichment culture	0.04 (AQDS) 4.6 (HA)	About 50% and 85% of toluene were recovered as $^{13}CO_2$ in HA- and AQDS-added cultures in 2 weeks, resp.; no recovery occurred in unadded cultures	[28]
MTBE	AQDS, HA	Aquifer sediments	1.61 (AQDS) 0.33 (HA)	The addition of AQDS or HA stimulated the anaerobic degradation of MTBE in aquifer sediments	[29]
CCl₄	Cyanocobalamin	Lactate/*Shewanella alga* strain BrY	0.13	No conversion of CT by *Shewanella alga* BrY in the absence RM, whereas 92% of CT conversion to CO within 3 weeks of incubation in RM-amended cultures compared to control	[7]
Carbon tetrachloride	Cobalamins	Propanediol, dextrose and acetate/enrichment culture	0.005, 0.01, 0.03, 0.05	CT degradation rates increased linearly with higher intracellular CNB12 content	[21]
Carbon tetrachloride	Cyanocobalamin	Dichloromethane/enrichment culture	34	Adding cyanocobalamin increased the rate of CT transformation in live cultures by at least tenfold but had a minor effect on the rate of CT used in autoclaved cultures	[30]
Chloroform	Riboflavin, Cobalamin	Methanogenic consortium	100, 20, 10, 5	At the highest molar vitamin: CF ratios tested of 0.2, the first-order rate constant of CF degradation was 5.3- and 91-fold higher in RF and CNB12 amended cultures, respectively, compared to the unamended control culture	[22]

Table 8.2 (continued)

Type of substrate[a]	Redox mediators[b]	Electron donor/system	Ratio pollutant/RM[c]	Results[d]	References
Poorly crystalline iron (hydr)oxide	Phenazines	Lactate, succinate, and pyruvate/*Shewanella oneidensis* MR1	0.001	MR1 grew more rapidly in the presence of either PCN than it did when provided with Fe(III) (hydr)oxide alone. Fine-grained magnetite formed rapidly, coinciding with fast iron reduction; in contrast, magnetite accumulated more slowly when PCN was omitted. Other phenazines tested (e.g., pyocyanine, phenazine methosulfate, and phenazine) stimulated Fe(III) mineral reduction by MR1 in the same way	[24]
Trichloroethene	Methyl viologen	Electrode/mixed culture	0.015	The reductive dechlorination of TCE to harmless end products such as ethene and ethane could be performed	[25]
CCl_4 $CHCl_3$	Porphyrins	Methanol/*Methanosarcina thermophila*	N/A	The cell exudates from the methanogen *Methanosarcina thermophila* are active in the degradation of CCl_4 and $CHCl_3$ and are confirmed to contain porphorinogen-type molecules, possibly corrinoids, hemes, and zinc-containing molecules	[19]
Tetrachloromethane	Cytochromes	Methanol/*Shewanella putrefaciens* 200	N/A	Respiratory cytochromes are involved in CT dehalogenation by *S. putrefaciens* 200, and increased cytochrome production following microaerobic growth results in increased dehalogenation ability	[20]
Carbon Tetrachloride	Pyridines	*Pseudomonas stutzeri* strain KC	N/A	Strain KC secretes pyridine-2,6-bis(thiocarboxylate) as a metabolite which has CCl_4 transformation activity	[23]

[a]*MTBE* methyl *tert*-butyl ether

[b]*AQDS* anthraquinone-2,6-disulfonate, *AQS* anthraquinone-2-sulfonate, *MQ* menadione, *SBR* sequential batch reactor

[c]Ratio pollutant/RM=molar ratio pollutant: redox mediator

[d]*VC* vinyl chloride, *RF* riboflavin, *CNB12* cyanocobalamin, *CF* chloroform, *PCN* phenazine-1-carboxamide, *TCE* trichloroethene

```
                          ┌─────────────────────┐
                          │  Soil organic matter │
                          └─────────────────────┘
                              ╱             ╲
                    20-30%  ╱                 ╲  60-80%
                          ╱                     ╲
              ┌─────────────────────┐   ┌─────────────────────┐
              │ Non-humic substances │   │  Humic substances   │
              └─────────────────────┘   └─────────────────────┘
                                                │
                                       Alkaline precipitation
                                           ╱         ╲
                             ┌──────────────────┐  ┌──────────────────┐
                             │  Alkaline soluble │  │ Insoluble residue │
                             │  humic substances │  │      Humin        │
                             └──────────────────┘  └──────────────────┘
                                   ╱       ╲
                     Acidic      ╱           ╲
                  precipitation ╱             ╲
              ┌──────────────────┐  ┌──────────────────┐
              │ Insoluble residue │  │   Soluble part   │
              │    Humic acid     │  │    Fulvic acid   │
              └──────────────────┘  └──────────────────┘
```
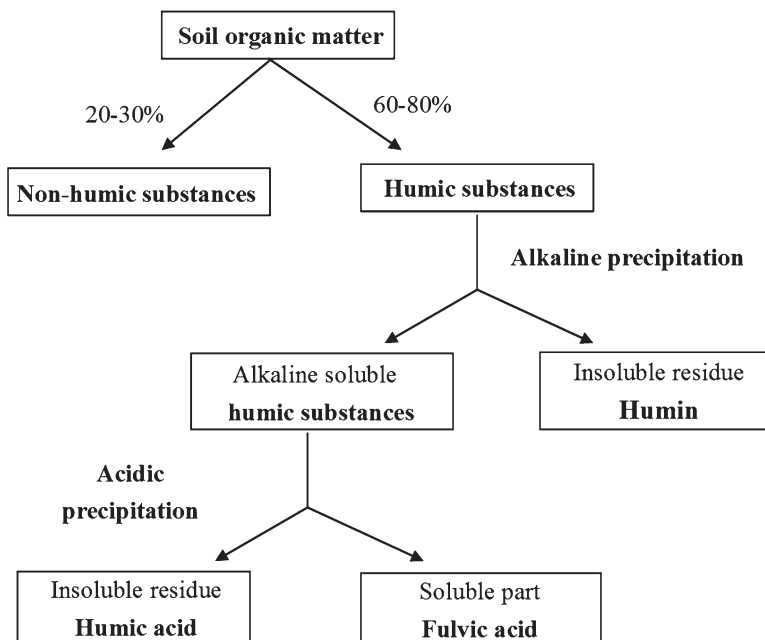
Fig. 8.3 Division of humic substances in dependence of their solubility

Although HSs are considered to be very inert, new evidence is accumulating indicating that they can have active roles in the abiotic and biological biotransformation of priority pollutants, e.g., electron acceptors for respiration, redox mediators for reduction processes, and electron donors to microorganisms. Furthermore, HSs are generally considered as nonhazardous materials and do not lead to the production of toxic by-products [33]. Until now, there are extensive studies on the redox-mediating effects of dissolved HSs, namely, HAs and FAs, supporting the microbial remediation of organic/inorganic compounds under anaerobic conditions [5, 6, 7, 34].

In the case of humin, it has generated relatively little research interest compared with the other humic fractions [35]. The humin comprises a relatively small proportion of organic carbon and a larger proportion of inorganic materials, and the organic carbon is strongly bonded with inorganic materials [35]. Because of the lack of an efficient extracting solvent for humin [36], although it typically represents more than 50% of the soil organic carbon, it is the least characterized fraction, and there is no consensus on its fundamental nature [37]. Early studies on the function of humin in the environment have been limited to the sorption of organic chemicals [38, 39]. Recently, the role of solid-phase humin as an RM has emerged as an important research topic. It has reported that humin works as an RM for microbial reductive dechlorination of pentachlorophenol (PCP) [11, 13, 40], microbial reductive debromination of tetrabromobisphenol A [12], microbial Fe(III) oxide reduction [11], microbial nitrate reduction [14], and microbial degradation of 2,2′,4,4′,5,5′-hexachlorobiphenyl [41]. Moreover, in some cases, humin not only works as an RM, but it's also requisite for the dechlorination to take place, whereas

the activity is unable to be maintained when humin is replaced with dissolved HSs and related compounds including 0.1 M NaOH-extracted humic acid from soil, Aldrich humic acid, or AQDS [11, 12].

The solid-phase humin, being an all-natural substance, is attractive for the use as an redox mediator in in situ remediation. Firstly, humin is an environmentally benign material compared to most of other RMs. In addition, for any environmental remediation project, cost always is the key point that needs to be concerned. Thus, in situ technologies that apply natural originated humin that do not need artificial production and abundant in the environment may be more cost effective.

8.2.3   Other Reported Solid-Phase RMs and Their Application

Metal-humic acid complexes were synthesized for their application as solid-phase RM in the biotransformation of pollutants [15, 42]. Zhang et al. [13] reported that insoluble Fe-humic acid complex functions as a solid-phase RM for anaerobic microbial dechlorination of PCP, although dissolved humic acids could not. Metal (Ca and Fe)-humic acid complexes significantly increased the biotransformation of iopromide in upflow anaerobic sludge blanket reactors [42]. After the experiments, 78% and 91% of the Fe- and Ca-humic acid complexes, respectively, initially added were retained in the amended reactors, which proved the stability and immobilization of metal-humic acid complexes.

Some studies have shown that the immobilization of HSs on anion exchange resins (AER) or alumina (nano)particles could enhance the bioremediation of contaminants as the solid-phase RM [43–46]. Quinoid RM, including 1,2-naphthoquinone-4-sulfonate (NQS) and AQDS, or HSs adsorbed on AER were demonstrated as effective solid-phase RM for the decolorization of azo dyes and reductive biotransformation of carbon tetrachloride [45, 46]. Alumina particles were used as the supporting materials for HSs, i.e. fulvic acid and leonardite, such HSs/alumina composite can function as solid-phase RM to enhance the dechlorination of carbon tetrachloride and decolorization of the recalcitrant azo dye [43, 44].

In addition, biochar, which is produced by heating biomass in a closed system with limited oxygen supply, has large internal surface areas and been promoted as an RM to stimulate microbial direct interspecies electron transfer [47] and significantly accelerate the microbial reductive dehalogenation of 2,2′,4,4′-tetrabromodiphenyl ether (BDE-47) [48] and PCP in anaerobic conditions [49].

8.3   RM-Assisted Bioelectrochemical Systems (BESs) as an Emerging Sustainable Bioremediation Process

BESs provide both oxidation and reduction approaches to remediate contaminated site. The advantage of BESs for remediation is that this technique does not require any chemical addition. Instead, electrodes serve as inexhaustible electron donors/

acceptors to stimulate microorganisms for transformation or degradation the pollutants. One of greatest challenges of the scaling up process of BESs is the difficulty in achieving high rates of EET between the microorganisms and the electrode [50, 51]. Several studies have shown that the anodic/cathodic electron transfer rate can be promoted when redox mediators were present in the BESs [52, 53].

8.3.1 RM-Assisted Anodic Reaction (Oxidative Reaction)

By using redox mediator, the extracellular electron transfer rate of microorganisms has often been even orders of magnitude higher than that of system with no RMs, leading to higher anodic substrate treatment efficiencies [54]. RMs are important for anode respiration microorganisms that are unable to effectively transfer electrons outside of the cell. So far, a large group of compounds either artificially synthesized or naturally presented were investigated for their suitability and behavior as RM assisting microbial anode respiration.

8.3.1.1 Microbial Fuel Cells (MFCs)

Microbial fuel cells (MFCs) are devices that produce electricity from different compounds using microorganisms as biocatalyst [55]. The MFCs are considered as energy-efficient remediation devices; besides easy biodegraded substrates such as acetate and lactate, several kinds of pollutants could be treated in MFCs, for example, heavy metals [56], petroleum hydrocarbon [57], polychlorinated biphenyls [58], or landfill leachate [59]. As shown in Fig. 8.4, the microorganisms transfer (directly or through RM) the electrons produced from these substrates to the anode, and the electrons flow to the cathode through an external circuit [60]. The anodic
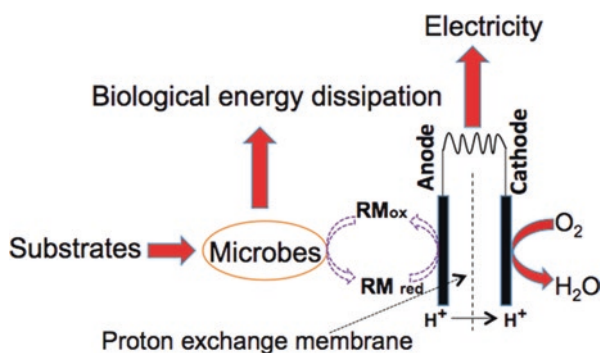

Fig. 8.4 Working principle of RM participated microbial fuel cell

electron transfer rate is one of important factors affecting the performance of MFCs for pollutant removal.

In MFCs, microorganisms switch from the natural electron acceptor, such as oxygen, nitrate, iron oxide, etc., to an insoluble electrode (anode) as the electron acceptor. This transfer can be assisted either via cell membrane components or soluble electron shuttles. Until now, a variety of common bacteria, for example, *Geobacter*, *Shewanella*, *Enterobacter*, and *Bacillus*, have been tested with respect to their capacity of the power generation in MFCs [61–64].

If the bacteria are incapable of releasing electrons to anode directly, the anode will finally accept the electrons from the RM [65]. Thus far, a lot of artificially synthesized RMs (neutral red (NR), phenazine, AQDS, or natural presented RMs (humic acid, iron minerals) were tested as the redox mediator to enhance anode performance (Table 8.3).

Table 8.3 Redox mediators used in MFCs

Electron donor	Microbial source	Redox mediator	Power (mW/m^2 anode surface)	Reference
Glucose	*Proteus vulgaris* B11	Thionine	4.5	[66]
Glucose	*Erwinia dissolvens*	Fe(III)CyDTA	0.27	[67]
Glucose	*Escherichia coli* K12	NR	0.16	[68]
Glucose	*Proteus vulgaris*	Thionine	85	[69]
Lactate	*Escherichia coli* K12	Mn^{4+}	91	[70]
Glucose	*Pseudomonas aeruginosa* KRP1	Pyocyanin	2.7	[71]
Lactate	*Shewanella oneidensis* DSP10	AQDS	>44.4	[72]
Cellulose	*Clostridium cellulolyticum*	Resazurin	0.0015	[73]
Glucose	*Escherichia coli* K12	Hydroquinone	1300	[74]
Glucose	*Klebsiella* sp. ME17	Quinone-like substances	1209	[75]
Glucose	*Saccharomyces cerevisiae*	Methylene blue	2.04	[52]
Lactate	Activated sludge	NR	5.3	[70]
Glucose	Domestic wastewater	Humic acid	52	[76]
Organic matter in sediments	Fresh water sediment	Colloidal iron oxyhydroxide	85.77	[77]
A mixture of benzene and phenanthrene	Anaerobically digested sludge	Riboflavin	26.2	[78]
Sucrose	Sewage sludge	Carbon quantum dots	126	[79]

8.3.1.2 Artificial Synthesized RM-Assisted Anodic Reaction

Artificially synthesized compounds, such as NR, AQDS, resazurin, thionine, and methylene blue (MB), have been supplemented to anode chamber to enhance EET rates. Indeed, Park and Zeikus have demonstrated that EET rates in a glucose-fed MFC with NR as anodic RM were enhanced by about tenfold compared to RM-free system [68]. Rahimnejad et al. found *Saccharomyces cerevisiae* (PTCC 5269), previously known as electrochemically inactive specie, could be acclimated with thionine or MB for facilitation of electron transfer [80]. Adelaja et al. showed the use of riboflavin as the RM in optimizing EET while maintaining good degradation efficiency of petroleum hydrocarbons [78]. Sund et al. examined the abilities of several RMs on promotion of EET in a cellulose fermentation anode; the result suggested resazurin showed best performance, probably because of its higher cell membrane penetration ability compared to other RMs examined [73]. Vishwanathan et al. demonstrated that addition of carbon quantum dots as a suspension in the anode chamber of an MFC resulted in a 22.5% enhancement in maximum power density [79].

8.3.1.3 Natural RM-Assisted Anodic Reaction

As described in earlier section, HSs as natural redox-active material are ubiquitous in the environment. Thygesen et al. reported that, by the addition of humic acids, maximum powers of glucose-fed and xylose-fed MFCs increased by 84% and 30%, respectively [76]. In another study, Sun et al. demonstrated compared with RM-free MFC, the MFC with added 1 g/L of HA showed 15% increase in maximum power density along with 258% increase in decolorization rates of Congo red [81]. These studies confirmed that HSs could mediate the electron transfer for anodic respiration.

Iron oxide compound is another RM commonly found in anaerobic environments; Zhou et al. demonstrated that colloidal iron oxyhydroxide instead of soluble ferric iron played an important role in voltage production through maintaining high-concentration ferrous iron in pore water of sediments as RM and for chemical oxidation on the anode [77].

In some instances, microorganisms, mostly gram-negative bacteria, might secrete RMs to promote EET; the so-called "self-mediated" EET is also drawing much interests. It has been shown that *Pseudomonas aeruginosa* produces pyocyanin and phenazine-1-carboxamide as RM [82]. Interestingly, Pham et al. reported phenazines produced by *Pseudomonas* sp. could enhance the EET capacity of a gram-positive bacterium *Brevibacillus* sp. PTH1 [83], indicating that RM may provide a synergic strategy in microbial community for anodic respiration. *Shewanella oneidensis* MR-1 is another important electroactive bacteria and has been reported to produce quinone-like compounds [84] and flavins [85, 86] as RMs. For example, Marsili et al. have reported that flavins in *Shewanella oneidensis* MR-1 biofilms increased the EET rate by at least 370% [86], while the ATP cost on flavin secretion was negligible compared with the resulting energy benefit.

8.3.1.4 Engineered RMs for Their Application in Anodic Reactions

Multiple studies have been demonstrated to improve the performance of RMs for paving the way to the real application of RMs in anode respiration. The engineered methods adopted in these studies are summarized as below.

8.3.1.4.1 Physical Methods

To prevent the NR lost, Mardiana et al. fixed it onto the surface of electrode via electropolymerization [87]. Xu et al. immobilized a redox mediator riboflavin (RF) onto carbon cloth using bioinspired and self-assembled peptide nanotubes (PNTs), increased by 263.3% of current density compared to the bare electrode [88]. Ding et al. demonstrated that polyaniline nanowire arrays as a solid-state RM could be electrochemically polymerized on an Au electrode, which allowed efficient EET of *Shewanella loihica* PV-4 [89].

8.3.1.4.2 Chemical Methods

Chen et al. achieved high-energy conversion efficiency by changing the molecular structure of phenazines to reduce the biological energy acquisition [90]. For promotion of electron transfer rate, Yong et al. successfully enhanced the riboflavin synthesized of *Shewanella oneidensis* MR-1, by adjusting the pH to 9 [91].

8.3.1.4.3 Biological Methods

Zheng et al. promoted RM (pyocyanin) production and EET rates of *Pseudomonas aeruginosa* through overexpression of rhlA, the key gene responsible for rhamnolipid (biosurfactant) synthesis [92]. By a similar manner, Yong [93] promoted electricity power output of MFCs by manipulation of electron shuttle (pyocyanin) synthesis pathways.

8.3.2 RM-Assisted Cathode Reaction (Reductive Reaction)

8.3.2.1 BES Cathodes as an Electron Donor Driving Microbial Reactions

BESs, in which the cathodes are employed as direct electron donors for the microbial reduction of oxidized contaminants in subsurface environments, have been attracting attention as a promising technology with environmental benefits [25, 94]. By this way, the energy and organic matter (as an electron donor) required were decreased in comparison with conventional biological contaminant treatment

method. The working principle of a BES was shown in Fig. 8.5. Generally, the cathode is set at a negative potential that is sufficient to support anaerobic respiration but too high for significant hydrogen production [95]. The BESs of the bioelectrochemical reduction of oxidized contaminants with electrodes serving as electron donors have been demonstrated for a variety of compounds such as nitrate [96], nitrobenzene [97], antibiotics [98–100], azo dyes [101–103], sulfate [104], U (VI) [105], perchlorate [94], chloroethenes [25, 51, 106, 107], and PCP [13]. By far, only few of pure cultures have been shown to be capable of receiving electrons directly from the electrodes [96, 106, 108, 109–111]. As RMs are used in anode chamber, they have also been utilized in cathode chamber to facilitate the electron transfer from cathode to microorganisms (Table 8.4).

8.3.2.2 Dissolved RM-Assisted Cathode Reaction

In biocathode, dissolved redox mediators, such as methyl viologen (MV) and AQDS, act to facilitate electron transfer between the cathodes and microorganisms and have been studied as a strategy for fine-tuning environmentally relevant
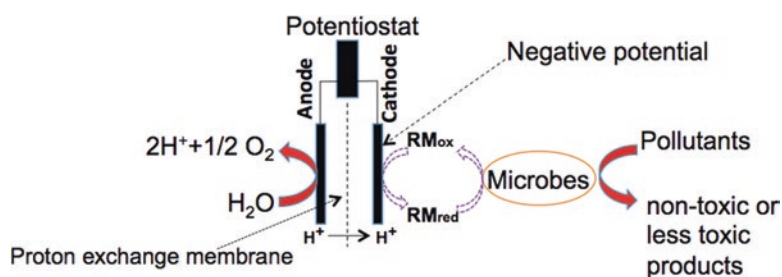
Fig. 8.5 Working principle of RM participated biocathode

Table 8.4 RMs used in cathode chamber of BESs

Electron acceptors	Redox mediator	Cathode potential (vs. SHE)	Microorganism	Reference
Fumarate	Neutral red	Not available	*Actinobacillus succinogenes*	[112]
Trichloroethene	Methyl viologen	−500	Mixed culture (*Dehalococcoides*)	[25]
Trichloroethene	AQDS	−250	Mixed culture (*Dehalococcoides*)	[107]
Perchlorate	AQDS	−300	Wastewater	[94]
1,2-dichloroethane	AQDS	−300	Mixed culture (*Dehalococcoides*)	[113]
PCP	Humin	−500	Mixed culture	[13]
Nitrate	Humin	−500	*Pseudomonas stutzeri*	[114]

microbial metabolisms such as dechlorination [25, 51]. Dissolved RMs, reversibly oxidized and reduced, accelerates reactions by lowering the activation energy [115], resulting in the enhancement of microbial transformation of pollutants. Aulenta et al. [25] showed that an electrochemical system with negatively polarized electrode, in combination with a low-potential MV as redox mediator, can efficiently transfer electrochemical reducing equivalents to dechlorinators which respiring trichloroethene (TCE), while no dechlorination happen if without MV as redox mediator. Also, Aulenta et al. [51] proved that, by the addition of humic acid analogue AQDS, the initial dechlorination rate increased more than three times than AQDS-free treatment. Perchlorate could be readily reduced by washed cell of *Dechloromonas* and *Azospira* species in cathode with AQDS as redox mediator; no perchlorate was reduced in the absence of AQDS [94].

8.3.2.3   Insoluble RM-Assisted Cathode Reaction

Solid-phase RMs have been attracting attention as a promising strategy for bioremediation by BESs, because of their ecological advantages of stable characteristics and effective retention within the system, which will reduce the investments in application of RMs in BES. The redox-mediating potential of naturally derived humin had been firstly reported that various humins obtained from soils and sediments functioned as solid-phase redox mediators in the microbial reductive dehalogenation of PCP [11]. Later, humin was also applied to cathode in BESs for the dechlorination of PCP. The PCP dechlorination rate was obviously enhanced by BES combined with humin, while no dechlorination metabolites was produced in the absence of humin, and microbial reduction of amorphous Fe (III) was also significantly enhanced by solid-phase humin in BES [13]. In another study, denitrification was enhanced electrochemically by solid-phase humin, and the electrons could be mediated to non-electrotrophic *P. stutzeri* by humin [114]. These findings suggest that solid-phase humin was versatile as a redox mediator in donating electrons to multiple microorganisms in BESs. Given that the nature-originated humin is ubiquitously and abundantly present in environments, utilization of solid-phase humin as RM may contribute greatly to the in situ bioelectrochemical remediation.

The other solid-phase RMs mentioned above, i.e., metal-humic acid complexes, HS immobilization on anion exchange resins (AERs) or alumina (nano)particles, and biochar, could be attractive for their application in the reductive biotransformation of several contaminants in BESs. However, the electron-mediating performance and stability of these RMs in BESs should be warranted for further investigation.

8.4 Conclusion

The results presented in the literature indicate great potentials for the application of RMs in the BESs for the bioremediation of real contaminated sites. Nonetheless, to warrant a successful application of RM-assisted BESs, several important topics should be considered in future research. (1) In order to tune desired microbial metabolisms for biotransformation of pollutants, studies about more pure culture are required to develop a deep understanding of electron transfer between RMs and cellular components of microbes, especially for solid-form RMs. (2) HSs, as one of promising RMs, are ubiquitous in the environment. The limitation of its application for BES remediation technologies is the intrinsic variability in composition and redox properties among different origins. Thus, it is important to study the functional group of HSs that mediate different microbial reactions; based on such information, we can enhance the performance of HS by manipulation of their composition. (3) To implement RM-assisted BESs at the field scale, engineering factors (conductivity of soil or water, BESs design, RM deliver method, etc.) that may be encountered in situ remediation need to be assessed to determine if they will affect the treatment process.

References

1. Thauer RK, Jungermann K, Decker K (1977) Energy-conservation in chemotropic anaerobic bacteria. Bacteriol Rev 41(1):100–180
2. He Z, Angenent LT (2006) Application of bacterial biocathodes in microbial fuel cells. Electroanalysis 18(19–20):2009–2015. https://doi.org/10.1002/elan.200603628
3. Madigen MT, Martinko JM (2000) Brock biology of microorganisms. Prentice-Hall, Upper Saddle River
4. Straub KL, Benz M, Schink B (2001) Iron metabolism in anoxic environments at near neutral pH. FEMS Microbiol Ecol 34(3):181–186. https://doi.org/10.1111/j.1574-6941.2001.tb00768.x
5. Van der Zee FR, Cervantes FJ (2009) Impact and application of electron shuttles on the redox (bio)transformation of contaminants: a review. Biotechnol Adv 27(3):256–277. https://doi.org/10.1016/j.biotechadv.2009.01.004
6. van der Zee FP, Bouwman RHM, Strik D, Lettinga G, Field JA (2001) Application of redox mediators to accelerate the transformation of reactive azo dyes in anaerobic bioreactors. Biotechnol Bioeng 75(6):691–701. https://doi.org/10.1002/bit.10073
7. Workman DJ, Woods SL, Gorby YA, Fredrickson JK, Truex MJ (1997) Microbial reduction of vitamin B_{12} by *Shewanella alga* strain BrY with subsequent transformation of carbon tetrachloride. Environ Sci Technol 31(8):2292–2297. https://doi.org/10.1021/es960880a
8. van der Zee FP, Bisschops IAE, Lettinga G, Field JA (2003) Activated carbon as an electron acceptor and redox mediator during the anaerobic biotransformation of azo dyes. Environ Sci Technol 37(2):402–408. https://doi.org/10.1021/es025885o

9. Mezohegyi G, Kolodkin A, Castro UI, Bengoa C, Stuber F, Font J, Fabregat A, Fortuny A (2007) Effective anaerobic decolorization of azo dye acid orange 7 in continuous upflow packed-bed reactor using biological activated carbon system. Ind Eng Chem Res 46(21):6788–6792. https://doi.org/10.1021/ie061692o

10. Guo J, Zhou J, Wang P, Wang D, Tian C, Salah Uddin M, Yu H (2007) Biocatalyst effects of immobilized anthraquinone on the anaerobic reduction of azo dyes by the salt-tolerant bacteria. Water Res 41(2):426–432. https://doi.org/10.1016/j.watres.2006.10.022

11. Zhang CF, Katayama A (2012) Humin as an electron mediator for microbial reductive dehalogenation. Environ Sci Technol 46(12):6575–6583. https://doi.org/10.1021/Es3002025

12. Zhang C, Li Z, Suzuki D, Ye L, Yoshida N, Katayama A (2013) A humin-dependent *Dehalobacter* species is involved in reductive debromination of tetrabromobisphenol A. Chemosphere 92(2013):1343–1348. https://doi.org/10.1016/j.chemosphere.2013.05.051

13. Zhang D, Zhang C, Li Z, Suzuki D, Komatsu DD, Tsunogai U, Katayama A (2014) Electrochemical stimulation of microbial reductive dechlorination of pentachlorophenol using solid-state redox mediator (Humin) immobilization. Bioresour Technol 164:232–240. https://doi.org/10.1016/j.biortech.2014.04.071

14. Zhang D, Zhang C, Xiao Z, Suzuki D, Katayama A (2014) Humin as an electron donor for enhancement of multiple microbial reduction reactions with different redox potentials in a consortium. J Biosci Bioeng 119(2):188–194. https://doi.org/10.1016/j.jbiosc.2014.07.010

15. Zhang C, Zhang D, Li Z, Akatsuka T, Yang S, Suzuki D, Katayama A (2014) Insoluble Fe-HA complex as a solid-phase electron mediator for microbial reductive dechlorination. Environ Sci Technol 48:6318–6325. https://doi.org/10.1021/es501056n

16. Russ R, Rau J, Stolz A (2000) The function of cytoplasmic flavin reductases in the reduction of azo dyes by bacteria. Appl Environ Microbiol 66(4):1429–1434. https://doi.org/10.1128/AEM.66.4.1429-1434.2000

17. Lovley DR, Fraga JL, Blunt-Harris EL, Hayes LA, Phillips EJP, Coates JD (1998) Humic substances as a mediator for microbially catalyzed metal reduction. Acta Hydrochim Hydrobiol 26(3):152–157. https://doi.org/10.1002/(sici)1521-401x(199805)26:3<152::aid-aheh152>3.0.co;2-d

18. Field JA, Cervantes FJ (2005) Microbial redox reactions mediated by humus and structurally related quinones, vol 52. Springer, Dordrecht, pp 343–352. https://doi.org/10.1007/1-4020-3252-8_17

19. Koons BW, Baeseman JL, Novak PJ (2001) Investigation of cell exudates active in carbon tetrachloride and chloroform degradation. Biotechnol Bioeng 74(1):12–17. https://doi.org/10.1002/bit.1090

20. Picardal FW, Arnold RG, Couch H, Little AM, Smith ME (1993) Involvement of cytochromes in the anaerobic biotransformation of tetrachloromethane by *Shewanella putrefaciens* 200. Appl Environ Microbiol 59(11):3763–3770

21. Zou S, Stensel HD, Ferguson JF (2000) Carbon tetrachloride degradation: effect of microbial growth substrate and vitamin B_{12} content. Environ Sci Technol 34(9):1751–1757. https://doi.org/10.1021/es990930m

22. Guerrero-Barajas C, Field JA (2005) Riboflavin- and cobalamin-mediated biodegradation of chloroform in a methanogenic consortium. Biotechnol Bioeng 89(5):539–550. https://doi.org/10.1002/bit.20379

23. Lee C-H, Lewis TA, Paszczynski A, Crawford RL (1999) Identification of an extracellular catalyst of carbon tetrachloride dehalogenation from *Pseudomonas stutzeri* strain KC as pyridine-2,6-bis(thiocarboxylate). Biochem Biophys Res Commun 261(3):562–566. https://doi.org/10.1006/bbrc.1999.1077

24. Hernandez ME, Kappler A, Newman DK (2004) Phenazines and other redox-active antibiotics promote microbial mineral reduction. Appl Environ Microbiol 70(2):921–928. https://doi.org/10.1128/AEM.70.2.921-928.2004

25. Aulenta F, Catervi A, Majone M, Panero S, Reale P, Rossetti S (2007) Electron transfer from a solid-state electrode assisted by methyl viologen sustains efficient microbial reduc-

tive dechlorination of TCE. Environ Sci Technol 41(7):2554–2559. https://doi.org/10.1021/es0624321

26. Albuquerque MGE, Lopes AT, Serralheiro ML, Novais JM, Pinheiro HM (2005) Biological sulphate reduction and redox mediator effects on azo dye decolourisation in anaerobic–aerobic sequencing batch reactors. Enzym Microb Technol 36(5):790–799. https://doi.org/10.1016/j.enzmictec.2005.01.005

27. Bradley PM, Chapelle FH, Lovley DR (1998) Humic acids as electron acceptors for anaerobic microbial oxidation of vinyl chloride and dichloroethene. Appl Environ Microbiol 64(8):3102–3105

28. Cervantes FJ, Dijksma W, Duong-Dac T, Ivanova A, Lettinga G, Field JA (2001) Anaerobic mineralization of toluene by enriched sediments with quinones and humus as terminal electron acceptors. Appl Environ Microbiol 67(10):4471–4478. https://doi.org/10.1128/AEM.67.10.4471-4478.2001

29. Finneran KT, Lovley DR (2001) Anaerobic degradation of methyl tert-butyl ether (MTBE) and tert-butyl alcohol (TBA). Environ Sci Technol 35(9):1785–1790. https://doi.org/10.1021/es001596t

30. Hashsham SA, Scholze R, Freedman DL (1995) Cobalamin-enhanced anaerobic biotransformation of carbon tetrachloride. Environ Sci Technol 29(11):2856–2863. https://doi.org/10.1021/es00011a023

31. Field JA, Cervantes FJ, van der Zee FP, Lettinga G (2000) Role of quinones in the biodegradation of priority pollutants: a review. Water Sci Technol 42(5–6):215–222

32. Stevenson FJ (1994) Humus chemistry: genesis, composition, reactions. Wiley, New York

33. Perminova IV, Kovalenko AN, Schmitt-Kopplin P, Hatfield K, Hertkorn N, Belyaeva EY, Petrosyan VS (2005) Design of quinonoid-enriched humic materials with enhanced redox properties. Environ Sci Technol 39(21):8518–8524. https://doi.org/10.1021/es050915j

34. Li M, Su Y, Chen Y, Wan R, Zheng X, Liu K (2016) The effects of fulvic acid on microbial denitrification: promotion of NADH generation, electron transfer, and consumption. Appl Microbiol Biotechnol 100(12):5607–5618. https://doi.org/10.1007/s00253-016-7383-1

35. Rice JA (2001) Humin. Soil Sci 166(11):848–857. https://doi.org/10.1097/00010694-200111000-00009

36. Simpson AJ, Song GX, Smith E, Lam B, Novotny EH, Hayes MHB (2007) Unraveling the structural components of soil humin by use of solution-state nuclear magnetic resonance spectroscopy. Environ Sci Technol 41(3):876–883. https://doi.org/10.1021/es061576c

37. Hayes MHB, Clapp CE (2001) Humic substances: considerations of compositions, aspects of structure, and environmental influences. Soil Sci 166(11):723–737

38. Wen B, Zhang JJ, Zhang SZ, Shan XQ, Khan SU, Xing BS (2007) Phenanthrene sorption to soil humic acid and different humin fractions. Environ Sci Technol 41(9):3165–3171. https://doi.org/10.1021/es062262s

39. Borisover M, Graber ER (2004) Hydration of natural organic matter: effect on sorption of organic compounds by humin and humic acid fractions vs original peat material. Environ Sci Technol 38(15):4120–4129. https://doi.org/10.1021/es035357s

40. Zhang CF, Zhang DD, Xiao ZX, Li ZL, Suzuki D, Katayama A (2015) Characterization of humins from different natural sources and the effect on microbial reductive dechlorination of pentachlorophenol. Chemosphere 131:110–116. https://doi.org/10.1016/j.chemosphere.2015.02.043

41. Zhang DD, Zhang N, Yu XW, Zhang ZC, Yang SM, Zhang CF (2017) Effect of humins from different sediments on microbial degradation of 2,2′,4,4′,5,5′-hexachlorobiphenyl (PCB$_{153}$), and their polyphasic characterization. RSC Adv 7(12):6849–6855. https://doi.org/10.1039/c6ra25934k

42. Cruz-Zavala AS, Pat-Espadas AM, Rangel-Mendez JR, Chazaro-Ruiz LF, Ascacio-Valdes JA, Aguilar CN, Cervantes FJ (2016) Immobilization of metal-humic acid complexes in anaerobic granular sludge for their application as solid-phase redox mediators in the bio-

transformation of iopromide in UASB reactors. Bioresour Technol 207:39–45. https://doi.org/10.1016/j.biortech.2016.01.125

43. Cervantes FJ, Gómez R, Alvarez LH, Martinez CM, Hernandez-Montoya V (2015) Efficient anaerobic treatment of synthetic textile wastewater in a UASB reactor with granular sludge enriched with humic acids supported on alumina nanoparticles. Biodegradation 26(4):289–298. https://doi.org/10.1007/s10532-015-9734-5

44. Alvarez LH, Jimenez-Bermudez L, Hernandez-Montoya V, Cervantes FJ (2012) Enhanced dechlorination of carbon tetrachloride by immobilized fulvic acids on alumina particles. Water Air Soil Pollut 223(4):1911–1920. https://doi.org/10.1007/s11270-011-0994-3

45. Cervantes FJ, Garcia-Espinosa A, Antonieta Moreno-Reynosa M, Rene Rangel-Mendez J (2010) Immobilized redox mediators on anion exchange resins and their role on the reductive decolorization of azo dyes. Environ Sci Technol 44(5):1747–1753. https://doi.org/10.1021/es9027919

46. Cervantes FJ, Gonzalez-Estrella J, Márquez A, Alvarez LH, Arriaga S (2011) Immobilized humic substances on an anion exchange resin and their role on the redox biotransformation of contaminants. Bioresour Technol 102(2):2097–2100. https://doi.org/10.1016/j.biortech.2010.08.021

47. Chen SS, Rotaru AE, Shrestha PM, Malvankar NS, Liu FH, Fan W, Nevin KP, Lovley DR (2014) Promoting interspecies electron transfer with biochar. Sci Rep 4:5019. https://doi.org/10.1038/srep05019

48. Chen J, Wang C, Pan Y, Farzana SS, Tam NFY (2018) Biochar accelerates microbial reductive debromination of 2,2′,4,4′-tetrabromodiphenyl ether (BDE-47) in anaerobic mangrove sediments. J Hazard Mater 341:177–186. https://doi.org/10.1016/j.jhazmat.2017.07.063

49. Yu LP, Yuan Y, Tang J, Wang YQ, Zhou SG (2015) Biochar as an electron shuttle for reductive dechlorination of pentachlorophenol by *Geobacter sulfurreducens*. Sci Rep 5:16221. https://doi.org/10.1038/srep16221

50. Rosenbaum MA, Franks AE (2014) Microbial catalysis in bioelectrochemical technologies: status quo, challenges and perspectives. Appl Microbiol Biotechnol 98(2):509–518. https://doi.org/10.1007/s00253-013-5396-6

51. Aulenta F, Maio VD, Ferri T, Majone M (2010) The humic acid analogue anthraquinone-2,6-disulfonate (AQDS) serves as an electron shuttle in the electricity-driven microbial dechlorination of trichloroethene to cis-dichloroethene. Bioresour Technol 101(24):9728–9733. https://doi.org/10.1016/j.biortech.2010.07.090

52. Rahimnejad M, Najafpour GD, Ghoreyshi AA, Shakeri M, Zare H (2011) Methylene blue as electron promoters in microbial fuel cell. Int J Hydrog Energy 36(20):13335–13341. https://doi.org/10.1016/j.ijhydene.2011.07.059

53. Rosenbaum M, Aulenta F, Villano M, Angenent LT (2011) Cathodes as electron donors for microbial metabolism: which extracellular electron transfer mechanisms are involved? Bioresour Technol 102(1):324–333. https://doi.org/10.1016/j.biortech.2010.07.008

54. Schroder U (2007) Anodic electron transfer mechanisms in microbial fuel cells and their energy efficiency. Phys Chem Phys 9(21):2619–2629. https://doi.org/10.1039/003627m

55. Min B, Logan BE (2004) Continuous electricity generation from domestic wastewater and organic substrates in a flat plate microbial fuel cell. Environ Sci Technol 38(21):5809–5814. https://doi.org/10.1021/es0491026

56. Kim C, Lee CR, Song YE, Heo J, Choi SM, Lim DH, Cho J, Park C, Jang M, Kim JR (2017) Hexavalent chromium as a cathodic electron acceptor in a bipolar membrane microbial fuel cell with the simultaneous treatment of electroplating wastewater. Chem Eng J 328:703–707. https://doi.org/10.1016/j.cej.2017.07.077

57. Wang X, Cai Z, Zhou Q, Zhang Z, Chen C (2012) Bioelectrochemical stimulation of petroleum hydrocarbon degradation in saline soil using U-tube microbial fuel cells. Biotechnol Bioeng 109(2):426–433. https://doi.org/10.1002/bit.23351

58. Yu H, Feng CH, Liu XP, Yi XY, Ren Y, Wei CH (2016) Enhanced anaerobic dechlorination of polychlorinated biphenyl in sediments by bioanode stimulation. Environ Pollut 211:81–89. https://doi.org/10.1016/j.envpol.2015.12.039

59. Puig S, Serra M, Coma M, Cabré M, Dolors Balaguer M, Colprim J (2011) Microbial fuel cell application in landfill leachate treatment. J Hazard Mater 185(2):763–767. https://doi.org/10.1016/j.jhazmat.2010.09.086

60. Babanova S, Hubenova Y, Mitov M (2011) Influence of artificial mediators on yeast-based fuel cell performance. J Biosci Bioeng 112(4):379–387. https://doi.org/10.1016/j.jbiosc.2011.06.008

61. Nevin KP, Richter H, Covalla SF, Johnson JP, Woodard TL, Orloff AL, Jia H, Zhang M, Lovley DR (2008) Power output and columbic efficiencies from biofilms of Geobacter sulfurreducens comparable to mixed community microbial fuel cells. Environ Microbiol 10(10):2505–2514. https://doi.org/10.1111/j.1462-2920.2008.01675.x

62. Kim HJ, Park HS, Hyun MS, Chang IS, Kim M, Kim BH (2002) A mediator-less microbial fuel cell using a metal reducing bacterium, Shewanella putrefaciense. Enzym Microb Technol 30(2):145–152. https://doi.org/10.1016/S0141-0229(01)00478-1

63. Samrot AV, Senthilkumar P, Pavankumar K, Akilandeswari GC, Rajalakshmi N, Dhathathreyan KS (2010) Electricity generation by *Enterobacter cloacae* SU-1 in mediator less microbial fuel cell. Int J Hydrog Energy 35(15):7723–7729. https://doi.org/10.1016/j.ijhydene.2010.05.047

64. Nimje VR, Chen C-Y, Chen J-L, Chen C-C, Jean J-S, Reddy AS, Fan C-W, Pan K-Y, Liu H-T (2009) Stable and high energy generation by a strain of *Bacillus subtilis* in a microbial fuel cell. J Power Sources 190(2):258–263. https://doi.org/10.1016/j.jpowsour.2009.01.019

65. Du Z, Li H, Gu T (2007) A state of the art review on microbial fuel cells: a promising technology for wastewater treatment and bioenergy. Biotechnol Adv 25(5):464–482. https://doi.org/10.1016/j.biotechadv.2007.05.004

66. Delaney GM, Bennetto HP, Mason JR, Roller SD, Stirling JL, Thurston CF (1984) Electron-transfer coupling in microbial fuel cells. 2. Performance of fuel cells containing selected microorganism-mediator-substrate combinations. J Chem Technol Biotechnol Biotechnol 34(1):13–27. https://doi.org/10.1002/jctb.280340104

67. Vega CA, Fernández I (1987) Mediating effect of ferric chelate compounds in microbial fuel cells with *Lactobacillus plantarum*, *Streptococcus lactis*, and *Erwinia dissolvens*. Bioelectrochem Bioenerg 17(2):217–222. https://doi.org/10.1016/0302-4598(87)80026-0

68. Park DH, Zeikus JG (2000) Electricity generation in microbial fuel cells using neutral red as an electronophore. Appl Environ Microbiol 66(4):1292–1297. https://doi.org/10.1128/AEM.66.4.1292-1297.2000

69. Choi Y, Kim N, Kim S, Jung S (2003) Dynamic behaviors of redox mediators within the hydrophobic layers as an important factor for effective microbial fuel cell operation. Bull Kor Chem Soc 24(4):437–440. https://doi.org/10.5012/bkcs.2003.24.4.437

70. Park DH, Zeikus JG (2003) Improved fuel cell and electrode designs for producing electricity from microbial degradation. Biotechnol Bioeng 81(3):348–355. https://doi.org/10.1002/bit.10501

71. Rabaey K, Ossieur W, Verhaege M, Verstraete W (2005) Continuous microbial fuel cells convert carbohydrates to electricity. Water Sci Technol 52(1–2):515–523

72. Ringeisen BR, Henderson E, Wu PK, Pietron J, Ray R, Little B, Biffinger JC, Jones-Meehan JM (2006) High power density from a miniature microbial fuel cell using *Shewanella oneidensis* DSP10. Environ Sci Technol 40(8):2629–2634. https://doi.org/10.1021/es052254w

73. Sund CJ, McMasters S, Crittenden SR, Harrell LE, Sumner JJ (2007) Effect of electron mediators on current generation and fermentation in a microbial fuel cell. Appl Microbiol Biotechnol 76(3):561–568. https://doi.org/10.1007/s00253-007-1038-1

74. Qiao Y, Li CM, Bao S-J, Lu Z, Hong Y (2008) Direct electrochemistry and electrocatalytic mechanism of evolved *Escherichia coli* cells in microbial fuel cells. Chem Commun 11:1290–1292. https://doi.org/10.1039/b719955d

75. Xia X, Cao X-X, Liang P, Huang X, Yang S-P, Zhao G-G (2010) Electricity generation from glucose by a *Klebsiella* sp. in microbial fuel cells. Appl Microbiol Biotechnol 87(1):383–390. https://doi.org/10.1007/s00253-010-2604-5

76. Thygesen A, Poulsen FW, Min B, Angelidaki I, Thomsen AB (2009) The effect of different substrates and humic acid on power generation in microbial fuel cell operation. Bioresour Technol 100(3):1186–1191. https://doi.org/10.1016/j.biortech.2008.07.067

77. Zhou YL, Yang Y, Chen M, Zhao ZW, Jiang HL (2014) To improve the performance of sediment microbial fuel cell through amending colloidal iron oxyhydroxide into freshwater sediments. Bioresour Technol 159:232–239. https://doi.org/10.1016/j.biortech.2014.02.082

78. Adelaja O, Keshavarz T, Kyazze G (2015) The effect of salinity, redox mediators and temperature on anaerobic biodegradation of petroleum hydrocarbons in microbial fuel cells. J Hazard Mater 283:211–217. https://doi.org/10.1016/j.jhazmat.2014.08.066

79. Vishwanathan AS, Aiyer KS, Chunduri LAA, Venkataramaniah K, Siva Sankara Sai S, Rao G (2016) Carbon quantum dots shuttle electrons to the anode of a microbial fuel cell. 3 Biotech 6(2):1–6. https://doi.org/10.1007/s13205-016-0552-1

80. Rahimnejad M, Najafpour GD, Ghoreyshi AA, Talebnia F, Premier GC, Bakeri G, Kim JR, Oh S-E (2012) Thionine increases electricity generation from microbial fuel cell using *Saccharomyces cerevisiae* and exoelectrogenic mixed culture. J Microbiol 50(4):575–580. https://doi.org/10.1007/s12275-012-2135-0

81. Sun J, Li W, Li Y, Hu Y, Zhang Y (2013) Redox mediator enhanced simultaneous decolorization of azo dye and bioelectricity generation in air-cathode microbial fuel cell. Bioresour Technol 142:407–414. https://doi.org/10.1016/j.biortech.2013.05.039

82. Rabaey K, Boon N, Höfte M, Verstraete W (2005) Microbial phenazine production enhances electron transfer in biofuel cells. Environ Sci Technol 39(9):3401–3408. https://doi.org/10.1021/es048563o

83. Pham TH, Boon N, Aelterman P, Clauwaert P, De Schamphelaire L, Vanhaecke L, De Maeyer K, Höfte M, Verstraete W, Rabaey K (2008) Metabolites produced by *Pseudomonas* sp. enable a gram-positive bacterium to achieve extracellular electron transfer. Appl Microbiol Biotechnol 77(5):1119–1129. https://doi.org/10.1007/s00253-007-1248-6

84. Newman DK, Kolter R (2000) A role for excreted quinones in extracellular electron transfer. Nature 405(6782):94–97. https://doi.org/10.1038/35011098

85. Canstein HV, Ogawa J, Shimizu S, Lloyd JR (2008) Secretion of flavins by *Shewanella* species and their role in extracellular electron transfer. Appl Environ Microbiol 74(3):615–623. https://doi.org/10.1128/AEM.01387-07

86. Marsili E, Baron DB, Shikhare ID, Coursolle D, Gralnick JA, Bond DR (2008) *Shewanella* secretes flavins that mediate extracellular electron transfer. Proc Natl Acad Sci USA 105(10):3968–3973. https://doi.org/10.1073/pnas.0710525105

87. Mardiana U, Innocent C, Jarrar H, Cretin M, Buchari, Gandasasmita S (2015) Electropolymerized neutral red as redox mediator for yeast fuel cell. Int J Electrochem Sci 10(11):8886–8898

88. Xu HD, Quan XC (2016) Anode modification with peptide nanotubes encapsulating riboflavin enhanced power generation in microbial fuel cells. Int J Hydrog Energy 41(3):1966–1973. https://doi.org/10.1016/j.ijhydene.2015.11.124

89. Ding C, Liu H, Zhu Y, Wan M, Jiang L (2012) Control of bacterial extracellular electron transfer by a solid-state mediator of polyaniline nanowire arrays. Energy Environ Sci 5(9):8517–8522. https://doi.org/10.1039/c2ee22269h

90. Chen J-J, Chen W, He H, Li D-B, Li W-W, Xiong L, Yu H-Q (2013) Manipulation of microbial extracellular electron transfer by changing molecular structure of phenazine-type redox mediators. Environ Sci Technol 47(2):1033–1039. https://doi.org/10.1021/es304189t

91. Yong Y-C, Cai Z, Yu Y-Y, Chen P, Jiang R, Cao B, Sun J-Z, Wang J-Y, Song H (2013) Increase of riboflavin biosynthesis underlies enhancement of extracellular electron transfer of Shewanella in alkaline microbial fuel cells. Bioresour Technol 130:763–768. https://doi.org/10.1016/j.biortech.2012.11.145

92. Zheng T, Xu Y-S, Yong X-Y, Yong Y-C, Li B, Yin D, Cheng Q-W, Yuan H-R (2015) Endogenously enhanced biosurfactant production promotes electricity generation from microbial fuel cells. Bioresour Technol 197:416–421. https://doi.org/10.1016/j.biortech.2015.08.136

93. Yong X, Shi D, Chen Y, Feng J, Xu L, Zhou J, Wang S, Yong Y, Sun Y, Ouyang P, Zheng T (2014) Enhancement of bioelectricity generation by manipulation of the electron shuttles synthesis pathway in microbial fuel cells. Bioresour Technol 152(1):220–224. https://doi.org/10.1016/j.biortech.2013.10.086

94. Thrash JC, Van Trump JI, Weber KA, Miller E, Achenbach LA, Coates JD (2007) Electrochemical stimulation of microbial perchlorate reduction. Environ Sci Technol 41(5):1740–1746. https://doi.org/10.1021/es062772m

95. Lovley DR (2011) Powering microbes with electricity: direct electron transfer from electrodes to microbes. Environ Microbiol Rep 3(1):27–35. https://doi.org/10.1111/j.1758-2229.2010.00211.x

96. Su W, Zhang L, Li D, Zhan G, Qian J, Tao Y (2012) Dissimilatory nitrate reduction by *Pseudomonas alcaliphila* with an electrode as the sole electron donor. Biotechnol Bioeng 109(11):2904–2910. https://doi.org/10.1002/bit.24554

97. Wang A-J, Cheng H-Y, Liang B, Ren N-Q, Cui D, Lin N, Kim BH, Rabaey K (2011) Efficient reduction of nitrobenzene to aniline with a biocatalyzed cathode. Environ Sci Technol 45(23):10186–10193. https://doi.org/10.1021/es202356w

98. Liang B, Cheng H-Y, Kong D-Y, Gao S-H, Sun F, Cui D, Kong F-Y, Zhou A-J, Liu W-Z, Ren N-Q, Wu W-M, Wang A-J, Lee D-J (2013) Accelerated reduction of chlorinated nitroaromatic antibiotic chloramphenicol by biocathode. Environ Sci Technol 47(10):5353–5361. https://doi.org/10.1021/es400933h

99. Lo WT, Hsu PK, Fang TH, Hu JH, Hsieh HY (2016) Phytoplankton communities impacted by thermal effluents off two coastal nuclear power plants in subtropical areas of northern Taiwan. Terr Atmos Ocean Sci 27(1):107–120. https://doi.org/10.3319/TAO.2015.09.24.01(Oc)

100. Kong D, Yun H, Cui D, Qi M, Shao C, Cui D, Ren N, Liang B, Wang A (2017) Response of antimicrobial nitrofurazone-degrading biocathode communities to different cathode potentials. Bioresour Technol 241:951–958. https://doi.org/10.1016/j.biortech.2017.06.056

101. Yun H, Liang B, Kong D-Y, Cheng H-Y, Li Z-L, Gu Y-B, Yin H-Q, Wang A-J (2017) Polarity inversion of bioanode for biocathodic reduction of aromatic pollutants. J Hazard Mater 331:280–288. https://doi.org/10.1016/j.jhazmat.2017.02.054

102. Gao S-H, Peng L, Liu Y, Zhou X, Ni B-J, Bond PL, Liang B, Wang A-J (2016) Bioelectrochemical reduction of an azo dye by a *Shewanella oneidensis* MR-1 formed biocathode. Int Biodeterior Biodegrad 115:250–256. https://doi.org/10.1016/j.ibiod.2016.09.005

103. Sun Q, Li ZL, Liu WZ, Cui D, Wang YZ, Chung JS, Wang AJ (2016) Assessment of the operational parameters in bioelectrochemical system in perspective of decolorization efficiency and energy conservation. Int J Electrochemicalence 11(3):2447–2460

104. Su W, Zhang L, Tao Y, Zhan G, Li D, Li D (2012) Sulfate reduction with electrons directly derived from electrodes in bioelectrochemical systems. Electrochem Commun 22(1):37–40. https://doi.org/10.1016/j.elecom.2012.04.030

105. Gregory KB, Lovley DR (2005) Remediation and recovery of uranium from contaminated subsurface environments with electrodes. Environ Sci Technol 39(22):8943–8947. https://doi.org/10.1021/es050457e

106. Strycharz SM, Woodard TL, Johnson JP, Nevin KP, Sanford RA, Löffler FE, Lovley DR (2008) Graphite electrode as a sole electron donor for reductive dechlorination of tetrachlorethene by *Geobacter lovleyi*. Appl Environ Microbiol 74(19):5943–5947. https://doi.org/10.1128/AEM.00961-08

107. Aulenta F, Reale P, Canosa A, Rossetti S, Panero S, Majone M (2010) Characterization of an electro-active biocathode capable of dechlorinating trichloroethene and cis-dichloroethene to ethene. Biosens Bioelectron 25(7):1796–1802. https://doi.org/10.1016/j.bios.2009.12.033

108. Gregory KB, Bond DR, Lovley DR (2004) Graphite electrodes as electron donors for anaerobic respiration. Environ Microbiol 6(6):596–604. https://doi.org/10.1111/j.1462-2920.2004.00593.x

109. Strycharz SM, Gannon SM, Boles AR, Franks AE, Nevin KP, Lovley DR (2010) Reductive dechlorination of 2-chlorophenol by *Anaeromyxobacter dehalogenans* with an electrode serving as the electron donor. Environ Microbiol Rep 2(2):289–294. https://doi.org/10.1111/j.1758-2229.2009.00118.x

110. Yu L, Yuan Y, Chen S, Zhuang L, Zhou S (2015) Direct uptake of electrode electrons for autotrophic denitrification by *Thiobacillus denitrificans*. Electrochem Commun 60:126–130. https://doi.org/10.1016/j.elecom.2015.08.025

111. Nguyen VK, Park Y, Yu J, Lee T (2016) Microbial selenite reduction with organic carbon and electrode as sole electron donor by a bacterium isolated from domestic wastewater. Bioresour Technol 212:182–189. https://doi.org/10.1016/j.biortech.2016.04.033

112. Park DH, Zeikus JG (1999) Utilization of electrically reduced neutral red by *Actinobacillus succinogenes*: physiological function of neutral red in membrane-driven fumarate reduction and energy conservation. J Bacteriol 181(8):2403–2410

113. Leitão P, Rossetti S, Danko AS, Nouws H, Aulenta F (2016) Enrichment of *Dehalococcoides mccartyi* spp. from a municipal activated sludge during AQDS-mediated bioelectrochemical dechlorination of 1,2-dichloroethane to ethene. Bioresour Technol 214:426–431. https://doi.org/10.1016/j.biortech.2016.04.129

114. Xiao Z, Awata T, Zhang C, Zhang D, Li Z, Katayama A (2016) Enhanced denitrification of *Pseudomonas stutzeri* by a bioelectrochemical system assisted with solid-phase humin. J Biosci Bioeng 122(1):85–91. https://doi.org/10.1016/j.jbiosc.2015.11.004

115. Liu H, Guo J, Guo Y, Qu J, Lian J, Jefferson W, Yang J (2012) Biological catalyzed denitrification by a functional electropolymerization biocarrier modified by redox mediator. Bioresour Technol 107:144–150. https://doi.org/10.1016/j.biortech.2011.12.071

Chapter 9
Bioelectrochemical System Integrated with Photocatalysis: Principle and Prospect in Wastewater Treatment

Shu-Sen Wang, Hafiz Muhammad Adeel Sharif, Hao-Yi Cheng, and Ai-Jie Wang

9.1 Introduction

The shortage of nonrenewable energy source and gradual increase of environmental pollution are two major problems for society. For this reason, more efforts have been put forward for renewable energy source and environmental restoration around the world.

To account these issues, microbial electrochemical technologies (METs) have become a research hotspot in the field of environment and resources nowadays because the pollutants degradation and enegergy recovery (electricity, hydrogen, etc.) can be done simultaneously by this technology [1, 2]. However, there are still some limitations in METs. For pollutants degradation, only simple organics, such as carbohydrates and volatile acids, can be efficiently removed, while the degradation of recalcitrant organics, such as aromatics and heterocycle compounds is difficult [3, 4]. Regarding energy production, in order to obtain high output power

S.-S. Wang · H. M. A. Sharif
Key Laboratory of Environmental Biotechnology, Research Center for Eco-Environmental Sciences, Chinese Academy of Sciences, Beijing, China

University of Chinese Academy of Sciences, Beijing, China

H.-Y. Cheng (✉)
Key Laboratory of Environmental Biotechnology, Research Center for Eco-Environmental Sciences, Chinese Academy of Sciences, Beijing, China
e-mail: hycheng@rcees.ac.cn

A.-J. Wang (✉)
Key Laboratory of Environmental Biotechnology, Research Center for Eco-Environmental Sciences, Chinese Academy of Sciences, Beijing, China

State Key Laboratory of Urban Water Resource and Environment, School of Environment, Harbin Institute of Technology, Harbin, China
e-mail: ajwang@rcees.ac.cn

or hydrogen production, precious metals catalysts are usually used in cathode materials for microbial fuel cell (MFC) and microbial electrolytic cell (MEC), which could ultimately increase the cost [5, 6]. In addition, in terms of hydrogen production, although MEC can achieve energy compensation by degradation of organic pollutants, the spontaneously hydrogen generation is still impossible because oxidation of organics by anode respiration bacteria lied at an energy level that is lower than that of hydrogen evolution (i.e. −300 mV for NAD/NADH vs −410 mV for H^+/H_2 at pH 7) [7].

Compared with the conductors, semiconductors have a special electronic band structure and energy levels. There is a forbidden band between the conduction band and the valence band. When irradiating by a certain wavelength of light, the electrons in the valence band of the semiconductor can be excited and transferred to the conduction band, leaving highly oxidative holes at valence band. Since This transition generates the electron and hole pair are capable of driving reducing and oxidizing reactions, semiconductors can introduce photo energy into chemical processes. Owing to the excellent photo-to-energy conversion characteristics and high efficiency for refractory organics degradation of semiconductors [8–10], introducing semiconductors into METs have attracted increasing attentions these years, which have been revealed to overcome those limitations of METs. For instance, using solar energy as an additional source of energy can overcome the energy barrier of hydrogen evolution and enable the hydrogen generation spontaneously. In addition, semiconductor involved photocatalytic oxidation technologies have been known as a powerful advanced oxidation approach. Therefore, introducing the photocatalyst into the METs can extend this technology to remove recalcitrant organic contaminants. Solar energy is a kind of sufficient and renewable resource. By use of solar energy, no supplementary energy is required, and ultimately no secondary pollution will be produced. Therefore, recently photoelectrochemical technology is more famous and promising for coupling with the MFC and MEC to form microorganism-light-electrochemical coupling technology [11–14]. In this chapter, different types of hybrid photoelectrochemical-bioelectrochemical systems are described. We want to make understanding about coupling system that is hybrid of photoelectrochemical and MFC or MEC as shown in Fig. 9.1.

9.2 Research Status of Microbial-photo-electrochemical Systems

9.2.1 Coupling Semiconductor Solar Cell with Microbial Electrochemical Reactor

Photosensitive semiconductors have the ability of converting solar energy into the electrical energy. The semiconductors have a special structure called p-n junction. When the photosensitive semiconductor is illuminated, the electrons with negative charge can be generated in negative (n) area; meanwhile the holes with positive charge can be generated in positive (p) area. When the negative area and positive
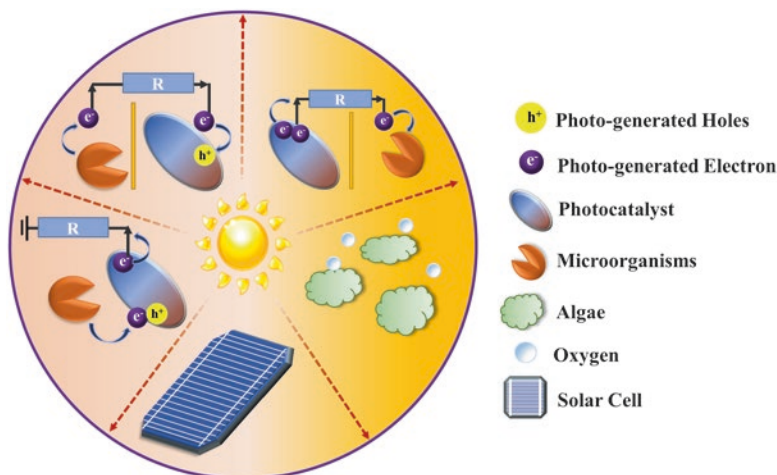
Fig. 9.1 Schematic summary of different types of microbial-photo-electrochemical systems
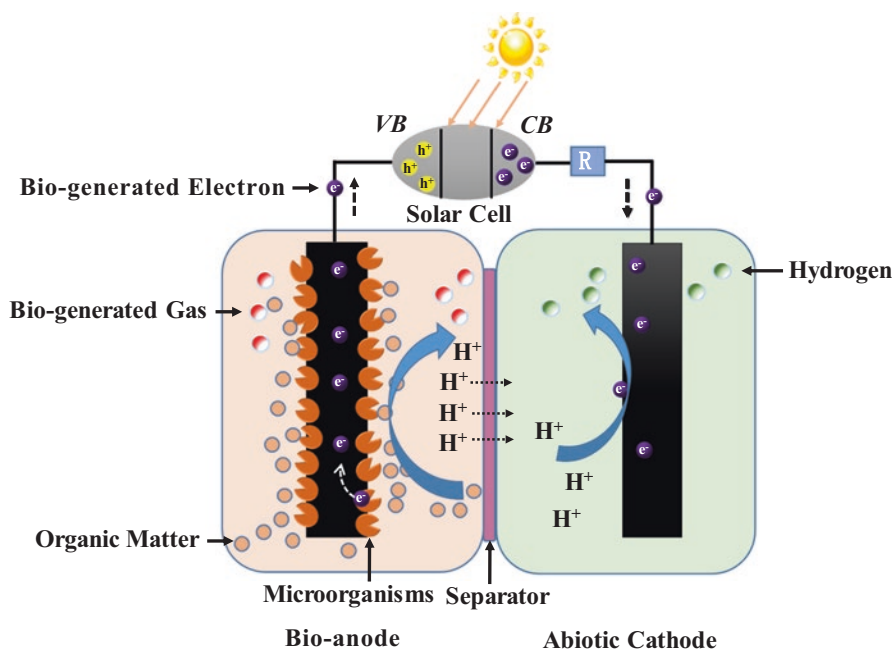
Fig. 9.2 Scheme of coupling system of solar cell and MFC

area are connected with electric wire, the electrons generated in the positive area will transfer to the negative area and result in the current generation. It can be seen that the p-side of the solar cell has the ability to attract electrons, while the n-side can provide electrons. If the solar cell is coupled with a microbial-electrochemical reactor (Fig. 9.2), the characteristics of the semiconductor p-n junction can be

utilized to improve the electron transfer capability. The photo-generated holes can attract the electrons generated at the bio-anode, which can increase the anode electric potential. Therefore, the oxidizability of the anode can be enhanced. Meanwhile, the photo-generated electrons can be transferred to the biocathode, which can lower the cathode potential and increase its reducing capability [15].

Chen et al. coupled silicon semiconductor solar cells with a MFC, building a photovoltaic cell – biofuel cell system [16]. Similar to the mechanism shown in Fig. 9.2, the electrons generated on the negative side of the solar cell can move to the cathode via the external circuit and react with electron acceptor in the cathode chamber. The photo-generated holes combined with the bio-electrons that are generated from the degradation of organics at the bioanode. The results showed that the highest power density of coupling system can reach to 275 mW/m^3, apparently higher than that of normal MFC with 140 mW/m^3. The coupling of solar cell with MFC can effectively improve the ability of cathode to accept electrons and enhance the anodic electron donating ability, which can significantly improve the power generation of MFC.

Solar-sensitive semiconductor can not only improve the electron transfer efficiency of MFC but also can help to generate hydrogen spontaneously. In this case, the MEC powered by solar illumination instead of electricity. Chae et al. built a dye-sensitized solar cell and MEC coupling system [17]. The experimental results showed that the system can use solar energy as the energy source and realize the spontaneous hydrogen production under sunlight illumination by the synergetic effect of dye-sensitized solar cells and MEC. The hydrogen generation rate reached 3.14 ± 0.20 mol H_2/mol acetate. Wang et al. proposed a type of cell that combined photoelectrochemical cell (PEC) with MFC [18]. The cathode of MFC can catch the electron generated by PEC and use the electron to reduce the oxygen. At the same time, the anode of MFC can transfer the electrons produced from organic degradation to the cathode of PEC for H_2 generation. This combination can use sunlight as the sole source of energy for pollutant degradation and hydrogen production. The current density of MFC using *Shewanella oneidens* reached 1.25 mA/cm^2; meanwhile, the solar to hydrogen conversion rate reached 1.54%.

9.2.2 Coupling Bio-electrode with Semiconductor Electrode

9.2.2.1 Coupling Bio-anode with Semiconductor Cathode

The cathode of the microbial electrochemical reactor often uses noble metal as electrode material to catalyze the reduction reaction [19–22], which suffers from high cost. The noble metal like Pt is expensive. And in most cases, it does not generate electrons so that the electrons for the reaction need to be provided from external circuit. There is another cheaper material, which is called photocatalyst or photosensitive semiconductor, which can promote reaction rate as well as generate electrons. The photosensitive semiconductor material can be used as the cathode to
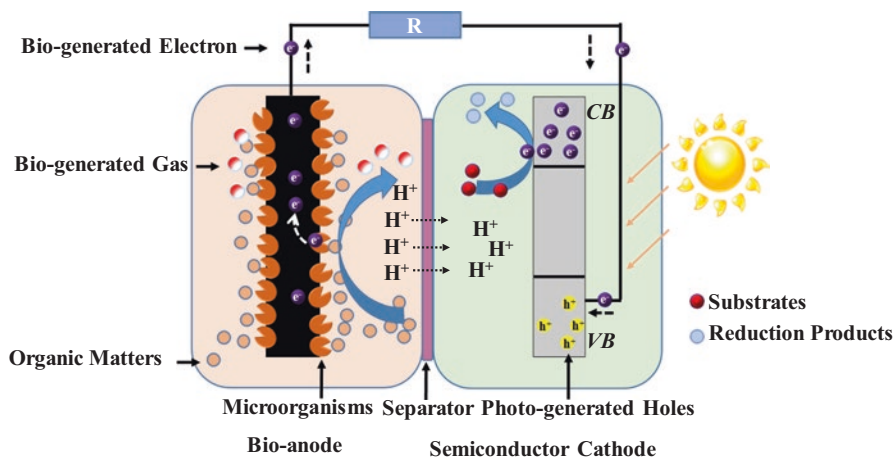
Fig. 9.3 Scheme of coupling system of bio-anode and semiconductor cathode

participate in the reduction reaction. By using this characteristic, the bio-anode/semiconductor cathode mode system gets coupled. The schematic is shown as in Fig. 9.3. As what we can see in Fig. 9.3, the microorganisms in the anode oxidize organic matters and transfer electrons via the electrode to the external circuit. Meanwhile the cathode semiconductor is excited by light to generate electron-hole pairs, and the holes can combine with the bio-generated electrons coming from the external circuit. The combination of the holes and bio-generated electrons can decrease the recombination rate of photo-generated holes and electrons, so that the redox reaction rate on the electrodes can be increased significantly. Compared with the traditional microbial electrochemical reactors, the coupling of the semiconductor cathode can promote the oxidation reaction of the bio-anode and the reduction of the semiconductor cathode. This means that some reactions which cannot happen in normal MFC can be carried out in this system.

Li et al. combined a semiconductor cathode with a microbial electrochemical reactor and investigated the reduction ability of Cr (VI) for the first time [23]. The anaerobic activated sludge was used to inoculate the electroactive microorganism, and the cathode was a natural rutile semiconductor. The experimental results showed that the introduction of light increased the output voltage and the reduction rate of Cr (VI). The maximum output voltage under illumination is 0.80 V, which was better than 0.55 V under dark conditions. The reduction rate of Cr (VI) under illumination was 1.6 times faster than dark condition. Lu et al. used the bio-anode rutile semiconductor cathode coupling system to study the properties of electrical production [24]. The experimental results showed that the maximum power density under illumination was 12.03 W/cm^3, which was nearly double of that under dark conditions (7.64 W/cm^3). Ding et al. used the same coupling system to study the reduction and degradation of methyl orange [25]. The experimental results showed that when they used rutile as a cathode instead of graphite, the internal resistance decreased

from 1429.0 Ω to 443.3 Ω and the initial current was increased from 0.110 mA to 0.165 mA. At the same time, the decoloration rate of methyl orange increased from 62.3% to 73.4% in 24 h. Lin et al. introduced the TiO_2 cathode into a MFC system, which greatly accelerated the rate of denitrification at the cathode [26]. The above studies indicates that the semiconductor cathode and bio-anode coupling system can effectively improve the oxidization capacity of the bio-anode and promote the reduction reaction of the semiconductor cathode and improve the electricity production characteristics of the system.

Qian et al. developed a microbial photoelectrochemical cell (MPC) by coupling a p-type Cu_2O nanotube array semiconductor cathode with *Shewanella oneidensis* MR-1 bio-anode. Under illumination, self-sustained generation of electricity was observed [27]. They explained the mechanism of this system as that the semiconductor cathode has a valence band potential higher than the anode potential so that electrons produced by electrochemical active bacteria can be transferred spontaneously from anode to the cathode and result in the current output under illumination. Under zero bias condition, the MPC generate current of 300 μA, which is much higher than that of pure photoelectrochemical system (0.6 μA) and traditional MEC (20 μA), indicating the synergistic effect between the semiconductor and the bio-anode can extract energy from organic pollutants and sunlight simultaneously.

Wang et al. constructed a coupling system with a $CuInS_2$ cathode and a bio-anode [28]. The results showed that the introduction of $CuInS_2$ strengthened the electron transfer and improves the cell efficiency with the maximum output current and power density of 0.62 mA/cm^2 and 0.11 mW/cm^2, respectively. Zang et al. combined MoS_3-modified silicon nanowires with biological anodes to increase the cathode potential and reduce the overpotential for hydrogen production, enabling the system to produce hydrogen spontaneously, continuously, and efficiently [29]. The average hydrogen evolution rate and maximum power density reached 7.5 ± 0.3 μmol/(h•cm^2), and 71 mW/m^2, respectively. More positive onset potential of the MoS3 modified cathode was observed compared to those unmodified ones, indicating introducing state-of-the-art semiconductors into the coupling system is an efficient way to enhance the system performance.

Chen et al. used the n-type TiO_2 nanorod array as the semiconductor cathode and coupled with the bio-anode to study the power generation and hydrogen production efficiency of the system [30]. The maximum power density of 6.0 mW/m^2 was obtained with the hydrogen evolution rate at cathode as 4.4 μL/h. This suggests that the bio-anode/semiconductor cathode coupling system is not limited to coupling with p-type semiconductors, which expands the design and applications of this coupling system.

9.2.2.2 Coupling Model of Semiconductor Anode and Biocathode

Semiconductors as anodes are the common form of photoelectrochemical cells. Photosensitive semiconductor-generated holes have strong oxidizing ability, which can break down the structure of refractory pollutants quickly and efficiently, and do
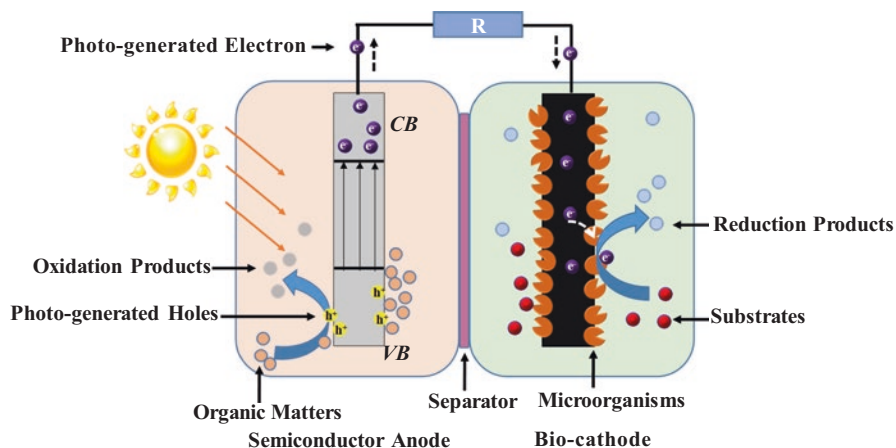
Fig. 9.4 Scheme of coupling system of semiconductor anode and biocathode

not produce secondary pollution. The electrons generated by the photo semiconductor can be supplied to the biological cathode for catalytic reduction reaction. Figure 9.4 shows the coupling mode between the semiconductor anode and the biocathode. The researchers have studied the performance of semiconductor-anode/biocathode MFC with different pollutants.

Brune et al. used an indium tin oxide (ITO) transparent conductive film glass containing nano-TiO_2 particles and coated with a porphyrin sensitizer as the electrode to couple with an enzyme-type bioelectrochemical cathode to improve the power generation performance [31]. When light impinged on the anode, the excited porphyrin sensitizer transfers the electrons to the conduction band of TiO_2 and then to the cathode through the ITO electrode. In this process, the electron-deficient porphyrin sensitizer was regenerated from the redox couple of the enzyme electrode to regenerate the electron, whereas the reduced coenzyme regenerates by the glucose dehydrogenase oxidizing the glucose or ethanol-supplied electrons. The results showed that the device can produce higher photocurrent and has good stability.

Han et al. used TiO_2 nanotube arrays as the semiconductor anode and bilirubin oxidase as the biocathode to construct a glucose-based, membrane-free, non-media single-chamber fuel cell [32]. The experimental results showed that the battery performance has been improved, and the open circuit voltage reached to 1.00 V and the maximum power density 47 1 $\mu W/cm^2$ was obtained. Du et al. constructed a coupling system of TiO_2 photo-anode and biological cathode [33]. The decolorization rate constant of methyl orange in this system reached 0.0120 min^{-1}, and the maximum power density reached 211.32 mW/m^2, which was similar to that of carbon brush cathode loaded with 50 mg Pt/C catalyst. Further, Du et al. investigated the key parameters of the system, such as electrolyte type, electrolyte concentration, and vapor phase composition in the anolyte. The results showed that the system had the highest degradation and conversion efficiency with acetate as the substrate [34]. Wang et al. coupled the TiO_2 semiconductor photoanode with the bioelectrochemi-

cal denitrification cathode and achieved the complete removal of various forms of nitrogen in the wastewater [35].

Since the research on biological cathodes started relatively late, the researches on the coupling systems of semiconductor anodes and biocathodes are still less. In addition, most of the pollutants studied in the current study are small-molecule organic compounds, which do not meet the capability of high efficiency and rapid degradation of complex organic compounds provided by the semiconductor photo-anode. It can be expected that the photoanode/biocathode coupling system that combines strong oxidation and selective reduction in one system would attract great attention in future studies.

9.2.3 Coupling of Semiconductor and Bio-electrode as Semiconductor-microbial Composite Electrode

Extracellular electron transfer (EET) of electrochemical active bacteria is the fundamental of traditional microbial electrochemical technologies [36, 37]. With the deep understanding of EET in recent years [38–40], it has become a new research hotspot of developing microbial photoelectrochemical system with semiconductor-microbial composite electrode.

Semiconductor-microbial composite electrode schematic was shown in Fig. 9.5. Photo-generated holes and electrons will be generated when the semiconductor is illuminated. The holes attract the electrons generated by the electroactivated microorganisms, which can not only help to separate the photo-generated holes and electrons but also accelerates the degradation rate of organic matters at anode, resulting the improvement of electricity production and pollution removal.

Qian et al. used a hematite nanoarray electrode as a photo-anode, and *S. oneidensis MR-1* strain was added to the electrolyte to construct a single-chamber, electrochemical system [41]. The results showed that there had been electron transfer between the hematite and the bacteria. Under the condition of illumination and with the presence of living bacteria, the current density of the system reached 0.25 mA/cm^2, which was 150% higher than that of the non-bacteria control group. The system was stable in 2 weeks. The direct electron transfers between the semiconductor and the anode respiration bacteria ensured the continuous energy output of the whole system, indicating the fuel cell can be constructed through a well-designed semiconductor-microbial composite electrode to achieve the purpose of obtaining energy from sunlight and pollutants.

Li et al. enriched electrochemical active biofilm on a α-Fe2O3 modified ITO electrode to form semiconductor-biofilm composite electrode [42]. The current in the system increased significantly under the condition of irradiation when the anode potential above −0.25 V. This was partly due to the fact that anode respiration bacteria can provide more electrons to the α-Fe$_2$O$_3$ surface by adjusting the respiration rate during illumination. As a result, the remaining biogenetic electrons after com-
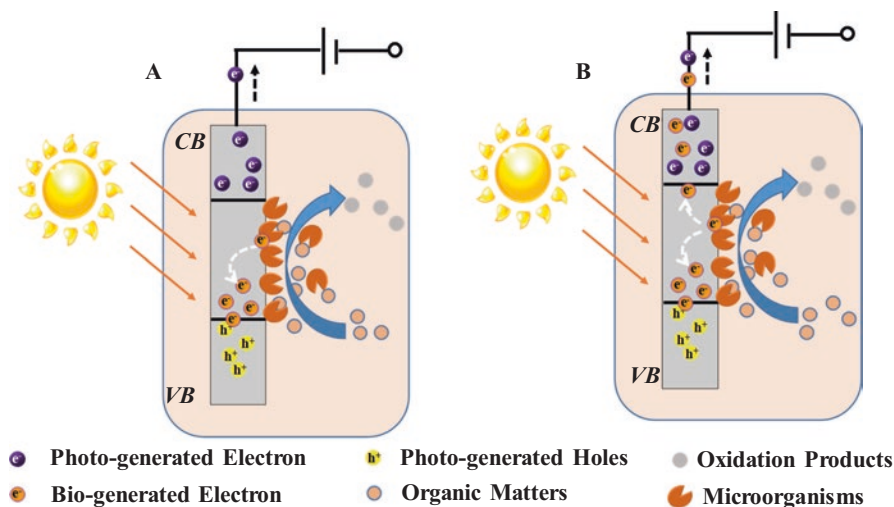
Fig. 9.5 (**a**) Scheme of semiconductor-microbial composite electrode with less bio-generated electrons which were only used to combine with the holes; (**b**) scheme of semiconductor-microbial composite electrode with more bio-generated electrons which were not only used to combine with the holes but also used to transfer to the external circuit

bining with photo-generated holes can flow out with the photo-generated electrons to increase the current density (Fig. 9.5b). It was noteworthy that, in traditional concept, the photo-induced holes can generate various strong oxidizing substances which may damage the surface of the bacteria cells, but the study observed that *Geobacter sulfurreducens* cells on the excited α-Fe$_2$O$_3$ surface can alive and maintain the electrochemical activity [42]. The possible reason was interpreted as that rapid interfacial electron transport and low hole potential avoid the generation of a large number of free radicals at the interface and the cells had a higher reductase activity under illumination than in the dark.

Zhou et al. constructed an anode that intimately couples anode-respiring bacteria (ARB) and nitrogen-doped TiO$_2$ (N-TiO$_2$) photocatalyst (ICPB-anode) to explor if and how ARB played a role in transporting photo-generated electrons [43]. In this work, the photo-generated electrons can be transferred to the external circuit by the ARB at the potential of +0.25 V. Carbon form was used as the basement material of anode in this work which was compromised by prolonged ethanol soaking to attenuate direct electron transfer from photocatalyst to carbon form. The N-TiO$_2$ was loaded firmly on the outside surface of the compromised carbon form, which the bacteria were cultured on the interface. Compared to the current density under dark condition, the ARB-N-TiO$_2$ anode can have an increasing of 3 A/m^2 (30%) with 50 mM acetate under light condition contributed by the photo-generated electrons. Additionally, the columbic efficiency was found to be increased by ~20% as well. Since the electrons generated by the N-TiO$_2$ cannot be transferred through the compromised carbon form directly, the conductive bacterial matrix was sug-

gested to be the way. Besides, R_{ohm} for the ICPB-anode decreased to $3.3 \times 10^2\ \Omega$, a ~98% decrease compared to that of the photo-anode ($1.7 \times 10^4\ \Omega$). The changes of the Rohm also mean the conductivity of the bacterial film had converted the photo-anode into a biofilm anode [44–46].

Up to now, there are only a few studies focusing on semiconductor-biofilm composite electrode. It can be seen from the works as mentioned above that this kind of microbial photoelectrochemical coupling system has good characteristics of simple structure and high efficiency. With the breakthrough of the electron transfer mechanism between semiconductors and microorganisms, this type of system will be also expected to become the research hotspots in the future.

9.2.4   Coupling System of Algae and MFC

For many years, the algae are considered as a promising resource for biofuel such as biodiesel, methane, hydrogen, and ethanol [47–50]. The microalgae usually grow in aquatic environments, which provide them with many nutrients in dissolved form, such as CO_2, P, and N [12, 51, 52]. Due to their simple structure, they harness solar energy quickly and efficiently through photosynthesis. They use sunlight and CO_2 to produce oils or sugars in a more efficient way than crop plants. What's more, the microalgae are versatile in producing oxygen.

With plenty of good energy conversion characterization, more and more researchers attempt to integrate algae into MFCs. One of the ideas is to convert solar energy to chemical energy by algae in the form of biomass, which is then fed into MFC as the electron donor for electricity production [53]. Because of the varied biomass content and composition of organics [54, 55], the power generation capacities in MFC feeding with different types of algae were unidentical. As the microalgae can produce oxygen, a limiting factor in MFC, and remove organics and nutrients from wastewater, integration of MFC with alive microalgae is of more interesting topic. The advances under this scope are described as below.

9.2.4.1   Two-chamber Algae MFC

The algae introduced into cathode of MFC can enhance the electricity generation ability and generate biomass simultaneously (Fig. 9.6). The substrate in the anode chamber can use plenty of kinds of organic matters for different aims. The microorganisms in the anode would degrade the organic matter and generate electrons, CO_2 and H^+. CO_2 levels of 5–20% were known to be the optimal carbon range for the growth of *Chlorella vulgaris* (*C. vulgaris*) which was treated as model algae [56, 57]. With light and CO_2, the algae performed photosynthesis, and the biomass and dissolved oxygen (DO) would increase. Meanwhile, some nutrients could be removed by the microorganisms and the microalgae.
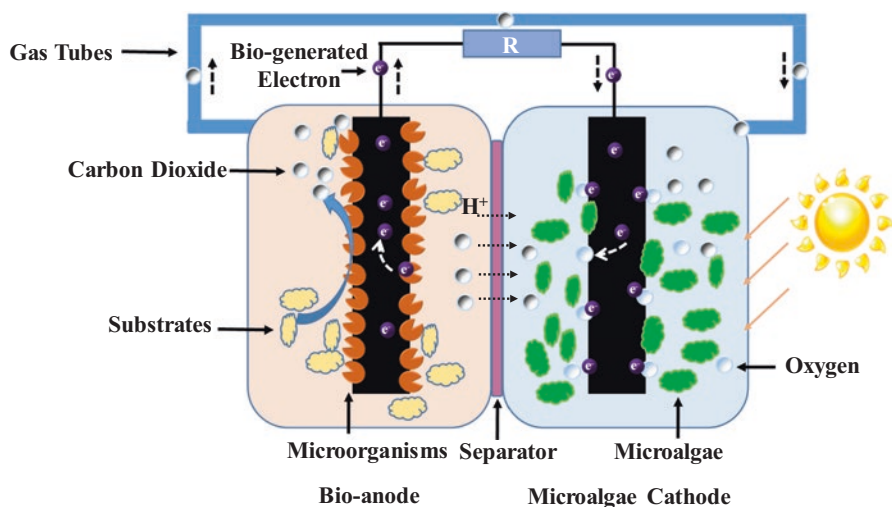
Fig. 9.6 Scheme of coupling model of bio-anode and microalgae-cathode MFC, in which the algae powder and extract lipid can be used as substrates to generate energy

The optimal CO_2 concentration is 5–20% for the growth of the most commonly used *C. vulgaris* [56, 57]. In lab-scale experiments, most of the microalgae MFC were designed by linking the anode chamber and cathode chamber with a gas tube to ensure the CO_2 produced at anode side can be transferred to the cathode side [58–60]. There would be a poor performance before the anode can provide enough CO_2. Therefore, the activity of anodic microorganisms and the substrates had a great influence on lag period of the microalgae-MFC system. However, Liu et al. [58] found that without the pipe connecting between the anode and cathode, the algae MFC can also generate electricity with light because of the diffusion of CO_2 generated in anode through the separator between the anode and cathode chamber, although the maximum power density was a little lower (146 mW/m²) than the pipe-linked system (187 mW/m²).

Illumination is another vital important parameter to the performance of algae-cathode MFC. Gouveia et al. [61] found that the increasing light intensity from 26 to 96 μE/(m²·s) led to 6-fold higher power generation. The illumination was likely to have effects on the performance of the cathode and the photosynthesis of algae. Wu et al. [62] tested some electrical parameters and the oxygen generation capability with different light intensities (0–3500 lx). The cathode resistance decreased from 3152.0 Ω to 136.7 Ω, and the cathode potential increased from −0.44 to V −0.33 V (vs. Ag/AgCl) when the light intensity increased to 1500 lx. A peak was reached when the light intensity increased from 1500 lx to 3500 lx. Meanwhile, the DO increased 76% (from 7.5 to 13.2 mg/L). Hu et al. [59] tested a series of light intensity (2.4, 5.0, 8.9, and 11.4 W/m²), and the result showed that the algae MFC (with *C. vulgaris* in the cathode) had the maximum power densities and CO_2 fixation rate under light intensity of 8.9 W/m² and 887.8 mg/(L·d), respectively. The

lipid productivity was increased with the light intensity from 2.4 W/m^2 to 11.4 W/m^2, but there were no significant differences in lipid productivities between light intensities of 8.9 W/m^2 and 11.4 W/m^2. The illumination surely has influence on the living activity and photosynthesis, thus controlling the performance of the algae MFC.

The same as normal microorganisms MFC, these kinds of alga MFCs have a good ability to degrade organics in the anode and generate electricity. Cui et al. established a double-chamber system. They introduced *C. vulgaris* to the cathode and used dry biomass of *Scenedesmus* (a green algae) as substrate in the anode [63]. Compared to the control group in which acetate was used as substrate in anode, the microalgae system generated higher current and power density in the same COD condition. This might be due to the high concentration of digestible free fatty acid in lyzed *Scenedesmus* powder feedstock. The power densities and the current densities were 1.17 W/m^2 and 2.55 A/m^2 for microalgae system in 968 ± 6 mg COD/L substrate concentration. The maximum power density reached 1926 ± 21.4 mW with 2490 ± 28 mg COD/L. The maximum *C. vulgaris* biomass concentration of 1247 ± 52 mg/L was obtained. Through the operation, the COD removal rate can reach to 85%.

Gajda et al. established a novel microalgae-MFC combination system, which anode was fed with microalgae grown in the cathode chamber, and achieved 128 μW of power output. This assembly simultaneously produced electricity and biomass and was considered to have a promising potential to generate electricity from the biomass produced in the cathode of MFCs.

To increase the energy utilization efficiency and save the energy used to degrade the biomass of algae, some researchers also attempted to extract the bio-oil matters and launch algae-extractive-fed MFC. Rashid et al. attempted to apply the extracted algae lipid to the anodic substrate, but the system only gained the OCV (open circuit voltage) of 21 mV [64]. Khandelwal et al. increased the OCV of algae-lipid-fed MFC [65]. This system successfully made a substance cycle and energy generation with higher OCV. The anode was fed by the lipid-extracted algae (LEA) which was extracted from the algae grown in the cathode by using the CO_2 generated in anode. The electron can be captured by the oxygen released by the alae under irradation condition. They used methanol-chloroform (2:1) by modified Bligh and Dyer extraction method to extract the lipid [66]. The acclimatized LEA-fed MFC did not take any start-up time and exhibited a voltage of 120 ± 11.5 mV after 1 day of operation, which further reached 300 mV with 1000 Ω of external resistance.

Some organic wastewaters are good electron donors. Nguyen et al. [60] reported a mix of algae-cathode and microorganism-anode MFC to treat the landfill leachate wastewater. When the mixture percentage of landfill leachate wastewater and domestic wastewater is 5:95 (v:v), it can reach the maximum cell voltage of 300 ± 11 mV. The best nutrient removal efficiency was obtained with 10% leachate. After a 5-day operation, the COD in anode decreased from 1552.9 ± 60.4 to 50.2 ± 4.9 mg/L (96.8% removal), while the COD in the cathode chamber decreased from 316 ± 60 to 149 ± 8 mg/L (52.9% removal). The NH_4^+-N can be used as nitrogen

nutrient for algae with removal efficiency of 98.7 ± 1.8%. At the same time, the cathode can reduce 61.46% of total phosphorous.

Colombo et al. [67] made an assembly to treat swine-farming wastewater. In this case, organics in swine-farming wastewater were degraded by anodic bacteria with giving electrons to the anode, while *Spirulina* was introduced into the cathode to produce oxygen which can be used as the electron acceptor. Compared to the air-cathode MFC, the algae-cathode MFC produced a similar current density of 5 A/m^2, and the COD removal rate also reached the same level of 89 ± 1% which means the algae can produce ample oxygen to capture the electrons. Meanwhile, the average growth rates of algae in cathode resulted in around 0.1 g/(L·d) (dry biomass concentration) which showed the economic value of this treatment system.

A double-chamber algae-cathode MFC was established by Commault et al. [68] in which anode effluent can be treated by the *C. vulgaris* at the cathode. The anode influent was synthetic wastewater that contained COD (2922 ± 66 mg/L), ammonium (135 ± 1 mg/L), nitrate (165 ± 24 mg/L), and phosphate (9.5 ± 0.4 mg/L). The maximum power density reached 34.2 ± 10.0 mW/m^2, which was two times higher than the no-algae MFC. A removal rate of 0.19 g/(L·d) COD and 5 mg/(L·d) ammonium was achieved in this algae-cathode MFC.

9.2.4.2   Single-chamber Algae MFC

The two-chamber algae MFC systems as above can realize the simultaneously removal of COD and some nutrient elements, but because of using the separation membrane and gas transfer tube, the costs of operation and reactor construction are expensive. For this, algae MFC with single-chamber configuration was developed (Fig. 9.7).

In order to minimize the adverse effect of algae on the anode (i.e. oxygen as competitive electron acceptor), Yang et al. proposed an algae biofilm microbial fuel cell (ABMFC), in which the microalgae was immobilized on a film [52]. In this system, the anode degraded organic matters while generating CO_2 and electrons. The cathode was designed to float on the water surface, which can use the oxygen generated from microalgae and provided from atmosphere as the electron as electron acceptor. With the help of the anode, the microalgae can carry out photosynthesis to reduce ammonium, nitrate, and phosphorous. In continuous mode, the removal efficiencies of TN, TP, and COD in the algae biofilm microbial fuel cell (ABMFC) reached 95.5%, 96.4%, and 81.9%, respectively. The highest power density of the ABMFC (62.93 mW/ m^2) was 18% higher than that of the MFC (52.33 mW/m^2), and a lipid productivity of 6.26 mg/(L·d) was obtained simultaneously.
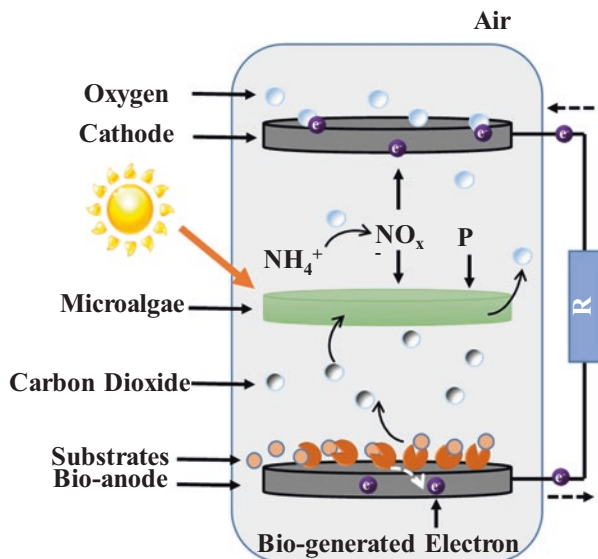
Fig. 9.7 Scheme of microorganisms MFC with microalgae, in which the microalgae grown on the middle space of the anode and cathode to capture CO_2 and nutrient compounds and released O_2

9.3 Conclusion and Overview

Compared with the traditional microbial electrochemical technology, the novel microbial photoelectrochemical coupling technology, which introduces the solar energy into a microbial electrochemical reactor, has more efficient pollutant degradation capability and stronger electric power generation capability. Additionally, the replacement of electricity with solar energy is also in line with the development of sustainable technology. This green system is expected to become a hot topic in the research field of environment and resources in future. At present, the development of microbial photoelectrochemical coupling technology is still in the laboratory research stage. More basic researches and process optimization are required, which would help to update and promote the application of this technology. The following aspects are likely play key roles in the further development of this technology:

(a) In electroactive microorganism aspects. The discovery of electrochemically active microorganisms or microalgae with more diverse functions will help to further expand the range of the applications of this technology.
(b) In electron transfer aspects. The understanding the direct and indirect electron transfer mechanism between microorganisms and semiconductors in detail will help to design the microbial-photo-electrochemical coupling system with higher efficiency.

(c) In material aspects. Research advances in semiconductor materials will help to increase the solar energy utilization efficiency of microbial-photo-electrochemical coupling system.

(d) In application aspects. The researches on process optimization, manipulation strategy, and scale-up of different coupling modes are of great significance to the engineering application of this technology.

References

1. Logan BE, Rabaey K (2012) Conversion of wastes into bioelectricity and chemicals by using microbial electrochemical technologies. Science 337(6095):686–690
2. Logan BE, Hamelers B, Rozendal R, Schröder U, Keller J, Freguia S, Aelterman P, Verstraete W, Rabaey K (2006) Microbial fuel cells: methodology and technology. Environ Sci Technol 40(17):5181–5192
3. Min B, Logan BE (2004) Continuous electricity generation from domestic wastewater and organic substrates in a flat plate microbial fuel cell. Environ Sci Technol 38(21):5809–5814
4. Mook WT, Aroua MKT, Chakrabarti MH, Noor IM, Irfan MF, Low CTJ (2013) A review on the effect of bio-electrodes on denitrification and organic matter removal processes in bio-electrochemical systems. J Ind Eng Chem 19(1):1–13
5. Rozendal RA, Hamelers HV, Euverink GJ, Metz SJ, Buisman CJ (2006) Principle and perspectives of hydrogen production through biocatalyzed electrolysis. Int J Hydrog Energy 31(12):1632–1640
6. Liu H, Grot S, Logan BE (2005) Electrochemically assisted microbial production of hydrogen from acetate. Environ Sci Technol 39(11):4317–4320
7. Cheng S, Logan BE (2007) Sustainable and efficient biohydrogen production via electrohydrogenesis. Proc Natl Acad Sci 104(47):18871–18873
8. Antoniadou M, Lianos P (2010) Production of electricity by photoelectrochemical oxidation of ethanol in a PhotoFuelCell. Appl Catal B Environ 99(1–2):307–313
9. Lianos P (2011) Production of electricity and hydrogen by photocatalytic degradation of organic wastes in a photoelectrochemical cell: the concept of the photofuelcell: a review of a re-emerging research field. J Hazard Mater 185(2–3):575–590
10. Zhou K, Hu X-Y, Chen B-Y, Hsueh C-C, Zhang Q, Wang J, Lin Y-J, Chang C-T (2016) Synthesized TiO2/ZSM-5 composites used for the photocatalytic degradation of azo dye: intermediates, reaction pathway, mechanism and bio-toxicity. Appl Surf Sci 383:300–309
11. Han H-X, Shi C, Yuan L, Sheng G-P (2017) Enhancement of methyl orange degradation and power generation in a photoelectrocatalytic microbial fuel cell. Appl Energy 204:382–389
12. Neethu B, Ghangrekar MM (2017) Electricity generation through a photo sediment microbial fuel cell using algae at the cathode. Water Sci Technol 76:3269–3327. https://doi.org/10.2166/wst.2017.485
13. Lai Y-C, Liang C-M, Hsu S-C, Hsieh P-H, Hung C-H (2017) Polyphosphate metabolism by purple non-sulfur bacteria and its possible application on photo-microbial fuel cell. J Biosci Bioeng 123(6):722–730
14. Kim HW, Lee KS, Razzaq A, Lee SH, Grimes CA, In SI (2018) Photocoupled bioanode: a new approach for improved microbial fuel cell performance. Energ Technol 6(2):257–262
15. Ajayi FF, Kim K-Y, Chae K-J, Choi M-J, Kim S-Y, Chang I-S, Kim IS (2009) Study of hydrogen production in light assisted microbial electrolysis cell operated with dye sensitized solar cell. Int J Hydrog Energy 34(23):9297–9304
16. Chen Z, Ding H, Chen W, Li Y, Zhang G, Lu A, Li X (2012) Photoelectric catalytic properties of silicon solar cell used in microbial fuel cell system. Acta Phys Sin 61(24):000543–000547

17. Chae K-J, Choi M-J, Kim K-Y, Ajayi FF, Chang I-S, Kim IS (2009) A solar-powered microbial electrolysis cell with a platinum catalyst-free cathode to produce hydrogen. Environ Sci Technol 43(24):9525–9530

18. Wang H, Qian F, Wang G, Jiao Y, He Z, Li Y (2013) Self-biased solar-microbial device for sustainable hydrogen generation. ACS Nano 7(10):8728–8735

19. Yang X, Lu J, Zhu Y, Shen J, Zhang Z, Zhang J, Chen C, Li C (2011) Microbial fuel cell cathode with dendrimer encapsulated Pt nanoparticles as catalyst. J Power Sources 196(24):10611–10615

20. Neburchilov V, Mehta P, Hussain A, Wang H, Guiot SR, Tartakovsky B (2011) Microbial fuel cell operation on carbon monoxide: cathode catalyst selection. Int J Hydrog Energy 36(18):11929–11935

21. Oh S, Booki Min A, Logan BE (2004) Cathode performance as a factor in electricity generation in microbial fuel cells. Environ Sci Technol 38(18):4900

22. Cetinkaya AY, Ozdemir OK, Koroglu EO, Hasimoglu A, Ozkaya B (2015) The development of catalytic performance by coating Pt-Ni on CMI7000 membrane as a cathode of a microbial fuel cell. Bioresour Technol 195:188

23. Li Y, Lu A, Ding H, Jin S, Yan Y, Wang C, Zen C, Wang X (2009) Cr (VI) reduction at rutile-catalyzed cathode in microbial fuel cells. Electrochem Commun 11(7):1496–1499

24. Lu A, Li Y, Jin S, Ding H, Zeng C, Wang X, Wang C (2009) Microbial fuel cell equipped with a photocatalytic rutile-coated cathode. Energy Fuel 24(2):1184–1190

25. Ding H, Li Y, Lu A, Jin S, Quan C, Wang C, Wang X, Zeng C, Yan Y (2010) Photocatalytically improved azo dye reduction in a microbial fuel cell with rutile-cathode. Bioresour Technol 101(10):3500–3505

26. Lin Z-Q, Yuan S-J, Li W-W, Chen J-J, Sheng G-P, Yu H-Q (2017) Denitrification in an integrated bioelectro-photocatalytic system. Water Res 109:88–93

27. Qian F, Wang G, Li Y (2010) Solar-driven microbial photoelectrochemical cells with a nanowire photocathode. Nano Lett 10(11):4686–4691

28. Wang S, Yang X, Zhu Y, Su Y, Li C (2014) Solar-assisted dual chamber microbial fuel cell with a CuInS 2 photocathode. RSC Adv 4(45):23790–23796

29. Zang G-L, Sheng G-P, Shi C, Wang Y-K, Li W-W, Yu H-Q (2014) A bio-photoelectrochemical cell with a MoS 3-modified silicon nanowire photocathode for hydrogen and electricity production. Energy Environ Sci 7(9):3033–3039

30. Chen Q-Y, Liu J-S, Liu Y, Wang Y-H (2013) Hydrogen production on TiO2 nanorod arrays cathode coupling with bio-anode with additional electricity generation. J Power Sources 238:345–349

31. Brune A, Jeong G, Liddell PA, Sotomura T, Moore TA, Moore AL, Gust D (2004) Porphyrin-sensitized nanoparticulate TiO2 as the photoanode of a hybrid photoelectrochemical biofuel cell. Langmuir 20(19):8366–8371

32. Han L, Bai L, Zhu C, Wang Y, Dong S (2012) Improving the performance of a membraneless and mediatorless glucose–air biofuel cell with a TiO2 nanotube photoanode. Chem Commun 48(49):6103–6105

33. Du Y, Feng Y, Qu Y, Liu J, Ren N, Liu H (2014) Electricity generation and pollutant degradation using a novel biocathode coupled photoelectrochemical cell. Environ Sci Technol 48(13):7634–7641

34. Du Y, Qu Y, Zhou X, Feng Y (2015) Electricity generation by biocathode coupled photoelectrochemical cells. RSC Adv 5(32):25325–25328

35. Wang Q, Xu J, Ge Y, Zhang Y, Feng H, Cong Y (2016) Efficient nitrogen removal by simultaneous photoelectrocatalytic oxidation and electrochemically active biofilm denitrification. Electrochim Acta 198:165–173

36. Bond DR, Lovley DR (2003) Electricity production by Geobacter sulfurreducens attached to electrodes. Appl Environ Microbiol 69(3):1548–1555

37. Reguera G, McCarthy KD, Mehta T, Nicoll JS, Tuominen MT, Lovley DR (2005) Extracellular electron transfer via microbial nanowires. Nature 435(7045):1098

38. Nakamura R, Kai F, Okamoto A, Newton GJ, Hashimoto K (2009) Self-constructed electrically conductive bacterial networks. Angew Chem Int Ed 48(3):508–511
39. Borole AP, Reguera G, Ringeisen B, Wang Z-W, Feng Y, Kim BH (2011) Electroactive biofilms: current status and future research needs. Energy Environ Sci 4(12):4813–4834
40. Strycharz-Glaven SM, Snider RM, Guiseppi-Elie A, Tender LM (2011) On the electrical conductivity of microbial nanowires and biofilms. Energy Environ Sci 4(11):4366–4379
41. Qian F, Wang H, Ling Y, Wang G, Thelen MP, Li Y (2014) Photoenhanced electrochemical interaction between Shewanella and a hematite nanowire photoanode. Nano Lett 14(6):3688–3693
42. Li D-B, Cheng Y-Y, Li L-L, Li W-W, Huang Y-X, Pei D-N, Tong Z-H, Mu Y, Yu H-Q (2014) Light-driven microbial dissimilatory electron transfer to hematite. Phys Chem Chem Phys 16(42):23003–23011
43. Zhou D, Dong S, Ki D, Rittmann BE (2018) Photocatalytic-induced electron transfer via anode-respiring bacteria (ARB) at an anode that intimately couples ARB and a TiO2 photocatalyst. Chem Eng J 338:745–751
44. Ha PT, Moon H, Kim BH, Ng HY, Chang IS (2010) Determination of charge transfer resistance and capacitance of microbial fuel cell through a transient response analysis of cell voltage. Biosens Bioelectron 25(7):1629–1634
45. Lovley DR (2011) Live wires: direct extracellular electron exchange for bioenergy and the bioremediation of energy-related contamination. Energy Environ Sci 4(12):4896–4906
46. Malvankar NS, Lau J, Nevin KP, Franks AE, Tuominen MT, Lovley DR (2012) Electrical conductivity in a mixed-species biofilm. Appl Environ Microbiol 78(16):5967–5971
47. Li Y, Horsman M, Wang B, Wu N, Lan CQ (2008) Effects of nitrogen sources on cell growth and lipid accumulation of green alga Neochloris oleoabundans. Appl Microbiol Biotechnol 81(4):629–636
48. Ugwu CU, Aoyagi H, Uchiyama H (2008) Photobioreactors for mass cultivation of algae. Bioresour Technol 99(10):4021
49. Hannon M, Gimpel J, Tran M, Rasala B, Mayfield S (2010) Biofuels from algae: challenges and potential. Biofuels 1(5):763
50. Brennan L, Owende P (2010) Biofuels from microalgae—a review of technologies for production, processing, and extractions of biofuels and co-products. Renew Sustain Energy Rev 14(2):557–577
51. Baicha Z, Salar-García MJ, Ortiz-Martínez VM, Hernández-Fernández FJ, Ríos APDL, Labjar N, Lotfi E, Elmahi M (2016) A critical review on microalgae as an alternative source for bioenergy production: a promising low cost substrate for microbial fuel cells. Fuel Process Technol 154:104–116
52. Yang Z, Pei H, Hou Q, Jiang L, Zhang L, Nie C (2018) Algal biofilm-assisted microbial fuel cell to enhance domestic wastewater treatment: nutrient, organics removal and bioenergy production. Chem Eng J 332:277–285
53. Velasquez-Orta SB, Curtis TP, Logan BE (2009) Energy from algae using microbial fuel cells. Biotechnol Bioeng 103(6):1068–1076
54. Becker EW (2007) Micro-algae as a source of protein. Biotechnol Adv 25(2):207–210
55. Ventura MR, Castañón JIR (1998) The nutritive value of seaweed (Ulva lactuca) for goats. Small Rumin Res 29(3):325–327
56. Rashid N, Song W, Park J, Jin HF, Lee K (2009) Characteristics of hydrogen production by immobilized cyanobacterium Microcystis aeruginosa through cycles of photosynthesis and anaerobic incubation. J Ind Eng Chem 15(4):498–503
57. Jafary T, Rahimnejad M, Ghoreyshi AA, Najafpour G, Hghparast F, Ramli WDW (2013) Assessment of bioelectricity production in microbial fuel cells through series and parallel connections. Energy Convers Manag 75(5):256–262
58. Liu T, Rao L, Yuan Y, Zhuang L (2015) Bioelectricity generation in a microbial fuel cell with a self-sustainable photocathode. Sci World J 2015:864568

59. Hu X, Zhou J, Liu B (2016) Effect of algal species and light intensity on the performance of an air-lift-type microbial carbon capture cell with an algae-assisted cathode. RSC Adv 6(30):25094–25100
60. Nguyen HT, Kakarla R, Min B (2017) Algae cathode microbial fuel cells for electricity generation and nutrient removal from landfill leachate wastewater. Int J Hydrog Energy 42(49):29433–29442
61. Gouveia L, Neves C, Sebastião D, Nobre BP, Matos CT (2014) Effect of light on the production of bioelectricity and added-value microalgae biomass in a photosynthetic alga microbial fuel cell. Bioresour Technol 154:171–177
62. Wu Y-C, Wang Z-J, Zheng Y, Xiao Y, Yang Z-H, Zhao F (2014) Light intensity affects the performance of photo microbial fuel cells with Desmodesmus sp. A8 as cathodic microorganism. Appl Energy 116:86–90
63. Cui Y, Rashid N, Hu N, Rehman MSU, Han J-I (2014) Electricity generation and microalgae cultivation in microbial fuel cell using microalgae-enriched anode and bio-cathode. Energy Convers Manag 79:674–680
64. Rashid N, Cui YF, Rehman MSU, Han JI (2013) Enhanced electricity generation by using algae biomass and activated sludge in microbial fuel cell. Sci Total Environ 456–457(7):91
65. Khandelwal A, Vijay A, Dixit A, Chhabra M (2017) Microbial fuel cell powered by lipid extracted algae: a promising system for algal lipids and power generation. Bioresour Technol 247:520–527
66. Ryckebosch E, Muylaert K, Foubert I (2012) Optimization of an analytical procedure for extraction of lipids from microalgae. J Am Oil Chem Soc 89(2):189–198
67. Colombo A, Marzorati S, Lucchini G, Cristiani P, Pant D, Schievano A (2017) Assisting cultivation of photosynthetic microorganisms by microbial fuel cells to enhance nutrients recovery from wastewater. Bioresour Technol 237:240–248
68. Commault AS, Laczka O, Siboni N, Tamburic B, Crosswell JR, Seymour JR, Ralph PJ (2017) Electricity and biomass production in a bacteria- Chlorella based microbial fuel cell treating wastewater. J Power Sources 356:348–355

Chapter 10
Bioelectro-Fenton System
for Environmental Pollutant Degradation

Li-Juan Zhang and Hu-Chun Tao

10.1 Fenton Process

The reaction of Fenton was initially established by the British chemist Fenton [1, 2] who invented a solution of hydrogen peroxide and iron salts. The solution, named Fenton's reagent, was able to oxidize tartaric acid in the presence of iron. The mechanism of a classic Fenton reaction was interpreted by Haber and Weiss [3], in which the decomposition of H_2O_2 led to a hydroxyl ion and a hydroxyl radical and the oxidation of a ferrous iron to a ferric ion in aqueous acidic medium. The Fenton reaction occurs as follows (where k is the kinetic rate constant):

$$Fe^{2+} + H_2O_2 + H^+ \rightarrow Fe^{3+} + {}^{\bullet}OH + H_2O \quad k = 63.0\,M^{-1} \bullet s^{-1} \qquad (10.1)$$

Fenton reaction is an advanced oxidation process (AOP) that was firstly utilized to treat organic toxicants in the early 1960s. It was then widely applied for removal of various organic contaminants from wastewater. Hydroxyl radical (${}^{\bullet}OH$), the strongest known oxidant (E^{θ} (${}^{\bullet}OH/H_2O$) = +2.80 V) (vs. standard hydrogen electrode unless otherwise specified), second to fluorine (E^{θ} (F_2/HF) = +3.05 V), is responsible for the major ${}^{\bullet}OH$-R reaction to destroy the target compound (R) to smaller or less harmful fragments and even to complete mineralization [4, 5]. A hydroxyl radical has several interesting characteristics, including short life span, electrophilic behavior, high reactivity, non-selectivity, and so on. It can react in aqueous solution by four different pathways: (i) addition, (ii) hydrogen abstraction, (iii) electron transfer, and (iv) radical interaction. The classic Fenton reaction can be interpreted by a redox chain model (Eq. 10.1–10.18) based on Haber-Weiss's theory [6, 7].

L.-J. Zhang · H.-C. Tao (✉)
Key Laboratory for Heavy Metal Pollution Control and Reutilization, School of Environment and Energy, Peking University Shenzhen Graduate School, Shenzhen, China
e-mail: taohc@pkusz.edu.cn

Chain propagation:

$$^{\bullet}OH + Fe^{2+} + H^+ \rightarrow Fe^{3+} + H_2O \qquad k = 3.0 \times 10^8\,M^{-1} \cdot s^{-1} \qquad (10.2)$$

$$Fe^{3+} + H_2O_2 \rightarrow Fe^{2+} + HO_2^{\bullet} + H^+ \qquad k = 3.1 \times 10^{-3} \qquad (10.3)$$

$$Fe - OOH^{2+} \rightarrow Fe^{2+} + HO_2^{\bullet} \qquad k = 2.7 \times 10^{-3}\,s^{-1} \qquad (10.4)$$

$$^{\bullet}OH + H_2O_2 \rightarrow H_2O + HO_2^{\bullet} \qquad k = 3.3 \times 10^7\,M^{-1} \cdot s^{-1} \qquad (10.5)$$

$$Fe^{2+} + HO_2^{\bullet} \rightarrow Fe - OOH^{2+} \qquad k = 1.2 \times 10^6\,M^{-1} \cdot s^{-1} \qquad (10.6)$$

$$Fe^{2+} + O_2^- + H^+ \rightarrow Fe - OOH^{2+} \qquad k = 1.0 \times 10^7\,M^{-1} \cdot s^{-1} \qquad (10.7)$$

$$HO_2^{\bullet} + Fe^{3+} \rightarrow Fe^{2+} + O_2 + H^+ \qquad k < 1.0 \times 10^3\,M^{-1} \cdot s^{-1} \qquad (10.8)$$

$$HO_2^{\bullet} \rightarrow O_2^{\bullet -} + H^+ \qquad k = 27\ M^{-1} \cdot s^{-1} \qquad (10.9)$$

$$O_2^- + H^+ \rightarrow HO_2^{\bullet} \qquad k = 1.0 \times 10^{10}\,M^{-1} \cdot s^{-1} \qquad (10.10)$$

$$HO_2^{\bullet} + HO_2^{\bullet} \rightarrow H_2O_2 + O_2 \qquad k = 8.3 \times 10^5\,M^{-1} \cdot s^{-1} \qquad (10.11)$$

$$HO_2^{\bullet} + O_2^- + H^+ \rightarrow H_2O_2 + O_2 \qquad k = 9.7 \times 10^7\,M^{-1} \cdot s^{-1} \qquad (10.12)$$

$$HO_2^{\bullet} + {}^{\bullet}OH \rightarrow H_2O + O_2 \qquad k = 7.1 \times 10^9\,M^{-1} \cdot s^{-1} \qquad (10.13)$$

$$^{\bullet}OH + O_2^{\bullet} + H^+ \rightarrow H_2O + O_2 \qquad k = 1.0 \times 10^{10}\,M^{-1} \cdot s^{-1} \qquad (10.14)$$

$$^{\bullet}OH + {}^{\bullet}OH \rightarrow H_2O_2 \qquad k = 5.2 \times 10^9\,M^{-1} \cdot s^{-1} \qquad (10.15)$$

Chain termination:

$$Fe^{3+} + O_2^{\bullet -} \rightarrow Fe^{2+} + O_2 \qquad k = 5.0 \times 10^7\,M^{-1} \cdot s^{-1} \qquad (10.16)$$

$$Fe^{2+} + O_2^{\bullet -} + 2H^+ \rightarrow Fe^{3+} + H_2O_2 \qquad k = 1.0 \times 10^7\,M^{-1} \cdot s^{-1} \qquad (10.17)$$

$$R^{\bullet} + HO^- \rightarrow ROH \qquad\qquad - \qquad (10.18)$$
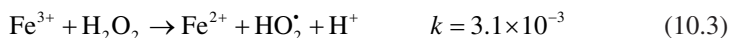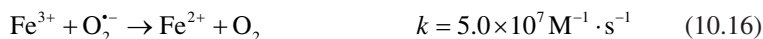
The redox chain model proposes the Fenton reaction as a complex process. The dominant oxidant of hydroxyl radical, as well as many other active species of hydrogen peroxide ($E^{\theta}(H_2O_2/H_2O)$ = +1.76 V) and hydroperoxyl ion ($E^{\theta}(HO_2^{\bullet}/H_2O)$ = +1.65 V) etc., plays synergic effects on the destruction of a wide variety of organic contaminants [4]. Unfortunately, the conventional Fenton reaction is

Table 10.1 Mechanisms of different Fenton-like processes

Process	Mechanism	Reference
UV/ photo-Fenton	Higher yield of hydroxyl radicals by the reaction of regenerated ferrous ions with H_2O_2	[8, 9]
	$Fe^{3+} + H_2O \xrightarrow{hv} Fe^{2+} + {}^{\bullet}OH + H^+$	
	$Fe^{2+} + H_2O_2 + H^+ \rightarrow Fe^{3+} + {}^{\bullet}OH + H_2O$	
US/ sono-Fenton	${}^{\bullet}OH$ and H_2O_2 production by both sonolysis of water in the cavities and Fenton reaction	[10]
	$H_2O \xrightarrow{{}^{\bullet)))}} H^{\bullet} + {}^{\bullet}OH$	
	${}^{\bullet}OH + {}^{\bullet}OH \rightarrow H_2O_2$	
	$H^{\bullet} + O_2 \rightarrow HO_2^{\bullet}$	
	$HO_2^{\bullet} + H^{\bullet} \rightarrow H_2O_2$	
	$HO_2^{\bullet} + HO_2^{\bullet} \rightarrow H_2O_2 + O_2$	
	$Fe^{2+} + H_2O_2 + H^+ \rightarrow Fe^{3+} + {}^{\bullet}OH + H_2O$	
MW-Fenton	Increased chemical reaction rate by a dielectric heating effect and decreased chemical activation energy by a thermal effect	[11]
Electro-Fenton	In situ generation of Fenton's reagent and ${}^{\bullet}OH$ at high levels	[12, 13]
	Anode: $2H_2O \rightarrow O_2 + 4H^+ + 4e^-$	
	Cathode: $O_2 + 2H^+ + 2e^- \rightarrow H_2O_2$ $Fe^{3+} + e^- \rightarrow Fe^{2+}$ $Fe^{2+} + H_2O_2 + H^+ \rightarrow Fe^{3+} + {}^{\bullet}OH + H_2O$	

plagued with high reagent dosage and accumulation of Fe^{3+} ions in practical applications. The generation of hydroxyl radical terminates as soon as all the initial Fe^{2+} ions are oxidized to Fe^{3+} ions. Thus, the Fenton reaction alone is not capable of further mineralizing the organic compounds upon iron depletion. Recent advances made in the improvement of conventional Fenton technology have led to various Fenton-like systems, such as electron-Fenton by applying external voltage, ultraviolet (UV)/photo-Fenton by exploiting light irradiation, ultrasonication (US)/sono-Fenton by introducing ultrasonication/sonolysis, and microwave (MW)-Fenton by employing radiation power. The mechanisms of each novel Fenton-like process are listed in Table 10.1. These processes are reported to be faster, more efficient, and sustainable in contaminant removal with higher ${}^{\bullet}OH$ yield and lower reagent dose. However, the cost-and-energy intensive operation, which often presents environmental challenges, holds back their industrial application.
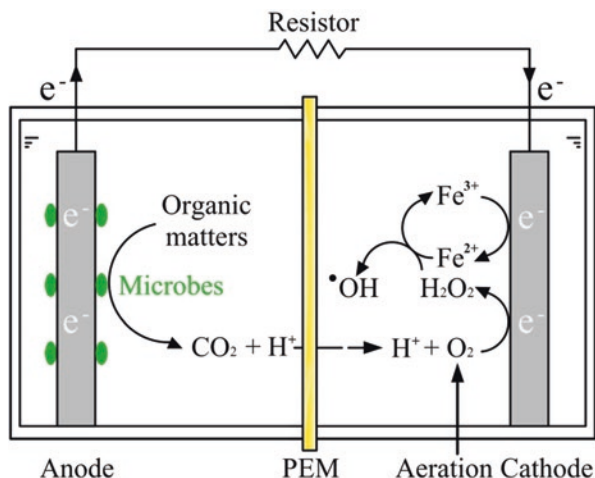
Fig. 10.1 Working principle of a bioelectro-Fenton system

10.2 Bioelectro-Fenton (BEF) System

The BEF system is an important innovation to combine the bioelectrochemical system (BES) and chemical Fenton. It was firstly proposed by X. P. Zhu and J. R. Ni (2009) for simultaneous electricity generation and *p*-nitrophenol degradation. As illustrated in Fig. 10.1, it is developed based on the electro-Fenton by replacing the traditional electricity input with the bioelectron flux. On the anode, the electrochemically active microbes act as biological catalysts to decompose the organic matters, releasing electrons and protons (Eq. 10.19). The electrons are transferred from the anode to the cathode via a closed electrical circuit. The protons migrate through a proton exchange membrane (PEM) between two chambers. On the cathode, continuous ˙OH formation (Eq. 10.1) is feasible by the reaction between in situ-produced H_2O_2 (Eq. 10.20) and regenerated Fe^{2+} (Eq. 10.21) under their respective favorable electrode potential [14]. The major electrode reactions are:

Anode:

$$CH_3COO^- + 4H_2O \rightarrow 2HCO_3^- + 9H^+ + 8e^- \quad E^\theta = -0.296 \text{ V}$$
$$\left(\text{Acetate as substrate,} \left[CH_3COO^- \right] \text{ and } \left[HCO_3^- \right] = 5.0 \text{ mM}, pH = 7.0 \right) \tag{10.19}$$

Cathode:

$$O_2 + 2H^+ + 2e^- \rightarrow H_2O_2 \quad E^\theta = +0.695 \text{ V}$$
$$\left(PO_2 = 0.2, \left[H_2O_2 \right] = 5.0 \text{ mM}, pH = 7.0 \right) \tag{10.20}$$
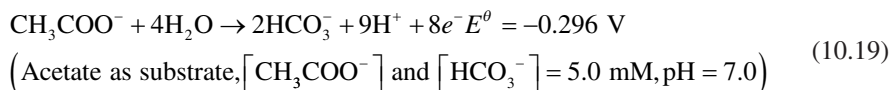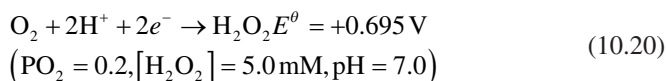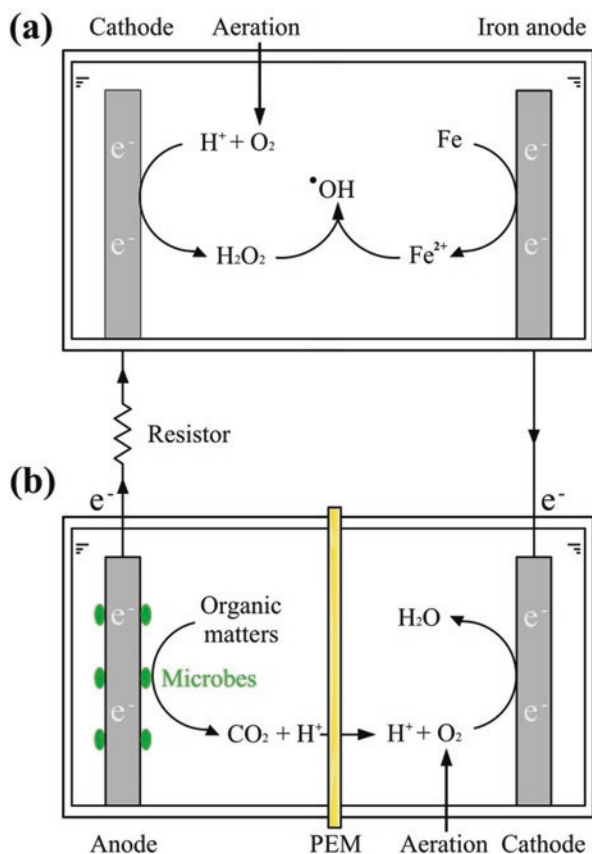
Fig. 10.2 Schematic diagram of (**a**) the electro-Fenton system powered by (**b**) an MFC

$$Fe^{3+} + e^- \rightarrow Fe^{2+} E^\theta = +0.771\,V$$
$$\left(\left[Fe^{3+} \right] = \left[Fe^{2+} \right], T = 303\,K, pH < 7.0 \right) \tag{10.21}$$
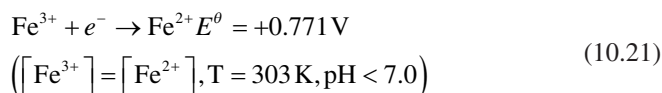
Microbial fuel cell (MFC), an expended concept of BES, can harvest electrical power from various organic wastes [15]. It has been well developed in powering miniature devices such as mini funs and a data collector in remote ocean [16, 17]. In the past decade, the power output of MFCs has increased to as high as several watts per surface area of electrode [18], making it practical to serve as a renewable power source for electro-Fenton. In an ex situ MFC-Fenton system (Fig. 10.2), which is operated in microbial electrolysis cell (MEC) mode, the Fenton reagent-producing electrode and electricity-generating bio-anode are arranged in separate reactors. With a sacrificial iron electrode, efficient and sustainable delivery of Fe^{2+} ions is achieved. The pH value can be self-maintained within an optimal range (pH = 2–3) [19]. An MFC turned out to be the most appropriate bioelectro-motive force to drive

the iron electrolysis for enhanced degradation of organic pollutants in an MEC. As a result, the combined BEF system dually benefits the environmental engineering: it simultaneously decomposes pollutants and produces electrical energy.

10.2.1 Iron Source

Iron source can significantly affect the performance of a BEF system. It acts as a catalyst to promote the generation of hydroxyl radical. As compiled in Table 10.2, various iron sources have been explored for the BEF process in both homogeneous and heterogeneous phases. In the homogeneous phase, the iron sources exist as soluble ferrous or ferric ions depending heavily on the acidic conditions, while in the heterogeneous phase, solid reagents serve as the iron sources in a broader range of pH values.

Direct dosing is the most usual way to add Fe^{2+} ions into BEF systems. An acidic environment is necessary not only to keep the Fe^{2+} dissolved but mostly to achieve the maximum effectiveness of $^\bullet OH$ generation (Eq. 10.1). Iron sulfate and chloride salts have been applied to dye degradation incorporated into in situ H_2O_2 production in MFC-Fenton systems [20]. The major challenges from the homogeneous iron sources include (1) difficult separation of dissolved iron from the other solutes in wastewater and (2) unable control of the iron concentration. For these reasons, Fernández de Dios et al. [21, 28] implemented a countermeasure by trapping ferric ions into alginate beads. The alginate beads were nontoxic and biodegradable, producing thermally irreversible and water-insoluble gels to be easily separated from the reaction solution. A desired concentration of iron could be achieved by dosing a fixed amount of iron alginate beads. More importantly, the porosity of alginate beads allowed H_2O_2 to well contact with the entrapped iron, supporting the catalyst in continuous and stable dye treatment. Iron phthalocyanine (FePc) resembles the active sites of catalytic catalysts to activate H_2O_2 and O_2 [22]. High-valent metal-oxo compounds, which are converted from a nucleophilic iron(III) peroxocomplex,

Table 10.2 Iron sources in bioelectro-Fenton systems

Iron source		Example	Reference
Homogeneous phase	Ferrous iron	$FeSO_4 \bullet 7H_2O$	[20]
	Ferric iron	$Fe_2(SO_4)_3$	[20–22]
		$FeCl_3$	
		FePc	
Heterogeneous phase	Zero-valent iron	Scrap iron	[18, 23]
		Iron plate	
	Iron oxide	Fe_2O_3	[24]
	Iron hydroxide	γ-FeOOH	[25]
	Natural iron ore	Limonite	[26, 27]
		Pyrrhotite	

participate as active species in the Fenton process. Effective degradation of recalcitrant pollutants can then be catalyzed by the active radicals. In order to prevent the loss of water-soluble FePc catalyst, some solid materials are employed to support FePc for easier separation and reuse. Ferric and ferrous irons, however, are limited in practical usage, substantially ascribed to the high cost and unavailability of these chemical sources.

Zero-valent iron is a cheaper alternative to in situ Fe^{2+} production. Fe^{2+} ions can be released from the heterogeneous metals into aqueous solution via acid corrosion ($Fe + 2H^+ \rightarrow Fe^{2+} + H_2$). Pure metals of both scrap iron and intact plate have been investigated for the treatment of wastewater containing toxic p-nitrophenol [18, 23]. Heterogeneous catalytic mechanism, which dominates the BEF reaction, can greatly speed up the transformation of Fe^{3+} and Fe^{2+} to improve the efficiency of Fenton reaction. It can also solve the problem of separating solid reagents from the aqueous phase, making it easier to remove and reuse the iron sources at the end of reaction. An unsolved issue herein is the strict pH conditions to release sufficient Fe^{2+} ions from insoluble iron sources in the strong oxidative Fenton process.

Iron oxide and hydroxide are often involved as adducts (e.g., ferryl ion FeO^{2+}) other than Fe^{2+} ions to initiate the classic Fenton reaction [25, 29]. These iron species were shown to be effective in catalyzing the degradation of target compounds at circumneutral pH, opening a promising perspective for BEF systems with less operational problems [30, 31]. The supply of iron source was supposed to be self-regulated by a composite cathode loaded with $Fe@Fe_2O_3$; a constant amount of ions was available all along the reaction period [32, 33]. More recently, natural iron ores such as limonite and pyrrhotite, which contain iron oxide of mixed valence, were applied as the cathodic heterogeneous Fenton catalysts toward the degradation of biorefractory organics [26, 27]. The natural ores are potentially more reactive because of the favorable surface-to-volume ratio of iron oxides, which exist as micrometric and/or nanometric particles. The excellent surface reactivity, structural stability, and flexible reusability can play a preeminent role in sorption and/or Fenton reactions. Compared with the most reported synthetic products, the natural iron ores are capable of promoting a simple, stable, and low-cost process in long-term runs, which stand a chance to push the BEF system to practice in due course.

10.2.2 Hydrogen Peroxide

In a BES, the spontaneous synthesis of H_2O_2 is feasible on cathode owing to the higher cathodic oxygen reduction potential than the anodic organic oxidation potential. Like with an MFC, exergonic reaction ($\Delta G^\theta = -431.83$ kJ mol^{-1} calculated for acetate from Eq. 10.19) occurs for H_2O_2 evolution without requirement for energy input [34]. With pKa = 11.62 at 25 °C, H_2O_2 is relatively stable in its protonated state under neutral pH conditions [35]. Thus, the dosing of H_2O_2 to the BES can be avoided upon in situ generation to make the BEF process sustainable, efficient, and cost-effective.

The surface morphology and electrical property of electrode have been widely considered important in mass production of H_2O_2. In year 2010, in situ generation of H_2O_2 was proved successful in a self-driven MFC-Fenton system using simple and inexpensive carbon-based materials [25]. A noble-metal-free composite cathode, which was composed of carbon nanotube (CNT) and γ-FeOOH, was fabricated to achieve two-electron reaction between O_2 and H_2O_2. The steady-state concentration and production rate of H_2O_2, however, were reported to be quite low at 3.24 mg L^{-1} and less than 0.1 mg L^{-1} h^{-1}. On a pure graphite rod as cathode, the H_2O_2 concentration could reach 78.85 mg L^{-1} with a production rate of 6.57 mg L^{-1} h^{-1} [36]. To realize a larger surface area and higher electrical conductivity, a three-dimensional electrode was fabricated with activated carbon particles. Many small regular or random graphite particles were stacked in an electric field, forming charged microelectrodes with strong electro-activity to catalyze H_2O_2 synthesis. The intensive micropores contributed to additional catalytic sites and high mass transfer toward cathodic oxygen reduction, leading to an increased H_2O_2 yield of 196.50 mg L^{-1} at a rate of 8.19 mg L^{-1} h^{-1} [37]. Extra power supply has a positive impact on H_2O_2 production. By applying a 0.40 V voltage to the three-dimensional particle cathode, i.e., in an MEC mode, a more than threefold increase in H_2O_2 concentration to 705.6 mg L^{-1} was achieved at a considerably high rate of 88.33 mg L^{-1} h^{-1} [38]. Transition metallic macrocycles, whose planar structure is able to increase the electron density of the central atom and improves the conductivity, have good redox abilities for oxygen reduction [39]. One latest study reported a composite electrode employing the FePc with aligned CNT on the surface of a stainless steel [40]. The significantly enhanced electrical properties of cathode resulted in an elevated number of hydroxyl radicals in the presence of FePc catalyst, which exhibits great potential for improving the overall efficiency of BEF system in the future. The bioelectrochemical activity of anode is also an important issue to be addressed in BESs that strives toward H_2O_2 synthesis. Based on in situ oxidation of microbial primary metabolites, e.g., H_2 which carries high electro-catalytic reactivity, electron transfer in electrochemically active bacteria (exo-electrogens) can be efficiently catalyzed by a metal-composite anode. The MFC has shown a substantial increase in current density from 1.0 to 1.5 mA cm^{-2} [41], giving rise to a remarkable potential for biomass-to-H_2O_2 conversion. In the MFC operating on a composite Pt/C anode with H_2-reducing microbes, the H_2O_2 concentration was greatly boosted to higher than 2000 mg L^{-1} during 12-h reaction period [42].

Sustainable energy for H_2O_2 generation is so far a key challenge confronting the MFC-Fenton system. A number of supplementary technologies have been explored to enhance the system sustainability. The H_2O_2 production rate of an MEC is one to two orders of magnitude higher than that of a conventional MFC [43], providing a promising alternative to meet the energy challenge in BESs. As mentioned above, the MEC has been found to be a suitable partner for Fenton process, though a small power supply (0.20–0.80 V) is required. In order to save the electrical energy spent on the MEC, an MFC stack was established as a renewable and powerful source [44]. With a single MFC as power supply, the maximum H_2O_2 production reached 73.17 mg L^{-1} h^{-1}. When more than three MFCs were stacked, the H_2O_2 was no lon-

ger the key limiting factor since its production was sufficient for the Fenton reaction. Development of sustainable energy has long been of great interest. Driven by the electrons harvested from the exo-electrogens and salinity-gradient between fresh- and seawater, a microbial reverse-electrodialysis electrolysis cell (MREC) was incorporated to the Fenton process [45]. The MREC-Fenton system combined a reverse-electrodialysis stack and an MEC, which replaced the electrical power source with renewable salinity-gradient energy. The energy consumption was lowered to only 25.93 kWh with per kilogram of total organic carbon (TOC) under optimal conditions, allowing efficient pollutant mineralization with enhanced H_2O_2 production at low cost. Recently, Ki et al. [46] evaluated the performance of primary sludge in anaerobic conversion to provide energy for H_2O_2 production. A maximum H_2O_2 concentration of 230 mg L^{-1} was achieved in the 6-h batch operation. This is the first demonstration of solid waste other than wastewater as substrates for H_2O_2 generation, which significantly advances the BES extracting energy from biomass-based materials in commercial and industrial viability.

In view of practical significance, though promising, more efforts should be made in H_2O_2-producing BES with a scaling-up design. The high internal resistance and extra operational cost of the membrane in a dual-chamber MFC hamper its wide application. A single-chamber MFC is possible to cut the capital cost of membranes. It can be stacked up and used as external power sources for MFC-Fenton to in situ produce H_2O_2. However, the distance between each unit might reduce the efficiency of assembled process. Moreover, implementation of continuous-flow operation is necessary to accelerate the industrial application.

10.3 Application of Bioelectro-Fenton System in Environmental Remediation

With its self-sufficient generation of energy and in situ formation of Fenton reagents, a BEF system overcomes the shortcomings of intensive reagent dosage, low reagent utilization efficiency, and excessive iron sludge production as well as extra energy input. The subsequent section is to review its widespread application in disposing biorefractory and/or toxic compounds, including various organic dyes, pharmaceuticals, agricultural and industrial chemicals, as well as many other emerging contaminants at low-energy consumption.

10.3.1 Decolorization

The highly concentrated organics in dye-containing wastewater can exert adverse impacts on environment and human health. Hence, it is important to treat the dye-containing wastewater below threshold limits before the discharge. Several physical

and/or chemical technologies, including flocculation, adsorption, and advanced oxidation, have been proposed to remove dyes from wastewater. However, most of these approaches are high in capital and operating cost. On the contrary, biological treatment is an economical alternative to remove chromaticity color of dyes, but the relatively slow rate of decolorization restricts its widespread utilization in practice.

Different energy-saving BESs have been proposed for the enhanced treatment of high-concentration dyes ranging from azo, anthraquinone, indigotine, polymeric, and triarylmethane to thiazine families. During the last decade and particularly since 2009, extensive efforts were invested to achieve coupling of anodic bio-oxidation of organic pollutants and cathodic Fenton degradation of dyes in an integrated and compact BEF system. Later, a BEF process driven by MFCs was implemented for complete Orange II decolorization [25]. The big advantage of such a hybrid system lies in the sustainable Fenton process driven by the bioelectrons from the biodegradable pollutants in wastewater. It thereafter offers an opportunity to harvest energy and valuable substances from abundant but largely abandoned wastes in water. However, the architecture and mechanism complex of two series technology requires more skillful manipulation and systematic investigation.

The organic dyes have different colors due to various functional groups. Reduction of dye chroma can be achieved by breaking down the bonds of the functional groups. As summarized in Table 10.3, the BEF reactions are efficient in decolorization of dyes upon $^{\bullet}$OH attack on the target chemical structures. Azo dye, featured for substituted aromatic rings joined by one or more N=N double bonds, is the most common organic dye that has been widely used in textile, leather, and plastic industries. Hence, tremendous research attentions have been focused on them. High decolorization efficiency of >80% is feasible for amaranth, methyl orange, and reactive black 5 within a shorter operating period of less than 2.0 h [20, 28, 47]. When the reaction time was extended to 6–30 h, a complete removal of chromaticity color was observed for Orange II and Orange G [25, 30, 45].

In contrast to the fast and easy decolorization, it is more difficult to mineralize the azo dyes because of their complicated structure and high molecular weight. Similar scenario occurred for other reported organic dyes of anthraquinone, triarylmethane, and thiazine containing one or more carbon rings. The cyclic carbons, especially the aromatic molecules with quite stable benzene rings, do not break apart easily to react with $^{\bullet}$OH radicals. Consequently, a higher concentration of residue TOC is usually detected in the treated effluent contaminated by the three abovementioned dyes. Extremely low decolorization efficiency of 19% was obtained for polycyclic aromatic dye of Poly R-478. In theory, the advanced oxidation of Poly R-478 compounds can be improved by increasing the concentration of Fenton's reagents. But too high a reactant concentration may trigger a scavenging effect of H_2O_2 and recombination of free radicals, which in reverse inhibit the overall decolorization process.

The BEF system is also a useful approach creating bioenergy from colored effluents treatment. The amount of power output is dependent on the types of dye contaminants and individual reactor design, ranging from several hundreds to near 1000 mW per square meter of electrode surface or dozens of milliwatt per cubic

Table 10.3 Dye removal and power output in bioelectro-Fenton systems

Target		Power output	Concentration level	Efficiency	Operating conditions	Reference
Anthraquinone	Acid blue 113	36 mW•m^{-3a}	100 mg•L^{-1}	71% decolorization in 90 min 29% TOC removal in 90 min	[Fe^{2+}] = 10 mg L^{-1} pH = 3.0 ER = 50 Ω O$_2$ purge	[48, 49]
Azo	Amaranth	28.3 W•m^{-3}	75 mg•L^{-1}	83% (with Fe^{2+}) or 76% (with Fe^{3+}) decolorization in 1.0 h	[Fe^{2+}] = 1.0 mM [Fe^{3+}] = 0.5 mM pH = 3.0 ER = 20 Ω O$_2$ purge	[20]
	Methyl orange	268 mW m^{-3}	5 mg•L^{-1}	87% decolorization in 2.0 h	[Fe@Fe$_2$O$_3$] = 0.5 g L^{-1} pH = 2.0 ER = 100 Ω Air sparge at 750 mL•min^{-1}	[47]
	Orange II	823 mW m^{-2b}	0.20 mM	100% decolorization in 30 h	[γ-FeOOH] = 1.0 g L^{-1} pH = 7.0 ER = 1000 Ω Air sparge at 100 mL•min^{-1}	[30]
		230 mW m^{-2}	0.10 mM	100% decolorization in 14 h 100% TOC removal in 43 h	[γ-FeOOH@CNT] = 66 g L^{-1} pH = 7.0 ER = 1000 Ω Air sparge at 100 mL•min^{-1}	[25]
		130 mW•m^{-2c}	2.0 mM	85% decolorization in 30 min	Iron plate pH = 3.0 ER = 1000 Ω 2.0 mM H$_2$O$_2$ addition	[19]

(continued)

Table 10.3 (continued)

Target		Power output	Concentration level	Efficiency	Operating conditions	Reference
Orange G		1.26 A m^{-2}	400 mg L^{-1}	100% decolorization in 6 h; 99.6% TOC removal in 6 h	[Fe^{2+}] = 10 mM; pH = 2.0; ER = 10 Ω; Air sparge at 8 mL•min^{-1}	[45]
Reactive black 5		1033 mV	50 mg L^{-1}	88% decolorization in 15 min	[Fe^{3+}@alginate gel bead] = 150 mg L^{-1}	[28]
Indigotine	Indigo carmine	1045 mV	20 mg L^{-1}	97% decolorization in 15 min	pH = 7.8; ER = 1000 Ω; Air sparge at 1.0 L•min^{-1}	
Polymeric	Poly R-478	1035 mV	80 mg L^{-1}	19% decolorization in 60 min		
Triarylmethane	Crystal violet	1.2 W m^{-3d}	10 mg L^{-1}	83% decolorization in 9 h; 82% TOC removal in 9 h	[Fe^{3+}@alginate gel beads] = 150 mg L^{-1}; pH = 2.0; ER = 1000 Ω; Air sparge at 2.0 L•min^{-1}	[21]
	Lissamine green B		10 mg L^{-1}	94% decolorization in 9 h; 70% TOC removal in 9 h		
Rhodamine B		307 mW m^{-2}	15 mg•L^{-1}	95% decolorization in 12 h; 90% TOC removal in 12 h	[Fe@Fe$_2$O$_3$] = 0.2 g L^{-1}; pH = 3.0; Short circuit; Air sparge at 300 mL•min^{-1}	[29]
Thiazine	Methylene blue	0.49 A m^{-2}	50 mg•L^{-1}	97% decolorization in 8 h; 99.6% TOC removal in 16 h	[Fe^{2+}] = 2.0 mM; pH = 3.0; ER = 5 Ω; Air sparge at 10 mL•min^{-1}	[44]

ER External resistance

[a]Power/current density is normalized by the working volume of cathode chamber (unless otherwise specified)

[b]Power/current density is normalized by the surface area of cathode electrode (unless otherwise specified)

[c]Power/current density is normalized by the surface area of anode electrode

[d]Power/current density is normalized by the working volume of anode chamber

meter of wastewater by the sample dyes. An enhanced voltage output of ~1000 mV can be harvested to self-sustain the combined system for highly efficient dye removal. In most applications, despite that the BEF system is economically and technically advantageous in treating high-strength dye-containing wastewater, the impacts of different operational and environmental factors have not yet been clearly demonstrated. Based on this fact, increasing interests are to be drawn in the research area of biotechnological dye treatment for more engineering practice.

10.3.2 PPCP/EDC Treatment

The discharge of emerging contaminants (ECs) into the environment has raised great concerns due to their negative effects on the ecosystem. Every day millions of gallons of treated and untreated sewage are discharged into the waterways of the world. This sewage contains various ECs of pharmaceuticals and personal care products (PPCPs) including prescription and over-the-counter (OTC) medications, nutraceuticals, detergents, perfumes, insect repellent, and steroids etc. Recent studies have shown that many of these compounds at low concentrations can have passive impacts on the endocrine systems of aquatic organisms. These compounds are collectively known as endocrine-disrupting compounds (EDCs). Other concerns regarding PPCPs include contamination of drinking water and development of antibiotic-resistant bacteria. Due to their stable and toxic nature, many of these compounds are resistant to the conventional biological treatment. Intensive research efforts have been undertaken in order to find effective methods to treat these compounds.

The BEF system has been confirmed as an integrated and sustainable approach for EC-contaminating wastewater treatment (Table 10.4). In the cathode chamber of a dual-chamber BEF reactor, electro-catalytic degradation of clinical medicines, e.g., paracetamol which is widely applied in pharmaceutical industries and daily life, was explored [50]. It was found that the stepwise degradation of paracetamol was completed via electrochemical reduction followed by chemical oxidation associated with Fenton processes (Fig. 10.3). The first-step Fenton reduction of paracetamol was coupled to the bioelectrochemical reactions on the anode. The second-step chemical Fenton process started with electrophilic attack by $^{\bullet}OH$ on the benzene ring of paracetamol and then underwent breakdown and hydroxylation of the benzene ring via $^{\bullet}OH$ addition and subsequent H_2O elimination, generating smaller dicarboxylic and carboxylic acids. For the sake of eliminating estrogenic risk, Xu's group [51, 52] evaluated the adsorption and oxidation removal of 17α-ethynyl estradiol (EE2) and 17β-estradiol (E2) by a cathodic BEF process. The production of H_2O_2 in the cathodic chamber and the adsorption by the electrode surface were responsible for the highest total removal of 81% E2 and 56% EE2 within 10 h. BEF was the dominant mechanism for the two estrogens' removal, and the majority of them were oxidized. The higher removal efficiency of E2 than EE2 was likely due to the presence of the ethynyl group in EE2 that stabilized the phe-

Table 10.4 PPCP/EDC oxidation and power output in bioelectro-Fenton systems

Target		Power output	Concentration level	Efficiency (%)	Operating conditions	Reference
Prescription and OTC medication	Paracetamol	2383 mA m^{-2}	10 mg L^{-1}	70% COD and 25% TOC removal in 9 h	[Fe^{2+}] = 5.0 mg L^{-1}	[50]
					pH = 2.0	
					ER = 20 Ω	
					Air sparge at 16.7 mL•min^{-1}	
Estrogen	17α-ethynyl estradiol (EE2)	4.35 W m^{-3a}	20 μg L^{-1}	56% removal in 10 h	[Fe@Fe$_2$O$_3$] = 0.2 g L^{-1}	[52]
					pH = 3.0	
	17β-estradiol (E2)		20 μg L^{-1}	81% removal in 10 h	ER = 1000 Ω	
					Air sparge at 100 mL•min^{-1}	
	Estrone (E1)	0.69 W m^{-3a}	1.0 mg L^{-1}	100% removal in 24 h	[Fe^{2+}] = 1.25 mM	[53]
Antimicrobial	Sulfamethazine			100% removal in 24 h	pH = 3.0	
	Triclocarban			99% removal in 24 h	ER = 10 Ω	
Industrial chemical	Bisphenol A			75% removal in 24 h	Air sparge	

^{a}Power/current density is normalized by the working volume of anode chamber
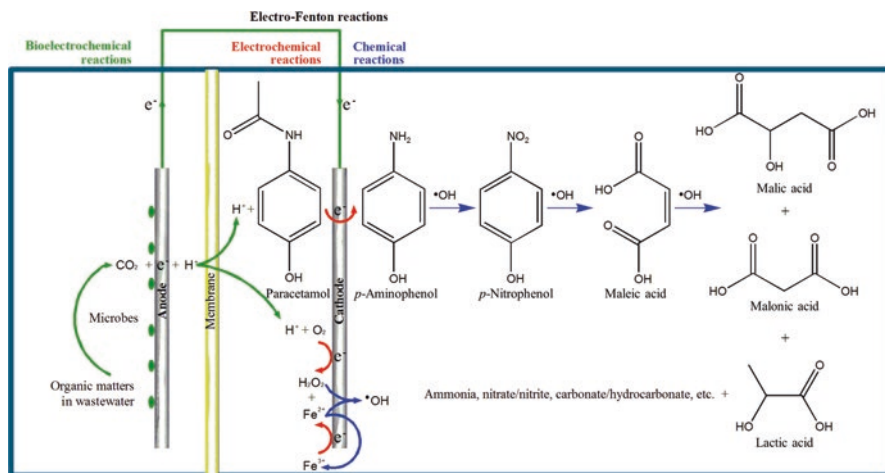
Fig. 10.3 Proposed pathway of cathodic paracetamol degradation. (Adapted from ref. [50], Copyright 2015, with permission from Elsevier)

nolic ring and resisted attack by reactive radicals. The enhanced removal of other EDCs includes estrone (E1), sulfamethazine, triclocarban, and bisphenol A, which is contributed by adsorption and $\bullet$OH destruction depending on the EC reactivity in Fenton reaction [53].

Even if the degradation of PPCPs leads to partial mineralization to CO_2 or other inorganic final products, previous studies realized the enhanced Fenton efficacies by employing real wastewater to feed the exo-electrogens for releasing bioelectrons. From an environmental point of view, the wastewater-powered BEF system for PPCP/EDC degradation has several advantages over conventional technologies. When comparing with anodic oxidation of ECs in common BESs, the cathodic BEF could prevent potential toxicity of these compounds and their metabolites to exo-electrogens on anode. When comparing traditional Fenton process with the BEF, the bioelectron fluxes extracted from the organic pollutants in wastewater facilitated the regeneration of Fe^{2+}; thus, no continuous addition of iron source was required. The cathodic degradation of ECs has been proved to be improved by the bioelectrons, and the power output of a BES driving the BEF can be improved by providing a lowered cathode potential with constant generation of hydrogen peroxide in reverse. A single-chamber MFC can be used as a power source for electron supply and aeration for this purpose. The average voltage output from Fenton-MFC was 20–30% higher than that without addition of Fenton reagents for paracetamol degradation, and a maximum power density of 4.35 W m^{-3} was produced with simultaneous EDC removal. Continuous flow of cathodic influent with pH control can further promote in situ H_2O_2 production and should be considered in future application of BEF systems.

10.3.3   Other Waste Treatment and Bioresource Production

To boost the practical engineering of BEF technique, integrated processes of both MFC-Fenton and MEC-Fenton have been applied to treat various industrial pollutants (Table 10.5), such as chemical materials of anilines, phenol, and *p*-nitrophenol, hazardous wastes of landfill leachate and arsenite, as well as complicated organics in swine, coking, medicinal herbs, and municipal wastewater [18, 33, 54]. The BEF systems show great advantages in applicability, capability, and sustainability.

The BEF system extends the practical merits of traditional BESs toward decontamination of biorefractory pollutants. The BOD_5/COD ratio, whose value is generally acceptable at 0.40, is an indicator of the biodegradability threshold from which solution can be considered environmentally remediable [55]. A BEF process has been considered as an efficiently alternative for advanced oxidation of organic pollutants. For instance, up to 96% of TOC could be removed from swine wastewater with a low BOD_5/COD ratio of 0.23. High NH_3-N removal efficiency of 88% and power output of 840 mA•m^{-2} were simultaneously obtained within 35 h [32]. As for an old-age landfill leachate with an even lower BOD_5/COD ratio of 0.18, 77% of color and 78% of COD were removed by a pyrrhotite-catalyzed cathode [27]. A longer operating period of 45 days was required for the lower bioavailable leachate, but the exemption from external voltage made the treatment cost-effective. Similar trend in TOC and COD removal was observed for sanitary landfill leachate in BES-driven electro-Fenton system using effluent from a partial nitrification-anaerobic ammonium oxidation process [56, 57]. In spite of the low organic matter biodegradability of mature landfill leachate, COD removal rates of 1077–1244 mg L^{-1} day^{-1} were reached with concomitant renewable electricity production of 43.5 ± 2.1 A m^{-3}. A considerable decrease in UV_{254} indicated the destruction of aromatic rings or unsaturated (double and triple) bonds in the molecular structure of leaching contaminants (e.g., humic and fulvic acids). When treating low-strength coking wastewater with an MFC-Fenton reactor, the TOC removal efficiency could be lowered to 54% in around 2 days [58]. Further, Tao et al. [26] tested the feasibility of natural limonite as an iron source to reduce the operating cost of BEF systems. Atmospheric oxygen and limonite powder were employed as the original materials of Fenton's reagents. Continuous addition of both H_2O_2 and Fe^{2+} was successfully avoided. Limonite mostly seemed like working as a heterogeneous catalyst, while the formation of H_2O_2 was basically constant due to a saturated concentration of dissolved oxygen. Following the pseudo-first-order kinetic, the *p*-nitrophenol degradation could achieve a high efficiency of 96% in 6 h under the optimal experimental conditions.

Arsenic contamination is of particular interest due to its high toxicity and mobility. The fate and transformation of arsenic in water should be regarded as one of the major environmental issues in the world. Wang et al. [31] demonstrated that the BEF system made it a potentially attractive method for the detoxification of As(III) from aqueous solution. In the presence of electrocogens, H_2O_2 was evolved through oxygen reduction to initiate the Fenton reactions with Fe^{2+} released from γ-FeOOH

Table 10.5 Degradation of biorefractory organics and power output in bioelectro-Fenton systems

Target		Power output	Concentration level	Efficiency	Operating conditions	Reference
Industrial pollutants	Anilines	–	4460 mg L^{-1}	93% TOC removal in 144 h	[Fe^{2+}] = 10 mM pH = 3.0 O$_2$ purge at 16 mL min^{-1}	[54]
	Phenol	1746 mW•m^{-2}	1.0 mM	77% TOC removal in 22 h	Sacrificial iron anode pH = 3.0 Short circuit Aeration	[18]
	p-Nitrophenol	238 mA•m^{-2}	0.25 mM	96% removal in 6 h	[Limonite] = 2.24 g L^{-1} pH = 2.0 ER = 20 Ω Air sparge at 100 mL min^{-1}	[26]
Real wastewater	Swine	840 mA•m^{-2}	[COD] = 1652 mg L^{-1}, [BOD$_5$/COD] = 0.23	77% COD removal 96% TOC removal	[Fe@Fe$_2$O$_3$] = 0.8 g L^{-1} pH = 3.0	[32]
			[NH$_3$-N] = 378 mg L^{-1}	88% NH$_3$-N removal in 35 h	ER = 100 Ω Air sparge at 300 mL min^{-1}	
	Coking	8.21 mA	[TOC] = 28.3 mg L^{-1}	54% TOC removal in 40 h	[γ-FeOOH] = 10 g L^{-1} pH = 7.0 Short circuit Air sparge at 200 mL min^{-1}	[58]
	Grease and oil Alcohol Propylene glycol Cellulose	60 mW m^{-2}	[COD] = 6183 mg L^{-1}, [BOD$_5$/COD] = 0.51	84% COD removal in 50 h	[Fe@Fe$_2$O$_3$] = 0.6 g L^{-1} pH = 3.0 ER = 100 Ω Air sparge at 300 mL min^{-1}	[33]

(continued)

Table 10.5 (continued)

Target		Power output	Concentration level	Efficiency	Operating conditions	Reference
Landfill leachate		4.2 W•m^{-3}	[COD] = 1022 mg L^{-1}, [BOD$_5$/COD] = 0.18	77% color and 78% COD removal in 45 days	Pyrrhotite pH = 2.7 ER = 500 Ω Air sparge	[27]
		44 A m^{-3a}	[COD] = 2401 mg L^{-1} [BOD$_5$/COD] <0.10	COD and TOC removal rate of 897 and 303 mg L^{-1} day^{-1} 51% UV$_{254}$ removal in 24 h	[Fe^{2+}] = 300 mg L^{-1} pH = 3.0 Air sparge	[56, 57]
Arsenite	As(III)	250 mV	1000 µg L^{-1}	96% removal in 72 h	[γ-FeOOH] = 26.7 g L^{-1} pH = 7.0 ER = 1000 Ω Air sparge at 100 mL min^{-1}	[31]
Organotin	Triphenyltin (TPT)	57 mW m^{-2b}	100 µM	78% removal 101 h	[Fe@Fe$_2$O$_3$] = 3.0 g L^{-1} pH = 3.0 ER = 2000 Ω Air sparge at 100 mL min^{-1}	[59]

[a]Power/current density is normalized by the working volume of anode chamber
[b]Power/current density is normalized by the surface area of anode electrode

under neutral pH conditions. As(III) was then quickly oxidized to less toxic species of As(V) by •OH radicals on the cathode. An apparent oxidation current efficiency was calculated to be as high as 73.1%. The γ-FeOOH dosage in the catholyte was an important factor governing the system performance. An increased dosage of γ-FeOOH could introduce more active sites onto the outer surface of iron mineral, on which the resulting As(V) product was bound as a surface complex. Another metal pollutant triphenyltin (TPT), as one of the most intensively used organotins, is widely used in industry and agriculture activities as plastic stabilizers, pesticides, and antifouling paints. With a general formula of $(C_6H_5)_3Sn$, TPT has caused serious environmental problems due to its high affinity for particulates and sediments in the aquatic system. It may enter the bodies of animals and plants via food chain, eventually threating the health of human beings. The effective degradation of TPT was carried out in a BEF system, in which a stepwise dephenylation of TPT might involve in Sn-C bonds breaking with final products of inorganic tin and CO_2 [59]. These BEF processes for metal detoxification may be practical in rural areas where electricity is limited for water and wastewater treatment on a small scale.

It is worth noting that, other than decontamination and detoxification, high concentrations of H_2O_2 and other high-value chemicals could be produced from certain BESs fed with real wastewater. For example, a considerably high concentration of 2.26 g L^{-1} H_2O_2 was produced from municipal wastewater. This amount of H_2O_2 could be potentially utilized for membrane cleaning in a membrane bioreactor for wastewater treatment [60]. The potential use of glucose as a simulated pollutant was evaluated to produce a high-value chemical of ethanol [61]. Simultaneous energy generation and bioethanol fermentation from glucose demonstrate an effective and economical way of wastewater treatment. Neither external electrical energy supply nor addition of H_2O_2 was required for the BEF system driven by an MFC. The maximum ethanol production rate was 11.52 g L^{-1} under an anaerobic condition, accompanied by a glucose removal efficiency of 68.81% and a maximum power density of 30.46 mW m^{-2} in a Fe@Fe_2O_3/graphite system. A scalable field study protocol and rationale for this advanced oxidation process, however, are necessary for practical engineering in real wastewater treatment plants.

10.4   Conclusions and Perspectives

As an advancing interdisciplinary field of microbiology, environmental engineering, electrochemistry, and material science, the BEF technology can offer a potentially sustainable solution to challenges in water pollution control. Its smaller footprint of integrated reactor allows a better adaption to the increasing energy and spatial constraint imposed by rapid urbanization. Hence, from an environmental point of view, the BEF system has several advantages in pollutant remediation:

1. Cost-effective. Compared with the Fenton process alone, the anodic extraction of electrons in a BEF system facilitates the cathodic regeneration of Fe^{2+} and in situ production of H_2O_2; thus no continuous addition of Fenton's reagents is required.
2. Energy saving. Compared with the chemical electro-Fenton process, the electrons are released spontaneously by the oxidation of organic matters at lowered anode potential (<0 V) other than water splitting driven by higher overpotential (>1.229 V).
3. Power output. The voltage output of BES can be improved by posing a stable cathode potential with constant generation of H_2O_2 in reverse. The voltage output from Fenton-assisted BES is higher than that without addition of Fenton reagents.
4. Wastewater treatment. Simultaneous wastewater treatment is applicable by coupling biodegradation of organic pollutants to AOP destruction of biorefractory or toxic contaminants.

Nevertheless, there still remains unresolved complexity of mechanism for the BEF process. Neither production yields of H_2O_2 nor complete mineralization of recalcitrant wastes has reached the utilization level of wastewater treatment plants. The enhanced capacity of high-quality effluent and net power production for a BEF system may ensure research interest continues to grow. And newly emerged technologies can hopefully shed light on the significance of existing BES-based hybrid systems and future outlook.

References

1. Fenton HJH (1876) On a new reaction of tartaric acid. Chem News 33:190
2. Fenton HJH (1894) Oxidation of tartaric acid in the presence of iron. J Chem Soc 65:899–910
3. Haber F, Weiss J (1934) The catalytic decomposition of hydrogen peroxide by iron salts. In: Proceedings of the Royal Society of London A: Mathematical, Physical and Engineering Sciences, vol 861. The Royal Society, pp 332–351
4. Bard AJ, Parsons R, Jordan J (1985) Standard potentials in aqueous solutions. Marcel Dekker, New York
5. Latimer WM (1952) Oxidation potentials, 2nd edn. Prentice-Hall, Englewood Cliffs
6. Walling C (1975) Fenton's reagent revisited. Acc Chem Res 8(4):125–131
7. Yuan BL, Wang HJ (2006) Principle and application of new wastewater treatment technologies. Chemical Industry Press, Beijing
8. Bauer R, Waldner G, Fallmann H, Hager S, Klare M, Krutzler T, Malato S, Maletzky P (1999) The photo-fenton reaction and the TiO2/UV process for waste water treatment – novel developments. Catal Today 53(1):131–144. https://doi.org/10.1016/s0920-5861(99)00108-x
9. Litter MI (1999) Heterogeneous photocatalysis – transition metal ions in photocatalytic systems. Appl Catal B-Environ 23(2–3):89–114. https://doi.org/10.1016/s0926-3373(99)00069-7
10. Wood RW, Loomis AL (1927) XXXVIII. The physical and biological effects of high-frequency sound-waves of great intensity. Lond Edinb Dublin Philos Mag J Sci 4(22):417–436
11. Caddick S (1995) Microwave-assisted organic-reactions. Tetrahedron 51(38):10403–10432. https://doi.org/10.1016/0040-4020(95)00662-r
12. Do JS, Chen CP (1994) In-situ oxidative-degradation of formaldehyde with hydrogen-peroxide electrogenerated on the modified graphites. J Appl Electrochem 24(9):936–942. https://doi.org/10.1007/bf00348785

13. Alverez-Gallegos A, Pletcher D (1999) The removal of low level organics via hydrogen per-oxide formed in a reticulated vitreous carbon cathode cell. Part 2: the removal of phenols and related compounds from aqueous effluents. Electrochim Acta 44(14):2483–2492. https://doi.org/10.1016/S0013-4686(98)00371-5
14. Logan BE (2008) Microbial fuel cells. Willey, Hoboken
15. Logan BE, Hamelers B, Rozendal RA, Schrroder U, Keller J, Freguia S, Aelterman P, Verstraete W, Rabaey K (2006) Microbial fuel cells: methodology and technology. Environ Sci Technol 40(17):5181–5192. https://doi.org/10.1021/es0605016
16. Reimers CE, Tender LM, Fertig S, Wang W (2001) Harvesting energy from the marine sediment-water interface. Environ Sci Technol 35(1):192–195. https://doi.org/10.1021/es001223s
17. Rezaei F, Richard TL, Brennan RA, Logan BE (2007) Substrate-enhanced microbial fuel cells for improved remote power generation from sediment-based systems. Environ Sci Technol 41(11):4053–4058. https://doi.org/10.1021/es070426e
18. Zhu X-P, Logan BE (2013) Using single-chamber microbial fuel cells as renewable power sources of electro-Fenton reactors for organic pollutant treatment. J Hazard Mater 252:198–203. https://doi.org/10.1016/j.jhazmat.2013.02.051
19. Liu X-W, Sun X-F, Li D-B, Li W-W, Huang Y-X, Sheng G-P, Yu H-Q (2012) Anodic Fenton process assisted by a microbial fuel cell for enhanced degradation of organic pollutants. Water Res 46(14):4371–4378. https://doi.org/10.1016/j.watres.2012.05.044
20. Fu L, You S-J, Zhang G-Q, Yang F-L, Fang X-H (2010) Degradation of azo dyes using in-situ Fenton reaction incorporated into H_2O_2-producing microbial fuel cell. Chem Eng J 160(1):164–169. https://doi.org/10.1016/j.cej.2010.03.032
21. Fernández de Dios MÁ, del Campo AG, Fernández FJ, Rodrigo M, Pazos M, Sanromán MÁ (2013) Bacterial–fungal interactions enhance power generation in microbial fuel cells and drive dye decolourisation by an ex situ and in situ electro-Fenton process. Bioresour Technol 148:39–46. https://doi.org/10.1016/j.biortech.2013.08.084
22. Yuan G-E, Li Y-B, Lv J-B, Zhang G-Q, Yang F-L (2017) Integration of microbial fuel cell and catalytic oxidation reactor with iron phthalocyanine catalyst for Congo red degradation. Biochem Eng J 120:118–124. https://doi.org/10.1016/j.bej.2017.01.005
23. Zhu X-P, Ni J-R (2009) Simultaneous processes of electricity generation and p-nitrophenol degradation in a microbial fuel cell. Electrochem Commun 11(2):274–277. https://doi.org/10.1016/j.elecom.2008.11.023
24. Zhuang L, Zhou S-G, Li Y-T, Liu T-L, Huang D-Y (2010) In situ Fenton-enhanced cathodic reaction for sustainable increased electricity generation in microbial fuel cells. J Power Sources 195(5):1379–1382. https://doi.org/10.1016/j.jpowsour.2009.09.011
25. Feng C-H, Li F-B, Mai H-J, Li X-Z (2010) Bio-electro-Fenton process driven by microbial fuel cell for wastewater treatment. Environ Sci Technol 44(5):1875–1880. https://doi.org/10.1021/es9032925
26. Tao H-C, Wei X-Y, Zhang L-J, Lei T, Xu N (2013) Degradation of p-nitrophenol in a BES-Fenton system based on limonite. J Hazard Mater 254:236–241. https://doi.org/10.1016/j.jhazmat.2013.03.061
27. Li Y, Lu A-H, Ding H-R, Wang X, Wang C-Q, Zeng C-P, Yan Y-H (2010) Microbial fuel cells using natural pyrrhotite as the cathodic heterogeneous Fenton catalyst towards the degradation of biorefractory organics in landfill leachate. Electrochem Commun 12(7):944–947. https://doi.org/10.1016/j.elecom.2010.04.027
28. Fernandez de Dios MA, Iglesias O, Bocos E, Pazos M, Sanroman MA (2014) Application of benthonic microbial fuel cells and electro-Fenton process to dye decolourisation. J Ind Eng Chem 20(5):3754–3760. https://doi.org/10.1016/j.jiec.2013.12.075
29. Zhuang L, Zhou S-G, Yuan Y, Liu M, Wang Y-D (2010) A novel bioelectro-Fenton system for coupling anodic COD removal with cathodic dye degradation. Chem Eng J 163(1):160–163. https://doi.org/10.1016/j.cej.2010.07.039

30. Feng C-H, Li F-B, Liu H-Y, Lang X-M, Fan S-S (2010) A dual-chamber microbial fuel cell with conductive film-modified anode and cathode and its application for the neutral electro-Fenton process. Electrochim Acta 55(6):2048–2054. https://doi.org/10.1016/j.electacta.2009.11.033

31. Wang X-Q, Liu C-P, Yuan Y, Li F-B (2014) Arsenite oxidation and removal driven by a bio-electro-Fenton process under neutral pH conditions. J Hazard Mater 275:200–209. https://doi.org/10.1016/j.jhazmat.2014.05.003

32. Xu N, Zhou S-G, Yuan Y, Qin H, Zheng Y, Shu C-W (2011) Coupling of anodic biooxidation and cathodic bioelectro-Fenton for enhanced swine wastewater treatment. Bioresour Technol 102(17):7777–7783. https://doi.org/10.1016/j.biortech.2011.06.030

33. Birjandi N, Younesi H, Ghoreyshi AA, Rahimnejad M (2016) Electricity generation through degradation of organic matters in medicinal herbs wastewater using bio-electro-Fenton system. J Environ Manag 180:390–400. https://doi.org/10.1016/j.jenvman.2016.05.073

34. Thauer RK, Jungermann K, Decker K (1977) Energy conservation in chemotrophic anaerobic bacteria. Bacteriol Rev 41(1):100–180

35. Qiang ZM, Chang JH, Huang CP (2002) Electrochemical generation of hydrogen peroxide from dissolved oxygen in acidic solutions. Water Res 36(1):85–94. https://doi.org/10.1016/s0043-1354(01)00235-4

36. Fu L, You S-J, Yang F-L, Gao M-M, Fang X-H, Zhang G-Q (2010) Synthesis of hydrogen peroxide in microbial fuel cell. J Chem Technol Biotechnol 85(5):715–719. https://doi.org/10.1002/jctb.2367

37. Chen J-Y, Li N, Zhao L (2014) Three-dimensional electrode microbial fuel cell for hydrogen peroxide synthesis coupled to wastewater treatment. J Power Sources 254:316–322. https://doi.org/10.1016/j.jpowsour.2013.12.114

38. Chen J-Y, Zhao L, Li N, Liu H (2015) A microbial fuel cell with the three-dimensional electrode applied an external voltage for synthesis of hydrogen peroxide from organic matter. J Power Sources 287:291–296. https://doi.org/10.1016/j.jpowsour.2015.04.071

39. Zagal JH, Bedioui F, Dodelet J-P (2006) N4-macrocyclic metal complexes. Springer, New York

40. Wang Y-T, Wang R-S (2017) A bio-electro-Fenton system employing the composite FePc/CNT/SS316 cathode. Materials 10(2). https://doi.org/10.3390/ma10020169

41. Schroder U, Niessen J, Scholz F (2003) A generation of microbial fuel cells with current outputs boosted by more than one order of magnitude. Angew Chem Int Ed 42(25):2880–2883. https://doi.org/10.1002/anie.200350918

42. You S-J, Wang J-Y, Ren N-Q, Wang X-H, Zhang J-N (2010) Sustainable conversion of glucose into hydrogen peroxide in a solid polymer electrolyte microbial fuel cell. ChemSusChem 3(3):334–338. https://doi.org/10.1002/cssc.200900245

43. Rozendal RA, Leone E, Keller J, Rabaey K (2009) Efficient hydrogen peroxide generation from organic matter in a bioelectrochemical system. Electrochem Commun 11(9):1752–1755. https://doi.org/10.1016/j.elecom.2009.07.008

44. Zhang Y-F, Wang Y, Angelidaki I (2015) Alternate switching between microbial fuel cell and microbial electrolysis cell operation as a new method to control H_2O_2 level in bioelectro-Fenton system. J Power Sources 291:108–116. https://doi.org/10.1016/j.jpowsour.2015.05.020

45. Li X-H, Jin X-D, Zhao N-N, Angelidaki I, Zhang Y-F (2017) Novel bio-electro-Fenton technology for azo dye wastewater treatment using microbial reverse-electrodialysis electrolysis cell. Bioresour Technol 228:322–329. https://doi.org/10.1016/j.biortech.2016.12.114

46. Ki D, Popat SC, Rittmann BE, Torres CI (2017) H2O2 production in microbial electrochemical cells fed with primary sludge. Environ Sci Technol 51(11):6139–6145. https://doi.org/10.1021/acs.est.7b00174

47. Ling T, Huang B, Zhao M-X, Yan Q, Shen W (2016) Repeated oxidative degradation of methyl orange through bio-electro-Fenton in bioelectrochemical system (BES). Bioresour Technol 203:89–95. https://doi.org/10.1016/j.biortech.2015.12.031

48. Asghar A, Salihoudin A, Raman AAA, Daud WMAW (2017) Cathode modification to enhance the performance of in-situ Fenton oxidation in microbial fuel cells. Environ Prog Sustain 36(2):382–393. https://doi.org/10.1002/ep.12468

49. Asghar A, Raman AAA, Daud AMAW (2017) In situ production of hydrogen peroxide in a microbial fuel cell for recalcitrant wastewater treatment. J Chem Technol Biotechnol 92(7):1825–1840. https://doi.org/10.1002/jctb.5192

50. Zhang L-J, Yin X-J, Li SFY (2015) Bio-electrochemical degradation of paracetamol in a microbial fuel cell-Fenton system. Chem Eng J 276:185–192. https://doi.org/10.1016/j.cej.2015.04.065

51. Xu N, Zeng Y-Q, Li J, Zhang Y-Y, Sun W-L (2015) Removal of 17 beta-estrodial in a bio-electro-Fenton system: contribution of oxidation and generation of hydroxyl radicals with the Fenton reaction and carbon felt cathode. RSC Adv 5(70):56832–56840. https://doi.org/10.1039/c5ra08053c

52. Xu N, Zhang Y-Y, Tao H-C, Zhou S-G, Zeng Y-Q (2013) Bio-electro-Fenton system for enhanced estrogens degradation. Bioresour Technol 138:136–140. https://doi.org/10.1016/j.biortech.2013.03.157

53. Wang Y-H, Feng C-J, Li Y, Gao J-Y, Yu C-P (2017) Enhancement of emerging contaminants removal using Fenton reaction driven by H2O2-producing microbial fuel cells. Chem Eng J 307:679–686. https://doi.org/10.1016/j.cej.2016.08.094

54. Li X-H, Jin X-D, Zhao N-N, Angelidaki I, Zhang Y-F (2017) Efficient treatment of aniline containing wastewater in bipolar membrane microbial electrolysis cell-Fenton system. Water Res 119:67–72. https://doi.org/10.1016/j.watres.2017.04.047

55. Olvera-Vargas H, Cocerva T, Oturan N, Buisson D, Oturan MA (2016) Bioelectro-Fenton: a sustainable integrated process for removal of organic pollutants from water: application to mineralization of metoprolol. J Hazard Mater 319:13–23. https://doi.org/10.1016/j.jhazmat.2015.12.010

56. Hassan M, Pous N, Xie B, Colprim J, Balaguer MD, Puig S (2017) Employing microbial electrochemical technology-driven electro-Fenton oxidation for the removal of recalcitrant organics from sanitary landfill leachate. Bioresour Technol 243:949–956. https://doi.org/10.1016/j.biortech.2017.07.042

57. Hassan M, Pous N, Xie B, Colprim J, Balaguer MD, Puig S (2017) Influence of iron species on integrated microbial fuel cell and electro-Fenton process treating landfill leachate. Chem Eng J 328:57–65. https://doi.org/10.1016/j.cej.2017.07.025

58. Wu B-G, Feng C-H, Huang L-Q, Lv Z-S, Xie D-H, Wei C-H (2014) Anode-biofilm electron transfer behavior and wastewater treatment under different operational modes of bioelectrochemical system. Bioresour Technol 157:305–309. https://doi.org/10.1016/j.biortech.2014.01.088

59. Yong X-Y, Gu D-Y, Wu Y-D, Yan Z-Y, Zhou J, Wu X-Y, Wei P, Jia H-H, Zheng T, Yong Y-C (2017) Bio-Electron-Fenton (BEF) process driven by microbial fuel cells for triphenyltin chloride (TPTC) degradation. J Hazard Mater 324:178–183. https://doi.org/10.1016/j.jhazmat.2016.10.047

60. Modin O, Fukushi K (2013) Production of high concentrations of H2O2 in a bioelectrochemical reactor fed with real municipal wastewater. Environ Technol 34(19):2737–2742. https://doi.org/10.1080/09593330.2013.788041

61. Birjandi N, Younesi H, Ghoreyshi AA, Rahimnejad M (2016) Electricity generation, ethanol fermentation and enhanced glucose degradation in a bio-electro-Fenton system driven by a microbial fuel cell. J Chem Technol Biotechnol 91(6):1868–1876. https://doi.org/10.1002/jctb.4780

Chapter 11
Bioelectroremediation of Sediments

Yonggang Yang and Meiying Xu

11.1 Sediment Bioremediation and Sediment Bioelectrochemical Systems (SBESs)

Contamination of the aquatic environment has become a worldwide problem, especially for the developing countries due to the fast urbanization process and unsustainable industry development. Water contamination causes many risks for human health, ecological balance, and society sustainability. Therefore, remediation of the contaminated aquatic environment has been paid unprecedented attention in the last decade.

Sediment was considered to be the most important and challenging component in aquatic environment remediation because plenty of contaminants from the water, land surface, and atmosphere eventually accumulate in aquatic sediments via various atmospheric or geochemical processes (e.g., surface runoff, adsorption, and precipitation) [1, 2]. Moreover, sediment accumulates most of the refractory contaminants such as polycyclic aromatic hydrocarbons (PAHs), polychlorinated biphenyls (PCBs), brominated flame retardants (BFRs), and heavy metals [3]. After being accumulated in sediment, those contaminants are then continually and long-termly released to the water body. Therefore, sediment is not only a sink but also a source of the contaminants in aquatic environment [1, 3].

Y. Yang
Guangdong Provincial Key Laboratory of Microbial Culture Collection and Application, Guangdong Institute of Microbiology, Guangzhou, China

M. Xu (✉)
Guangdong Provincial Key Laboratory of Microbial Culture Collection and Application, Guangdong Institute of Microbiology, Guangzhou, China

Guangdong Open Laboratory of Applied Microbiology, Guangzhou, China

State Key Laboratory of Applied Microbiology Southern China, Guangzhou, China
e-mail: xumy@gdim.cn

Apart from the contaminants, sediments usually contain high concentration of organics and biomass generated from hydrobiological or microbial metabolisms [4, 5]. It has been reported that marine sediments can accumulate 2.52–28.8 mg C m^{-2} of organic carbon every day, and that for lake sediments could be about 21.6 mg m^{-2} day^{-1} [6]. The typical energy density of such sediments is 6.1×10^4 J/L (based on a complete oxidation of 2.0% organic carbon content) [5]. Therefore, sediment is also considered as a huge energy reserve if the chemical energy stored in sediments could be extracted.

Many physicochemical methods such as dredging, capping, aeration, or electrochemical degradation have been practically used in sediment remediation [1, 6]. However, those methods are not suitable for wide and in situ applications because of their high energy consumption, cost inefficiency, and secondary contamination [1, 6]. Bioremediation refers to technologies that stimulate environmental cleanup by regulating or enhancing the contaminant degradation by microbes, plant, or protozoon [2]. In sediments, microbial metabolism is the key driving force in contaminant degradation. However, biodegradation efficiency in sediments is usually lower than that in aerobic and aquatic environments. One of the most important reasons is the low availability of electron acceptors in sediments [1, 3, 7]. Replenishing electron acceptors (e.g., nitrate, oxygen, Fe oxides) in sediment bioremediation has been demonstrated to be an effective method for the bioremediation of various contaminated sediments [8, 9]. In the past two decades, electrodes in bioelectrochemical systems (BESs) have been intensively used as artificial electron acceptors to stimulate biodegradation [2, 4, 10].

BESs deployed in sediments were termed as sediment BESs (SBESs). Sediment microbial fuel cells (SMFCs) are the mostly used SBESs that can simultaneously stimulate sediment remediation and harvest bioelectric energy from sediments. In 2001 and 2002, Tender and his research group reported the first SMFCs deployed in benthic sediments in situ and ex situ [4, 10]. To date, over 100 researches on SBESs have been published, and about 1/3 focused on sediment remediation. Figure 11.1 showed a brief profile of those publications. It can be seen that SBESs have been paid increasing interests in the past decade. Both the power output and system volume increased in recent years.

SBESs have been operated in sediments from various environments including rivers, lakes, marines, and salt marshes, and various contaminants have been tested in SBESs. Almost all studies showed enhanced contaminant degradation efficiency. In addition to sediment remediation, many reports have successfully managed to use the electricity generated by SBES to power electronics (e.g., ultrasonic receiver, cell phone, environmental sensors) in laboratory or practical environments [11–14]. Several reports have shown that enlarged or field-deployed SBESs could function as self-sustainable, long-term devices for simultaneous bioremediation and power supply, especially in remote or contaminated aquatic environments [5, 15]. Therefore, SBESs hold the possibility to be the first applicable BES in the near future. On the other hand, the evaluation and optimization of SBES are more challenging compared with other aquatic BESs due to the heterogeneity and low matter diffusion efficiency in sediments, slow bacterial metabolism, as well as benthos activities and
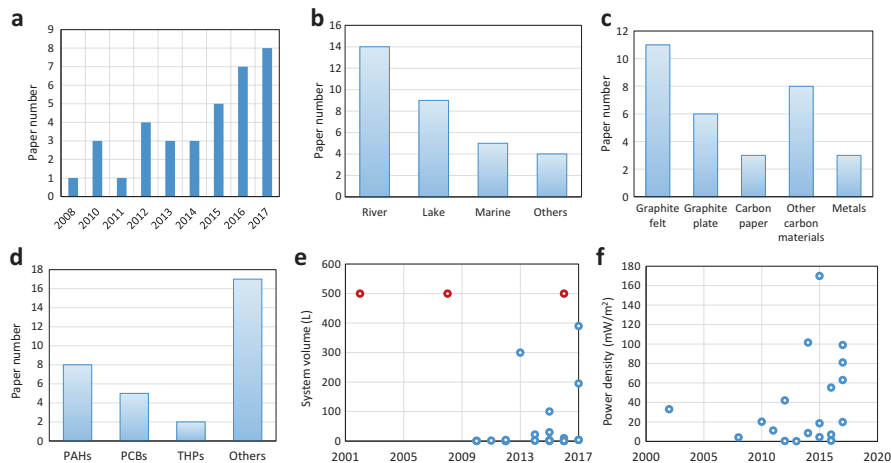
Fig. 11.1 The brief information of SBESs for sediment bioremediation. (**a**) Published papers in the last 10 years; (**b**) the sediments sources of the SBESs; (**c**) anode materials; (**d**) target contaminants of the SBES; (**e**) system volume (the red circles indicate in situ application); (**f**) power densities

some other unpredictable factors in field application. In this section, the structures, biogeochemical mechanisms, contaminant-degrading capacities, microbial ecological properties, and future challenges of SBESs will be introduced and discussed.

11.2   Structures and Principles of Different SBESs

In addition to SMFCs, several new types of SBESs including bioelectrochemical sediment caps (BSCs) [16, 17], plant-sediment microbial fuel cells (PSMFC), and bioelectro-snorkels (BSKs) have been developed recently for sediment remediation [18–21] (Fig. 11.2). Despite different structures and biogeochemical processes, microbial metabolisms and extracellular electron transfer (EET) in sediment are the core driven force in all of those SBESs.

11.2.1   Sediment Microbial Fuel Cells (SMFC)

Typically, the anode of SMFCs is embedded in anaerobic sediments, and the cathode is located in aerobic overlying water. Many microorganisms in the sediment can degrade contaminants and donate electrons to anode by their extracellular electron transfer (EET) pathway. The sediment-water interface can function as a natural layer to separate the anodic and cathodic environments. Driven by the natural

Fig. 11.2 Different types
of SBESs
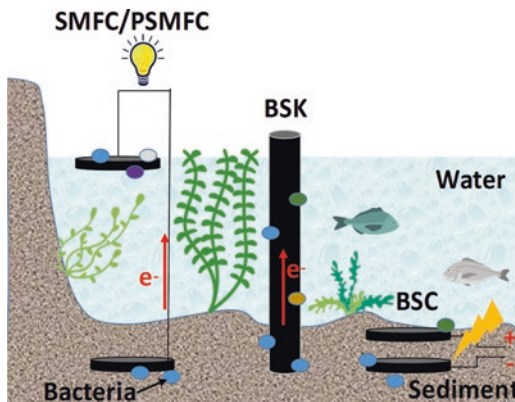
potential gradient between sediment and overlying water, the anodic electrons can flow via a conductive metal wire to form H_2O with protons and oxygen at the cathode. It can be seen that the outer frame and membrane, the most valuable components in a MES, are not needed in SMFCs. Therefore, SBES assembly is simpler and cheaper relative to most aquatic MESs [22].

SMFCs are expected to be long-term bioremediation or power supply devices in aquatic environments. Many factors such as microbial redox activities, sulfites, heavy metals, and high salinity would cause corrosion of the electrodes or metal wires. Therefore, SMFC materials should be corrosion resistant. To date, most studies used various carbon-based electrodes (e.g., carbon plate, felt, cloth, mesh, or brush) which have been proven corrosion resistant and suitable for long-term operation, and their power density are comparable to metal electrodes [1, 6]. Stainless steel has been used as SMFC electrodes in several reports but was still found to be corroded in long-term operation [23]. High-cost catalysts (e.g., Pt, copper, and iron) are usually unfeasible as the high concentration of sulfides or other toxic compounds accumulated on SMFC electrode surface in practical environments [1]. In addition to electrodes, the connection wires, especially the connecting knots of the wires and electrodes, should be also carefully protected. Holmes used watertight #20 AWG marine-grade wire screwed into holes in graphite electrodes, and the holes were then filled with silver epoxy and sealed with marine epoxy, by which SMFCs were operated over 7 months under both experimental and in situ marine sediments without corrosion [24]. Similar connection method was also adopted in a SMFC deployed in heavily contaminated freshwater sediments and sustained stable electricity generation for over 2 years [5]. Titanium wire was also frequently used. However, a coating layer (e.g., epoxy, polytetrafluorethylene (PTFE)) should be used to prevent corrosion of titanium wire and electron loss to the surrounding water [25, 26]. It should be noted that the concerns on corrosion of the electrode and wires are not only related to SMFCs but also to other SBESs.

11.2.2 Sediment Microbial Fuel Cell Stacks

For a single SMFC deployed in natural environments, the theoretically maximum voltage is ~1.0 V, while the practical values usually ranged from 0.3 to 0.8 V, which is much lower than the requirement of commercial monitors or electronics [27]. Like chemical fuel cells or batteries, MFCs can be operated as single unit or as parallel/serially stacked units for higher power output [28]. Stacking SMFC units in parallel can increase the current and in series can increase the voltage output. Currently, little is known on the SMFC stack. In fact, the parallel-stacked SMFC means an enlarged electrode area which will decrease the internal resistance and increase the voltage to some extent. Therefore, stacking provides a simple method to elevate the power level of SMFCs. A noteworthy drawback of serial SMFC stacks is that the electrode reversal and charge crossover will cause significant potential loss of the stack [28, 29]. On the other hand, the stacked SMFC means a larger effective area in terms of the electrode-dependent remediation [30]. The stack model can increase the electrode potential and electron transfer rate near the electrode; therefore, higher remediation efficiency can be expected. In support, a recent report showed higher substrate-consuming rate in parallel MFC stacks than that in serial MFC stacks [31]. However, before the field application of SMFCs stack, many questions such as the distance between anodes or cathodes, the area ratio of cathode to anode, and the optimal unit numbers remain to be investigated.

11.2.3 Plant-Sediment Microbial Fuel Cells (PSMFC)

In some cases, low availability and low diffusion efficiency of electron donor in sediments are important limits for the long-time performance of SMFCs. Aquatic plants were considered as a proper method to address those limits, as the plant roots located in sediments could directly generate rhizodeposits (including sugars, organic acids, polymeric carbohydrates, enzymes, and dead cell material) which subsequently serve as electron donors for the anodic bacteria [32]. Moreover, the plants could also be grown in cathodic part as the root-excreted oxygen is favorable for cathodic reaction. It has been reported that the growth of many plants such as *Glyceria maxima*, *Spartina anglica*, and *Arundinella anomala* in anodic sediments could significantly increase the power output and speed up heavy metal and organic contaminant removal in SMFCs [33–35]. The rhizodeposits account for approximately 20–40% of plant photosynthetic productivity. In terms of that, PSMFC is a technique converting solar energy into electricity. It has been estimated that net power generation of 21 GJ ha^{-1} year^{-1} (67 mW/m^2) could be achieved by a PSMFC, which is comparable to the net energy yield by traditional biomass electricity production systems, such as digestion of energy crops (2.8–70 GJ ha^{-1} year^{-1}) and

biomass combustion (27–91 GJ ha^{-1} year^{-1}) [6]. However, several field or laboratory experiments (rice paddy in Japan) of PSMFC showed no significant increase in power density compared to SMFC without plants, indicating the enhancement of plants on SMFC may be effected by a variety of factors such as the plant, solar radiation level, sediment composition, and temperature [32].

11.2.4 Electricity-Stimulating Systems (ESSs)

ESSs represent a group of technology that uses electric power to stimulate the bioremediation of sediments. The major difference between ESS and other SBES is that ESS consumes electricity, while the other SBESs are electricity generating or nonconsuming. One or two electrodes of ESSs were polarized at a certain potential by a potentiostat for a more specific or rapid degradation of contaminants. For example, when the electrode in the sediment was polarized at a negative potential (e.g., −0.4 V), it could serve as electron donors for microbial reduction of chlorinated organic compounds, azo dyes, Cr, and U, and when polarized at a positive potential, it could serve as electron acceptors to drive microbial oxidization of PAHs, benzene compounds, and antibiotics [16, 17]. Sun et al. recently assembled a novel ESS termed bioelectrochemical sediment caps (BSCs) by embedding two polarized electrodes (with an applied voltage of 4 V) into the cap layer [19]. Traditional sediment caps represent a thin layer of sand, activated carbon, or apatite that sequesters contaminants and further retards the movement of contamination from the sediments. In BSCs, the cathodic water electrolysis generated hydrogen which could serve as electron donor for microbial or chemical reduction of contaminants, while the anodic water electrolysis generated oxygen to serve as electron acceptor for the oxidization of contaminants [18, 19]. It can be seen that BSCs combine the advantages of both sediment caps and ESSs. Higher salinity or electron mediators could be used to further enhance the performance of BSCs. However, significant pH differences generated between the two electrode zones which might limit the long-term performance of BESCs. Despite the merits shown by lab-scale BESCs, the energy cost should be considered in long-term scaled-up application.

11.2.5 Bioelectro-snorkels (BESnK)

BESnk was firstly developed by Erable et al. as a wastewater treatment device modified from MFC [36]. Typically, a BESnk was a graphite rod (or other conductive rods) with the bottom part inserted in sediments (or activated sludge) and the top part exposed to overlying water [20, 36, 37]. BESnk could be considered as a conductive bridge linking the anaerobic sediment environment and aerobic overlying water environment, so that the electrons generated by the bottom bacteria can flow along BESnk to the overlying water. In comparison with SMFCs, BESnk cannot

generate electricity. However, its simple structure, rapid electron transfer, and larger redox effects on local environment render a higher bioelectrodegradation efficiency in sediment remediation and wastewater treatment [38].

11.3 Common Biogeochemical Process in SBES

11.3.1 Anodic Biogeochemical Process

The biological and physicochemical properties of sediments from freshwater, marine, mash, or paddy vary largely, which means the electron donors, electricity-generating microbes, and electron acceptors are different among those sediments. Despite that, all kinds of sediments, even though the sterilized sediments, can generate electricity in SBES [39]. SBES anodes have been found to serves as a favorable electron acceptor for both microorganisms and reductive chemicals in the anaerobically heterogeneous sediments.

11.3.1.1 Electron Donors

Several field-deployed or scaled-up SBES have shown that SBES could generate electricity for several years [3, 5, 14]. A lifetime of 8.9 years was estimated of a 100 L SBES contained contaminated river sediments, indicating there are sufficient electron donors in sediments for SBES [5]. Generally, sulfides and organic matters are the main electron donors for SBES electricity generation [39].

Organic and inorganic sulfur compounds were not only the key factor causing odor and blackish of water body but also an important electron donors for SMES electricity generation. Sulfur-redox cycle is one of the most complex processes in sediments, especially on the anode surface (Fig. 11.3). Firstly, sulfate in the sediment and water body was reduced to sulfide by sulfate-reducing bacteria and then accumulated in sediments. When an anode was added, the sulfides can be either electrochemically (at redox potentials over -0.15 V) or microbiologically (e.g., *Thiobacillus* species) oxidized to elemental sulfur on the anode surface. Therefore, elemental sulfur accumulation was often observed on SBES anodes which may block further electron transfer from microbes or sulfides. Sulfur-oxidizing bacteria play a key role to succeed in further electron transfer. Those bacteria (e.g., *Desulfuromonas palmitatis*, *Desulfobulbus propionicus*) can oxidize sulfur to sulfate using anode as electron acceptor [39–41]. It has been estimated that sulfides oxidization could account for about 40% of the electrons in SBES electricity generation which will vary according to the sulfides amount and microbial composition in sediments [24, 39].

Organic matter oxidization contributes the most electrons of SBES electricity generation. Typically, electricity-generating bacteria can only use small molecular
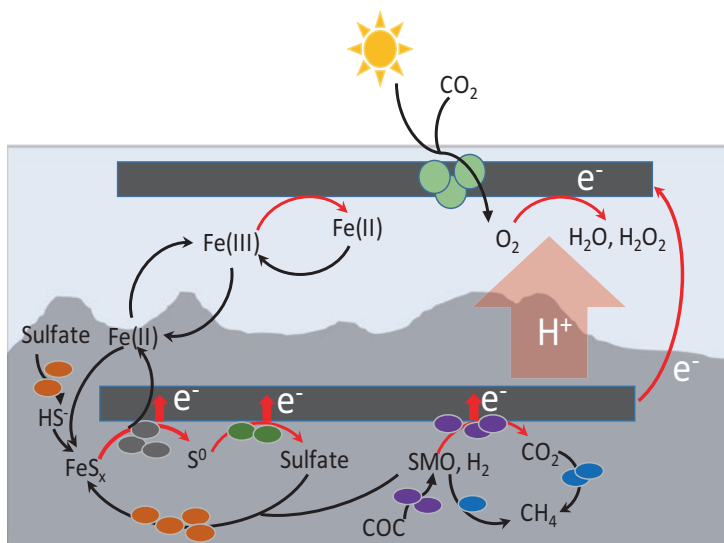
Fig. 11.3 Biogeochemical pathways of electrons at the anode and cathode in SBESs

organics (SMO) in electrode respiration. For example, *Geobacter* species use toluene, acetate, and H_2; *Shewanella* species use lactate, formate and H_2; and *Rhodoferax ferrireducens* uses glucose, sucrose fructose, and xylose [7, 42–44]. Despite those SMOs being ubiquitous in sediments, it was considered that the existing SMO (generally below 1 mM) will be rapidly depleted and most of the SMO come from the fermentation and hydrolysis of complex compounds by fermenters or other non-electricity-generating bacteria [45, 46]. The depletion of SMO by electricity-generating bacteria could alleviate the feedback inhibition of SMO to the fermentation or degradation of complex compounds. It can be seen that the main role of electricity-generating bacteria is to motivate the biodegradation of complex organic compounds (COC) rather than directly decompose them (Fig. 11.3). Organic matter are generally considered harmless for SBES, and higher concentration of organic matter can provide electrons for long-term electricity generation. Therefore, many studies added organics such as acetate, glucose, cellulose, or wheat straw to SBES [16, 47, 48]. However, Zhao et al. recently showed that higher organic contents (up to 16%) in sediments will cause unstable electricity generation, more methane emission, and higher worm activities [49].

Current studies using different kinds of sediment have demonstrated that electron donors are generally sufficient for long-term SBES operation. Moreover, additional organic electron donors may cause secondary contaminants or suppress the degradation of the local contaminants. Therefore there is no need to amending electron donors to SBES if bioremediation is the main object.

11.3.1.2 Competing Electron Acceptors

In addition to electrode, various inherent chemicals have been used as the electron acceptors by microbes in sediments. Dissolved oxygen in water column can be depleted within several micrometers below the water-sediment interface. In the deeper anaerobic environments, many other chemicals including sulfate, nitrate, humics, metal oxides, and CO_2 would compete with anode for electrons [50, 51]. The anode potential of spontaneously operated SMFC ranged from −0.2 to 0.2 V, which is relatively higher than the sulfate (SO_4^{2-}/H_2S, −0.21 V) and CO_2 (CO_2/CH_4, −0.24 V) reduction [6]. Consistently, several reports have shown that SMFC depressed the sulfate reduction and methane emission [6, 20, 25]. However, this is not always the case due to the large variation of sediment environments. For example, an in situ experiment in a specific riparian zone showed that the methane emission was depressed by SMFC deployed at upstream but slightly increased at downstream SMFC [52]. Moreover, in contrast to the assumed competing relationship between SMFC and other electron acceptors, several studies have shown that SBES performed better in the presence of some electron acceptors (e.g., Fe(III), humics) possibly because the redox intermediates of those compounds served as electron mediators or changed the local environment for electrode reduction. For example, Zhou et al. managed to improve the performance of SMFC through amending colloidal iron oxyhydroxide into freshwater sediments as the Fe(III)/Fe(II) redox species mediate electron transfer to electrode [46]. And the transformation of mineral oxides may accelerate the sediment conductivity and thus increase electricity generation [53, 54]. As another example, the redox cycle of sulfur species can release sulfate to the cathode, decreasing the cathodic pH and thus increasing the SBES performance.

11.3.2 Cathode Processes

Due to the low chemical diffusion efficiency in sediments, anode biogeochemical reactions were considered the main limit for SBES. Moreover, most recalcitrant contaminants (e.g., PAHs, PCBs, PBDEs) accumulate in sediments. Therefore, almost all SBES studies focused on the anode biogeochemical processes. However, it is possible that cathode suffers more charge transfer resistance in contaminated or nutrient-rich water bodies wherein the dissolved oxygen is low and microbe density is high. To maintain electricity generation, the electron acceptor redox potential should be higher than that of anode. Oxygen was the most favorable electron acceptor for SBES due to its high redox potential and inexhaustibility in natural water bodies. Improving the cathodic oxygen reduction could not only enhance SBES electricity generation but also the anodic biodegradation. Therefore, many synthetic cathodic catalysts and improved cathode configuration have been reported. The

photosynthetic activity plays an important role in SBES cathode performance. Wang et al. improved the cathode performance by immobilizing oxygen-generating algae (*Chlorella vulgaris*) on cathode [55] (Fig. 11.3). He et al. increased the cathode oxygen concentration by developing a rotating cathode [56]. However, in addition to oxygen, PCBs, Cr(VI), Fe(III), sulfate, and nitrate could also function singly or multiply as electron acceptors at cathode [57, 58], which should be paid more attention in the future studies.

11.4   Bioelectroremediation of Sediments

About 30% of the reported SBESs researches dealt with the contaminant removal function of SMES, while the others focused on the power recovery, material or structure optimization, or microbial ecology effects of SMES. Table 11.1 summaries the brief information of the SBESs with aims to stimulate contaminant degradation. Among the diverse types of contaminants in sediments, POPs such as PAHs, PBDEs, and polychlorinated biphenyls (PCBs) were the mainly interested contaminants in the reported SMESs, followed by sulfur compounds, TOC, cellulose, and some other normal water quality indexes. POPs became the mainly targeted contaminants in SMES studies because of their wide existence, high toxicity, and low biodegradability by traditional bioremediation methods. Moreover, those contaminants generally have high hydrophobicity, and most of them are deposited and absorbed in sediments rather than water bodies.

11.4.1   SBES for PAHs Degradation

All the reported SMESs showed much higher removal efficiency on PAHs compared to the natural processes. Most of those reports used sediments from freshwater environments as inoculums. A 60-day experiment using a scaled-up SMFC showed 0.34-, 0.79-, and 0.4-fold higher removal efficiency on the benzo(a)pyrene (BaP), benzo(k)fluoranthene, and total PAHs in the river sediments. SMFCs operated for a longer term could generally further remove PAHs [59]. For example, Yan et al. reported that the BaP was decreased from 1.6 to 1.2 mg/Kg (wet sediment) after a 50-day treatment in SMFC and further to 0.8 mg/Kg at day 230, while no significant removal was observed in control [33]. It was also noted that the removal efficiency decreased over treatment time, as the removal efficiency at day 367 was comparable to that at day 230. A 970-day experiment also showed a BaP removal rate of 2 μg/Kg/day within the initial 180 days but only 0.19 μg/Kg/day in the following 800 days [3]. In addition to the decreased electricity generation, another proposed reason for the decreased PAHs degradation speed is the adsorption or transformation of PAHs or their byproducts into humic matters (humification) [3, 60]. Fertilized sediments generally showed no removal on PAHs, suggested that

Table 11.1 Contaminants degradation in different SBESs

SBES types	Sediment sources	Contaminants	Anode materials	Power densities	Scale (L)	Running time (days)	References
SMFC	River	Benzo(a)pyrene, benzo(k) fluoranthene, total PAHs	Carbon mesh	81 mW/m^2	195	60	[59]
SMES	Marine	Toluene	Graphite plate	431 mA/m^2	0.25	100	[25]
SMFC	River	TOC, ROOM, LOI	Graphite felt	18.6 mW/m^3	100	730	[5]
SMFC	River	68 organic compounds	Graphite felt	4.32 mW/m^2	30	30	[68]
SMFC	Lake	Pyrene, BaP	Graphite felt	1.1 mW/m^2	10	365	[33]
PSMFC	Lake	Pyrene, BaP	Graphite felt	1.02 mW/m^2	10	365	[33]
SMFC	Lake	BaP	Graphite felt	19.8 mW/m^2	4	970	[3]
SMFC	Lake	Phenanthrene, pyrene	Stainless steel	0.35 mW/m^2	4	240	[60]
ESS	River	PCB1, PCB61	Ti foil	49 mA/m^2	0.1	88	[17]
ESS	River	PCB61	Carbon paper	2.9 A/m^2	0.1	110	[16]
SMFC	Lake	ROOM	Graphite felt	4.08 mW/m^2	In situ	180	[15]
SMFC	Stream	TOC	Graphite felt	20.2 mA m^2	0.25	120	[75]
SMFC	Stream	CH$_4$, N$_2$O, SO$_4^{2-}$, Cl$^-$	Graphite plate	10 mA/m^2	In situ	42	[52]
SMFC	Marine	Sulfides	Graphite disks	33 mW/m^2	In situ	224	[4]
ESS	River	Naphthalene	Graphite felt	/	0.6	69	[18]
		Phenanthrene					
ESS	River	Tetrachlorobenzene	Carbon cloth	/	0.6	100	[19]
SMES	Harbor	Toluene, benzene, naphthalene	Graphite sticks	/	0.5	12	[7]
ESS	Fishing facility	CH$_4$	Graphite	34.9 mA/m^2	2	15	[76]
BSK	Marine	TPHs	Graphite rods	/	0.12	417	[20]
SMFC	River	TOC, PCB	Graphite brush	18.30 W/m^3	3.14	60	[63]
SMFC	Pond	COD	Graphite plates	0.1 mW/m^2	300	28	[77]

(continued)

Table 11.1 (continued)

SBES types	Sediment sources	Contaminants	Anode materials	Power densities	Scale (L)	Running time (days)	References
SMFC	Stream	LOI, DOM, cellulose	Graphite felt	0.68 mW/m^2	1.4	330	[66]
SMFC	River	TOC, DOC	Graphite fiber brush	99 mW/m^2	3.9	60	[62]
SMFC	Lake	NO_3^-, NO_2^-	Carbon paper	42 mW/m^2	0.5	38	[58]
SMFC	Lake	LOI, ROOM	Stainless steel	11.2 mW/m^2	1.4	160	[78]
SMFC	Lake	Volatile fatty acid	Graphite plates	55.2 mW/m^2	0.65	100	[49]
SMFC	Beach	TPHs	Carbon cloth	2162 mW/m^3	0.1	66	[67]
SMFC	Lake	LOI, ROOM	Graphite felt	101.5 mW/m^2	1	110	[46]
SMFC	River	Benzo(a)pyrene, benzo(k) fluoranthene, benzo(b) fluoranthene	Carbon mesh	63 mW/m^2	390	72	[69]
SMFC	Pond	COD, TN, NX^n	Graphite plate	8.47 mW/m^2	22	45	[48]
SMFC	River	BDE209	Carbon paper	280 mW/m^2	0.12	70	[64]

PAHs could only be removed by microbial degradation rather than chemical reaction in natural sediments [16]. However, the PAHs degradability of microbes in natural sediments usually decreases with the ring number in PAHs. Therefore, the concentration of PAHs with more ring number is generally higher in sediments. Recent results in our lab showed an interesting fact the SBES-enriched microbial consortia have equal or even higher degradability on PAHs with more rings. The study using a 3.5 V BSCs showed comparable efficiency with oxygen exposure for PAHs removal. Another advantage of BSCs is that the anode potential can be exchanged so that the PAHs could be degraded via either oxidative or reductive reaction [18].

Some other methods have been used to compare or integrate with SBES for a better PAHs degradation, for example, metal oxides. Fe is the most abundant metal element in subsurface environments. SMFC electrodes are generally thermodynamically more favorable than solid iron oxides in microbial respiration. Yan et al. have shown that SMFC performed higher phenanthrene and pyrene degradation efficiency than amorphous ferric hydroxide [60]. The degradation was further increased by using both SMFC and amorphous ferric hydroxide in treatment. The electron transfer rate at the microbe-electrode interface is a key factor determining the cur-

rent generation and substrate degradation. Therefore, chemicals stimulating the microbe-electrode electron transfer would increase biodegradation. Zhou et al. used several kinds of iron compounds including colloidal iron oxyhydroxide, ferric oxyhydroxide, goethite, and magnetite to stimulate the electron transfer and organic degradation in the anodic sediment [46]. Among those compounds, colloidal iron oxyhydroxide showed the highest current density and substrate degradation. Zero-valent Fe (Fe^0) was also used to enhance the biodegradation and current generation in SMFCs mostly due to its highly oxidative activity [61]. In addition to role of iron species as electron donors (Fe^0) or acceptors (iron minerals), the redox cycle of Fe^{2+}/Fe^{3+} catalyzed by biological or chemical reactions is also believed to have a role in SMFC sediments [46, 62]. Rhizosphere oxygenation and root exudates have been demonstrated to play a key role in sediment phytoremediation. And some of the exudates may serve as co-substrates to stimulate PAHs degradation. It was recently shown that the removal efficiency of pyrene and BaP was enhanced by onefold by grown sweet flag (*Acorus calamus*) in a SMFC [33]. Two other reasons could also account for the enhanced degradation in PSMFCs: (1) the redox potential increased from −50 to over 100 mV when SMFC or sweet flag was added in the sediments; (2) the microbial community was significantly changed by growing the sweet flag.

11.4.2 SBES for Polyhalogenated Aromatic Compounds (PACs)

PACs are another group of recalcitrant contaminants with high toxicity and wide existence in sediments. Chun et al. applied different voltages on two electrodes vertically inserted in sediments to stimulate the PCB degradation [17]. The degradation efficiency increased with the applied voltage. Fertilized sediments showed no degradation. Therefore, the PCB was mainly degraded by microbes even though high voltages were used (4.0 V). However, H_2 or O_2 was generated at cathode or anode, respectively, when the applied voltage is bigger than 2.2 V. Therefore, both oxidative and reductive degradation was stimulated within the system. In contrast to the vertical electrodes, Sun et al. used two horizontal settled electrodes to form bioelectrochemical caps to stimulate the removal of 1,2,3,5-tetrachlorobenzene (TeCB) in sediments [19]. Considering that the microbial PCB degradation is generally initiated by reductive dechlorination, Yu et al. tried to use a negatively poised electrode (−0.3 V) as electron donor to reduce PCBs; however, no obvious PCB61 removal was observed within 1 year [16]. In contrast, a positive electrode (0.2 V) showed 58% removal efficiency within 120 days, 1.5-fold higher than that of natural degradation. They also showed that the microbial PCB dechlorination occurred primarily at para and meta positions but rarely at ortho position [16]. Those reports suggested that an anaerobic oxidative pathway possibly contributed to the PCB degradation in sediments, although it has not been evidenced. Surfactant has been used in desorption of the contaminants with high hydrophobicity in sediments. It was

recently showed that the addition of surfactants (sodium dodecyl sulfate and Tween 80) could further increase the PCB degradation rate by 28.6% relative to a normal SMFC or 200% relative for natural degradation [63].

Similar to the PAHs and PCBs, PBDEs are a group of emerging contaminants with several members listed as POPs. High PBDE concentrations were commonly detected in the sediments contaminated by electronic wastes mostly in Guangdong and Zhejiang, China. Yang et al. have showed that the electrode respiration in SBES could enhance the debromination of BDE-209 by 1.5-fold [64, 65]. However the degradation products such as BDE-207 206 and BDE-183 could not be mineralized under anaerobic condition suggesting a subsequent aerobic treatment is needed.

11.4.3   Other Contaminants

Cellulose generated from the aquatic plants is an important component of the organic content in sediments. Due to the low degradable nature, cellulose is also an important reason for the contamination of water environments. Recent studies showed that adding cellulose to sediment enhanced the electricity generation of SMFC, indicating that some microbes in the SMFC could degrade cellulose to generate electricity [48]. A 330-day study showed that SMFC could enhance the sediment cellulose removal efficiency by 34.4%. A nanotube cathode could further increase the removal efficiency and electricity generation. Moreover, the cellulose activity in SMFC increased tenfold relative to that in natural sediments [66].

Toluene is also a common contaminant in sediments. Some bacteria (e.g., *Geobacter*, *Pseudomonas*) could use toluene as electron donor for electricity generation [7]. Daghio et al. found that adding toluene could significantly increase the electricity of SMFCs with a 16 mg/kg sediment/day degradation rate [25]. However, no electricity increase was observed after four batches. It was presumed that the toluene was inaccessible to the electrode-respiring bacteria when the electrode biofilm thickness increased. Sulfate was then used as electron acceptor by the thick biofilms for toluene degradation. The results also indicated that the electrode was more thermodynamic favorable than sulfate. By using [^{14}C]-toluene, Zhang et al. demonstrated that both toluene and benzene degradation could be enhanced within SMFC, and toluene could be completely oxidized to CO_2 under anaerobic sediments [7].

Two studies made efforts to stimulate the total petroleum hydrocarbons (TPHs) in sediments with SBESs. Morris and Jin reported an 11-fold (24% vs 2%) higher TPH degradation efficiency in SMFCs compared with natural sediments after 66 days [67]. Compared to SMFC, BSK was considered to be more efficient in biodegradation but no electricity generation. Viggi et al. reported a long-term (400 days)

treatment of the TPH-contaminated sediments with BSKs [20]. After 200 days, 20% of the TPH was removed in BSK, while no significant removal was observed in natural or sterilized sediments. However, after 400 days, all reactors showed over 80% removal efficiency, indicating that the sediment itself had degradation capacity on TPH and BSK could stimulate the degradation process.

Despite that the degradation capacity of SBES on various organic contaminants has been demonstrated, almost all of those SBESs dealt with only one or a group of contaminants by using different reactors. There are no comparability of those reports. A key question for SBES application still remains unanswered: which kinds of contaminants are more suitable to be treated by SBES? Xia et al. analyzed 68 putative organic compounds belonged to 12 groups (alkanoates, aldehydes, ketones, alcohols, carboxylic acids and phthalate, alkenes and benzene homologs, alkanes, heterocyclic compounds, silanes, and others) in the SMFC-treated contaminated sediments [68]. The results showed a general trend that chemicals with higher polarity were more readily to be degraded in SMFC. A contrary trend (i.e., higher degradation efficiency of chemicals with lower polarity) was observed by using nitrate as artificial electron acceptor in the sediments. The results indicated that SMFCs are not proper for environments contaminated by low-polar chemicals such as petroleum pollution sites. A combination of SMFCs with soluble electron acceptors such as nitrate or sulfate would be more versatile for sediment bioremediation.

11.4.4 The Anodic Spatiotemporal Process in SBES

The spatiotemporal process is one central but less studied issue in the SBES-based bioremediation. Li et al. recently reported that the TOC decreased 17% at the anode surface, while no significant degradation occurred at 10 cm away from the anode within 18 days. At day 72, comparable TOC degradation was detected at the site 10 cm from anode [69]. Assuming that the degradation rate was linear with the distance, the effecting zone of the anode expanded at a speed of 0.25 cm/day. Several soil MFC reported the spatiotemporal property of the degradation processes. Wang et al. reported that the PAHs beyond 3 cm were not degraded after a 25-day treatment [70]. Biochar, graphite, and some conductive minerals have been used to stimulate electron transfer due to their possible role of bridging electron donors or acceptors in sediments [71–73]. A recent report showed a 70–300 cm effecting distance by using a graphite granule anode after 120 days, which largely elevated the practical bioremediation feasibility of SBES [74]. The spatiotemporal process of SBES depends on many factors including the electricity density, external resistor, and chemical and biological compositions of the sediments, but little has been known to date. Therefore, more efforts should be made on this issue.

11.4.5 Cathode-Stimulated Remediation

In contrast to the anodic processes, only several reports studied the pollutants removal by SMFC cathodes, including sulfate, nitrate, and TOC [58, 69]. Moreover, the anodic sediment environment is the main characteristic that distinguishes SMFCs from the other BESs, while the SMFC cathode processes are similar to those in the other types of MFCs, as introduced in other sections.

11.5 Microbial Mechanisms of the Bioelectroremediation in SBES

11.5.1 Microbial Communities

Electrodes are an exotic electron acceptor for the natural microbial communities in sediments. Therefore, the microbial communities will be shaped in response to SBES electrodes. Generally, the diversity decreases after SBES deployment [24, 79]. However, the specific composition enriched by different SBES varied largely from each other (Table 11.2), which could be attributed to many reasons: sediment composition, electrode potential, electrode material, or electron transfer rate. To date, most bacteria enriched by the anode belonged to *Proteobacteria* phylum; only one SMFC operated under high temperature (60 °C, marine sediment) showed the highest abundance of *Firmicutes* [80]. At the class level, *Deltaproteobacteria* showed the highest abundance in most reports, regardless of the sediment types (freshwater, marine, or lake). However, other classes belonging to *Proteobacteria* phylum such as *Alphaproteobacteria*, *Betaproteobacteria*, *Gammaproteobacteria*, and *Epsilonproteobacteria* were also enriched as the most abundant bacteria in several reports. Many operation factors such as substrate, electrode potential, or temperature could change the bacterial class composition. For example, adding Fe(III) to a SMFC changed the major microbial class from *Gamma-* to *Deltaproteobacteria* [62]. Growing plant *Acorus Calamus* in the SMFCs can change the most abundant anodic class from *Delta-* to *Betaproteobacteria*, and the most abundant family shifted from *Geobacteraceae* to *Anaerolineaceae* [33]. However, there was another report which showed that growing *Canna indica* did not change the SMFC microbial community at the class level [34], indicating the community shift could be attributed to many factors. Moreover, PCR-DGGE was a popular microbial community analyzing method before next-generation sequencing. However, two reports using PCR-DGGE method showed *Alphaproteobacteria* as the most abundant class which was rarely detected in the reports using next-generation sequencing method [21, 58]. It is possible that the two methods have different bias in microbial community analysis. The genus-level shifts in microbial community are much more susceptible to the geochemical and operational factors in SMFCs. *Geobacter* was one of the most frequently detected genus in SMFCs. Recent reports showed that

Table 11.2 Microbial communities in contaminant-degrading SBESs

SBES type	Sediment source	Phylum	Class	Genus	G/Sᵃ	References
SMFC	River	Proteobacteria	*Gammaproteobacteria*	*Longilinea*	+/−	[69]
SBES	Marine	*Proteobacteria*	*Deltaproteobacteria*	NA	−/−	[25]
SMFC	River	*Proteobacteria*	*Gammaproteobacteria*	*Geobacter*	+/+	[62]
			Deltaproteobacteria (Fe added)	*Pseudomonas* (Fe added)	+/+	
SMFC	Lake	*Proteobacteria*	*Alphaproteobacteria*	*Denitrifying* bacterium W73c	−/−	[58]
SMFC	Lake	*Proteobacteria*	*Deltaproteobacteria*	*Geobacter*	+/−	[33]
PSMFC			*Betaproteobacteria*	*Longilinea*	+/−	[33]
SMFC	Bog	*Proteobacteria*	*Deltaproteobacteria*	*Geobacter*	+/−	[79]
SMFC	Marine	*Firmicutes*	NA	*Thermincola*	+/−	[80]
SBES	River	*Proteobacteria*	*Epsilonproteobacteria*	*Arcobacter*	+/+	[16]
			Deltaproteobacteria	*Pseudomonas*	+/+	[16]
SMFC	Marine	*Proteobacteria*	*Deltaproteobacteria*	*Desulfuromonas*	+/−	[24]
				Desulfuromusa (AQDS added)	+/−	
SMFC	Salt marsh	*Proteobacteria*	*Deltaproteobacteria*	*Geobacter*	+/−	
SMFC	River	*Proteobacteria*	*Deltaproteobacteria*	*Geobacter*	+/−	
SMFC	Wetland	*Proteobacteria*	*Deltaproteobacteria*	*Geobacter*	+/−	[34]
PSMFC				*Desulfobulbus*	+/−	
SMFC	Marine	*Proteobacteria*	*Deltaproteobacteria*	*Geobacter*	+/−	[4]
SMFC	Lake	*Proteobacteria*	*Deltaproteobacteria*	*Desulfobulbus*	−/−	[49]
SMFC	Lake	*Proteobacteria*	*Deltaproteobacteria*	*Longilinea*	+/−	[59]
SMFC	Lake	*Proteobacteria*	*Betaproteobacteria*	*Thiobacillus*	−/−	[41]
SMFC	Fishing facility	*Proteobacteria*	NA	*Thiobacillus*	+/−	[76]
ESS			NA	*Geobacter* (−0.2 V)		
				Thiobacillus (+0.3 V)		
BSK	Marine	*Proteobacteria*	*Deltaproteobacteria*	NA	NA	[20]
BSK	Marine	*Proteobacteria*	*Alphaproteobacteria*	NA	−/−	[21]
SMFC	Lake	*Proteobacteria*	*Alphaproteobacteria*	NA	+/+	[81]
SMFC	Lake	*Proteobacteria*	*Deltaproteobacteria*	NA	+/+	[3]

NA indicates no available information

ᵃDetection of *Geobacter* or *Shewanella* species: + indicates detected; − indicates not detected

Geobacter could be largely effected by the electrode redox potential and the electron donor [16]. *Geobacter* dominated on the anode polarized under −200 mV but was overcome by *Thiobacillus* on the anode of +500 mV (vs SHE) [76]. In the SBES by Yu et al., *Geobacter* increased from 1.8% in the seed sediment to 3.4% in non-acetate SBES and to 5.6% in acetate-added SBES, despite the electrode potential was polarized at +400 (vs SHE) [16]. Although *Geobacter* is a model

metal-reducing organism, its abundance significantly decreased by adding Fe(III) to a SMFC, while the versatile respiring bacteria *Pseudomonas* increased to be the most abundant genus [62], possibly due to that more little organic acids were needed as electron donor to reducing the additional Fe(III). Some other microbial community shifts according to the operation factors can be seen in Table 11.2. *Geobacter* and *Shewanella* were two mostly used electrode-respiring model organisms, and they were widely observed in various subsurface environments. Therefore, their detection in SMFC was also noted in Table 11.2. It can be seen that *Geobacter* was detected in most (16/21) SMFC reports, while *Shewanella* was detected in only four reports. It is possible that *Shewanella* was more suitable to survive in redox-fluctuant environments rather than the stable and oligotrophic sediments.

In contrast to bacteria, the role of archaea in SBES was unclear to date. *Thermophilic* archaea such as *Thermoplasmatales*, *Desulfurococcales*, *Thermoproteales*, and *Thermococcales* were founded in SMFC and PSMFC sediments but were decreased compared with the original sediments, indicating those archaea did not participate in the electricity generation. Considering the competition between methane generation and electricity generation, the abundance of methanogens may have important effects on the performance of SBES. Lu et al. showed that the methanogen abundance was increased relative to the other archaea in SMFC, and most of the methanogens were hydrogenotrophic [34]. Similarly, hydrogenotrophic methanogens was the main methanogens in SMFCs with different levels of organic content [49]. In a SMFC operated for 970 days, the methanogens were significantly decreased compared with the control sediment, indicating an inhibition of electricity generation on methane generation [3].

Similar to the studies on biodegradation, most reported SBES microbial communities were grown on the anodes or sediments. Only one report studied the microbial communities on SMFCs operated in marine or salt mash sediments [24]. *Cycloclasticus* and *Methylotroph* I were dominated communities in the marine cathode, while *Rhodobacter* capable of photosynthesis dominated in the salt marsh cathode.

11.5.2 Functional Gene Communities

The functional gene or enzyme-based results are more reliable in understanding the enhancement of SMFC on the contamination biodegradation. However, only several reports showed available information on the functional gene or enzymes in SBESs [3, 64]. GeoChip is a powerful tool to test the almost all biogeochemical process-related genes in various environments. Yang et al. firstly used the GeoChip 4.0 to understand the anode-enhanced PBDE degradation. Over 9000 genes were detected, and 87.9% of them were detected in the BES but not detected in the normal anaerobic reactor. Almost all functional genes (including the genes in carbon, nitrogen, phosphorus, sulfur cycling, electron transfer, and aromatic hydrocarbon

degradation) were upregulated under electricity-generating condition [64]. Yan et al. recently integrated 16S rRNA sequencing and Geochip 5.0 to analyze the bioelectrochemical BaP degradation in SMFC. A highly clustered gene network was observed in SMFC. The genes involved in electron transfer, carbon cycling, organic contamination degradation, and aromatic degradation were significantly enriched [3]. In addition to GeoChip, other methods (e.g., q-PCR and enzyme activity measurement) also evidenced that many functional genes or enzymes including dissimilatory sulfite reductase (*dsrA*), benzylsuccinate synthase (*bssA*), cellulose, and catalase upregulated on the anode of SMFCs or soil MFCs, compared to the natural sediments [25, 66, 74]. Those reports explained a confusing phenomenon in SBES researches that the degradation of almost all contaminants, regardless of oxidative or reductive, could be stimulated in SBESs, although the removal efficiencies were different. Lacking favorable electron acceptor is the main limit for the biodegradation in anaerobic sediments. The SBES provides an electron pathway from contaminants firstly to the anode and finally to the oxygen in the overlying water. The high redox potential of anodes driven by the oxygen reduction at cathode can provide much more energy for the sediment microbial community. As a result, the functional gene expression, microbial metabolism, and the cellular proliferation will be stimulated by the electrode respiration in SBESs, which can explain the stimulation of SBESs on various contaminants.

11.6 Future Development and Applications

Increasing reports have evidenced that SBESs is a promising technology to stimulate sediment bioremediation with simultaneous power recovery. How to operate SBESs in practical environments is the most urgent and challenging problem for a further development of SBESs. The first and most important step to address this problem is to deploy a SBES in a practical environment. Many unexpected problems will arise after the field deployment which may cause failure or cost much more money or labor force than that in laboratory experiment. Many of the problems can be avoided by careful considerations and designs before filed application. Firstly, the general environment of the operation sites must be evaluated before a field deployment, including the temperature range, sediment thickness and composition, water flow speed, tidal cycle, human activities, as well as the government management. Secondly, the structures and materials of the SBESs should be evaluated and optimized before application, including the SBES type, electrode material, electrode area, wire-electrode connection, system stabilization, and protection from biodisturbance. Thirdly is the operation mode. If high power output or large bioremediation zone is needed, parallel stack of multiple SMFCs will be a better choice than single or serially connected SMFCs. Moreover, a combination of different SBESs or SBESs and some other remediation methods should be considered based on their different degradation preferences.

References

1. Li WW, Yu HQ (2015) Stimulating sediment bioremediation with benthic microbial fuel cells. Biotechnol Adv 33:1–12
2. Kronenberg M, Trably E, Bernet N et al (2017) Biodegradation of polycyclic aromatic hydrocarbons: using microbial bioelectrochemical systems to overcome an impasse. Environ Pollut 231:509–523
3. Yan Z, He Y, Cai H et al (2017) Interconnection of key microbial functional genes for enhanced benzo[a]pyrene biodegradation in sediments by microbial electrochemistry. Environ Sci Technol 51:8519–8529
4. Tender LM, Reimers CE, Stecher HA et al (2002) Harnessing microbially generated power on the seafloor. Nat Biotechnol 20:821–825
5. Yang Y, Lu Z, Lin X et al (2015) Enhancing the bioremediation by harvesting electricity from the heavily contaminated sediments. Bioresour Technol 179:615–618
6. De Schamphelaire L, Rabaey K, Boeckx P et al (2008) Outlook for benefits of sediment microbial fuel cells with two bio-electrodes. Microb Biotechnol 1:446–462
7. Zhang T, Gannon SM, Nevin KP et al (2010) Stimulating the anaerobic degradation of aromatic hydrocarbons in contaminated sediments by providing an electrode as the electron acceptor. Environ Microbiol 12:1011–1020
8. Lovley DR (1995) Bioremediation of organic and metal contaminants with dissimilatory metal reduction. J Ind Microbiol 14:85–93
9. Lovley DR (2002) Dissimilatory metal reduction: from early life to bioremediation. ASM News 68:231–237
10. Reimers CE, Tender LM, Fertig S et al (2001) Harvesting energy from the marine sediment-water interface. Environ Sci Technol 35:192–195
11. Donovan C, Dewan A, Heo D et al (2008) Batteryless, wireless sensor powered by a sediment microbial fuel cell. Environ Sci Technol 42:8591–8596
12. Shantaram A, Beyenal H, Raajan R et al (2005) Wireless sensors powered by microbial fuel cells. Environ Sci Technol 39:5037–5042
13. Zhang F, Tian L, He Z (2011) Powering a wireless temperature sensor using sediment microbial fuel cells with vertical arrangement of electrodes. J Power Sources 196:9568–9573
14. Tender LM, Gray SA, Groveman E et al (2008) The first demonstration of a microbial fuel cell as a viable power supply: powering a meteorological buoy. J Power Sources 179:571–575
15. Hong SW, Kim HJ, Choi YS et al (2008) Field experiments on bioelectricity production from Lake sediment using microbial fuel cell technology. Bull Kor Chem Soc 29:2189–2194
16. Yu H, Feng CH, Liu XP et al (2016) Enhanced anaerobic dechlorination of polychlorinated biphenyl in sediments by bioanode stimulation. Environ Pollut 211:81–89
17. Chun CL, Payne R, Sowers KR et al (2013) Electrical stimulation of microbial PCB degradation in sediment. Water Res 47:141–152
18. Yan F, Reible DD (2012) PAH degradation and redox control in an electrode enhanced sediment cap. J Chem Technol Biotechnol 87:1222–1228
19. Sun M, Yan F, Zhang RL et al (2010) Redox control and hydrogen production in sediment caps using carbon cloth electrodes. Environ Sci Technol 44:8209–8215
20. Viggi CC, Presta E, Bellagamba M et al (2015) The "Oil-Spill Snorkel": an innovative bioelectrochemical approach to accelerate hydrocarbons biodegradation in marine sediments. Front Microbiol 6:881
21. Matturro B, Viggi CC, Aulenta F et al (2017) Cable Bacteria and the bioelectrochemical snorkel: the natural and engineered facets playing a role in hydrocarbons degradation in marine sediments. Front Microbiol 8:952
22. Zhang YF, Angelidaki I (2016) Microbial electrochemical systems and technologies: it is time to report the capital costs. Environ Sci Technol 50:5432–5433
23. Erable B, Lacroix R, Etcheverry L et al (2013) Marine floating microbial fuel cell involving aerobic biofilm on stainless steel cathodes. Bioresour Technol 142:510–516

24. Holmes DE, Bond DR, O'Neill RA et al (2004) Microbial communities associated with electrodes harvesting electricity from a variety of aquatic sediments. Microb Ecol 48:178–190
25. Daghio M, Vaiopoulou E, Patil SA et al (2016) Anodes stimulate anaerobic toluene degradation via sulfur cycling in marine sediments. Appl Environ Microbiol 82:297–307
26. Hsu L, Chadwick B, Kagan J et al (2013) Scale up considerations for sediment microbial fuel cells. RSC Adv 3:15947–15954
27. Wang HM, Park JD, Ren ZJ (2015) Practical energy harvesting for microbial fuel cells: a review. EnvironSci Technol 49:3267–3277
28. Ewing T, Ha PT, Babauta JT et al (2014) Scale-up of sediment microbial fuel cells. J Power Sources 272:311–319
29. Zhuang L, Zhou SG (2009) Substrate cross-conduction effect on the performance of serially connected microbial fuel cell stack. Electrochem Commun 11:937–940
30. Karra U, Huang GX, Umaz R et al (2013) Stability characterization and modeling of robust distributed benthic microbial fuel cell (DBMFC) system. Bioresour Technol 144:477–484
31. Zhao NN, Angelidaki I, Zhang Y (2017) Electricity generation and microbial community in response to short-term changes in stack connection of self-stacked submersible microbial fuel cell powered by glycerol. Water Res 109:367–374
32. Nitisoravut R, Regmi R (2017) Plant microbial fuel cells: a promising biosystems engineering. Renew Sust Energ Rev 76:81–89
33. Yan ZS, Jiang HL, Cai HY et al (2015) Complex interactions between the Macrophyte Acorus Calamus and microbial fuel cells during pyrene and benzo[a]pyrene degradation in sediments. Sci Rep 5:10709
34. Lu L, Xing DF, Ren ZJ (2015) Microbial community structure accompanied with electricity production in a constructed wetland plant microbial fuel cell. Bioresour Technol 195:115–121
35. Liu ST, Song HL, Li XN et al (2013) Power generation enhancement by utilizing plant Photosynthate in microbial fuel cell coupled constructed wetland system. Int J Photoener 2:15158–15166
36. Erable B, Etcheverry L, Bergel A (2011) From microbial fuel cell (MFC) to microbial electrochemical snorkel (MES): maximizing chemical oxygen demand (COD) removal from wastewater. Biofouling 27:319–326
37. Yang Y, Guo J, Sun G et al (2013) Characterizing the snorkeling respiration and growth of Shewanella decolorationis S12. Bioresour Technol 128C:472–478
38. Lovley DR (2011) Live wires: direct extracellular electron exchange for bioenergy and the bioremediation of energy-related contamination. Energy Environ Sci 4:4896–4906
39. Ryckelynck N, Stecher H, Reimers CE (2005) Understanding the anodic mechanism of a seafloor fuel cell: interactions between geochemistry and microbial activity. Biogeochemistry 76:113–139
40. Dutta PK, Keller J, Yuan Z et al (2009) Role of sulfur during acetate oxidation in biological anodes. Environ Sci Technol 43:3839–3845
41. Zhang T, Bain TS, Barlett MA et al (2014) Sulfur oxidation to sulfate coupled with electron transfer to electrodes by Desulfuromonas strain TZ1. Microbiology 160:123–129
42. Mahadevan R, Palsson BO, Lovley DR (2011) In situ to in silico and back: elucidating the physiology and ecology of Geobacter spp. using genome-scale modelling. Nat Rev Microbiol 9:39–50
43. Koch C, Harnisch F (2016) What is the essence of microbial Electroactivity? Front Microbiol 7:1890
44. Koch C, Harnisch F (2016) Is there a specific ecological niche for electroactive microorganisms? ChemElectroChem 3:1282–1295
45. Lovley DR (2006) Bug juice: harvesting electricity with microorganisms. Nat Rev Microbiol 4:497–508
46. Zhou YL, Yang Y, Chen M et al (2014) To improve the performance of sediment microbial fuel cell through amending colloidal iron oxyhydroxide into freshwater sediments. Bioresour Technol 159:232–239

47. Rezaei F, Richard TL, Brennan RA et al (2007) Substrate-enhanced microbial fuel cells for improved remote power generation from sediment-based systems. Environ Sci Technol 41:4053–4058

48. Sajana TK, Ghangrekar MM, Mitra A (2014) Effect of presence of cellulose in the freshwater sediment on the performance of sediment microbial fuel cell. Bioresour Technol 155:84–90

49. Zhao Q, Li R, Ji M et al (2016) Organic content influences sediment microbial fuel cell performance and community structure. Bioresour Technol 220:549–556

50. Lowy DA, Tender LM, Zeikus JG et al (2006) Harvesting energy from the marine sediment-water interface II – kinetic activity of anode materials. Biosens Bioelectron 21:2058–2063

51. Lowy DA, Tender LM (2008) Harvesting energy from the marine sediment-water interface III. Kinetic activity of quinone- and antimony-based anode materials. J Power Sources 185:70–75

52. Friedman ES, McPhillips LE, Werner JJ et al (2015) Methane emission in a specific riparian-zone sediment decreased with bioelectrochemical manipulation and corresponded to the microbial community dynamics. Front Microbiol 6:1523

53. Lu AH, Li Y, Jin S (2012) Interactions between semiconducting minerals and Bacteria under light. Elements 8:125–130

54. Kato S, Hashimoto K, Watanabe K (2011) Methanogenesis facilitated by electric syntrophy via (semi)conductive iron-oxide minerals. Environ Microbiol 14:1646–1654

55. Wang H, Liu DM, Lu L et al (2012) Degradation of algal organic matter using microbial fuel cells and its association with trihalomethane precursor removal. Bioresour Technol 116:80–85

56. He Z, Shao H, Angenent LT (2007) Increased power production from a sediment microbial fuel cell with a rotating cathode. Biosens Bioelectron 22:3252–3255

57. Babauta JT, Hsu L, Atci E et al (2014) Multiple cathodic reaction mechanisms in seawater cathodic biofilms operating in sediment microbial fuel cells. ChemSusChem 7:2898–2906

58. Zhang Y, Angelidaki I (2012) Bioelectrode-based approach for enhancing nitrate and nitrite removal and electricity generation from eutrophic lakes. Water Res 46:6445–6453

59. Li H, Tian Y, Qu Y et al (2017) A pilot-scale benthic microbial electrochemical system (BMES) for enhanced organic removal in sediment restoration. Sci Rep 7:39802

60. Yan Z, Song N, Cai H et al (2012) Enhanced degradation of phenanthrene and pyrene in freshwater sediments by combined employment of sediment microbial fuel cell and amorphous ferric hydroxide. J Hazard Mater 199–200:217–225

61. Zhang HK, Zhu DW, Song TS et al (2015) Effects of the presence of sheet iron in freshwater sediment on the performance of a sediment microbial fuel cell. Int J Hydrog Energ 40:16566–16571

62. Xu X, Zhao Q, Wu M et al (2017) Biodegradation of organic matter and anodic microbial communities analysis in sediment microbial fuel cells with/without Fe(III) oxide addition. Bioresour Technol 225:402–408

63. Xu X, Zhao QL, Wu MS (2015) Improved biodegradation of total organic carbon and polychlorinated biphenyls for electricity generation by sediment microbial fuel cell and surfactant addition. RSC Adv 5:62534–62538

64. Yang Y, Xu M, He Z et al (2013) Microbial electricity generation enhances decabromodiphenyl ether (BDE-209) degradation. PLoS One 8:e70686

65. Xu MY, Chen XJ, Qiu MD et al (2012) Bar-coded pyrosequencing reveals the responses of PBDE-degrading microbial communities to Electron donor amendments. PLoS One 7:e30439

66. Zhu D, Wang DB, Song TS et al (2016) Enhancement of cellulose degradation in freshwater sediments by a sediment microbial fuel cell. Biotechnol Lett 38:271–277

67. Morris JM, Jin S (2012) Enhanced biodegradation of hydrocarbon-contaminated sediments using microbial fuel cells. J Hazard Mater 13:474–477

68. Xia C, Xu M, Liu J et al (2015) Sediment microbial fuel cell prefers to degrade organic chemicals with higher polarity. Bioresour Technol 190:420–423

69. Li HN, He WH, Qu YP et al (2017) Pilot-scale benthic microbial electrochemical system (BMES) for the bioremediation of polluted river sediment. J Power Sources 356:430–437

70. Wang X, Cai Z, Zhou QX et al (2012) Bioelectrochemical stimulation of petroleum hydrocarbon degradation in saline soil using U-tube microbial fuel cells. Biotechnol Bioeng 109:426–433
71. Li X, Wang X, Ren ZJ et al (2015) Sand amendment enhances bioelectrochemical remediation of petroleum hydrocarbon contaminated soil. Chemosphere 141:62–70
72. Li X, Wang X, Zhao Q et al (2016) Carbon fiber enhanced bioelectricity generation in soil microbial fuel cells. Biosens Bioelectron 85:135–141
73. Chen S, Rotaru AE, Shrestha PM et al (2014) Promoting interspecies electron transfer with biochar. Sci Rep 4:5019
74. Lu L, Yazdi H, Jin S et al (2014) Enhanced bioremediation of hydrocarbon-contaminated soil using pilot-scale bioelectrochemical systems. J Hazard Mater 274:8–15
75. Hong SW, Kim HS, Chung TH (2010) Alteration of sediment organic matter in sediment microbial fuel cells. Environ Pollut 158:185–191
76. Ueno Y, Kitajima Y (2012) Suppression of methane gas emission from sediment using a bioelectrochemical system. Environ Eng Manag J 11:1833–1837
77. Sajana TK, Ghangrekar MM, Mitra A (2013) Application of sediment microbial fuel cell for in situ reclamation of aquaculture pond water quality. Aquac Eng 57:101–107
78. Song TS, Yan ZS, Zhao ZW et al (2011) Construction and operation of freshwater sediment microbial fuel cell for electricity generation. Bioprocess Biosyst Eng 34:621–627
79. Yates MD, Kiely PD, Call DF et al (2012) Convergent development of anodic bacterial communities in microbial fuel cells. ISME J 6:2002–2013
80. Mathis BJ, Marshall CW, Milliken CE et al (2008) Electricity generation by thermophilic microorganisms from marine sediment. Appl Microbiol Biotechnol 78:147–155
81. Martins G, Peixoto L, Ribeiro DC et al (2010) Towards implementation of a benthic microbial fuel cell in lake Furnas (Azores): phylogenetic affiliation and electrochemical activity of sediment bacteria. Bioelectrochemistry 78:67–71

Chapter 12
Microbial Electro-respiration Enhanced Biodegradation and Bioremediation: Challenges and Future Perspectives

Check for updates

Yixuan Wang, Houyun Yang, Xianwei Liu, and Yang Mu

12.1 Challenges and Perspectives

The microbial electro-respiration (MER) process provides new opportunities for various biodegradation and bioremediation applications. Meanwhile, it is also an open system that can be readily incorporated with other technologies, such as solar energy and salinity gradient energy production and activated sludge processes, to enable higher reaction performance or energy efficiency [1–3]. In light of the great potential and remaining challenges of the MER for diverse and still-expanding applications, we expect that the MER enhanced biodegradation and bioremediation will become a research focus in biological wastewater treatment area in the coming decade.

However, this emerging technology is still confronted with some problems now, which need to be well addressed in the future.

Y. Wang · X. Liu · Y. Mu (✉)
CAS Key Laboratory of Urban Pollutant Conversion, Department of Chemistry,
University of Science and Technology of China, Hefei, China
e-mail: yangmu@ustc.edu.cn

H. Yang
CAS Key Laboratory of Urban Pollutant Conversion, Department of Chemistry,
University of Science and Technology of China, Hefei, China

School of Environment and Energy Engineering, Key Laboratory of Anhui Province of Water
Pollution Control and Wastewater Reuse, Anhui Jianzhu University, Hefei, China

12.1.1 Understanding and Manipulation of Extracellular Electron Transfer

The extracellular electron transfer (EET) between microorganisms (named electroactive bacteria) and electrodes is the core process of the MER. Take the most common electroactive bacteria *Shewanella*, *Geobacter*, and *Pseudomonas* as examples, a large number of studies have shown that the pathways of EET mainly include the direct electron transfer (DET) via cell membrane-associated compounds (cytochrome *c* and "nanowire") and mediated electron transfer (MET) via soluble electron shuttles [4, 5]. However, the complex processes and mechanisms involved in the above three kinds of EET pathways are not yet clear, which need to be further investigated. What are the key molecules involved in the EET process? What are the key biological pathways involved in the EET? Besides for the well-known three EET pathways to us, are there any other ways of electron transfer between microorganism and electrode? In addition, microbes can also accept electrons from extracellular donors instead of transmitting electrons to extracellular receptors [6]. However, the biochemical mechanisms of microorganisms obtaining electrons from the cathode have been less explored, and it is still unclear completely. For these reasons, various novel methodologies need be established in the future to further understand the EET mechanisms between microorganism and electrode. In particular, high-throughput and system biology methods could be used to systematically investigate the molecular mechanisms of EET through regulation of genetic and metabolic network analysis [7].

In order to enhance the degradation of pollutants, in the past decades, researchers have made unremitting efforts to explore new methods to promote EET of microorganisms. Qiao et al. modified the anode material with carbon nanotubes and polyaniline to enhance the EET efficiency of microorganisms [8]. The EET ability of microorganisms could be enhanced through the reformation of the metabolic pathway of *Escherichia coli* [9]. However, due to the complexity and diversity of EET, the understanding of the EET manipulation mechanisms is still relatively limited, which leads to a lack of appropriate regulatory methods. On the basis of previous studies, it is possible to make more efforts from the following aspects: (1) Manipulation at microbial molecular scale. Based on the systematic analysis of the electron-releasing and EET mechanisms of the electroactive bacteria, synthetic biological technology could be adopted for directional transformation of electroactive bacteria, greatly promoting their EET ability. On one hand, by means of metabolic engineering, the metabolic pathway of microorganism can be directed transformed to obtain genetically engineered bacteria, so that the intracellular electrons can be more efficiently released to the outside of the cells. On the other hand, poor permeability of biofilms is the key bottleneck for the transfer of intracellular electrons to the external world. The artificial heterologous expression of certain large pore cell membrane proteins in the electroactive bacteria can be considered to promote the EET of microorganisms [10]. (2) Regulation at microbial cell scale. Biofilm developed on the surface of the electrode is particularly important for electron transfer

between microbes and electrode. Based on this, methodologies such as the development of artificially conducted biofilms and three-dimensional carbon nanomaterial electrodes can be considered to enhance the performance of biofilms practically for the electron transfer between biofilm and electrode [11]. (3) Interface regulation of electrode materials. The formation of biofilms on the electrode surface is largely limited to the interfacial properties of the electrode materials, such as specific surface area, charge property, functional group, hydrophobicity, etc. which can affect the formation of biofilms and the process of EET of microbes, thus affecting the removal efficiency of contaminants [12]. On one hand, it can be considered to modify the electrode interface using conventional chemical methods, such as acid, alkali, high temperature, electrochemical oxidation, etc. On the other hand, the interfacial properties of electrodes can be changed by the modification with various materials, such as carbon nanomaterials, metal oxides, and conductive polymers, to realize the effective EET regulation of microbes [13, 14].

12.1.2 Monitoring and Simulation of the MER Process

The MER-based pollutant removal is a complex and dynamic process, including not only the mass transfer process of the pollutant but also the electron transfer between microorganism and electrode. Therefore, the real-time monitoring of MER process may be essential. In addition, mathematic simulation might be able to provide us the deeper understanding on the MER process. However, very few studies have been explored on such aspects in the past.

In terms of monitoring, in order to ensure the stable operation of MER process, it is necessary to construct the online and real-time monitoring on the reactor. (1) Macroscopically, the sensitivity of reactor monitoring systems needs to be further improved. At present, researchers can only conduct online monitoring of a few common parameters, such as temperature and pH, and the monitoring sensitivity is poor. In addition, most of the monitoring methods cannot obtain comprehensive and complete reactor information. The effectiveness and sensitivity of the monitoring technology need to be further improved for providing more comprehensive, accurate, reliable, and timely reactor information and optimizing reactor operation. (2) Microscopically, the real-time monitoring of microorganism metabolism needs to be established. In general, in order to understand the interaction between microorganism and electrode, it always needs to destruct the samples of biofilm which has already formed on the electrode and will further affect the subsequent operation of the reactors. Thus, it needs to develop new techniques to monitor the process of microbial activity in real time, which may not affect the operation of the reactors. For example, Franks et al. proposed that the use of confocal laser scanning microscopy to real-time monitor biofilm formation [15].

In terms of simulation, construction models on the MER processes can provide a theoretical basis for biochemical reactions and mass variations in biofilm systems and are of great significance for the in-depth understanding of the microscopic

mechanisms of microbial bioremediation and degradation. Currently, limited studies have been focused on this aspect [16, 17], and in the future, we should consider not only the competitive/synergistic relationship between electroactive and non-electroactive microorganisms but also the coupling of electrochemical and biochemical processes.

1. Microscopic scale. With the deepening of the research, it is discovered that the electron transfer between the microorganism and electrode is the essence of the MER. Development of the mathematical models to simulate this electron transfer process would be highly useful for the better understanding the MER-based biodegradation and bioremediation.
2. Mesoscopic scale. In typical MER-based biodegradation and bioremediation, biofilm formed on the electrode includes not only electroactive bacteria but also other non-electroactive bacteria. Mathematic models are powerful tools for understanding the performance of biofilms, where the electrochemical and biochemical processes can be connected to each other by simulations.
3. Macro scale. The construction of macroscopic models can provide an in-depth understanding of numerous processes in the reactor systems, including mass transfer and hydrodynamic processes. Recently, Wang et al. constructed a hydrodynamic model on a bioelectrochemical reactor to make it possible to monitor and control the mixing in the reactor [18]. Overall, the in-depth understanding of the MER-based biodegradation and bioremediation could be further achieved by constructing different-scale mathematic models.

12.1.3 Integration with Other Technologies

The MER-based pollutant removal has been shown several limitations such as low removal efficiency and difficult to be mineralized, which seriously limits its applications in biodegradation of pollutants. In order to overcome those shortages, the MER process has been coupled with other technologies to enhance pollutant removal and mineralization efficiency, which remarkably expand its practical applications. For instance, the MER process was already integrated into several anaerobic systems, including upflow anaerobic blanket reactor, anaerobic fluidized bed, and anaerobic baffled reactor [19–21], for improving the biodegradation of persistent organic pollutants. In addition, the MER coupled with photocatalysis or Fenton process has also been successfully constructed to significantly increase the removal and mineralization efficiencies of toxic pollutants [22, 23]. Nevertheless, the clear understanding of mechanisms of such coupled systems still lacked, which restrict to develop more novel coupled systems. In the next step, the research can focus on the following points:

1. The electroactive bacteria and other functional degradable microorganisms always coexist in the coupled systems, and the microbial metabolic network would be quite different from the traditional biological systems. Consequently,

the characteristics of metabolic networks of various microorganisms and their cooperative mechanisms in coupled systems need to be fully elucidated.

2. Conversion and degradation mechanisms of pollutants need be further explored in the coupled systems. Compared to the single system, the mechanisms of pollutant conversion and degradation would be more complex in the coupled systems, which make it more difficult to be understood. Therefore, different advanced analysis methods should be adopted or developed to face this challenge in the future.

3. Developing more MER coupled technologies. With the rapid development of industrialization, the species of pollutants in wastewater increased, including a variety of low-level toxic emerging organic pollutants, which are difficult to be deep eliminated by existing technologies. As a consequence, this would bring us a high level of motivation to develop more novel MER coupled technologies.

12.1.4   Scaling Up of MER-Based Technology

Although the MER-based technology has been shown the potential promising for pollutant biodegradation and environmental bioremediation, the vast majority of studies on this technology still remain at the lab-scale, due to a range of factors limiting its large-scale application, such as high amplification cost, time-consuming, poor stability, and difficulty to carry out field studies. The first large-scale test of BESs was conducted at Foster's brewery in Yatala, Queensland, by the Advanced Water Management Center at the University of Queensland. The reactor consisted of 12 modules, each 3 m high, with a total volume of approximately 1 m^3. Little is known about the BES performance, other than low solution conductivity, limiting current density and excess biochemical oxygen demand. The first pilot-scale BES for hydrogen production using organic wastewater was conducted by Penn State researchers. The reactor contained 24 modules, each with six pairs of electrodes, and was approximately 1 m^3 in total volume [24].

However, in order to realize the large-scale engineering application of the MER-based technology, more unremitting efforts should be put into various aspects in the future.

1. Selection of electrode and membrane materials. It is essential to find low-cost and high-stability electrode and membrane materials, which can affect the cost and long-term stability of the whole system. Carbon materials seem to be the best choice, based on the adsorption capacity, biocompatibility, and cost of materials. However, low conductivity and biological fouling during the long-running process restrict its development [25]. Besides, the price of proton and cation exchange membranes is very expensive, and the phenomenon of membrane blockage and fouling is inevitable in the long running of the system. As a consequence, it is imminent to develop different low-cost and antifouling membranes, which depend on the advances of material science. In addition, high surface,

porous three-dimensional electrode materials need be further developed in order to offer enough surface area for the thin biofilm of electroactive bacteria.

2. Design of system configuration. Many reactor configurations have been reported at the lab-scale, such as tube, cubic, and bottle shapes. However, there are various limitations in the configuration of these reactors in the process of large-scale applications, such as significant increase in the internal resistance, enlarging the reactor dead zone, and aggravation of the uneven distribution of hydraulic distribution especially on the surface of electrodes. These limitations would seriously decrease the efficiency of systems, resulting in much lower performance compared to the lab-scale reactors. Therefore, design of new reactor configurations is of the essence to deal with the above problems. One point to be focused on is that the hydrodynamic of the system needs to be further studied, so as to optimize the reactor kinetics and guide reactor design [26]. In addition, the existence of membrane will remarkably increase the ohmic resistance and the cost of reactors, therefore the design of membrane-free MER systems might be another focus in the next step [27].

3. Life cycle assessment (LCA) on the MER-based technology. LCA is a universally accepted approach of determining the environmental consequences of a particular product over its entire production cycle, which is necessary to avoid unintended consequences of a new technology or mitigation strategy [28]. It is necessary to conduct analyses of potential life cycle impacts of the MER-based technology, aiming to avoid unintended consequences of this technology. Currently, there are few evaluations on the MER-based technology with regard to their life cycle in terms of performance and economic as well as comparison to existing technologies. Therefore, it is essential to have a complete "cradle-to-grave" life cycle assessment of the MER-based technology, which not only gives an idea to the researchers and policy makers of all the necessary scientific/technical points but also serves as a guiding tool to the practitioners of this technology.

4. Field-scale study. With the scale-up and engineering application of the MER-based technology, field-scale study is unavoidable although it is more expensive and time-consuming than lab-scale study. It is the only reasonable way to determine the suitable deployment location and configuration of the MER-based technology and evaluate whether microorganisms can sustain growth over time within a specific treatment zone. Moreover, due to extreme environmental conditions and complexity of microbial ecology in the real wastewater, manipulating the MER-based technology could be extremely challenging even with positive testing results obtained in labs. Thus, future field studies should be conducted to address the following issues such as material selection, reactor design, operating mode, and site conditioning, based on a balanced consideration of the process robustness and stability, remediation efficiency, economical feasibility, and environmental sustainability.

References

1. Strik DP, Timmers RA, Helder M, Steinbusch KJ, Hamelers HV, Buisman CJ (2011) Microbial solar cells: applying photosynthetic and electrochemically active organisms. Trends Biotechnol 29(1):41–49

2. Hatzell MC, Cusick RD, Logan BE (2014) Capacitive mixing power production from salinity gradient energy enhanced through exoelectrogen-generated ionic currents. Energy Environ Sci 7(3):1159–1165

3. Liu XW, Wang YP, Huang YX, Sun XF, Sheng GP, Zeng RJ, Li F, Dong F, Wang SG, Tong ZH (2011) Integration of a microbial fuel cell with activated sludge process for energy-saving wastewater treatment: taking a sequencing batch reactor as an example. Biotechnol Bioeng 108(6):1260–1267

4. Logan BE (2009) Exoelectrogenic bacteria that power microbial fuel cells. Nat Rev Microbiol 7(5):375

5. Lovley DR (2006) Bug juice: harvesting electricity with microorganisms. Nat Rev Microbiol 4(7):497

6. Choi O, Sang BI (2016) Extracellular electron transfer from cathode to microbes: application for biofuel production. Biotechnol Biofuels 9(1):11

7. Rivalland C, Madhkour S, Salvin P, Robert F (2015) Electrochemical and microbial monitoring of multi-generational electroactive biofilms formed from mangrove sediment. Bioelectrochemistry 106:125–132

8. Qiao Y, Bao SJ, Li CM (2010) Electrocatalysis in microbial fuel cells—from electrode material to direct electrochemistry. Energy Environ Sci 3(5):544–553

9. Yong YC, Yu YY, Yang Y, Li CM, Jiang R, Wang X, Wang JY, Song H (2012) Increasing intracellular releasable electrons dramatically enhances bioelectricity output in microbial fuel cells. Electrochem Commun 19:13–16

10. Yong YC, Yu YY, Li CM, Zhong JJ, Song H (2011) Bioelectricity enhancement via overexpression of quorum sensing system in Pseudomonas aeruginosa-inoculated microbial fuel cells. Biosens Bioelectron 30(1):87–92

11. Yong YC, Yu YY, Zhang X, Song H (2014) Highly active bidirectional electron transfer by a self-assembled electroactive reduced-graphene-oxide-hybridized biofilm. Angew Chem Int Ed 53(17):4480–4483

12. Qi M, Liang B, Chen R, Sun X, Li Z, Ma X, Zhao Y, Kong D, Wang J, Wang A (2018) Effects of surface charge, hydrophilicity and hydrophobicity on functional biocathode catalytic efficiency and community structure. Chemosphere 202:105–110

13. Bian R, Jiang Y, Wang Y, Sun JK, Hu J, Jiang L, Liu H (2018) Highly boosted microbial extracellular electron transfer by semiconductor nanowire array with suitable energy level. Adv Funct Mater 1707408:1–7

14. Shkil H, Schulte A, Guschin DA, Schuhmann W (2011) Electron transfer between genetically modified hansenula polymorpha yeast cells and electrode surfaces via Os-complex modified redox polymers. ChemPhysChem 12(4):806–813

15. Franks AE, Nevin KP, Jia H, Izallalen M, Woodard TL, Lovley DR (2009) Novel strategy for three-dimensional real-time imaging of microbial fuel cell communities: monitoring the inhibitory effects of proton accumulation within the anode biofilm. Energy Environ Sci 2(1):113–119

16. Kato Marcus A, Torres CI, Rittmann BE (2007) Conduction-based modeling of the biofilm anode of a microbial fuel cell. Biotechnol Bioeng 98(6):1171–1182

17. Picioreanu C, Head IM, Katuri KP, van Loosdrecht MC, Scott K (2007) A computational model for biofilm-based microbial fuel cells. Water Res 41(13):2921–2940

18. Wang YZ, Wang YK, He CS, Yang HY, Sheng GP, Shen JY, Mu Y, Yu HQ (2015) Hydrodynamics of an electrochemical membrane bioreactor. Sci Rep 5:10387

19. Kim T, An J, Jang JK, Chang IS (2015) Coupling of anaerobic digester and microbial fuel cell for COD removal and ammonia recovery. Bioresour Technol 195:217–222

20. Cui D, Guo YQ, Lee HS, Wu WM, Liang B, Wang AJ, Cheng HY (2014) Enhanced decolorization of azo dye in a small pilot-scale anaerobic baffled reactor coupled with biocatalyzed electrolysis system (ABR–BES): a design suitable for scaling-up. Bioresour Technol 163:254–261
21. Shen J, Xu X, Jiang X, Hua C, Zhang L, Sun X, Li J, Mu Y, Wang L (2014) Coupling of a bioelectrochemical system for p-nitrophenol removal in an upflow anaerobic sludge blanket reactor. Water Res 67:11–18
22. Feng CH, Li FB, Mai HJ, Li XZ (2010) Bio-electro-Fenton process driven by microbial fuel cell for wastewater treatment. Environ Sci Technol 44(5):1875–1880
23. Xu X, Zhou B, Ji F, Zou Q, Yuan Y, Jin Z, Zhao D, Long J (2015) Nitrification, denitrification, and power generation enhanced by photocatalysis in microbial fuel cells in the absence of organic compounds. Energy Fuel 29(2):1227–1232
24. Logan BE (2010) Scaling up microbial fuel cells and other bioelectrochemical systems. Appl Microbiol Biotechnol 85(6):1665–1671
25. Zhou M, Chi M, Luo J, He H, Jin T (2011) An overview of electrode materials in microbial fuel cells. J Power Sources 196(10):4427–4435
26. Wang YR, Gong L, Jiang JK, Chen ZG, Yu HQ, Mu Y (2017) Response of anodic biofilm to hydrodynamic shear in two-chamber bioelectrochemical systems. Electrochim Acta 258:1304–1310
27. Liu H, Logan BE (2004) Electricity generation using an air-cathode single chamber microbial fuel cell in the presence and absence of a proton exchange membrane. Environ Sci Technol 38(14):4040–4046
28. Pant D, Singh A, Van Bogaert G, Gallego YA, Diels L, Vanbroekhoven K (2011) An introduction to the life cycle assessment (LCA) of bioelectrochemical systems (BES) for sustainable energy and product generation: relevance and key aspects. Renew Sust Energ Rev 15(2):1305–1313